CANCER MODELS

EDITED BY: Michael Breitenbach and Jens Hoffmann
PUBLISHED IN: Frontiers in Oncology

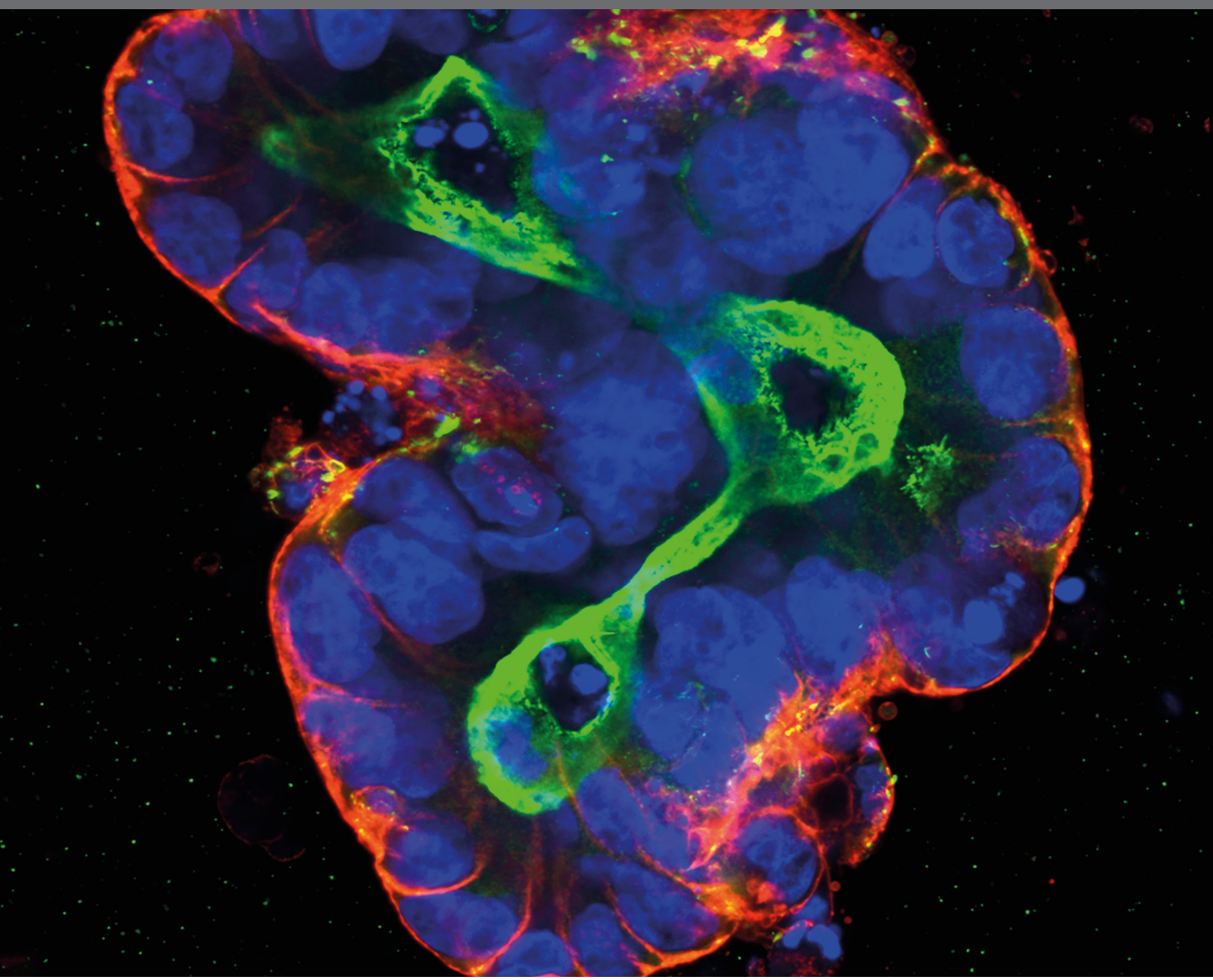

frontiers Research Topics

ISSN 1664-8714
ISBN 978-2-88945-701-4
DOI 10.3389/978-2-88945-701-4

About Frontiers

Frontiers is more than just an open-access publisher of scholarly articles: it is a pioneering approach to the world of academia, radically improving the way scholarly research is managed. The grand vision of Frontiers is a world where all people have an equal opportunity to seek, share and generate knowledge. Frontiers provides immediate and permanent online open access to all its publications, but this alone is not enough to realize our grand goals.

Frontiers Journal Series

The Frontiers Journal Series is a multi-tier and interdisciplinary set of open-access, online journals, promising a paradigm shift from the current review, selection and dissemination processes in academic publishing. All Frontiers journals are driven by researchers for researchers; therefore, they constitute a service to the scholarly community. At the same time, the Frontiers Journal Series operates on a revolutionary invention, the tiered publishing system, initially addressing specific communities of scholars, and gradually climbing up to broader public understanding, thus serving the interests of the lay society, too.

Dedication to Quality

Each Frontiers article is a landmark of the highest quality, thanks to genuinely collaborative interactions between authors and review editors, who include some of the world's best academicians. Research must be certified by peers before entering a stream of knowledge that may eventually reach the public - and shape society; therefore, Frontiers only applies the most rigorous and unbiased reviews.
Frontiers revolutionizes research publishing by freely delivering the most outstanding research, evaluated with no bias from both the academic and social point of view. By applying the most advanced information technologies, Frontiers is catapulting scholarly publishing into a new generation.

What are Frontiers Research Topics?

Frontiers Research Topics are very popular trademarks of the Frontiers Journals Series: they are collections of at least ten articles, all centered on a particular subject. With their unique mix of varied contributions from Original Research to Review Articles, Frontiers Research Topics unify the most influential researchers, the latest key findings and historical advances in a hot research area! Find out more on how to host your own Frontiers Research Topic or contribute to one as an author by contacting the Frontiers Editorial Office: researchtopics@frontiersin.org

CANCER MODELS

Topic Editors:
Michael Breitenbach, University of Salzburg, Austria
Jens Hoffmann, EPO Experimental Pharmacology & Oncology Berlin-Buch GmbH, Germany

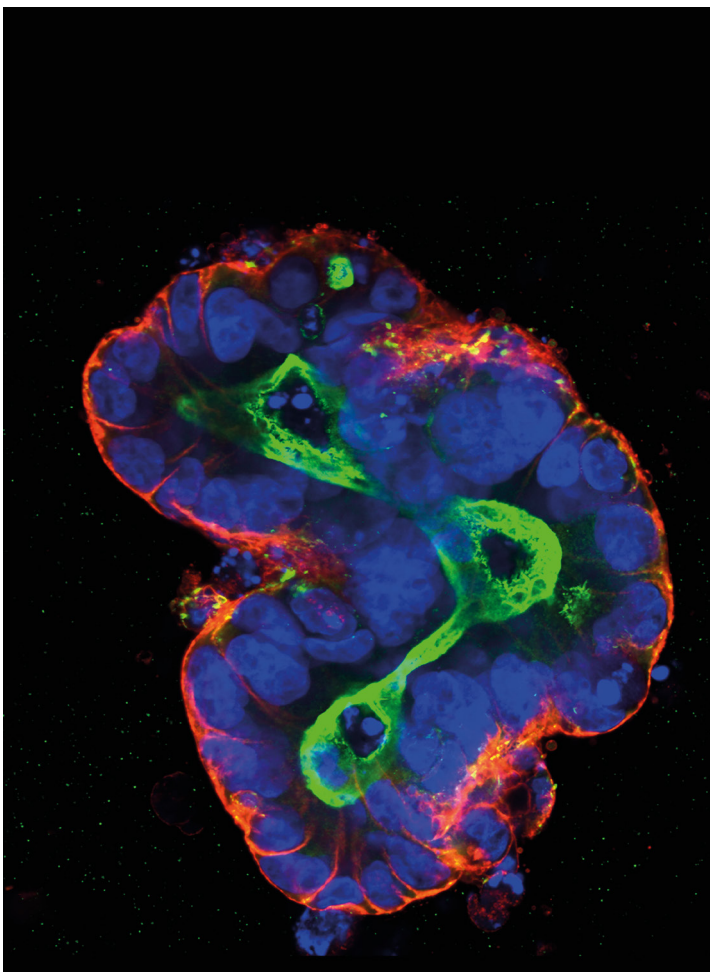

Immunofluorescence micrograph of a patient-derived 3D (PD3D®) organoid stained for EpCAM (red), Ezrin (green) and nuclei (DAPI, blue). For details see Gaebler et al. (2017).

Cancer research, like research on other diseases, highly depends on representative and reliable model systems. In the Research Topic "Cancer Models", we collected original papers and review articles addressing the topic of tumor modeling from molecular biology, biochemistry, microorganisms, cells and organoids, fishes, animals and xenografts, up to computational cancer models and patient data analysis.

This representative eBook describes that there is not a single molecular defined tumor but rather a heterogenic and highly variable complex of different individual diseases. This is what makes research on cancer so difficult, expensive, and explains the broad number of models needed for research.

Our authors describe new next-generation sequencing-based methods to analyze complex patterns of chromosomal aberrations in order to understand the molecular biology of tumorigenesis as well as the role of cellular senescence and dormancy in the aetiology of tumor formation and development of therapy resistance of tumors. The current developments on 3D cultures are thoroughly reviewed, as these models help to overcome the current limitations of cell cultures and allow a more accurate mimicry of the native cancer tissue, including cellular heterogeneity and restore specific biochemical and morphological. Reviews about tumor models in zebrafish, different transgenic mouse strains and pigs conclude the book. In the final two chapters of this volume, the authors discuss the theoretical and mathematical models developed in cancer research.

Citation: Breitenbach, M., Hoffmann, J., eds. (2019). Cancer Models. Lausanne: Frontiers Media. doi: 10.3389/978-2-88945-701-4

Table of Contents

IV. MODELING CANCER IN FISH, MICE, AND PIGS

V. COMPUTATIONAL MODELS IN CANCER RESEARCH

frontiers in Oncology

EDITORIAL
published: 03 October 2018
doi: 10.3389/fonc.2018.00401

Editorial: Cancer Models

Michael Breitenbach[1] *and Jens Hoffmann*[2]*

[1] *Department of Biosciences, University of Salzburg, Salzburg, Salzburg, Austria,* [2] *Experimental Pharmacology and Oncology Berlin-Buch GmbH, Berlin, Germany*

Keywords: tumor models, PDX (patient-derived xenografts), tumor cell, Transgene mouse, 3D cell biology

Editorial on the Research Topic

Cancer Models

Cancer is still a major concern for public health and is a cause of death while being psychologically the most dreaded disease. Until recent times, the diagnosis of a progressed form of cancer invariably meant that there was little chance for long-term survival. This notion has changed recently thanks to the tremendous efforts in cancer research and development (compared to other diseases) supported by enormous public and private financing. To illustrate this, just consider the "moonshot initiative" announced by US President Obama in 2016 (1).

Cancer research, like research in other diseases, highly depends on representative and reliable model systems. However, cancer is not the single molecule-defined tumor, but rather a heterogenic and highly variable complex of different individual diseases. This makes research on cancer highly difficult, expensive, and explains the enormous resources needed.

Looking back on more than 100 years of cancer research, the models used have changed constantly and extended permanently to all the new stages of drug discovery including target identification, lead structure optimization, tolerability, toxicity, biomarker discovery, and individual patient prediction. Today, the selection of the most appropriate model to best reflect the given tumor entity is one of the major challenges for the cancer researchers.

From the available volumes on the research topic "Cancer Models," we collected original papers and review articles that addressed the topic of tumor modeling from perspectives such as molecular biology, biochemistry, microorganisms, cells, and organoids, fishes, animals, and xenografts, up to computational cancer models and patient data analysis.

Next-generation sequencing-based methods have recently revealed complex patterns of chromosomal aberrations, which are beyond explanation by classical models of karyotypic evolution. The term chromothripsis has been introduced to describe the phenomenon of temporarily and spatially confined genomic instability. This results in dramatic chromosomal rearrangements of segments of one or a few chromosomes. Simultaneously, misrepaired DNA double-strand breaks are causing another phenomenon called chromoplexy, which is characterized by the presence of chained translocations and interlinking deletion bridges in chromosomes.

Steininger et al. have been new models for the molecular biology underlying tumorigenesis. They developed a technology for genome-wide identification of chromosomal translocations based on the analysis of translocation-associated changes in spatial proximities of chromosome territories. Using the sequence data from a cutaneous T-cell lymphoma for genome-wide chromosome conformation capture (Hi-C), they fine-mapped chromosomal breakpoints and correlated them with gene-associated biological processes like transcription. As identification and functional analysis of chromosomal aberrations are basic for cancer research, such genome-wide high-resolution analyses of structural chromosomal aberrations will gain increasing importance.

OPEN ACCESS

Edited and reviewed by:
Paolo Pinton,
University of Ferrara, Italy

***Correspondence:**
Jens Hoffmann
Jens.Hoffmann@epo-berlin.com

Specialty section:
This article was submitted to Molecular and Cellular Oncology, a section of the journal Frontiers in Oncology

Received: *15 August 2018*
Accepted: *03 September 2018*
Published: *03 October 2018*

Citation:
Breitenbach M and Hoffmann J (2018) Editorial: Cancer Models. Front. Oncol. 8:401. doi: 10.3389/fonc.2018.00401

In this light, Tosato et al. describe a model for the functional validation of gene translocations in yeast models. Genetic fusions between NUP145 and TOP2 in the human orthologs are associated with acute myeloid leukemia (AML). This translocant yeast strain can be used as a model to provide new grounds for a possible involvement of p53 in cell transformation toward AML.

A better understanding of tumor cell biology has led to the development of new model systems for certain functional processes that are related to the development and growth of cancer.

Some of these new methods and models are reviewed in the chapters of Schosserer et al., Lorz et al., Valenzuela et al., and Auer et al. In the individual cancers, the mechanisms for tumor hypoxia and senescence and cytoskeletal organization vary. Thus, specialized pharmacological agents need to be applied after characterizing a specific tumor with new and advanced biochemical methods. This includes tumor neo-antigens, specific ways of deregulation in the tumor, genomic sequencing of the tumor and the patient, and various omics methods applied to the tumor material and to patient-derived xenografts. Precision medicine means that a large amount of the data just mentioned is now being used to construct a pathway model of the individual tumor with the help of new bioinformatics methods, often called "big data" or "data science."

A very important and relevant topic in cancer research in the twenty-first century is the role of cellular senescence and dormancy in the etiology of tumor formation and of therapy resistance of tumors. No fewer than three of the chapters published in the present volume deal with this topic: Schosserer et al., Yadav et al., and Valenzuela et al. Cellular senescence of cultured human cells was discovered by Hayflick (2) and termed senescence. Ever since that discovery, the "Hayflick phenomenon" or "Hayflick aging" was discussed as a possible cause of organismic aging. For a long time, it was unclear if Hayflick aging is perhaps an artifact of cell culture–because lowering the oxygen partial pressure during cell culture to the low levels occurring in peripheral tissue can indeed substantially increase the lifespan of a cell. Biochemical markers of senescence were discovered, such as the senescence-associated beta-galactosidase (3) and the senescence-associated secretory phenotype (4) and relatively recently, it was shown beyond doubt that senescent cells do occur *in vivo* in old individuals and constitute one cause of organismic aging. The latter fact was shown by eliminating the senescent cells by selectively inducing apoptosis of these cells without general induction of apoptosis in the mouse. Compounds able to do this are called senolytics (5). Even naturally aged mice regained juvenile organ characteristics by this treatment, for instance in the kidney (4, 6). Senescent cells are found in tumors (7) and, quite frequently, chemotherapy spares those cells and leads to an often deadly relapse of the disease. The senescent cells can, through release of cytokines (the senescent cell secretome), induce cancerous growth in surrounding cells. An important aim for cancer therapy would be not only to kill the fast dividing cancer cells, but also to kill, like in the experiments of Baar et al. (6), the senescent cells contained in the tumors. This relatively new development completely replaces the old theory that senescence was primarily "invented" by evolution to avoid the formation of tumors (8).

The importance of cellular senescence in cancer biology is further stressed in the hypothesis and theory chapter by Valenzuela et al. These authors explain the role of the senescence associated secretory phenotype (SASP) in the MET and in the formation of metastases. In this process, which is intimately connected also to aging and the permanent low level of inflammation in aged individuals, platelets play a central role, which was not studied intensively in the past.

While classical 2D cell culture models have been the mainstay for cancer research, current limitations of cell cultures are now partially overcome by 3D cell cultures that allow a more accurate mimicry of the native cancer tissue, since they preserve cellular heterogeneity and restore some of the specific biochemical and morphological features similar to the corresponding tissue *in vivo*. This is a fundamental advantage, because both morphology and cell-environment crosstalk strongly influence gene expression and, therefore, cell behavior.

They have gained an important role for research on tumor micro-environmental regulation of proliferation, invasion, cell-cell interaction and metabolism, used between cellular monolayers and animal models. The 3D cell cultures have served as a model for a variety of experimental therapy studies using radiotherapy, chemotherapy, as well as cell- and antibody-based immunotherapy. The current developments in 3D cultures are thoroughly reviewed by Gaebler et al. in this volume.

Modeling of tumor disease in animals goes back to more than 100 years to the first experiments with the transplantation of syngeneic tumors in inbred mouse strains (9). These models are mainly replaced by "human" tumor models, the pros and cons of which have been described in more details by Klinghammer et al. (10).

A relatively new animal model, in between cell culture and mammalian models, is based on the zebrafish (*Danio rerio*). The zebrafish model, treated here in the chapter written by Kirchberger et al., offers the important advantage of extracorporeal fertilization, and a very well-researched translucent embryo, as well as short generation time and a well-developed genetical toolbox. All this makes this little fish an ideal model system for studying development. Cancer, after all, is a deviation from normal development, caused by aberrations in gene expression. In a zebrafish melanoma model, it could be shown that at the base of cancer formation is the de-differentiation of epithelial cells to form embryonic neural crest cells (11). Due to the small size, short generation time, and extracorporeal development of the fish, it was possible to perform several large-scale screens (in a typical case more than 26,000 compounds) of chemical libraries to find compounds that could inhibit specific cancers or metastasis in transgenic fish containing patient-derived xenografts (12).

Using mouse models to study human tumor growth dates back to the late 1960s. Development of immune-deficient mouse strains like nude or severe combined immunodeficiency (SCID) allowed a continuous improvement of these models, which

can be used for xenotransplanting human cell lines or human tumors directly as patient-derived xenotransplants (=PDX) or transplant human cell lines [for review see Behrens et al. (13)].

Two further animal models are treated in separate chapters in this volume. As we know now, it is in nearly all cases impossible to study the very early stages of the disease in humans due to the very long time interval between a primary causative mutational event and the first detection of a tumor in the clinic. However, it is possible to look at these early stages of tumor development in certain highly sophisticated transgenic mouse models, which allow the researchers to induce expression of an oncogenic mutation in an otherwise healthy animal at a specific time and in a specific organ (see the chapter by Lampreht-Tratar et al. on "transgenic mouse models in cancer research").

Genomically, mice and humans are reasonably closely related as about 80% of all protein coding genes of humans share closely related orthologs with the mouse, including most of the recognized genes involved in cancer. What makes the mouse model so attractive is the short generation time (10 weeks) and average life expectancy (2.5 years in commonly used laboratory mice), the possibilities for reverse genetics, meaning the possibility to introduce at will nearly all genetic alterations desired to study cancer biology, and the frequent occurrence of cancer even in the absence of cancerogenic agents, with an exponential increase in old age, like in humans. Of course, not all questions posed by human cancers can be answered in one animal model.

The domestic pig is an additional new animal model for cancer, which is treated in detail in the chapter on the Oncoming Cancer Model by Schachtschneider et al. in the present volume. This chapter very well describes both the differences and shortcomings of the mouse cancer model and the surprising similarities between the human and pig cancer biology. We name just a few important experimental findings pertaining to the comparison of these cancer models. First, the loss of heterozygosity (LOH) mechanism, which is very common in human cancers, in particular in adenomatous polyposis coli (APC) leading to colon cancer appears to be very infrequent in mice. Second, the cytochrome P450 system of mice is very different from the human system, making a detailed comparison of the cancerogenic potential of xenobiotics is difficult in the mouse. On the other hand, the cytochrome P450 system is very similar in swine and humans. Liver cirrhosis and hepatocellular carcinoma (HCC) can be efficiently induced in pigs and the experimental therapeutical possibilities (surgical as well as chemotherapeutic) can be well studied in the pig. Generally, the large size of the pig make it easier to study therapeutic approaches, typical comorbidities and the interaction of cancers with the microbiome are similar to the ones found in human patients.

So it appears that the three animal model systems presented here together with several others not mentioned presently can all lead the way to answering different open questions in cancer biology complementing each other. In all three animals, the complete sequence of the genome is known and the techniques of genetic manipulation needed for cancer research are well developed. These techniques include reverse genetics including the modern CRISPR/Cas9 system in several forms, the creation of conditional mutations in cancer-relevant genes, and the cloning of animals by somatic cell nuclear transfer (SCNT).

We just have to mention that during the last 10 years, the biggest impact and improvement in cancer survival were without any doubt the introduction of new ways to raise the patient's immune defense against cancer cells as a new form of therapy. This was achieved not only through the newly developed humanized antibodies that recognize cancer cells through binding to neo-antigens, but also due to more subtle interference with the natural regulators of the immune system, for instance IL2, aiming at the induction of apoptosis of tumor cells without imposing a general cytostatic load onto the patient. Spectacular examples of cancers where 5-year survival was extremely low and a complete cure is now possible include certain forms of melanoma (14). Models for tumor immunology are extremely challenging and will be addressed in a separate research topic.

In our times, literature data are becoming more and more important for cancer research. New mathematical models analyzing literature data can be used to identify or validate new tumor targets. For example, hypoxia is an important topic in cancer research that was investigated continuously over several decades, starting with the seminal papers of Warburg (15). Rausch et al. summarize the results of 18 publications dealing with the correlation of breast cancer incidence with adipocytes and severe obesity. Adipocytes are a source of several hormones like adiponectin, which is positively correlated with breast cancer incidence and progression. By downstream signaling via HIF-1apha, adiponectin can contribute to the formation of the breast tumors.

In the final two chapters of this volume, the authors are dealing with theoretical and mathematical models developed in cancer research. Ogilvie et al. in their "Perspective" contribution present meta-theoretical considerations on mathematical models in cancer research and treat questions like these: What are the basic and most important prerequisites which are to be met, if a theoretical model shall benefit cancer research? Which are the results that were produced up to now? What has been modeled and what is currently impossible to describe meaningfully in a theoretical model? This chapter deals primarily with the possibility (or currently "impossibility") to use bioinformatics models to create a truly personalized medicine (16, 17). This would be based on the ever increasing datasets provided by the "omics" methods as applied to tumor material, the genome of the tumor and of the patient, and the metabolic pathways revealed by metabolomics. Lorz et al., in their chapter, present original research done with a mathematical model based on partial differential equations dealing with growth of cancer cell lines *in vitro* under the influence of variable parameters like initial cell density and, most importantly, concentrations of cell cycle inhibitors (anti-mitotic agents). During the *in silico* experiment, the cells populate three different compartments:

proliferation (active cell division), quiescence (blocked cell division and survival), and apoptosis (programmed cell death). The simulations correctly predict under which conditions the actively dividing tumor cells will die out and the kinetics of the transitions between the three compartments. Of note, the quiescent (dormant) state, corresponding to a reversible cell cycle arrest, is a necessary component of the model. It has been covered in three other chapters in the present book (see above) and plays a central role in contemporary cancer research.

AUTHOR CONTRIBUTIONS

All authors listed have made a substantial, direct and intellectual contribution to the work, and approved it for publication.

FUNDING

This work was supported by grant P26713 of the Austrian Science Fund (FWF) to MB.

REFERENCES

1. Sindzinski A. The moonshot initiative and the future of cancer research. *J Natl Cancer Inst.* (2017) 109:djx276. doi: 10.1093/jnci/djx276
2. Hayflick L, Moorhead PS. The serial cultivation of human diploid cell strains. *Exp Cell Res.* (1961) 25:585–621.
3. Dimri GP, Lee X, Basile G, Acosta M, Scott G, Roskelley C, et al. A biomarker that identifies senescent human cells in culture and in aging skin *in vivo*. *Proc Natl Acad Sci USA.* (1995) 92:9363–7. doi: 10.1073/pnas.92.20.9363
4. de Keizer PL. The fountain of youth by targeting senescent cells? *Trends Mol Med.* (2017) 23:6–17. doi: 10.1016/j.molmed.2016.11.006
5. Zhu Y, Tchkonia T, Pirtskhalava T, Gower AC, Ding H, Giorgadze N, et al. The Achilles' heel of senescent cells: from transcriptome to senolytic drugs. *Aging Cell* (2015) 4:644–58. doi: 10.1111/acel.12344
6. Baar MP, Brandt RMC, Putavet DA, Klein JDD, Derks KWJ, Bourgeois BRM, et al. Targeted apoptosis of senescent cells restores tissue homeostasis in response to chemotoxicity and aging. *Cell* (2017) 169:132–47. doi: 10.1016/j.cell.2017.02.031
7. Collado M, Serrano M. The power and the promise of oncogene-induced senescence markers. *Nat Rev Cancer* (2006) 6:472–6. doi: 10.1038/nrc1884
8. Campisi J. Senescent cells, tumor suppression, and organismal aging: good citizens, bad neighbors. *Cell* (2005) 120:513–22. doi: 10.1016/j.cell.2005.02.003
9. Ehrlich P, Apolant H. Beobachtungen über maligne Mäusetumoren. *Berliner Klinische Wochenschrift* (1905) 42:871–4.
10. Klinghammer K, Walther W, Hoffmann J. Choosing wisely-Preclinical test models in the era of precision medicine. *Cancer Treat Rev.* (2017) 55:36–45. doi: 10.1016/j.ctrv.2017.02.009
11. Kaufman CK, Mosimann C, Fan ZP, Yang S, Thomas AJ, Ablain J, et al. A zebrafish melanoma model reveals emergence of neural crest identity during melanoma initiation. *Science* (2016) 351:6272. doi: 10.1126/science.aad2197
12. Ridges S, Heaton WL, Joshi D, Choi H, Eiring A, Batchelor L, et al. Zebrafish screen identifies novel compound with selective toxicity against leukemia. *Blood* (2012) 119:5621–31. doi: 10.1182/blood-2011-12-398818
13. Behrens D, Rolff J, Hoffmann J. Predictive In Vivo Models for Oncology. *Handb Exp Pharmacol* (2016) 232:203–21. doi: 10.1007/164_2015_29
14. Barlas S. The white house launches a cancer moonshot: despite funding questions, the progress appears promising. *P & T* (2016) 41:290–5.
15. Warburg O. On respiratory impairment in cancer cells. *Science* (1956) 124:269–70.
16. Angermueller C, Pärnamaa T, Parts L, Stegle O. Deep learning for computational biology. *Mol Syst Biol.* (2016) 12:878. doi: 10.15252/msb.20156651
17. Schork NJ. Personalized medicine: time for one-person trials. *Nature* (2015) 520:609–11. doi: 10.1038/520609a

Conflict of Interest Statement: The authors declare that the research was conducted in the absence of any commercial or financial relationships that could be construed as a potential conflict of interest.

frontiers in Oncology

REVIEW
published: 25 September 2017
doi: 10.3389/fonc.2017.00211

The Linkage between Breast Cancer, Hypoxia, and Adipose Tissue

Linda K. Rausch[1,2], Nikolaus C. Netzer[1,2,3], Josef Hoegel[4] and Stephan Pramsohler[1]*

[1] Hermann Buhl Institute for Hypoxia and Sleep Medicine Research, Bad Aibling, Germany, [2] Department of Sports Science, University Innsbruck, Innsbruck, Austria, [3] Division of Sports Medicine and Rehabilitation, Department of Medicine, University Ulm, Ulm, Germany, [4] Institute of Human Genetics, University of Ulm, Ulm, Germany

Objective: The development of breast cancer cells is linked to hypoxia. The hypoxia-induced factor HIF-1α influences metastasis through neovascularization. Hypoxia seems to decrease the responsiveness to hormonal treatment due to loss of estrogen receptors (ERs). Obesity is discussed to increase hypoxia in adipocytes, which promotes a favorable environment for tumor cells in mammary fat tissue, whereas, tumor cells profit from good oxygen supply and are influenced by its deprivation as target regions within tumors show. This review gives an overview of the current state on research of hypoxia and breast cancer in human adipose tissue.

Methods: A systematic literature search was conducted on PubMed (2000–2016) by applying hypoxia and/or adipocytes and breast cancer as keywords. Review articles were excluded as well as languages other than English or German. There was no restriction regarding the study design or type of breast cancer. A total of 35 papers were found. Eight studies were excluded due to missing at least two of the three keywords. One paper was removed due to Russian language, and one was dismissed due to lack of adherence. Seven papers were identified as reviews. After applying exclusion criteria, 18 articles were eligible for inclusion.

Results: Two articles describe the impairment of mammary epithelial cell polarization through hypoxic preconditioning. A high amount of adipocytes enhances cancer progression due to the increased expression of HIF-1α which causes the loss of ER α protein as stated in four articles. Four articles analyzed that increased activation of HIF's induces a series of transcriptions resulting in tumor angiogenesis. HIF inhibition, especially when combined with cytotoxic chemotherapy, holds strong potential for tumor suppression as stated in further four articles. In two articles there is evidence of a strong connection between hypoxia, oxidative stress and a poor prognosis for breast cancer via HIF regulated pathways. Acute hypoxia seems to normalize the microenvironment in breast cancer tissue and has proven to affect tumor growth positively as covered in two articles.

Conclusion: This review indicates that the development of breast cancer is influenced by hypoxia. A high amount of adipocytes enhances cancer progression due to the increased expression of HIF-1α.

Keywords: hypoxia, adipocytes, breast cancer, HIF-1α, HIF-2α

OPEN ACCESS

Edited by:
Michael Breitenbach, University of Salzburg, Austria

Reviewed by:
Maja Cemazar, Institute of Oncology Ljubljana, Slovenia
Luisa Lanfrancone, Istituto Europeo di Oncologia, Italy

****Correspondence:***
Linda K. Rausch
l.rausch@hermann-buhl-institut.de

Specialty section:
This article was submitted to Molecular and Cellular Oncology, a section of the journal Frontiers in Oncology

Received: *14 June 2017*
Accepted: *28 August 2017*
Published: *25 September 2017*

Citation:
Rausch LK, Netzer NC, Hoegel J and Pramsohler S (2017) The Linkage between Breast Cancer, Hypoxia, and Adipose Tissue. Front. Oncol. 7:211. doi: 10.3389/fonc.2017.00211

INTRODUCTION

Breast cancer is the most commonly diagnosed cancer in women (1). In 2012, over a million new cases were identified and figures are rising due to late diagnosis at already quite advanced cancer stages (World Cancer Research Fund International, 2012) (2). Breast cancer represents 25% of all cancer types in women and is the fifth most common cause of death. It is classified into three main groups (3). The hormone receptor (HR) positive group, which expresses estrogen receptor (ER) or progesterone receptor (PR); the epidermal growth factor receptor 2 (HER2) positive group and the triple-negative breast cancer (TNBC) group without expression of ER, PR, and HER2. 90% of breast cancer patients die in consequence of metastasis most commonly found in bone tissue (4).

Several prospective, epidemiological studies show that there is a direct relationship between obesity and cancer (5–9). Especially, the manifestation of breast cancer seems to be linked to obesity (10). Notably, female obese breast cancer patients show a less sufficient response to the same dosage of chemotherapy compared to female lean breast cancer patients (11). In premenopausal women, the risk for breast cancer is reduced with increasing body mass index (BMI). Thus, postmenopausal women are at higher risk for breast cancer development if BMI is increased (10). There is a strong association between BMI and breast cancer in ER−/PR+ receptor positive breast cancer types as found in a dose–response meta-analysis (12). This could be due to an increase in sex-hormones triggered by an increase in estradiol production of adipose tissue, caused by a higher activity of aromatase enzymes (13). Adipose tissue is divided into brown adipose tissue (BAT) and white adipose tissue (WAT). BAT is only 50 g compared to kilograms of WAT, which is an endocrine organ producing a large number of adipokines and cytokines (14). In the presence of hypertrophy, the protein synthesis of white adipocytes is changed toward producing pro-inflammatory adipokines, such as tumor necrosis factor-alpha. On the contrary, adiponectin is an anti-inflammatory adipokine with cardio-protective and anti-tumor actions. Dysfunctional adipose tissue in obesity causes defective adipokines with increased levels of pro-inflammatory factors (14). The currently available therapies for advanced breast cancer stages in obese women seem to achieve a rather poor clinical outcome. Conclusively, a long-lasting reduced-calorie diet seems to lower the risk for breast cancer (15).

It remains difficult to identify single impact factors as dietary changes, energy balance, amount of physical activity, and obesity on cancer development and progression (16, 17). It also remains unclear if the higher amount of adipose tissue and the resulting tissue hypoxia in obesity contributes to the development of cancer. Especially, the elevated activation of HIF's seems to increase metastasis and worsen the prognosis of patient survival (18). Intra-tumoral partial pressure of oxygen (PO_2) is decreased by 20% compared to healthy tissue (19). PO_2 values below 10 mmHg have shown to drive cancer growth, metastasis, and mortality. In cancer tissue, oxygen supply can be restrained due to the proliferation of vessels. Therefore, HIF's, as the key factors of hypoxic cancer cells, seem to stimulate inflammation and angiogenesis (18).

The concurrence of adipose tissue hypoxia to cancer development is not fully explained, but tumors are most likely surrounded by adipose tissue (20–22). Hence, it is likely that such a malignant environment may promote tumor development (22).

METHODS

A literature search was conducted according to preferred reporting items for review and meta-analysis protocols (PRISMA-2015) statement. *Via* PubMed (2000–2016) search and manual searches of reference lists, studies examining the relationship between hypoxia, adipocytes, and breast cancer were identified. The keywords for the search were (*hypoxia* and/or *adipocyte*) and *breast cancer*. Articles had to be in English or German language. Review articles were excluded. There was no restriction regarding study design or certain breast cancer types. After this search, a total of 35 papers were identified. After title and abstract evaluation, eight studies were excluded due to lack of coherences with the topic. Out of four papers not offering open access, one paper was excluded due to Russian language, and another paper was also excluded due to lack of coherence. After assessing full-text articles for eligibility, seven papers were identified as reviews. Finally, 18 articles were eligible for inclusion in this review and selected for analysis. **Figure 1** shows a flow diagram according to PRISMA-2015 protocols displaying the process of literature identification, screening, eligibility, and inclusion.

RESULTS

After the final evaluation of the 18 included articles, six on-topic categories were identified. Two studies identify the impact of hypoxic conditioning on malignant and non-malignant mammary epithelial cells. Two studies examine the role of hypoxic adipocytes in the development of breast cancer cells. Five studies approach the activation of HIF's occurring in hypoxic adipocytes, which promotes breast cancer cell growth. Two studies identify the distinct biochemical responses of the body responsible for HIF inhibition. Three studies investigate medical interventions for HIF inhibition and limitation of breast cancer cell growth. Two studies express alternatives to drug cure of breast cancer inhibiting breast cancer *via* HIF pathways. **Table 1** displays a study summary of HIF-related effects through different physiological and biochemical pathways on breast cancer progression.

HYPOXIC PRECONDITIONING

The most important element for tumor growth is the development of tumor vasculature (41–43). This vasculature is highly disorganized and constantly changing due to blood vessel gain and loss. A consequence of this alteration is the fluctuation of oxygen- and glucose levels, which result in heterogeneous states of hypoxia, anaerobic, and aerobic glycolysis (42). If a cell happens

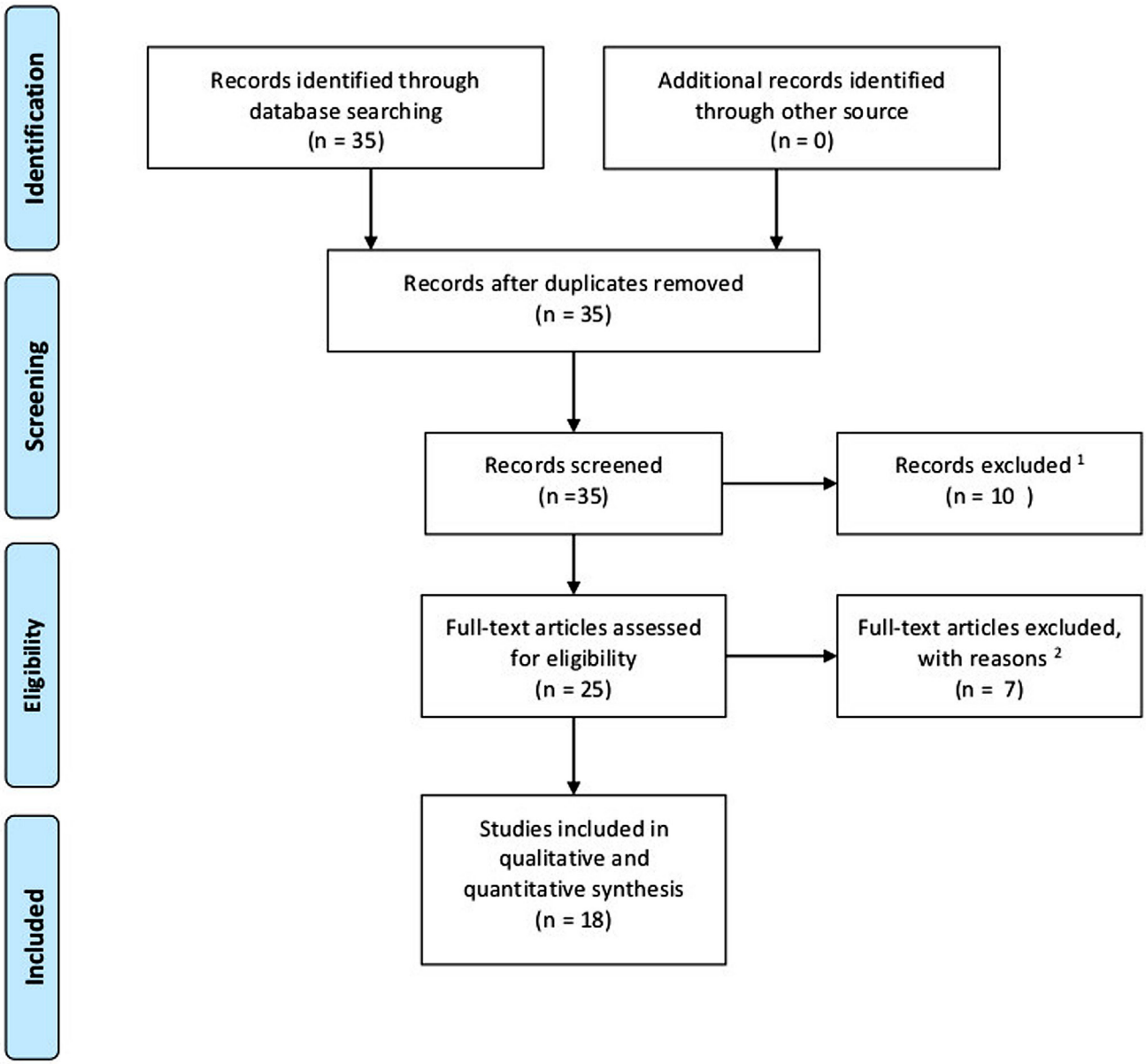

FIGURE 1 | Flow diagram according to PRISMA-2015 protocols displaying process of literature identification, screening, eligibility, and inclusion. [1]Language other than English or German; at least two of the three keywords missing. [2]Fulltexts identified as reviews.

to be above its diffusion limit of oxygen, chronic hypoxia occurs (44). Transient hypoxia occurs due to local oxygen depletion (44). As a result of the fluctuant oxygenation within a tumor, it is possible that the hypoxia-induced glycolysis pre-conditions cancer cells for aerobic glycolysis (45). Increased glycolysis with and without the presence of oxygen is an important indicator for cancer and the connecting link between multidrug-resistant breast cancer cells and hypoxia (46–49). Milane et al. (39) extracted proteins of TNBC and ovarian cancer cell lines pre-exposed to either normoxic or hypoxic conditions. The TNBC cell line MDA-MB-231 experienced the most significant hypoxic transformation with an increase in all glycolytic proteins glucose transporters (GLUT-1 and GLUT-3), hexokinase 1 and 2, phosphofructokinase (PFK), aldolase, glyceraldehyde-3-phosphate dehydrogenase (GAPDH), phosphoglycerate kinase (PGK), enolase, pyruvate kinase, and lactate dehydrogenase (LDH). That indicates that each cell line has a time-specific threshold for hypoxic transformation inducing glycolysis (39). This finding is based on malignant breast cancer cells, but little is known about the effects of hypoxia on non-malignant cells. Vaapil et al. (35) cultivated normal human primary breast epithelial cells and non-malignant mammary epithelial MCF-10A cells under hypoxia and normoxia. The breast epithelial cells with high HIF-levels were found to be immature compared to the well-oxygenated

TABLE 1 | Study summary of HIF-related effects through different physiological and biochemical pathways on breast cancer progression.

	HIF activity	Physiological Effects	Effects on cancer progression
Denzel et al. (23)	↓	Reduced pulmonary metastasis	↓
Yao-Borengasser et al. (24)	↓	Reduction of ER gene expression	↓
Xiang et al. (25)	↓	Inhibition of HSP90	↓
Liapis et al. (26)	↓	Evofosfamide binds to hypoxic bone cell	↓
Samanta et al. (27)	↓	Paclitaxel or gemcitabine alternate HIF expression in triple-negative breast cancers (TNBCs)	↓
Hardman et al. (28)	↓	Dietary with omega three fatty acids	↓
Wang et al. (29)	↑	Increase of microvesicles	↑
Chaturvedi et al. (30)	↑	Increased signaling between BCCs and mesenchymal stem cells (MSCs)	↑
Gehmert et al. (31)	↑	Hypoxia and inflammation lead to migration of MSCs	↑
Seifert et al. (32)	↑	TCDD inhibits ERα signaling in MCF7 cells	↑
Luo et al. (33)	↑	Reprogramming of glucose metabolism	↑
Siclari et al. (34)	↑	Encoding adrenomedullin	↑
Vaapil et al. (35)	↑	Promoting metastasis	↑
Pahlman et al. (36)	↑	Failed lactation in mammary epithelium	↑
Krutilina et al. (37)	↑	Increase of micRNA	↑
Martinez-Outschoorn et al. (38)	↑	Endorsed autophagy	↑
Milane et al. (39)	↑	Increased glycolysis	↑
Jones et al. (40)	↑	Moderate-intensity exercise	↓

cells. Due to the fact that constant cell proliferation is followed by high HIF-levels in certain compartments of the tumor, cellular differentiation of non-malignant human mammary epithelial cells is restrained (35).

Hypoxic preconditioning impairs polarization and organization of mammary epithelial cells and enhances cancer manifestation and progression.

THE ROLE OF HYPOXIC ADIPOCYTES IN THE DEVELOPMENT OF BREAST CANCER CELLS

Obesity is accompanied with the development of hypoxic fat tissue and an increase of oxidative stress (50, 51). Conditioned by rising cell size, oxygen (O_2) diffusion is decreased and vascular growth impaired in the hypoxic fat tissue (52). The mitochondrial production of excessive free fatty acids leads to increased procreation of reactive oxygen species (ROS), which causes oxidative stress (53, 54). As a consequence, the production of adipokines, cell signaling proteins secreted by adipose tissue, is defective and leads to angiogenesis and inflammation (50). This reaction chain creates a pro-malignancy setting in epithelial tissue for the development of breast cancer cells. Gehmert et al. (31) isolated mesenchymal stem cells (MSCs) from subcutaneous fat tissue. Breast cancer cells were injected into mammary fat pad and it showed that MSCs migrated primarily toward an inflammatory milieu in tumor stroma and vasculature independent of biological processes causing inflammation. It is suggested that the migration of MSCs depends on cancer-secreted cytokines due to the lack of inflammatory response by the immune system (31). Furthermore, Yao-Borengasser et al. (24) co-cultured the progressive breast cancer cell line MCF7 with human adipocytes. The MCF7 cell line is the most investigated cell line to analyze the cross talk of estrogen and ERα protein (estrogen receptor alpha protein) (32). They found a decreased level of ERα protein caused by deregulated adipocytes under hypoxic cell conditions. In human adipocyte cells, HIF-1α gene expression was increased and accompanied by a reduction of ER gene expression. With the loss of ERα protein, the tumor progresses and hormone therapy is less efficient (24). Seifert et al. also analyzed MCF7 cell lines cultivated under mild hypoxic conditions (5% of O_2 for a duration of 6 h) (32). These cell lines were exposed to TCDD (2,3,7,8-tetrachlorodibenzo-para-dioxin), a pollutant causing a variety of biochemical and toxic effects, accumulating in adipose tissue. The prevalence of breast cancer cells was significantly higher due to the positive correlation with increased TCDD serum levels. TCDD reduces the hypoxia-induced stabilization and activation of HIF-1α (32).

Denzel et al. states that drug inhibition of the pro-angiogenic HIF-1α pathway only leads to temporary improvement and breast cancer resists treatment after a limited time frame (23). The effect of HIF on changes in human adipocytes inclines with extended exposure time (55, 56). They investigated cellular functions of adiponectin in breast cancer cells creating an adiponectin null mouse model of mammary cancer. The treatment of adiponectin leads to a reduction of human breast cancer cells due to adiponectins' cancer-protective functions. Vessel density is restrained through tumor vasculature because of adiponectin deficit. This limits the supply of oxygen and nutrients (23). Therefore, high adiponectin levels in women are associated with a lower risk of breast cancer and tumor metastasis (57, 58).

A high amount of adipocytes enhances cancer progression due to the increased expression of HIF-1α which causes the loss of ERα protein. Thus, a high amount of the peptide hormone adiponectin appears to be cancer protective.

ACTIVATION OF HIF's AND THE IMPACT ON BREAST CANCER CELL GROWTH

HIF-1α and HIF-2α are linked to breast cancer metastasis and poor patients' survival (21, 59). The expression of HIF-1α and

HIF-2α occurs differently during separate phases of mammary gland development and function (36). Selective inhibition of HIF-1α expression in mammary epithelium leads to lactation failure and in breast cancer models to increased tumor growth (60–62). Pahlman et al. investigated the separate phases using different mouse models with MCF-7 breast cancer cells. They found that the regulation and expression of the two factors and its subunits is not merely dependent on the availability of oxygen (36). Under hypoxic condition, HIFs are stabilized. In a malignant setting, the activation of HIF-induced transcriptions is implemented in extracellular proteolytic activity, invasion, and angiogenesis (36). Wang et al. cultivated TNBC cell lines that were exposed to hypoxia (29). These cells increased their production of microvesicles due to HIF expression. Microvesicles contain proteins that stimulate the invasion and metastasis of breast cancer cells (63). Chaturvedi et al. found that tumor growth, which promotes signals between TBNC's and MSCs is stimulated by HIF activity (30). HIF activates transcription genes, which encode proteins that play a role in proliferation of breast cancer cells. As stated by Luo et al., some of these proteins only interact with HIF-1α, but not with HIF-2α. The consequence is the reprogramming of the glucose metabolism of breast cancer cells which generates macromolecular blocks, such as amino acids and acetyl CoA, that release more breast cancer cells (33). Furthermore, Siclari et al. (34) identify adrenomedullin as a 52-amino acid peptide for which gene transcription is increased by the HIF-1α pathway. This peptide stimulates angiogenesis and proliferation. Many cancer types release adrenomedullin and its receptors which is indirectly connected to poor survival probability (64).

Taken together, increased activation of HIF's induces a series of transcriptions resulting in tumor invasion and angiogenesis. Adrenomedullin is one of them which plays a major role.

INHIBITION OF HIF's AND THE IMPACT ON BREAST CANCER CELL GROWTH

Tumor hypoxia contributes to a great degree to treatment failure and increased patients' mortality for a broad range of malignancies (65). Hypoxic regions within a solid tumor contain cancer cells that resist conventional chemotherapy or radiotherapy (66). This leads to cancer recurrence and metastasis (67). HIF's activate two main transcription processes. First, the gene expression of vascular endothelial growth factors (VEGFs) which contributes to vascularization (68, 69) and, second, the expression of proteins regulating the change from mainly oxidative to glycolytic metabolism (70). The identification of chemical HIF inhibitors and their mechanisms has been a relevant target in anti-cancer research (71). The difficulty in analyzing the development of HIF inhibitors is the lack of specificity. In the ER−/PR+ cancer group, there are already appropriate receptor-blocking inhibitors in use while we still lack comparable methods for TNBCs (72). This type of cancer is associated with increased mortality compared to other types. Inhibition of HIF's and its target genes in consequence could provide a feasible method for tumor suppression.

Xiang et al. showed that in human breast cancer cell cultures the drug Ganetesip inhibits, among others, the expression of the heat shock protein 90 (HSP90). The lack of HSP90 leads to a degeneration of HIF-1α (25). The distribution of HIF-1α was decreased by 35% in breast cancer cells and the expression of VEGFs was reduced as well. The inhibition of HSP90 resulted in a reduction of tumor weight and -growth (25). Another prodrug exhibiting hypoxia-selective cytotoxicity on breast cancer cells is Evofosfamide (TH-302). Liapis et al. show that by binding to hypoxic bone cells, the drug is able to destroy 50–90% of hypoxic cancer cells in bone tissue (26). The advantage of Evofosfamide therapy seems to be greatest when combined with cytotoxic chemotherapy. The combination of chemotherapy and HIF inhibiting drugs is also suggested by Samanta et al. This is based on the finding that paclitaxel as well as gemcitabine change the activity of HIF expression and transcription in human TNBC cell lines (27).

HIF inhibition, especially when combined with cytotoxic chemotherapy, holds strong potential for tumor suppression as well as for the reduction of metastasis.

SELF-REGULATING MECHANISMS OF THE HUMAN BODY AND ITS IMPACT ON HIF EXPRESSION

The human body offers several regulating mechanisms affecting HIF expression and in consequence tumor progression. One important regulating mechanism seems to be the distinct expression profiles of microRNAs that are associated with molecular subgroups and pathological characteristics in breast cancer (73). Krutilina et al. (37) link the expression of microRNAs to a HIF-1α dependent hypoxic response. A growing number of microRNAs have been described as oncogenes and tumor suppressors. Within solid tumors, microRNAs have proven to be downregulated which causes a higher expression of HIF-1α. In consequence, the downregulation of microRNAs withholds a higher probability for metastasis (74–76). One of the most frequently deregulated microRNAs-encoding genes in human cancer is the polycistronic MIR17HG gene, which encodes six microRNAs including miR-18a. Increased expression of miR-18a in MDA-MB-231 breast cancer cell lines has shown to reduce primary tumor growth and lung metastasis and miR-18a inhibition promotes tumor growth and lung metastasis (37). Besides other self-regulating mechanisms of the human body, the regulation of autophagy heavily affects the development and growth of breast cancer. Autophagy is a catabolic process responsible for the systematic degradation and recycling of cellular components (38). Yao-Borengasser et al. show that hypoxia and oxidative stress promote autophagy and support a pro-malignancy setting in epithelial tissue for the development of breast cancer cells (24, 77). Furthermore, as stated by Martinez-Outschoorn et al. (38) in some cases, autophagy promotes tumor progression while in other cases autophagy has shown to have tumor-suppressive effects. Increased HIF expression promotes autophagy and stromal caveolin-1 is degraded. Caveolin-1 appears to be tumor

suppressive and low levels carry a poor prognosis for tumor development for the patient (78–80).

The human body offers a range of tumor affecting mechanisms that are not fully understood. Nevertheless, there seems to be a strong connection between hypoxia, oxidative stress, and a poor prognosis for breast cancer via HIF-regulated pathways.

ALTERNATIVES TO DRUG CURE OF BREAST CANCER INHIBITING BREAST CANCER CELL GROWTH

Physical activity is discussed as a supportive factor for breast cancer therapy and has proven to be quite effective (81, 82). Jones et al. (40) investigated effects of moderate aerobic exercise on tumor characteristics, such as vascularization, angiogenesis, and metabolism. MDA-MB-231 breast cancer cell line implanted mice were randomly assigned to voluntary wheel running. Moderate aerobic exercise has shown to increase intra tumor vascularization, which leads to normalization of tissue environment. This is one of the first studies to evaluate the impact of an exercise intervention on the microenvironment in cancer tissue (40). In contrast to other studies exercise-induced high concentration of HIF is associated with a normalization of cancer microenvironment. This is thought to improve oxygenation and removal of by-products in the long run. In several other studies, regular moderate-intensity exercise is associated with a 30–50% reduction in the risk of mortality in cancer, a fact which supports this finding (83, 84). Physical exercise as well as dietary interventions has shown to affect tumor growth and progression. Hardman et al. investigated the effect of an omega-3 fatty acids enriched diet on mice bearing MDA-MB-231 breast cancer cells. This dietary delays tumor growth and vascularization which could be ought to the reduction of oxygen radicals and HIF expression in consequence (28).

Acute hypoxia seems to normalize the microenvironment in breast cancer tissue and has proven to affect tumor growth and progression positively.

CONCLUSION

There seems to be a strong linkage between adipose tissue hypoxia and the development, growth, and progression of breast cancer. HIF-1α and its target genes play a strong role in driving breast cancer cell proliferation. A high amount of adipocytes enhances cancer progression due to the increased expression of HIF-1α which causes the loss of ERα protein. Thus, a high amount of the peptide hormone adiponectin appears to be cancer protective. On the other hand, tissue hypoxia seems to provide a feasible pathway for the identification of cancer cells and their degeneration. Physical activity shows to improve tissue hypoxia and to reduce adipose tissue and is very likely to improve prognosis as well as therapy outcome in breast cancer (85).

AUTHOR CONTRIBUTIONS

LR and SP: literature search and analysis and writing manuscript; JH: writing manuscript; and NN: designing research strategy, optimization of keywords, and revising manuscript.

REFERENCES

1. James FR, Wootton S, Jackson A, Wiseman M, Copson ER, Cutress RI. Obesity in breast cancer – what is the risk factor? *Eur J Cancer* (2015) 51(6):705–20. doi:10.1016/j.ejca.2015.01.057
2. World Cancer Research Fund International (2012)
3. Smid M, Wang Y, Zhang Y, Sieuwerts AM, Yu J, Klijn JG, et al. Subtypes of breast cancer show preferential site of relapse. *Cancer Res* (2008) 68(9): 3108–14. doi:10.1158/0008-5472.CAN-07-5644
4. Coleman RE. Clinical features of metastatic bone disease and risk of skeletal morbidity. *Clin Cancer Res* (2006) 12(20 Pt 2):6243s–9s. doi:10.1158/1078-0432.CCR-06-0931
5. Calle EE, Rodriguez C, Walker-Thurmond K, Thun MJ. Overweight, obesity, and mortality from cancer in a prospectively studied cohort of U.S. adults. *N Engl J Med* (2003) 348(17):1625–38. doi:10.1056/NEJMoa021423
6. Calle EE, Kaaks R. Overweight, obesity and cancer: epidemiological evidence and proposed mechanisms. *Nat Rev Cancer* (2004) 4(8):579–91. doi:10.1038/nrc1408
7. Renehan AG, Tyson M, Egger M, Heller RF, Zwahlen M. Body-mass index and incidence of cancer: a systematic review and meta-analysis of prospective observational studies. *Lancet* (2008) 371(9612):569–78. doi:10.1016/S0140-6736(08)60269-X
8. Wiseman M. The second World Cancer Research Fund/American Institute for Cancer Research expert report. Food, nutrition, physical activity, and the prevention of cancer: a global perspective. *Proc Nutr Soc* (2008) 67(3):253–6. doi:10.1017/S002966510800712X
9. Vainio H, Kaaks R, Bianchini F. Weight control and physical activity in cancer prevention: international evaluation of the evidence. *Eur J Cancer Prev* (2002) 11(Suppl 2):S94–100.
10. Reeves GK, Pirie K, Beral V, Green J, Spencer E, Bull D. Cancer incidence and mortality in relation to body mass index in the Million Women Study: cohort study. *BMJ* (2007) 335(7630):1134. doi:10.1136/bmj.39367.495995.AE
11. Wolin KY, Carson K, Colditz GA. Obesity and cancer. *Oncologist* (2010) 15(6):556–65. doi:10.1634/theoncologist.2009-0285
12. Ma J, Li H, Giovannucci E, Mucci L, Qiu W, Nguyen PL, et al. Prediagnostic body-mass index, plasma C-peptide concentration, and prostate cancer-specific mortality in men with prostate cancer: a long-term survival analysis. *Lancet Oncol* (2008) 9(11):1039–47. doi:10.1016/S1470-2045(08)70235-3
13. de Pergola G, Silvestris F. Obesity as a major risk factor for cancer. *J Obes* (2013) 2013:291546. doi:10.1155/2013/291546
14. Divella R, de Luca R, Abbate I, Naglieri E, Daniele A. Obesity and cancer: the role of adipose tissue and adipo-cytokines-induced chronic inflammation. *J Cancer* (2016) 7(15):2346–59. doi:10.7150/jca.16884
15. Spindler SR. Rapid and reversible induction of the longevity, anticancer and genomic effects of caloric restriction. *Mech Ageing Dev* (2005) 126(9):960–6. doi:10.1016/j.mad.2005.03.016
16. Pallavi R, Giorgio M, Pelicci PG. Insights into the beneficial effect of caloric/dietary restriction for a healthy and prolonged life. *Front Physiol* (2012) 3:318. doi:10.3389/fphys.2012.00318
17. Imayama I, Ulrich CM, Alfano CM, Wang C, Xiao L, Wener MH, et al. Effects of a caloric restriction weight loss diet and exercise on inflammatory biomarkers in overweight/obese postmenopausal women: a randomized controlled trial. *Cancer Res* (2012) 72(9):2314–26. doi:10.1158/0008-5472.CAN-11-3092
18. Semenza GL. Hypoxia-inducible factors in physiology and medicine. *Cell* (2012) 148(3):399–408. doi:10.1016/j.cell.2012.01.021
19. Vaupel P, Hockel M, Mayer A. Detection and characterization of tumor hypoxia using pO_2 histography. *Antioxid Redox Signal* (2007) 9(8):1221–35. doi:10.1089/ars.2007.1628

20. Semenza GL. Advances in cancer biology and therapy. *J Mol Med (Berl)* (2013) 91(4):409. doi:10.1007/s00109-013-1024-2
21. Bos R, Zhong H, Hanrahan CF, Mommers EC, Semenza GL, Pinedo HM, et al. Levels of hypoxia-inducible factor-1 alpha during breast carcinogenesis. *J Natl Cancer Inst* (2001) 93(4):309–14. doi:10.1093/jnci/93.4.309
22. Schindl M, Schoppmann SF, Samonigg H, Hausmaninger H, Kwasny W, Gnant M, et al. Overexpression of hypoxia-inducible factor 1alpha is associated with an unfavorable prognosis in lymph node-positive breast cancer. *Clin Cancer Res* (2002) 8(6):1831–7.
23. Denzel MS, Hebbard LW, Shostak G, Shapiro L, Cardiff RD, Ranscht B. Adiponectin deficiency limits tumor vascularization in the MMTV-PyV-mT mouse model of mammary cancer. *Clin Cancer Res* (2009) 15(10):3256–64. doi:10.1158/1078-0432.CCR-08-2661
24. Yao-Borengasser A, Monzavi-Karbassi B, Hedges RA, Rogers LJ, Kadlubar SA, Kieber-Emmons T. Adipocyte hypoxia promotes epithelial-mesenchymal transition-related gene expression and estrogen receptor-negative phenotype in breast cancer cells. *Oncol Rep* (2015) 33(6):2689–94. doi:10.3892/or.2015.3880
25. Xiang L, Gilkes DM, Chaturvedi P, Luo W, Hu H, Takano N, et al. Ganetespib blocks HIF-1 activity and inhibits tumor growth, vascularization, stem cell maintenance, invasion, and metastasis in orthotopic mouse models of triple-negative breast cancer. *J Mol Med (Berl)* (2014) 92(2):151–64. doi:10.1007/s00109-013-1102-5
26. Liapis V, Zinonos I, Labrinidis A, Hay S, Ponomarev V, Panagopoulos V, et al. Anticancer efficacy of the hypoxia-activated prodrug evofosfamide (TH-302) in osteolytic breast cancer murine models. *Cancer Med* (2016) 5(3):534–45. doi:10.1002/cam4.599
27. Samanta D, Gilkes DM, Chaturvedi P, Xiang L, Semenza GL. Hypoxia-inducible factors are required for chemotherapy resistance of breast cancer stem cells. *Proc Natl Acad Sci U S A* (2014) 111(50):E5429–38. doi:10.1073/pnas.1421438111
28. Hardman WE, Sun L, Short N, Cameron IL. Dietary omega-3 fatty acids and ionizing irradiation on human breast cancer xenograft growth and angiogenesis. *Cancer Cell Int* (2005) 5(1):12. doi:10.1186/1475-2867-5-12
29. Wang et al. (2014)
30. Chaturvedi P, Gilkes DM, Takano N, Semenza GL. Hypoxia-inducible factor-dependent signaling between triple-negative breast cancer cells and mesenchymal stem cells promotes macrophage recruitment. *Proc Natl Acad Sci U S A* (2014) 111(20):E2120–9. doi:10.1073/pnas.1406655111
31. Gehmert S, Gehmert S, Bai X, Klein S, Ortmann O, Prantl L. Limitation of in vivo models investigating angiogenesis in breast cancer. *Clin Hemorheol Microcirc* (2011) 49(1–4):519–26. doi:10.3233/CH-2011-1502
32. Seifert A, Taubert H, Hombach-Klonisch S, Fischer B, Navarrete Santos A. TCDD mediates inhibition of p53 and activation of ERalpha signaling in MCF-7 cells at moderate hypoxic conditions. *Int J Oncol* (2009) 35(2):417–24.
33. Luo W, Chang R, Zhong J, Pandey A, Semenza GL. Histone demethylase JMJD2C is a coactivator for hypoxia-inducible factor 1 that is required for breast cancer progression. *Proc Natl Acad Sci U S A* (2012) 109(49):E3367–76. doi:10.1073/pnas.1217394109
34. Siclari et al. (2014)
35. Vaapil M, Helczynska K, Villadsen R, Petersen OW, Johansson E, Beckman S, et al. Hypoxic conditions induce a cancer-like phenotype in human breast epithelial cells. *PLoS One* (2012) 7(9):e46543. doi:10.1371/journal.pone.0046543
36. Pahlman S, Lund LR, Jogi A. Differential HIF-1alpha and HIF-2alpha expression in mammary epithelial cells during fat pad invasion, lactation, and involution. *PLoS One* (2015) 10(5):e0125771. doi:10.1371/journal.pone.0125771
37. Krutilina R, Sun W, Sethuraman A, Brown M, Seagroves TN, Pfeffer LM, et al. MicroRNA-18a inhibits hypoxia-inducible factor 1alpha activity and lung metastasis in basal breast cancers. *Breast Cancer Res* (2014) 16(4):R78. doi:10.1186/bcr3693
38. Martinez-Outschoorn UE, Trimmer C, Lin Z, Whitaker-Menezes D, Chiavarina B, Zhou J, et al. Autophagy in cancer associated fibroblasts promotes tumor cell survival: Role of hypoxia, HIF1 induction and NFkappaB activation in the tumor stromal microenvironment. *Cell Cycle* (2010) 9(17):3515–33. doi:10.4161/cc.9.17.12928
39. Milane L, Duan Z, Amiji M. Role of hypoxia and glycolysis in the development of multi-drug resistance in human tumor cells and the establishment of an orthotopic multi-drug resistant tumor model in nude mice using hypoxic pre-conditioning. *Cancer Cell Int* (2011) 11:3. doi:10.1186/1475-2867-11-3
40. Jones LW, Viglianti BL, Tashjian JA, Kothadia SM, Keir ST, Freedland SJ, et al. Effect of aerobic exercise on tumor physiology in an animal model of human breast cancer. *J Appl Physiol (1985)* (2010) 108(2):343–8. doi:10.1152/japplphysiol.00424.2009
41. Cairns R, Papandreou I, Denko N. Overcoming physiologic barriers to cancer treatment by molecularly targeting the tumor microenvironment. *Mol Cancer Res* (2006) 4(2):61–70. doi:10.1158/1541-7786.MCR-06-0002
42. Guppy M. The hypoxic core: a possible answer to the cancer paradox. *Biochem Biophys Res Commun* (2002) 299(4):676–80. doi:10.1016/S0006-291X(02)02710-9
43. Vaupel P. Tumor microenvironmental physiology and its implications for radiation oncology. *Semin Radiat Oncol* (2004) 14(3):198–206. doi:10.1016/j.semradonc.2004.04.008
44. Cosse J-P, Michiels C. Tumour hypoxia affects the responsiveness of cancer cells to chemotherapy and promotes cancer progression. *Anticancer Agents Med Chem* (2008) 8(7):790–7. doi:10.2174/187152008785914798
45. Lu H, Forbes RA, Verma A. Hypoxia-inducible factor 1 activation by aerobic glycolysis implicates the Warburg effect in carcinogenesis. *J Biol Chem* (2002) 277(26):23111–5. doi:10.1074/jbc.M202487200
46. Lum JJ, Bui T, Gruber M, Gordan JD, DeBerardinis RJ, Covello KL, et al. The transcription factor HIF-1alpha plays a critical role in the growth factor-dependent regulation of both aerobic and anaerobic glycolysis. *Genes Dev* (2007) 21(9):1037–49. doi:10.1101/gad.1529107
47. Lopez-Lazaro M. The warburg effect: why and how do cancer cells activate glycolysis in the presence of oxygen? *Anticancer Agents Med Chem* (2008) 8(3):305–12. doi:10.2174/187152008783961932
48. Seagroves TN, Ryan HE, Lu H, Wouters BG, Knapp M, Thibault P, et al. Transcription factor HIF-1 is a necessary mediator of the pasteur effect in mammalian cells. *Mol Cell Biol* (2001) 21(10):3436–44. doi:10.1128/MCB.21.10.3436-3444.2001
49. Semenza GL. HIF-1 mediates the Warburg effect in clear cell renal carcinoma. *J Bioenerg Biomembr* (2007) 39(3):231–4. doi:10.1007/s10863-007-9081-2
50. Hosogai N, Fukuhara A, Oshima K, Miyata Y, Tanaka S, Segawa K, et al. Adipose tissue hypoxia in obesity and its impact on adipocytokine dysregulation. *Diabetes* (2007) 56(4):901–11. doi:10.2337/db06-0911
51. Rausch ME, Weisberg S, Vardhana P, Tortoriello DV. Obesity in C57BL/6J mice is characterized by adipose tissue hypoxia and cytotoxic T-cell infiltration. *Int J Obes (Lond)* (2008) 32(3):451–63. doi:10.1038/sj.ijo.0803744
52. Ye J, Gao Z, Yin J, He Q. Hypoxia is a potential risk factor for chronic inflammation and adiponectin reduction in adipose tissue of ob/ob and dietary obese mice. *Am J Physiol Endocrinol Metab* (2007) 293(4):E1118–28. doi:10.1152/ajpendo.00435.2007
53. Wojtczak L, Schonfeld P. Effect of fatty acids on energy coupling processes in mitochondria. *Biochim Biophys Acta* (1993) 1183(1):41–57. doi:10.1016/0005-2728(93)90004-Y
54. Fridlyand LE, Philipson LH. Reactive species and early manifestation of insulin resistance in type 2 diabetes. *Diabetes Obes Metab* (2006) 8(2):136–45. doi:10.1111/j.1463-1326.2005.00496.x
55. Wang B, Wood IS, Trayhurn P. Dysregulation of the expression and secretion of inflammation-related adipokines by hypoxia in human adipocytes. *Pflugers Arch* (2007) 455(3):479–92. doi:10.1007/s00424-007-0301-8
56. Gatterer H, Haacke S, Burtscher M, Faulhaber M, Melmer A, Ebenbichler C, et al. Normobaric intermittent hypoxia over 8 months does not reduce body weight and metabolic risk factors – a randomized, single blind, placebo-controlled study in normobaric hypoxia and normobaric sham hypoxia. *Obes Facts* (2015) 8(3):200–9. doi:10.1159/000431157
57. Mantzoros C, Petridou E, Dessypris N, Chavelas C, Dalamaga M, Alexe DM, et al. Adiponectin and breast cancer risk. *J Clin Endocrinol Metab* (2004) 89(3):1102–7. doi:10.1210/jc.2003-031804
58. Chen DC, Chung YF, Yeh YT, Chaung HC, Kuo FC, Fu OY, et al. Serum adiponectin and leptin levels in Taiwanese breast cancer patients. *Cancer Lett* (2006) 237(1):109–14. doi:10.1016/j.canlet.2005.05.047
59. Helczynska K, Larsson AM, Holmquist Mengelbier L, Bridges E, Fredlund E, Borgquist S, et al. Hypoxia-inducible factor-2alpha correlates to distant recurrence and poor outcome in invasive breast cancer. *Cancer Res* (2008) 68(22):9212–20. doi:10.1158/0008-5472.CAN-08-1135

60. Seagroves TN, Hadsell D, McManaman J, Palmer C, Liao D, McNulty W, et al. HIF1alpha is a critical regulator of secretory differentiation and activation, but not vascular expansion, in the mouse mammary gland. *Development* (2003) 130(8):1713–24. doi:10.1242/dev.00403
61. Schwab LP, Peacock DL, Majumdar D, Ingels JF, Jensen LC, Smith KD, et al. Hypoxia-inducible factor 1alpha promotes primary tumor growth and tumor-initiating cell activity in breast cancer. *Breast Cancer Res* (2012) 14(1):R6. doi:10.1186/bcr3087
62. Liao D, Corle C, Seagroves TN, Johnson RS. Hypoxia-inducible factor-1alpha is a key regulator of metastasis in a transgenic model of cancer initiation and progression. *Cancer Res* (2007) 67(2):563–72. doi:10.1158/0008-5472.CAN-06-2701
63. Galindo-Hernandez O, Villegas-Comonfort S, Candanedo F, González-Vázquez MC, Chavez-Ocaña S, Jimenez-Villanueva X, et al. Elevated concentration of microvesicles isolated from peripheral blood in breast cancer patients. *Arch Med Res* (2013) 44(3):208–14. doi:10.1016/j.arcmed.2013.03.002
64. Garayoa M, Martínez A, Lee S, Pío R, An WG, Neckers L, et al. Hypoxia-inducible factor-1 (HIF-1) up-regulates adrenomedullin expression in human tumor cell lines during oxygen deprivation: a possible promotion mechanism of carcinogenesis. *Mol Endocrinol* (2000) 14(6):848–62. doi:10.1210/mend.14.6.0473
65. Brown JM, Wilson WR. Exploiting tumour hypoxia in cancer treatment. *Nat Rev Cancer* (2004) 4(6):437–47. doi:10.1038/nrc1367
66. Chang J, Erler J. Hypoxia-mediated metastasis. *Adv Exp Med Biol* (2014) 772:55–81. doi:10.1007/978-1-4614-5915-6_3
67. Saggar JK, Yu M, Tan Q, Tannock IF. The tumor microenvironment and strategies to improve drug distribution. *Front Oncol* (2013) 3:154. doi:10.3389/fonc.2013.00154
68. Forsythe JA, Jiang BH, Iyer NV, Agani F, Leung SW, Koos RD, et al. Activation of vascular endothelial growth factor gene transcription by hypoxia-inducible factor 1. *Mol Cell Biol* (1996) 16(9):4604–13. doi:10.1128/MCB.16.9.4604
69. Ceradini DJ, Kulkarni AR, Callaghan MJ, Tepper OM, Bastidas N, Kleinman ME, et al. Progenitor cell trafficking is regulated by hypoxic gradients through HIF-1 induction of SDF-1. *Nat Med* (2004) 10(8):858–64. doi:10.1038/nm1075
70. Semenza GL. HIF-1 mediates metabolic responses to intratumoral hypoxia and oncogenic mutations. *J Clin Invest* (2013) 123(9):3664–71. doi:10.1172/JCI67230
71. Hu Y, Liu J, Huang H. Recent agents targeting HIF-1alpha for cancer therapy. *J Cell Biochem* (2013) 114(3):498–509. doi:10.1002/jcb.24390
72. Cleator S, Heller W, Coombes RC. Triple-negative breast cancer: therapeutic options. *Lancet Oncol* (2007) 8(3):235–44. doi:10.1016/S1470-2045(07)70074-8
73. Lujambio A, Lowe SW. The microcosmos of cancer. *Nature* (2012) 482(7385):347–55. doi:10.1038/nature10888
74. Iorio MV, Ferracin M, Liu CG, Veronese A, Spizzo R, Sabbioni S, et al. MicroRNA gene expression deregulation in human breast cancer. *Cancer Res* (2005) 65(16):7065–70. doi:10.1158/0008-5472.CAN-05-1783
75. Persson H, Kvist A, Rego N, Staaf J, Vallon-Christersson J, Luts L, et al. Identification of new microRNAs in paired normal and tumor breast tissue suggests a dual role for the ERBB2/Her2 gene. *Cancer Res* (2011) 71(1):78–86. doi:10.1158/0008-5472.CAN-10-1869
76. Foekens JA, Sieuwerts AM, Smid M, Look MP, de Weerd V, Boersma AW, et al. Four miRNAs associated with aggressiveness of lymph node-negative, estrogen receptor-positive human breast cancer. *Proc Natl Acad Sci U S A* (2008) 105(35):13021–6. doi:10.1073/pnas.0803304105
77. Zhang H, Bosch-Marce M, Shimoda LA, Tan YS, Baek JH, Wesley JB, et al. Mitochondrial autophagy is an HIF-1-dependent adaptive metabolic response to hypoxia. *J Biol Chem* (2008) 283(16):10892–903. doi:10.1074/jbc.M800102200
78. Lee SW, Reimer CL, Oh P, Campbell DB, Schnitzer JE. Tumor cell growth inhibition by caveolin re-expression in human breast cancer cells. *Oncogene* (1998) 16(11):1391–7. doi:10.1038/sj.onc.1201661
79. Witkiewicz AK, Dasgupta A, Sotgia F, Mercier I, Pestell RG, Sabel M, et al. An absence of stromal caveolin-1 expression predicts early tumor recurrence and poor clinical outcome in human breast cancers. *Am J Pathol* (2009) 174(6):2023–34. doi:10.2353/ajpath.2009.080873
80. Sloan EK, Ciocca DR, Pouliot N, Natoli A, Restall C, Henderson MA, et al. Stromal cell expression of caveolin-1 predicts outcome in breast cancer. *Am J Pathol* (2009) 174(6):2035–43. doi:10.2353/ajpath.2009.080924
81. Cummings SR, Tice JA, Bauer S, Browner WS, Cuzick J, Ziv E, et al. Prevention of breast cancer in postmenopausal women: approaches to estimating and reducing risk. *J Natl Cancer Inst* (2009) 101(6):384–98. doi:10.1093/jnci/djp018
82. Friedenreich CM, Orenstein MR. Physical activity and cancer prevention: etiologic evidence and biological mechanisms. *J Nutr* (2002) 132(11 Suppl):3456S–64S. doi:10.1503/cmaj.051073
83. Holick CN, Newcomb PA, Trentham-Dietz A, Titus-Ernstoff L, Bersch AJ, Stampfer MJ, et al. Physical activity and survival after diagnosis of invasive breast cancer. *Cancer Epidemiol Biomarkers Prev* (2008) 17(2):379–86. doi:10.1158/1055-9965.EPI-07-0771
84. Irwin ML, Smith AW, McTiernan A, Ballard-Barbash R, Cronin K, Gilliland FD, et al. Influence of pre- and postdiagnosis physical activity on mortality in breast cancer survivors: the health, eating, activity, and lifestyle study. *J Clin Oncol* (2008) 26(24):3958–64. doi:10.1200/JCO.2007.15.9822
85. McNeely ML, Campbell KL, Rowe BH, Klassen TP, Mackey JR, Courneya KS. Effects of exercise on breast cancer patients and survivors: a systematic review and meta-analysis. *Can Med Assoc J* (2006) 175(1):34–41. doi:10.1503/cmaj.051073

Conflict of Interest Statement: We declare that the research was conducted in the absence of any commercial or financial relationships that could be construed as a potential conflict of interest.

frontiers in Oncology

ORIGINAL RESEARCH
published: 29 September 2017
doi: 10.3389/fonc.2017.00231

Bridge-Induced Translocation between *NUP145* and *TOP2* Yeast Genes Models the Genetic Fusion between the Human Orthologs Associated With Acute Myeloid Leukemia

Valentina Tosato[1,2,3], Nicole West[4], Jan Zrimec[2], Dmitri V. Nikitin[5], Giannino Del Sal[6], Roberto Marano[6], Michael Breitenbach[7] and Carlo V. Bruschi[3,7]*

[1] Ulisse Biomed S.r.l., AREA Science Park, Trieste, Italy, [2] Faculty of Health Sciences, University of Primorska, Izola, Slovenia, [3] Yeast Molecular Genetics, ICGEB, AREA Science Park, Trieste, Italy, [4] Clinical Pathology, Hospital Maggiore, Trieste, Italy, [5] Biology Faculty, M.V. Lomonosov Moscow State University, Moscow, Russia, [6] Department of Life Sciences, University of Trieste, Trieste, Italy, [7] Genetics Division, Department of Cell Biology, University of Salzburg, Salzburg, Austria

OPEN ACCESS

Edited by:
Bernd Kaina, Johannes Gutenberg-Universität Mainz, Germany

Reviewed by:
Takaomi Sanda, National University of Singapore, Singapore
Gavin P. McStay, New York Institute of Technology, United States

***Correspondence:**
Valentina Tosato
v.tosato@ulissebiomed.com

Specialty section:
This article was submitted to Molecular and Cellular Oncology, a section of the journal Frontiers in Oncology

Received: *15 June 2017*
Accepted: *07 September 2017*
Published: *29 September 2017*

Citation:
Tosato V, West N, Zrimec J, Nikitin DV, Del Sal G, Marano R, Breitenbach M and Bruschi CV (2017) Bridge-Induced Translocation between NUP145 and TOP2 Yeast Genes Models the Genetic Fusion between the Human Orthologs Associated With Acute Myeloid Leukemia. Front. Oncol. 7:231. doi: 10.3389/fonc.2017.00231

In mammalian organisms liquid tumors such as acute myeloid leukemia (AML) are related to spontaneous chromosomal translocations ensuing in gene fusions. We previously developed a system named bridge-induced translocation (BIT) that allows linking together two different chromosomes exploiting the strong endogenous homologous recombination system of the yeast *Saccharomyces cerevisiae*. The BIT system generates a heterogeneous population of cells with different aneuploidies and severe aberrant phenotypes reminiscent of a cancerogenic transformation. In this work, thanks to a complex pop-out methodology of the marker used for the selection of translocants, we succeeded by BIT technology to precisely reproduce in yeast the peculiar chromosome translocation that has been associated with AML, characterized by the fusion between the human genes *NUP98* and *TOP2B*. To shed light on the origin of the DNA fragility within *NUP98,* an extensive analysis of the curvature, bending, thermostability, and B-Z transition aptitude of the breakpoint region of *NUP98* and of its yeast ortholog *NUP145* has been performed. On this basis, a DNA cassette carrying homologous tails to the two genes was amplified by PCR and allowed the targeted fusion between *NUP145* and *TOP2,* leading to reproduce the chimeric transcript in a diploid strain of *S. cerevisiae*. The resulting translocated yeast obtained through BIT appears characterized by abnormal spherical bodies of nearly 500 nm of diameter, absence of external membrane and defined cytoplasmic localization. Since Nup98 is a well-known regulator of the post-transcriptional modification of P53 target genes, and *P53* mutations are occasionally reported in AML, this translocant yeast strain can be used as a model to test the constitutive expression of human *P53*. Although the abnormal phenotype of the translocant yeast was never rescued by its expression, an exogenous *P53* was recognized to confer increased vitality to the translocants, in spite of its usual and well-documented toxicity to wild-type yeast strains. These results obtained in yeast could provide new grounds for the interpretation of past observations made in leukemic patients indicating a possible involvement of *P53* in cell transformation toward AML.

Keywords: acute myeloid leukemia, bridge-induced translocation, gene fusion, yeast, nucleoporin, P53

INTRODUCTION

Nucleoporins have important roles in many cellular pathways such as the nucleocytoplasmic transport (1), mitotic spindle assembly checkpoint (2), and chromatin metabolism (3). The sporadic rearrangement of their encoding genes lead to aberrant chimeric proteins often implicated in hematologic malignancies such as the acute myeloid leukemia (AML) (4). In particular, the amino terminus of Nup98 is known to be involved in the fusions with at least 28 different partners provoking different types of leukemia (5). In the past, several mouse models of retroviral-introduced artificial fusions have been developed (6, 7) and potential therapeutic targets for specific Nup98 fusions-mediated transformation are under studies (8), but the exact role of the Nup98 chimeras in cell immortalization remains still unclear (9, 10). Moreover, previous works were mostly focused on the clinical effects of the chimeric fusion rather than on the genetic etiology of the disease. We, therefore, planned an experiment to verify whether a chromosomal translocation involving *NUP98* might be reproduced in a model organism such as *Saccharomyces cerevisiae* using our previously published bridge-induced translocation (BIT) system (11, 12). Among all the different possible chimeras leading to hematopoietic malignancies, we focused on a peptide resulting from the fusion between the genes *NUP98* and *TOP2B* that had been found in a patient with primary AML (13). The choice of these two loci required a substantial long period of time and was dictated (i) by the necessity of a detailed sequence description of a translocation breakpoint in human cells, (ii) by the fact that these two genes (*NUP98* and *TOP2B*) have orthologs in yeast and, (iii) by the topological orientation of these orthologs allowing the formation of a viable translocated yeast cell. The patient described in this paper (13) achieved complete histologic remission but relapsed 15 months after diagnosis and showed a 90% blast cell infiltration in the bone marrow. The blast cells were resistant to a combination of Ara-C and topotecan, usually efficient in cases without a complete response (14), with a negative outcome (13). In this work, the precise DNA junction between the two genes had been clearly described, providing partial sequences of the *NUP98/TOP2B* fusion. The breakpoint within *NUP98* (Chromosome 11) occurred at nucleotide 1,199 of the intron 13 with a consequent deletion of two base pairs, while the breakpoint of *TOP2B* (Chromosome 3) occurred within nucleotide 687 within intron 25, with a duplication of four base pairs (13). An important point is that at least two different reciprocal chimeric transcripts (*TOP2B–NUP98*) were identified, suggesting that a precise reciprocal construct is not essential for the leukemic transformation process. This observation is confirmed by other analyses of *NUP98* fusions, where the reciprocal transcript was never found in leukemic patients (15, 16). Since BIT produces always non-reciprocal chromosome translocations (17, 18), the demonstration that the reciprocal transcript(s) did not play a role in the oncogenic transformation reinforced the idea to use BIT in the modeling of this particular translocation. BIT allows to precisely link together through a linear DNA cassette two targeted *loci* on different chromosomes, exploiting the Rad52/Rad54-dependent endogenous homologous recombination system (HRS) of the yeast cell (11, 18). The efficiency of the resulting translocation event depends on the length of the homologous ends, on the selected yeast strain and on the DNA stability of the targeted *loci* (19). Using BIT followed by a pioneering pop-out technology we succeeded to generate an *in vivo* perfect fusion between the genes *NUP145* (ortholog to human *NUP98*) and *TOP2* (ortholog to human *TOP2B*). Extensive conformational and physicochemical analyses of the DNA region around the breakpoints detected similarities and differences between yeast and mammalian DNA and enlightened the basis of the DNA weakness of *NUP98*. BIT produced a peculiar NUP-TOP translocated yeast strain (TNT), suggestively resembling a "leukemic yeast," which can be easily manipulated to investigate the genetic origin of the leukemic translocation process and the molecular players involved. Aged TNT cells are phenotypically characterized by huge, abnormal, spherical bodies (SBs), which can be stained by the RNA-intercalator Pyronin Y (PY). Differently from other types of tumors, *P53* is rarely mutated in hematological malignancies while it is vice versa recurrently overexpressed (20–22). After constitutive expression of human *P53* in TNT, in spite of the lack of a phenotypic reversion, an increased vitality and vigorous growth were observed. These data were completely unexpected since constitutively expressed *P53* was found to be toxic in the parental wild-type (WT) yeast strain, in agreement with previous observations (23). Therefore, these results obtained in the model translocant yeast indicate that the human P53 is an energy booster for aneuploid yeast cells and, corroborating previous clinical data, suggest that P53 might be an indicator of cell transformation to AML (24, 25) and its presence predictive of adverse prognosis (22). Moreover, we propose that the unusual phenotype of aged TNTs, characterized by huge RNA-rich SBs, could be related to the translocation involving Nup145. Further insights on the role of this nucleoporin in the function, size, and integrity of cytoplasmatic bodies are currently under investigation.

Abbreviations: BIT, bridge-induced translocation; AML, acute myeloid leukemia; HRS, homologous recombination system; 5-FOA, 5-fluoroorotic acid; TEM, transmission electron microscopy; TNT, translocant NUP-TOP; NPC, nuclear pore complex; TIDD, thermally induced duplex destabilization; SB, spherical body.

MATERIALS AND METHODS

Strains and Media

The diploid strain San1, constructed in our laboratory (11, 26) by mating Fas20 (α, ade1 ade2 ade8 can1R leu2 trp1, ura3-52) (26) and YPH250 (a, ade2-101^o leu2-Δ1 lys2-801a his3-Δ200 trp1-Δ1 ura3-52, ATCC 96519), was used to obtain the TNTs and as control strain throughout this work. To plot the growth curves, the cells were counted every 2 h and the values expressed in 10^7 cells/ml. Each value is the result of three independent readings and its error bar is reported accordingly.

Yeast peptone dextrose (YPD), supplemented with geneticin (G418, final conc. 200 μg/ml, Gibco), and Synthetic Complete (SC)—URA were used as selective media. To select for the TNTs, the SE drop-out-medium (with ammonium glutamate instead of ammonium sulfate) was prepared as previously described (27).

5-Fluoroorotic acid (5-FOA) plates were prepared optimizing the protocol from Akada (28) with an increased amount of 5-FOA up to 1.2 g/l and a decreased amount of uracil (final concentration ≤20 mg/l) to minimize background.

Translocants Construction and Analysis

Plasmid pFA6aKlura (29) was used to amplify the gene *URA3* from *Kluyveromyces lactis* (KlURA). while the plasmid pFA6aKANMX4 (30) was used as template to amplify the kanamycin gene. URA prototroph and G418-resistant transformants were obtained using the lithium-acetate transformation for the PCR-based gene replacement method (30). To obtain different constructs we prepared a template with 320 bp of *NUP145* that were cut PstI/BamHI and cloned upstream the *KlURA* gene on the pFA6aKlura plasmid while 150 bp of *NUP145* were cut SacI/EcoRI and cloned downstream the same plasmid as shown in Figure S1D in Supplementary Material. All the primers used to amplify the constructs and to verify them are listed in Table S1 in Supplementary Material. The constructs were all amplified by High-Fidelity PCR (Kapa Biosystems), purified and verified by sequencing (BMR sequencing service, Padova). The total amount of cells per transformation was 2.2×10^8 and the efficiency (E) of each transformation was determined dividing the frequency (ν) for the DNA amount in microgram used in the transformation process (ν/μg DNA) (19).

Chromosome separation by contour-clamped homogeneous electric field (CHEF) and Southern hybridization were performed as previously reported (11) using probes amplified with primers listed in Table S1 in Supplementary Material. For the Gene Copy Number by quantitative PCR, the DNA was extracted using the Wizard Genomic DNA purification kit (Promega), then it was diluted from 10 to 50 ng/μl and quantified with a GeneQuant Pro spectrophotometer (NanoDrop1000, Thermo scientific) in order to define a standard curve, using as reference genes *ACT1* on chromosome VI and *SSE2* on chromosome II (31). Copy number of unknown samples was calculated from the standard curve by using the equation copy number $= 10^{(Ct - b)/m}$, where b and m represents y intercept and slope, respectively.

The DNA copy number and the RT-PCR were run in a Rotor-GENE Q PCR (Qiagen) using the Rotor-Gene SYBR green KIT (Qiagen) and standard programs recommended by the supplier.

The data analysis of the RT-PCR was performed repeating the experiments at least three times and the relative gene expression (RGE) was calculated with the comparative C (T) method (32) using *ACT1* as internal control gene and either the WT San1 or the translocant (both transformed with the empty pJL49) as reference strain to calculate the ΔC (T) values.

POP-OUT Selection of the Translocants and Stability Checking

The translocants carrying the *KlURA* marker and labeled with the *KAN* gene on the translocated chromosome were grown for 2 days in non-selective medium and then overnight, from a fresh inoculum, in YPD + G418. The cells were plated on 5-FOA in serial dilutions from 3.2×10^7/plate to 1×10^5/plate using as positive control the auxotrophic strain San1 and as negative control a prototrophic WT yeast strain. After replica plating to eliminate the background, the putative POP-OUT clones were re-streaked on SC-URA and on 5-FOA and verified by Southern blot, colony PCR, and genomic-PCR. In the case of a positive POP-OUT response (with consequent elimination of the marker), a DNA stretch (named "scar" because it was the result of homologous recombination even if it did not contain any exogenous DNA) of 659 bp was amplified with primers FwNUP and REVTOP (Table S1 in Supplementary Material) and sequenced. In all the figures, if not differently specified, the standard DNA ladder was always the 1 kb Plus (Invitrogen). Stability tests of the translocated chromosome were performed growing each TNT translocant in non-selective medium, plating 100 μl of a 2×10^3/ml dilution on 40 YPD plates and replicating them on G418 after 2 days.

Microscopy

DAPI and *FUN-1* staining (Molecular Probes, OR, USA) were performed as previously described (17) using a Leica DMBL photomicroscope equipped with a CCD computer-driven camera at 60× and 100× magnifications. The endocytosis assay was performed using the dye lucifer yellow (LY, Sigma; final conc. 4 mg/ml) with an optimized Riezman protocol (33), as previously described (34), and detecting the fluorescence in the FITC channel. The PY (Sigma) staining on yeast cells was performed dissolving the powder in an acid solution (15% acetic acid in water) and diluting it several times with water, reaching 1 μg/ml as optimal working concentration. The yeast cells were then centrifuged, washed twice with water (to eliminate the background generated by the medium), and resuspended in a maximum of 50–100 ng/ml PY solution. The amount of PY was never exceeded to avoid signal interference from the nuclear DNA, as also previously suggested at the FOM2011 Conference by Rybak (35).[1] When cell wall visualization was needed, Calcofluor White M2R (final concentration 25 μM) was added to the yeast cell suspension already labeled with PY. After incubation at 30°C in the dark for few minutes, fluorescence was detected exciting PY and Calcofluor with green and UV light, respectively.

After 4 weeks of continuous growth, the morphology of TNTs was analyzed through transmission electron microscopy (TEM). The fixation step with glutaraldehyde was followed by a postfixation step with osmium tetroxide and by a dehydration step with increasing percentages of ethanol. Then the samples were embedded within the epoxy resin Derr 332-732. After a three-day resin polymerization, the samples were cut in 10–20 nm-thick sections with an ultramicrotome (Leica Ultracut UCT) equipped with a diamond blade (Drukker). Sections were thus laid down in a holder grid and incubated 10 min at room temperature with a 0.1% (w/v) lead citrate solution and a 2% (w/v) uranyl acetate solution; after each incubation, the grid was washed 20 times by immersion in water. Finally, samples were observed with a transmission electron microscope EM 208 (Philips) equipped with a Morada 4,008 × 2,672 pixels 14 Bit-camera and an acquiring system Olympus Soft Imaging Solutions GmbH.

Bioinformatics

Physicochemical and conformational properties of the DNA breaking strands were predicted with different models: (i) relative

[1] http://www.focusonmicroscopy.org/2011/PDF/412_Rybak.pdf.

DNA duplex stability (*dG*) with the thermodynamic nearest-neighbor model and unified free energy parameters at 37°C (36); (ii) thermally induced duplex destabilization (TIDD) with the TIDD server[2] (37) using the M5P model with 6 bp neighboring regions and a threshold of 0.1 Å; (iii) B-to-A (*BA*) and B-to-Z (*BZ*) transitions according to the dinucleotide model parameters described in Lisser and Margalit (38); (iv) DNA bending, complexity, and curvature analysis were performed using the bend.it® server (39) with a curvature/complexity window size of 50–70 nt and a cubic spline smoothing. Sequence complexity, calculated according to the Shannon entropy or Kolmogorov methods, had been previously defined (40). Bending was considered as produced by a rolling of adjacent base pairs over one another about their long axes with the tilting of base pairs about their short axes that could make a contribution. By contrast, curvature was defined as relatively macroscopic DNA bend, representing the intrinsic tendency of DNA to follow a non-linear pathway over an appreciable length, which is a result of variation of local bends in phase with the DNA helix (41); (v) DNA persistence length (*z,* proportional to bending rigidity) and DNA helical repeats (*h*, number of bps per helix turn) with the model based on cyclization experiments of short DNA fragments (42). The structural properties were predicted in windows of 100 bp, except with TIDD, where 20 nt was used, and the bending/curvature, where windows from 70 to 100 nt were used. To build the control range, five known fragile sequences under ongoing spontaneous breaks (three from *TEL1/ETV6*, one from *PML2*, and one from the *RARA* gene) have been analyzed with the same programs.

Sequences aligning and comparisons were verified with the NCBI database using the specialized BLAST bl2seq. Functionally, conserved aminoacids (aa) were found and represented with the Seq2Logo programme exploiting the Kullback–Leibler logo type and the Hobohm 1 clustering method, correcting the displayed frequencies for low number of observations as described (43). Regulatory DNA motifs were identified running SCOPE 2.1.0 [Dartmouth College, NH, USA; (44)] on both DNA strands.

RESULTS

Identification of the Translocation Breakpoint in Yeast

In *Homo sapiens* (*Hs*) Nup98 is coded together with Nup96 by the same open reading frame and produced by autopeptidase cleavage. In *S. cerevisae* (*Sc*) the whole length of the protein is 1,317 amino acids-long and it is composed of 605 residues of N-terminal Nup145 (ortholog to Nup98) and of 712 residues of C-terminal Nup145 (ortholog to Nup96). We found that the identity (BLASTp) between *Hs*Nup98 and *Sc*Nup145 is on average 36% with peaks of 72% within short regions while the identity between *Hs*Top2B and *Sc*Top2 is on average much higher (**Figure 1A**) since topoisomerases are well conserved, with structural insights from the yeast enzymes that are likely to apply to the human ones (45). The most conserved region (90% positives) between Nup98 and Nup145 is represented by a hydrophobic stretch of 11 residues immediately before the breakpoint. Exploiting the good level of homology between yeast and human sequences, it was, therefore, easy to pinpoint the corresponding, virtual breakpoint in *S. cerevisiae* (**Figure 1**) and to design the primers (Table S1 in Supplementary Material) for a BIT cassette amplification that would model the chromosomal translocation etiology of the leukemic transformation in yeast (**Figure 2**).

Construction of the Translocation "NUP-TOP" (TNT)

To generate the translocation between *nup* and *top* loci, we implemented a methodology based on the following steps and briefly summarized in **Figure 2**: (a) amplification of a DNA cassette carrying the selection marker and two homologies toward *nup145* (Chromosome VII) and *top2* (Chromosome XIV) loci; (b) transformation of the yeast diploid strain San1 and selection for the correct translocants on G418 plates; (c) POP-OUT of the marker and verification of the precise fusion of the two coding sequences. *KlURA3,* the orotidine-5′-phosphate decarboxylase gene from *K. lactis,* whose loss can be easy counter-selected on 5-FOA, was chosen as selective marker (see Materials and Methods for details). We planned to perform the POP-OUT of the marker exploiting the homologous recombination between direct repeats (**Figure 2**). Since the recombination frequency between 40 bp repeats in yeast vegetative cultures was calculated as 2.9×10^{-6}, with a 100-fold variation range, probably due to the intrinsic property of the selected sequence (28), we decided to test a set of constructs differing among them for the length of the repeat (from 40 to 800 bp) and for the length of the homologous ends (from 40 to 100 bp, see Table S1 in Supplementary Material). When the short repeat (40 bp) and the standard length of homology of a BIT cassette [65 bp (11, 19)] were used, the efficiency of the translocation NUP-TOP was very poor (0.6%) while when the repeats were extended up to 800 bp, even single site integration (SSI) events were favored against BIT [data not shown; for a detailed description of the differences between BIT and SSI pathways see Ref. (46)]. The optimal length of the repeat was found to be around 150 bp while the ideal length of the homologies for an efficient targeting was 100 bp. Using this optimized BIT cassette, we were able to find 6 clones, out of 177 screened, with both ends integrated in the corrected loci (Table S2 in Supplementary Material). Surprisingly, none of them gave rise to the amplification of the bridge either by colony or genomic PCR even using two different sets of primers chosen on the two chromosomes around the translocation breakpoint (Table S1 in Supplementary Material). Moreover, sequencing of the junctions showed point mutations and/or rearrangements in four out of these six clones and Southern blot hybridization revealed that only one of them (cl. 112) had the translocant of the expected size (Figure S1C in Supplementary Material). We assumed that, in the majority of clones, a faulty recombination had happened among different copies of the cassette inside the cell leading to an unwanted concatemer (Figure S1B in Supplementary Material). This hypothesis was verified by colony PCR with primers k1 and k2 (Figure S1B in Supplementary Material) and was confirmed by quantitative PCR analysis, which detected at least 10 copies of the cassette. The concatemer was also generated with short repeats

[2]http://tidd.immt.eu.

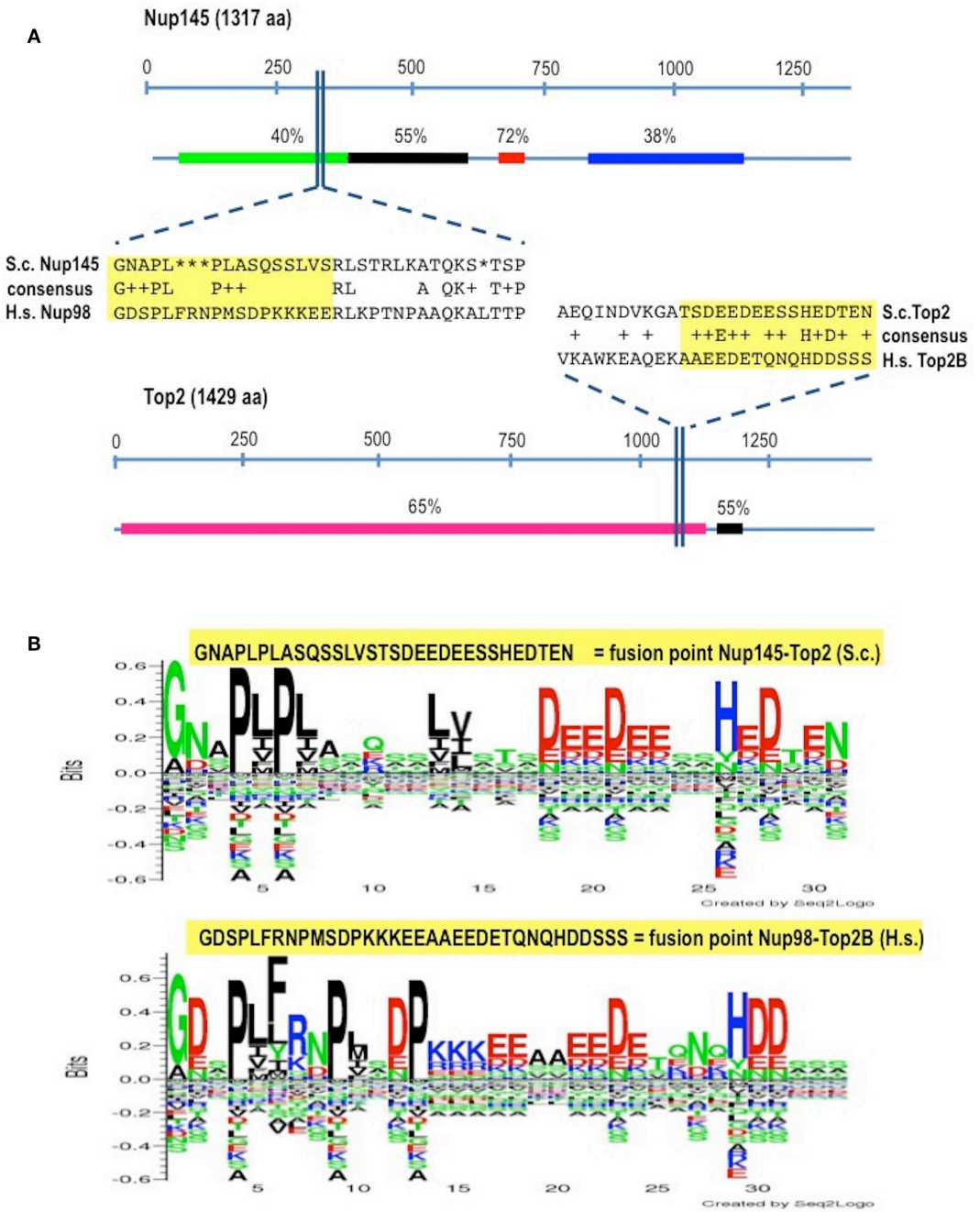

FIGURE 1 | Identification of the virtual breakpoints within the yeast proteins Nup145 and Top2 through an alignment with the human orthologs. **(A)** Breakpoints within the yeast proteins and their homology in percentages with the human orthologs (line below each protein) are shown. In the windows, a partial sequence alignment between yeast (S.c.) and human (H.s.) proteins and the relative consensus are presented. The parts of the proteins that are going to be fused together resulting in chimeras are outlined in yellow. aa, amino acids. **(B)** The fusion points in yeast (top panel) and in human (bottom panel) are represented by the Seq2Logo server. Large symbols represent frequently observed amino acids, big stack represents conserved positions and small stack represents variable positions. The *Y*-axis describes the amount of information in bits. The *X*-axis shows the position in the alignment.

of at least 40 bp (data not shown). In order to reduce the length of the concatemer and to get the correct TNT, clone 112 was left growing in rich, non-selective medium for 1 week. Then it was diluted and plated on YPD, -URA, and 5-FOA medium. Among all the clones screened, one (cl.15) that was strongly flocculating, grew on YPD and on -URA, negligibly on 5-FOA, and had the expected size (2,460 bp) of the correct bridge between *nup145* and *top2* loci. This clone was verified by sequencing and Southern blot and it was subsequently used for the POP-OUT of the marker *KlURA* (**Figure 2**).

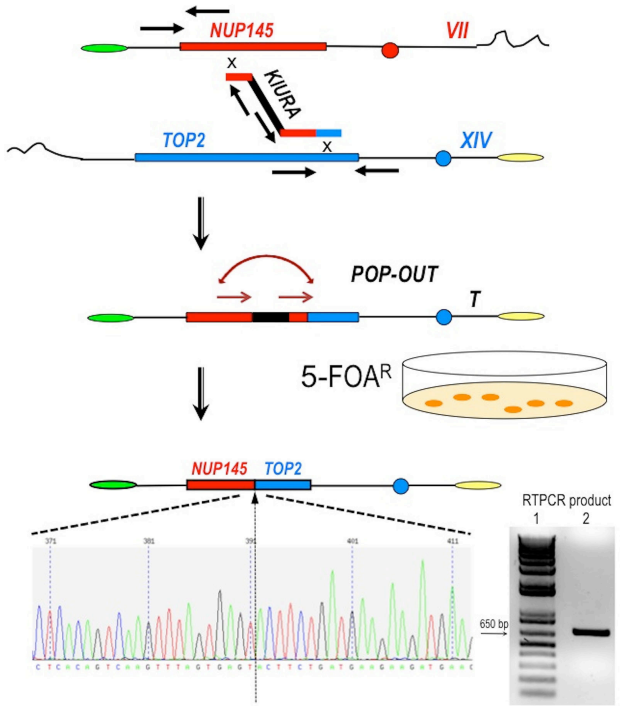

FIGURE 2 | Scheme of the procedure to obtain a perfect fusion between *NUP145* and *TOP2*. The first step is represented by the bridge-induced translocation between *NUP145* (Chromosome VII, shown in red) and *TOP2* (Chromosome XIV, shown in blue) triggered by a BIT cassette. The *URA3* gene from *Kluyveromyces lactis* (KlURA) was used as selection marker between the two homologous ends. Its POP-OUT, indicated by sequential arrows, was verified by selection on 5-FOA plates. The original chromatogram of one clone showing the perfect fusion between the two genes and the relative amplified chimeric transcript from one translocant (T) are also reported. Since the primers used in the RTPCR (sequence in Table S1 in Supplementary Material) are 418 and 241 bp far from the junction point, respectively, the size of the amplicon shown here is exactly 659 bp (lane 2 of the gel); lane 1:1 kb Plus ladder (Invitrogen).

Before the POP-OUT, the translocated chromosome of the TNT strain was labeled to avoid false positives on 5-FOA (clones that grow on 5-FOA because they have lost the whole translocated chromosome and not the *KlURA* marker only). We, therefore, introduced the KAN gene within the right arm of the translocated chromosome, between *PHO91* and *YNR014W* (Figure S2 in Supplementary Material—for the primers sequence and their exact location see Table S1 in Supplementary Material).

The POP-OUT was performed as described in Section "Materials and Methods" and happened with an approximate frequency of 1×10^{-6}. The 659 bp-scar left by the *KlURA* gene was amplified with primers FwNUP and RevTOP (Table S1 and Figure S1 in Supplementary Material; **Figure 2**) and sequenced. The POP-OUT resulted in the wanted, perfect junction between chromosome VII (position 338787) and chromosome XIV (position 460959) (the partial sequence and chromatogram is reported in **Figure 2**). We repeated the procedure (KAN labeling, POP-OUT followed by replica and selection) three different times obtaining nine TNTs (Translocants "NUP-TOP"). All of them were analyzed in details.

Characterization of the Translocants

Translocants NUP-TOP were confirmed by DNA sequencing of the junction between chromosome VII and XIV and they were afterward analyzed by contour-clamped homogeneous electric field (CHEF) followed by Southern blot and sequential hybridizations (Figure S3 in Supplementary Material). Six out of nine translocants (clones 1, 2, 6, 7, 8, 10) showed a correct size of the translocated chromosome while three (clones 3, 4, 9) showed unexpected bands suggesting either spurious clones (as in clone 4) or abnormal rearrangements (for details, see the hybridizations panels of Figure S3 in Supplementary Material). The correct TNTs were further analyzed to check their phenotype while the expression of their chimeric transcript was verified by RT-PCR (**Figure 2**). The translocated chromosome was very stable also without selection, with 0.03% average of chromosome loss frequency in all the TNTs. Interestingly, when the translocants were left growing for at least 2 weeks, peculiar SBs started to mature within the cells. These structures have neither been found in other aged BIT yeast translocants (47) nor in human AML cells where only rod-shaped inclusions composed of fused lysosomes/primary neutrophilic granules, named Auer bodies, can be detected within the cytoplasm (48). DAPI (**Figure 3A**), and especially the RNA-specific dye PY (**Figure 3B**; Figure S4 in Supplementary Material), easily stained SBs, indicating an accumulation of RNA within the TNTs cells. The difference between the PY staining of the WT and of the translocants is remarkable (Figure S4 in Supplementary Material). To better investigate the SBs, a series of 4-week-old TNTs (**Figure 3C**) was observed in details by means of TEM. SBs appeared as big, interspersed cytoplasmic aggregates, lacking a surrounding membrane (**Figure 4**). The content of SBs is poorly electron dense, due probably to a progressive loss of material during the fixation procedure.

Spherical bodies are very different from stress granules as size, localization and number and are more similar to P-bodies (49) although they seem to condense into punctate patches (**Figure 4**).

Genotypic and Phenotypic Investigation of the Translocation Loci

NUP145 and *TOP2* are both essential genes in budding yeast and *NUP145* has been reported as haploinsufficient in rich medium (50). Synthetic lethality (BioGRID, Biological General Repository for Interaction Datasets) or genetic interactions (DRYGIN, Data Repository of Yeast Genetic Interactions) are not known between these two genes. Thus, to verify the phenotype of the NUP-TOP translocants in our genetic background, we performed the gene deletion of *NUP145* and *TOP2*. While *TOP2* deletion resulted, as expected, in a haploproficient phenotype (with approximately 90% of successful one-copy deletion), we confirmed that also in our genetic background *NUP145* is not only essential (51) but also haploinsufficient (50) since the heterozygous full gene deletion was never achieved even extending the homologies (data not shown). However, we succeeded in the partial deletion of one copy of *NUP145* with a frequency of 9.8%. Performing this deletion (with primers FwNupKlura, RevNUP-KO-Klura; Table S1 in Supplementary Material), a fragment of 861 bp at the 5′

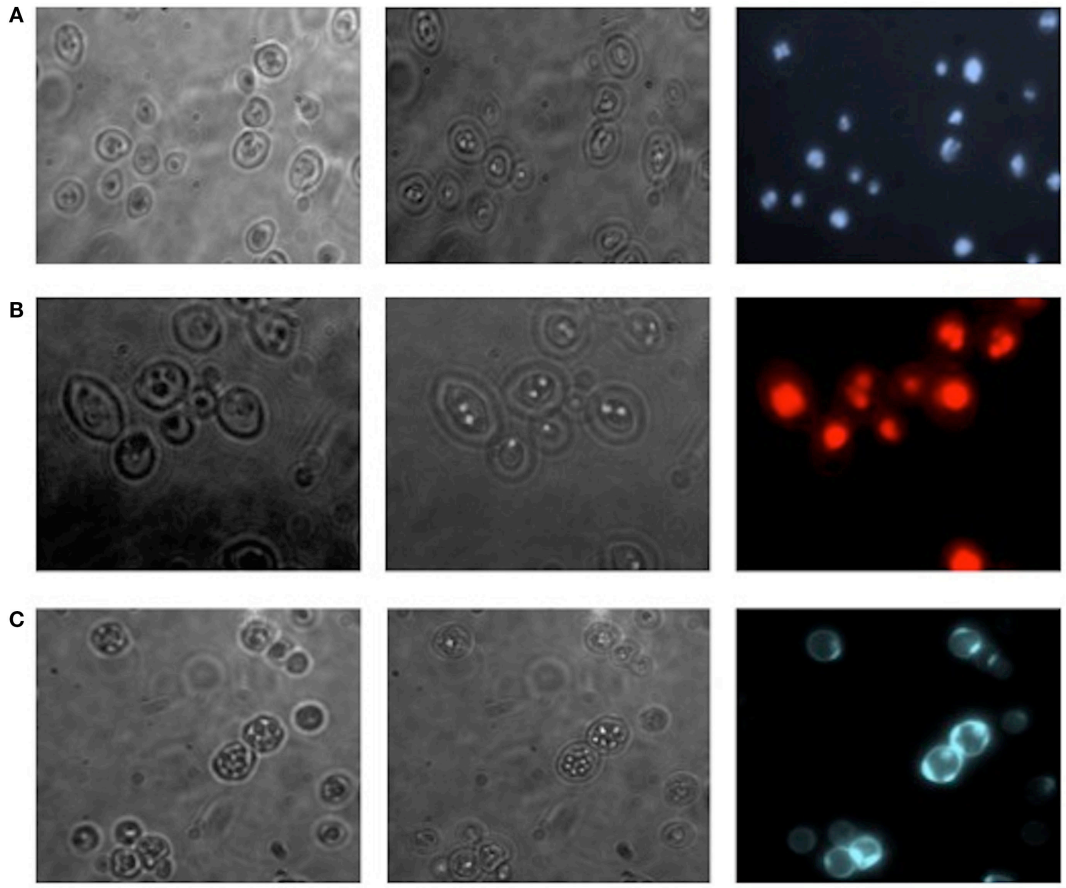

FIGURE 3 | Fluorescent microscopy of aged (3 weeks old) NUP-TOP translocants. The spherical bodies, whose number increased with aging, can be visualized also without fluorescence using different focus lengths (the first two pictures of each panel), but they become more evident after staining with DAPI **(A)** and Pyronin Y **(B)**. After 4 weeks, all the cells of all the TNTs translocant strains contain a variable number of SBs. Cell aging is testified by the numerous scars on the cell wall that are visible after calcofluor treatment **(C)**.

end was left in homozygous condition, exactly as in the TNTs, suggesting that this gene portion is sufficient to avoid haploinsufficiency in rich medium. These data support early observations (52, 53) proposing that 200 bp at the 5′ end of *NUP145* are necessary to avoid haploinsufficiency in minimal medium (SC-LEU). We concluded that the 287 aa haplosufficient N-terminal region of Nup145, which contains also the GLFG (gly-leu-phe-gly) structural domain and which is part of the chimeric construct after the NUP-TOP translocation, is essential for diploid cells survival. Moreover, the overexpression of both *NUP145* and *TOP2* was verified in different background strains in the past (for a detailed description of the phenotypes and a list of references, see the Saccharomyces Genome Database at www.yeastgenome.org/), but the presence of the phenotype observed in TNTs was never reported.

To verify the possible influence of secondary structures on the fragility of the *NUP98* sequences, we performed extensive bioinformatics analyses of the region around the breakpoints to identify putative motifs responsible for non-B DNA conformations.

Bioinformatic Analysis of the Breakpoints

The programme SCOPE—algorithm BEAM—(54) identified a direct, non-degenerate repeat (5′-ACTAGA-3′) leading to a slipped (hairpin) structure exactly at the breakpoint, within intron 13 (Chr. 11) of *NUP98* (Figure S5 in Supplementary Material). Running the same program with the algorithm SPACER it was possible to detect an inverted, degenerated repeat (5′-ACAAYRTTG-3′) within the breakpoint of intron 25 (Chr. 3) of *TOP2B* (data not shown). While the hairpin structure is responsible for non-B DNA, the degenerated inverted repeats are often found in rearrangement events in eukaryotes (55).

Since not only hairpins-prone repeats (56) but also repeated bending (57) can affect nicking at non-B DNA conformations and can, therefore, induce chromosomal translocations through non-homologous end joining (58), or homologous recombination (59) we analyzed the curvature and bending of the DNA within the *nup* locus.

The bend.it analysis of *NUP98* genomic DNA revealed high GC content and high bending immediately before and after the region of the intron 13 that spontaneously breaks (**Figures 5A–C**). A

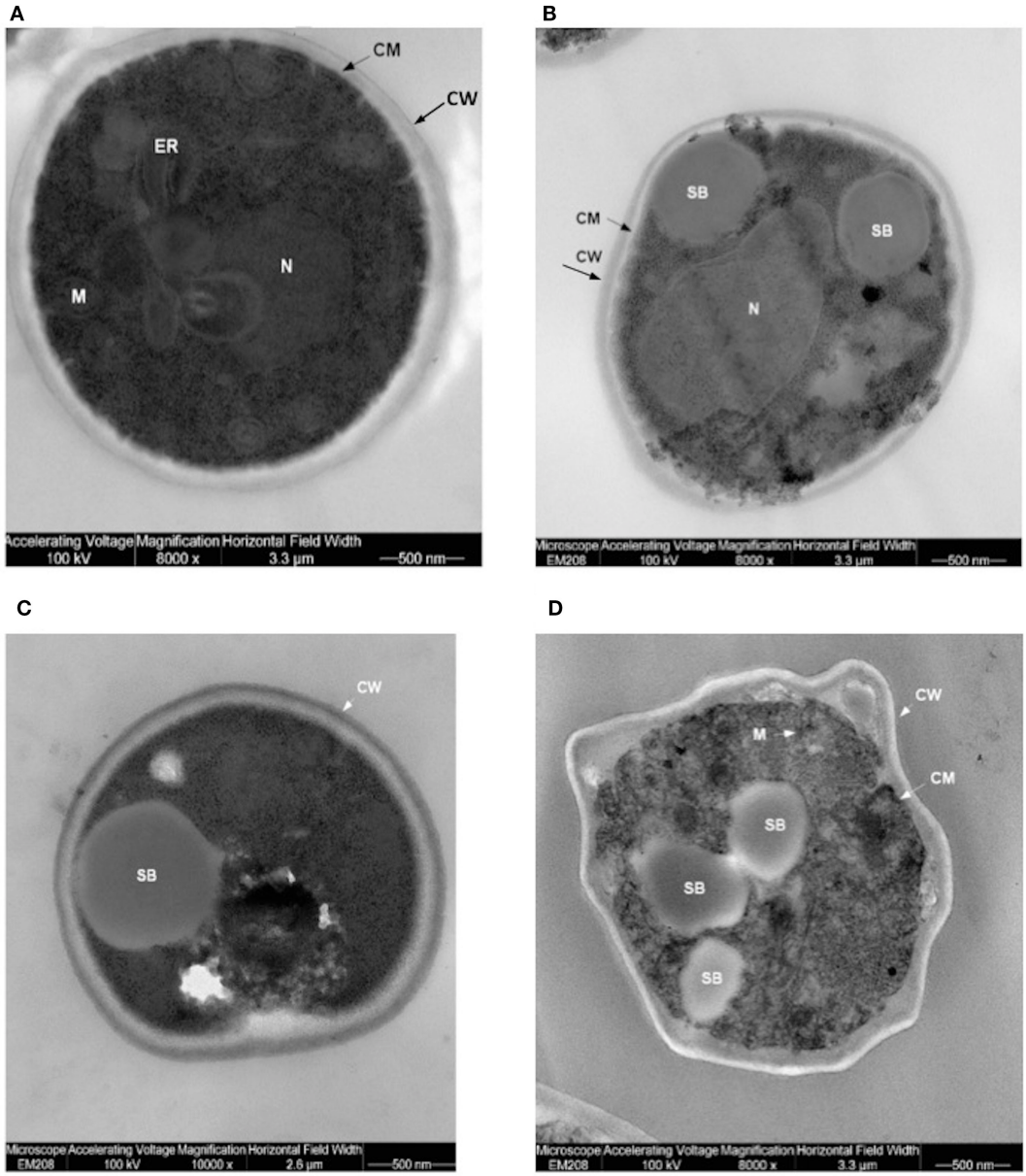

FIGURE 4 | Trasmission electron microscopy (TEM) of aged (4 weeks old) translocants compared to the wild type (WT) strain: **(A)** WT San1, **(B)** TNT10, **(C)** TNT 10/P53, and **(D)** TNT 10/H273. N, nucleus; SB, spherical body; CW, cell wall; CM, cell membrane; M, mitochondria; ER, endoplasmic reticulum.

sudden fall of bendability and a specular increase of curvature correspond exactly to the breakpoint. Similarly, *NUP145* shows high bendability, high GC content, and low curvature from the 5′ end until the breakpoint (**Figures 5D–F**). Then, after this, dramatic changes occur and the curvature suddenly increases. Therefore, the comparison of the DNA complexity in TNTs and in the translocant *NUP98-TOP2B* (**Figures 5G,H**) may predict the point of junction between the two chromosomes. Peaks of high GC content are usually associated with high thermostability and low homologous recombination (60) while fast re-associating DNA shows low complexity. High GC content, which correlates with high local bending, means also a denser, less flexible DNA and easy B-Z DNA transition. Analysis of computationally predicted physicochemical structural properties of *NUP98* showed that bulky changes occur around the breakpoint (**Figure 6**). In the profile of TIDD (37), the intensity of destabilizations increase of 80% around the breakpoint (in particular the number of TIDD events rise from 1,500 to 6,000, **Figures 6F**) and a similar trend could be observed in the predicted DNA thermodynamic stability with a 60% change (from −150 to −115 kcal/mol), in the B to Z transitions (from 1,270 to 1,450 kJ/mol) and in the B to A transitions (from 300 to −160 kJ/mol) with over 70% variations around the breakpoint (**Figures 6E,A,B** respectively). These results clearly and conjointly indicate an overall "weakening"

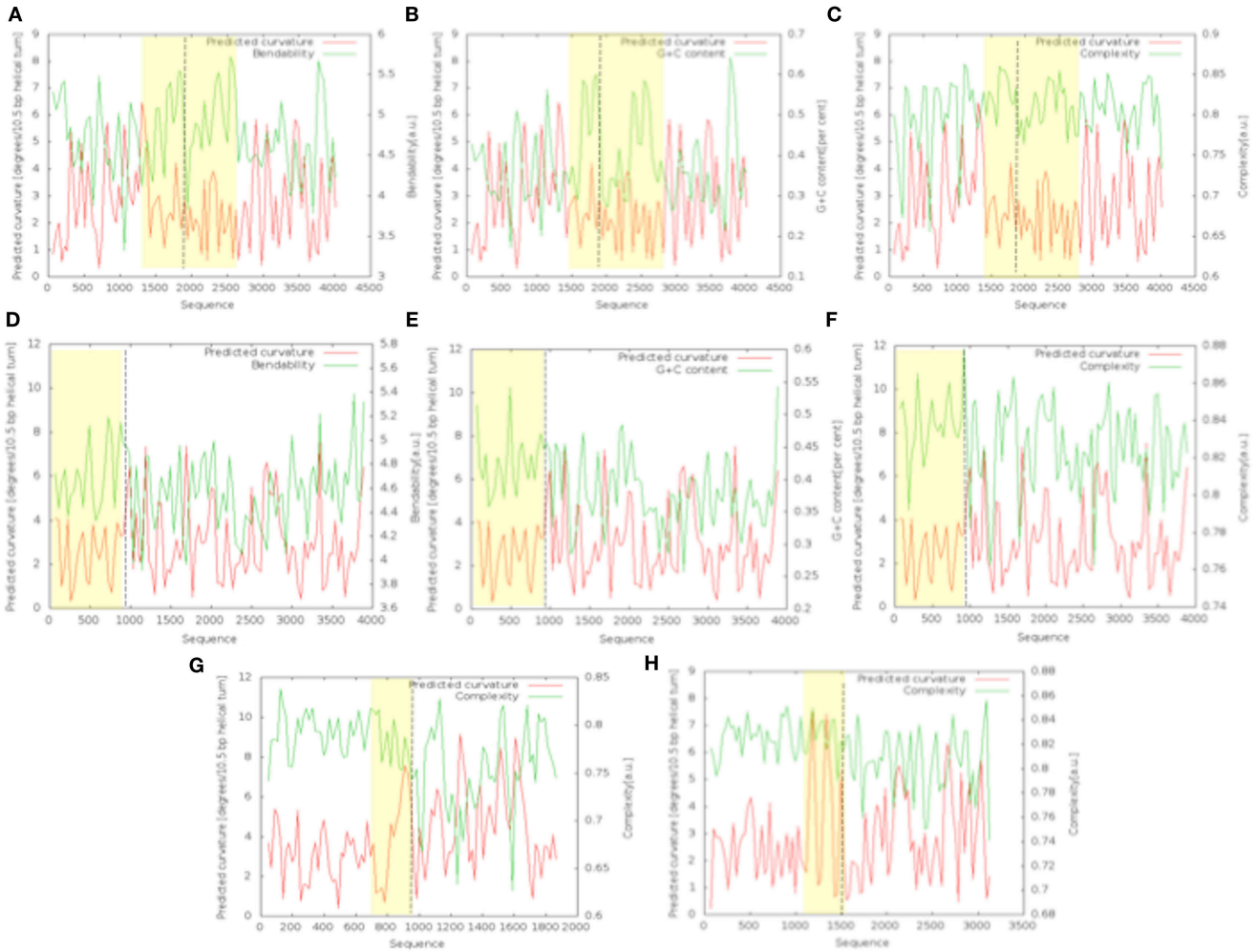

FIGURE 5 | Bend.it analysis. The upper panel refers to the analysis of the genomic DNA around the breakpoint (in the figure at 1,982 bp) within *NUP98*. The panel in the middle refers to the analysis of the breakpoint (in the figure at 982 bp) within *NUP145*. **(A–C)** (*NUP98)* and **(D–F)** (*NUP145)* show the bendability, the GC content and the complexity of the genomic region against the curvature, respectively. The bottom panel refers to the comparison between the cDNA complexity of the junctions *NUP145-TOP2* **(G)** and *NUP98-TOP2B* **(H)**. The breakpoints in the graphics are at 883 bp **(G)** and 1,666 bp (H). In all the panels, the *Y*-axis is reported as degrees/10.5 bp helical turn. Dashed lines indicate the breakpoints while the peculiar regions discussed in the text are outlined in yellow.

of this genomic region. Conversely, *NUP145* did not display pronounced physicochemical changes around the homologous region of the artificially induced breakpoint except with predicted B to A transition (**Figure 6A**). However, conformational properties such as the helical repeats and the persistence length have a similar trend either within *NUP98* or *NUP145* (**Figures 6C,D**). In both genes, the persistence length increased from 475 to 490–500 nm while helical repeats decreased from approximately 10.52 bp/turn to 10.44–10.46 bp/turn immediately before the breakpoint (**Figures 6C,D**).

Study of the Effect of Human *P53* Expression in TNTs

In AML, the frequency of *P53* mutations ranges from 4 to 15% (61) and it is, therefore, very low if compared with other types of cancer, such as the high-grade serous carcinoma of the ovary, where *P53* mutation rates are close to 100%. Nevertheless, poor prognosis is usually associated with *P53* mutations in hematopoietic malignancies and in particular in myeloid leukemia (61). Recently, by using next-generation sequencing, frequent mutations of *P53*, *NOTCH1* and *ATM* have been identified in chronic lymphocytic leukemia (62). The P53 protein is usually mutated in the hotspot region of the DNA binding domain (aa 273–280) and in particular in the position H273. The high frequency (around 95%) of this mutation was also confirmed by a leukemic specific profile from a comprehensive analysis of 268 mutations of *P53* in 254 patients (63). Many abnormalities of the P53 network have been implicated in the pathogenesis of AML (64) and, moreover, the activity of nucleoporins (in particular Nup98) and both topoisomerases can be modulated by P53 (65–67). The observation that increased expression of P53

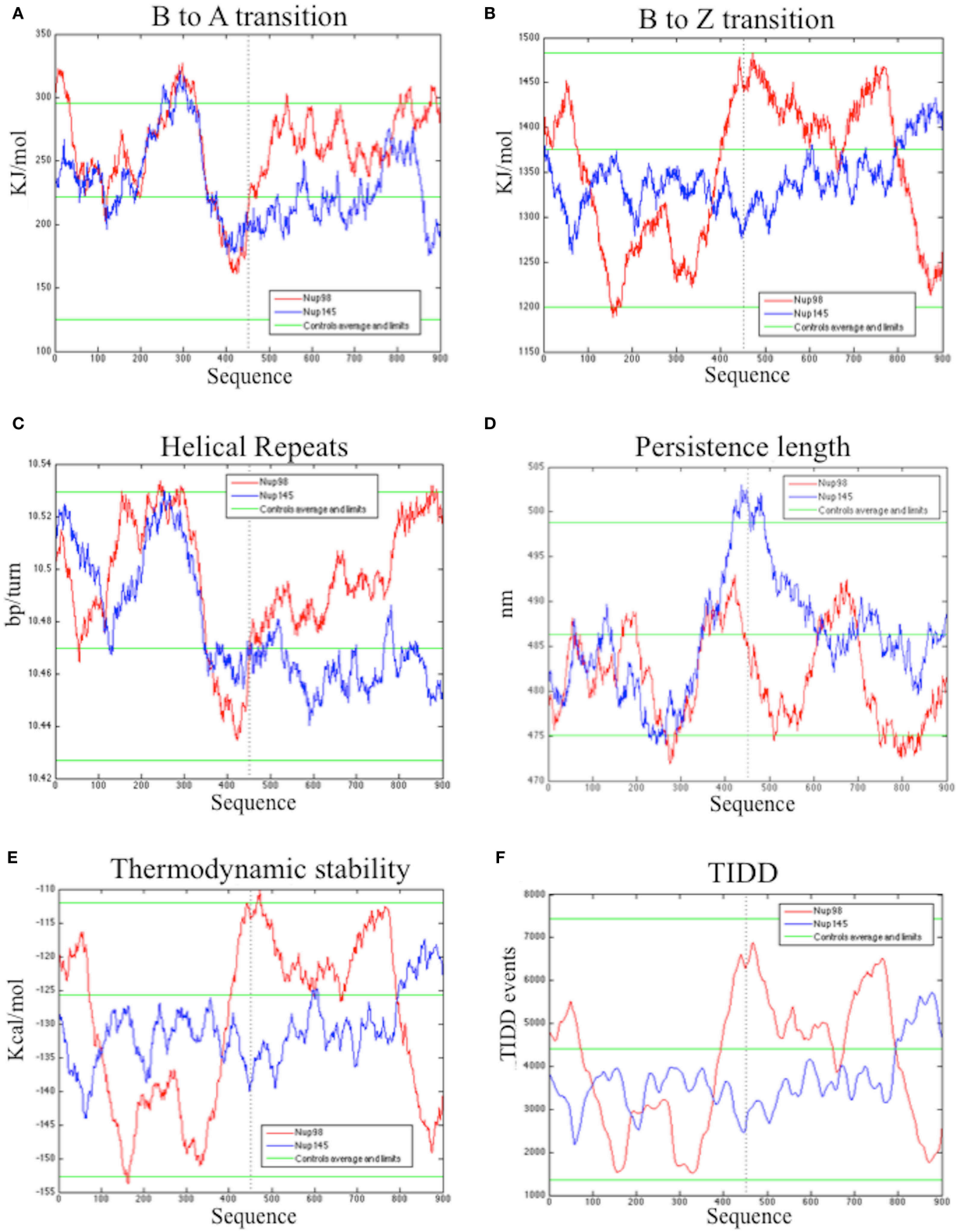

FIGURE 6 | Bioinformatic analysis of the physicochemical and conformational properties of the sequences around the breakpoints of *NUP98* (red color) and *NUP145* loci (blue color). The three green lines in each graphic correspond to an average, maximum and minimum value of five control sequences (see Materials and Methods for details). **(A)** B to A transition, **(B)** B to Z transition, **(C)** Helical repeats, **(D)** Persistence length, **(E)** Thermodynamic stability, **(F)** thermally induced duplex destabilization (TIDD). The *X*-axis is labeled with numbers representing the nucleotide sequence; the *Y*-axis is labeled, in the different panels, with kiloJoule per mole (kJ/mol), nanometers (nm), kilocalories per mole (kcal/mol), base pairs per helical turn (bp/turn).

protein can be present in several types of human leukemia cells at different stages of differentiation, and in particular in AML (levels 10- to 100-fold those of fresh normal low-density human bone marrow cells), was reported a long time ago (21). More recently, other authors demonstrated that high levels of P53 protein carry an adverse prognosis, regardless of mutation status (22). More than half of patients with AML showed P53 protein expression by flow cytometry (68), P53 increased quantification in 256 AML patients was shown in proteomic profiling (69). Furthermore, it was assessed (24) that strong P53 expression in bone marrow progenitor cells was significantly associated with higher AML risk ($P = 0.0006$) and shorter survival ($P = 0.00175$) rendering P53 as the stronger predictor of transformation to AML (25). A *P53* ortholog seems not to be present, or at least has never been identified, in *S. cerevisiae*. However, the P53 pathway is very well conserved in yeast. Moreover, *S. cerevisiae* has proven to be an efficient model system for studies of the tumor suppressor P53 and in particular of its transcriptional activity (70), apoptosis induction (71) and modulation of the Warburg effect (18, 72) that are important prognosis predictors in leukemia (73). We, therefore, transformed the translocant yeast with a constitutive plasmid carrying human *P53*. The cDNA of P53 and of P53/H273 were cloned without the untranslated regions (UTRs), which may impair translation in yeast (23), in the constitutive vector pJL49 (see Materials and Methods). After the resultant constructs were sequenced TNTs were transformed with the pJL49 + P53 and pJL + P53/H273 constructs and also with an empty pJL49 vector to generate a negative control strain. We verified that P53 did not have any revertant effect on the TNTs phenotype since the SBs were clearly visible also when *P53* was expressed in the translocants (**Figure 4C**). Moreover, since it is known that P53 participates in the regulation of clathrin-mediated endocytosis (74) and since we demonstrated in the past that BIT translocants usually show impaired endocytosis (34), we tested endocytosis in TNTs with and without *P53* expression. P53 did not strongly modify the endocytosis in TNTs (**Figure 7A**), although it seemed to slightly improve it. These results correlate with an increased vitality of the P53-expressing translocants, as suggested by the fluorescent *FUN-1* assay on the cylindrical intra-vacuolar structures (**Figure 7B**). In effect, when TNT cells were transformed with P53 they showed a strong staining of the vacuole, similarly to the WT strain, indicating a vigorous and unexpected fitness (**Figure 7B**). To corroborate this hypothesis, we verified that the constitutive expression of *P53* favored the growth of the translocants albeit impairing the proliferation of the WT strain (**Figure 8A**). All BIT translocants usually grow less and at a lower density than the WT strains from which they derive (46), frequently showing endocytosis defects (34) and short chromosomal life span (47). It was already known that induced overexpression of human *P53* inhibits wild yeast proliferation probably because of its transcriptional activity on selective yeast genes involved in cell cycle arrest or cell death (23, 75, 76). Besides, it was demonstrated that Nup98 regulates the expression of P53 target genes in mammalian cells (77). Each *NUP98* fusion differs from the others with respect to P53 expression. For example, it is known that in case of *NUP98* fused with *HOXD13*, *JARID1A*, and *HOXA9,* the HOXA cluster genes are upregulated (5) and that *HOX5* under expression limits *P53* expression in tumors (78). Moreover, the complete loss of one or both alleles of *P53* can accelerate the development of AML in a *NUP98–HOXD13* mouse model (79). On the contrary, topoisomerase II interacts directly with the C-terminal region of P53 (80), although we presently ignore how this interaction can be affected in the *NUP98-TOP2* translocation.

For these reasons, we compared the expression of putative P53 targets in TNTs translocants with and without P53 expression. We decided to quantify the expression of six yeast genes that code for proteins directly interacting with P53 like the autophagy-related Atg17 (81) and the chromatin remodeling Rtf1 (82) or that are orthologs of human regulators of P53 such as Sir2 (83), Pak1/Prk1 (84), Mtbp/Boi1 (85), and the cyclin-dependent kinase Cdc28 (86). The majority of these genes were similarly expressed in the translocants with and without P53 expression (**Figure 8B**); nevertheless, a substantial increase (1.79-folds) of the *CDC28* transcript was detectable in P53-expressing translocants (**Figure 8B**). To verify whether this increase was a peculiarity of the translocants, we measured the *CDC28* expression in the WT strain transformed with *P53*. Also in this case, an increase of 1.8-folds of *CDC28* expression was detected (**Figure 8C**) suggesting that the effect of P53 on *CDC28* is independent on the *NUP-TOP* translocation effect. The expression of *P53* and of the mutant *P53/H273* was verified in two different TNT strains. The two genes were expressed at comparable level in both TNTs and in the WT strain (**Figure 8D**).

DISCUSSION

The nucleoporin Nup98 is an essential component of the nuclear pore complex (NPC) and takes part into the nuclear-cytoplasmic traffic, including mRNA export. Several chromosomal rearrangements such as translocations and inversions, with 28 consequent Nup98 gene fusions, are associated with a wide array of hematopoietic malignancies (5). Because in the past we developed the BIT system to generate *ad hoc* translocations without strain preengineering, just by exploiting the strong homologous recombination of yeast cells (11, 87), we decided to reproduce in *S. cerevisiae* a deeply characterized translocation in humans, responsible of AML, between *NUP98* and *TOP2B* (13). This modeling of the translocation event allowed us to investigate the genetic etiology of AML that can be affected by the physico-chemical properties of the genomic regions around the breakpoints and by the so-called position effect (88) or position-effect variegation (89). Before triggering the translocation between the yeast orthologs *NUP145* and *TOP2,* we investigated the DNA conformational properties around the *NUP145* breakpoint, comparing them with those of *NUP98* (**Figure 5**; Figure S5 in Supplementary Material). It is presently not known why the genomic sequences of *NUP98* are so prone to break, but it has been postulated that introns act as recombination enhancers within coding sequences, increasing the efficiency of selection at nearby sites. Hotspots can be the results of an antagonistic co-evolution between distinct, but tightly linked, DSB inducers and DSB-cut regions (90). It is well known that many of the translocation breakpoints are within a region of predicted non-B DNA conformation. Cruciforms, triplexes, hairpins, slipped conformations, quadruplexes, and left-handed

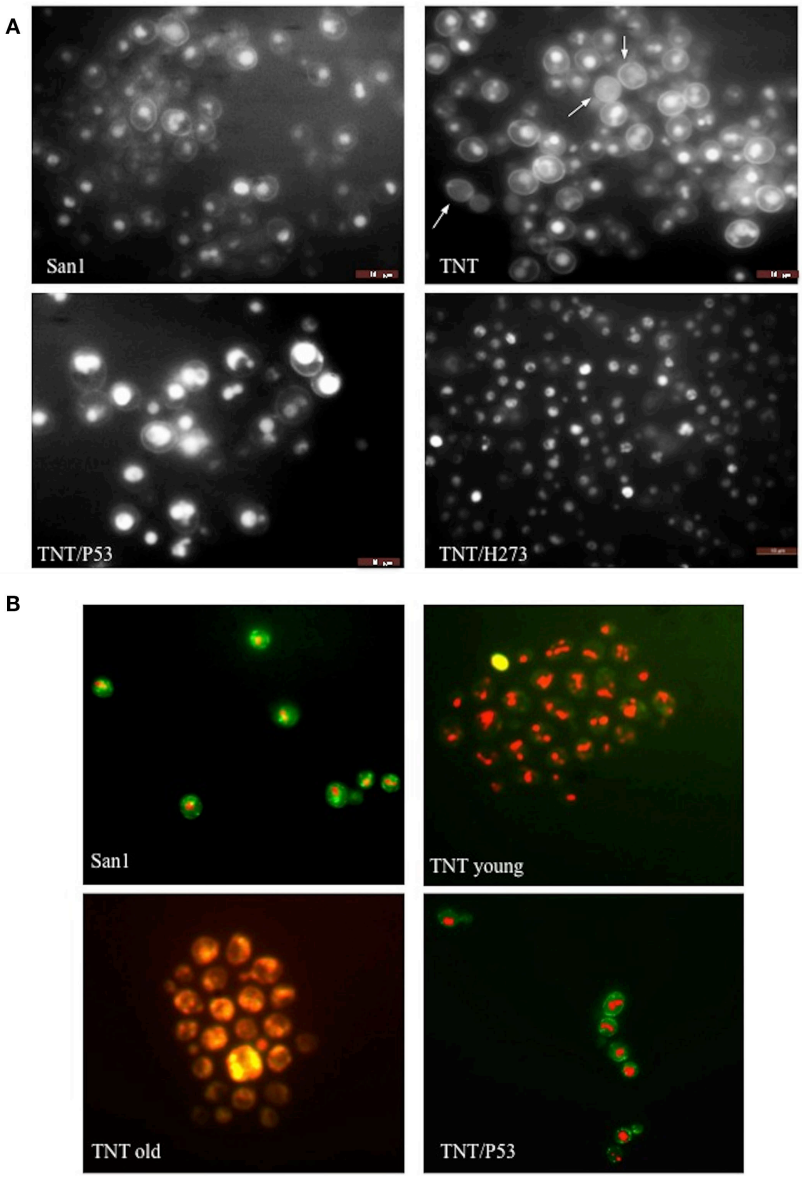

FIGURE 7 | Fluorescent microscopy of **(A)** endocytosis **(B)** and cell viability. In **(A)**, lucifer yellow (LY) was used to test endocytosis in the wild type (WT) San1, in TNT cells, in TNTs transformed with P53 (TNT/P53) and with P53 mutated in H273 (TNT/H273). LY gives a high background staining of the cell wall of the translocants with a defective accumulation of the fluorescent molecule in the vacuole. The white arrows indicate cells with almost complete loss of endocytosis (roughly 10% of the cells). P53 restores a good level of endocytosis in the translocants. In **(B)**, the *FUN-1* staining reveals comparable viability of both San1 and the TNT cells transformed with P53. The TNT cells without P53 appeared already suffering when young cultures (2 days old) and very sick when old cultures (3 weeks old). The dead cells are stained in yellow. After 4 weeks, 5% of the cells appeared dead (yellow) and all them appeared as very sick (orange color).

Z-DNA are formed by repeats in these regions and are usually responsible for genomic instability leading to translocations, inversions, deletions, or insertions [for an extensive review, see Ref. (91)]. The bendability is a local parameter representing the ability of DNA to bend (usually toward the major groove) as a result of thermal fluctuations (41) or DNA–protein interactions such as the one with P53 (92). Bended segments are usually associated with active transcription and play a role in chromatin organization by influencing nucleosome positioning (93). Comparable features of high bending and very low curvature before a breakpoint can be detected in both *NUP145* and *NUP98*. These results are in agreement with preliminary observations indicating that high bending is a sign of genome integrity (94). In our analysis, a strong bending drop as well as an 80% increase of TIDD events between bent segments can both predict the exact breakpoint (**Figures 5** and **6**). These data agree with the typical straight conformation of other fragile sites that are characterized by poor thermal stability and are flanked either side by highly bent DNA

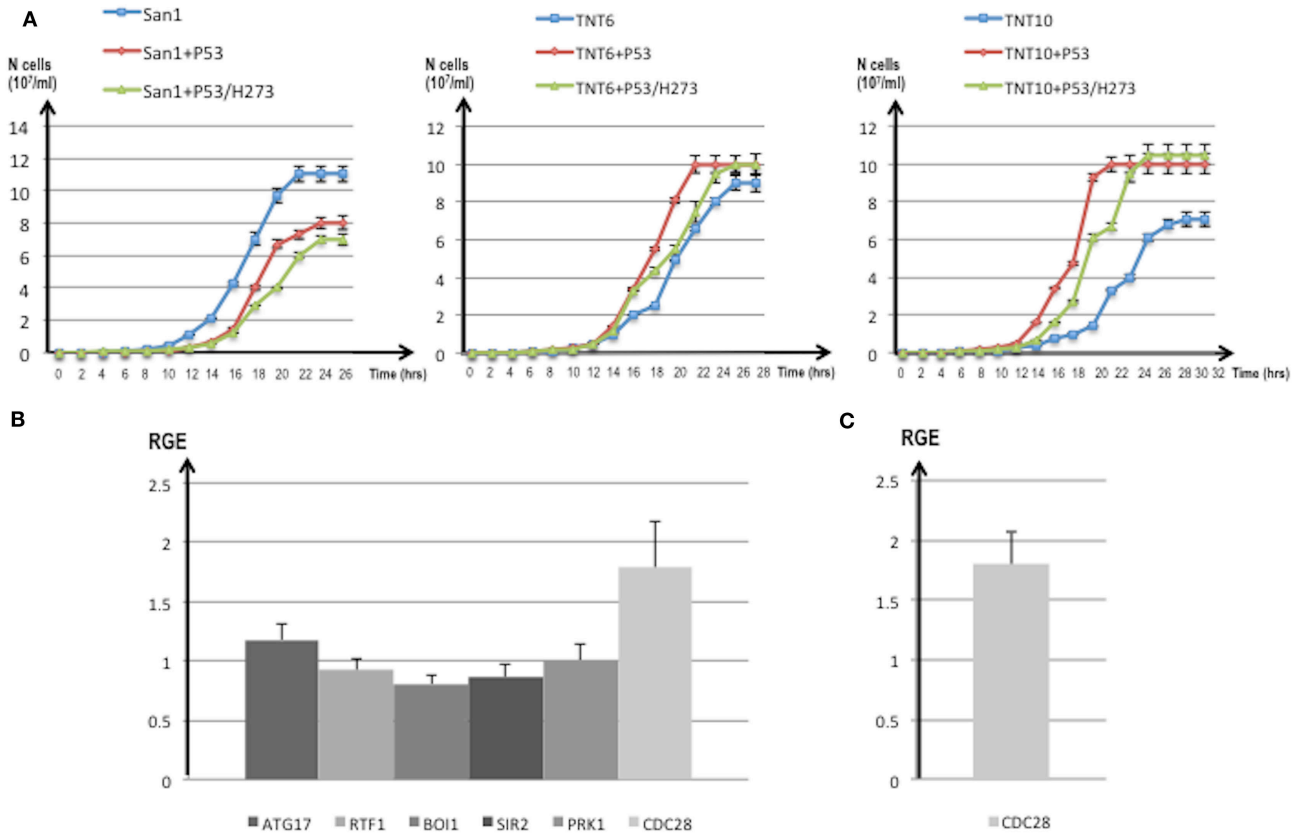

FIGURE 8 | **(A)** Growth curves of translocants number 6 (TNT6) and 10 (TNT10) and of the wild type (WT) San1. The curves without P53 (blue), with P53 (red), and with the P53 mutant H273 (green) are shown for San1 (left), TNT6 (center), and TNT 10 (right panel). On the *X*-axis, the growth time (in hours), and on the *Y*-axis the cell number (10^7/ml) are reported. Each aliquot was retrieved every 2 h and cell density determined by counting each aliquot three times on a Neubauer Improved Cell counting chamber. Error bars are reported accordingly. **(B)** Relative gene expression (RGE) of six genes (*ATG17*, *RTF1*, *BOI1, SIR2*, *PRK1*, *CDC28*) measured in TNT6 with P53. As reference, TNT6 transformed with an empty PJL49 plasmid was used (see Materials and Methods for details on the comparative method). *CDC28* increases 1.79-folds. **(C)** RGE of *CDC28* in San1 transformed with P53. The increase of *CDC28* is 1.8-folds respect to San1 transformed with an empty plasmid. The bars represent the average of three independent readings (bar errors are reported and calculated as standard error). **(D)** The expression of the mutant *P53/H273* was normalized respect to the WT form of *P53* taken as 1 in the WT strain San1 and in two different translocants (TNT6 and TNT10). RGE was calculated using *ACT1* as reference gene and following the procedure described in Section "Materials and Methods." Error bars are reported accordingly.

segments (95). Bending strongly affects recombination, especially site-specific recombination (96, 97), and, resulting as Z-DNA formation (98), it can thus affect BIT efficiency. BIT has usually a frequency varying from 4 to 10% using homologies of 65 nt (11). Its frequency variability depends primarily on the genomic sites chosen as targets. It is much easier to target inter-genic regions, promoters, terminators, pre-telomeric sequences (17, 19) and *vice versa* it is difficult to target intragenic or GC rich regions (Tosato and Noel, personal communication). Usually, coding regions correlate not only with low recombination rates but also with weak nucleosome positioning and strong DNA complexity patterns (99) that were in fact detected at the 5′end of *NUP145* (**Figures 5G**). The *nup-top* translocation represents in this sense an exception because using a standard BIT cassette, with 65 nt of homology and no repeats, the translocation frequency was high (8.3%; Table S2 in Supplementary Material) despite the targeting of intragenic regions with high GC content (**Figure 5**). In particular, the locus *top2* seemed to be the hotspot for recombination (Table S2 in Supplementary Material). The initial difficulty to find a stable TNT (0.6%) was, therefore, due to the artificial repeated region added to the cassette for the POP-OUT induction and not to the poor recombinogenicity of the genomic targets, as also testified by the strong intra-recombination of 5′end *NUP145* segments leading to the concatemer. We, thus, demonstrated in this work that it is feasible, although with low frequency, to obtain a perfect fusion *in vivo*, without any DNA sequence scar, between two selected genomic loci exploiting BIT followed by a selectable POP-OUT of the marker.

When *P53* was expressed in the NUP-TOP translocant yeast, BIT was still possible even if with lower frequency, but there was a different distribution of integration events. With a constitutive expression of *P53*, ectopic integrations (obtained regardless of the homology) more than doubled (Table S2 in Supplementary Material). It is well documented that P53 suppresses homologous recombination and modulates the recombination pathways (100, 101), giving an explanation to

the high rate of ectopic integrants that were found when P53 is expressed (Table S2 in Supplementary Material). P53 seems, moreover, to be less toxic for BIT translocants than for the WT (**Figure 7**) and its presence is almost beneficial for the translocants, increasing their vitality (**Figure 8A**). The toxicity of P53 in yeast is mainly related to gene repression of thioredoxin (Trx1/2), a highly conserved multifunctional anti-oxidative and anti-apoptotic protein family required for the detoxification of reactive oxygen species (ROS) (23). *P53* protects against metabolic stress by upregulation of oxidative phosphorylation and modulation of antioxidants (102) and, when expressed in yeast, induces ROS accumulation, which represents the major cause of cell death (23). We previously demonstrated that BIT translocants have a very high deregulated oxidative stress response network resulting in extremely high and persistent ROS levels (47) and that BIT may induce adaptation with improved phenotypic fitness with respect to stressful conditions (46). We, therefore, speculate that all the ROS-related toxic effects of P53 could be negligible in adapted translocant cells. This theory is supported by our findings on the *CDC28* gene that is overexpressed in TNTs/P53. The increase in the levels of *CDC28* expression is present in cells that are able to re-enter the cell cycle more efficiently after stress (103). In order to verify whether the stress in our cells was given by the expression of *P53* or by the translocation event *per se,* we measured the level of expression of *CDC28* in the WT overexpressing *P53*. The overexpression was the same in the WT and in the translocants suggesting that the constitutive expression of *P53* is generally stressful for the yeast cell, independently of the translocation event and that P53 does not further worsen the stressful condition of the translocants. On the other hand, we noticed that the expression of human *P53* did not considerably affect the vitality (and the transformability) of the WT yeast strain subjected to BIT transformation (Table S2 in Supplementary Material). We know from previous studies that heat shock, required for DNA uptake, induces a transient G1 arrest in yeast cells for a period of approximately 1 h (104), and that once the heat shock proteins are induced and thermo-tolerance is acquired, the normal cell cycle resumes (105). Normal cell cycle progression in yeast relies on activation of the cyclin-dependent kinase Cdc28 and plasmid-driven overexpression of *CDC28* can suppress delay on cell cycle progression observed upon stress (103). Therefore, we can postulate that the long-lasting induction of *CDC28* by P53 is beneficial for stressed cells to recover after heat shock to re-enter the cell cycle more efficiently after DNA transformation.

Finally, neither P53 nor its H273-mutant was able to rescue the unusual phenotype typical of the aged translocants. SBs started to appear in TNTs as interspersed cytoplasmic aggregates, without any membrane, after 3 weeks of continuous growth. In budding yeast, as in higher eukaryotes, processing bodies (P-bodies) are dynamic *foci* within the cytoplasm that are not solid aggregates, as the stress granules, but liquid-like droplets (106) containing untranslating mRNAs and proteins involved in mRNA decay (107). Their size depends on the extension of defects in mRNA decapping and, more generally, to environmental perturbations (108). However, in the case of cellular stress, the size usually varies from 0.1 to 0.3 μm^2 (106) that is comparable with the size of the SBs observed within the aged TNTs (**Figure 4**). Recently, it has been demonstrated that the *C. elegans* germ P-granules, which share a lot of similarities with P-bodies, associate with Nup98 and need an intact Nup98 for integrity and function (109). We still do not know whether the Nup98 ortholog, Nup145, is as well important for P-bodies in yeast, but our study indicates a role of this nucleoporin outside the nucleus and related to RNA-rich bodies within the cytoplasm. Nup98 is already known to be a tumor suppressor because it stabilizes P53 target genes (77). Here, we propose that its oncogenic properties could also involve dysregulation of RNA turnover in the cytoplasm supporting the hypothesis that P-body disassembly and subsequent mRNA deregulation might be linked to certain types of cancers (110). However, notwithstanding many studies, the exact mechanism by which P-bodies impact the development and progression of cancer is largely unknown and a thorough understanding of their roles in carcinogenesis could help in the identification of new targets for cancer therapy (111).

CONCLUSION

Our data suggest that Nup98 could be related to P-bodies regulation in yeast and, therefore, be responsible for mRNA turnover in the cytoplasm. We suppose that other leukemic translocations involving Nup98 might be characterized by the same defects of cytoplasmic mRNA dysregulation. We confirmed that, like *NUP98* in humans, *NUP145* is haploinsufficient in yeast. It is likely that this *NUP-TOP* induced translocation generates secondary chromosomal rearrangements as we demonstrated in the past for other BIT events (17) and as shown by the Southern hybridizations of the translocated clones (Figure S3 in Supplementary Material). Possibly, secondary aneuploidies resulting from *NUP145* haploinsufficiency could generate genome instability, as already surmised for *NUP98* translocations in human cells (5). Last, but certainly not least, this work points out a role of *P53* in these Nup98-translocated cells, although the inactivation of *P53* is a frequent event in tumorigenesis (61, 71). Here, we demonstrated that in the yeast model expression of *P53* improved vitality, endocytosis and growth of translocated cells, fostering considerations on its possible role in translocation-related tumors.

AUTHOR CONTRIBUTIONS

VT and DN had the idea and conceived the strategies; VT designed and performed the majority of the experiments; NW helped in the PCRs and microscopy; JZ performed the bioinformatics analysis; GS and RM contributed to the P53 data; VT, MB, and CB analyzed the data and wrote the paper.

ACKNOWLEDGMENTS

The Authors wish to thank Claudio Gamboz (Transmission Electron Microscopy Service, University of Trieste) for technical help and Alberto Inga (CIBIO, Trento) for fruitful suggestions. A particular thank to Jean-Luc Parrou (Toulouse, France) for having provided the plasmid pJL49.

FUNDING

This work was supported by FWF project P26713 (to MB). JZ was a Post-Doctoral fellow supported by the Slovenian Research Agency (ARRS, Ljubljana).

SUPPLEMENTARY MATERIAL

The Supplementary Material for this article can be found online at http://journal.frontiersin.org/article/10.3389/fonc.2017.00231/full#supplementary-material.

REFERENCES

1. Kabachinski G, Schwartz TU. The nuclear pore complex-structure and function at a glance. *J Cell Sci* (2015) 128:423–9. doi:10.1242/jcs.083246
2. Mossaid I, Fahrenkrog B. Complex commingling: nucleoporins and the spindle assembly checkpoint. *Cells* (2015) 4:706–25. doi:10.3390/cells4040706
3. Ptak C, Wozniak RW. Nucleoporins and chromatin metabolism. *Curr Opin Cell Biol* (2016) 40:153–60. doi:10.1016/j.ceb.2016.03.024
4. Takeda A, Yaseen NR. Nucleoporins and nucleocytoplasmic transport in hematologic malignancies. *Semin Cancer Biol* (2014) 27:3–10. doi:10.1016/j.semcancer.2014.02.009
5. Gough SM, Slape CI, Aplan PD. *NUP98* gene fusions and hematopoietic malignancies: common themes and new biologic insights. *Blood* (2011) 118:6247–57. doi:10.1182/blood-2011-07-328880
6. Lin YW, Slape C, Zhang Z, Aplan PD. *NUP98-HOXD13* transgenic mice develop a highly penetrant, severe myelodysplastic syndrome that progresses to acute leukemia. *Blood* (2005) 106:287–95. doi:10.1182/blood-2004-12-4794
7. Kroon E, Thorsteinsdottir U, Mayotte N, Nakamura T, Sauvageau G. *NUP98-HOXA9* expression in hemopoietic stem cells induces chronic and acute myeloid leukemias in mice. *EMBO J* (2001) 20:350–61. doi:10.1093/emboj/20.3.350
8. Qiu JJ, Zeisig BB, Li S, Liu W, Chu H, Song Y, et al. Critical role of retinoid/rexinoid signaling in mediating transformation and therapeutic response of NUP98-RARG leukemia. *Leukemia* (2015) 29:1153–62. doi:10.1038/leu.2014.334
9. Takeda A, Goolsby C, Yaseen NR. *NUP98-HOXA9* induces long-term proliferation and blocks differentiation of primary human CD34+ hematopoietic cells. *Cancer Res* (2006) 66:6628–37. doi:10.1158/0008-5472.CAN-06-0458
10. Fahrenkrog B, Martinelli V, Nilles N, Fruhmann G, Chatel G, Juge S, et al. Expression of leukemia-associated Nup98 fusion proteins generates an aberrant nuclear envelope phenotype. *PLoS One* (2016) 11:e0152321. doi:10.1371/journal.pone.0152321
11. Tosato V, Waghmare S, Bruschi CV. Non-reciprocal chromosomal bridge-induced translocation (BIT) by targeted DNA integration in yeast. *Chromosoma* (2005) 114:15–27. doi:10.1007/s00412-005-0332-x
12. Nikitin D, Tosato V, Zavec AB, Bruschi CV. Cellular and molecular effects of non-reciprocal chromosome translocation in *S. cerevisiae*. *Proc Natl Acad Sci U S A* (2008) 105:9703–8. doi:10.1073/pnas.0800464105
13. Nebral K, Schmidt HH, Haas OA, Strehl S. NUP98 is fused to topoisomerase (DNA) IIbeta 180 kDa (TOP2B) in a patient with acute myeloid leukemia with a new t(3;11)(p24;p15). *Clin Cancer Res* (2005) 11:6489–94. doi:10.1158/1078-0432.CCR-05-0150
14. Prébet T, Jean E, Autret A, Charbonnier A, Rey J, Etienne A, et al. Combination of cytarabine and topotecan in patients treated for acute myeloid leukemia with persistent disease after frontline induction. *Leuk Lymphoma* (2012) 53:2186–91. doi:10.3109/10428194.2012.685733
15. Slape C, Aplan PD. The role of *NUP98* gene fusions in hematologic malignancy. *Leuk Lymphoma* (2004) 45:1341–50. doi:10.1080/10428190310001659325
16. Kobzev YN, Martinez-Climent J, Lee S, Chen J, Rowley JD. Analysis of translocations that involve the *NUP98* gene in patients with 11p15 chromosomal rearrangements. *Genes Chromosomes Cancer* (2004) 41:339–52. doi:10.1002/gcc.20092
17. Rossi B, Noel P, Bruschi CV. Different aneuploidies arise from the same bridge-induced chromosomal translocation event in *Saccharomyces cerevisiae*. *Genetics* (2010) 186:775–90. doi:10.1534/genetics.110.120683
18. Tosato V, Grüning NM, Breitenbach M, Arnak R, Ralser M, Bruschi CV. Genomic instability and Warburg effect: two yeast models for cancer cells. *Front Oncol* (2013) 2:212. doi:10.3389/fonc.2012.00212
19. Tosato V, Sidari S, Bruschi CV. Bridge-induced chromosome translocation in yeast relies upon a Rad54/Rdh54-dependent, Pol32-independent pathway. *PLoS One* (2013) 8:e60926. doi:10.1371/journal.pone.0060926
20. Koníková E, Kusenda J. P53 protein expression in human leukemia and lymphoma cells. *Neoplasma* (2001) 48:290–8.
21. Koeffler HP, Miller C, Nicolson MA, Raynard J, Bosselman RA. Increased expression of P53 in human leukemia cells. *Proc Natl Acad Sci U S A* (1986) 83:4035–9. doi:10.1073/pnas.83.11.4035
22. Kornblau SM, Barnett J, Qiu Y, Chen W, Faderl S, Coombs KR, et al. P53 protein expression levels are prognostic in AML and predict for mutational status. *Blood* (2007) 110:2397.
23. Hadj Amor IY, Smaoui K, Chaabène I, Mabrouk I, Djemal L, Elleuch H, et al. Human p53 induces cell death and downregulates thioredoxin expression in *Saccharomyces cerevisiae*. *FEMS Yeast Res* (2008) 8:1254–62. doi:10.1111/j.1567-1364.2008.00445.x
24. Saft L, Karimi M, Ghaderi M, Matolcdy A, Mufti GJ, Kulasekararaj A, et al. P53 protein expression independently predicts outcome in patients with lower risk myelodisplastic syndromes with del(5q). *Haematologica* (2014) 99:104–9. doi:10.3324/haematol.2013.098103
25. Nagy EE, Finna C, Demian S, Chira L, Horvath E. P53 protein as a survival biomarker in myelodysplastic syndromes: immunohistochemical morphometric study. *Farmacia* (2016) 64:104–11.
26. Bruschi CV, Howe GA. High frequency FLP-independent homologous DNA recombination of 2 mu plasmid in the yeast Saccharomyces cerevisiae. *Curr Genet* (1988) 14:191–9. doi:10.1007/BF00376739
27. Cheng TH, Chang CR, Joy P, Yablok S, Gartenberg MR. Controlling gene expression in yeast by inducible site-specific recombination. *Nucleic Acids Res* (2000) 28:E108. doi:10.1093/nar/28.24.e108
28. Akada R, Kitagawa T, Kaneko S, Toyonaga D, Ito S, Kakihara Y, et al. PCR-mediated seamless gene deletion and marker recycling in *Saccharomyces cerevisiae*. *Yeast* (2006) 23:399–405. doi:10.1002/yea.1365
29. Delneri D, Gardner DC, Bruschi CV, Oliver SG. Disruption of seven hypothetical aryl alcohol dehydrogenase genes from *Saccharomyces cerevisiae* and construction of a multiple knock-out strain. *Yeast* (1999) 15:1681–9. doi:10.1002/(SICI)1097-0061(199911)15:15<1681::AID-YEA486>3.0.CO;2-A
30. Wach A, Brachat A, Pohlmann R, Philippsen P. New heterologous modules for classical or PCR-based gene disruptions in *Saccharomyces cerevisiae*. *Yeast* (1994) 10:1793–808. doi:10.1002/yea.320101310
31. Teste MA, Duquenne M, François JM, Parrou JL. Validation of reference genes for quantitative expression analysis by real-time RT-PCR in *S. cerevisiae*. *BMC Mol Biol* (2009) 10:99. doi:10.1186/1471-2199-10-99
32. Schmittgen TD, Livak KJ. Analyzing real-time PCR data by the comparative C(T) method. *Nat Protoc* (2008) 3:1101–8. doi:10.1038/nprot.2008.73
33. Riezman H. Endocytosis in yeast: several of the yeast secretory mutants are defective in endocytosis. *Cell* (1985) 40:1001–9. doi:10.1016/0092-8674(85)90360-5
34. Nikitin DV, Bruschi CV, Sims J, Breitenbach M, Rinnerthaler M, Tosato V. Chromosome translocation may lead to PRK1-dependent anticancer drug resistance in yeast via endocytic actin network deregulation. *Eur J Cell Biol* (2014) 93:145–56. doi:10.1016/j.ejcb.2014.03.003
35. Rybak P, Kwiatek J, Pierzynska-Mach A, Zawrotniak M, Dobricki J. *Paradoxical Pattern of RNA Staining with Pyronin Y in Live and Intact Cells – The Role of Fluorescence Quenching and Photobleaching*. Konstanz, Germany: FOM (2011). p. 2–A.
36. SantaLucia J Jr. A unified view of polymer, dumbbell, and oligonucleotide DNA nearest-neighbor thermodynamics. *Proc Natl Acad Sci U S A* (1998) 95:1460–5. doi:10.1073/pnas.95.4.1460
37. Zrimec J, Lapanje A. Fast prediction of DNA melting bubbles using DNA thermodynamic stability. *IEEE/ACM Trans Comput Biol Bioinform* (2015) 12:1137–45. doi:10.1109/TCBB.2015.2396057

38. Lisser L, Margalit H. Determination of common structural features in *E. coli* promoters by computer analysis. *Eur J Biochem* (1994) 223:823–30. doi:10.1111/j.1432-1033.1994.tb19058.x
39. Vlahovicek K, Kaján L, Pongor S. DNA analysis servers: plot.it, bend.it, model.it and IS. *Nucleic Acids Res* (2003) 31:3686–7. doi:10.1093/nar/gkg559
40. Gabrielian A, Bolshoy A. Sequence complexity and DNA curvature. *Comput Chem* (1999) 23:263–74. doi:10.1016/S0097-8485(99)00007-8
41. Goodsell GD, Dickerson RE. Bending and curvature calculations in B-DNA. *Nucleic Acids Res* (1994) 22:5497–503. doi:10.1093/nar/22.24.5497
42. Geggier S, Kotlyar A, Vologodskii A. Temperature dependence of DNA persistence length. *Nucleic Acids Res* (2011) 39:1419–26. doi:10.1093/nar/gkq932
43. Thomsen MC, Nielsen M. Seq2Logo: a method for construction and visualization of amino acid binding motifs and sequence profiles including sequence weighting, pseudo counts and two-sided representation of amino acid enrichment and depletion. *Nucleic Acids Res* (2012) 40:W281–7. doi:10.1093/nar/gks469
44. Chakravarty A, Carlson JM, Khetani RS, Gross RH. A novel ensemble learning method for de novo computational identification of DNA binding sites. *BMC Bioinformatics* (2007) 8:249. doi:10.1186/1471-2105-8-249
45. Nitiss JL. DNA topoisomerase II and its growing repertoire of biological functions. *Nat Rev Cancer* (2009) 9:327–37. doi:10.1038/nrc2608
46. Tosato V, Sims J, West N, Colombin M, Bruschi CV. Post-translocational adaptation drives evolution through genetic selection and transcriptional shift in *S. cerevisiae*. *Curr Genet* (2017) 63:281–92. doi:10.1007/s00294-016-0635-x
47. Sims J, Bruschi CV, Bertin C, Breitenbach M, Schroeder S, Eisenberg T, et al. Extreme oxidative stress levels are detected at the end of the chronological life span of translocant yeast. *Mol Genet Genomics* (2016) 291:423–35. doi:10.1007/s00438-015-1120-9
48. Freeman JA. Origin of auer bodies. *Blood* (1966) 27:499–510.
49. Lui J, Castelli LM, Pizzinga M, Simpson CE, Hoyle NP, Bailey KL, et al. Granules harboring translationally active mRNAs provide a platform for P-body formation following stress. *Cell Rep* (2014) 9:944–54. doi:10.1016/j.celrep.2014.09.040
50. Deutschbauer AM, Jaramillo DF, Proctor M, Kumm J, Hillenmeyer ME, Davis RW, et al. Mechanisms of haploinsufficiency revealed by genome-wide profiling in yeast. *Genetics* (2005) 169:1915–25. doi:10.1534/genetics.104.036871
51. Teixeira MT, Siniossoglou S, Podtelejnikov S, Benichou JC, Mann M, Dujon B, et al. Two functionally distinct domains generated by in vivo cleavage of Nup145p: a novel biogenesis pathway for nucleoporins. *EMBO J* (1997) 16:5086–97. doi:10.1093/emboj/16.16.5086
52. Wente SR, Blobel G. *NUP145* encodes a novel yeast glycine-leucine-phenylalanine-glycine (GLFG) nucleoporin required for nuclear envelope structure. *J Cell Biol* (1994) 125:955–69. doi:10.1083/jcb.125.5.955
53. Emtage JL, Bucci M, Watkins JL, Wente SR. Defining the essential functional regions of the nucleoporin Nup145p. *J Cell Sci* (1997) 110:911–25.
54. Carlson JM, Chakravarty A, DeZiel CE, Gross RH. SCOPE: a web server for practical *de novo* motif discovery. *Nucleic Acids Res* (2007) 35:W259–64. doi:10.1093/nar/gkm310
55. Fan WH, Woelfle MA, Mosig G. Two copies of a DNA element, 'Wendy', in the chloroplast chromosome of *Chlamydomonas reinhardtii* between rearranged gene clusters. *Plant Mol Biol* (1995) 29:63–80. doi:10.1007/BF00019119
56. Lobachev KS, Rattray A, Narayanan V. Hairpin- and cruciform-mediated chromosome breakage: causes and consequences in eukaryotic cells. *Front Biosci* (2007) 12:4208–20. doi:10.2741/2381
57. Kouzine F, Levens D. Supercoil-driven DNA structures regulate genetic transactions. *Front Biosci* (2007) 12:4409–23. doi:10.2741/2398
58. Lieber MR, Lu H, Gu J, Schwarz K. Flexibility in the order of action and in the enzymology of the nuclease, polymerases, and ligase of vertebrate non-homologous DNA end joining: relevance to cancer, aging, and the immune system. *Cell Res* (2008) 18:125–33. doi:10.1038/cr.2007.108
59. Gonçalves MA, van Nierop GP, Holkers M, de Vries AA. Concerted nicking of donor and chromosomal acceptor DNA promotes homology-directed gene targeting in human cells. *Nucleic Acids Res* (2012) 40:3443–55. doi:10.1093/nar/gkr1234
60. Gruss A, Moretto V, Ehrlich SD, Duwat P, Dabert P. GC-rich DNA sequences block homologous recombination in vitro. *J Biol Chem* (1991) 266:6667–9.
61. Melo MB, Ahmad NN, Lima CS, Pagnano KB, Bordin S, Lorand-Metze I, et al. Mutations in the p53 gene in acute myeloid leukemia patients correlate with poor prognosis. *Hematology* (2002) 7:13–9. doi:10.1080/10245330290020090
62. Athanasakis E, Melloni E, Rigolin GM, Agnoletto C, Voltan R, Vozzi D, et al. The p53 transcriptional pathway is preserved in ATM mutated and NOTCH1 mutated chronic lymphocytic leukemias. *Oncotarget* (2014) 5:12635–45. doi:10.18632/oncotarget.2211
63. Zenz T, Vollmer D, Trbusek M, Smardova J, Benner A, Soussi T, et al. TP53 mutation profile in chronic lymphocytic leukemia: evidence for a disease specific profile from a comprehensive analysis of 268 mutations. *Leukemia* (2010) 24:2072–9. doi:10.1038/leu.2010.208
64. Wojcik I, Szybka M, Golanska E, Rieske P, Blonski JZ, Robak T, et al. Abnormalities of the P53, MDM2, BCL2 and BAX genes in acute leukemias. *Neoplasma* (2005) 52:318–24.
65. Yarbrough ML, White MA, Fontoura BMA. Shaping the p53 response with nucleoporins. *Mol Cell* (2012) 48:665–6. doi:10.1016/j.molcel.2012.11.027
66. Yeo CQX, Alexander I, Lin Z, Lim S, Anig OA, Kumar R, et al. P53 maintains genomic stability by preventing interference between transcription and replication. *Cell Rep* (2016) 15:132–46. doi:10.1016/j.celrep.2016.03.011
67. Gobert C, Bracco L, Rossi F, Olivier M, Tazi J, Lavelle F, et al. Modulation of DNA topoisomerase I activity by p53. *Biochemistry* (1996) 35:5778–86. doi:10.1021/bi952327w
68. Cavalcanti GB, Vasconcelos FC, Pinto de Faria G, Scheiner MA, de Almeida Dobbin J, Klumb CE, et al. Coexpression of p53 protein and MDR functional phenotype in leukemias: the predominant association in chronic myeloid leukemia. *Cytometry B Clin Cytom* (2004) 61:1–8. doi:10.1002/cyto.b.20013
69. Kornbalu SM, Tibes R, Qiu YH, Chen W, Kantarjian HM, Andreeff M, et al. Functional proteomic profiling of AML predicts response and survival. *Blood* (2009) 113:154–64. doi:10.1182/blood-2007-10-119438
70. Leão M, Gomes S, Soares J, Bessa C, Maciel C, Ciribilli Y, et al. Novel simplified yeast-based assays of regulators of p53-MDMX interaction and p53 transcriptional activity. *FEBS J* (2013) 280:6498–507. doi:10.1111/febs.12552
71. Guaragnella N, Palermo V, Galli A, Moro L, Mazzoni C, Giannattasio S. The expanding role of yeast in cancer research and diagnosis: insights into the function of the oncosuppressors p53 and BRCA1/2. *FEMS Yeast Res* (2014) 14:2–16. doi:10.1111/1567-1364.12094
72. Diaz-Ruiz R, Rigoulet M, Devin A. The Warburg and Crabtree effects: on the origin of cancer cell energy metabolism and of yeast glucose repression. *Biochim Biophys Acta* (2011) 1807:568–76. doi:10.1016/j.bbabio.2010.08.010
73. Hong M, Xia Y, Zhu Y, Zhao H-H, Zhu H, Xie Y, et al. TP53-induced glycolysis and apoptosis regulator protects from spontaneous apoptosis and predicts poor prognosis in chronic lymphocytic leukemia. *Leuk Res* (2016) 50:72–7. doi:10.1016/j.leukres.2016.09.013
74. Endo Y, Sugiyama A, Li SA, Ohmori K, Ohata H, Yoshida Y, et al. Regulation of clathrin-mediated endocytosis by p53. *Genes Cells* (2008) 13:375–86. doi:10.1111/j.1365-2443.2008.01172.x
75. Coutinho I, Pereira G, Leão M, Gonçalves J, Côrte-Real M, Saraiva L. Differential regulation of p53 function by protein kinase C isoforms revealed by a yeast cell system. *FEBS Lett* (2009) 583:3582–8. doi:10.1016/j.febslet.2009.10.030
76. Nigro JM, Sikorski R, Reed SI, Vogelstein B. Human p53 and CDC2Hs genes combine to inhibit the proliferation of *Saccharomyces cerevisiae*. *Mol Cell Biol* (1992) 12:1357–65. doi:10.1128/MCB.12.3.1357
77. Singer S, Zhao R, Barsotti AM, Ouwehand A, Fazollahi M, Coutavas E, et al. Nuclear pore component Nup98 is a potential tumor suppressor and regulates posttranscriptional expression of select p53 target genes. *Mol Cell* (2012) 48:799–810. doi:10.1016/j.molcel.2012.09.020
78. Raman V, Martensen SA, Reisman D, Evron E, Odenwald WF, Jaffee E, et al. Compromised HOXA5 function can limit p53 expression in human breast tumors. *Nature* (2000) 405:974–8. doi:10.1038/35016125
79. Xu H, Menendez S, Schlegelberger B, Bae N, Aplan PD, Göhring G, et al. Loss of p53 accelerates the complications of myelodysplastic syndrome in a NUP98-HOXD13-driven mouse model. *Blood* (2012) 120:3089–97. doi:10.1182/blood-2012-01-405332
80. Cowell IG, Okorokov AL, Cutts SA, Padget K, Bell M, Milner J, et al. Human topoisomerase IIα and IIβ interact with the C-terminal region of P53. *Exp Cell Res* (2000) 225:86–94. doi:10.1006/excr.1999.4772

81. Morselli E, Shen S, Ruckenstuhl C, Bauer MA, Mariño G, Galluzzi L, et al. p53 inhibits autophagy by interacting with the human ortholog of yeast Atg17, RB1CC1/FIP200. *Cell Cycle* (2011) 10:2763–9. doi:10.4161/cc.10.16.16868
82. Koerte A, Cong T, Li X, Wahane K, Cai M. Suppression of the yeast mutation rft1-1 by human p53. *J Biol Chem* (1995) 270:22556–64. doi:10.1074/jbc.270.38.22556
83. Smith J. Human Sir2 and the "silencing" of p53 activity. *Trends Cell Biol* (2002) 12:404–6. doi:10.1016/S0962-8924(02)02342-5
84. Thiagalingam S, Kinzler KW, Vogelstein B. PAK1, a gene that can regulate p53 activity in yeast. *Proc Natl Acad Sci U S A* (1995) 92:6062–6. doi:10.1073/pnas.92.13.6062
85. Boyd MT, Vlatkovic N, Haines DS. A novel cellular protein (MTBP) binds to MDM2 and induces a G1 arrest that is suppressed by MDM2. *J Biol Chem* (2000) 275:31883–90. doi:10.1074/jbc.M004252200
86. Hixon ML, Flores AI, Wagner MW, Gualberto A. Ectopic expression of cdc2/cdc28 kinase subunit *Homo sapiens* 1 uncouples cyclin B metabolism from the mitotic spindle cell cycle checkpoint. *Mol Cell Biol* (1998) 18:6224–37. doi:10.1128/MCB.18.11.6224
87. Tosato V, Nicolini C, Bruschi CV. DNA bridging of yeast chromosomes VIII leads to near-reciprocal translocation and loss of heterozygosity with minor cellular defects. *Chromosoma* (2009) 118:179–91. doi:10.1007/s00412-008-0187-z
88. Kleinjan DJ, van Heyningen V. Position effect in human genetic disease. *Hum Mol Genet* (1998) 7:1611–8. doi:10.1093/hmg/7.10.1611
89. Elgin SCR, Reuter G. Position-effect variegation, heterochromatin formation, and gene silencing in *Drosophila*. *Cold Spring Harb Perspect Biol* (2013) 5:a017780. doi:10.1101/cshperspect.a017780
90. Friberg U, Rice WR. Cut Thy neighbor: cyclic birth and death of recombination hotspots via genetic conflict. *Genetics* (2008) 179:2229–38. doi:10.1534/genetics.107.085563
91. Bacolla A, Wells RD. Non-B DNA conformations as determinants of mutagenesis and human disease. *Mol Carcinog* (2009) 48:273–85. doi:10.1002/mc.20507
92. Pan Y, Nussinov R. p53-Induced DNA bending: the interplay between p53-DNA and p53-p53 interactions. *J Phys Chem* (2008) 112:6716–24. doi:10.1021/jp800680w
93. Drew HR, Travers AA. DNA bending and its relation to nucleosome positioning. *J Mol Biol* (1985) 186:773–90. doi:10.1016/0022-2836(85)90396-1
94. Gonzalez-Huici V, Szakal B, Urulangodi M, Psakhye I, Castellucci F, Menolfi D, et al. DNA bending facilitates the error-free DNA damage tolerance pathway and upholds genome integrity. *EMBO J* (2014) 33:327–40. doi:10.1002/embj.201387425
95. Palin AH, Critcher R, Fitzgerald DJ, Anderson JN, Farr CJ. Direct cloning and analysis of DNA sequences from a region of the Chinese hamster genome associated with aphidicolin-sensitive fragility. *J Cell Sci* (1998) 111:1623–34.
96. Snyder UK, Thompson JF, Landy A. Phasing of protein-induced DNA bends in a recombination complex. *Nature* (1989) 341:255–7. doi:10.1038/341255a0
97. Luetke KH, Sadowski PD. The role of DNA bending in Flp-mediated site-specific recombination. *J Mol Biol* (1995) 251:493–506. doi:10.1006/jmbi.1995.0451
98. Arican E, Ekimler S, Tosato V, Bruschi CV. Characterization of bridge induced translocation (Bit) driven by Z-DNA formation in *Saccharomyces cerevisiae* via non-B DB and SIDD/Z-DNA web-based servers. *Fresen Environ Bull* (2016) 25:1365–71.
99. Bolshoy A, Shapiro K, Trifonov EN, Ioshikhes I. Enhancement of the nucleosomal pattern in sequences of lower complexity. *Nucleic Acids Res* (1997) 25:3248–54. doi:10.1093/nar/25.16.3248
100. Romanova LY, Willers H, Blagosklonny MV, Powell SN. The interaction of p53 with replication protein A mediates suppression of homologous recombination. *Oncogene* (2004) 23:9025–33. doi:10.1038/sj.onc.1207982
101. Linke SP, Sengupta S, Khabie N, Jeffries BA, Buchhop S, Miska S, et al. p53 interacts with hRAD51 and hRAD54, and directly modulates homologous recombination. *Cancer Res* (2003) 63:2596–605.
102. Sinthupibulyakit C, Ittarat W, St Clair WH, St Clair DK. p53 protects lung cancer cells against metabolic stress. *Int J Oncol* (2010) 37:1575–81. doi:10.3892/ijo_00000811
103. Nadal-Ribelles M, Solé C, Xu Z, Steinmetz LM, de Nadal E, Posas F. Control of Cdc28 CDK1 by a stress-induced lncRNA. *Mol Cell* (2014) 53:549–61. doi:10.1016/j.molcel.2014.01.006
104. Shin DY, Matsumoto K, Iida H, Uno I, Ishikawa T. Heat shock response of *Saccharomyces cerevisiae* mutants altered in cyclic AMP-dependent protein phosphorylation. *Mol Cell Biol* (1987) 7:244–50. doi:10.1128/MCB.7.1.244
105. Mendenhall MD, Hodge AE. Regulation of Cdc28 cyclin-dependent protein kinase activity during the cell cycle of the yeast *Saccharomyces cerevisiae*. *Microbiol Mol Biol Rev* (1998) 62:1191–243.
106. Kroschwald S, Maharana S, Mateju D, Malinovska L, Nüske E, Poser I, et al. Promiscuous interactions and protein disaggregases determine the material state of stress-inducible RNP granules. *Elife* (2015) 4:e06807. doi:10.7554/eLife.06807
107. Decker CJ, Parker R. P-bodies and stress granules: possible roles in the control of translation and mRNA degradation. *Cold Spring Harb Perspect Biol* (2012) 4:a012286. doi:10.1101/cshperspect.a012286
108. Nissan T, Parker R. Analyzing P-bodies in *Saccharomyces cerevisiae*. *Methods Enzymol* (2008) 448:507–20. doi:10.1016/S0076-6879(08)02625-6
109. Voronina E, Seydoux G. The *C. elegans* homolog of nucleoporin Nup98 is required for the integrity and function of germline *P. granules*. *Development* (2010) 137:1441–50. doi:10.1242/dev.047654
110. Cougot N, Daguenet E, Baguet A, Cavalier A, Thomas D, Bellaud P, et al. Overexpression of MLN51 triggers P-body disassembly and formation of a new type of RNA granules. *J Cell Sci* (2014) 127:4692–701. doi:10.1242/jcs.154500
111. Anderson P, Kedersha N, Ivanov P. Stress granules, P-bodies and cancer. *Biochim Biophys Acta* (2015) 1849:861–70. doi:10.1016/j.bbagrm.2014.11.009

Conflict of Interest Statement: The authors declare that the research was conducted in the absence of any commercial or financial relationship that could be construed as a potential conflict of interest.

frontiers in Oncology

ORIGINAL RESEARCH
published: 30 May 2018
doi: 10.3389/fonc.2018.00183

Genome-Wide Analysis of Interchromosomal Interaction Probabilities Reveals Chained Translocations and Overrepresentation of Translocation Breakpoints in Genes in a Cutaneous T-Cell Lymphoma Cell Line

*Anne Steininger[1†], Grit Ebert[1†], Benjamin V. Becker[2], Chalid Assaf[3], Markus Möbs[4], Christian A. Schmidt[5], Piotr Grabarczyk[5], Lars R. Jensen[6], Grzegorz K. Przybylski[7], Matthias Port[2], Andreas W. Kuss[6] and Reinhard Ullmann[2]**

[1] Max Planck Institute for Molecular Genetics, Berlin, Germany, [2] Bundeswehr Institute of Radiobiology Affiliated to the University of Ulm, Munich, Germany, [3] Department of Dermatology and Venerology, Helios Klinikum Krefeld, Krefeld, Germany, [4] Berlin Institute of Health, Institute of Pathology, Charité – Universitätsmedizin Berlin, Corporate Member of Freie Universität Berlin, Humboldt-Universität zu Berlin, Berlin, Germany, [5] Clinic for Internal Medicine C, University Medicine Greifswald, Greifswald, Germany, [6] Human Molecular Genetics, Department of Functional Genomics, University Medicine Greifswald, Greifswald, Germany, [7] Institute of Human Genetics, Polish Academy of Sciences, Poznan, Poland

In classical models of tumorigenesis, the accumulation of tumor promoting chromosomal aberrations is described as a gradual process. Next-generation sequencing-based methods have recently revealed complex patterns of chromosomal aberrations, which are beyond explanation by these classical models of karyotypic evolution of tumor genomes. Thus, the term chromothripsis has been introduced to describe a phenomenon, where temporarily and spatially confined genomic instability results in dramatic chromosomal rearrangements limited to segments of one or a few chromosomes. Simultaneously arising and misrepaired DNA double-strand breaks are also the cause of another phenomenon called chromoplexy, which is characterized by the presence of chained translocations and interlinking deletion bridges involving several chromosomes. In this study, we demonstrate the genome-wide identification of chromosomal translocations based on the analysis of translocation-associated changes in spatial proximities of chromosome territories on the example of the cutaneous T-cell lymphoma cell line Se-Ax. We have used alterations of intra- and interchromosomal interaction probabilities as detected by genome-wide chromosome conformation capture (Hi-C) to infer the presence of translocations and to fine-map their breakpoints. The outcome of this analysis was subsequently compared to datasets on DNA copy number alterations and gene expression. The presence of chained translocations within the Se-Ax genome, partly connected by intervening deletion bridges, indicates a role of chromoplexy in the etiology of this cutaneous T-cell lymphoma. Notably, translocation breakpoints were significantly overrepresented in genes, which highlight gene-associated biological

OPEN ACCESS

Edited by:
Michael Breitenbach, University of Salzburg, Austria

Reviewed by:
Luisa Lanfrancone, Istituto Europeo di Oncologia s.r.l., Italy
Wei Chen, Southern University of Science and Technology, China

***Correspondence:**
Reinhard Ullmann
reinhard1ullmann@bundeswehr.org

†Present address:
Anne Steininger, Steglitz, Berlin, Germany;
Grit Ebert, TMF – Technology, Methods, and Infrastructure for Networked Medical Research, Berlin, Germany

Specialty section:
This article was submitted to Molecular and Cellular Oncology, a section of the journal Frontiers in Oncology

Received: *14 November 2017*
Accepted: *09 May 2018*
Published: *30 May 2018*

Citation:
Steininger A, Ebert G, Becker BV, Assaf C, Möbs M, Schmidt CA, Grabarczyk P, Jensen LR, Przybylski GK, Port M, Kuss AW and Ullmann R (2018) Genome-Wide Analysis of Interchromosomal Interaction Probabilities Reveals Chained Translocations and Overrepresentation of Translocation Breakpoints in Genes in a Cutaneous T-Cell Lymphoma Cell Line. Front. Oncol. 8:183. doi: 10.3389/fonc.2018.00183

processes like transcription or other gene characteristics as a possible cause of the observed complex rearrangements. Given the relevance of chromosomal aberrations for basic and translational research, genome-wide high-resolution analysis of structural chromosomal aberrations will gain increasing importance.

Keywords: chromosome conformation capture, chromoplexy, chromosomal translocations, deep sequencing, cutaneous T-cell lymphoma

INTRODUCTION

The analysis of structural chromosomal aberrations is of relevance for both basic and translational research. Several chromosomal markers are already routinely used in clinical tests for genotype-based sub-classification of tumors or to assist in therapeutic decisions. In addition, the identification of recurrent aberrations can highlight driver genes of tumorigenesis, which represent promising starting points for the development of targeted therapies. Apart from clinical applications, the characterization of chromosomal aberrations can shed light on the underlying mutational mechanisms and in this way contribute to a better understanding of the cause and course of intra-individual evolution of tumors.

According to classical models of tumorigenesis, complex abnormal karyotypes emerge through the stepwise acquisition of chromosomal rearrangements followed by expansion of those mutated clones with highest proliferative capacity (1). Yet, the conception of intra-individual karyotypic evolution has been biased by the limited perspective as provided by the low resolution of genome-wide datasets on structural chromosomal rearrangements for a long time. The lack of appropriate techniques capable of capturing karyotypic complexity both genome-wide and with high resolution has hampered the identification of mechanisms alternative to the well-documented gradual process. The introduction of array-based comparative genomic hybridization [(arrayCGH) (2, 3)] has mitigated this technical shortcoming for unbalanced structural chromosomal aberrations, but the situation has remained unsatisfactory for balanced chromosomal rearrangements. Until recently, their characterization required time-consuming cloning of breakpoints or, in case of translocations, depended on sophisticated sorting of derivative chromosomes followed by hybridization of sorted chromosomes on DNA microarrays (4–6). This situation has changed with the advent of next-generation sequencing (NGS), which has set the stage for the development of new protocols for the analysis of structural chromosome aberrations (7). Initially, these analyses have mainly focused on alterations of sequencing depth across the genome or along sorted chromosomes to define DNA copy number changes and translocation breakpoints (8), respectively. Later protocols have taken advantage of paired-end reads and used their mapping position and orientation with respect to the human reference genome to infer the presence and location of structural chromosome aberrations (9). Despite the development of paired-end NGS protocols, the identification of structural chromosomal aberrations such as balanced translocations has remained challenging. This is mainly due to the fact that strategies based on standard paired-end sequencing protocols have to rely on those few sequenced chimeric fragments that span the chromosomal breakpoints. Hence, reliable detection of such rearrangements using standard NGS protocols requires considerable sequencing depth (10). Furthermore, even in case of sufficient sequencing depth, translocation breakpoints in the very vicinity of regions with low mappability, such as repetitive elements, segmental duplications or DNA segments with extreme bias of base composition might be missed or erroneously aligned (11). An alternative strategy capable to overcome these problems is based on the fact that chromosomal rearrangements such as translocations disrupt nuclear architecture and modify spatial proximities of chromosome territories. These modifications of nuclear organization can be monitored by chromosome conformation capture assays such as Hi-C (12–14). This technique combines proximity ligation and NGS to infer nuclear neighborhood of chromosomal regions (see **Figure 1** for explanation). The closer two chromosomal segments are within the nucleus, the more frequent Hi-C will detect interactions between them.

In general, interaction frequencies between two regions on the same chromosome decrease with linear distance and interactions between two chromosomes are considerably rare when compared to intra-chromosomal ones. In case of a translocation, regions of two or more chromosomes come into close contact. This results in an abrupt increase of interaction frequencies between the segments adjacent to the translocation breakpoints and makes Hi-C an ideal approach for the detection of balanced translocations (10, 15–17).

The application of array- and sequencing-based approaches as described above unveiled an unprecedented complexity of structural chromosomal aberrations in tumor genomes. In several cases, the observed mutational patterns were hardly compatible with a stepwise accumulation of chromosomal aberrations as described by the classical model of tumorigenesis (18). For example, regionally confined clusters of numerous chromosomal aberrations with limited DNA copy number states in the absence of general genomic instability have suggested a single catastrophic event as the underlying cause of this complex pattern of aberrations instead of a series of consecutive events. Meanwhile, it has been shown that this phenomenon, termed chromothripsis, can be encountered in a broad range of tumor types, where it can affect 2–3% of patients (19). In 2015, Zhang and colleagues succeeded to demonstrate that micronuclei formation and DNA damage confined to these structures can produce similar patterns of chromosomal changes as typical for chromothripsis (20). Multiple simultaneously arising DNA double-strand breaks also account for the emergence of chromoplexy, which is characterized by chained translocations and interlinking deletion bridges involving numerous chromosomes (21). The complex patterns of

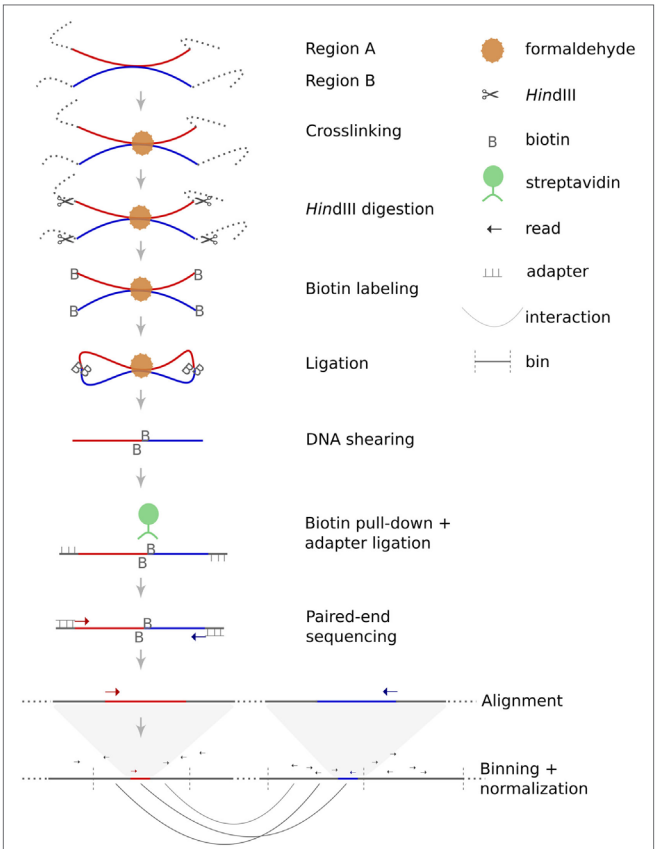

FIGURE 1 | Principle of Hi-C. Hi-C is a variant of the chromosome conformation capture assay dedicated to the identification of genome-wide intrachromosomal and interchromosomal interaction probabilities. The method starts with crosslinking of chromatin within the nuclei. Restriction enzyme digestion (in this case HindIII) generates sticky ends which are filled-in and labeled with biotin. During the following ligation step, free DNA ends are re-ligated, which can either restore the original DNA sequence or can lead to chimeric products. The likelihood of such chimeric products depends on their spatial proximity. Afterward, crosslinking is reversed and DNA is sheared. Size selection and pull-down of biotin-labeled fragments are performed to increase specificity. Next, sequencing adapters are ligated to each fragment before sequencing. Finally, paired-end sequences are mapped to the human reference genome to deduce spatial proximities from the frequency of chimeric sequences.

chromosomal aberrations typical for chromoplexy are unlikely result of a stepwise process, as this would require the repeated use of the same chromosomal breakpoints (18, 21). It is still unclear what triggers these simultaneously arising DNA strand breaks in the context of chromoplexy (18).

In this study, we have employed chromosomal interaction probabilities to fine-map translocations in a cell line derived from a patient with Sézary syndrome. The etiology of this highly malignant cutaneous T-cell lymphoma is poorly understood (22) and thorough investigation of structural chromosomal aberrations promises more insights into its development and progression (23). We demonstrate the presence of chained translocations partly connected by interlinking deletion bridges, which suggests the manifestation of chromoplexy and argues against a gradual appearance of these chromosomal aberrations. The overrepresentation of chromosomal translocation breakpoints within genes highlights the possible impact of spatial proximities of genes and biological processes associated with genes on the emergence of chromosomal translocations in this cutaneous T-cell lymphoma.

MATERIALS AND METHODS

Hi-C is a high-throughput variant of the chromosome conformation capture assay and facilitates the genome-wide investigation of interaction probabilities of genomic segments within the nucleus. The technology is based on crosslinking of chromatin, fragmentation of DNA followed by re-ligation. Depending on their spatial distribution, not only the original DNA fragments but also fragments in spatial proximity will re-ligate. These chimeric fragments can be detected by paired-end sequencing and their frequency can be used to calculate the interaction probability of these fragments within the nucleus. The principle of Hi-C is schematically depicted in **Figure 1**. For this study, we have used a Hi-C protocol published in detail by Lieberman-Aiden and colleagues (13).

Fixation, Cell Lysis, and Restriction Enzyme Digestion

In brief, 20–25 million Se-Ax cells (24) were cross-linked with formaldehyde (Thermo Fisher Scientific, Waltham, MA, USA). Crosslinking was stopped by addition of 125 mM glycine (Merck Millipore, Darmstadt, Germany). After washing cells in ice-cold DPBS buffer (Lonza, Basel, Switzerland), cell pellets were flash frozen and stored at −80°C. For lysis, cells were resuspended in Hi-C lysis buffer and lysed using a Dounce homogenizer (Fisher Scientific GmbH, Schwerte, Germany). After centrifugation, pellets were washed twice in NEB buffer 2 (New England Biolabs, Ipswhich, MA, USA), finally resuspended in 370 µl NEB buffer 2 and 50 µl were transferred to seven tubes each. In order to remove proteins not cross-linked to DNA, 38 µl 1%SDS (Sigma-Aldrich, St. Louis, MO, USA) was added to each tube and incubated for 10 min at 65°C. Afterward, SDS was inactivated by the addition of 44 µl 10% Triton X-100 (Sigma-Aldrich, St. Louis, MO, USA). In each but one tube 400 U HindIII (New England Biolabs, Ipswhich, MA, USA) were added and DNA was digested overnight at 37°C with rotation. The next day, the tube with undigested DNA and one HindIII treated sample were removed to verify HindIII digestion efficiency.

Endlabeling, Re-Ligation, Reversal of Crosslinking, and DNA Purification

For the remaining tubes a fill-in reaction was performed to blunt the sticky ends as generated by HindIII digestion. For later enrichment of re-ligated fragments, Biotin-dCTP (Invitrogen, Carlsbad, CA, USA) was incorporated during this fill-in reaction. Fragments were re-ligated with 15 U T4 DNA ligase per tube for 4 h at 16°C. Reversal of crosslinking was made by addition of 25 µl Proteinase K (20 mg/ml, Thermo Fisher Scientific, Waltham, MA, USA) and incubation overnight at 65°C. After RNA digestion with 50 µl RNase A (10 mg/ml, Thermo Fisher Scientific, Waltham, MA,

USA) for 45 min at 37°C, DNA was purified by means of standard phenol chroroform isoamylalcohol treatment (Sigma-Aldrich, St. Louis, MO, USA) and ethanol (Merck Millipore, Darmstadt, Germany) precipitation. DNA of the separate tubes was conflated and concentration measured with a Qubit fluorometric assay (Thermo Fisher Scientific, Waltham, MA, USA).

Removal of Biotin From Unligated DNA Ends, Enrichment of Re-Ligated Fragments and Preparation of Sequencing Libraries

In order to remove biotin-labeling from unligated fragments, samples were treated for 2 h at 12°C with 5 U T4 DNA polymerase (New England Biolabs, Ipswhich, MA, USA), whose exonuclease activity removed the biotin at the ends of the unligated fragments while keeping the centrally positioned biotin of ligated fragments untouched. Library generation was done according to the manufacturer's protocols, with minor adaptions concerning the pull-down of biotin-labeled fragments to eliminate unligated fragments. In brief, 5 µg DNA was sheared with the Covaris S2 system (Covaris, Woburn, MA, USA), DNA end-repaired and size selected by means of Agencourt AMPure XP Reagent beads (Beckman Coulter Genomics, Danvers, MA, USA). Afterward, size and quantity was verified employing a 2100 Bioanalyzer (Agilent Technologies, Santa Clara, CA, USA). Unligated fragments were depleted by pull-down of biotin-labeled fragments with 50 µl streptavidin beads (10 mg/ml, Life Technologies, Carlsbad, CA, USA). The resulting DNA-coated beads were resuspended in 34 µl TE buffer (Life Technologies, Carlsbad, CA, USA). After A-tailing, i.e., addition of a dATP to the repaired DNA ends, and ligation of sequencing adapters, 5 µl of DNA-coated beads were used for 10 cycles of PCR amplification with primers complementary to the ligated sequencing adapters. These amplicons were sequenced using the SOLiD 5500X1 Sequencing Instrument (Life Technologies, Carlsbad, CA, USA) using the paired-end protocol with 75 and 35 nucleotides for the forward and reverse strand, respectively.

Processing and Quality Control of Hi-C Data

Forward and reverse sequence reads were separately aligned to the human reference genome (hg19) by means of LifeScope Genomic Analysis Software 2.5.1. The resulting file was imported into the software tool HOMER v.4.7 (25), where the dataset was filtered for possible PCR artifacts, reads with low mapping quality and reads derived from sites lacking HindIII motifs. For visualization of chromosomal interaction probabilities as heatmaps, reads that passed the above-mentioned filters were summarized to genomic bins of 100 and 250 kb in size and read counts were normalized. The normalization strategy as implemented in HOMER proceeds on the assumption that each region within the genome should have the same visibility and for that reason equalizes possible artifactual effects caused by differences in GC content, accessibility of DNA and unequal distribution of HindIII sites. Significantly interacting genomic bins were determined employing HOMER's analyzeHiC module (FDR = 0.001; bin interaction distance >25 Mb). Visualization of interaction frequencies in heatmaps was done in JAVA Treeview (26). Translocations were preselected by visual inspection of the interaction heatmaps. Translocation breakpoints were fine-mapped by evaluating read distribution within a 2 Mb window surrounding the breakpoints in order to identify the HindIII fragment next to the breakpoint.

Comparison of Translocation Breakpoint Regions With Data on Higher Order Chromatin Conformation, DNA Copy Number Alterations, and Search for Expressed Fusion Genes

Given the hypothesis that spatial proximity might promote the emergence of translocations, we have processed public Hi-C data on the B-lymphocyte cell line GM12878 (27) in the same ways as the data for Se-Ax and evaluated the presence of significant interchromosomal interactions as defined by HOMER (FDR = 0.001) connecting the translocation partner chromosomes by means of Circos (28). Additionally, we have visually inspected various public data on chromatin interaction deposited at the 4DGenome database (29) (https://4dgenome.research.chop.edu/) to identify possible interactions between our intervals of interest in other cell lines.

Data on DNA copy number alterations in Se-Ax that have been generated by means of arrayCGH in a previous study (30) were visualized for each translocation within a 2 Mb interval surrounding the breakpoint by means of R and the R packages reshape2 (31) and ggplot2 (32). The expression of fusion genes was tested using previously published RNA-Seq data (33, 34). Translocation breakpoints were verified by screening paired-end sequencing data for Se-Ax (33, 34) and the analysis of these data by Breakdancer (35).

Analysis of Chromosomal Breakpoint Overrepresentation Within Genes

Overrepresentation of translocation breakpoints within genes was tested at the resolution of single HindIII fragments by calculating the likelihood that the same number of randomly distributed HindIII fragments map to genes as it has been observed for HindIII fragments located next to the translocation breakpoints. In a first step, we have cataloged all HindIII restriction sites within the human genome by means of Galaxy Emboss command *fuzznuc* (36, 37). Gaps in the human genome assembly (38) were subtracted with BEDtools (39). From the resulting dataset, the Unix command *shuf* was employed to generate 100,000 permutations of 32 HindIII fragments and the BEDtools command "intersectBed" was used to compute the frequency of overlap with RefSeq genes (40).

To calculate the *p*-value for Monte Carlo resampling according to Ref. (41), the number of permutation datasets that feature an equal or greater count of HindIII fragment regions with gene overlap as observed (> = 24) were used as the expected overlap.

RESULTS

Hi-C analysis was based on 91.9 million read pairs that passed processing and quality filtering in HOMER. A genome-wide survey of structural aberrations is presented in **Figure 2**. This heatmap depicts the ratio of observed interaction frequencies and the expected frequencies based on a background model. Translocations are indicated by higher than expected frequencies of interchromosomal interactions (red color). Correspondingly, intrachromosomal interaction frequencies of the chromosomes involved in the translocation are decreased (blue color). The color gradient indicates the orientation of the breakpoint; i.e., interaction intensities decrease with distance from chromosomal breakpoints. In total, we identified 22 translocations, from which we were able to fine-map 32 breakpoints to a single HindIII fragment (**Table 1**; note that only 32 of the 34 breakpoints as listed in **Table 1** were considered for the following analysis as in two cases breakpoints mapped to the same HindIII fragment). A comparison of Hi-C data with whole-genome sequencing data generated by a different laboratory using a different batch of Se-Ax cells (33, 34) revealed an overlap of 25 breakpoints. These have been highlighted in **Table 1**. A comparison of translocation breakpoints with array CGH data generated in a previous study by our laboratory with a resolution of ~100 kb (30) revealed that 11 of those breakpoints not identified by whole-genome sequencing were flanked by either deletions ($n = 7$) or duplications ($n = 4$). Other translocation breakpoints solely identified by Hi-C analysis were in close vicinity to other translocations, suggesting the presence of a complex rearrangement (t1/t10; t7/t8; t8/t15; and t13/t14). Yet, it has to be emphasized that non-overlapping

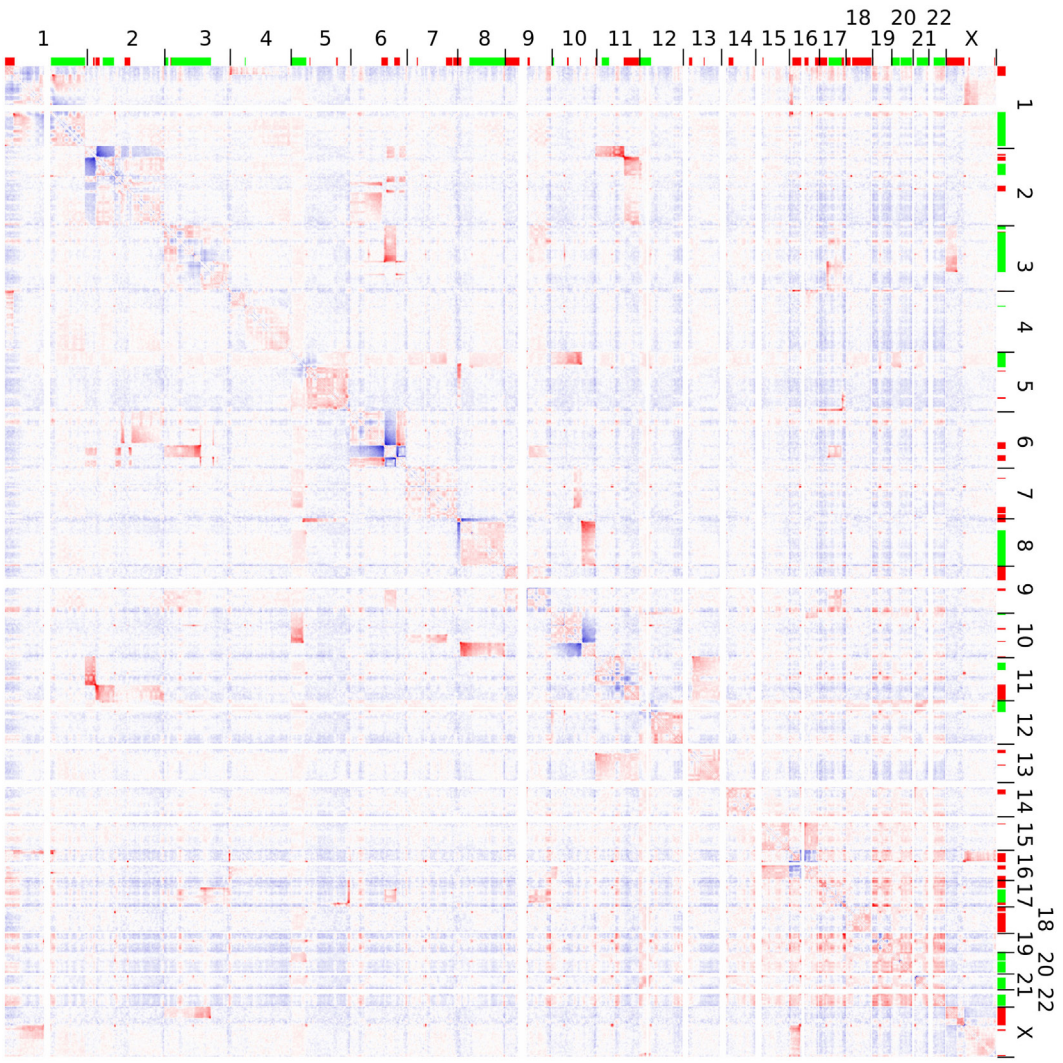

FIGURE 2 | Genome-wide interaction frequencies in Se-Ax. Higher and lower than expected normalized interaction frequencies are shown with 2.5 Mb resolution in red and blue, respectively. The chromosome numbers are given at the top and to the right; together with information on DNA copy number losses (red) and gains (green) as detected by array comparative genomic hybridization. Translocations are characterized by interchromosomal interactions higher than expected, while their corresponding intrachromosomal interactions are decreased. A more detailed view of selected chromosomes is provided in **Figure 3**.

TABLE 1 | Translocation breakpoints (hg19).

ID	Partner ID	Chromosome	Start	Stop	Genes
t1	t1_1p35.3	chr1	28238215	28248287	RPA2
	t1_4p16.3	chr4	4050000[b]	4150000	BC042823
t2	t2_1q21.3	chr1	150769818	150781274	CTSK
	t2_16p13.13[a]	chr16	11004475	11019710	CIITA
t3	t3_2q14.2[a]	chr2	120270564	120285427	SCTR
	t3_6q16.1[a]	chr6	98127299	98143928	LOC101927314
t4	t4_2q22.1[a]	chr2	137227625	137228172	—
	t4_6q21[a]	chr6	114395987	114399043	HDAC2-AS2
t5	t5_11q14.3[a]	chr11	88350000[b]	88450000	GRM5
	t5_2p22.3[a]	chr2	32260000[b]	32360000	Several genes
t6	t6_11q14.3[a]	chr11	88350000[b]	88450000	GRM5
	t6_2p22.3[a]	chr2	32230000[b]	32330000	Several genes
t7	t7_3q13.2	chr3	112240000[b]	112340000	Several genes
	t7_6q21[a]	chr6	106400000[b]	106500000	—
t8	t8_3q13.2	chr3	113435703	113437137	NAA50
	t8_17q11.2	chr17	28807394	28808819	GOSR1
t9	t9_3q24[a]	chr3	143214724	143222670	SLC9A9
	t9_Xp21.1[a]	chrX	36597000	36600264	—
t10	t10_16p13.13	chr16	11954332	11955153	—
	t10_4p16.3	chr4	3315595	3322490	RGS12
t11	t11_5p13.2[a]	chr5	37046678	37051545	NIPBL
	t11_8p23.1[a]	chr8	10977335	10981039	XKR6
t12	t12_10q23.31[a]	chr10	91799056	91801084	—
	t12_5q13.2[a]	chr5	37046678	37051545	NIPBL
t13	t13_17q25.1	chr17	70991114	71006897	SLC39A11
	t13_5q31.3	chr5	143656972	143667413	KCTD16
t14	t14_5q35.2[a]	chr5	176114621	176120288	—
	t14_17q24.3[a]	chr17	70537801	70539618	LINC00673
t15	t15_6q24.2[a]	chr6	143380000[b]	143480000	AIG1
	t15_17q11.2[a]	chr17	28770000[b]	28870000	CPD, GOSR1
t16	t16_10q22.1	chr10	71038330	71050820	HK1
	t16_7q31.33	chr7	126890674	126899921	GRM8
t17	t17_10q23.33[a]	chr10	95298787	95314132	—
	t17_8p23.1[a]	chr8	10977335	10981039	XKR6
t18	t18_12p12.2	chr12	20833396	20843983	PDE3A
	t18_10p14	chr10	7970549	7976904	TAF3
t19	t19_13q12.3[a]	chr13	31132320	31134497	HMGB1
	t19_11p15.5[a]	chr11	1444072	1449221	BRSK2
t20	t20_12p12.3	chr12	18675961	18680225	PIK3C2G
	t20_Xq28	chrX	147292149	147300244	—
t21	t21_17q25.3[a]	chr17	75511241	75516019	—
	t21_19p13.3	chr19	3737154	3750893	TJP3
t22	t22_17q24.3	chr17	69185554	69188239	CASC17
	t22_9q21.13	chr9	74350000[b]	74600000	Several genes

[a]*Identified in an independent Se-Ax cell batch by whole-genome sequencing.*

[b]*Not mapped to a single HindIII interval.*

Start and stop define the HindIII interval covering the breakpoint.

breakpoints may also be owed to private mutations emerging during cultivation of Se-Ax cells in different laboratories over longer time or other technical reasons, in particular differences in resolution.

As an example for the complexity of chromosomal aberrations, a zoom-in depicting interchromosomal interactions for chromosomes 2, 6, and 11 is given in **Figure 3**. Additionally, chromosomal deletions and duplications identified by arrayCGH analysis of Se-Ax are indicated in both heatmaps.

Deletions adjacent to transclocation breakpoints have been encountered 12 times (out of 32 breakpoints; **Figure 4**). The Circos plot depicted in **Figure 5** demonstrates chained translocations

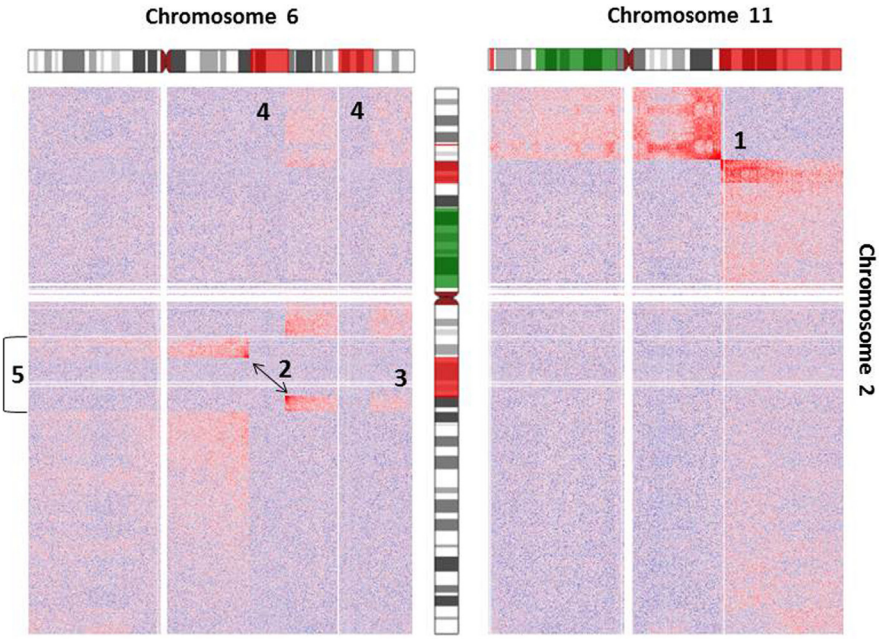

FIGURE 3 | Heatmap of normalized interchromosomal interaction frequencies between chromosomes 2 and 6 and chromosomes 2 and 11. Two heatmaps are shown, which demonstrate the presence of a translocation t(2;6) (left) and t(2;11) (right), respectively. Both derivative chromosomes lead to higher than expected interchromosomal interaction frequencies, which are indicated by the red color gradient. Alterations of DNA copy number state as detected by array comparative genomic hybridization is indicated by coloring of the chromosome ideograms (red = deletion, green = gain). While the breakpoint of reciprocal translocation t(2;11) is easily identifiable [1], the identification of t(2;6) [2] is complicated by additional deletions of chromosome 2 [3] and chromosome 6 [4] and an inversion of chromosome 2 [5]. Orientation of chromosomal rearrangements can be inferred from the color gradient [interaction intensities (i.e., red color) decrease with distance from chromosomal breakpoints].

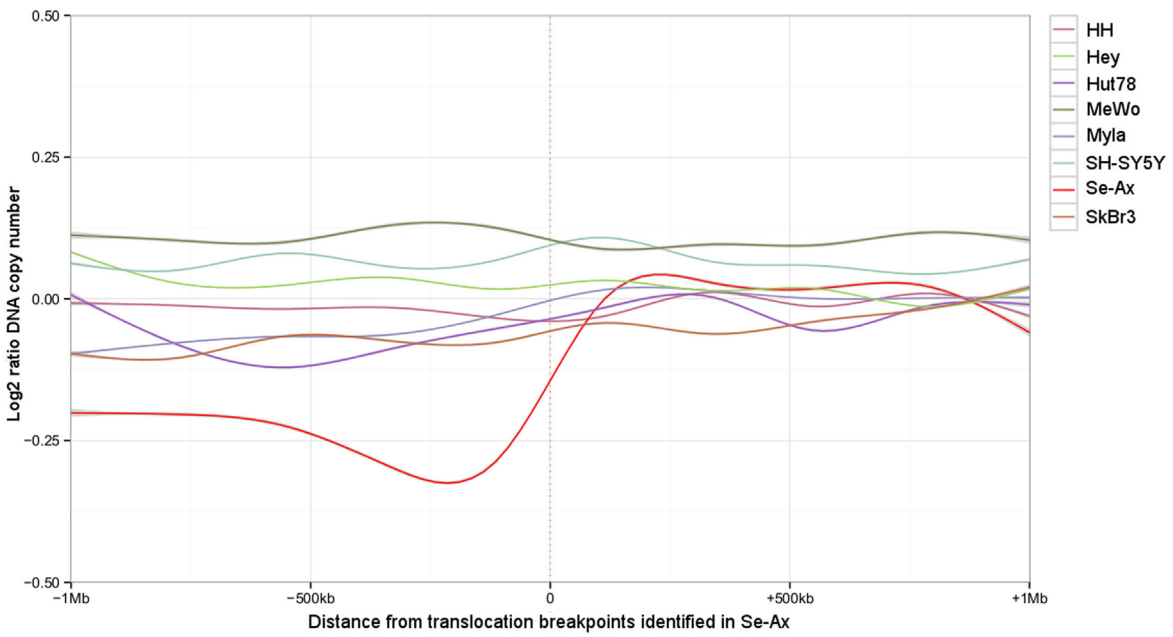

FIGURE 4 | Deletions adjacent to the translocation breakpoints identified in Se-Ax. Smoothed log2 ratios of DNA copy number within a 2 Mb interval surrounding the translocation breakpoints are shown for Se-Ax (red line). DNA copy numbers of additional cell lines for the very same intervals are displayed for comparison (see insert box for color legend).

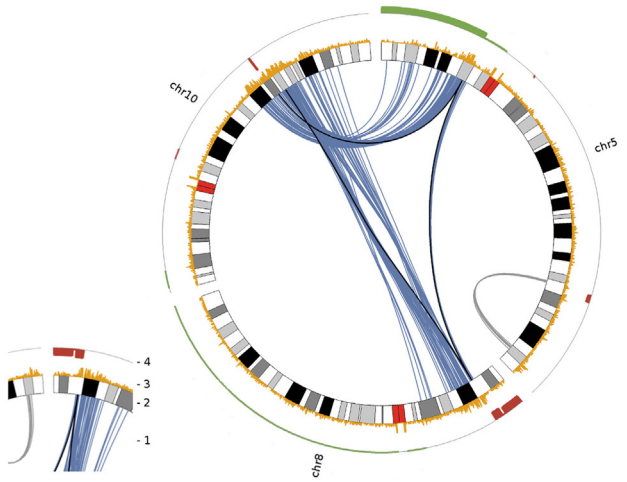

FIGURE 5 | Circos plot visualizing chained translocations between chromosomes 5, 8 and 10. In this Circos plot chromosomes are radially aligned. Arcs within this circle indicate significant interchromosomal and long distance intrachromosomal interactions. Following the numbering given in the small insert to the left: (1) significant interchromosomal interactions (blue lines; FDR <0.001), significant long distance intrachromosomal interactions (gray lines; >25 Mb, FDR <0.001) and translocations as given in **Table 1** (black lines); (2) radially aligned chromosome ideograms; (3) count of significant interactions per 50 kb bin (all interaction distances; max = 10); (4) DNA copy number status in red (deletion) and green (gain) as detected by array comparative genomic hybridization.

with shared breakpoints between several chromosomes on the example of chromosome 5, 8, and 10.

In order to evaluate the impact of spatial proximity of chromosomes on the emergence of translocations, we screened public Hi-C datasets for interactions between those chromosomal intervals affected by translocations in Se-Ax. We failed to get any clues on higher interaction probabilities between regions encompassing the translocation regions, neither in the data of the lymphoblastoid cell line GM12878, which we processed the same way as the Se-Ax data, nor in the datasets from the 4DGenome database. Permutation analysis revealed a significant overrepresentation of translocation breakpoint-associated HindIII fragments within genes ($p = 0.00208$, 100,000 permutations). For one of the possible fusion genes (*AIG1/GOSR1*), transcripts were identified in the corresponding published RNA-Seq data (33).

DISCUSSION

The genome-wide identification and fine-mapping of chromosomal aberrations in tumor cells is instrumental in getting insights into the molecular mechanisms underlying their formation. On the example of a cutaneous T-cell lymphoma cell line we demonstrated the usefulness of Hi-C for the identification of balanced chromosomal translocations. We could show that the abrupt and prominent change of chromosomal interaction probabilities caused by derivative chromosomes facilitates the identification of translocation partners, their orientation to each other as well as their chromosomal breakpoints. Thereby, the observed changes of interaction probabilities were not confined to the area surrounding the breakpoints, but have extended several megabases beyond (**Figures 2** and **3**). This makes the detection of translocations by Hi-C sensitive, robust, and less prone to artifacts, particularly if the chromosomal breakpoints are next to repetitive sequences, segmental duplications or DNA copy number aberrations. Consequently, the analysis of translocations by Hi-C overcomes some of the limitations of alternative deep sequencing approaches described above. Resolution and sensitivity of this approach might be further increased by recent modifications of the Hi-C protocol (27), by using more sequencing reads and more frequently cutting enzymes (e.g., 4 bp instead of 6 bp) (42) or DNase as an alternative (43). A current limitation of the presented approach is that the presence of translocations has been identified by visual inspection of interaction matrices and that their chromosomal breakpoints were pinned down to the level of single restriction enzyme recognition sites by scrutinizing read distribution within the preselected chromosomal intervals later on. There is need for automation and objectivation of this process and very recently, first software tools dedicated to this task have already been presented (44). Although the focus of this study is on balanced translocations, the observation of higher than expected interaction probabilities between chromosomal segments can also be employed for the detection of DNA copy number alterations and inversions, but particularly for small inversions higher sequencing depth is needed for their robust detection (10). Hi-C analysis with sufficient sequencing depth and read length would also facilitate the determination of haplotype phase (45, 46), which would allow the correct assignment of chromosomal breakpoints to either the maternally or paternally derived chromosomes.

In line with previous reports, the Hi-C data presented in this study have revealed a highly complex karyotype in the investigated cell line. Strikingly, several of the translocation breakpoints seem to be chained and associated with chromosomal deletions. Such patterns of rearrangements have already been observed in other tumors (47, 48), including one case of cutaneous T-cell lymphoma (49), and the term chromoplexy has been coined to describe this phenomenon (21). Simultaneously arising DNA double-strand breaks are a prerequisite for chromoplexy, but the triggers of the temporarily and spatially confined genomic instability have not been identified yet (18). Notably, the majority of breakpoints map within genes ($p = 0.00208$), which suggests that transcription or other biological processes associated with genic sequences could be involved in this mutational event (50). Irrespective of the cause of genomic instability the fusion of DNA double-strand breaks requires their spatial proximity, either before DNA damage (contact first) or thereafter, when broken ends might migrate to some sort of repair center (breakage first) (51). Although our comparison of translocation breakpoints with public chromatin interaction data did not produce any conclusive results, there is evidence in the literature that nuclear neighborhood of chromosomes impacts the frequency of translocations (52, 53). Against this background, transcription factories could be the possible scene of the observed punctuated accumulation of chromosomal translocations, as

genes from different chromosomes cluster together in these nuclear structures (54, 55).

In summary, we have demonstrated the power of genome-wide chromosome conformation capture analysis to detect chromosomal translocations. We present evidence that several translocations identified in the investigated cutaneous T-cell lymphoma cell line likely emerged simultaneously leading to karyotypic features typical of chromoplexy. Overrepresentation of breakpoints within genic sequences highlights the role of transcription or gene-associated biological processes in the emergence of the observed pattern of structural chromosomal rearrangements.

AUTHOR CONTRIBUTIONS

AS, GE, LRJ and AWK generated Hi-C data, which were analyzed by AS, GE and RU. GKP compared Hi-C results to whole genome sequencing data. CA, MM, GE, MP, CAS, BVB, PG LRJ, GKP and AWK contributed to data interpretation and critically reviewed the manuscript. AS and RU designed the study and wrote the manuscript.

ACKNOWLEDGMENTS

We thank Robert Weissmann for excellent bioinformatic support of Hi-C data.

FUNDING

This project was funded by the German Ministry of Defence. CA was funded by the Wilhelm-Sander Stiftung (2011-066.1) and GKP by the National Science Centre (decision No 2013/08/M/NZ2/00962).

REFERENCES

1. Yates LR, Campbell PJ. Evolution of the cancer genome. *Nat Rev Genet* (2012) 13(11):795–806. doi:10.1038/nrg3317
2. Solinas-Toldo S, Lampel S, Stilgenbauer S, Nickolenko J, Benner A, Dohner H, et al. Matrix-based comparative genomic hybridization: biochips to screen for genomic imbalances. *Genes Chromosomes Cancer* (1997) 20(4):399–407. doi:10.1002/(SICI)1098-2264(199712)20:4<399::AID-GCC12>3.0.CO;2-I
3. Pinkel D, Segraves R, Sudar D, Clark S, Poole I, Kowbel D, et al. High resolution analysis of DNA copy number variation using comparative genomic hybridization to microarrays. *Nat Genet* (1998) 20(2):207–11. doi:10.1038/2524
4. Veltman IM, Veltman JA, Arkesteijn G, Janssen IM, Vissers LE, de Jong PJ, et al. Chromosomal breakpoint mapping by arrayCGH using flow-sorted chromosomes. *Biotechniques* (2003) 35(5):1066–70.
5. Fiegler H, Gribble SM, Burford DC, Carr P, Prigmore E, Porter KM, et al. Array painting: a method for the rapid analysis of aberrant chromosomes using DNA microarrays. *J Med Genet* (2003) 40(9):664–70. doi:10.1136/jmg.40.9.664
6. Kalscheuer VM, FitzPatrick D, Tommerup N, Bugge M, Niebuhr E, Neumann LM, et al. Mutations in autism susceptibility candidate 2 (AUTS2) in patients with mental retardation. *Hum Genet* (2007) 121(3–4):501–9. doi:10.1007/s00439-006-0284-0
7. Abel HJ, Duncavage EJ. Detection of structural DNA variation from next generation sequencing data: a review of informatic approaches. *Cancer Genet* (2013) 206(12):432–40. doi:10.1016/j.cancergen.2013.11.002
8. Chen W, Kalscheuer V, Tzschach A, Menzel C, Ullmann R, Schulz MH, et al. Mapping translocation breakpoints by next-generation sequencing. *Genome Res* (2008) 18(7):1143–9. doi:10.1101/gr.076166.108
9. Chen W, Ullmann R, Langnick C, Menzel C, Wotschofsky Z, Hu H, et al. Breakpoint analysis of balanced chromosome rearrangements by next-generation paired-end sequencing. *Eur J Hum Genet* (2010) 18(5):539–43. doi:10.1038/ejhg.2009.211
10. Harewood L, Kishore K, Eldridge MD, Wingett S, Pearson D, Schoenfelder S, et al. Hi-C as a tool for precise detection and characterisation of chromosomal rearrangements and copy number variation in human tumours. *Genome Biol* (2017) 18(1):125. doi:10.1186/s13059-017-1253-8
11. Paterson AL, Weaver JM, Eldridge MD, Tavare S, Fitzgerald RC, Edwards PA, et al. Mobile element insertions are frequent in oesophageal adenocarcinomas and can mislead paired-end sequencing analysis. *BMC Genomics* (2015) 16:473. doi:10.1186/s12864-015-1685-z
12. Dekker J, Marti-Renom MA, Mirny LA. Exploring the three-dimensional organization of genomes: interpreting chromatin interaction data. *Nat Rev Genet* (2013) 14(6):390–403. doi:10.1038/nrg3454
13. Lieberman-Aiden E, van Berkum NL, Williams L, Imakaev M, Ragoczy T, Telling A, et al. Comprehensive mapping of long-range interactions reveals folding principles of the human genome. *Science* (2009) 326(5950):289–93. doi:10.1126/science.1181369
14. Belton J-M, McCord RP, Gibcus J, Naumova N, Zhan Y, Dekker J. Hi-C: a comprehensive technique to capture the conformation of genomes. *Methods* (2012) 58(3):268–76. doi:10.1016/j.ymeth.2012.05.001
15. Burton JN, Adey A, Patwardhan RP, Qiu R, Kitzman JO, Shendure J. Chromosome-scale scaffolding of de novo genome assemblies based on chromatin interactions. *Nat Biotechnol* (2013) 31(12):1119–25. doi:10.1038/nbt.2727
16. Engreitz JM, Agarwala V, Mirny LA. Three-dimensional genome architecture influences partner selection for chromosomal translocations in human disease. *PLoS One* (2012) 7(9):e44196. doi:10.1371/journal.pone.0044196
17. Barutcu AR, Lajoie BR, McCord RP, Tye CE, Hong D, Messier TL, et al. Chromatin interaction analysis reveals changes in small chromosome and telomere clustering between epithelial and breast cancer cells. *Genome Biol* (2015) 16:214. doi:10.1186/s13059-015-0768-0
18. Zhang CZ, Leibowitz ML, Pellman D. Chromothripsis and beyond: rapid genome evolution from complex chromosomal rearrangements. *Genes Dev* (2013) 27(23):2513–30. doi:10.1101/gad.229559.113
19. Stephens PJ, Greenman CD, Fu B, Yang F, Bignell GR, Mudie LJ, et al. Massive genomic rearrangement acquired in a single catastrophic event during cancer development. *Cell* (2011) 144(1):27–40. doi:10.1016/j.cell.2010.11.055
20. Zhang CZ, Spektor A, Cornils H, Francis JM, Jackson EK, Liu S, et al. Chromothripsis from DNA damage in micronuclei. *Nature* (2015) 522(7555):179–84. doi:10.1038/nature14493
21. Baca SC, Prandi D, Lawrence MS, Mosquera JM, Romanel A, Drier Y, et al. Punctuated evolution of prostate cancer genomes. *Cell* (2013) 153(3):666–77. doi:10.1016/j.cell.2013.03.021
22. Bagherani N, Smoller BR. An overview of cutaneous T cell lymphomas. *F1000Res* (2016) 5. doi:10.12688/f1000research.8829.1
23. Elenitoba-Johnson KS, Wilcox R. A new molecular paradigm in mycosis fungoides and Sezary syndrome. *Semin Diagn Pathol* (2017) 34(1):15–21. doi:10.1053/j.semdp.2016.11.002
24. Kaltoft K, Bisballe S, Rasmussen HF, Thestrup-Pedersen K, Thomsen K, Sterry W. A continuous T-cell line from a patient with Sézary syndrome. *Arch Dermatol Res* (1987) 279(5):293–8. doi:10.1007/BF00431220
25. Heinz S, Benner C, Spann N, Bertolino E, Lin YC, Laslo P, et al. Simple combinations of lineage-determining transcription factors prime cis-regulatory elements required for macrophage and B cell identities. *Mol Cell* (2010) 38(4):576–89. doi:10.1016/j.molcel.2010.05.004
26. Saldanha AJ. Java Treeview – extensible visualization of microarray data. *Bioinformatics* (2004) 20(17):3246–8. doi:10.1093/bioinformatics/bth349
27. Rao SS, Huntley MH, Durand NC, Stamenova EK, Bochkov ID, Robinson JT, et al. A 3D map of the human genome at kilobase resolution reveals principles of chromatin looping. *Cell* (2014) 159(7):1665–80. doi:10.1016/j.cell.2014.11.021
28. Krzywinski M, Schein J, Birol I, Connors J, Gascoyne R, Horsman D, et al. Circos: an information aesthetic for comparative genomics. *Genome Res* (2009) 19(9):1639–45. doi:10.1101/gr.092759.109

29. Teng L, He B, Wang J, Tan K. 4DGenome: a comprehensive database of chromatin interactions. *Bioinformatics* (2015) 31(15):2560–4. doi:10.1093/bioinformatics/btv158
30. Steininger A, Mobs M, Ullmann R, Kochert K, Kreher S, Lamprecht B, et al. Genomic loss of the putative tumor suppressor gene E2A in human lymphoma. *J Exp Med* (2011) 208(8):1585–93. doi:10.1084/jem.20101785
31. Wickham H. Reshaping data with the reshape package. *J Stat Softw* (2007) 21(12):1–20. doi:10.18637/jss.v021.i12
32. Wickham H. *ggplot2: Elegant Graphics for Data Analysis*. New York: Springer-Verlag (2009).
33. Izykowska K, Zawada M, Nowicka K, Grabarczyk P, Braun FCM, Delin M, et al. Identification of multiple complex rearrangements associated with deletions in the 6q23–27 region in Sezary syndrome. *J Invest Dermatol* (2013) 133(11):2617–25. doi:10.1038/jid.2013.188
34. Izykowska K, Przybylski GK, Gand C, Braun FC, Grabarczyk P, Kuss AW, et al. Genetic rearrangements result in altered gene expression and novel fusion transcripts in Sezary syndrome. *Oncotarget* (2017) 8(24):39627–39. doi:10.18632/oncotarget.17383
35. Chen K, Wallis JW, McLellan MD, Larson DE, Kalicki JM, Pohl CS, et al. BreakDancer: an algorithm for high-resolution mapping of genomic structural variation. *Nat Methods* (2009) 6(9):677–81. doi:10.1038/nmeth.1363
36. Afgan E, Baker D, van den Beek M, Blankenberg D, Bouvier D, Cech M, et al. The Galaxy platform for accessible, reproducible and collaborative biomedical analyses: 2016 update. *Nucleic Acids Res* (2016) 44(W1):W3–10. doi:10.1093/nar/gkw343
37. Rice P, Longden I, Bleasby A. EMBOSS: the European molecular biology open software suite. *Trends Genet* (2000) 16(6):276–7. doi:10.1016/S0168-9525(00)02024-2
38. Karolchik D, Hinrichs AS, Furey TS, Roskin KM, Sugnet CW, Haussler D, et al. The UCSC table browser data retrieval tool. *Nucleic Acids Res* (2004) 32(Database issue):D493–6. doi:10.1093/nar/gkh103
39. Quinlan AR, Hall IM. BEDTools: a flexible suite of utilities for comparing genomic features. *Bioinformatics* (2010) 26(6):841–2. doi:10.1093/bioinformatics/btq033
40. O'Leary NA, Wright MW, Brister JR, Ciufo S, Haddad D, McVeigh R, et al. Reference sequence (RefSeq) database at NCBI: current status, taxonomic expansion, and functional annotation. *Nucleic Acids Res* (2016) 44(D1):D733–45. doi:10.1093/nar/gkv1189
41. Phipson B, Smyth GK. Permutation P-values should never be zero: calculating exact P-values when permutations are randomly drawn. *Stat Appl Genet Mol Biol* (2010) 9:Article39. doi:10.2202/1544-6115.1585
42. Lajoie BR, Dekker J, Kaplan N. The Hitchhiker's guide to Hi-C analysis: practical guidelines. *Methods* (2015) 72:65–75. doi:10.1016/j.ymeth.2014.10.031
43. Ramani V, Cusanovich DA, Hause RJ, Ma W, Qiu R, Deng X, et al. Mapping 3D genome architecture through in situ DNase Hi-C. *Nat Protoc* (2016) 11(11):2104–21. doi:10.1038/nprot.2016.126
44. Chakraborty A, Ay F. Identification of copy number variations and translocations in cancer cells from Hi-C data. *Bioinformatics* (2018) 34(2):338–45. doi:10.1093/bioinformatics/btx664
45. Edge P, Bafna V, Bansal V. HapCUT2: robust and accurate haplotype assembly for diverse sequencing technologies. *Genome Res* (2017) 27(5):801–12. doi:10.1101/gr.213462.116
46. Selvaraj S, Dixon JR, Bansal V, Ren B. Whole-genome haplotype reconstruction using proximity-ligation and shotgun sequencing. *Nat Biotechnol* (2013) 31(12):1111–8. doi:10.1038/nbt.2728
47. Dzamba M, Ramani AK, Buczkowicz P, Jiang Y, Yu M, Hawkins C, et al. Identification of complex genomic rearrangements in cancers using CouGaR. *Genome Res* (2017) 27(1):107–17. doi:10.1101/gr.211201.116
48. Mansfield AS, Murphy SJ, Harris FR, Robinson SI, Marks RS, Johnson SH, et al. Chromoplectic TPM3-ALK rearrangement in a patient with inflammatory myofibroblastic tumor who responded to ceritinib after progression on crizotinib. *Ann Oncol* (2016) 27(11):2111–7. doi:10.1093/annonc/mdw405
49. Choi J, Goh G, Walradt T, Hong BS, Bunick CG, Chen K, et al. Genomic landscape of cutaneous T cell lymphoma. *Nat Genet* (2015) 47(9):1011–9. doi:10.1038/ng.3356
50. Kim N, Jinks-Robertson S. Transcription as a source of genome instability. *Nat Rev Genet* (2012) 13(3):204–14. doi:10.1038/nrg3152
51. Meaburn KJ, Misteli T, Soutoglou E. Spatial genome organization in the formation of chromosomal translocations. *Semin Cancer Biol* (2007) 17(1):80–90. doi:10.1016/j.semcancer.2006.10.008
52. Zhang Y, McCord RP, Ho Y-J, Lajoie BR, Hildebrand DG, Simon AC, et al. Chromosomal translocations are guided by the spatial organization of the genome. *Cell* (2012) 148(5):908–21. doi:10.1016/j.cell.2012.02.002
53. Mathas S, Kreher S, Meaburn KJ, Johrens K, Lamprecht B, Assaf C, et al. Gene deregulation and spatial genome reorganization near breakpoints prior to formation of translocations in anaplastic large cell lymphoma. *Proc Natl Acad Sci U S A* (2009) 106(14):5831–6. doi:10.1073/pnas.0900912106
54. Iborra FJ, Pombo A, Jackson DA, Cook PR. Active RNA polymerases are localized within discrete transcription 'factories' in human nuclei. *J Cell Sci* (1996) 109(Pt 6):1427–36.
55. Osborne CS. Molecular pathways: transcription factories and chromosomal translocations. *Clin Cancer Res* (2014) 20(2):296–300. doi:10.1158/1078-0432.CCR-12-3667

Conflict of Interest Statement: The authors declare that the research was conducted in the absence of any commercial or financial relationships that could be construed as a potential conflict of interest.

frontiers in Oncology

HYPOTHESIS AND THEORY
published: 28 August 2017
doi: 10.3389/fonc.2017.00188

The Potential Role of Senescence As a Modulator of Platelets and Tumorigenesis

Claudio A. Valenzuela[1], Ricardo Quintanilla[1], Rodrigo Moore-Carrasco[2] and Nelson E. Brown[1]**

[1] Center for Medical Research, University of Talca Medical School, Talca, Chile, [2] Faculty of Health Sciences, University of Talca, Talca, Chile

In addition to thrombus formation, alterations in platelet function are frequently observed in cancer patients. Importantly, both thrombus and tumor formation are influenced by age, although the mechanisms through which physiological aging modulates these processes remain poorly understood. In this context, the potential effects of senescent cells on platelet function represent pathophysiological mechanisms that deserve further exploration. Cellular senescence has traditionally been viewed as a barrier to tumorigenesis. However, far from being passive bystanders, senescent cells are metabolically active and able to secrete a variety of soluble and insoluble factors. This feature, known as the senescence-associated secretory phenotype (SASP), may provide senescent cells with the capacity to modify the tissue environment and, paradoxically, promote proliferation and neoplastic transformation of neighboring cells. In fact, the SASP-dependent ability of senescent cells to enhance tumorigenesis has been confirmed in cellular systems involving epithelial cells and fibroblasts, leaving open the question as to whether similar interactions can be extended to other cellular contexts. In this review, we discuss the diverse functions of platelets in tumorigenesis and suggest the possibility that senescent cells might also influence tumorigenesis through their ability to modulate the functional status of platelets through the SASP.

Keywords: cancer, fibrinolysis, platelets, senescence, thrombosis

OPEN ACCESS

Edited by:
Michael Breitenbach, University of Salzburg, Austria

Reviewed by:
Frederique Gaits-Iacovoni, Institut national de la santé et de la recherche médicale, France
Valentina Tosato, International Centre for Genetic Engineering and Biotechnology, Italy

****Correspondence:***
Rodrigo Moore-Carrasco
rmoore@utalca.cl;
Nelson E. Brown
nbrown@utalca.cl

Specialty section:
This article was submitted to Molecular and Cellular Oncology, a section of the journal Frontiers in Oncology

Received: *12 May 2017*
Accepted: *09 August 2017*
Published: *28 August 2017*

Citation:
Valenzuela CA, Quintanilla R, Moore-Carrasco R and Brown NE (2017) The Potential Role of Senescence As a Modulator of Platelets and Tumorigenesis. Front. Oncol. 7:188. doi: 10.3389/fonc.2017.00188

INTRODUCTION

Platelets are key blood components that are continuously generated in the bone marrow through fragmentation of the edges of megakaryocytes (1). In addition to their canonical role in hemostasis, platelets participate in a variety of pathological processes, including chronic inflammation and cancer (2). As the incidence of both cancer and chronic inflammatory disorders rise in an age-dependent manner, the influence that aging may exert on platelet function has become particularly relevant (3). So far, however, the mechanisms involved in this age-dependent modulation of platelets or other components of the hemostasis cascade remain poorly characterized. Similarly, the age-dependent factors that modulate the interaction between platelets and cancer cells are largely unknown. Based on the capacity of senescent cells to actively modify the tissue microenvironment through the secretion of pro-inflammatory mediators, herein we speculate about the existence of a functional link between cellular senescence and platelets that may help explain the increased incidence of cancer and thrombotic diseases in older individuals.

THE COMPLEX INVOLVEMENT OF PLATELETS IN CANCER

The functional connection between cancer and platelets has been recognized since the late nineteenth century, when an association between the occurrence of certain solid tumors and the development of venous thrombosis and blood hypercoagulability was first described (4). Accordingly, defects in platelet function or reduced platelet counts have both been associated with a reduced ability of tumors to metastasize (5, 6). We now know that platelets may contribute to the establishment of various hallmarks of cancer, including the ability of cancer cells to sustain proliferation, to resist apoptosis and to promote angiogenesis and metastasis (1) (for an overview of the contribution of platelets to the hallmarks of cancer, see **Figure 1**). It is presently unclear, however, to what extent these contributions are the result of a direct action of platelets on tumor cells or, alternatively, may be part of an underlying inflammatory process inherent to many tumors. Inflammatory cells and soluble mediators of inflammation are important constituents of the tumor microenvironment. In some tumors, inflammatory conditions are present before the occurrence of malignant transformation (7). Yet in other types of tumors, the inflammatory microenvironment emerges during the process of neoplastic transformation (8). Regardless of its origin, an environment rich in inflammatory cells and growth factors is thought to promote proliferation, angiogenesis, and/or metastasis of cancer cells (1, 7).

Platelets participate in diverse inflammatory processes that may be associated with cancer (9, 10). One of the crucial

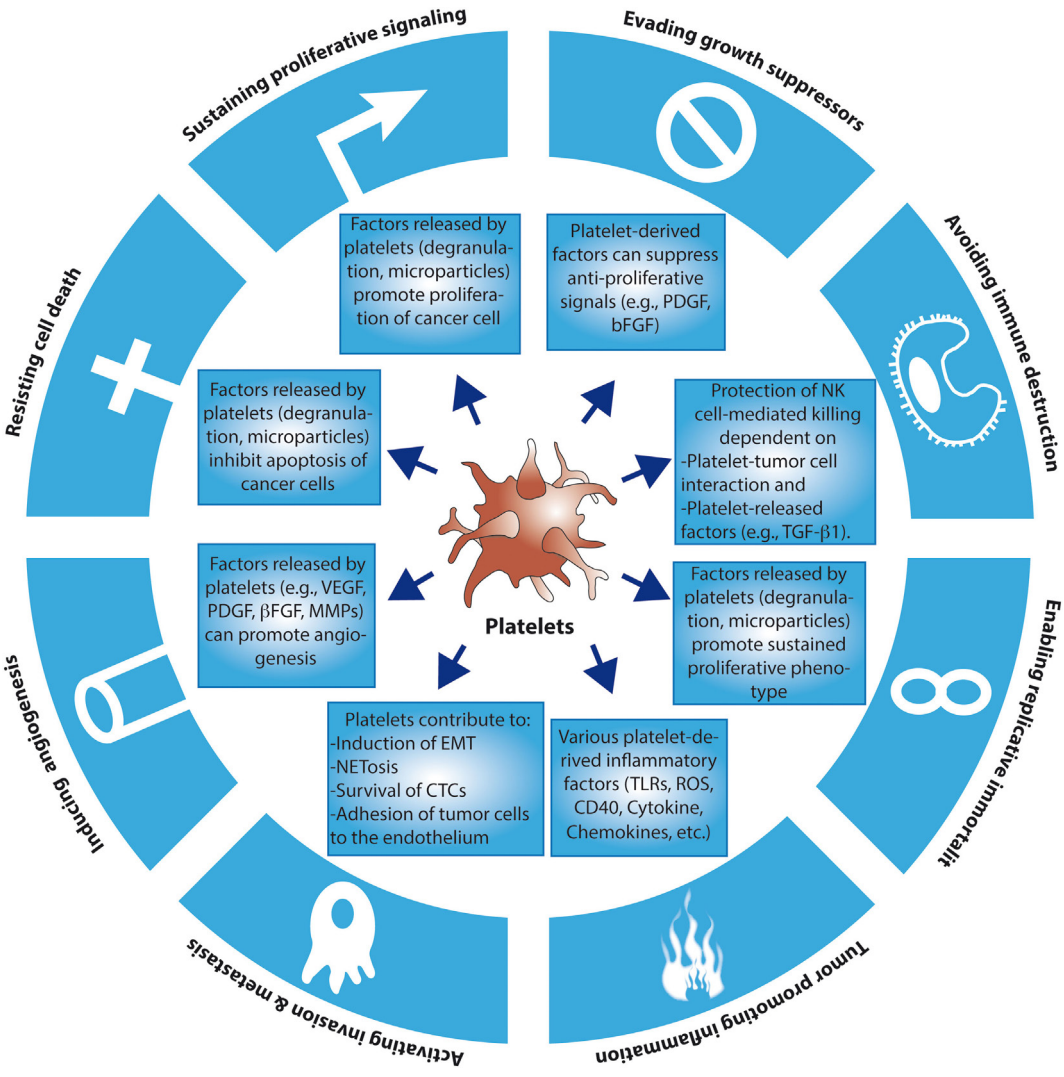

FIGURE 1 | The contributions of platelets to the hallmarks of cancer. So far, there is evidence that platelets may contribute to the emergence of several of the hallmarks of cancer through the release of soluble factors and microparticles, or through direct cancer cell–platelet interactions. For simplicity reasons, more complex and intricate mechanisms have been excluded. EMT, epithelial–mesenchymal transition; CTCs, circulating tumor cells; TLRs, toll-like receptors; ROS, reactive oxygen species; NKs, natural killers.

inflammatory mechanisms involving platelets is NETosis. In this process, neutrophils release part of their intracellular content (chromatin, histones, enzymes, etc.) to the extracellular milieu. These components can then form a mesh that captures circulating microbes and impedes their tissue adhesion and colonization (11, 12). Mechanistically, granulocyte colony-stimulating factor (CSF-G) released by tumor cells is thought to increase the production of inflammatory neutrophils and promote neutrophil–platelet interaction (*via* P-selectin), which in turn is required to stimulate NETosis and a hyper-coagulation/pro-thrombotic state (13). More recently, NETosis has also been shown to play a role at different stages of tumorigenesis, including metastasis (14, 15), and the establishment of paraneoplastic syndromes leading to organ failure and thrombosis (16). Other components of innate immunity that have been associated with cancer are the inflammatory responses mediated by toll-like receptors (TLRs). Classic mediators of TLR activation are tissue damage-associated proteins, particularly members of the HMGB1 (high-mobility group box1). Whereas under normal conditions these proteins are bound to chromatin, they can be released by necrotic cells or secreted by macrophages under inflammatory or tissue damaging conditions (17). Importantly, Le-Xing et al. demonstrated that toll-like receptor 4 (TLR4), present in platelets and other cells of myeloid origin, is crucial for the interaction between tumor cells and platelets (18). Taken together, these examples illustrate the importance of platelets in the regulation of diverse pro-tumorigenic inflammatory processes.

In addition to the general roles of platelets in inflammation, activated platelets may also participate more directly in tumor growth and metastasis. The alpha granules of platelets are the source of various trophic factors, including growth factors, chemokines, adhesion molecules, and angiogenic factors, which may promote tumor progression once they are released by activated platelets (19). In fact, the levels of many of these factors have been used as prognostic determinants in cancer patients (20, 21). In addition to these paracrine actions, tumor growth and metastasis also seem to depend on the ability of platelets to physically interact with tumor cells through specific integrin complexes. For example, blockade of GpIIb/IIIa—a fibrinogen-binding integrin complex that is required for platelet aggregation and binding to tumor cells—reduces the number of metastatic nodules in the lung (22). Consistent with this observation, mice deficient in β3-integrin also display reduced metastasis (6). Altogether, these data indicate that integrin-mediated tumor cell–platelet interaction is necessary for platelet activation during metastasis (23). As mentioned above, TLR4 can also enhance tumor cell–platelet interactions, a function that is, at least in part, dependent on the release of endogenous ligand HMGB1 by tumor or damaged cells (18).

The growth factor-enriched microenvironment generated by platelet degranulation can also render tumor cells more resistant to chemotherapeutic agents (**Figure 1**). For example, in a group of patients with recurrent ovarian cancer, an increased number of platelets were associated with a reduction in overall survival and resistance to chemotherapy (24, 25). A similar phenomenon occurs in gastric cancer, where increases in both the number and volume of platelets were associated with a reduced response to chemotherapy (26, 27). Platelets also increase the overall survival of 5-fluorouracil- and paclitaxel-treated colon adenocarcinoma cells (28). In this case, the presence of platelets induces the expression of anti-apoptotic proteins and reduces the expression of pro-apoptotic proteins in cancer cells (28). This prosurvival effect seems to correlate with the ability of platelets to change the profile of factors secreted by cancer cells themselves, which may explain the reduced apoptotic effect of 5-fluorouracil y paclitaxel (28). Interestingly, the anti-tumorigenic effects of thrombocytopenia may also be explained by the presence of micro-hemorrhages that improve chemotherapy response (29–32). In addition to influencing anti-cancer therapy response, platelet function itself can be altered in the course of chemotherapy. For example, Kedzierska et al. described hematological alterations in patients with breast cancer before, during and after chemotherapy (33), demonstrating that the size, number, and aggregation capacities of platelets obtained from patients undergoing chemotherapy were higher compared to healthy controls (33). These changes appear to be a compensatory mechanism that hinders the correct distribution of the chemotherapeutic drugs within the tumor. Recently, Holmes et al. (34) also described changes in the secretory profile of platelets in patients with breast cancer. They observed a differential regulation in the release of angiogenic factors, especially vascular endothelial growth factor (VEGF), by platelets from individuals with cancer versus healthy individuals. Interestingly, these authors also showed that platelets from individuals undergoing chemotherapy released more angiogenic factors compared to individuals with cancer but not subjected to chemotherapy treatment (34).

Platelets may also promote distant colony formation (metastasis) by allowing the survival of tumor cells in the circulation [circulating tumor cells (CTCs)] (35). Under normal conditions, CTCs are rapidly eliminated from circulation by the host immune system or the activation of apoptosis (following lack of substrate attachment, a form of apoptosis known as anoikis). However, CTCs that become coated with platelets are protected from immune-dependent cell lysis (36). In this scenario, adhesion molecules present on the surface of activated platelets, including GpIIb/IIIa integrin, mediate the formation of heteroaggregates with tumor cells that remain shielded from immunological detection and natural killer (NK) cell-mediated lysis (35, 37). At least in part, this immunological tolerance may be also explained by platelet-derived secreted factors, such as TGF-β1, that impair NK cell anti-tumor activity (38).

Platelets may also facilitate the adhesion of tumor cells to the endothelium, generating a locally protected tumor microenvironment that promotes migration of tumor cells. The establishment of this microenvironment also seems depend on granulocyte recruitment (39) and a platelet-induced increase in endothelial permeability (40). It has been shown that this effect depends on the ability of activated platelets to secrete nucleotides that act on P2Y2 receptors expressed on the surface of endothelial cells. It is important to mention that platelets are also considered a major source of VEGF, an angiogenic factor that is released upon activation (41). In addition, platelet-derived TGF-β1 enables tumor cells to undergo a process that resembles the epithelial–mesenchymal transition, thus facilitating invasion and dissemination

(42). Finally, platelet-derived microparticles also play a role in tumor growth, migration, and metastasis (43). CTCs can increase the production of platelet-associated microparticles that promote invasiveness and metastasis (44). Among other proteins, microparticles also contain tissue factor, which is important for the generation of thrombin and the subsequent activation of protease-activated receptor-1 receptors on platelets, leading to VEGF secretion and angiogenesis (45). Taken together, the role of platelets in tumor invasion and metastasis is complex and can be explained by both direct actions on cancer cells or through collaborative effects with other cell types. So far, platelet-assisted dissemination of cancer cells has been demonstrated in the context of several human cancers, including colorectal (46), lung (47), breast (48), kidney (49), and pancreatic (50) cancers.

Tumor-derived factors leading to platelet production and activation are similarly variable and, in general, poorly understood. Several pro-inflammatory cytokines released by tumor cells, or tumor-associated stromal cells, are able to increase the number of platelets by stimulating the formation and fragmentation of megakaryocytes (51). Among the most recent findings, Stone et al. (24) reported that thrombocytosis in patients with ovarian cancer was associated with cytokine production by tumor and host tissues. In particular, tumor-derived interleukin-6 (IL-6) led to an increase in the number of activated platelets (24). Similarly, local secretion of soluble mediators by tumor cells enhances platelet activation and aggregation. For example, colorectal cancer cells induce platelet aggregation *via* the release of ADP and MMP-2 (52). Platelet aggregation, in turn, correlated with overexpression of GPIIb/IIIa and P-selectin in platelets, allowing the formation of tumor cell–platelet interactions (5, 52). Some of these mechanisms also involve the generation of thrombin (e.g., colon carcinoma cells) (53). Other mechanisms of cancer-dependent platelet activation that involve cell-to-cell contact include the overexpression of podoplanin, a trans-membrane protein (also known as "aggrus") that is expressed in several tumor types (54). Podoplanin binds the c-type lectin receptor on the surface of platelets, triggering their activation (55, 56). Similarly, the release of cathepsin B by B16 melanoma cells can also trigger the activation of platelets (57).

AGING AND PLATELETS

So far, the role of the physiological process of aging as a modulator of platelet function, or as a factor that may influence the interaction between platelets and tumor cells, remains poorly understood (58). Early studies found that plasma concentrations and activities of various coagulation factors (fibrinogen, von Willebrand factor, factors V, VII, VIII, and IX) increase with the physiological process of aging (3, 59, 60). Among these factors, fibrinogen is particularly relevant because it represents a primary risk factor for thrombotic disorders (61, 62). Interestingly, fibrinogen levels also increase in response to the pro-inflammatory cytokine IL-6. As levels of IL-6 were also strongly correlated with aging (63), these findings might suggest that high levels of fibrinogen in the elderly could be, at least in part, a reflection of an age-dependent inflammatory state. Similarly, the fibrinolytic system is also affected by aging. Thus, several studies have shown that the levels of PAI-1 (plasminogen activator inhibitor-1), a major inhibitor of fibrinolysis, increase with age (3, 64).

In addition to the above-mentioned hemostatic factors, platelets and endothelial cells are also affected by aging. Decrease in bleeding time (a surrogate for platelet activity) and elevation of markers of platelet activation have both been correlated with physiological aging (65). Moreover, platelets from older individuals display a greater aggregation response to ADP and collagen compared to younger individuals (66). Similarly, endothelial cells isolated from older individuals display important changes that may predispose these individuals to thrombotic disease. These changes include an age-dependent decline in endothelial production of prostacyclin and nitric oxide (67, 68).

Taken together, changes in virtually all aspects of hemostasis have been associated with physiological aging. As older adults often show signs of chronic inflammation, it is likely that changes in hemostasis—particularly those involving platelet function—may be part of a more general inflammatory process. So far, however, the age-dependent mechanisms involved in the modulation of hemostasis and platelet function are not completely understood. In the next sections, we advance the idea that cellular senescence might explain, at least in part, some of the hemostatic changes that lead to thrombosis and cancer.

CELLULAR SENESCENCE

Typical hallmarks of physiological aging include impaired tissue regeneration and repair, a functional impairment of progenitor cells, and alterations of the immune system (69). While the specific cellular changes associated with each one of these hallmarks will vary depending on the tissue analyzed, cellular senescence is rapidly emerging as an underlying process that may help explain some of these changes. In keeping with this idea, senescent cells accumulate in several tissues derived from aged animals (70, 71).

Cellular senescence was described more than 50 years ago as a process that limits the proliferation of primary human cells propagated *in vitro* (72). Simply stated, cellular senescence refers to a type of permanent and stable cell cycle arrest induced by numerous stimuli, including DNA damage, oxidative stress, activation of certain oncogenes, and therapeutic stress (including chemotherapy and radiotherapy). Because senescent cells cease to proliferate, cellular senescence was initially regarded as a functional equivalent of apoptosis in its ability to suppress tumor formation (73). However, recent work indicates that the physiological relevance of cellular senescence extends far beyond tumor suppression, into processes as diverse as embryonic development, wound healing, and tissue repair (74–77). Moreover, as discussed in the next section, the presence of senescent cells in tissues may actually promote the acquisition of neoplastic features by adjacent cells or otherwise foster the generation of a pro-inflammatory environment (78).

Morphologically, senescent cells appear large and "flattened" (79) and are typically positive for β-galactosidase activity at pH 6.0, a reflection of the high content of lysosomes in these cells (78, 80). Another prominent feature of senescent cells is the presence of "senescence-associated heterochromatin

foci," which correspond to regions of chromatin condensation (heterochromatin) that appear as bright and dense foci in the nuclei of senescent cells (81, 82). The cell cycle exit observed in senescent cells is generally associated with a typical DNA content of G1 phase, that is, a failure to initiate DNA replication even when growth conditions are adequate. The initial transition from cycling to cell cycle arrest involves a reduction in the activity of cyclin/cyclin-dependent kinases (CDKs) complexes, leading ultimately to the activation of the p53 and pRB tumor suppressor pathways (83, 84). For example, the transcription factor p53 can be stabilized in response to various stressful stimuli, increasing the expression of various target genes that trigger cellular senescence or, in extreme cases, apoptosis. One of these targets, $p21^{Cip1/WAF1}$, is a potent inhibitor of cyclin/CDK complexes. Similarly, $p16^{INK4a}$, another inhibitor of CDKs, is highly expressed in senescent cells (83, 85). The upregulation of both types of CDK inhibitors results in the inhibition of CDKs and the subsequent activation (through hypo-phosphorylation) of the pRB pathway, event that effectively blocks the G1-S transition (86) (see **Figure 2**).

Historically, the extent to which cellular senescence contributes to organismal aging and age-driven tissue dysfunction has been difficult to establish, in part due to the lack of markers that could specifically detect senescent cells in aging tissues (87). Nonetheless, the use of combinations of markers has provided convincing evidence that senescent cells do accumulate in aged tissues, as well as in sites of tissue injury and repair (71, 74, 88). For example, markers of DNA damage and de-repression of the *INK4/ARF* locus—which encodes for the tumor suppressive proteins $p16^{INK4A}$ and $p19^{ARF}$—increase with chronological aging. Accordingly, the levels of $p16^{INK4A}$ correlate with the aging of numerous tissues from mice and humans (89, 90). Moreover, for at least some tissues (e.g., liver, skin, lung, and spleen), a good correlation between the proportion of cells with DNA damage, and the proportion of cells displaying senescence-associated β-galactosidase activity, has been found (71).

Taken together, the current evidence indicates that in addition to functioning as a barrier against tumor formation, cellular senescence is also active during embryonic development, tissue repair, and organismal aging. The involvement of cellular senescence in these physiological processes is currently thought to depend on the ability of senescent cells to produce and secrete a variety of factors that can impinge on neighboring cells and the extracellular matrix (ECM), a function that only becomes evident in the context of complex tissues. As mentioned in the following sections, these non-cell autonomous capabilities of senescent cells are also emerging as key contributors to the pathogenesis of age-related conditions, including chronic inflammation, fibrosis, and, paradoxically, cancer.

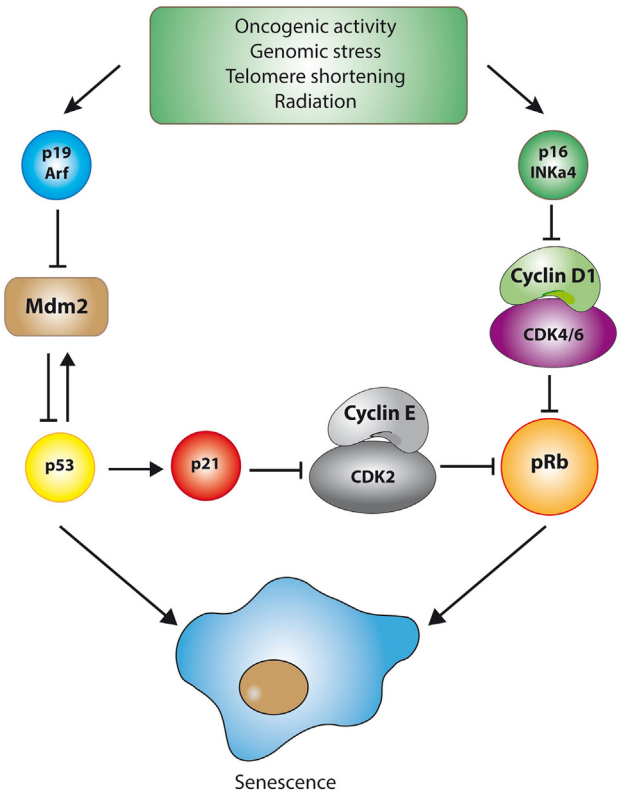

FIGURE 2 | The p53 and pRB pathways during senescence. Cellular senescence is triggered by the activation of one of two major tumor suppressive pathways, namely the p53 or the pRB pathway. Although the details may vary, activation of these pathways is marked by the inhibition of cyclin-dependent kinases (CDKs), the key enzymes involved in cell cycle progression. For example, stabilization of the transcription factor p53 in response to DNA damage (which is dependent on p19/ARF-mediated inhibition of MDM2, an E3-ubiquitin ligase that targets p53 for degradation) is followed by the p53-dependent transcription of genes involved in the orchestration of cellular senescence. One of these target genes, $p21^{Cip1/WAF1}$, is a potent inhibitor of cyclin/CDK complexes, particularly cyclin E/CDK2 complexes. Similarly, $p16^{INK4a}$, another inhibitor of CDKs that highly expressed in some senescent cells, inhibits cyclin D1/CDK4/6 complexes. The upregulation of both types of CDK inhibitors results in the inhibition of CDKs and the subsequent activation of the pRB pathway, which effectively blocks the G1-S cell cycle transition.

THE SENESCENCE-ASSOCIATED SECRETORY PHENOTYPE (SASP)

In addition to cell cycle arrest, the establishment of a mature senescent phenotype involves extensive metabolic reprogramming, as well as the implementation of complex traits such as the SASP (91, 92). The SASP refers to the almost universal capacity of senescent cells to produce and secrete a variety of soluble and insoluble factors, including extracellular proteases, cytokines, chemokines, and growth factors. This ability of senescent cells to potentially modify the tissue microenvironment (neighboring cells and the ECM) *via* SASP adds a further layer of complexity to the implications of cellular senescence to tissue homeostasis and disease (93–96).

A common feature of aging and age-related diseases is chronic inflammation. The term "inflamm-aging" has been coined to describe a low-grade, chronic, and systemic inflammation associated with aging and aging phenotypes in the absence of evidence of infection (97). In line with this concept, many of the factors secreted by senescent cells are also well-known

pro-inflammatory molecules with the potential to induce chronic inflammation in certain biological contexts (69, 98). Indeed, early microarray analyses revealed that senescent fibroblasts display an expression profile that resembles the one displayed by fibroblasts in early stages of wound repair (99). More recently, a unique type of inflammation triggered by senescent cells, the senescence-inflammatory response, has been identified (100). Interestingly, similar to chronic inflammation produced by other mechanisms, the inflammatory "secretoma" produced by senescent cells also seems to depend on activation of the NF-κB and C/EBP-β transcriptional regulators (101). Examples of conserved components of the SASP with known pro-inflammatory actions include IL-6 (102), IL-1-α (103) macrophage inflammatory protein, various metalloproteinases (MMP-2, -4, -1), GM-CSF, and cathepsin B (93, 104).

As expected, the SASP can have complex effects on tissue microenvironments. Thus, some components of the SASP can propagate or reinforce the senescent phenotype through autocrine or paracrine mechanisms, leading to further secretion and amplification of the SASP (105). In addition, SASP factors may attract immune cells, which in turn can orchestrate the elimination of senescent cells and the termination of a senescence-associated inflammatory response. Importantly, clearance of senescent cells seems to dictate the net effect of cellular senescence at the organismal level (106). While transient and limited cellular senescence can be beneficial in the context of the normal tissue remodeling that occurs during embryonic development and wound healing, chronic accumulation of senescent cells—owing to age-dependent deterioration of the innate or adaptive immunity—can have important detrimental consequences. For example, pro-inflammatory cytokines secreted by senescent cells may promote chronic inflammation and, depending on the biological context, lead to pathological conditions characterized by an excess of fibrosis (e.g., liver cirrhosis) (74, 107). Moreover, the SASP, particularly its inflammatory component, can accelerate tumor initiation and progression by fostering a pro-tumorigenic microenvironment (106, 108). Accordingly, clearance of tumor cells (or cells of the tumor stroma) undergoing genetically or drug-induced senescence leads to long-term regression and reduced recurrence of tumors in mouse models of liver and breast tumorigenesis (107, 109–113).

The complex heterotypic interactions in which senescent cells can participate were anticipated by early *in vitro* experiments showing that senescent fibroblasts can enhance proliferation and tumorigenesis of epithelial cells of various types (114–117). For example, factors secreted by senescent fibroblasts, such as amphiregulin and GROα, stimulate the proliferation of premalignant prostate epithelial cells (93, 114). Similarly, high levels of IL-6 and IL-8, also produced by senescent fibroblasts, can promote invasion of weakly malignant keratinocytes (118). Importantly, coinjection of senescent fibroblasts with either premalignant or malignant mammary epithelial cells can lead to, or accelerate, tumor formation in mice (116). Furthermore, normal human prostate epithelial cells undergoing senescence can also enhance *in vivo* tumorigenicity of low- or non-tumorigenic prostate cancer cells, suggesting that factors released by senescent epithelial cells can also be protumorigenic (119). It is worth mentioning that the SASP-dependent ability of senescent cells to promote tumorigenesis has been mainly reported in cellular systems involving co-cultures of epithelial cells and fibroblasts. Therefore, it remains unknown if similar interactions can be observed in other cellular contexts. Finally, it is important to emphasize that not all components of a SASP are pro-tumorigenic. Some SASP components have anti-angiogenic effects or are even able to induce apoptosis or senescence in non-senescent neighboring cells (120, 121).

THE POTENTIAL ROLE OF THE SASP IN HEMOSTASIS

Based on the emerging physiological and pathological processes in which the SASP might be involved, it is conceivable that senescent cells may also affect hemostasis through mechanisms that include, but are not limited to, changes in the production and functional status of platelets. As mentioned elsewhere in this review, IL-6 is one of the most prominent pro-inflammatory cytokines present in the SASP (102). Interestingly, IL-6 has been postulated as a central mediator of age-associated inflammatory pathways (63), with serum concentrations of IL-6 increasing with age (122). Moreover, IL-6 upregulates the synthesis of hemostatic factors, such as fibrinogen, and may also directly activate platelets (63, 123). Thus, it is tempting to speculate that the high levels of IL-6 (and other pro-inflammatory factors, such as IL-1β and TNF-α) detected in aged individuals could reflect, at least in part, an increased rate of secretion of this cytokine

TABLE 1 | Senescence-associated secretory phenotype (SASP) factors with potential effect on platelets aggregation and the fibrinolytic system.

SASP component	Function
Interleukin-6	Upregulates the production of hepatic thrombopoetin, elevating the number of platelets number (24)
IL-11	Contributes to megakaryopoiesis and thus indirectly to thrombopoiesis (51, 128)
PAI-1	Main inhibitor of tissue plasminogen activator and urokinase (24), regulates the dissolution of fibrin and also inhibits the degradation of the extracellular matrix by reducing plasmin generation (129)
MMP-2	Released by tumor cells and activated platelets *in vitro* (130)
GM-CSF	Contributes to megakaryopoiesis and thus indirectly to thrombopoiesis (51)
Fibronectin	Involved in cell adhesion and migration processes, including embryogenesis, wound healing, blood coagulation, host defense, and metastasis (131)
THPO	Necessary for megakaryocyte proliferation and maturation, as well as for thrombopoiesis (132)
Granulocyte colony-stimulating factor (G-CSF)	Cancer cell releases high levels of G-CSF primed neutrophils to release NETs, activating platelets (133), and also contributes to megakaryopoiesis and thus indirectly to thrombopoiesis (51)
MMP1	Activates protease-activated receptor-1 (PAR-1) by cleaving the receptor and promotes platelet aggregation through PAR-1 (134)

by senescent cells—or by other cells responding to senescent cells—in the context of a senescence-induced chronic inflammation. An age-dependent increase of pro-inflammatory factors would, in turn, contribute to platelet activation and a higher proclivity to thrombus formation. Therefore, we postulate that cellular senescence (as a result of physiological aging or secondary to therapeutic stress) might play an important role in the regulation of platelet function. By regulating the activation of platelets, senescent cells could provide yet another mechanism contributing to the higher prevalence of chronic inflammation (and cancer) in aged individuals.

While direct interaction between senescent cells and platelets remains to be experimentally confirmed, components of the SASP have already been linked to the modulation of the process of fibrinolysis *via* the plasminogen activation pathway (93, 124). Thus, increased plasma levels of PAI-1 (plasminogen activator inhibitor-1) are associated with a variety of age-associated conditions, including thrombogenic endothelial dysfunction (93). Supporting the connection between cellular senescence and thrombogenesis, PAI-1 mRNA and protein levels are also constitutively upregulated in senescent endothelial cells (125). In addition, fibroblasts and endothelial cells isolated from elderly donors or from patients with Werner syndrome—a disease characterized by premature aging and atherosclerosis—also display elevated levels of PAI-1 (126). Taking together, these data support the existence of a close association between aging, cellular senescence, and the deterioration of the fibrinolytic system.

Finally, senescent cells also secrete insoluble proteins that are normally present in the ECM and accumulate as a consequence of chronic inflammatory processes. One prominent example is fibronectin, a component of the connective tissue that is also found on cell surfaces, plasma, and other body fluids. Importantly, it has been demonstrated that fibronectin stabilizes the hemostatic clot, controls the diameter of the fibrin fiber, and also enhances platelet adhesion (127).

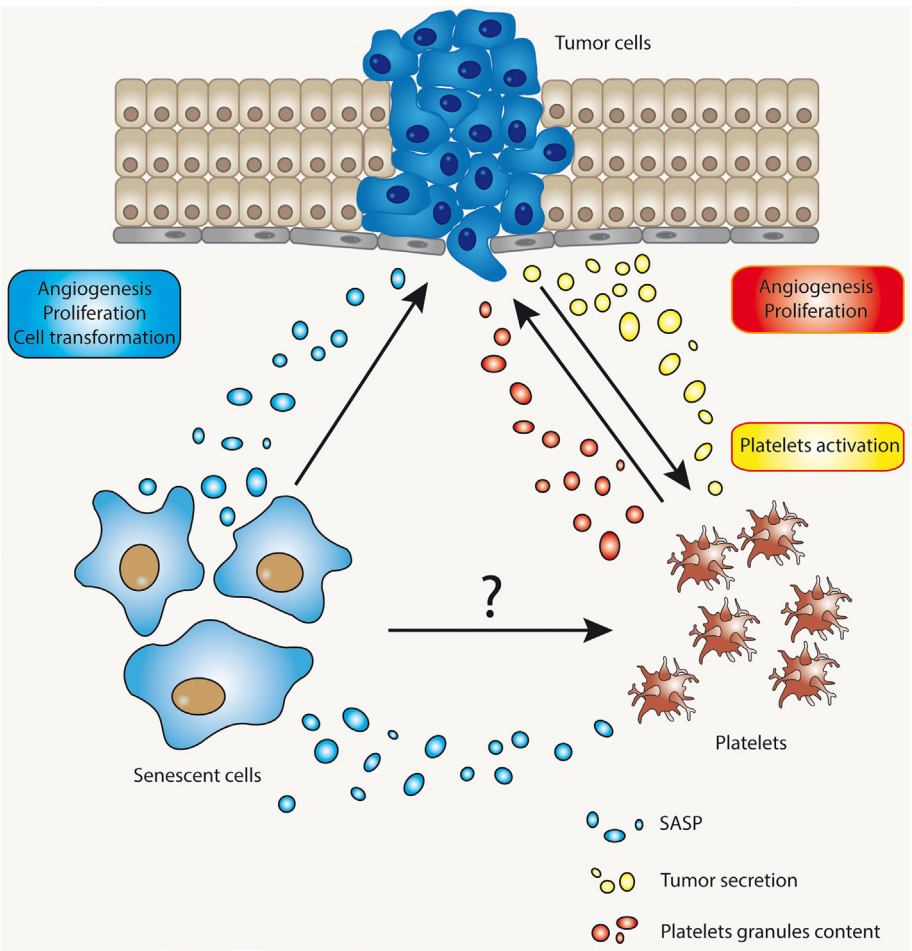

FIGURE 3 | The complex interaction between senescent cells, tumor cells, and platelets. The interaction between tumor cells and platelets is already well known. Tumor cells may affect platelet activation through several mechanisms and, reciprocally, activated platelets may release factors that impinge on proliferation and metastasis of tumor cells, or cells in the process of becoming tumorigenic. Senescent cells, on the other hand, might cause alterations in microenvironment through their ability to develop a secretory phenotype [senescence-associated secretory phenotype (SASP)]. SASP's components, for example, could alter the functional status of platelets or the process of fibrinolysis.

Taken together, the data support a model in which SASP components could modulate various aspects of hemostasis, including the functional status of platelets. Local activation of platelets, in turn, could contribute propitiate chronic inflammation, accelerate tumor progression, and enhance thrombus formation. A selection of senescence-associated secreted factors that could modify the function or production of platelets is listed in **Table 1**.

CONCLUDING REMARKS

The functional interaction between cancer cells and platelets has been well established. Most of the efforts aimed to clarify these interactions have been focused on the ability of tumor cells (or tumor-associated stromal cells) to produce and secrete pro-inflammatory factors that can result in the activation of platelets. Active platelets—acting synergistically with other components of the tumor stroma—can then promote or enhance tumor progression and metastasis. Paradoxically, many of the factors secreted by tumor cells or tumor-associated inflammatory cells with a known effect on platelet activity are also produced and secreted by cells undergoing senescence, a process originally regarded as tumor suppressive. Indeed, the evidence indicates that cellular senescence may also play an active role in driving, rather than suppressing, tumor formation, a non-cell autonomous role that seems to be largely dependent on the SASP. Accordingly, factors released by senescent cells may help create a pro-tumorigenic microenvironment that enhances proliferation and migration of neighbor cells (135). Although still controversial, this model would be in line with the observation that the prevalence of most cancers increases with age.

Alterations in hemostasis involving platelet dysfunction or alterations in the process fibrinolysis are at the core of thrombogenesis (136). As with cancer, thrombogenesis is most commonly observed in older individuals, who presumably harbor a higher proportion of senescent cells in their tissues. We, therefore, postulate that cellular senescence, either as a result of normal aging or secondary to stress, could play an important role in the regulation of platelet function. **Figure 3** depicts the potential relationship between senescent cells, platelets, and cells at risk of becoming tumorigenic. According to this model, senescent cells have the ability to modify the microenvironment in ways that may enhance tumorigenesis. Similarly, senescent cells might also regulate the activity of platelets, the process of fibrinolysis, or both. By regulating the activation of platelets, senescent cells may provide yet another mechanism to enhance tumorigenesis. Whether or not these circuits are relevant to tumorigenesis and/or thrombogenesis remains to be fully elucidated.

AUTHOR CONTRIBUTIONS

CV contributed to writing the manuscript, figures, and the final submission. RQ contributed to writing specific sections of the manuscript. RM-C and NB contributed to writing, editing, and discussing the manuscript. All authors read and approved the final manuscript.

FUNDING

This work was supported by the National Fund for Scientific & Technological Development (FONDECYT) Grant 1140389 (NBV), and the Regional Funds for Innovation and Competiveness (FIC-R) number 30388034 (NBV).

REFERENCES

1. Franco AT, Corken A, Ware J. Platelets at the interface of thrombosis, inflammation, and cancer. *Blood* (2015) 126(5):582–8. doi:10.1182/blood-2014-08-531582
2. Mohebali D, Kaplan D, Carlisle M, Supiano MA, Rondina MT. Alterations in platelet function during aging: clinical correlations with thromboinflammatory disease in older adults. *J Am Geriatr Soc* (2014) 62(3):529–35. doi:10.1111/jgs.12700
3. Franchini M. Hemostasis and aging. *Crit Rev Oncol Hematol* (2006) 60(2):144–51. doi:10.1016/j.critrevonc.2006.06.004
4. Varki A. Trousseau's syndrome: multiple definitions and multiple mechanisms. *Blood* (2007) 110(6):1723–9. doi:10.1182/blood-2006-10-053736
5. Kim YJ, Borsig L, Varki NM, Varki A. P-selectin deficiency attenuates tumor growth and metastasis. *Proc Natl Acad Sci U S A* (1998) 95(16):9325–30. doi:10.1073/pnas.95.16.9325
6. Bakewell SJ, Nestor P, Prasad S, Tomasson MH, Dowland N, Mehrotra M, et al. Platelet and osteoclast beta3 integrins are critical for bone metastasis. *Proc Natl Acad Sci U S A* (2003) 100(24):14205–10. doi:10.1073/pnas.2234372100
7. Mantovani A, Allavena P, Sica A, Balkwill F. Cancer-related inflammation. *Nature* (2008) 454(7203):436–44. doi:10.1038/nature07205
8. Crusz SM, Balkwill FR. Inflammation and cancer: advances and new agents. *Nat Rev Clin Oncol* (2015) 12(10):584–96. doi:10.1038/nrclinonc.2015.105
9. Jenne CN, Kubes P. Platelets in inflammation and infection. *Platelets* (2015) 26(4):286–92. doi:10.3109/09537104.2015.1010441
10. Thomas MR, Storey RF. The role of platelets in inflammation. *Thromb Haemost* (2015) 114(3):449–58. doi:10.1160/TH14-12-1067
11. Brinkmann V, Reichard U, Goosmann C, Fauler B, Uhlemann Y, Weiss DS, et al. Neutrophil extracellular traps kill bacteria. *Science* (2004) 303(5663):1532–5. doi:10.1126/science.1092385
12. Urban CF, Reichard U, Brinkmann V, Zychlinsky A. Neutrophil extracellular traps capture and kill *Candida albicans* yeast and hyphal forms. *Cell Microbiol* (2006) 8(4):668–76. doi:10.1111/j.1462-5822.2005.00659.x
13. Demers M, Krause DS, Schatzberg D, Martinod K, Voorhees JR, Fuchs TA, et al. Cancers predispose neutrophils to release extracellular DNA traps that contribute to cancer-associated thrombosis. *Proc Natl Acad Sci U S A* (2012) 109(32):13076–81. doi:10.1073/pnas.1200419109
14. Demers M, Wong SL, Martinod K, Gallant M, Cabral JE, Wang Y, et al. Priming of neutrophils toward NETosis promotes tumor growth. *Oncoimmunology* (2016) 5(5):e1134073. doi:10.1080/2162402X.2015.1134073
15. Cedervall J, Zhang YY, Olsson AK. Tumor-induced NETosis as a risk factor for metastasis and organ failure. *Cancer Res* (2016) 76(15):4311–5. doi:10.1158/0008-5472.CAN-15-3051
16. Cedervall J, Zhang Y, Huang H, Zhang L, Femel J, Dimberg A, et al. Neutrophil extracellular traps accumulate in peripheral blood vessels and compromise organ function in tumor-bearing animals. *Cancer Res* (2015) 75(13):2653–62. doi:10.1158/0008-5472.CAN-14-3299
17. Andersson U, Tracey KJ. HMGB1 is a therapeutic target for sterile inflammation and infection. *Annu Rev Immunol* (2011) 29:139–62. doi:10.1146/annurev-immunol-030409-101323
18. Yu LX, Yan L, Yang W, Wu FQ, Ling Y, Chen SZ, et al. Platelets promote tumour metastasis via interaction between TLR4 and tumour cell-released high-mobility group box1 protein. *Nat Commun* (2014) 5:5256. doi:10.1038/Ncomms6256

19. Tesfamariam B. Involvement of platelets in tumor cell metastasis. *Pharmacol Ther* (2016) 157:112–9. doi:10.1016/j.pharmthera.2015.11.005
20. Peterson JE, Zurakowski D, Italiano JE Jr, Michel LV, Connors S, Oenick M, et al. VEGF, PF4 and PDGF are elevated in platelets of colorectal cancer patients. *Angiogenesis* (2012) 15(2):265–73. doi:10.1007/s10456-012-9259-z
21. Italiano JE, Richardson JL, Patel-Hett S, Battinelli E, Zaslavsky A, Short S, et al. Angiogenesis is regulated by a novel mechanism: pro- and antiangiogenic proteins are organized into separate platelet alpha granules and differentially released. *Blood* (2008) 111(3):1227–33. doi:10.1182/blood-2007-09-113837
22. Amirkhosravi A, Mousa SA, Amaya M, Blaydes S, Desai H, Meyer T, et al. Inhibition of tumor cell-induced platelet aggregation and lung metastasis by the oral GpIIb/IIIa antagonist XV454. *Thromb Haemost* (2003) 90(3):549–54. doi:10.1160/TH03-02-0102
23. Lonsdorf AS, Kramer BF, Fahrleitner M, Schonberger T, Gnerlich S, Ring S, et al. Engagement of alphaIIbbeta3 (GPIIb/IIIa) with alphanubeta3 integrin mediates interaction of melanoma cells with platelets: a connection to hematogenous metastasis. *J Biol Chem* (2012) 287(3):2168–78. doi:10.1074/jbc.M111.269811
24. Stone RL, Nick AM, McNeish IA, Balkwill F, Han HD, Bottsford-Miller J, et al. Sood paraneoplastic thrombocytosis in ovarian cancer. *N Engl J Med* (2012) 366(7):610–8. doi:10.1056/NEJMoa1110352
25. Bottsford-Miller J, Choi H-J, Dalton HJ, Stone RL, Cho MS, Haemmerle M, et al. Differential platelet levels affect response to taxane-based therapy in ovarian cancer. *Clin Cancer Res* (2015) 21(3):602–10. doi:10.1158/1078-0432.ccr-14-0870
26. Lian L, Xia Y-Y, Zhou C, Shen X-M, Li X-L, Han S-G, et al. Mean platelet volume predicts chemotherapy response and prognosis in patients with unresectable gastric cancer. *Oncol Lett* (2015) 10(6):3419–24. doi:10.3892/ol.2015.3784
27. Sun K-Y, Xu J-B, Chen S-L, Yuan Y-J, Wu H, Peng J-J, et al. Novel immunological and nutritional-based prognostic index for gastric cancer. *World J Gastroenterol* (2015) 21(19):5961–71. doi:10.3748/wjg.v21.i19.5961
28. Radziwon-Balicka A, Medina C, O'Driscoll L, Treumann A, Bazou D, Inkielewicz-Stepniak I, et al. Platelets increase survival of adenocarcinoma cells challenged with anticancer drugs: mechanisms and implications for chemoresistance. *Br J Pharmacol* (2012) 167(4):787–804. doi:10.1111/j.1476-5381.2012.01991.x
29. Demers M, Ho-Tin-Noé B, Schatzberg D, Yang JJ, Wagner DD. Increased efficacy of breast cancer chemotherapy in thrombocytopenic mice. *Cancer Res* (2011) 71(5):1540–9. doi:10.1158/0008-5472.can-10-2038
30. Ho-Tin-Noe B, Goerge T, Cifuni SM, Duerschmied D, Wagner DD. Platelet granule secretion continuously prevents intratumor hemorrhage. *Cancer Res* (2008) 68(16):6851–8. doi:10.1158/0008-5472.CAN-08-0718
31. Ho-Tin-Noe B, Carbo C, Demers M, Cifuni SM, Goerge T, Wagner DD. Innate immune cells induce hemorrhage in tumors during thrombocytopenia. *Am J Pathol* (2009) 175(4):1699–708. doi:10.2353/ajpath.2009.090460
32. Goerge T, Ho-Tin-Noe B, Carbo C, Benarafa C, Remold-O'Donnell E, Zhao BQ, et al. Inflammation induces hemorrhage in thrombocytopenia. *Blood* (2008) 111(10):4958–64. doi:10.1182/blood-2007-11-123620
33. Kedzierska M, Czernek U, Szydlowska-Pazera K, Potemski P, Piekarski J, Jeziorski A, et al. The changes of blood platelet activation in breast cancer patients before surgery, after surgery, and in various phases of the chemotherapy. *Platelets* (2013) 24(6):462–8. doi:10.3109/09537104.2012.711866
34. Holmes CE, Levis JE, Schneider DJ, Bambace NM, Sharma D, Lal I, et al. Platelet phenotype changes associated with breast cancer and its treatment. *Platelets* (2016) 27(7):703–11. doi:10.3109/09537104.2016.1171302
35. Palumbo JS, Talmage KE, Massari JV, La Jeunesse CM, Flick MJ, Kombrinck KW, et al. Platelets and fibrin(ogen) increase metastatic potential by impeding natural killer cell-mediated elimination of tumor cells. *Blood* (2005) 105(1):178–85. doi:10.1182/blood-2004-06-2272
36. Nieswandt B, Hafner M, Echtenacher B, Männel DN. Lysis of tumor cells by natural killer cells in mice is impeded by platelets. *Cancer Res* (1999) 59(6):1295–300.
37. Borsig L, Wong R, Feramisco J, Nadeau DR, Varki NM, Varki A. Heparin and cancer revisited: mechanistic connections involving platelets, P-selectin, carcinoma mucins, and tumor metastasis. *Proc Natl Acad Sci U S A* (2001) 98(6):3352–7. doi:10.1073/pnas.061615598
38. Kopp HG, Placke T, Salih HR. Platelet-derived transforming growth factor-beta down-regulates NKG2D thereby inhibiting natural killer cell antitumor reactivity. *Cancer Res* (2009) 69(19):7775–83. doi:10.1158/0008-5472.CAN-09-2123
39. Labelle M, Begum S, Hynes RO. Platelets guide the formation of early metastatic niches. *Proc Natl Acad Sci U S A* (2014) 111(30):E3053–61. doi:10.1073/pnas.1411082111
40. Schumacher D, Strilic B, Sivaraj KK, Wettschureck N, Offermanns S. Platelet-derived nucleotides promote tumor-cell transendothelial migration and metastasis via P2Y2 receptor. *Cancer Cell* (2013) 24(1):130–7. doi:10.1016/j.ccr.2013.05.008
41. Di Vito C, Navone SE, Marfia G, Abdel Hadi L, Mancuso ME, Pecci A, et al. Platelets from glioblastoma patients promote angiogenesis of tumor endothelial cells and exhibit increased VEGF content and release. *Platelets* (2016) 29:1–10. doi:10.1080/09537104.2016.1247208
42. Labelle M, Begum S, Richard O. Hynes: direct signaling between platelets and cancer cells induces an epithelial-mesenchymal-like transition and promotes metastasis. *Cancer Cell* (2011) 20(5):576–90. doi:10.1016/j.ccr.2011.09.009
43. Baj-Krzyworzeka M, Majka M, Pratico D, Ratajczak J, Vilaire G, Kijowski J, et al. Platelet-derived microparticles stimulate proliferation, survival, adhesion, and chemotaxis of hematopoietic cells. *Exp Hematol* (2002) 30(5):450–9. doi:10.1016/S0301-472X(02)00791-9
44. Dashevsky O, Varon D, Brill A. Platelet-derived microparticles promote invasiveness of prostate cancer cells via upregulation of MMP-2 production. *Int J Cancer* (2009) 124(8):1773–7. doi:10.1002/ijc.24016
45. Ma L, Perini R, McKnight W, Dicay M, Klein A, Hollenberg MD, et al. Proteinase-activated receptors 1 and 4 counter-regulate endostatin and VEGF release from human platelets. *Proc Natl Acad Sci U S A* (2005) 102(1):216–20. doi:10.1073/pnas.0406682102
46. Hwang SG, Kim KM, Cheong JH, Kim HI, An JY, Hyung WJ, et al. Impact of pretreatment thrombocytosis on blood-borne metastasis and prognosis of gastric cancer. *Eur J Surg Oncol* (2012) 38(7):562–7. doi:10.1016/j.ejso.2012.04.009
47. Maráz A, Furák J, Varga Z, Kahán Z, Tiszlavicz L, Hideghéty K. Thrombocytosis has a negative prognostic value in lung cancer. *Anticancer Res* (2013) 33(4):1725–9.
48. Taucher S, Salat A, Gnant M, Kwasny W, Mlineritsch B, Menzel RC, et al. Study: impact of pretreatment thrombocytosis on survival in primary breast cancer. *Thromb Haemost* (2003) 89(6):1098–106. doi:10.1267/THRO03061098
49. Erdemir F, Kilciler M, Bedir S, Ozgok Y, Coban H, Erten K. Clinical significance of platelet count in patients with renal cell carcinoma. *Urol Int* (2007) 79(2):111–6. doi:10.1159/000106322
50. Brown KM, Domin C, Aranha GV, Yong S, Shoup M. Increased preoperative platelet count is associated with decreased survival after resection for adenocarcinoma of the pancreas. *Am J Surg* (2005) 189(3):278–82. doi:10.1016/j.amjsurg.2004.11.014
51. van Es N, Sturk A, Middeldorp S, Nieuwland R. Effects of cancer on platelets. *Semin Oncol* (2014) 41(3):311–8. doi:10.1053/j.seminoncol.2014.04.015
52. Medina C, Jurasz P, Santos-Martinez MJ, Jeong SS, Mitsky T, Chen R, et al. Platelet aggregation-induced by caco-2 cells: regulation by matrix metalloproteinase-2 and adenosine diphosphate. *J Pharmacol Exp Ther* (2006) 317(2):739–45. doi:10.1124/jpet.105.098384
53. Pearlstein E, Ambrogio C, Gasic G, Karpatkin S. Inhibition of the platelet-aggregating activity of two human adenocarcinomas of the colon and an anaplastic murine tumor with a specific thrombin inhibitor, dansylarginine N-(3-ethyl-1,5-pentanediyl)amide. *Cancer Res* (1981) 41(11 Pt 1):4535–9.
54. Schacht V, Dadras SS, Johnson LA, Jackson DG, Hong YK, Detmar M. Up-regulation of the lymphatic marker podoplanin, a mucin-type transmembrane glycoprotein, in human squamous cell carcinomas and germ cell tumors. *Am J Pathol* (2005) 166(3):913–21. doi:10.1016/S0002-9440(10)62311-5
55. Suzuki-Inoue K. Essential in vivo roles of the platelet activation receptor CLEC-2 in tumour metastasis, lymphangiogenesis and thrombus formation. *J Biochem* (2011) 150(2):127–32. doi:10.1093/jb/mvr079

56. Fujita N, Takagi S. The impact of Aggrus/podoplanin on platelet aggregation and tumour metastasis. *J Biochem* (2012) 152(5):407–13. doi:10.1093/jb/mvs108
57. Honn K, Cavanaugh P, Evens C, Taylor J, Sloane B. Tumor cell-platelet aggregation: induced by cathepsin B-like proteinase and inhibited by prostacyclin. *Science* (1982) 217(4559):540–2. doi:10.1126/science.7046053
58. Sabin RJ, Anderson RM. Cellular senescence – its role in cancer and the response to ionizing radiation. *Genome Integr* (2011) 2(1):1–9. doi:10.1186/2041-9414-2-7
59. Hager K, Setzer J, Vogl T, Voit J, Platt D. Blood coagulation factors in the elderly. *Arch Gerontol Geriatr* (1989) 9(3):277–82. doi:10.1016/0167-4943(89)90047-2
60. Sagripanti A, Carpi A. Natural anticoagulants, aging, and thromboembolism. *Exp Gerontol* (1998) 33(7–8):891–6. doi:10.1016/S0531-5565(98)00047-3
61. Kannel WB, Wolf PA, Castelli WP, D'Agostino RB. Fibrinogen and risk of cardiovascular disease: the framingham study. *JAMA* (1987) 258(9):1183–6. doi:10.1001/jama.1987.03400090067035
62. Wilhelmsen L, Svärdsudd K, Korsan-Bengtsen K, Larsson B, Welin L, Tibblin G. Fibrinogen as a risk factor for stroke and myocardial infarction. *N Engl J Med* (1984) 311(8):501–5. doi:10.1056/NEJM198408233110804
63. Ershler WB. Interleukin-6: a cytokine for gerontolgists. *J Am Geriatr Soc* (1993) 41(2):176–81. doi:10.1111/j.1532-5415.1993.tb02054.x
64. Gleerup G, Winther K. The effect of ageing on platelet function and fibrinolytic activity. *Angiology* (1995) 46(8):715–8. doi:10.1177/000331979504600810
65. Zahavi J, Jones NAG, Leyton J, Dubiel M, Kakkar VV. Enhanced in vivo platelet "release reaction" in old healthy individuals. *Thromb Res* (1980) 17(3):329–36. doi:10.1016/0049-3848(80)90067-5
66. Kasjanovová D, Baláž V. Age-related changes in human platelet function in vitro. *Mech Ageing Dev* (1986) 37(2):175–82. doi:10.1016/0047-6374(86)90074-6
67. Celermajer DS, Sorensen KE, Bull C, Robinson J, Deanfield JE. Endothelium-dependent dilation in the systemic arteries of asymptomatic subjects relates to coronary risk factors and their interaction. *J Am Coll Cardiol* (1994) 24(6):1468–74. doi:10.1016/0735-1097(94)90141-4
68. Taddei S, Virdis A, Ghiadoni L, Salvetti G, Bernini G, Magagna A, et al. Age-related reduction of NO availability and oxidative stress in humans. *Hypertension* (2001) 38(2):274–9. doi:10.1161/01.hyp.38.2.274
69. López-Otín C, Blasco MA, Partridge L, Serrano M, Kroemer G. The hallmarks of aging. *Cell* (2013) 153(6):1194–217. doi:10.1016/j.cell.2013.05.039
70. Krishnamurthy J, Ramsey MR, Ligon KL, Torrice C, Koh A, Bonner-Weir S, et al. p16INK4a induces an age-dependent decline in islet regenerative potential. *Nature* (2006) 443(7110):453–7. doi:10.1038/nature05092
71. Wang C, Jurk D, Maddick M, Nelson G, Martin-Ruiz C, Von Zglinicki T. DNA damage response and cellular senescence in tissues of aging mice. *Aging Cell* (2009) 8(3):311–23. doi:10.1111/j.1474-9726.2009.00481.x
72. Hayflick L. The limited in vitro lifetime of human diploid cell strains. *Exp Cell Res* (1965) 37:614–36. doi:10.1016/0014-4827(65)90211-9
73. Sherr CJ. Principles of tumor suppression. *Cell* (2004) 116(2):235–46. doi:10.1016/S0092-8674(03)01075-4
74. Krizhanovsky V, Yon M, Dickins RA, Hearn S, Simon J, Miething C, et al. Senescence of activated stellate cells limits liver fibrosis. *Cell* (2008) 134(4):657–67. doi:10.1016/j.cell.2008.06.049
75. Munoz-Espin D, Canamero M, Maraver A, Gomez-Lopez G, Contreras J, Murillo-Cuesta S, et al. Programmed cell senescence during mammalian embryonic development. *Cell* (2013) 155(5):1104–18. doi:10.1016/j.cell.2013.10.019
76. Rajagopalan S, Long EO. Cellular senescence induced by CD158d reprograms natural killer cells to promote vascular remodeling. *Proc Natl Acad Sci U S A* (2012) 109(50):20596–601. doi:10.1073/pnas.1208248109
77. Storer M, Mas A, Robert-Moreno A, Pecoraro M, Ortells MC, Di Giacomo V, et al. Keyes: senescence is a developmental mechanism that contributes to embryonic growth and patterning. *Cell* (2013) 155(5):1119–30. doi:10.1016/j.cell.2013.10.041
78. Campisi J, d'Adda di Fagagna F. Cellular senescence: when bad things happen to good cells. *Nat Rev Mol Cell Biol* (2007) 8(9):729–40. doi:10.1038/nrm2233
79. Zhao H, Halicka HD, Traganos F, Jorgensen E, Darzynkiewicz Z. New biomarkers probing depth of cell senescence assessed by laser scanning cytometry. *Cytometry A* (2010) 77(11):999–1007. doi:10.1002/cyto.a.20983
80. Gary RK, Kindell SM. Quantitative assay of senescence-associated beta-galactosidase activity in mammalian cell extracts. *Anal Biochem* (2005) 343(2):329–34. doi:10.1016/j.ab.2005.06.003
81. Aird KM, Zhang R. Detection of senescence-associated heterochromatin foci (SAHF). *Methods Mol Biol* (2013) 965:185–96. doi:10.1007/978-1-62703-239-1_12
82. Narita M, Nunez S, Heard E, Narita M, Lin AW, Hearn SA, et al. Rb-mediated heterochromatin formation and silencing of E2F target genes during cellular senescence. *Cell* (2003) 113(6):703–16. doi:10.1016/S0092-8674(03)00401-X
83. Beausejour CM, Krtolica A, Galimi F, Narita M, Lowe SW, Yaswen P, et al. Reversal of human cellular senescence: roles of the p53 and p16 pathways. *EMBO J* (2003) 22(16):4212–22. doi:10.1093/emboj/cdg417
84. Purvis JE, Karhohs KW, Mock C, Batchelor E, Loewer A, Lahav G. p53 dynamics control cell fate. *Science* (2012) 336(6087):1440–4. doi:10.1126/science.1218351
85. Adams PD. Healing and hurting: molecular mechanisms, functions, and pathologies of cellular senescence. *Mol Cell* (2009) 36(1):2–14. doi:10.1016/j.molcel.2009.09.021
86. Bazarov AV, Lee WJ, Bazarov I, Bosire M, Hines WC, Stankovich B, et al. The specific role of pRb in p16 (INK4A) – mediated arrest of normal and malignant human breast cells. *Cell Cycle* (2012) 11(5):1008–13. doi:10.4161/cc.11.5.19492
87. Sharpless NE, Sherr CJ. Forging a signature of in vivo senescence. *Nat Rev Cancer* (2015) 15(7):397–408. doi:10.1038/nrc3960
88. Jun JI, Lau LF. Cellular senescence controls fibrosis in wound healing. *Aging (Albany NY)* (2010) 2(9):627–31. doi:10.18632/aging.100201
89. Baker DJ, Perez-Terzic C, Jin F, Pitel KS, Niederlander NJ, Jeganathan K, et al. Opposing roles for p16Ink4a and p19Arf in senescence and ageing caused by BubR1 insufficiency. *Nat Cell Biol* (2008) 10(7):825–36. doi:10.1038/ncb1744
90. Collado M, Serrano M. Senescence in tumours: evidence from mice and humans. *Nat Rev Cancer* (2010) 10(1):51–7. doi:10.1038/nrc2772
91. Chien Y, Scuoppo C, Wang X, Fang X, Balgley B, Bolden JE, et al. Control of the senescence-associated secretory phenotype by NF-kappaB promotes senescence and enhances chemosensitivity. *Genes Dev* (2011) 25(20):2125–36. doi:10.1101/gad.17276711
92. Tchkonia T, Zhu Y, van Deursen J, Campisi J, Kirkland JL. Cellular senescence and the senescent secretory phenotype: therapeutic opportunities. *J Clin Invest* (2013) 123(3):966–72. doi:10.1172/JCI64098
93. Coppe JP, Desprez PY, Krtolica A, Campisi J. The senescence-associated secretory phenotype: the dark side of tumor suppression. *Annu Rev Pathol* (2010) 5:99–118. doi:10.1146/annurev-pathol-121808-102144
94. Parrinello S, Coppe JP, Krtolica A, Campisi J. Stromal-epithelial interactions in aging and cancer: senescent fibroblasts alter epithelial cell differentiation. *J Cell Sci* (2005) 118(Pt 3):485–96. doi:10.1242/jcs.01635
95. Rodier F, Campisi J. Four faces of cellular senescence. *J Cell Biol* (2011) 192(4):547–56. doi:10.1083/jcb.201009094
96. Salama R, Sadaie M, Hoare M, Narita M. Cellular senescence and its effector programs. *Genes Dev* (2014) 28(2):99–114. doi:10.1101/gad.235184.113
97. Franceschi C, Campisi J. Chronic inflammation (inflammaging) and its potential contribution to age-associated diseases. *J Gerontol A Biol Sci Med Sci* (2014) 69(Suppl 1):S4–9. doi:10.1093/gerona/glu057
98. Rodier F, Coppe J-P, Patil CK, Hoeijmakers WAM, Munoz DP, Raza SR, et al. Persistent DNA damage signalling triggers senescence-associated inflammatory cytokine secretion. *Nat Cell Biol* (2009) 11(8):973–9. doi:10.1038/ncb1909
99. Shelton DN, Chang E, Whittier PS, Choi D, Funk WD. Microarray analysis of replicative senescence. *Curr Biol* (1999) 9(17):939–45. doi:10.1016/S0960-9822(99)80420-5
100. Pribluda A, Elyada E, Wiener Z, Hamza H, Goldstein RE, Biton M, et al. A senescence-inflammatory switch from cancer-inhibitory to cancer-promoting mechanism. *Cancer Cell* (2013) 24(2):242–56. doi:10.1016/j.ccr.2013.06.005

101. Bernal GM, Wahlstrom JS, Crawley CD, Cahill KE, Pytel P, Liang H, et al. Loss of Nfkb1 leads to early onset aging. *Aging (Albany NY)* (2014) 6(11):931–42. doi:10.18632/aging.100702
102. Kuilman T, Michaloglou C, Vredeveld LC, Douma S, van Doorn R, Desmet CJ, et al. Oncogene-induced senescence relayed by an interleukin-dependent inflammatory network. *Cell* (2008) 133(6):1019–31. doi:10.1016/j.cell.2008.03.039
103. Orjalo AV, Bhaumik D, Gengler BK, Scott GK, Campisi J. Cell surface-bound IL-1α is an upstream regulator of the senescence-associated IL-6/IL-8 cytokine network. *Proc Natl Acad Sci U S A* (2009) 106(40):17031–6. doi:10.1073/pnas.0905299106
104. Lasry A, Ben-Neriah Y. Senescence-associated inflammatory responses: aging and cancer perspectives. *Trends Immunol* (2015) 36(4):217–28. doi:10.1016/j.it.2015.02.009
105. Acosta JC, Banito A, Wuestefeld T, Georgilis A, Janich P, Morton JP, et al. A complex secretory program orchestrated by the inflammasome controls paracrine senescence. *Nat Cell Biol* (2013) 15(8):978–90. doi:10.1038/ncb2784
106. Lujambio A. To clear, or not to clear (senescent cells)? That is the question. *Bioessays* (2016) 38(Suppl 1):S56–64. doi:10.1002/bies.201670910
107. Xue W, Zender L, Miething C, Dickins RA, Hernando E, Krizhanovsky V, et al. Senescence and tumour clearance is triggered by p53 restoration in murine liver carcinomas. *Nature* (2007) 445(7128):656–60. doi:10.1038/nature05529
108. Watanabe S, Kawamoto S, Ohtani N, Hara E. Impact of senescence-associated secretory phenotype and its potential as a therapeutic target for senescence-associated diseases. *Cancer Sci* (2017) 108(4):563–9. doi:10.1111/cas.13184
109. Lujambio A, Akkari L, Simon J, Grace D, Tschaharganeh DF, Bolden JE, et al. Non-cell-autonomous tumor suppression by p53. *Cell* (2013) 153(2):449–60. doi:10.1016/j.cell.2013.03.020
110. Iannello A, Thompson TW, Ardolino M, Lowe SW, Raulet DH. p53-dependent chemokine production by senescent tumor cells supports NKG2D-dependent tumor elimination by natural killer cells. *J Exp Med* (2013) 210(10):2057–69. doi:10.1084/jem.20130783
111. Demaria M, O'Leary MN, Chang JH, Shao LJ, Liu S, Alimirah F, et al. Cellular senescence promotes adverse effects of chemotherapy and cancer relapse. *Cancer Discov* (2017) 7(2):165–76. doi:10.1158/2159-8290.CD-16-0241
112. Kang TW, Yevsa T, Woller N, Hoenicke L, Wuestefeld T, Dauch D, et al. Senescence surveillance of pre-malignant hepatocytes limits liver cancer development. *Nature* (2011) 479(7374):547–51. doi:10.1038/nature10599
113. Liu Y, Hawkins OE, Su YJ, Vilgelm AE, Sobolik T, Thu YM, et al. Targeting aurora kinases limits tumour growth through DNA damage-mediated senescence and blockade of NF-κB impairs this drug-induced senescence. *EMBO Mol Med* (2013) 5(1):149–66. doi:10.1002/emmm.201201378
114. Bavik C, Coleman I, Dean JP, Knudsen B, Plymate S, Nelson PS. The gene expression program of prostate fibroblast senescence modulates neoplastic epithelial cell proliferation through paracrine mechanisms. *Cancer Res* (2006) 66(2):794–802. doi:10.1158/0008-5472.CAN-05-1716
115. Dilley TK, Bowden GT, Chen QM. Novel mechanisms of sublethal oxidant toxicity: induction of premature senescence in human fibroblasts confers tumor promoter activity. *Exp Cell Res* (2003) 290(1):38–48. doi:10.1016/S0014-4827(03)00308-2
116. Krtolica A, Parrinello S, Lockett S, Desprez P-Y, Campisi J. Senescent fibroblasts promote epithelial cell growth and tumorigenesis: a link between cancer and aging. *Proc Natl Acad Sci U S A* (2001) 98(21):12072–7. doi:10.1073/pnas.211053698
117. Ohuchida K, Mizumoto K, Murakami M, Qian L-W, Sato N, Nagai E, et al. Radiation to stromal fibroblasts increases invasiveness of pancreatic cancer cells through tumor-stromal interactions. *Cancer Res* (2004) 64(9):3215–22. doi:10.1158/0008-5472.can-03-2464
118. Coppe J-P, Boysen M, Sun CH, Wong BJF, Kang MK, Park N-H, et al. A role for fibroblasts in mediating the effects of tobacco-induced epithelial cell growth and invasion. *Mol Cancer Res* (2008) 6(7):1085–98. doi:10.1158/1541-7786.mcr-08-0062
119. Bhatia B, Multani AS, Patrawala L, Chen X, Calhoun-Davis T, Zhou JJ, et al. Evidence that senescent human prostate epithelial cells enhance tumorigenicity: cell fusion as a potential mechanism and inhibition by p16INK4a and hTERT. *Int J Cancer* (2008) 122(7):1483–95. doi:10.1002/ijc.23222
120. Nickoloff BJ, Lingen MW, Chang BD, Shen M, Swift M, Curry J, et al. Tumor suppressor maspin is up-regulated during keratinocyte senescence, exerting a paracrine antiangiogenic activity. *Cancer Res* (2004) 64(9):2956–61. doi:10.1158/0008-5472.Can-03-2388
121. Wajapeyee N, Serra RW, Zhu X, Mahalingam M, Green MR. Oncogenic BRAF induces senescence and apoptosis through pathways mediated by the secreted protein IGFBP7. *Cell* (2008) 132(3):363–74. doi:10.1016/j.cell.2007.12.032
122. Ferrucci L, Corsi A, Lauretani F, Bandinelli S, Bartali B, Taub DD, et al. The origins of age-related proinflammatory state. *Blood* (2005) 105(6):2294–9. doi:10.1182/blood-2004-07-2599
123. Oleksowicz L, Mrowiec Z, Zuckerman D, Isaacs R, Dutcher J, Puszkin E. Platelet activation induced by interleukin-6: evidence for a mechanism involving arachidonic acid metabolism. *Thromb Haemost* (1994) 72(2):302–8.
124. Davalos AR, Coppe J-P, Campisi J, Desprez P-Y. Senescent cells as a source of inflammatory factors for tumor progression. *Cancer Metastasis Rev* (2010) 29(2):273–83. doi:10.1007/s10555-010-9220-9
125. Comi P, Chiaramonte R, Maier JA. Senescence-dependent regulation of type 1 plasminogen activator inhibitor in human vascular endothelial cells. *Exp Cell Res* (1995) 219(1):304–8. doi:10.1006/excr.1995.1232
126. Markiewicz M, Richard E, Marks N, Ludwicka-Bradley A. Impact of endothelial microparticles on coagulation, inflammation, and angiogenesis in age-related vascular diseases. *J Aging Res* (2013) 2013:734509. doi:10.1155/2013/734509
127. Wang Y, Reheman A, Spring CM, Kalantari J, Marshall AH, Wolberg AS, et al. Plasma fibronectin supports hemostasis and regulates thrombosis. *J Clin Invest* (2014) 124(10):4281–93. doi:10.1172/JCI74630
128. Dams-Kozlowska H, Kwiatkowska-Borowczyk E, Gryska K, Mackiewicz A. Designer cytokine hyper interleukin 11 (H11) is a megakaryopoietic factor. *Int J Med Sci* (2013) 10(9):1157–65. doi:10.7150/ijms.5638
129. Yamamoto K, Takeshita K, Saito H. Plasminogen activator inhibitor-1 in aging. *Semin Thromb Hemost* (2014) 40(6):652–9. doi:10.1055/s-0034-1384635
130. Jurasz P, Sawicki G, Duszyk M, Sawicka J, Miranda C, Mayers I, et al. Matrix metalloproteinase 2 in tumor cell-induced platelet aggregation: regulation by nitric oxide. *Cancer Res* (2001) 61(1):376–82.
131. Wang Y, Carrim N, Ni H. Fibronectin orchestrates thrombosis and hemostasis. *Oncotarget* (2015) 6(23):19350–1. doi:10.18632/oncotarget.5097
132. Ryu T, Nishimura S, Miura H, Yamada H, Morita H, Miyazaki H, et al. Thrombopoietin-producing hepatocellular carcinoma. *Intern Med* (2003) 42(8):730–4. doi:10.2169/internalmedicine.42.730
133. Fuchs TA, Brill A, Duerschmied D, Schatzberg D, Monestier M, Myers DD Jr, et al. Extracellular DNA traps promote thrombosis. *Proc Natl Acad Sci U S A* (2010) 107(36):15880–5. doi:10.1073/pnas.1005743107
134. Seizer P, May AE. Platelets and matrix metalloproteinases. *Thromb Haemost* (2013) 110(5):903–9. doi:10.1160/TH13-02-0113
135. Campisi J. Aging, cellular senescence, and cancer. *Annu Rev Physiol* (2013) 75:685–705. doi:10.1146/annurev-physiol-030212-183653
136. Badimon L, Padro T, Vilahur G. Atherosclerosis, platelets and thrombosis in acute ischaemic heart disease. *Eur Heart J Acute Cardiovasc Care* (2012) 1(1):60–74. doi:10.1177/2048872612441582

Conflict of Interest Statement: The authors declare that the research was conducted in the absence of any commercial or financial relationships that could be construed as a potential conflict of interest.

frontiers in Oncology

REVIEW
published: 23 November 2017
doi: 10.3389/fonc.2017.00278

The Dual Role of Cellular Senescence in Developing Tumors and Their Response to Cancer Therapy

Markus Schosserer[1,2], Johannes Grillari[1,2,3,4] and Michael Breitenbach[5]*

[1] Department of Biotechnology, University of Natural Resources and Life Sciences, Vienna, Austria, [2] Austrian Cluster for Tissue Regeneration, Vienna, Austria, [3] Christian Doppler Laboratory for Biotechnology of Skin Aging, Vienna, Austria, [4] Evercyte GmbH, Vienna, Austria, [5] Department of Cell Biology, Division of Genetics, University of Salzburg, Salzburg, Austria

Cellular senescence describes an irreversible growth arrest characterized by distinct morphology, gene expression pattern, and secretory phenotype. The final or intermediate stages of senescence can be reached by different genetic mechanisms and in answer to different external and internal stresses. It has been maintained in the literature but never proven by clearcut experiments that the induction of senescence serves the evolutionary purpose of protecting the individual from development and growth of cancers. This hypothesis was recently scrutinized by new experiments and found to be partly true, but part of the gene activities now known to happen in senescence are also needed for cancer growth, leading to the view that senescence is a double-edged sword in cancer development. In current cancer therapy, cellular senescence is, on the one hand, intended to occur in tumor cells, as thereby the therapeutic outcome is improved, but might, on the other hand, also be induced unintentionally in non-tumor cells, causing inflammation, secondary tumors, and cancer relapse. Importantly, organismic aging leads to accumulation of senescent cells in tissues and organs of aged individuals. Senescent cells can occur transiently, e.g., during embryogenesis or during wound healing, with beneficial effects on tissue homeostasis and regeneration or accumulate chronically in tissues, which detrimentally affects the microenvironment by de- or transdifferentiation of senescent cells and their neighboring stromal cells, loss of tissue specific functionality, and induction of the senescence-associated secretory phenotype, an increased secretory profile consisting of pro-inflammatory and tissue remodeling factors. These factors shape their surroundings toward a pro-carcinogenic microenvironment, which fuels the development of aging-associated cancers together with the accumulation of mutations over time. We are presenting an overview of well-documented stress situations and signals, which induce senescence. Among them, oncogene-induced senescence and stress-induced premature senescence are prominent. New findings about the role of senescence in tumor biology are critically reviewed with respect to new suggestions for cancer therapy leveraging genetic and pharmacological methods to prevent senescence or to selectively kill senescent cells in tumors.

Keywords: aging, cancer, cellular senescence, cancer-associated fibroblasts, senescence-associated secretory phenotype, stress-induced premature senescence, senolytic compounds, modulation of protein synthesis

OPEN ACCESS

Edited by:
Tao Liu,
University of New South Wales, Australia

Reviewed by:
Luisa Lanfrancone, Istituto Europeo di Oncologia, Italy
James C. Neil, University of Glasgow, United Kingdom

****Correspondence:***
Markus Schosserer
markus.schosserer@boku.ac.at

Specialty section:
This article was submitted to Molecular and Cellular Oncology, a section of the journal Frontiers in Oncology

Received: *29 September 2017*
Accepted: *06 November 2017*
Published: *23 November 2017*

Citation:
Schosserer M, Grillari J and Breitenbach M (2017) The Dual Role of Cellular Senescence in Developing Tumors and Their Response to Cancer Therapy. Front. Oncol. 7:278. doi: 10.3389/fonc.2017.00278

INTRODUCTION

In current cancer research, the tumor microenvironment is coming more and more into the focus as it is able to either promote or inhibit carcinogenesis and metastasis by providing cancer cells with growth factors and supply of oxygen and nutrients. The stroma of tumors is enriched for chemokines, which attract and activate various other cell types, including cancer-associated fibroblasts (CAF). These cells closely interact with cancer cells, secrete cytokines, remodel the extracellular matrix and thereby promote malignancy (1). Importantly, age is one of the main risk factors for many types of cancer and is accompanied by an accumulation of senescent cells in various tissues of the body. As senescent cells actively shape their tissue microenvironment in a similar fashion as CAF toward a pro-tumorigenic state (2), cellular senescence (together with the well-known mutation accumulation over a lifetime) is probably one of the main contributors to age-associated cancer development.

Cellular senescence, a state of irreversible growth arrest, was discovered by Leonard Hayflick more than 50 years ago (3). A whole new field of investigation was opened up by this seminal discovery that was over the last 50 years closely intertwined with research in organismic aging, which was of obvious primary interest, but also with several other closely related fields, like oxidative stress research, origin of reactive oxygen species (ROS), role of mitochondria in aging, role of telomeres and telomerase in aging, and the genetics of stress response and stress defense. From early on in this field, the hypothesis was entertained that (i) the phenomenon observed in mammalian cell culture indeed occurs *in vivo* and drives normal organismic aging and (ii) induction of senescence was positively selected for in evolution for several reasons, among them to protect cells and organisms from cancer. Both of these ideas were highly speculative, but over the last 20 years were shown to be correct in part (2, 4–8). On the other hand, reports that establish a beneficial and important role of cellular senescence in embryogenesis (9, 10) and wound healing (11) imply that senescence might have evolved for other reasons as well.

The basic arguments about the role of senescence in cancer protection are as follows: senescent cells have lost the ability to undergo cell division permanently, although they may be metabolically fully active. This would certainly protect individuals carrying a primary cancer from further cancerous growth. However, this has to be seen in a different way nowadays as compared to the time when this "anticancer hypothesis" was first published (8), as knowledge of the genetics of cancer and senescence increased rapidly over the last few years. By this, we mean on the one hand the sequence of mutational events that takes place in growing tumors (12, 13), and on the other hand the knowledge of biochemical senescence markers in senescent cells *in vivo* (6, 14–17). Most importantly, senescent cells may be prone to genetic and epigenetic instability (18, 19), which is also a hallmark of cancer cells (12). In addition, the senescence-associated secretory phenotype (SASP) directly causes transformation of neighboring cells and destruction of the extracellular matrix, other hallmarks of cancer growth, which help to spread malignant cells in the body (2, 20, 21). Thus, cellular senescence can be viewed as a typical example for antagonistic pleiotropy: at young age, senescence might protect cells from transformation into primary tumors; however, at old age senescent cells generate a pro-tumorigenic microenvironment.

In this review, we will summarize mechanisms of senescence induction, especially in the context of aging-associated cancers and tumor therapy. While cellular senescence was originally believed to be caused by telomere shortening alone, increasing evidence suggested additional inducers of senescence. These inducers of senescence include the activation of DNA damage response pathways by cytotoxic compounds or ROS as well as activation of oncogenes. The contribution of senescent cells to a pro-oncogenic microenvironment will be discussed and compared to other cancer-associated cells, such as CAF. Finally, we will introduce current and future therapy options targeting cancer-, non-senescent-, and senescent cells and discuss their potential influence on cell fate decisions within the tumor stroma.

MECHANISMS OF CELLULAR SENESCENCE INDUCTION AND THEIR CONNECTION WITH CANCER BIOLOGY

Biomarkers of Cellular Senescence

For a long time, since the discovery of replicative senescence in cell culture (3) until relatively recently [summarized in Ref. (22)], it was not clear if replicative senescence is (i) an artifact of cell culture, caused perhaps by unphysiological oxygen partial pressure; or (ii) if replicative senescence does occur *in vivo*, and, if yes, if it is causative for organismic aging (as opposed to cellular aging), and (iii) if it is related to the development of human (or mouse) cancers.

To clarify these questions, it was necessary to identify reliable and sufficiently specific biochemical markers of cellular senescence in order to find a tool for monitoring and influencing senescence. One of the earliest markers found that was also believed to be the major cause for aging is telomere shortening (23). Other useful biochemical markers were identified in the form of loss of lamin B1, which is implicated in structural changes of the nucleus with senescence (24), as well as senescence-associated beta-galactosidase (SA β-GAL) (6). The present view is that the increase in SA-β-GAL is an indication of the proliferation of the lytic compartment in senescent cells due to increase of GLB1 (25). Therefore, this marker is not entirely specific for the process. Recently, staining of cells and tissues by Sudan Black B was introduced as novel marker for cellular senescence that is also applicable to paraffin sections. Sudan Black B stains lipofuscin, which are aggregates of oxidized proteins, lipids, and metals (15, 17). Interestingly, this staining method appears to be specific for cellular senescence, although lipofuscin would also be expected to accumulate in non-senescent cells during chronological aging.

An upcoming, highly promising method for the label-free detection of senescent cells *in vitro* and *in situ* is vibrational (micro)spectroscopy. Indeed, first proof of principle for Raman- and near-infrared spectroscopy, followed by multivariate statistics has been achieved as it was able to distinguish different cell types and cellular states in a non-invasive manner. First results

on different human fibroblast strains, which were cultivated in 2D and 3D and subjected to serial passaging to induce replicative senescence, are very promising and allowed classification of cells at high confidence (26, 27). However, it needs to be determined if these methods are also applicable to other cell types, as well as to other inducers of cellular senescence. In the future, vibrational spectroscopy might allow to distinguish *in vivo* and in real time different cell types within the tumor stroma (28, 29), such as cancer cells, normal epithelial cells, and different subtypes of CAF, as well as determine how these cells respond to therapy by induction of either senescence or apoptosis (30).

Presently, expression of $p16^{INK4A}$, one of the protein inhibitors of the cell cycle regulator cyclin dependent kinase (CDK), is the most reliable senescence marker known (14). While the senescence response also requires the main tumor suppressor proteins p53 and retinoblastoma protein (Rb), $p16^{INK4A}$ seems to be expressed exclusively in senescent cells. Reporter constructs based on the promoter of $p16^{INK4A}$ have successfully been used to detect senescent cells *in vivo*, but more importantly, also to test the physiological relevance of senescent cells in organismic aging (31, 32). Interestingly, $p16^{INK4A}$ shares the same gene locus with two other important proteins involved in senescence and cancer.

The INK/ARF Locus—At the Crossroads between Cancer and Senescence

The potent tumor suppressor proteins $p16^{INK4A}$, $p15^{INK4B}$, and $p14^{ARF}$ are all transcribed from the same gene locus and are frequently targeted for deletion or epigenetic inhibition in numerous cancers. Although $p16^{INK4A}$ and $p14^{ARF}$ are both able to arrest the cell cycle and share exons 2 and 3, they comprise different amino acids and thus exert different biological functions due to alternative reading frames. Mouse models lacking either $p16^{INK4A}$, $p19^{ARF}$, which is the mouse homolog of human $p14^{ARF}$, or both, always show increased incidence of various tumors, while human cancers frequently display either deletion of the whole gene locus, affecting both alternative reading frames, or specific silencing of either the $p16^{INK4A}$ or $p14^{ARF}$ promoter by methylation (33).

$p16^{INK4A}$ and $p15^{INK4B}$ bind to CDK4 and CDK6 and thereby promote allosteric changes, which inhibit CDK4/6-mediated phosphorylation of Rb. Thus, expression of $p16^{INK4A}$ and $p15^{INK4B}$ maintains Rb in a hypophosporylated state, which induces G1 cell cycle arrest (34). $p14^{ARF}$ on the other hand stabilizes p53, the other main cellular tumor suppressor besides Rb, by trapping MDM2 in the nucleolus. This leads to increased p21 transcription and consequently to cell cycle arrest. However, $p14^{ARF}$ can also act in a p53-independent manner by interaction with numerous other target proteins (33, 34).

Although different inducers of cellular senescence seem to converge on $p16^{INK4A}$ in most cell types, and $p14^{ARF}$ might or might not be co-regulated depending on the tissue context, the precise individual contributions of these pathways to the senescent state are not resolved yet.

Replicative Senescence

The induction of cellular senescence was for a long time attributed to telomere shortening alone, for instance by serial passaging of cell cultures (23). Multiple cell divisions cause the telomeres to shorten to a critical length, which activates a persistent DNA damage response, leading to an upregulation of growth-inhibitory genes, such as $p16^{INK4A}$ and p53, and repression of genes promoting the progression of the cell cycle (35). Before also other inducers of cellular senescence were discovered, the contribution of replicative senescence to aging *in vivo* was heavily debated.

One of the main reasons for this was the lack of suitable model systems, as 2D cell cultures alone hardly reflect the physiological state of an organism and mice have exceptionally long telomeres that complicate the interpretation of replicative senescence contribution. For instance, mice lacking TERC, the RNA component of telomerase, show progressive telomere shortening with age, although this does not manifest in any phenotype in the F1 and F2 generation. Clearly, this suggests that in wild-type mice (with long telomers) telomere shortening does not contribute to organismic aging. Only in the F3 generation, when the telomeres shortened to a critical length, a partial progeroid phenotype appears, which encompasses increased incidence of neoplasia. This phenotype is further pronounced in the F6 generation, when mice are in addition already short lived and sterile (36). Although these mouse studies indicate a contribution of telomere shortening to organismal aging and appearance of aging-associated neoplasia, in humans only few studies could correlate telomere length with longevity and improved health at old age (37–39). In numerous other studies, telomere length of various cell types including blood leukocytes was not found to be a reliable predictor of biological age and mortality (38).

Similarly, although the accumulation of short telomeres with age is expected to be associated with genomic instability and thus also with increased cancer incidence (39), this is not always the case in humans. On the contrary, some individuals with constitutively long telomeres in somatic cells show an increased propensity of major cancers at increasing age, while many cancer cells have short telomeres. Aviv and coauthors recently proposed a Two-Hit-Hypothesis that resolves this "Telomere Length Paradox" as follows: the first hit of mutations leading to cancer happens at stem cell level is, therefore, telomere length independent and leads to the expansion of fast-growing clones. Then, additional hits that are telomere length dependent and might occur much later in life induce the transformation of these expanding, but still benign clones into cancer. Thus, cells from individuals with constitutively long telomeres have a much longer expansion phase before entering cellular senescence and thereby suffer from an increased hazard of acquiring a second hit required for malignant transformation (40). Although this model is indeed able to explain many aspects of the correlation of telomere length with cancer incidence, experimental evidence is still lacking and probably hard to obtain due to difficulties with standardized absolute measurements of telomere length across different labs.

Stress-Induced Premature Senescence (SIPS) and Therapy-Induced Senescence (TIS)

Besides the shortening of telomeres, senescence can also be induced by exposure of cells to acute or chronic sublethal doses of exogenous or endogenous stressors (**Figure 1**), causing a

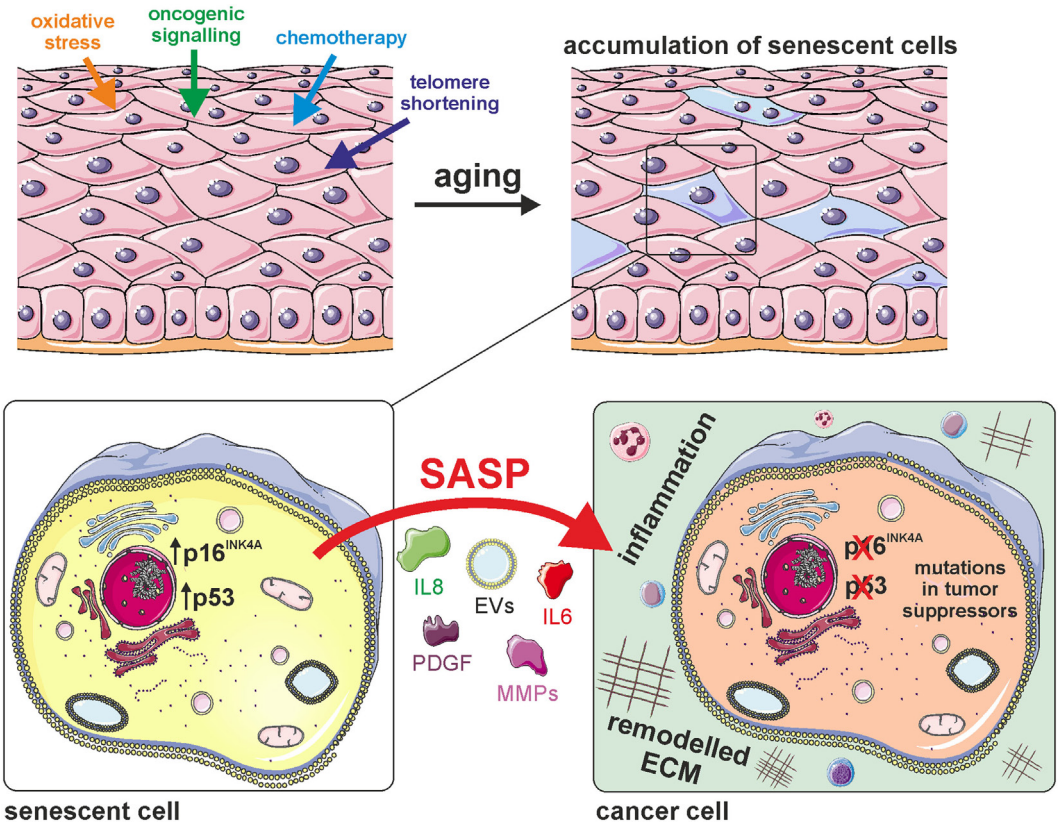

FIGURE 1 | Cellular senescence generates a pro-tumorigenic microenvironment. Cellular senescence is induced by various stimuli that lead to the accumulation of senescent cells in aged tissues. The senescent state is characterized by activation of the potent tumor suppressors $p16^{INK4A}$ and/or p53, as well as by secretion of various cytokines (e.g., IL-6, IL-8), growth factors [e.g., platelet-derived growth factor (PDGF)], matrix-metalloproteinases (MMPs), and extracellular vesicles (EVs). This senescence-associated secretory phenotype (SASP) generates a pro-tumorigenic microenvironment by inducing extracellular matrix remodeling and inflammation.

state of "stress-induced premature senescence" (41), "stress or aberrant signaling-induced senescence," (35) or "accelerated cellular senescence" (42). Irrespective of the inducer, SIPS-cells are irreversibly growth arrested and express typical senescence markers, including SA β-GAL, $p16^{INK4A}$, and telomere-associated persistent DNA damage foci (43). SIPS is likely the most important inducer of cellular senescence *in vivo*, since many cell types never exhaust their maximum replicative potential during organismal life span and thus do not enter replicative senescence, but are nevertheless exposed to various exogenous and endogenous stressors throughout life, which include ROS produced by the cell itself, cytotoxic compounds from the environment, radiation, or others.

Of high importance in the context of this review is the fact that many cytotoxic compounds as well as high dose radiation, which are currently used in cancer therapy to induce cell death, are also able to initiate senescence. Induction of senescence in cancer cells is often intended, as lower doses than for the induction of cell death are required and immediate severe side effects of therapy are minimized (44). These side effects include immunosuppression, fatigue, anemia, nausea, diarrhea, and alopecia (45). Furthermore, even cancer cells deficient in apoptosis pathways or lacking p53 and Rb retain their ability to undergo cellular senescence, rendering them sensitive to chemotherapy (46). This specific and important form of SIPS is referred to as "therapy-induced senescence." Typical cytotoxic drugs in clinical use that induce DNA damage and thereby cellular senescence encompass Bleomycin, Camptothecin, Cisplatin, Doxorubicin, and Etoposide among others, with Doxorubicin and Cisplatin being most effective in initiating the senescence response. Biopsies from breast and lung tumors confirm that senescent cancer cells are indeed present *in vivo* in response to chemotherapy (42, 44, 47).

While induction of cellular senescence in tumor cells is beneficial for the therapeutic outcome, treatment-induced bystander senescence in other cells of the tumor stroma or even in distant tissues is not intended, as senescent cells might promote tumor relapse, secondary tumors, and tissue degeneration (35, 45). Demaria and coworkers could clearly establish that Doxorubicin and Paclitaxel induce senescence in normal mouse and human fibroblasts *in vitro*. Furthermore, systemic administration of either doxorubicin, paclitaxel, cisplatin, or temozolomide in mice induced cellular senescence *in vivo* in different cell types of skin, lung, and liver (45).

Oncogene-Induced Senescence (OIS)

Oncogene activation and chemotherapy also induce premature senescence that is similar to replicative senescence regarding cell morphology and the expression profile of molecular markers (**Figure 1**). OIS was discovered by Serrano and coworkers more than 20 years ago (48, 49). It came as a surprise, because the paper essentially showed that the same dominant point mutation, which was found in many human tumors (H-rasV12) and was shown to be causative for cancer growth in combination with other mutations (for instance in the gene myc), was in isolation causing cell cycle arrest and cellular senescence, a nearly opposite phenotype compared to cancer growth. 20 years after this seminal discovery, we today see a bit more clearly the biological role of senescence in cancer biology. The above-mentioned point mutation in H-rasV12 or the corresponding mutation in yeast (RAS2-ala18, val19) cause a massive increase in ROS, which are inferred to transmit a signal causing senescence in the human case, and loss of growth regulation and subsequently apoptotic cell death in yeast (50, 51).

Oncogene-induced senescence does occur not only in cell culture, but also in tumors *in vivo* (52). Senescent cells in tumors are detected mostly in early pre-invasive stages of the tumor, but in later invasive stages are no longer detectable (53). OIS leads to SIPS *in vivo* and can induce tumorous growth in surrounding stroma cells. However, the molecular markers of OIS and the composition of the SASP depend on the experimental conditions and *in vivo* on the exact type of cancer. In one example (54), this included expression of the stem cell marker $CD34^+$ in skin cancers derived from keratinocytes in the mouse model.

Taken together, the results available to date indicate that senescent cells produced by OIS in tumors can be both growth inhibiting and, in the long term, cancer causing. Many open questions remain, for instance: is the senescent state in tumor cells reversible *in vivo*? What are the phenotypic differences between OIS in tumors and senescence in development and regeneration? What is the mechanistic cause leading cells to choose senescence rather than apoptosis in OIS? What are the reasons and consequences of the strong pro-inflammatory phenotype of senescent cells in tumors?

SENESCENT CELLS GENERATE A PRO-TUMORIGENIC MICROENVIRONMENT

The Composition of the SASP

We have to acknowledge the fact that cellular senescence in certain cancers *in vivo* and in cancer-derived cell cultures *in vitro* can on the one hand exert an anticancer activity, because senescence is a permanent cell cycle arrest, and on the other hand, the secretion of various cytokines and chemokines by senescent cells induces de-differentiation and consequently increased cell division and even metastasis in neighboring cells (21, 22, 55, 56). This phenomenon is dubbed SASP and is studied in a large number of experimental systems, including not only senescent cells in old individuals and in tumors but also in wound healing and in embryogenesis (9–11). In the large majority of cases studied, the SASP does occur and the secreted soluble factors comprise interleukins, inflammatory cytokines, and growth factors. Interleukin-1 (IL-1) and interleukin-6 (IL-6) are expressed by senescent epithelial cells, fibroblasts, and other cell types and can induce either cellular senescence or tumor formation in neighboring cells. Chemokines secreted by senescent cells encompass interleukin-8 (IL-8), MCP-1, -2, -3, and -4, HCC-4, eotaxin-3, and MIP-1α and -3α (21). Interestingly, OIS cells secrete a range of CXCR-2-binding chemokines, which reinforce the senescent arrest in an autocrine manner (57). The SASP is also enriched for almost all IGF-binding proteins and their regulatory factors, which can induce senescence and apoptosis in neighboring cells (21, 58), as well as platelet-derived growth factors (PDGF) and vascular endothelial growth factors promoting wound healing. PDGF-A was shown to be enriched in the secretome of senescent mouse embryonic fibroblasts and to promote myofibroblast differentiation. As a consequence, clearance of senescent cells in the p16-3MR mouse model retarded the closure of wounds (11). In this mouse model, the $p16^{INK4A}$ promoter, which is specific for senescent cells, drives both expression of *Renilla* luciferase and herpes simplex thymidine kinase (TK). By addition of gancyclovir, a suicide substrate of TK, only those cells are killed which activate the $p16^{INK4A}$ promoter (11, 32).

In addition to soluble signaling factors, the SASP comprises proteases of the matrix metalloproteinase and serine protease family, which facilitate tissue repair by degradation of collagen and regulate the activity of other SASP factors (21, 59). Furthermore, the large insoluble glycoprotein fibronectin is preferentially transcribed and secreted by senescent cells. Fibronectin interacts with various other macromolecules, such as components of the cytoskeleton, cell surface receptors, and extracellular matrix components and thereby modulates processes such as cell adhesion and proliferation (60, 61).

Although not as well characterized as soluble proteins, also other macromolecules such as lipids and carbohydrates, as well as nucleic acids and proteins enclosed in extracellular vesicles (EVs), are SASP members. Senescent cells secrete increased amounts of small extracellular vesicles (sEVs) that promote proliferation of cancer cells and exert other effects on bystander cells (62, 63). The mode of action is partially attributed to EphA2, which is phosphorylated upon cellular senescence and specifically packaged into sEVs. Together with Ephrin-1, which is expressed by cancer cells, reverse signaling *via* Erk is initiated and proliferation of cancer cells is stimulated (62). EVs also contain miRNAs that are able to exert paracrine effects on gene expression of other cells. Since miRNA expression patterns differ significantly between senescent and non-senescent cells (64), miRNAs will probably soon be recognized as novel and important SASP members.

Importantly, the composition of the SASP significantly varies from cell type to cell type and thereby might differently influence bystander cells (44, 59).

Actions of the SASP on Surrounding Cells and the Extracellular Matrix

Effects of the SASP on surrounding cells strictly depend on the tissue context. In most cases the SASP was reported to stimulate tumor growth (**Figure 1**), but on the other hand immune cells are attracted which participate in the clearance of cancer cells (65). Another example for context specific roles of senescent cells is

liver cancer: oncogene-induced senescent hepatocytes secrete CCL2, which attracts $CCR2^+$ myeloid cells that further differentiate into macrophages and clear pre-malignant cells. If, however, hepatocellular carcinoma is already established, cancer cells block the maturation of the attracted $CCR2^+$ myeloid cells into macrophages and thereby also inhibit NK cells. In this scenario, the presence of senescent cells promotes tumor outgrowth and thus worsens the prognosis for patients (66).

Despite its role in inducing bystander senescence, the SASP has also an important function in tissue plasticity and stemness. Ritschka and coworkers demonstrated that the SASP promotes the expression of stem cell markers *in vitro* and *in vivo* and transient exposure to the SASP induces stem cell functions. Chronic exposure, however, had an opposite effect, probably due to paracrine senescence induction in stem- and progenitor cells (54). The close relationship between senescence and tissue regeneration is further emphasized by a mouse model of ectopic expression of the transcription factors OCT4, SOX2, KLF4, and cMYC (OSKM), which are required for the induction of pluripotency. In these mice, tissues harboring a high proportion of senescent cells also displayed a high *in vivo* reprogramming efficiency and *vice versa*. Mosteiro and coworkers identified IL-6 as critical SASP factor for reprogramming, as well as tissue damage as a possible inducer (67).

The importance of typical SASP factors for tissue regeneration and wound healing might explain their evolutionary conservation and, in addition, SASP factors promote epithelial to mesenchymal transition, a hallmark during the development of carcinomas and angiogenesis (21). Therefore, we propose that not only senescence itself is antagonistically pleiotropic but also the corresponding SASP, as it might be beneficial in young individuals for wound healing and tissue regeneration, while tumor promoting in the elderly.

The Extracellular Matrix Is an Important Contributor to a Pro-Carcinogenic Microenvironment

Remodeling of the extracellular matrix by metalloproteinases of the SASP might create a beneficial microenvironment for tumor growth, as migration is facilitated and contact inhibition is blunted (**Figure 1**).

An interesting model organism to study the development of pro- and antitumorigenic microenvironments by modulation of the extracellular matrix is the naked mole rat. These animals are exceptionally long lived and suppress the development of cancer by expression of high molecular mass hyaluronic acid that renders the extracellular matrix highly viscous and thereby cells become extremely sensitive to contact inhibition (68). Interestingly, this phenomenon is associated with elevated expression of $p16^{INK4A}$ (69), and naked mole rat fibroblasts are more tolerant to cellular stress than mouse fibroblasts, because they halt cell proliferation at much lower doses of stressors (70). Thus, a denser extracellular matrix might promote increased expression of $p16^{INK4A}$, which allows cells to sense lower doses of toxic compounds and consequently enter a state of cell cycle arrest.

In order to further interrogate the complex relationship between cellular senescence, cancer formation, and the extracellular matrix, it would be very interesting to determine if this cell cycle arrest is irreversible and thereby resembles cellular senescence, as well as to test for presence of senescent cells in naked mole rats *in vivo*.

Senescent Cells and CAF: United by a Similar Secretory Phenotype?

Cancer-associated fibroblasts are a heterogeneous population of fibroblasts within the tumor stroma that is only poorly characterized so far. Most of these cells originate from normal local fibroblasts, which are stimulated by members of the PDGF or TGF-β family, but also normal endothelial or epithelial cells that underwent epidermal to mesenchymal transition, as well as bone-marrow derived mesenchymal stem cells contribute to the CAF population. Tumor cells release paracrine factors that attract CAF, support their survival within the tumor microenvironment, and stimulate their secretory phenotype. In contrast to normal fibroblasts, CAF express more factors associated with degradation of the ECM and increased angiogenesis, but also chemokines promoting tumor cell proliferation, migration, and invasion (1).

Two prominent sub-populations within CAF, namely senescent fibroblasts and myofibroblasts, both express α-smooth muscle actin and promote tumor cell mobility and thereby malignancy by secretion of soluble factors. Gene expression profiles between the two CAF subtypes differ, with myofibroblasts and non-senescent cells stimulating collagenous ECM deposition and thereby causing poor prognosis (71).

The tumor-promoting effects of CAF are mainly attributed to CXCL12, which is expressed and secreted by CAF (72), but is also an important SASP component (73). CXCL12 induces tumor proliferation, angiogenesis at the tumor site, and invasion, leading *in vivo* to increased tumor development and metastasis (1). Other tumor-promoting chemokines, which are secreted by CAF as well as by senescent cells, are SDF-1, GROα, GROβ, IL-8, MCP-1, and MCP-8 (1, 21, 74). miR-335 is upregulated in both CAF and normal senescent fibroblasts and is able to modulate secretion patterns of both cell types (75).

Taken together, these data clearly indicate similar secretory phenotypes and underlying regulatory networks of CAF and senescent cells, which generate a pro-tumorigenic microenvironment. Thus, senescent cells can serve as an important *in vitro* model for microenvironments favoring tumor growth. This is especially relevant for the evaluation of current cancer therapies, which mostly rely on cytotoxic compounds and/or radiation that drive cancer cells into either apoptosis or TIS. However, senescence is also induced in non-cancer cells, which further promotes the SASP and thereby exacerbates deleterious side effects (**Figure 2**).

UPCOMING INNOVATIVE THERAPEUTIC APPROACHES

Targeting Cancer and Senescence Simultaneously by Modulation of Protein Synthesis

Protein synthesis is highly upregulated in cancer in order to support fast tumor growth (12) and is conducted by ribosomes, which are complex nanomachines assembled in the nucleolus.

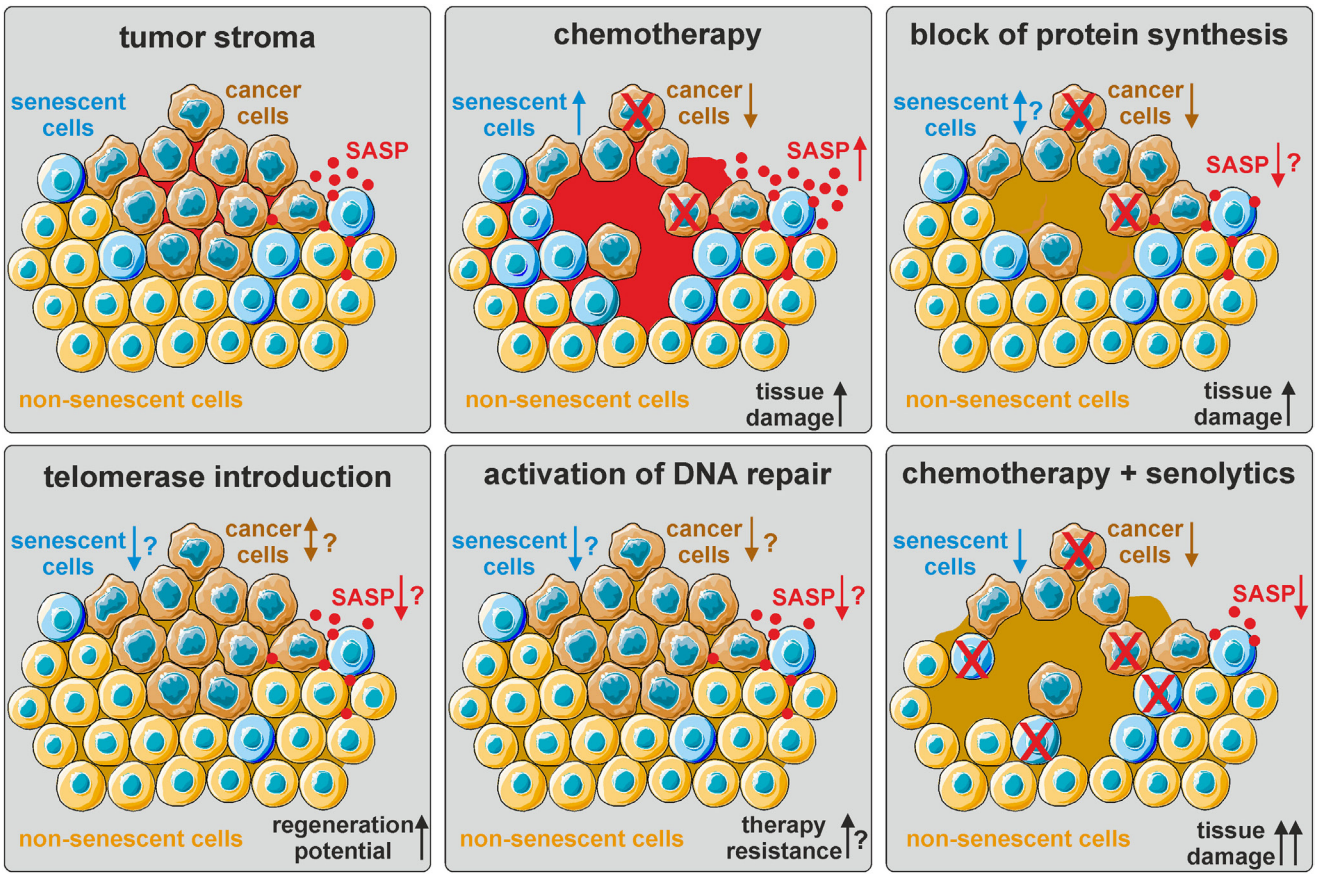

FIGURE 2 | The influence of current and hypothetical therapy options on the tumor stroma. The tumor stroma is comprised of tumor cells (brown), normal non-senescent cells (orange), and senescent cells (blue), as well as other cell types (not depicted here). The senescence-associated secretory phenotype (SASP) generates a pro-tumorigenic microenvironment (red). Chemotherapy eliminates cancer cells by inducing DNA damage, but also induces cellular senescence and thereby promotes secondary tumor formation and relapse *via* SASP upregulation. Block of protein synthesis also eliminates cancer cells, but might additionally mitigate the SASP. The effect on the number of senescent cells is not known. Telomerase (re-)introduction in normal cells might delay the onset of cellular senescence and promote tissue regeneration, but also facilitate cancer development. Activation of DNA repair pathways in non-senescent cells might prevent senescence and cancer formation, but also render cancer cells more resistant to chemo- and radiation therapy. Thus, a combinatorial approach of eliminating cancer cells by chemotherapy and senescent cells by senolytics might be most promising. However, increased tissue damage combined with decreased regenerative ability by SASP factors needs to be considered.

Ribosome biogenesis and consequently nucleolar size are directly correlated with cell cycle and protein synthesis. Thus, the morphology of nucleoli serves as an important surrogate marker for tumor pathologists to predict the clinical outcome of cancer (76). In contrast to cancer, bulk protein synthesis slows down during organismal aging (77). Although it is already established that senescent cells display decreased levels of protein degradation (78), the capacity of senescent cells to newly synthesize proteins was not studied so far. Surprisingly, primary fibroblasts from Hutchinson–Gilford Progeria patients and from old donors display elevated protein translation and nucleolar expansion compared to fibroblasts from healthy young donors (79), while long-lived *Caenorhabditis elegans* mutants have smaller nucleoli and less ribosomal RNA expression than their wild-type counterparts (80). Replicative senescent fibroblasts are characterized by a single enlarged nucleolus, while proliferating cells have an increased number of small nucleoli (81–83). However, although senescent cells undergo vast nuclear remodeling (18, 19), the relative positions of nucleolus-associated chromosomal domains only change marginally during senescence (84). Interestingly, the nuclear proteome is drastically remodeled in SIPS compared to untreated proliferating cells with an accumulation of ribosomal proteins and depletion of ribosome biogenesis factors. Taken together, these findings indicate a kinetic shift of ribosome assembly in senescent cells (85) and firmly establish that increased ribosome and protein syntheses, as well as nucleolar expansion, are hallmarks of both cancer and accelerated aging.

Thus, therapies targeting protein synthesis instead of inducing generalized DNA damage are supposed to be more selective for cancer cells, avoid the induction of senescence in non-cancer cells, and slow down organismal aging and aging-associated pathologies (**Figure 2**). Indeed, inhibition of ribosome biogenesis, for instance by RNA polymerase I inhibitors, selectively kills

cancer cells and is thereby considered to be a promising novel therapeutic option (86).

Another approach, which could simultaneously target tumor progression and organismal aging, is the inhibition of mTOR by Rapamycin or Rapamycin-analogs as inhibitors of protein synthesis. Rapamycin, even if administered late in life, extends organismal life span in mice (87) and blocks secretion of pro-tumorigenic components of the SASP, such as IL-6. This effect is achieved by specific translational repression of IL-6, as well as on transcription level *via* a feedback loop involving IL1A and NF-κB signaling. Importantly, Rapamycin also reduced tumor formation in a xenograft model *in vivo* (88). Thus, it would be very interesting to evaluate if other drugs that inhibit protein synthesis are also able to limit cancer progression while mitigating negative paracrine effects of senescent cells. Potential drug targets include several nucleolar proteins required for ribosome biogenesis.

One of these factors is Nucleophosmin 1 (B23), which is upregulated in adenomas and cancers of the colon (89) and translocates from the nucleolus to the nucleoplasm upon SIPS. B23 gene silencing by RNAi induces reductions in cell viability as well as increased abundance of senescent cells. Knockdown of p53 rescues this phenotype, indicating that p53 is required for B23-knockdown-mediated senescence (85).

Another remarkable nucleolar factor orchestrating the nucleolar stress response and linking cellular senescence and cancer initiation is nucleomethylin (NML). NML introduces specific m^1A 28S ribosomal RNA methylation in human and mouse cells and contributes to 60S subunit formation. Depletion of NML activates the p53 pathway and thereby regulates cellular proliferation (90). Interestingly, NML is important for the induction of drug-induced senescence in tumor cells. Upon depletion of NML, the probability of cells to escape senescence increases, which might cause relapse after chemotherapy. Indeed, downregulation of NML correlates with poor survival of breast cancer cell patients (91).

A very recent report describes NOLC1, which is a nucleolar protein with increased expression in cellular senescence and decreased expression in liver cancer. Strikingly, NOLC1 overexpression promotes the onset of senescence and represses hepatocellular carcinoma proliferation, both *in vitro* and in xenograft models. NOLC1 overexpression decreases rRNA synthesis and alters the morphology of nucleoli toward ring-like structures (92).

Taken together, these studies demonstrate that more and more genes are emerging, which establish a clear link between nucleolar stress, cellular senescence, and cancer, although most mechanistic details of these pathways remain elusive. Still, ribosome biogenesis and protein synthesis are important novel drug targets allowing decoupling of cancer therapy and bystander senescence induction.

Strategies to Decrease Cellular Senescence and Thereby Cancer

Telomerase—A Two-Edged Sword that Delays Senescence but Promotes Cancer

Telomerase is a reverse transcriptase that is mainly expressed in germ-, stem-, and cancer cells and counteracts telomere shortening induced by multiple cell divisions. Ectopic overexpression of telomerase is able to immortalize a wide range of different cell types (93–95). Although re-activation of telomerase is in many cases one of the critical steps in carcinogenesis, activation of telomerase by pharmacological compounds or gene therapy is still considered a promising strategy to promote tissue regeneration and delay various senescence-associated pathologies.

Several studies have already firmly established the dual role of telomerase in cancer and aging. Ectopic overexpression of TERT, the catalytic subunit of telomerase, promotes both tumor formation (96) and longevity in the mouse (97, 98). The increase in longevity is only observed in a tumor-resistant genetic background (97) or if telomerase expression is initiated late in life by gene therapy. In this scenario, TERT extends life span in 1- and 2-year-old mice, blunts the age-dependent loss of adipose tissue mass, bone density and coordination, but does not increase cancer incidence (98). The authors argue that the tumorigenic activity of telomerase is strongly repressed in aged organisms.

Nonetheless, pharmacological or gene therapy-mediated activation of telomerase to ameliorate aging-associated pathologies, including several forms of cancer, is heavily debated in the field. One side argues that re-expression of telomerase in old organisms, in synergy with caloric restriction (99) or in non-proliferative tissues, such as the heart, is not only safe, but also promotes tissue regeneration, such as after myocardial infarction (100). Others believe that expression of telomerase still poses the risk of increased cancer incidence by loss of a main tumor suppressor checkpoint (**Figure 2**). The role of telomerase in cancer and senescence was already extensively reviewed elsewhere (101).

Promotion of DNA Damage Repair to Reduce Senescence and Cancer Incidence

Apart from the activation of telomerase, a few other interventions were described in literature that are able to postpone the onset of cellular senescence and increase stress resistance in experimental models (**Figure 2**).

Our group could demonstrate that ectopic overexpression of $SNEV^{Prp19/Pso4}$ extends the replicative life span of human endothelial cells (102, 103), as well as the organismal life span of fruit flies (104). Although $SNEV^{Prp19/Pso4}$ participates also in pre-mRNA splicing (105) and in the ubiquitin/proteasome-pathway (106), we believe that its involvement in DNA damage repair is responsible for the increased stress resistance and fitness. Indeed, $SNEV^{Prp19/Pso4}$ and other DNA repair factors are also partially required for adipogenic differentiation of human adipose stromal cells and fat accumulation in *Caenorhabditis elegans* (107). Thus, enhancement of DNA damage repair, for instance by (not yet existing) small molecules activating $SNEV^{Prp19/Pso4}$, could potentially mitigate the accumulation of senescent cells upon aging or cancer therapy with cytotoxic compounds. Interestingly, $SNEV^{Prp19/Pso4}$ expression is elevated in breast cancer cells, but tumors with high $SNEV^{Prp19/Pso4}$ levels display reduced metastatic potential (102). Thus, animal experiments are required in order to evaluate benefits and detrimental effects of $SNEV^{Prp19/Pso4}$ overexpression regarding cancer incidence, metastasis, life span, and fitness at old age. In addition, it should be considered that improved DNA repair capacity in tumor cells is expected to reduce the efficacy of chemo- and radiation therapy.

Another promising approach that is already in clinical trials for the treatment of lung cancer is introduction of p53 by gene therapy (108). Thereby, cancer cells are sensitized for chemo- and radiation therapy. Since mouse experiments suggest that p53 overexpression (Super-p53 mouse) protects from cancer but does not shorten life span (109), it would be very interesting to evaluate if p53 gene therapy increases numbers of senescent cancer and non-cancer cells in human biopsies.

The problem with these hypothetical therapeutic interventions is the fact that activation of certain pathways or genes is usually more difficult to achieve by pharmaceuticals than their inactivation. Furthermore, it is very hard to predict how compounds targeting cancer affect senescence and *vice versa*, as pathways are tightly intertwined. Thus, selective clearance of senescent cells is in our view currently the most promising strategy to counteract aging- and therapy-associated senescence.

Elimination of Senescent Cells Mitigates Side Effects of Cancer Therapy

Genetic Clearance of Senescent Cells

The idea is to selectively kill senescent cells and to analyze if this can lead to rejuvenation of the organism, recovery from typical diseases of old age, which are believed to be caused by an accumulation of senescent cells, or recovery from the aging phenotypes which are caused by chemotherapy in cancer patients (44, 110). Basically, two approaches, namely, genetic clearance of senescent cells and senolytic compounds have been developed over the last years and both have proved to be highly successful in the mouse model (7, 11, 31, 32), but have not yet reached clinical application.

Genetic clearance of senescent cells relies on the genomic integration of either the *INC-ATTAC* (7, 31) or p16-3MR (11, 32) reporter construct, which were developed independently by two different labs, and enable recognition of $p16^{INK4A}$ -expressing cells in senescence accelerated mice, but also in naturally aged mice, both at cellular and organismic level. In addition, both constructs allow conditional induction of apoptosis specifically in $p16^{INK4A}$ positive cells upon systemic administration of either AP20187 (for *INC-ATTAC*) or ganciclovir (for p16-3MR). Importantly, clearance of senescent cells by *INC-ATTAC* increased life span, but did not decrease tumor incidence. However, mice having a tumor at the time of death showed increased survival (7). Genetic clearance of senescent cells in p16-3MR mice that were systemically treated with Doxorubicin was able to mitigate side effects of that drug, such as cardiac dysfunction, generalized increase of inflammation, and loss of hematopoetic stem cell function. In addition, genetic clearance of senescent cells reduced the incidence of cancer relapse and metastasis, as well as fatigue after Doxorubicin treatment (45). Thus, clearance of senescent cells might have clinical potential to reduce short-term and long-term side effects of current cancer therapy.

The downside of this approach is the fact that genetic clearance of senescent cells is not equally efficient in all organs (7, 31) and senescent cells lacking $p16^{INK4A}$ cannot be targeted. Thus, it would be very interesting to compare the current mouse models to other *in vivo* models that rely on different senescence markers. However, these models do not yet exist.

Senolytics—Translation of Genetic Mouse Models into Clinical Application

With the knowledge that specific elimination of senescent cells is able to slow organismal aging, several groups underwent the endeavor to screen for substances that specifically kill cells that are senescent, but not proliferating or reversibly growth arrested. Dasatinib and quercetin were identified as one of the first "senolytic" compounds and evaluated in the *INC-ATTAC* system *in vivo* (111). The results show that senescent cells are indeed eliminated, but the senolytic drugs which are presently known are not sufficiently specific, they also attack non-senescent cells (111, 112).

Therefore, an interesting strategy to specifically target senescent cells was introduced by Doerr and coworkers. The authors found that TIS-induced lymphoma cells have a much higher glucose- and energy demand, as well as elevated proteotoxic stress than non-senescent cells or TIS-cells that do not produce SASP (113). Mitochondria are required to fulfill the high energy demands of senescent cells and, indeed, depletion of mitochondria was able to reduce senescence phenotypes including the SASP *in vitro* and even prevent the onset of senescence in mouse livers *in vivo* (114). Thus, this specific metabolic condition of senescent cells, which is maintained by mitochondria, could be exploited to design a novel class of senolytics.

Another new approach was recently presented based on a cell penetrating peptide, FOXO4-DRI. FOXO4 is a member of the FOXO (FOX other) family of transcription factors which is expressed exclusively in senescent cells and prevents cell death by binding to p53 thereby retaining p53 in the nucleus. The peptide, FOXO4-DRI (FOXO4 D-amino acids retro inverso) is modeled after a unique sequence in the interaction surface of FOXO4 with p53. It contains only D-amino acids and is, therefore, not degradable in the cell. Penetration into cells is afforded by fusion with a hydrophilic and basic short sequence of the HIV-TAT protein. The interaction surface of FOXO4 is exactly mimicked by the side chains of the D-amino acids and the peptide with high affinity prevents binding between FOXO4 and p53, which in a "natural" way leads to efficient apoptotic death of the cells after nuclear export and transfer to mitochondria of p53. The mouse experiments show that (i) in normally aged mice, kidney function is restored to near youthful levels (tested by plasma urea and creatinine), and the same is true for skin and fur phenotypes; (ii) in mice that were treated with doxorubicin and developed senescence phenotypes, especially liver damage, this disease phenotype was also repaired by the FOXO4-DRI peptide. The side effects monitored in the mice and in cultured cells were negligible when compared to other senolytic drugs (32).

In our view, these experimental results combined show now for the first time in senescence research that the accumulation of senescent cells is indeed causally contributing to at least some aging diseases and probably to aging in general. More importantly, in the context of the present review article, senescent cells in tumors and in tumor patients after chemotherapy can be treated by eliminating senescent cells, which is a very promising suggestion for the future of cancer therapy (**Figure 2**). However, it should be considered that elimination of senescent cells might

impair tissue regeneration and, therefore, limit the repair of damage that was inflicted by chemotherapy. The correct timing, dosing, and patient selection by, e.g., specific companion diagnostics of senescent cell elimination and chemotherapy will be crucial in order to maximize therapy success and minimize side effects.

CONCLUSION AND OUTLOOK

For a long time, cellular senescence was purely seen as *in vitro* phenomenon and its influence on human aging was very controversial in the field, until quite recently several groups could clearly establish that senescent cells indeed contribute to aging-associated diseases and ultimately to organismal life- and health span. In the last few years, senescence has come also more and more into focus in cancer research, as senescence is frequently induced by current tumor therapies, being beneficial for arresting apoptosis-resistant cancer cells, but on the other hand inducing senescence in other cells and thereby promoting cancer relapse and secondary tumors. In addition, the accumulation of senescent cells with age might at least partially explain increasing cancer incidence with age.

Since the secretory phenotypes of senescent cells and CAF are similar, cellular senescence serves as an interesting model system for a pro-tumorogenic microenvironment that could be utilized for drug screenings. Furthermore, pharmaceutically targeting senescent cells might not only be a novel tool in battling aging-associated pathologies, but also a complementation to cancer therapy to eliminate senescent cancer and non-cancer cells and mitigate side effects. The coming years will show if a better understanding of the complex interplay between cellular senescence and cancer will indeed revolutionize therapy options.

AUTHOR CONTRIBUTIONS

MS and MB wrote the manuscript. MS designed figures. JG provided ideas regarding the concept of the manuscript and critically revised the manuscript. All authors read, corrected, and approved the final version of the manuscript. MS prepared and submitted all required files.

ACKNOWLEDGMENTS

Parts of **Figures 1** and **2** were produced using Servier Medical Art (http://www.servier.com) under Creative Commons BY 3.0 licence.

FUNDING

This work was supported by the Austrian Science Fund (FWF: I2514 to JG and P26713 to MB), the Austrian Federal Ministry of Science, Research and Economy, the National Foundation for Research, Technology and Development, and the Christian Doppler Research Society.

REFERENCES

1. Mishra P, Banerjee D, Ben-Baruch A. Chemokines at the crossroads of tumor-fibroblast interactions that promote malignancy. *J Leukoc Biol* (2011) 89:31–9. doi:10.1189/jlb.0310182
2. Campisi J. Senescent cells, tumor suppression, and organismal aging: good citizens, bad neighbors. *Cell* (2005) 120:513–22. doi:10.1016/j.cell.2005.02.003
3. Hayflick L, Moorhead PS. The serial cultivation of human diploid cell strains. *Exp Cell Res* (1961) 25:585–621. doi:10.1016/0014-4827(61)90192-6
4. Erusalimsky JD, Kurz DJ. Cellular senescence in vivo: its relevance in ageing and cardiovascular disease. *Exp Gerontol* (2005) 40:634–42. doi:10.1016/j.exger.2005.04.010
5. Herbig U, Ferreira M, Condel L, Carey D, Sedivy JM. Cellular senescence in aging primates. *Science* (2006) 311:1257. doi:10.1126/science.1122446
6. Dimri GP, Lee X, Basile G, Acosta M, Scott G, Roskelley C, et al. A biomarker that identifies senescent human cells in culture and in aging skin in vivo. *Proc Natl Acad Sci U S A* (1995) 92:9363–7. doi:10.1073/pnas.92.20.9363
7. Baker DJ, Childs BG, Durik M, Wijers ME, Sieben CJ, Zhong J, et al. Naturally occurring p16 Ink4a-positive cells shorten healthy lifespan. *Nature* (2016) 530:184–9. doi:10.1038/nature16932
8. Campisi J. Aging and cancer: the double-edged sword of replicative senescence. *J Am Geriatr Soc* (1997) 45:482–8. doi:10.1111/j.1532-5415.1997.tb05175.x
9. Muñoz-Espín D, Cañamero M, Maraver A, Gómez-López G, Contreras J, Murillo-Cuesta S, et al. Programmed cell senescence during mammalian embryonic development. *Cell* (2013) 155:1104–18. doi:10.1016/j.cell.2013.10.019
10. Storer M, Mas A, Robert-Moreno A, Pecoraro M, Ortells MC, Di Giacomo V, et al. Senescence is a developmental mechanism that contributes to embryonic growth and patterning. *Cell* (2013) 155:1119–30. doi:10.1016/j.cell.2013.10.041
11. Demaria M, Ohtani N, Youssef SA, Rodier F, Toussaint W, Mitchell JR, et al. An essential role for senescent cells in optimal wound healing through secretion of PDGF-AA. *Dev Cell* (2014) 31:722–33. doi:10.1016/j.devcel.2014.11.012
12. Hanahan D, Weinberg RA. Hallmarks of cancer: the next generation. *Cell* (2011) 144:646–74. doi:10.1016/j.cell.2011.02.013
13. Knudson AG. Mutation and cancer: statistical study of retinoblastoma. *Proc Natl Acad Sci U S A* (1971) 68:820–3. doi:10.1073/pnas.68.4.820
14. Krishnamurthy J, Torrice C, Ramsey MR, Kovalev GI, Al-Regaiey K, Su L, et al. Ink4a/Arf expression is a biomarker of aging. *J Clin Invest* (2004) 114:1299–307. doi:10.1172/JCI22475
15. Georgakopoulou EA, Tsimaratou K, Evangelou K, Fernandez Marcos PJ, Zoumpourlis V, Trougakos IP, et al. Specific lipofuscin staining as a novel biomarker to detect replicative and stress-induced senescence. A method applicable in cryo-preserved and archival tissues. *Aging (Albany NY)* (2013) 5:37–50. doi:10.18632/aging.100527
16. Brown JP, Wei W, Sedivy JM. Bypass of senescence after disruption of p21CIP1/WAF1 gene in normal diploid human fibroblasts. *Science* (1997) 277:831–4. doi:10.1126/science.277.5327.831
17. Evangelou K, Lougiakis N, Rizou SV, Kotsinas A, Kletsas D, Muñoz-Espín D, et al. Robust, universal biomarker assay to detect senescent cells in biological specimens. *Aging Cell* (2017) 16:192–7. doi:10.1111/acel.12545
18. De Cecco M, Criscione SW, Peckham EJ, Hillenmeyer S, Hamm EA, Manivannan J, et al. Genomes of replicatively senescent cells undergo global epigenetic changes leading to gene silencing and activation of transposable elements. *Aging Cell* (2013) 12:247–56. doi:10.1111/acel.12047
19. Criscione SW, De Cecco M, Siranosian B, Zhang Y, Kreiling JA, Sedivy JM, et al. Reorganization of chromosome architecture in replicative cellular senescence. *Sci Adv* (2016) 2:e1500882. doi:10.1126/sciadv.1500882
20. Franceschi C, Campisi J. Chronic inflammation (inflammaging) and its potential contribution to age-associated diseases. *J Gerontol A Biol Sci Med Sci* (2014) 69(Suppl 1):S4–9. doi:10.1093/gerona/glu057
21. Coppe JP, Desprez PY, Krtolica A, Campisi J. The senescence-associated secretory phenotype: the dark side of tumor suppression. *Annu Rev Pathol* (2010) 5:99–118. doi:10.1146/annurev-pathol-121808-102144

22. de Keizer PLJ. The fountain of youth by targeting senescent cells? *Trends Mol Med* (2017) 23:6–17. doi:10.1016/j.molmed.2016.11.006
23. Harley CB, Futcher AB, Greider CW. Telomeres shorten during ageing of human fibroblasts. *Nature* (1990) 345:458–60. doi:10.1038/345458a0
24. Freund A, Laberge R-M, Demaria M, Campisi J. Lamin B1 loss is a senescence-associated biomarker. *Mol Biol Cell* (2012) 23:2066–75. doi:10.1091/mbc.E11-10-0884
25. Lee BY, Han JA, Im JS, Morrone A, Johung K, Goodwin EC, et al. Senescence-associated β-galactosidase is lysosomal β-galactosidase. *Aging Cell* (2006) 5:187–95. doi:10.1111/j.1474-9726.2006.00199.x
26. Eberhardt K, Beleites C, Marthandan S, Matthäus C, Diekmann S, Popp J. Raman and infrared spectroscopy distinguishing replicative senescent from proliferating primary human fibroblast cells by detecting spectral differences mainly due to biomolecular alterations. *Anal Chem* (2017) 89:2937–47. doi:10.1021/acs.analchem.6b04264
27. Eberhardt K, Matthäus C, Winter D, Wiegand C, Hipler U, Diekmann S, et al. Raman and infrared spectroscopy differentiate senescent from proliferating cells in a human dermal fibroblast 3D skin model. *Analyst* (2017). doi:10.1039/c7an00592j
28. Diem M, Mazur A, Lenau K, Schubert J, Bird B, Miljković M, et al. Molecular pathology via IR and Raman spectral imaging. *J Biophotonics* (2013) 6:855–86. doi:10.1002/jbio.201300131
29. Brauchle E, Noor S, Holtorf E, Garbe C, Schenke-Layland K, Busch C. Raman spectroscopy as an analytical tool for melanoma research. *Clin Exp Dermatol* (2014) 39:636–45. doi:10.1111/ced.12357
30. Brauchle E, Thude S, Brucker SY, Schenke-Layland K. Cell death stages in single apoptotic and necrotic cells monitored by Raman microspectroscopy. *Sci Rep* (2014) 4:4698. doi:10.1038/srep04698
31. Baker DJ, Wijshake T, Tchkonia T, LeBrasseur NK, Childs BG, van de Sluis B, et al. Clearance of p16Ink4a-positive senescent cells delays ageing-associated disorders. *Nature* (2011) 479:232–6. doi:10.1038/nature10600
32. Baar MP, Brandt RM, Putavet DA, Klein JD, Derks KW, Bourgeois BR, et al. Targeted apoptosis of senescent cells restores tissue homeostasis in response to chemotoxicity and aging. *Cell* (2017) 169:132–47.e16. doi:10.1016/j.cell.2017.02.031
33. Ko A, Han SY, Song J. Dynamics of ARF regulation that control senescence and cancer. *BMB Rep* (2016) 49:598–606. doi:10.5483/BMBRep.2016.49.11.120
34. Kim WY, Sharpless NE. The regulation of INK4/ARF in cancer and aging. *Cell* (2006) 127:265–75. doi:10.1016/j.cell.2006.10.003
35. Shay JW, Roninson IB. Hallmarks of senescence in carcinogenesis and cancer therapy. *Oncogene* (2004) 23:2919–33. doi:10.1038/sj.onc.1207518
36. Rudolph KL, Chang S, Lee HW, Blasco M, Gottlieb GJ, Greider C, et al. Longevity, stress response, and cancer in aging telomerase-deficient mice. *Cell* (1999) 96:701–12. doi:10.1016/S0092-8674(00)80580-2
37. Terry DF, Nolan VG, Andersen SL, Perls TT, Cawthon R. Association of longer telomeres with better health in centenarians. *J Gerontol A Biol Sci Med Sci* (2008) 63:809–12. doi:10.1093/gerona/63.8.809
38. Sanders JL, Newman AB. Telomere length in epidemiology: a biomarker of aging, age-related disease, both, or neither? *Epidemiol Rev* (2013) 35:112–31. doi:10.1093/epirev/mxs008
39. Willeit P, Willeit J, Mayr A, Weger S, Oberhollenzer F, Brandstätter A, et al. Telomere length and risk of incident cancer and cancer mortality. *JAMA* (2010) 304:69–75. doi:10.1001/jama.2010.897
40. Aviv A, Anderson JJ, Shay JW. Mutations, cancer and the telomere length paradox. *Trends Cancer* (2017) 3:253–8. doi:10.1016/j.trecan.2017.02.005
41. Toussaint O, Royer V, Salmon M, Remacle J. Stress-induced premature senescence and tissue ageing. *Biochem Pharmacol* (2002) 64:1007–9. doi:10.1016/S0006-2952(02)01170-X
42. Wu PC, Wang Q, Grobman L, Chu E, Wu DY. Accelerated cellular senescence in solid tumor therapy. *Exp Oncol* (2012) 34:298–305.
43. Hewitt G, Jurk D, Marques FDM, Correia-Melo C, Hardy T, Gackowska A, et al. Telomeres are favoured targets of a persistent DNA damage response in ageing and stress-induced senescence. *Nat Commun* (2012) 3:708. doi:10.1038/ncomms1708
44. Ewald JA, Desotelle JA, Wilding G, Jarrard DF. Therapy-induced senescence in cancer. *J Natl Cancer Inst* (2010) 102:1536–46. doi:10.1093/jnci/djq364
45. Demaria M, O'Leary MN, Chang J, Shao L, Liu S, Alimirah F, et al. Cellular senescence promotes adverse effects of chemotherapy and cancer relapse. *Cancer Discov* (2017) 7:165–76. doi:10.1158/2159-8290.CD-16-0241
46. Schmitt CA, Fridman JS, Yang M, Lee S, Baranov E, Hoffman RM, et al. A senescence program controlled by p53 and p16INK4a contributes to the outcome of cancer therapy. *Cell* (2002) 109:335–46. doi:10.1016/S0092-8674(02)00734-1
47. Roninson IB. Tumor cell senescence in cancer treatment. *Cancer Res* (2003) 63:2705–15. doi:10.1016/j.mce.2006.03.017
48. Serrano M, Lin AW, McCurrach ME, Beach D, Lowe SW. Oncogenic ras provokes premature cell senescence associated with accumulation of p53 and p16INK4a. *Cell* (1997) 88:593–602. doi:10.1016/S0092-8674(00)81902-9
49. Collado M, Blasco MA, Serrano M. Cellular senescence in cancer and aging. *Cell* (2007) 130:223–33. doi:10.1016/j.cell.2007.07.003
50. Heeren G, Jarolim S, Laun P, Rinnerthaler M, Stolze K, Perrone GG, et al. The role of respiration, reactive oxygen species and oxidative stress in mother cell-specific ageing of yeast strains defective in the RAS signalling pathway. *FEMS Yeast Res* (2004) 5:157–67. doi:10.1016/j.femsyr.2004.05.008
51. Rinnerthaler M, Büttner S, Laun P, Heeren G, Felder TK, Klinger H, et al. Yno1p/Aim14p, a NADPH-oxidase ortholog, controls extramitochondrial reactive oxygen species generation, apoptosis, and actin cable formation in yeast. *Proc Natl Acad Sci U S A* (2012) 109:8658–63. doi:10.1073/pnas.1201629109
52. Sarkisian CJ, Keister BA, Stairs DB, Boxer RB, Moody SE, Chodosh LA. Dose-dependent oncogene-induced senescence in vivo and its evasion during mammary tumorigenesis. *Nat Cell Biol* (2007) 9:493–505. doi:10.1038/ncb1567
53. Collado M, Serrano M. The power and the promise of oncogene-induced senescence markers. *Nat Rev Cancer* (2006) 6:472–6. doi:10.1038/nrc1884
54. Ritschka B, Storer M, Mas A, Heinzmann F, Ortells MC, Morton JP, et al. The senescence-associated secretory phenotype induces cellular plasticity and tissue regeneration. *Genes Dev* (2017) 31:172–83. doi:10.1101/gad.290635.116
55. Velarde MC, Demaria M, Campisi J. Senescent cells and their secretory phenotype as targets for cancer therapy. *Interdiscip Top Gerontol* (2013) 38:17–27. doi:10.1159/000343572
56. Loaiza N, Demaria M. Cellular senescence and tumor promotion: is aging the key? *Biochim Biophys Acta* (2016) 1865:155–67. doi:10.1016/j.bbcan.2016.01.007
57. Acosta JC, O'Loghlen A, Banito A, Guijarro MV, Augert A, Raguz S, et al. Chemokine signaling via the CXCR2 receptor reinforces senescence. *Cell* (2008) 133:1006–18. doi:10.1016/j.cell.2008.03.038
58. Wajapeyee N, Serra RW, Zhu X, Mahalingam M, Green MR. Oncogenic BRAF induces senescence and apoptosis through pathways mediated by the secreted protein IGFBP7. *Cell* (2008) 132:363–74. doi:10.1016/j.cell.2007.12.032
59. Coppé J-P, Patil CK, Rodier F, Sun Y, Muñoz DP, Goldstein J, et al. Senescence-associated secretory phenotypes reveal cell-nonautonomous functions of oncogenic RAS and the p53 tumor suppressor. *PLoS Biol* (2008) 6:2853–68. doi:10.1371/journal.pbio.0060301
60. Grillari J, Hohenwarter O, Grabherr RM, Katinger H. Subtractive hybridization of mRNA from early passage and senescent endothelial cells. *Exp Gerontol* (2000) 35:187–97. doi:10.1016/S0531-5565(00)00080-2
61. Kumazaki T, Kobayashi M, Mitsui Y. Enhanced expression of fibronectin during in vivo cellular aging of human vascular endothelial cells and skin fibroblasts. *Exp Cell Res* (1993) 205:396–402. doi:10.1006/excr.1993.1103
62. Takasugi M, Okada R, Takahashi A, Virya Chen D, Watanabe S, Hara E. Small extracellular vesicles secreted from senescent cells promote cancer cell proliferation through EphA2. *Nat Commun* (2017) 8:15729. doi:10.1038/ncomms15728
63. Lehmann BD, Paine MS, Brooks AM, McCubrey JA, Renegar RH, Wang R, et al. Senescence-associated exosome release from human prostate cancer cells. *Cancer Res* (2008) 68:7864–71. doi:10.1158/0008-5472.CAN-07-6538
64. Hackl M, Brunner S, Fortschegger K, Schreiner C, Micutkova L, Mück C, et al. miR-17, miR-19b, miR-20a, and miR-106a are down-regulated in human aging. *Aging Cell* (2010) 9:291–6. doi:10.1111/j.1474-9726.2010.00549.x
65. Xue W, Zender L, Miething C, Dickins RA, Hernando E, Krizhanovsky V, et al. Senescence and tumour clearance is triggered by p53 restoration in murine liver carcinomas. *Nature* (2007) 445:656–60. doi:10.1038/nature05529
66. Eggert T, Wolter K, Ji J, Ma C, Yevsa T, Klotz S, et al. Distinct functions of senescence-associated immune responses in liver tumor surveillance and tumor progression. *Cancer Cell* (2016) 30:533–47. doi:10.1016/j.ccell.2016.09.003
67. Mosteiro L, Pantoja C, Alcazar N, Marión RM, Chondronasiou D, Rovira M, et al. Tissue damage and senescence provide critical signals for cellular reprogramming in vivo. *Science* (2016) 354:aaf4445. doi:10.1126/science.aaf4445

68. Tian X, Azpurua J, Hine C, Vaidya A, Myakishev-Rempel M, Ablaeva J, et al. High-molecular-mass hyaluronan mediates the cancer resistance of the naked mole rat. *Nature* (2013) 499:346–9. doi:10.1038/nature12234
69. Tian X, Azpurua J, Ke Z, Augereau A, Zhang ZD, Vijg J, et al. INK4 locus of the tumor-resistant rodent, the naked mole rat, expresses a functional p15/p16 hybrid isoform. *Proc Natl Acad Sci U S A* (2015) 112:1053–8. doi:10.1073/pnas.1418203112
70. Lewis KN, Mele J, Hornsby PJ, Buffenstein R. Stress resistance in the naked mole-rat: the bare essentials – a mini-review. *Gerontology* (2012) 58:453–62. doi:10.1159/000335966
71. Mellone M, Hanley CJ, Thirdborough S, Mellows T, Garcia E, Woo J, et al. Induction of fibroblast senescence generates a non-fibrogenic myofibroblast phenotype that differentially impacts on cancer prognosis. *Aging (Albany NY)* (2016) 9:114–32. doi:10.18632/aging.101127
72. Orimo A, Gupta PB, Sgroi DC, Arenzana-Seisdedos F, Delaunay T, Naeem R, et al. Stromal fibroblasts present in invasive human breast carcinomas promote tumor growth and angiogenesis through elevated SDF-1/CXCL12 secretion. *Cell* (2005) 121:335–48. doi:10.1016/j.cell.2005.02.034
73. Begley L, Monteleon C, Shah RB, Macdonald JW, Macoska JA. CXCL12 overexpression and secretion by aging fibroblasts enhance human prostate epithelial proliferation in vitro. *Aging Cell* (2005) 4:291–8. doi:10.1111/j.1474-9726.2005.00173.x
74. Wang T, Notta F, Navab R, Joseph J, Ibrahimov E, Xu J, et al. Senescent carcinoma-associated fibroblasts upregulate IL8 to enhance prometastatic phenotypes. *Mol Cancer Res* (2017) 15:3–14. doi:10.1158/1541-7786.MCR-16-0192
75. Kabir TD, Leigh RJ, Tasena H, Mellone M, Coletta RD, Parkinson EK, et al. A miR-335/COX-2/PTEN axis regulates the secretory phenotype of senescent cancer-associated fibroblasts. *Aging (Albany NY)* (2016) 8:1608–35. doi:10.18632/aging.100987
76. Derenzini M, Montanaro L, Treré D. What the nucleolus says to a tumour pathologist. *Histopathology* (2009) 54:753–62. doi:10.1111/j.1365-2559.2008.03168.x
77. Rattan SI. Synthesis, modifications, and turnover of proteins during aging. *Exp Gerontol* (1996) 31:33–47. doi:10.1016/0531-5565(95)02022-5
78. Cristofalo VJ, Lorenzini A, Allen RG, Torres C, Tresini M. Replicative senescence: a critical review. *Mech Ageing Dev* (2004) 125:827–48. doi:10.1016/j.mad.2004.07.010
79. Buchwalter A, Hetzer MW. Nucleolar expansion and elevated protein translation in premature aging. *Nat Commun* (2017) 8:328. doi:10.1038/s41467-017-00322-z
80. Tiku V, Jain C, Raz Y, Nakamura S, Heestand B, Liu W, et al. Small nucleoli are a cellular hallmark of longevity. *Nat Commun* (2016) 8:16083. doi:10.1038/ncomms16083
81. Bemiller PM, Lee LH. Nucleolar changes in senescing WI-38 cells. *Mech Ageing Dev* (1978) 8:417–27. doi:10.1016/0047-6374(78)90041-6
82. Mehta IS, Figgitt M, Clements CS, Kill IR, Bridger JM. Alterations to nuclear architecture and genome behavior in senescent cells. *Ann N Y Acad Sci* (2007) 1100:250–63. doi:10.1196/annals.1395.027
83. Hein N, Sanij E, Quin J, Hannan KM, Ganley A, Hannan RD. The nucleolus and ribosomal genes in aging and senescence. In: Nagata T, editor. *Senescence*. Rijeka: InTech (2012). p. 171–208.
84. Dillinger S, Straub T, Németh A. Nucleolus association of chromosomal domains is largely maintained in cellular senescence despite massive nuclear reorganisation. *PLoS One* (2017) 12:e0178821. doi:10.1371/journal.pone.0178821
85. Kar B, Liu B, Zhou Z, Lam YW. Quantitative nucleolar proteomics reveals nuclear re-organization during stress-induced senescence in mouse fibroblast. *BMC Cell Biol* (2011) 12:33. doi:10.1186/1471-2121-12-33
86. Bywater MJ, Poortinga G, Sanij E, Hein N, Peck A, Cullinane C, et al. Inhibition of RNA polymerase I as a therapeutic strategy to promote cancer-specific activation of p53. *Cancer Cell* (2012) 22:51–65. doi:10.1016/j.ccr.2012.05.019
87. Harrison DE, Strong R, Sharp ZD, Nelson JF, Astle CM, Flurkey K, et al. Rapamycin fed late in life extends lifespan in genetically heterogeneous mice. *Nature* (2009) 460:392–5. doi:10.1038/nature08221
88. Laberge R-M, Sun Y, Orjalo AV, Patil CK, Freund A, Zhou L, et al. MTOR regulates the pro-tumorigenic senescence-associated secretory phenotype by promoting IL1A translation. *Nat Cell Biol* (2015) 17:1049–61. doi:10.1038/ncb3195
89. Wong JC, Hasan MR, Rahman M, Yu AC, Chan SK, Schaeffer DF, et al. Nucleophosmin 1, upregulated in adenomas and cancers of the colon, inhibits p53-mediated cellular senescence. *Int J Cancer* (2013) 133:1567–77. doi:10.1002/ijc.28180
90. Waku T, Nakajima Y, Yokoyama W, Nomura N, Kako K, Kobayashi A, et al. NML-mediated rRNA base methylation links ribosomal subunit formation to cell proliferation in a p53-dependent manner. *J Cell Sci* (2016) 129:2382–93. doi:10.1242/jcs.183723
91. Yang L, Song T, Chen L, Soliman H, Chen J. Nucleolar repression facilitates initiation and maintenance of senescence. *Cell Cycle* (2015) 14:3613–23. doi:10.1080/15384101.2015.1100777
92. Yuan F, Zhang Y, Ma L, Cheng Q, Li G, Tong T. Enhanced NOLC1 promotes cell senescence and represses hepatocellular carcinoma cell proliferation by disturbing the organization of nucleolus. *Aging Cell* (2017) 16:726–37. doi:10.1111/acel.12602
93. Wolbank S, Stadler G, Peterbauer A, Gillich A, Karbiener M, Streubel B, et al. Telomerase immortalized human amnion- and adipose-derived mesenchymal stem cells: maintenance of differentiation and immunomodulatory characteristics. *Tissue Eng Part A* (2009) 15:1843–54. doi:10.1089/ten.tea.2008.0205
94. Wieser M, Stadler G, Jennings P, Streubel B, Pfaller W, Ambros P, et al. hTERT alone immortalizes epithelial cells of renal proximal tubules without changing their functional characteristics. *Am J Physiol Renal Physiol* (2008) 4:F1365–75. doi:10.1152/ajprenal.90405.2008
95. Bodnar AG, Ouellette M, Frolkis M, Holt SE, Chiu CP, Morin GB, et al. Extension of life-span by introduction of telomerase into normal human cells. *Science* (1998) 279:349–52. doi:10.1126/science.279.5349.349
96. González-Suárez E, Geserick C, Flores JM, Blasco MA. Antagonistic effects of telomerase on cancer and aging in K5-mTert transgenic mice. *Oncogene* (2005) 24:2256–70. doi:10.1038/sj.onc.1208413
97. Tomás-Loba A, Flores I, Fernández-Marcos PJ, Cayuela ML, Maraver A, Tejera A, et al. Telomerase reverse transcriptase delays aging in cancer-resistant mice. *Cell* (2008) 135:609–22. doi:10.1016/j.cell.2008.09.034
98. Bernardes de Jesus B, Vera E, Schneeberger K, Tejera AM, Ayuso E, Bosch F, et al. Telomerase gene therapy in adult and old mice delays aging and increases longevity without increasing cancer. *EMBO Mol Med* (2012) 4:691–704. doi:10.1002/emmm.201200245
99. Vera E, Bernardes de Jesus B, Foronda M, Flores JM, Blasco MA. Telomerase reverse transcriptase synergizes with calorie restriction to increase health span and extend mouse longevity. *PLoS One* (2013) 8:e53760. doi:10.1371/journal.pone.0053760
100. Bär C, Bernardes de Jesus B, Serrano R, Tejera A, Ayuso E, Jimenez V, et al. Telomerase expression confers cardioprotection in the adult mouse heart after acute myocardial infarction. *Nat Commun* (2014) 5:5863. doi:10.1038/ncomms6863
101. Bernardes de Jesus B, Blasco MA. Telomerase at the intersection of cancer and aging. *Trends Genet* (2013) 29:513–20. doi:10.1016/j.tig.2013.06.007
102. Voglauer R, Chang MW-F, Dampier B, Wieser M, Baumann K, Sterovsky T, et al. SNEV overexpression extends the life span of human endothelial cells. *Exp Cell Res* (2006) 312:746–59. doi:10.1016/j.yexcr.2005.11.025
103. Dellago H, Khan A, Nussbacher M, Gstraunthaler A, Schosserer M, Mück C, et al. ATM-dependent phosphorylation of SNEV is involved in extending cellular life span and suppression of apoptosis. *Aging (Albany NY)* (2012) 4:290–304. doi:10.18632/aging.100452
104. Garschall K, Dellago H, Gáliková M, Schosserer M, Flatt T, Grillari J. Ubiquitous overexpression of the DNA repair factor dPrp19 reduces DNA damage and extends Drosophila life span. *NPJ Aging Mech Dis* (2017) 3:5. doi:10.1038/s41514-017-0005-z
105. Grillari J, Ajuh P, Stadler G, Löscher M, Voglauer R, Ernst W, et al. SNEV is an evolutionarily conserved splicing factor whose oligomerization is necessary for spliceosome assembly. *Nucleic Acids Res* (2005) 33:6868–83. doi:10.1093/nar/gki986
106. Löscher M, Fortschegger K, Ritter G, Wostry M, Voglauer R, Schmid JA, et al. Interaction of U-box E3 ligase SNEV with PSMB4, the beta7 subunit of the 20 S proteasome. *Biochem J* (2005) 388:593–603. doi:10.1042/BJ20041517
107. Khan A, Dellago H, Terlecki-Zaniewicz L, Karbiener M, Weilner S, Hildner F, et al. SNEV(hPrp19/hPso4) regulates adipogenesis of human adipose stromal cells. *Stem Cell Reports* (2017) 8:21–9. doi:10.1016/j.stemcr.2016.12.001

108. Wang Z, Sun Y. Targeting p53 for novel anticancer therapy. *Transl Oncol* (2010) 3:1–12. doi:10.1593/tlo.09250
109. García-Cao I, García-Cao M, Martín-Caballero J, Criado LM, Klatt P, Flores JM, et al. "Super p53" mice exhibit enhanced DNA damage response, are tumor resistant and age normally. *EMBO J* (2002) 21:6225–35. doi:10.1093/emboj/cdf595
110. Henderson TO, Ness KK, Cohen HJ. Accelerated aging among cancer survivors: from pediatrics to geriatrics. *Am Soc Clin Oncol Educ Book* (2014) 2014:e423–30. doi:10.14694/EdBook_AM.2014.34.e423
111. Zhu Y, Tchkonia T, Pirtskhalava T, Gower AC, Ding H, Giorgadze N, et al. The Achilles' heel of senescent cells: from transcriptome to senolytic drugs. *Aging Cell* (2015) 14:644–58. doi:10.1111/acel.12344
112. Zhu Y, Doornebal EJ, Pirtskhalava T, Giorgadze N, Wentworth M, Fuhrmann-Stroissnigg H, et al. New agents that target senescent cells: the flavone, fisetin, and the BCL-XL inhibitors, A1331852 and A1155463. *Aging (Albany NY)* (2017) 9(3):955–63. doi:10.18632/aging.101202
113. Dörr JR, Yu Y, Milanovic M, Beuster G, Zasada C, Däbritz JHM, et al. Synthetic lethal metabolic targeting of cellular senescence in cancer therapy. *Nature* (2013) 501:421–5. doi:10.1038/nature12437
114. Correia-Melo C, Marques FDM, Anderson R, Hewitt G, Hewitt R, Cole J, et al. Mitochondria are required for pro-ageing features of the senescent phenotype. *EMBO J* (2016) 35:724–42. doi:10.15252/embj.201592862

Conflict of Interest Statement: JG is cofounder and shareholder of Evercyte GmbH and TAmiRNA GmbH. All other authors declare no competing interests.

frontiers in Oncology

REVIEW
published: 19 March 2018
doi: 10.3389/fonc.2018.00072

The Biology and Therapeutic Implications of Tumor Dormancy and Reactivation

Amit S. Yadav[1†], Poonam R. Pandey[2†], Ramesh Butti[1], N. N. V. Radharani[1], Shamayita Roy[1], Shaileshkumar R. Bhalara[1], Mahadeo Gorain[1], Gopal C. Kundu[1] and Dhiraj Kumar[1,3]*

[1] Laboratory of Tumor Biology, Angiogenesis and Nanomedicine Research, National Centre for Cell Science, Pune, India, [2] Laboratory of Genetics, National Institute on Aging-Intramural Research Program, National Institutes of Health, Baltimore, MD, United States, [3] Department of Cancer Biology, The University of Texas MD Anderson Cancer Center, Houston, TX, United States

Advancements in the early detection of cancer coupled with improved surgery, radiotherapy, and adjuvant therapy led to substantial increase in patient survival. Nevertheless, cancer metastasis is the leading cause of death in several cancer patients. The majority of these deaths are associated with metastatic relapse kinetics after a variable period of clinical remission. Most of the cancer recurrences are thought to be associated with the reactivation of dormant disseminated tumor cells (DTCs). In this review, we have summarized the cellular and molecular mechanisms related to DTCs and the role of microenvironmental niche. These mechanisms regulate the dormant state and help in the reactivation, which leads to metastatic outgrowth. Identification of novel therapeutic targets to eliminate these dormant tumor cells will be highly useful in controlling the metastatic relapse-related death with several cancers.

Keywords: cancer metastasis, dormancy, reactivation, tumor microenvironment, epithelial to mesenchymal transition

OPEN ACCESS

Edited by:
Michael Breitenbach, University of Salzburg, Austria

Reviewed by:
Markus Schosserer, University of Natural Resources and Life Sciences, Vienna, Austria
Walter Berger, Medizinische Universität Wien, Austria

***Correspondence:**
Dhiraj Kumar
dkumar@mdanderson.org

[†]These authors have contributed equally to this work.

Specialty section:
This article was submitted to Molecular and Cellular Oncology, a section of the journal Frontiers in Oncology

Received: *09 November 2017*
Accepted: *02 March 2018*
Published: *19 March 2018*

Citation:
Yadav AS, Pandey PR, Butti R, Radharani NNV, Roy S, Bhalara SR, Gorain M, Kundu GC and Kumar D (2018) The Biology and Therapeutic Implications of Tumor Dormancy and Reactivation. Front. Oncol. 8:72. doi: 10.3389/fonc.2018.00072

INTRODUCTION

Metastasis is a continuous biological process consists of an orderly sequence of basic steps including local invasion, intravasation, extravasation, and colonization. These classical events of metastasis help in understanding the complex array of biological properties that are necessary for the progression of primary malignancy to overt metastasis (1, 2). It involves dissemination of malignant cells from the primary tumor to the distant sites and their proliferation at metastatic sites, which leads to failure of vital organs (1, 2). The kinetics of the metastasis have been highly explored in the past decade. Despite significant research efforts and discoveries made in recent years, the precise reasons for tumor relapse remain largely unknown. There has been significant progress in basic cancer research and clinical oncology; however, metastasis remains to be a key challenge in cancer therapy. Systemic studies on understanding the cellular and molecular mechanisms involved in metastasis might be useful in developing novel diagnostic and therapeutic strategies for metastasis prevention. However, biological, clonal and genetic heterogeneity within or between tumors are the biggest challenges in metastasis research (1, 2). The differential progression of certain cancer subtypes under the distinct selective conditions exists in various tissues leads to metastatic speciation. Disseminated cancer cells might exhibit slow growth in order to adapt to the host microenvironment for the metastatic expansion (3–7). These processes are mirrored by several cancer relapse kinetics in a tissue-specific manner and by the manifestation of distinct organ tropism (3–7). Metastasis might be developed

without clinical symptoms after a long period of postsurgery (8). During this period, circulating tumor cells (CTCs) or disseminated tumor cells (DTCs) stay in the dormant state through inhibition of cell proliferation and activation of cell survival pathways (9, 10). The dormant tumor cells remain at low numbers after primary tumor resection. These cells are undetectable for long period and may be the reason for continued asymptomatic residual disease progression and treatment resistance (11–14). However, by understanding more about the biology of dormant cancer cells, the potential treatment strategies can be developed to combat the asymptomatic residual disease. The therapies targeting the mechanism of tissue-specific metastasis might open up new clinical avenues for the management of various cancer progression (15). However, to determine whether dormant solitary cells or micrometastases are valid targets for therapy, the cellular and molecular biology of tumor dormancy and reactivation need to be explored. This review emphasizes on the cancer dormancy, metastatic reactivation and the molecular mechanisms underlying these phenomena.

TUMOR AND METASTATIC DORMANCY

Tumor dormancy is a clinical process that eventually associates with local recurrences or cancer metastases. During this process, the residual disease might be present even after the treatment of primary tumors either in the forms of CTCs, DTCs, and/or micrometastases which have the capability of evading the treatment and survive in a quiescent state. Traditional chemotherapies are most effective on proliferative cells, however, ineffective toward the dormant cells (16). The dormancy nature of the tumor may be reflected by cellular or tumor mass dormancy. In cellular dormancy, cells halt in the G0 phase of the cell cycle and under favorable environmental conditions, they get reactivated by escaping from G0 cell cycle arrest (17). Moreover, during tumor mass dormancy tumor kept constant at a limited size owing to a balance between cell proliferation and cell death. Additionally, angiogenesis and immune response play an important role in maintaining the tumor mass dormancy (18). Dormant cells remain asymptomatic for months, years or even decades and eventually they undergo clinically detectable overt metastatic relapse as shown in **Figure 1** (19). Interestingly, dormant cancer cells have also been observed in the primary tumors that undergo epithelial to mesenchymal transition (EMT) to develop migratory and invasive phenotypes (20). In primary tumor dormancy development, somatic mutations play a critical role to withstand apoptosis, senescence, and evade the immune system and trigger neoangiogenesis. In addition, cells undergoing metastatic dormancy are also governed by extracellular matrix (ECM) niches that induce positive signals such as Wnt and Notch and attenuate negative signals like bone morphogenetic protein (BMP) (21). On the contrary, tumor cells at premetastatic sites may undergo dormancy due to delayed adaptation and complex interaction with the local microenvironment (**Figure 2**).

Several signaling pathways such as RAS-MEK-ERK/MAPK and PI3K-Akt play a crucial role during the process of cancer dormancy (17). Additionally, stress signals, including oxidative response and activation of unfolded protein response (UPR) also have a major contribution to metastatic dormancy and

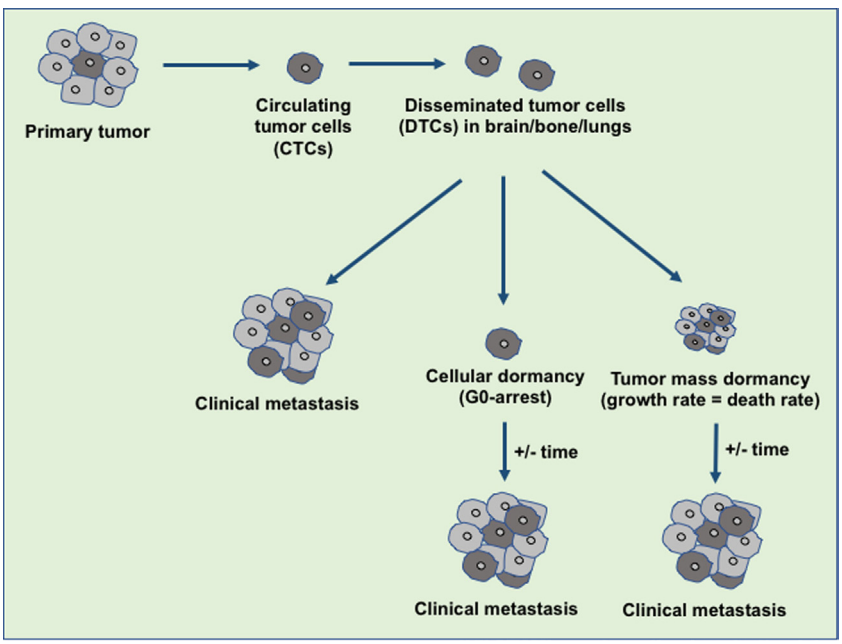

FIGURE 1 | An overview of disseminated tumor cells (DTCs) in dormancy and clinical metastasis relapse. During the metastasis, the disseminated primary tumor cells developed the secondary tumor in the distant organ sites immediately or at a later stage. The tumor microenvironment or the intrinsic factors decide the fate of the DTCs either to develop clinical metastasis or to maintain the dormant state. Over the years, these dormant tumor cells escape from dormancy state and develop the clinical metastasis.

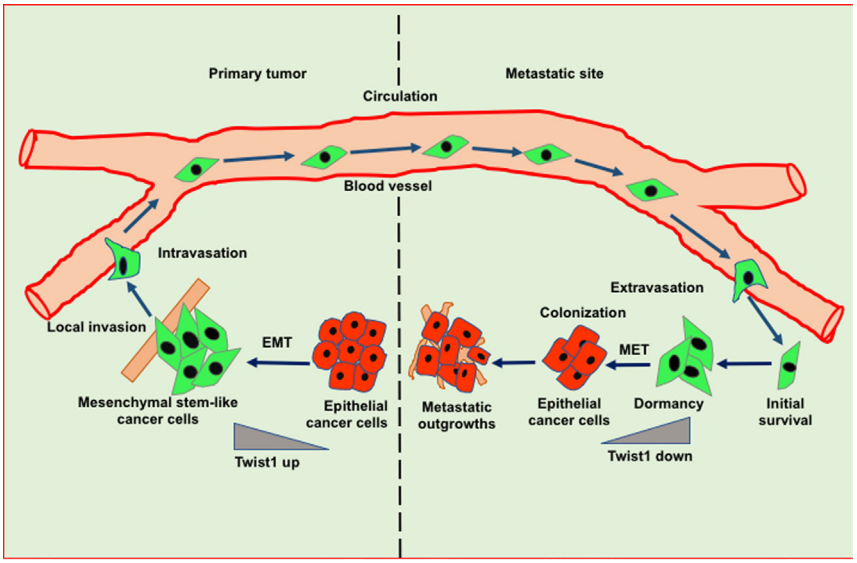

FIGURE 2 | Role of epithelial to mesenchymal transition (EMT) and mesenchymal to epithelial transition (MET) in invasion-metastasis cascade. Cancer cells undergo EMT to acquire stemness and invasion potential leading to cancer cell dissemination. In the target organ, disseminated cancer cells encounter inhibitory signals resulted in the arrest in cell cycle thereby leading to dormancy. Cancer cells undergo MET in order to acquire epithelial features such as proliferation to form metastatic outgrowth in the target organs.

reactivation (21). In addition to various signaling pathways, DNA repair mechanism, and genomic instability also contribute to cancer dormancy (22). It is reported that primary tumor microenvironment may generate a dormant subpopulation, which is capable of evading therapy and responsible for metastatic relapse. It has been shown that metabolic pathway plays a crucial role in dormancy. Studies have demonstrated that altered lipid metabolism coupled with accumulation of reactive oxygen species helps in metastatic recurrence (23).

METASTATIC NICHE IN TUMOR DORMANCY AND REACTIVATION

Several reports suggest that cancer cells undergo a protracted period of dormancy by the inhibitory molecular cues derived from primary tumors or restrains caused by target organ microenvironment (24–27). Bidirectional interaction of metastatic tumor cells with microenvironmental niches are imperative for the reactivation of dormant metastatic cells as well as the induction of mesenchymal to epithelial transition (MET) to sculpt the formation of macrometastases. Premetastatic niche provides a favorable microenvironment during metastasis development. Metastatic niche formation includes inflammation, immunosuppression, angiogenesis/vascular permeability, organotropism, lymphangiogenesis, and cellular reprogramming (28). Further, attachment of tumor cells to native basement membrane facilitates their survival, functional differentiation and growth arrest. This suggests that basement membrane is able to contribute to dormancy properties of DTCs. The DTCs often home to the distant organs where the primary basement membrane is mostly vascular in nature such as bone marrow, lung, liver, and brain (29, 30). Studies have shown a close association between DTCs and vascular basement membrane by using the mouse models of breast tumor dissemination (31). Ghajar et al. have shown that endothelial-derived thrombospondin-1 (TSP-1) induces the quiescence in breast cancer cells and this suppressive cue lost during neovasculature. The time-lapse analysis showed that sprouting vessels permit and accelerate breast cancer cell outgrowth (31). Further, they have shown that recreation of the organotypic microvascular niche of lung and bone marrow promotes dormancy and quiescence (31). It has also been shown that attachment with microvasculature in the perivascular niche is necessary for DTCs survival in mouse brain (32). These data support that endothelial cells help in dormancy induction whereas neovascularization in perivascular niche supports reactivation of dormant cells that leads to metastatic outgrowth.

A recent report suggests that a subset of macrophages (TAMs), known as metastasis-associated macrophages (MAMs), are enriched in metastatic breast cancer as compared to primary tumors. Flt1-regulated signaling in these MAMs upregulates inflammatory gene signature which is imperative for cancer cell survival during metastatic seeding (33). In addition to TAMs, circulating VEGFR1$^+$ and bone marrow-derived CD11b$^+$Gr1$^+$ myeloid cells are involved in premetastatic niche formation (34–36). Myeloid cells expressed versican, an ECM proteoglycan, plays a key role in inducing proliferation of cancer cells to form metastatic outgrowth in the lung (35). CYP4A-induced TAMs promote premetastatic niche formation and metastasis in the lung by recruitment of VEGFR1$^+$ myeloid cells (36). Moreover, induction of TGF-β in myeloid cells by natural killer T cell-derived interleukin (IL)-3 suppresses immune responses and controls tumor recurrence (37). Other stromal cells such as fibroblasts and endothelial cells present at premetastatic

niche also play an important role in this phenomenon. Cancer-associated fibroblasts show activated phenotype and are integral components of premetastatic niche. Studies show that breast cancer metastasis-associated fibroblasts secrete higher level of IL-6 that promotes malignant growth (38). Furthermore, systemic factors derived from primary tumors induce the fibronectin synthesis by fibroblasts to form premetastatic niche by recruiting a fibronectin-binding integrin $\alpha4\beta1^+$ hematopoietic progenitor cells. These hematopoietic progenitor cells remodel the local microenvironment by producing MMP-9 and other factors and stimulating angiogenesis (34, 39, 40). Hence, the metastatic niche plays a pivotal role in the survival, maintenance, and reactivation of DTCs.

MET AND METASTATIC REACTIVATION

Epithelial to mesenchymal transition-driven mesenchymal features in cancer cells enable them to invade and metastasize to the distant organs. Several studies suggest that EMT-inducing transcription factors such as Twist and Snail show inhibitory effects on cancer cell proliferation, however, these factors induce migratory potential by downregulating the cadherin junctions (41). A reverse phenomenon of EMT known as MET helps in the tumor relapse or dormancy reactivation through the restoration of epithelial features. Interestingly, during MET tumor cells actively proliferate and regain adhesive junctions to communicate with the surrounding niche of the metastatic sites (**Figure 2**) (42). Recent reports have shown that blockade of the TGFβ/Smad2 pathway by versican promotes MET phenotype (43). Induction of MET in breast cancer cells is associated with increased metastatic colonization. Tsai et al. have found that attenuation of Twist1 expression promotes the metastatic outgrowth by inducing MET and proliferation of cancer cells (44). Additionally, Prrx1 another EMT transcription factor confers the migratory and invasive properties of cancer cells. Various studies showed that loss of Prrx1 contributes to metastatic colonization by stimulating MET phenotype. Moreover, downregulation of Prrx1 is associated with metastatic disease and poor survival of patients (45). Several studies showed that accumulation of genetic and epigenetic changes in tumor cells facilitated them to revert dormancy and undergo metastatic reactivation. Posttranslational modification of histones is extensively studied epigenetic change which has been observed in transcriptional activation of various EMT/MET-associated genes. The recent report suggests that H3K27me3-demethylase KDM6A expression toggles during EMT and MET processes. KDM6A catalytically removes di- and tri-methyl groups from H3K27me3 suppressive mark of the H3K4me3/H3K27me3 bivalent promoters; to promote the expression of target genes associated with differentiation, proliferation and cellular adhesion (46). Collectively, these studies suggest that the stromal cell signaling and MET contribute to metastatic reactivation.

MECHANISMS OF CELLULAR DORMANCY

Metastatic dormancy is a result of growth arrest either in a single DTC termed as cellular dormancy or in micrometastatic lesions called as tumor mass dormancy. Cellular dormancy marked by a quiescent state in DTCs is associated with the decline in Ki67 expression, a proliferation marker or G0/G1 cell cycle arrest. There are various cellular and molecular mechanisms through which DTCs undergo dormancy which is discussed below.

Stress-Induced Signaling and UPR in Cellular Dormancy

Mitogen, stress signal, and other factors present in the premetastatic niche may be responsible for cell cycle arrest and dormancy. Crosstalk between mitogen and stress-induced signaling pathways are crucial for cellular dormancy. Studies have shown that a set of genes selectively affects the growth at the secondary site including MKK4, MKK6, and Nm23-H1. Interestingly, MKK4 and MKK6 are upstream activators of p38 while, Nm23-H1 indirectly downregulates ERK1/2 by inhibiting EDG2 LPA receptor, a strong activator of ERK1/2 (47). Hence, ERK/p38 signaling ratio seems to have a crucial role in cancer cell dormancy and reactivation (**Figure 3**). Several studies showed that the enhanced levels of p38 MAPK over ERK1/2 upon downregulation of uPAR induces dormancy in squamous cell carcinoma (48, 49). Researchers have demonstrated that Minibrain-related kinase/dual specificity tyrosine phosphorylation-regulated kinase 1B (Mirk/DYRK1B) blocks cyclin D1 and CDK4 which further regulates the survival signals and cell cycle arrest in pancreatic and ovarian cancer cells (50–52). Likewise, MAPKK4 has been shown to exert dormancy by the upregulation of JNK pathway in prostate and ovarian cancer cells (53, 54).

Several reports have shown that the upregulation of various UPR-associated genes like Grp78, Grp94, PDI, heat shock protein 47 (HSP47), and cyclophilin B in dormant cells play a crucial role in metastatic dormancy (55–58). Ranganathan et al. showed that stress-induced p38 activation leads to upregulation of the endoplasmic reticulum (ER) chaperone BiP. Further, this factor increases the activation of the ER stress-activated PERK signaling that results in higher survival and therapy resistance in dormant cells (56). Additionally, p38 kinase-mediated activation UPR also induces the expression of the ER stress-regulated transcription factor ATF6 and promotes mTOR-mediated survival of the dormant cells (59). Moreover, the mechanistic analysis in DTCs derived from bone marrow of breast cancer patient revealed that the expression of Grp78, a UPR protein, upregulated in low oxygen and glucose conditions and promotes higher proliferation and sustained survival (58).

Microenvironmental factors like BMPs and growth arrest-specific 6 (GAS6) derived from mesenchymal cells and osteoclasts, respectively, can curb proliferation and induce dormancy in cancer cells (**Figure 3**). By using the prostate cancer bone metastasis model, Kobayashi et al. have demonstrated that BMP7 promotes dormancy. BMP7 induces the expression of metastasis suppressor gene N-myc, leading to the activation of p38 MAPK, p21, and cell cycle arrest (60). Moreover, Shiozawa et al. reported that the activation of the GAS6 receptor in prostate cancer cells in the bone marrow environment plays a critical role in establishing metastatic tumor cell dormancy (61). The recent study has demonstrated that latency competent cancer cells from early-stage human lung and breast carcinoma cells can self-imposed in a

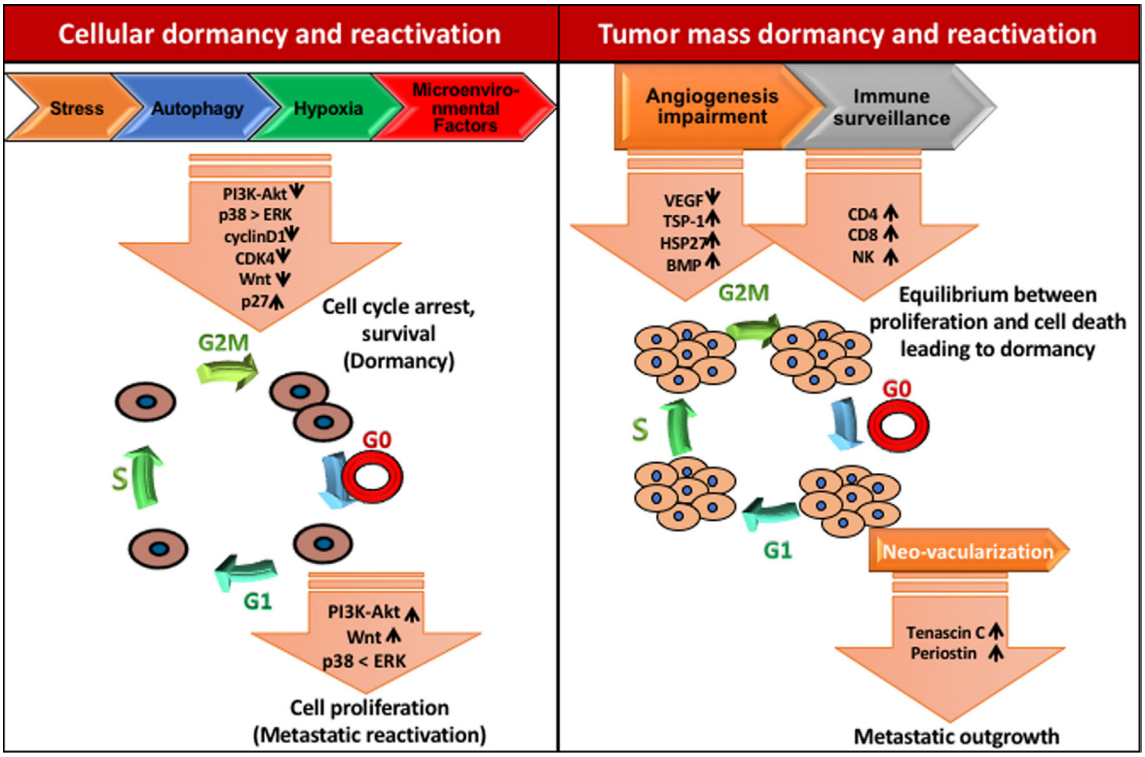

FIGURE 3 | Mechanisms of tumor dormancy. Solitary cell dormancy (cellular dormancy, left) is caused by cell cycle arrest and induction of survival mediated by various signaling cascades including downregulation of PI3K-Akt, ERK, and Wnt signaling and upregulation of p38 MAPK signaling. Tumor mass dormancy (right) is a result of the balance between proliferation and cell death due to less blood supply and immune surveillance.

dormant stage by downregulating Wnt signaling and inducing Sox-dependent stem-like state (62). Altogether, these results suggest that stress signaling helps in the single cell dormancy by arresting proliferation and enhancing survival of DTCs in the premetastatic niche.

Hypoxia and Dormancy

In the tumor microenvironment, hypoxia plays a critical role during tumor development and metastasis. Fluegan et al. have explored the influence of hypoxia on the fate of DTCs. They report that hypoxia enhances the expression of key dormancy genes like NR2F1, DEC2, p27 in head and neck squamous cell carcinoma (HNSCC) and primary breast tumor. Posthypoxic solitary DTCs in patient-derived xenografts and transgenic mice show NR2F1^{hi}/DEC2^{hi}/p27^{hi}/TGFβ2^{hi} population with dormant phenotype. NR2F1 and HIF1α involved in the regulation of p27 expression in posthypoxic dormant DTCs. Moreover, hormone receptor-dependent breast cancer cells exhibit higher affinity toward NR2F1-dependent dormancy (63). Harper et al. have delineated the molecular mechanism by which HER2 aberrantly activates a program for early dissemination and generation of DTCs. These early DTCs exhibit p-p38^{lo}p-Atf2^{lo}Twist1^{hi}E-cad^{lo} expression pattern and an EMT-like dissemination program without complete loss of epithelial feature which was recovered after inhibition of HER2 and Wnt signaling (**Figure 3**). Interestingly, the dormancy feature in these early DTCs was p38-independent and even after being Twist1^{hi}E-cad^{lo} and dormant, they were able to initiate metastasis (64). These data indicate that the development of dormancy feature is governed by several intrinsic and extrinsic programs and by contextual cues.

miRNAs in Cellular Dormancy

miRNAs play an important role in the various biological process. It has been shown that miRNAs may affect the hallmarks of cancer, including sustained proliferation, blocking growth inhibition signals, resisting cell death, inducing invasion, metastasis, and angiogenesis (65). Ono et al. have described the role of miRNA derived from bone marrow mesenchymal stem cells in the induction of dormancy in metastatic breast cancer cells isolated from bone marrow of the mice. This study showed that higher expression of miR-23b in metastatic breast cancer cells leads to dormant phenotype by downregulation of MARCKS gene, associated with cell cycle progression and motility (66). The data also showed a consensus set of 19 miRs with the potential role in governing the phenotypic switch of human dormant breast carcinoma, glioblastoma, osteosarcoma, and liposarcoma to outgrowth. They have shown that loss of dormancy-associated miRs (DmiRs, 16/19) reactivate the fast growth of the dormant tumors. However, reestablishment of a single DmiR (miR-580, 588, or 190) results in the phenotypic switch of fast-growing angiogenic tumor toward prolonged dormancy (67).

Autophagy and Dormancy

Autophagy is an extremely conserved self-degradation process, which has an important role in cancer stem cells (CSCs) regulation and tumor cell survival. Several reports suggest that DTCs possess CSCs properties, which prompted researchers to explore the potential role of autophagy in cancer cell dormancy and stress response. Various groups have shown that autophagy helps in the survival of DTCs for protracted periods (68, 69). Autophagy supports DTCs survival by sustaining amino acid levels, ATP production and blocking energetic catastrophe (69–71). Further, induction of autophagy has linked to dormancy. Liang et al. have shown that the activation of LKB1-AMPK leads to induction of ULK1, which initiates autophagy. Further, this pathway activates p27kip1-dependent growth arrest (G1 arrest) and downregulation of this signaling induces apoptotic cell death (72). They have proposed a novel mechanism which links autophagy stimulation, growth arrest and apoptosis. In recent finding, Lu et al. have shown the role of tumor suppressor protein, aplasia Ras homolog member I (ARH1) which partly induces autophagy by inhibiting PI3K/Akt pathway. This study shows that reexpression of ARH1 in SKOv3 ovarian cancer xenograft results in tumor regression likely due to autophagy. However, the xenograft exhibited prolonged growth arrest indicating the onset of dormancy which was reversed after subsequent knockdown of ARH1 (73). These studies link the onset of autophagy with growth arrest/quiescence program and survival which proposing a key role of autophagy in dormancy.

MECHANISMS OF TUMOR MASS DORMANCY

In contrast to single cell dormancy, tumor mass dormancy is governed by a balance between the rate of proliferation and apoptosis in micrometastatic lesions. The tumor mass dormancy is induced by slow proliferation, restrained blood supply and active immune response. Recent studies reveal that the frequency of osteolytic bone metastasis depends on metastatic niche environment rather than the number of cancer cells (74, 75). Moreover, stromal factors such as TGFβ and BMPs have potential role in the regulation of tumor initiation, proliferation and maintenance of the quiescent state. Bragado et al. have suggested that TGFβ2 induces slow cycling and quiescence in cells by suppressing CDK4 and inducing p27 in HNSCC (76). Interestingly, it has been shown in multiple myeloma that a small population of $Ki67^{+}$ cells coexists with dormant cells, proposing that for the reactivation defined niches are essential (77, 78). Unfortunately, the mechanisms behind long-term metastatic dormancy are highly unexplored. However, sustenance of tumor mass dormancy relies on the cellular mechanisms that induce slow cycling.

Micrometastatic lesions require the higher blood supply to grow beyond 1–2 mm, which leads to the induction of vessel formation by secretion of angiogenic factors like VEGF (79). Therefore, the antiangiogenic signaling mechanisms could be an interesting factor, which maintains the tumor mass dormancy (31, 80). These studies show that upregulation of TSP-1, an angiogenic inhibitor induces poor vascularization and dormancy in breast cancer, glioblastoma, osteosarcoma, and liposarcoma under *in vivo* conditions (81). Chaperons like HSP27 also regulate the angiogenesis and dormancy. Ablation of HSP27 in breast cancer prompts the long-term *in vivo* dormancy while its upregulation results in dormancy exit and enhanced vascular density (80).

Clearance of tumor cells by immune system contributes to another mechanism of tumor mass dormancy. Cancer cells coevolve in a microenvironment where the immune system is suppressed. However, DTCs do not have such support and eventually, most of these cells die due to the natural immune response. It has also been reported that immune system regulates the number of DTCs as well as the size of micrometastatic lesions (82). Additionally, the presence of DTCs in bone marrow of breast cancer patients showed the correlation with the higher immune cell subpopulations including NK cells, macrophages and T lymphocytes. All these cell types are known to be involved in rejection of primary tumors and metastasis, which leads to tumor dormancy (83).

MECHANISMS OF METASTATIC REACTIVATION

Dormant cancer cells may be subjected to reactivation to initiate metastasis in response to specific signals from their specialized niche, which maintains the balance between the self-renewal and production of differentiated progeny (84–88). Cancer cells start preconditioning the host microenvironment even before seeding by secreting various soluble factors (39, 89). Heparanase, osteopontin, and lysyl oxidase facilitate the invasion, survival, and proliferation of metastatic breast cancer cells (90–92). After extravasation, DTCs may encounter different niches including perivascular niche. It has been shown that attachment of DTCs on the abluminal surface of mature blood vessels promotes dormancy through endothelium-derived TSP-1, while neovascularization creates a local microenvironment favoring metastatic reactivation. After neovascular sprouting, vessel homeostasis gets disrupted and endothelial cells start secreting tumor-promoting signals and growth factors like ECM proteins, periostin and active TGFβ that leads to micrometastatic outgrowth (31). It has been reported that ECM protein tenascin C activates Notch and Wnt signaling leading to enhanced metastatic outgrowth (93, 94). TGFβ helps in the production of periostin from stromal fibroblasts and endothelial cells in the neovascular area that supports metastatic outgrowth (31, 95). Further, Gao et al. have reported that Coco a secreted antagonist of TGFβ ligand reactivates solitary breast cancer cells at organ-specific metastatic sites by shielding metastasis-initiating cells from inhibitory signals provided by lung-derived BMP proteins. A large group of patients expressing Coco showed predicted relapse to lung but not to brain and bone due to the absence of bioactive BMP (96). Hence, the metastasis-initiating cells may promote the permissive niche comprising of matrix proteins which are involved in activation of specific signaling pathways such as Wnt and Notch that in turn activate their self-renewal. Recent report suggests that the TAM family of receptor tyrosine kinases TYRO3, AXL, and MERTK have a potential role in dormancy regulation in prostate cancer. MERTK stimulates

the reactivation of dormant prostate cancer cells through MAP kinase-dependent mechanism, which involves p27, pluripotency transcription factors, and histone methylation (97).

THERAPEUTIC IMPLICATIONS OF DORMANCY AND REACTIVATION

Recent achievements in cancer therapy and increased overall survival motivate the researchers to look for new diagnostics for the patients at high risk of late metastasis and therapeutic system targeting DTCs. The limitation of current conventional and adjuvant therapies to prevent relapse, is they basically target growing tumor cells rather than DTCs. The systemic nature of the metastatic disease along with the heterogeneity of metastatic tumors, complex inter-connected pathways and the resistance against therapy makes its pharmacological management very difficult. Hence, there is a need to focus on preventing metastasis (98, 99). Bone-modifying drugs have been used clinically for management of bone metastasis-related morbidity. However, when they used in the preventive adjuvant setting against cancer, inconclusive results were observed (98–100). A detailed understanding of the mechanism of metastatic dormancy and colonization along with innovative therapeutics must be developed to solve this medical dilemma. For this, therapeutic agents that can inhibit metastasis by targeting metastatic cell-autonomous functions and mechanisms responsible for dormancy and their survival would serve as a new opportunity to prevent minimal residual disease (**Figure 4**). Since DTCs are highly dependent on signaling, hence targeting these pathways may be helpful in enhancing the efficacy of adjuvant therapy and managing the metastatic relapse. Based on existing reports, targeting Src, Akt, or Tor by using their inhibitors alone or in combination with chemotherapy can be a potential approach for the treatment of minimal residual disease. Studies under *in vivo* preclinical and 3D *in vitro* model of dormancy demonstrated that targeting the Src family kinase and MEK1/2 using their specific inhibitors resulted in apoptosis in a large fraction of the dormant cells and delayed metastatic outgrowth in breast cancer (101). Inhibition of Src kinase family signaling or Src knockdown leads to the nuclear localization of cyclin-dependent kinase inhibitor p27 resulting in prevention of metastatic outgrowth; however, it did not affect the survival of the dormant cells. MEK1/2 inhibitors that block the downstream ERK1/2 signaling suppresses DTCs survival. Several studies have shown that the various phenotypic and functional similarities are shared between metastasis-initiating cells and CSCs. Hence, CSCs targeted therapies may be effective in the treatment of metastatic disease. Moreover, stem cell signaling pathways also induce resistance to chemotherapy. Thus, combination therapy targeting stem cell pathways like Notch and Wnt along with canonical oncogenic pathway or reactivating BMP signaling may be effective in metastatic disease therapy. It has been shown that autophagy promotes the survival of the dormant cancer cells. Interestingly, inhibition of autophagy reduces clonogenic survival of lung, cervical, and breast cancer cell (102). Therefore, autophagy can also be considered as a therapeutic target in cancer metastasis.

Immunotherapy is being explored extensively for cancer management. Saudemont et al. have shown NK cells-based immune therapy targets dormant cells. Their study demonstrated that NK cells activated by CXCL10 can kill dormant tumor cells which are able to resist CTL-mediated lysis (103). As discussed

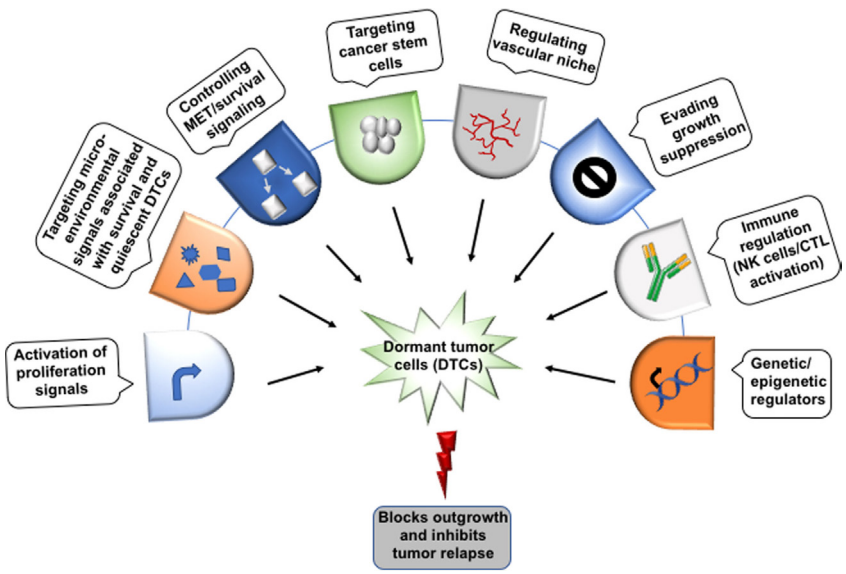

FIGURE 4 | Therapeutic implications of dormant tumor cells. The possible target sites to eliminate the dormant tumor cells (DTCs) in order to regulate metastatic relapse. Though the direct evidence to target the dormant cells yet needs to identify extensively. Moreover, the dormant cells can be targeted at several checkpoints including epigenetic regulators (DNMT1, EZH2), immune cells (NK cells/CTL) activation, evading growth suppression, vascular niche, quiescent cancer stem cells, survival signaling, and the microenvironment signals (bone morphogenetic protein 4/7, CXCL12, TRAIL, growth arrest-specific 6, TGFβ-2, BME, and thrombospondin 1) that help in the maintenance of the dormant state.

earlier, secretory molecules and cytokines in microenvironment also play a key role in the regulation of dormancy (**Figure 4**). Osteopontin, an ECM protein has been reported in the progression of various cancers (91, 104, 105). Boyerinas et al. have shown that stromal osteopontin helps in anchoring leukemia cells in bone marrow premetastatic niche and support dormancy by inducing cell cycle arrest. Neutralizing the osteopontin resulted in the proliferation of dormant cells and enable them sensitive to chemotherapy (106). Hence, the better understanding of the mechanism governing dormancy and reactivation and the role of metastatic niche may help in the identification of new potential therapeutic targets for the treatment of minimal residual disease.

FUTURE DIRECTION

Tumor dormancy and reactivation has become an interesting point as a key element of tumor evolution and metastatic relapse. Although metastasis-initiating cells undergo dormancy and ultimately get reactivated under the influence of microenvironment signals, various key questions are still unanswered. It will be interesting to explore the phenotypic and functional similarities between DTCs and CSCs, the role of MET, microenvironmental niches and genetic and epigenetic changes in metastasis-initiating cells in metastatic reactivation. Current approaches and models to investigate the molecular basis of metastasis have been very successful. Nevertheless, new approaches need to be discovered in order to gain an in-depth understanding of tumor dormancy and reactivation. Lineage-tracing studies utilizing newly developed reporter systems can provide critical understanding in this area by using the transgenic mouse models which mimic the natural conditions. Moreover, recently invented genetic screening strategy can be useful in quick identification of mediators involved in dormancy and reactivation. Future studies need to be conducted to assess the efficacy of screening the shRNA libraries for the recognition of regulators of dormancy and their potential use in various tumor types and clinical samples.

Advance strategies for characterization of various aspects of CTCs and better access to samples of metastases will be required to complete this goal. With the current progress in the field of metastasis, these questions will be addressed rapidly by designing and implementing the improved strategies for cancer treatment.

AUTHOR CONTRIBUTIONS

DK, AY, PP, and RB drafted the manuscript, composed the figures, and critically revised the manuscript. DK and GK conceived the manuscript and finalized the draft. NR, SR, SB, and MG have written some part and revised the manuscript. All authors read and approved the final manuscript.

ACKNOWLEDGMENTS

We would like to thank Anuradha Bulbule for useful discussion and reading the manuscript. We apologize to many colleagues whose contributions could not site due to lack of space.

REFERENCES

1. Gupta GP, Massagué J. Cancer metastasis: building a framework. *Cell* (2006) 127(4):679–95. doi:10.1016/j.cell.2006.11.00
2. Hanahan D, Weinberg RA. Hallmarks of cancer: the next generation. *Cell* (2011) 144(5):646–74. doi:10.1016/j.cell.2011.02.013
3. Bos PD, Zhang XH, Nadal C, Shu W, Gomis RR, Nguyen DX, et al. Genes that mediate breast cancer metastasis to the brain. *Nature* (2009) 459(7249): 1005–9. doi:10.1038/nature08021
4. Lu X, Mu E, Wei Y, Riethdorf S, Yang Q, Yuan M, et al. VCAM-1 promotes osteolytic expansion of indolent bone micrometastasis of breast cancer by engaging α4β1-positive osteoclast progenitors. *Cancer Cell* (2011) 20(6):701–14. doi:10.1016/j.ccr.2011.11.002
5. Zhang XH, Wang Q, Gerald W, Hudis CA, Norton L, Smid M, et al. Latent bone metastasis in breast cancer tied to Src-dependent survival signals. *Cancer Cell* (2009) 16(1):67–78. doi:10.1016/j.ccr.2009.05.017
6. Padua D, Zhang XH, Wang Q, Nadal C, Gerald WL, Gomis RR, et al. TGFbeta primes breast tumors for lung metastasis seeding through angiopoietin-like 4. *Cell* (2008) 133(1):66–77. doi:10.1016/j.cell.2008.01.046
7. Nguyen DX, Bos PD, Massagué J. Metastasis: from dissemination to organ-specific colonization. *Nat Rev Cancer* (2009) 9(4):274–84. doi:10.1038/nrc2622
8. Manjili MH. Tumor dormancy and relapse: from a natural byproduct of evolution to a disease state. *Cancer Res* (2017) 77(10):2564–9. doi:10.1158/0008-5472.CAN-17-0068
9. Braun S, Naume B. Circulating and disseminated tumor cells. *J Clin Oncol* (2005) 23(8):1623–6. doi:10.1200/JCO.2005.10.073
10. Ross JS, Slodkowska EA. Circulating and disseminated tumor cells in the management of breast cancer. *Am J Clin Pathol* (2009) 132(2):237–45. doi:10.1309/AJCPJI7DEOLKCS6F
11. Páez D, Labonte MJ, Bohanes P, Zhang W, Benhanim L, Ning Y, et al. Cancer dormancy: a model of early dissemination and late cancer recurrence. *Clin Cancer Res* (2012) 18(3):645–53. doi:10.1158/1078-0432.CCR-11-2186
12. Gay LJ, Malanchi I. The sleeping ugly: tumour microenvironment's act to make or break the spell of dormancy. *Biochim Biophys Acta* (2017) 1868(1): 231–8. doi:10.1016/j.bbcan.2017.05.002
13. Gao XL, Zhang M, Tang YL, Liang XH. Cancer cell dormancy: mechanisms and implications of cancer recurrence and metastasis. *Onco Targets Ther* (2017) 10:5219–28. doi:10.2147/OTT.S140854
14. Dasgupta A, Lim AR, Ghajar CM. Circulating and disseminated tumor cells: harbingers or initiators of metastasis? *Mol Oncol* (2017) 11(1):40–61. doi:10.1002/1878-0261.12022
15. Body JJ, Casimiro S, Costa L. Targeting bone metastases in prostate cancer: improving clinical outcome. *Nat Rev Urol* (2015) 12(6):340–56. doi:10.1038/nrurol.2015.90
16. Aguirre-Ghiso JA. Models, mechanisms and clinical evidence for cancer dormancy. *Nat Rev Cancer* (2007) 7(11):834–46. doi:10.1038/nrc2256
17. Yeh AC, Ramaswamy S. Mechanisms of cancer cell dormancy-another hallmark of cancer? *Cancer Res* (2015) 75(23):5014–22. doi:10.1158/0008-5472.CAN-15-1370
18. Todenhöfer T, Hennenlotter J, Faber F, Wallwiener D, Schilling D, Kühs U, et al. Significance of apoptotic and non-apoptotic disseminated tumor cells in the bone marrow of patients with clinically localized prostate cancer. *Prostate* (2015) 75(6):637–45. doi:10.1002/pros.22947
19. Gomis RR, Gawrzak S. Tumor cell dormancy. *Mol Oncol* (2016) 11:62–78. doi:10.1016/j.molonc.2016.09.009
20. Patel P, Chen EI. Cancer stem cells, tumor dormancy, and metastasis. *Front Endocrinol* (2012) 3:125. doi:10.3389/fendo.2012.00125
21. Giancotti FG. Mechanisms governing metastatic dormancy and reactivation. *Cell* (2013) 155(4):750–64. doi:10.1016/j.cell.2013.10.029
22. Evans EB, Lin SY. New insights into tumor dormancy: targeting DNA repair pathways. *World J Clin Oncol* (2015) 6(5):80–8. doi:10.5306/wjco.v6.i5.80
23. Havas KM, Milchevskaya V, Radic K, Alladin A, Kafkia E, Garcia M, et al. Metabolic shifts in residual breast cancer drive tumor recurrence. *J Clin Invest* (2017) 127(6):2091–105. doi:10.1172/JCI89914

24. Shachaf CM, Kopelman AM, Arvanitis C, Karlsson Å, Beer S, Mandl S, et al. MYC inactivation uncovers pluripotent differentiation and tumour dormancy in hepatocellular cancer. *Nature* (2004) 431(7012):1112–7. doi:10.1038/nature03043
25. Holmgren L, O'Reilly MS, Folkman J. Dormancy of micrometastases: balanced proliferation and apoptosis in the presence of angiogenesis suppression. *Nat Med* (1995) 1(2):149–53. doi:10.1038/nm0295-149
26. Eyles J, Puaux AL, Wang X, Toh B, Prakash C, Hong M, et al. Tumor cells disseminate early, but immunosurveillance limits metastatic outgrowth, in a mouse model of melanoma. *J Clin Invest* (2010) 120(6):2030–9. doi:10.1172/JCI42002
27. Rabinovsky R, Uhr JW, Vitetta ES, Yefenof E. Cancer dormancy: lessons from a B cell lymphoma and adenocarcinoma of the prostate. *Adv Cancer Res* (2007) 97:189–202. doi:10.1016/S0065-230X(06)97008-0
28. Liu Y, Cao X. Characteristics and significance of the pre-metastatic niche. *Cancer Cell* (2016) 30(5):668–81. doi:10.1016/j.ccell.2016.09.011
29. Ghajar CM. Metastasis prevention by targeting the dormant niche. *Nat Rev Cancer* (2015) 15(4):238–47. doi:10.1038/nrc3910
30. Chambers AF, Groom AC, MacDonald IC. Dissemination and growth of cancer cells in metastatic sites. *Nat Rev Cancer* (2002) 2(8):563–72. doi:10.1038/nrc865
31. Ghajar CM, Peinado H, Mori H, Matei IR, Evason KJ, Brazier H, et al. The perivascular niche regulates breast tumour dormancy. *Nat Cell Biol* (2013) 15(7):807–17. doi:10.1038/ncb2767
32. Kienast Y, von Baumgarten L, Fuhrmann M, Klinkert WE, Goldbrunner R, Herms J, et al. Real-time imaging reveals the single steps of brain metastasis formation. *Nat Med* (2010) 16(1):116–22. doi:10.1038/nm.2072
33. Qian BZ, Zhang H, Li J, He T, Yeo EJ, Soong DY, et al. FLT1 signaling in metastasis-associated macrophages activates an inflammatory signature that promotes breast cancer metastasis. *J Exp Med* (2015) 212(9):1433–48. doi:10.1084/jem.20141555
34. Kaplan RN, Riba RD, Zacharoulis S, Bramley AH, Vincent L, Costa C, et al. VEGFR1-positive haematopoietic bone marrow progenitors initiate the pre-metastatic niche. *Nature* (2005) 438(7069):820–7. doi:10.1038/nature04186
35. Gao D, Joshi N, Choi H, Ryu S, Hahn M, Catena R, et al. Myeloid progenitor cells in the premetastatic lung promote metastases by inducing mesenchymal to epithelial transition. *Cancer Res* (2012) 72(6):1384–94. doi:10.1158/0008-5472.CAN-11-2905
36. Chen XW, Yu TJ, Zhang J, Li Y, Chen HL, Yang GF, et al. CYP4A in tumor-associated macrophages promotes pre-metastatic niche formation and metastasis. *Oncogene* (2017) 36(35):5045–57. doi:10.1038/onc.2017.118
37. Terabe M, Matsui S, Park JM, Mamura M, Noben-Trauth N, Donaldson DD, et al. Transforming growth factor-beta production and myeloid cells are an effector mechanism through which CD1d-restricted T cells block cytotoxic T lymphocyte-mediated tumor immunosurveillance: abrogation prevents tumor recurrence. *J Exp Med* (2003) 198(11):1741–52. doi:10.1084/jem.20022227
38. Studebaker AW, Storci G, Werbeck JL, Sansone P, Sasser AK, Tavolari S, et al. Fibroblasts isolated from common sites of breast cancer metastasis enhance cancer cell growth rates and invasiveness in an interleukin-6–dependent manner. *Cancer Res* (2008) 68(21):9087–95. doi:10.1158/0008-5472.CAN-08-0400
39. Psaila B, Lyden D. The metastatic niche: adapting the foreign soil. *Nat Rev Cancer* (2009) 9(4):285–93. doi:10.1038/nrc2621
40. van Deventer HW, Wu QP, Bergstralh DT, Davis BK, O'Connor BP, Ting JP, et al. C-C chemokine receptor 5 on pulmonary fibrocytes facilitates migration and promotes metastasis via matrix metalloproteinase 9. *Am J Pathol* (2008) 173(1):253–64. doi:10.2353/ajpath.2008.070732
41. Thiery JP, Acloque H, Huang RY, Nieto MA. Epithelial-mesenchymal transitions in development and disease. *Cell* (2009) 139(5):871–90. doi:10.1016/j.cell.2009.11.007
42. Yao D, Dai C, Peng S. Mechanism of the mesenchymal–epithelial transition and its relationship with metastatic tumor formation. *Mol Cancer Res* (2011) 9(12):1608–20. doi:10.1158/1541-7786.MCR-10-0568
43. Gao D, Vahdat LT, Wong S, Chang JC, Mittal V. Microenvironmental regulation of epithelial–mesenchymal transitions in cancer. *Cancer Res* (2012) 72(19):4883–9. doi:10.1158/0008-5472.CAN-12-1223
44. Tsai JH, Donaher JL, Murphy DA, Chau S, Yang J. Spatiotemporal regulation of epithelial-mesenchymal transition is essential for squamous cell carcinoma metastasis. *Cancer Cell* (2012) 22(6):725–36. doi:10.1016/j.ccr.2012.09.022
45. Ocaña OH, Córcoles R, Fabra Á, Moreno-Bueno G, Acloque H, Vega S, et al. Metastatic colonization requires the repression of the epithelial-mesenchymal transition inducer Prrx1. *Cancer Cell* (2012) 22(6):709–24. doi:10.1016/j.ccr.2012.10.012
46. Taube JH, Sphyris N, Johnson KS, Reisenauer KN, Nesbit TA, Joseph R, et al. The H3K27me3-demethylase KDM6A is suppressed in breast cancer stem-like cells, and enables the resolution of bivalency during the mesenchymal-epithelial transition. *Oncotarget* (2017) 8(39):65548–65. doi:10.18632/oncotarget.19214
47. Sosa MS, Avivar-Valderas A, Bragado P, Wen HC, Aguirre-Ghiso JA. ERK1/2 and p38α/β signaling in tumor cell quiescence: opportunities to control dormant residual disease. *Clin Cancer Res* (2011) 17(18):5850–7. doi:10.1158/1078-0432.CCR-10-2574
48. Aguirre-Ghiso JA, Estrada Y, Liu D, Ossowski L. ERK(MAPK) activity as a determinant of tumor growth and dormancy; regulation by p38(SAPK). *Cancer Res* (2003) 63(7):1684–95.
49. Aguirre-Ghiso JA, Liu D, Mignatti A, Kovalski K, Ossowski L. Urokinase receptor and fibronectin regulate the ERK(MAPK) to p38(MAPK) activity ratios that determine carcinoma cell proliferation or dormancy *in vivo*. *Mol Biol Cell* (2001) 12(4):863–79. doi:10.1091/mbc.12.4.863
50. Deng X, Ewton DZ, Friedman E. Mirk/Dyrk1B maintains the viability of quiescent pancreatic cancer cells by reducing levels of reactive oxygen species. *Cancer Res* (2009) 69(8):3317–24. doi:10.1158/0008-5472.CAN-08-2903
51. Jin K, Ewton DZ, Park S, Hu J, Friedman E. Mirk regulates the exit of colon cancer cells from quiescence. *J Biol Chem* (2009) 284(34):22916–25. doi:10.1074/jbc.M109.035519
52. Ewton DZ, Hu J, Vilenchik M, Deng X, Luk KC, Polonskaia A, et al. Inactivation of mirk/dyrk1b kinase targets quiescent pancreatic cancer cells. *Mol Cancer Ther* (2011) 10(11):2104–14. doi:10.1158/1535-7163.MCT-11-0498
53. Hickson JA, Huo D, Vander Griend DJ, Lin A, Rinker-Schaeffer CW, Yamada SD. The p38 kinases MKK4 and MKK6 suppress metastatic colonization in human ovarian carcinoma. *Cancer Res* (2006) 66(4):2264–70. doi:10.1158/0008-5472.CAN-05-3676
54. Vander Griend DJ, Kocherginsky M, Hickson JA, Stadler WM, Lin A, Rinker-Schaeffer CW. Suppression of metastatic colonization by the context-dependent activation of the c-Jun NH2-terminal kinase kinases JNKK1/MKK4 and MKK7. *Cancer Res* (2005) 65(23):10984–91. doi:10.1158/0008-5472.CAN-05-2382
55. Bartkowiak K, Effenberger KE, Harder S, Andreas A, Buck F, Peter-Katalinic J, et al. Discovery of a novel unfolded protein response phenotype of cancer stem/progenitor cells from the bone marrow of breast cancer patients. *J Proteome Res* (2010) 9(6):3158–68. doi:10.1021/pr100039d
56. Ranganathan AC, Zhang L, Adam AP, Aguirre-Ghiso JA. Functional coupling of p38-induced up-regulation of BiP and activation of RNA-dependent protein kinase-like endoplasmic reticulum kinase to drug resistance of dormant carcinoma cells. *Cancer Res* (2006) 66(3):1702–11. doi:10.1158/0008-5472.CAN-05-3092
57. Chery L, Lam HM, Coleman I, Lakely B, Coleman R, Larson S, et al. Characterization of single disseminated prostate cancer cells reveals tumor cell heterogeneity and identifies dormancy associated pathways. *Oncotarget* (2014) 5(20):9939–51. doi:10.18632/oncotarget.2480
58. Bartkowiak K, Kwiatkowski M, Buck F, Gorges TM, Nilse L, Assmann V, et al. Disseminated tumor cells persist in the bone marrow of breast cancer patients through sustained activation of the unfolded protein response. *Cancer Res* (2015) 75(24):5367–77. doi:10.1158/0008-5472.CAN-14-3728
59. Schewe DM, Aguirre-Ghiso JA. ATF6alpha-Rheb-mTOR signaling promotes survival of dormant tumor cells *in vivo*. *Proc Natl Acad Sci U S A* (2008) 105(30):10519–24. doi:10.1073/pnas.0800939105
60. Kobayashi A, Okuda H, Xing F, Pandey PR, Watabe M, Hirota S, et al. Bone morphogenetic protein 7 in dormancy and metastasis of prostate cancer stem-like cells in bone. *J Exp Med* (2011) 208(13):2641–55. doi:10.1084/jem.20110840
61. Shiozawa Y, Pedersen EA, Patel LR, Ziegler AM, Havens AM, Jung Y, et al. GAS6/AXL axis regulates prostate cancer invasion, proliferation, and survival in the bone marrow niche. *Neoplasia* (2010) 12(2):116–27. doi:10.1593/neo.91384

62. Malladi S, Macalinao DG, Jin X, He L, Basnet H, Zou Y, et al. Metastatic latency and immune evasion through autocrine inhibition of WNT. *Cell* (2016) 165(1):45–60. doi:10.1016/j.cell.2016.02.025
63. Fluegen G, Avivar-Valderas A, Wang Y, Padgen MR, Williams JK, Nobre AR, et al. Phenotypic heterogeneity of disseminated tumour cells is preset by primary tumour hypoxic microenvironments. *Nat Cell Biol* (2017) 19(2): 120–32. doi:10.1038/ncb3465
64. Harper KL, Sosa MS, Entenberg D, Hosseini H, Cheung JF, Nobre R, et al. Mechanism of early dissemination and metastasis in Her2+ mammary cancer. *Nature* (2016) 540:588–92. doi:10.1038/nature20609
65. Peng Y, Croce CM. The role of MicroRNAs in human cancer. *Signal Transduct Target Ther* (2016) 1:15004. doi:10.1038/sigtrans.2015.4
66. Ono M, Kosaka N, Tominaga N, Yoshioka Y, Takeshita F, Takahashi RU, et al. Exosomes from bone marrow mesenchymal stem cells contains a microRNA that promotes dormancy in metastatic breast cancer cells. *Sci Signal* (2014) 7(332):ra63. doi:10.1126/scisignal.2005231
67. Almog N, Ma L, Schwager C, Brinkmann BG, Beheshti A, Vajkoczy P, et al. Consensus micro RNAs governing the switch of dormant tumors to the fast-growing angiogenic phenotype. *PLoS One* (2012) 7(8):e44001. doi:10.1371/journal.pone.0044001
68. Lu Z, Luo RZ, Lu Y, Zhang X, Yu Q, Khare S, et al. The tumor suppressor gene ARHI regulates autophagy and tumor dormancy in human ovarian cells. *J Clin Invest* (2008) 118(12):3917–29. doi:10.1172/JCI35512
69. Sosa MS, Bragado P, Aguirre-Ghiso JA. Mechanisms of disseminated cancer cell dormancy: an awakening field. *Nat Rev Cancer* (2014) 14(9):611–22. doi:10.1038/nrc3793
70. Galluzzi L, Pietrocola F, Levine B, Kroemer G. Metabolic control of autophagy. *Cell* (2014) 159(6):1263–76. doi:10.1016/j.cell.2014.11.006
71. Lum JJ, Bauer DE, Kong M, Harris MH, Li CY, Lindsten T, et al. Growth factor regulation of autophagy and cell survival in the absence of apoptosis. *Cell* (2005) 120(2):237–48. doi:10.1016/j.cell.2004.11.046
72. Liang J, Saho SH, Xu ZX, Hennessy B, Ding Z, Larrea M, et al. The energy sensing LKB1-AMPK pathway regulates p27kip1 phosphorylation mediatiing the decision to enter autophagy or apoptosis. *Nat Cell Biol* (2007) 9(2):218–24. doi:10.1038/ncb1537
73. Lu Z, Yang H, Sutton MN, Yang M, Clarke CH, Liao WS, et al. ARHI (DIRAS3) induces autophagy in ovarian cancer cells by downregulating the epidermal growth factor receptor, inhibiting PI3K and Ras/MAP signaling and activating the FOXo3a-mediated induction of Rab7. *Cell Death Differ* (2014) 21(8):1275–89. doi:10.1038/cdd.2014.48
74. Wang N, Reeves KJ, Brown HK, Fowles AC, Docherty FE, Ottewell PD, et al. The frequency of osteolytic bone metastasis is determined by conditions of the soil, not the number of seeds; evidence from in vivo models of breast and prostate cancer. *J Exp Clin Cancer Res* (2015) 34:124. doi:10.1186/s13046-015-0240-8
75. Wang H, Yu C, Gao X, Welte T, Muscarella AM, Tian L, et al. The osteogenic niche promotes early-stage bone colonization of disseminated breast cancer cells. *Cancer Cell* (2015) 27(2):193–210. doi:10.1016/j.ccell.2014.11.017
76. Bragado P, Estrada Y, Parikh F, Krause S, Capobianco C, Farina HG, et al. TGF-β2 dictates disseminated tumour cell fate in target organs through TGF-β-RIII and p38α/β signalling. *Nat Cell Biol* (2013) 15(11):1351–61. doi:10.1038/ncb2861
77. Lawson DA, Bhakta NR, Kessenbrock K, Prummel KD, Yu Y, Takai K, et al. Single-cell analysis reveals a stem-cell program in human metastatic breast cancer cells. *Nature* (2015) 526(7571):131–5. doi:10.1038/nature15260
78. Lawson MA, McDonald MM, Kovacic N, Hua Khoo W, Terry RL, Down J, et al. Osteoclasts control reactivation of dormant myeloma cells by remodelling the endosteal niche. *Nat Commun* (2015) 6:8983. doi:10.1038/ncomms9983
79. Gao D, Nolan DJ, Mellick AS, Bambino K, McDonnell K, Mittal V. Endothelial progenitor cells control the angiogenic switch in mouse lung metastasis. *Science* (2008) 319(5860):195–8. doi:10.1126/science.1150224
80. Straume O, Shimamura T, Lampa MJ, Carretero J, Øyan AM, Jia D, et al. Suppression of heat shock protein 27 induces long-term dormancy in human breast cancer. *Proc Natl Acad Sci U S A* (2012) 109(22):8699–704. doi:10.1073/pnas.1017909109
81. Lawler J. Thrombospondin-1 as an endogenous inhibitor of angiogenesis and tumor growth. *J Cell Mol Med* (2002) 6(1):1–12. doi:10.1111/j.1582-4934.2002.tb00307.x
82. Müller M, Gounari F, Prifti S, Hacker HJ, Schirrmacher V, Khazaie K. EblacZ tumor dormancy in bone marrow and lymph nodes: active control of proliferating tumor cells by CD8+ immune T cells. *Cancer Res* (1998) 58(23):5439–46.
83. Feuerer M, Rocha M, Bai L, Umansky V, Solomayer EF, Bastert G, et al. Enrichment of memory T cells and other profound immunological changes in the bone marrow from untreated breast cancer patients. *Int J Cancer* (2001) 92(1): 96–105. doi:10.1002/1097-0215(200102)9999:9999<:AID-IJC1152>3.0.CO;2-Q
84. Alvarez-Buylla A, Lim DA. For the long run: maintaining germinal niches in the adult brain. *Neuron* (2004) 41(5):683–6. doi:10.1016/S0896-6273(04)00111-4
85. Hsu YC, Fuchs E. A family business: stem cell progeny join the niche to regulate homeostasis. *Nat Rev Mol Cell Biol* (2012) 13(2):103–14. doi:10.1038/nrm3272
86. Kumar D, Gorain M, Kundu G, Kundu GC. Therapeutic implications of cellular and molecular biology of cancer stem cells in melanoma. *Mol Cancer* (2017) 16(1):7. doi:10.1186/s12943-016-0578-3
87. Morrison SJ, Spradling AC. Stem cells and niches: mechanisms that promote stem cell maintenance throughout life. *Cell* (2008) 132(4):598–611. doi:10.1016/j.cell.2008.01.038
88. Kumar D, Kumar S, Gorain M, Tomar D, Patil HS, Radharani NN, et al. Notch1-MAPK signaling axis regulates CD133+ cancer stem cell-mediated melanoma growth and angiogenesis. *J Invest Dermatol* (2016) 136(12): 2462–74. doi:10.1016/j.jid.2016.07.024
89. Weilbaecher KN, Guise TA, McCauley LK. Cancer to bone: a fatal attraction. *Nat Rev Cancer* (2011) 11(6):411–25. doi:10.1038/nrc3055
90. Cox TR, Rumney RMH, Schoof EM, Perryman L, Høye AM, Agrawal A, et al. The hypoxic cancer secretome induces pre-metastatic bone lesions through lysyl oxidase. *Nature* (2015) 522(7554):106–10. doi:10.1038/nature14492
91. Bandopadhyay M, Bulbule A, Butti R, Chakraborty G, Ghorpade P, Ghosh P, et al. Osteopontin as a therapeutic target for cancer. *Expert Opin Ther Targets* (2014) 18(8):883–95. doi:10.1517/14728222.2014.925447
92. Kelly T, Suva LJ, Huang Y, MacLeod V, Miao HQ, Walker RC, et al. Expression of heparanase by primary breast tumors promotes bone resorption in the absence of detectable bone metastases. *Cancer Res* (2005) 65(13):5778–84. doi:10.1158/0008-5472.CAN-05-0749
93. O'Connell JT, Sugimoto H, Cooke VG, MacDonald BA, Mehta AI, LeBleu VS, et al. VEGF-A and Tenascin-C produced by S100A4+ stromal cells are important for metastatic colonization. *Proc Natl Acad Sci U S A* (2011) 108(38):16002–7. doi:10.1073/pnas.1109493108
94. Oskarsson T, Acharyya S, Zhang XH, Vanharanta S, Tavazoie SF, Morris PG, et al. Breast cancer cells produce tenascin C as a metastatic niche component to colonize the lungs. *Nat Med* (2011) 17(7):867–74. doi:10.1038/nm.2379
95. Malanchi I, Santamaria-Martínez A, Susanto E, Peng H, Lehr HA, Delaloye JF, et al. Interactions between cancer stem cells and their niche govern metastatic colonization. *Nature* (2011) 481(7379):85–9. doi:10.1038/nature10694
96. Gao H, Chakraborty G, Lee-Lim AP, Mo Q, Decker M, Vonica A, et al. The BMP inhibitor Coco reactivates breast cancer cells at lung metastatic sites. *Cell* (2012) 150(4):764–79. doi:10.1016/j.cell.2012.06.035
97. Cackowski FC, Eber MR, Rhee J, Decker AM, Yumoto K, Berry JE, et al. Mer tyrosine kinase regulates disseminated prostate cancer cellular dormancy. *J Cell Biochem* (2017) 118(4):891–902. doi:10.1002/jcb.25768
98. Coleman RE. Bone cancer in 2011: prevention and treatment of bone metastases. *Nat Rev Clin Oncol* (2011) 9(2):76–8. doi:10.1038/nrclinonc.2011.198
99. Coleman RE. Adjuvant bone-targeted therapy to prevent metastasis: lessons from the AZURE study. *Curr Opin Support Palliat Care* (2012) 6(3):322–9. doi:10.1097/SPC.0b013e32835689cd
100. Smith MR, Coleman RE, Klotz L, Pittman K, Milecki P, Ng S, et al. Denosumab for the prevention of skeletal complications in metastatic castration-resistant prostate cancer: comparison of skeletal-related events and symptomatic skeletal events. *Ann Oncol* (2015) 26(2):368–74. doi:10.1093/annonc/mdu519
101. El Touny LH, Vieira A, Mendoza A, Khanna C, Hoenerhoff MJ, Green JE. Combined SFK/MEK inhibition prevents metastatic outgrowth of dormant tumor cells. *J Clin Invest* (2014) 124(1):156–68. doi:10.1172/JCI70259
102. Apel A, Herr I, Schwarz H, Rodemann HP, Mayer A. Blocked autophagy sensitizes resistant carcinoma cells to radiation therapy. *Cancer Res* (2008) 68:1485–94. doi:10.1158/0008-5472.CAN-07-0562

103. Saudemont A, Jouy N, Hetuin D, Quesnel B. NK cells that are activated by CXCL10 can kill dormant tumor cells that resist CTL-mediated lysis and can express B7-H1 that stimulates T cells. *Blood* (2005) 105(6):2428–35. doi:10.1182/blood-2004-09-3458
104. Ahmed M, Behera R, Chakraborty G, Jain S, Kumar V, Sharma P, et al. Osteopontin: a potentially important therapeutic target in cancer. *Expert Opin Ther Targets* (2011) 15(9):1113–26. doi:10.1517/14728222.2011.594438
105. Kumar S, Sharma P, Kumar D, Chakraborty G, Gorain M, Kundu GC. Functional characterization of stromal osteopontin in melanoma progression and metastasis. *PLoS One* (2013) 8(7):e69116. doi:10.1371/journal.pone.0069116
106. Boyerinas B, Zafrir M, Yesilkanal AE, Price TT, Hyjek EM, Sipkins DA. Adhesion to osteopontin in the bone marrow niche regulates lymphoblastic leukemia cell dormancy. *Blood* (2013) 121(24):4821–31. doi:10.1182/blood-2012-12-475483

Conflict of Interest Statement: The authors declare that the research was conducted in the absence of any commercial or financial relationships that could be construed as a potential conflict of interest.

frontiers in Oncology

REVIEW
published: 11 September 2017
doi: 10.3389/fonc.2017.00203

Three-Dimensional Patient-Derived *In Vitro* Sarcoma Models: Promising Tools for Improving Clinical Tumor Management

*Manuela Gaebler[1†], Alessandra Silvestri[2†], Johannes Haybaeck[3,4], Peter Reichardt[1], Caitlin D. Lowery[5], Louis F. Stancato[5], Gabriele Zybarth[2] and Christian R. A. Regenbrecht[2]**

[1] HELIOS Klinikum Berlin-Buch GmbH, Department of Interdisciplinary Oncology, Berlin, Germany, [2] cpo – Cellular Phenomics & Oncology Berlin-Buch GmbH, Berlin, Germany, [3] Medical Faculty, Department of Pathology, Otto-von-Guericke University Magdeburg, Magdeburg, Germany, [4] Institute of Pathology, Medical University Graz, Graz, Austria, [5] Eli Lilly and Company, Oncology Translational Research, Lilly Corporate Center, Indianapolis, IN, United States

OPEN ACCESS

Edited by:
Paolo Pinton,
University of Ferrara, Italy

Reviewed by:
Ritva Tikkanen,
Justus Liebig Universität Gießen, Germany
Walter Berger,
Medical University of Vienna, Austria
Bernd Ulrich Kölsch,
Essen University Hospital, Germany

***Correspondence:**
Christian R. A. Regenbrecht
christian.regenbrecht@cellphenomics.com

[†]These authors have contributed equally to this work.

Specialty section:
This article was submitted to Molecular and Cellular Oncology, a section of the journal Frontiers in Oncology

Received: 12 June 2017
Accepted: 21 August 2017
Published: 11 September 2017

Citation:
Gaebler M, Silvestri A, Haybaeck J, Reichardt P, Lowery CD, Stancato LF, Zybarth G and Regenbrecht CRA (2017) Three-Dimensional Patient-Derived In Vitro Sarcoma Models: Promising Tools for Improving Clinical Tumor Management. Front. Oncol. 7:203. doi: 10.3389/fonc.2017.00203

Over the past decade, the development of new targeted therapeutics directed against specific molecular pathways involved in tumor cell proliferation and survival has allowed an essential improvement in carcinoma treatment. Unfortunately, the scenario is different for sarcomas, a group of malignant neoplasms originating from mesenchymal cells, for which the main therapeutic approach still consists in the combination of surgery, chemotherapy, and radiation therapy. The lack of innovative approaches in sarcoma treatment stems from the high degree of heterogeneity of this tumor type, with more that 70 different histopathological subtypes, and the limited knowledge of the molecular drivers of tumor development and progression. Currently, molecular therapies are available mainly for the treatment of gastrointestinal stromal tumor, a soft-tissue malignancy characterized by an activating mutation of the tyrosine kinase KIT. Since the first application of this approach, a strong effort has been made to understand sarcoma molecular alterations that can be potential targets for therapy. The low incidence combined with the high level of histopathological heterogeneity makes the development of clinical trials for sarcomas very challenging. For this reason, preclinical studies are needed to better understand tumor biology with the aim to develop new targeted therapeutics. Currently, these studies are mainly based on *in vitro* testing, since cell lines, and in particular patient-derived models, represent a reliable and easy to handle tool for investigation. In the present review, we summarize the most important models currently available in the field, focusing in particular on the three-dimensional spheroid/organoid model. This innovative approach for studying tumor biology better represents tissue architecture and cell–cell as well as cell–microenvironment crosstalk, which are fundamental steps for tumor cell proliferation and survival.

Keywords: sarcoma, preclinical model, *in vitro* organoid culture, patient-derived *in vitro* model, drug screening, sarcoma treatment, personalized medicine

INTRODUCTION

Cancer is a group of diseases with a multitude of genomic aberrations typically classified by the cell of origin. Solid malignant neoplasms are predominantly carcinomas, which derive from epithelial cells, while a far less frequent group of solid neoplasms originates from mesenchymal cells. Normal mesenchymal cells form the soft and connective tissues as well as the bones. Tumors stemming from

these cells are called sarcomas. They are malignant in most cases, and while their incidence in adults ranges from 1 to 2% (1–4), they account for up to 15% of all childhood and adolescence cancers (2, 3). Two main groups can be subdivided: soft-tissue sarcomas (STS) are more common in adults and represent 87% of all sarcomas, while sarcomas of the bone [osteosarcomas, Ewing sarcomas (EWS), and chondrosarcomas] occur more often below the age of 20 years (4, 5). Currently, the American cancer registry reports 4.2 cases per 100,000 for STS and 1.0 per 100,000 for sarcomas of the bone (6). Similar incidence rates have been reported for Europe (5, 7–9). Based on these numbers and according common definitions (10), sarcomas meet the criteria of rare diseases.

As for any rare disease, diagnostics and treatment should take place in specialized centers (7–9). Despite increased survival resulting from numerous multidisciplinary curative and palliative treatment options including surgery, monodrug or multidrug chemotherapy and/or targeted therapy, radiation therapy, hyperthermia, and isolated limb perfusion in a neoadjuvant or adjuvant setting (7–9), the disease outcome is often fatal. Currently, the 5-year relative survival rate for a patient with sarcoma considering the type, stage, localization, and age is about 60% (5) but dramatically dropping to 10% when only patients with advanced stages are considered (11). Due to the limited availability of tumor tissue for research and the complexity of the disease, progress in clinical management of sarcomas is lagging behind that of carcinomas. Since the lack of effective treatment options contributes to the low survival rate, the need for improving the treatment is evident.

Risk Factors for Sarcoma Development

Sarcomas could stem from virtually any mesenchymal cell in the body, and new pathological and molecular methods used for tumor classification currently allow for the distinction of more than 70 histopathological subtypes (1, 2, 12, 13). This high degree of heterogeneity combined with low incidence makes systematic research of sarcomas scientifically challenging.

A large group of sarcomas develop spontaneously, but environmental and predisposing genomic factors have been found to increasing the risk of contracting this kind of tumor. For example, Kaposi sarcomas are known to be HIV or human herpes virus 8 induced (14). Common risk factors known to be causative for many malignancies such as exposure to certain environmental pollutants and chemicals, ionizing radiation (often in form of a previous radiotherapy), and inherited genetic aberrations are also confirmed to play a role in sarcomas (**Table 1**). Sarcomas can be classified based on their genomics into genetically simple and genetically complex sarcomas (15, 16). Sarcomas of the genetically simple category (hypomutated) are characterized by only one disease-specific "driver" aberration such as a translocation or mutation (**Table 2**) and are more common in younger patients. Most of the known translocations result in fusion genes which code for transcription or growth factors (15). Identifying these translocations is of great value to the pathologist, as they allow for a confirmed diagnosis where simple histopathology alone is not definite. For example, detecting the amplification of *MDM2* helps to confirm the diagnosis of a well-differentiated or dedifferentiated liposarcoma (17, 18). The genetically complex group (hypermutated) is made up by more or less chaotic karyotypes with high mutation frequencies in key oncogenes and tumor suppressor genes like *TP53* or *RB1* (15, 16). These complex genomic aberrations are commonly found in adult patients and/or as secondary lesions after radiation exposure (15) (**Table 2**).

Moreover, there are ongoing discussions about other potential risk factors for sarcoma development. Congenital or acquired immunodeficiency and, interestingly, also hernias seem to have suggestive evidence (3, 4). While often a trauma is reported in the patients' medical history, publication showed that there is no such causative link between injury and sarcoma development, except for fibrosarcoma, dermatofibrosarcoma, and for patients with Gardner's syndrome who underwent surgery (19).

Gastrointestinal Stromal Tumors (GISTs): Model for Developing New Targeted Therapies in Sarcoma

Gastrointestinal stromal tumors represent approximately 18% of all sarcomas and are the most common mesenchymal neoplasms of the gastrointestinal tract. Historically, GISTs have a poor prognosis with tumor recurrence within 5 years after complete

TABLE 1 | Common risk elevating factors for sarcoma development.

Risk factor		Resulting sarcoma subtype	Reference
Environmental pollutant/ chemical	Ionizing radiation, previous or environmental	Especially osteosarcoma, angiosarcoma	(3, 5)
	Herbicides (e.g., phenoxyacetic acids, chlorophenol)	Non-specific	(5, 15)
	Vinyl chloride	Hepatic angiosarcoma	(15)
	Dioxins	Non-specific	(3)
Infection	HIV, human herpes virus 8	Kaposi's sarcoma	(14)
Genetic disorder	Li–Fraumeni syndrome	Any cancer, 30% sarcomas, osteosarcoma and various soft-tissue sarcomas heaped among sarcomas	(3, 5, 12, 15)
	Neurofibromatosis type 1	Especially MPNST	(3, 4)
	Rb-mutation (13q14)	Especially osteosarcoma, if retinoblastoma has been survived	(3, 4)
	Paget disease	Osteosarcoma in adults	(5)
	Werner syndrome	Osteosarcoma	(4)
	Bloom syndrome	Osteosarcoma	(4)
	Gardner syndrome	Fibrosarcoma	(19)

Shown are the most likely resulting sarcomas depending on risk factor but omitting carcinomas and other types of cancer even if they are more prevalent.

TABLE 2 | Common known aberrations of certain sarcoma subtypes.

Sarcoma subtype	Type of aberration	Locus	Reference
Gastrointestinal stromal tumors	Mutation	*cKIT* (exon 9 or 11) or *PDGFR-alpha*	(13)
Liposarcoma, well differentiated, and dedifferentiated	Amplification	*MDM2* (suppressor of p53)	(17, 18)
Myxoid liposarcoma	Translocation	FUS–DDIT3 [t(12:16) (q13;p11)]	(15)
		EWSR1–DDIT3 [t(12;22) (q13;q12)]	(15)
Alveolar rhabdomyosarcoma	Translocation	PAX3–FOXO1A [t(2:13) (q35:q14)]	(15)
		PAX7–FOXO1A [t(1:13) (p36:q14)]	(15)
Synovial sarcoma	Translocation	SS18-SSX [t(X;18)(p11:q11)]	(3, 15)
Ewing sarcoma	Translocation	EWSR1-FLI1 [t(11:22) (q24;q12)]	(15)
		EWSR1–ERG [t(21;22) (q22;q12)]	(15)
		EWSR1–ETV1 [t(7;22) (p22;q12)]	(15)
		EWSR1–ETV4 [t(17;22) (q21;q12)]	(15)
		EWSR1–FEV [t(2;22) (q33;q12)]	(15)
Myxoid chondrosarcoma	Translocation	EWSR1–NR4A3 [t(9;22) (q22-31;q11-12)]	(15)

resection in up to 50% of patients. An important improvement in the management of this neoplasm was achieved in 1998 due to the discovery of oncogenic mutations in the tyrosine kinase KIT (20). The subsequent development and exploitation of kinase inhibitors that specifically downregulate this aberrant signal transduction pathway improved GIST patient outcome (21, 22) and made this approach a model for treating sarcoma by targeting altered intracellular signaling molecules. In some cases, a specific treatment can now be selected to target a mutation in a molecular pathway if a drug targeting this pathway is available, even if this drug was originally approved for a different tumor type. An important example is imatinib, a kinase inhibitor originally approved for the treatment of patients with BCR-ABL-positive chronic myeloid leukemia, which is also a very effective inhibitor of KIT and thus showed increased efficacy in KIT-mutated GIST. However, further investigation of mutation status in GIST has revealed a specific mutation (PDGFRA D842V) that according to current guidelines mostly prohibits the use of imatinib (9) as patients with this mutation harbor a primary resistance to this drug (21).

Cells of Origin of Sarcoma

Irrespective of the clinical characteristics and in contrast to carcinomas, which arise from epithelial cells and are well defined by their tissue of origin, sarcomas are a group of highly heterogeneous tumors and evidence suggest that they develop directly from mesenchymal stem cells (MSCs) (23). MSCs are multipotent precursor cells of mesenchymal tissues such as bone, cartilage, fat, and muscle; several studies indicate their involvement in sarcomagenesis. Based on the wide variety of sarcoma subtypes, the origin of these tumors can be explained by two different hypotheses: the development of malignant alterations in a committed cell, distinct for every sarcoma subtype, or the presence of a common multipotent cell of origin that after transformation can differentiate into specific lineages (**Figure 1**).

According to the first hypothesis, tumors with a distinct phenotype and grade develop based on the basis of the lineage and of the differentiation stage when the initiating mutation occurs. This hypothesis is supported by studies in which the comparison between gene expression profiles of sarcomas and tissue-specific differentiation stages of MSCs showed a signature overlap in tumor and normal tissue according to their lineage of differentiation (25–29). One of the limitations of these analyses is the fact that they are based on *in vitro* cell culturing, which is known to induce alterations in the gene expression profile, thereby introducing a bias in the results. Moreover, it has been demonstrated that cells of a specific sarcoma subtype can differentiate into multiple lineages *in vitro* when specific inducing factors are added, thus indicating that not only the cell of origin but also the tumor microenvironment is fundamental for determining the final tumor phenotype.

Increasing evidence indicates that sarcomagenesis might be initiated by an aberration in a multipotent cell, and this hypothesis is currently favored by most researchers in the field. Several studies have demonstrated that mouse and human transformed MSCs can give rise to sarcomas after transplantation into mice. Miura and coworkers (30) showed that murine bone marrow-derived mesenchymal stem cells (BMMSCs) undergo spontaneous malignant transformation after prolonged culture (passage 29–54). Moreover, when injected in mice, these cells can form fibrosarcomas.

To test if MSCs are able not only to develop tumors when injected in mice after transformation but also to directly transform *in vivo*, Li et al. (31) transplanted bone marrow or MSC from male C57BL/6J mice into transgenic mice expressing a non-mammalian beta-gal enzyme (ROSA), chicken h-actin-enhanced GFP, and into WT littermates with bone marrow or MSC from male C57BL/6J mice as a control. After 18–24 months from transplantation, fibrosarcomas were the most common tumor detected, and immunohistochemistry analysis demonstrated that these tumors were derived from the transplanted bone marrow.

Compared to murine cells, human BMMSCs showed senescence without immortalization indicating that human MSCs cannot spontaneously transform (30); therefore, to translate the results obtained in mouse models, transformation of human MSC prior to inoculation is required. Genetic approaches aimed to knock out tumor suppressor genes and overexpress specific oncogenes have been used to induce MSCs transformation. The most common way to transform normal cells into malignant counterparts is the endogenous expression of human telomerase reverse transcriptase, simian virus 40 large T antigen (SV40-LT), and oncogenic H-RAS (32–34). Li et al. (35) applied this approach to study the origin of osteosarcoma. By using hMSC, they established cell lines by serially introducing these genetic alterations, and the effect of this manipulation

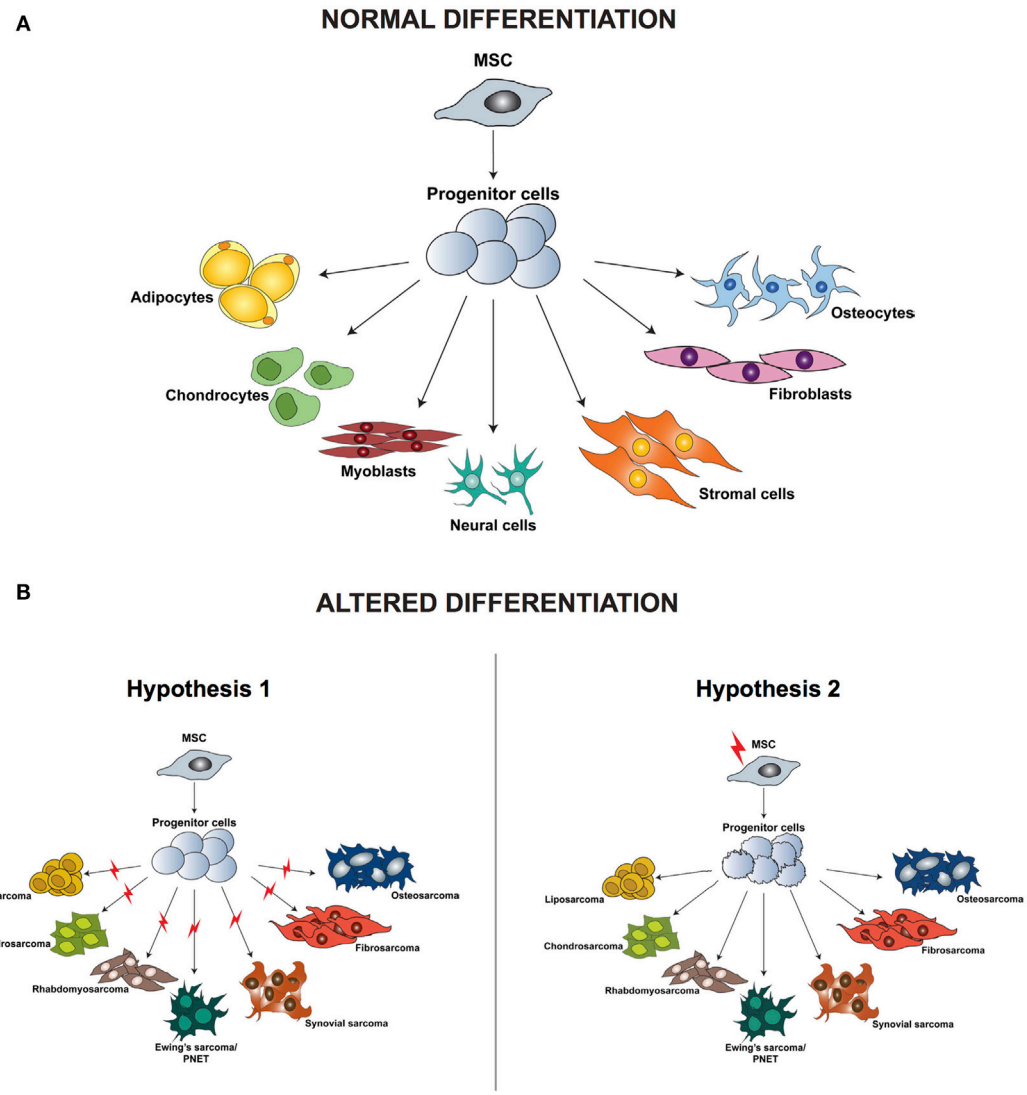

FIGURE 1 | Differentiation of normal mesenchymal stem cells **(A)** and altered differentiation **(B)**. **(B)** The difference between the two hypotheses, whereby the initiating aberration occurs either at a later stage of differentiation (hypothesis 1) or hits the stem cell (hypothesis 2). Modified from the study by Teicher (24).

on cellular phenotype, gene expression profiles, karyotype, and multilineage differentiation capacity was compared to osteosarcoma. They showed that two distinct genotypic and phenotypic sarcoma cell lines developed from these genetic events and that the transformed cells were characterized by increased motility. Moreover, transformed cells could be induced, so that osteogenic, adipogenic, and chondrogenic differentiation occurred, demonstrating that their multilineage differentiation potential was maintained.

Other groups studied MSC as cell of origin of osteosarcoma. Mohseny et al. (36) deeply characterized murine MSCs, transformed MSCs, and derived osteosarcoma cells lines genetically, phenotypically, and functionally, as well as for mRNA and protein expression. They identified aneuploidization, translocation, and homozygous loss of the *cdkn2* region as the key mediators of MSC transformation. In a cohort of 88 osteosarcoma patients, they showed a correlation between CDKN2A/p16 protein expression and prognosis, thus linking murine MSC model to human osteosarcoma. The genetic alterations that were found in both the *in vitro* cultured tumorigenic MSCs and the derived mouse tumors demonstrated that osteosarcoma could originate from MSCs. Interestingly, the fact that these cells could differentiate *in vitro* to chondrocytes and adipocytes but were prone to form osteosarcomas *in vivo* reveals the importance of the tumor microenvironment in determining the final tumor phenotype.

Finally, it has been shown that a subgroup of these multipotent cells express not only mesenchymal markers but also stem cell markers such as OCT3/4, NANOG, and SOX (37, 38) and that they are associated with drug resistance and metastasis development (39, 40). Taken together, these data suggest that MSCs might be not only the sarcoma initiating cells but also, due to their stemness, the cells responsible for maintaining tumor growth.

Requirement of New Preclinical *In Vitro* Models for Improving Sarcoma Outcome

Besides earlier detection by novel imaging techniques, the overall survival of sarcoma patients has not improved in the last 30 years. This is mainly due to the lack of understanding of the biological consequences of the genomic alterations involved in sarcomagenesis. Therefore, it is clear that a better understanding of human sarcoma tumorigenesis and metastasis is pivotal to improve the management of sarcoma patients in terms of new therapeutic targets and approaches. Since each sarcoma subtype is characterized by a low incidence, the development of clinical trials is challenging, and the results are often biased by the limited number of patients involved (16). These limitations related to the nature of sarcomas make interdisciplinary approaches indispensable and the development of reliable preclinical models for molecular analysis and research of potential targetable nodes a priority. Even with technologies such as next-generation sequencing finding their way into the field of pathology, only the detailed understanding of the biology of sarcomas will foster new insights and as consequence translate to more effective therapeutic regimens in the clinic.

Recently, the efficacy of molecular methods in improving sarcoma diagnosis was tested in a multicenter, prospective study. For this study, the diagnosis of 384 patients from 32 French sarcoma centers using histopathology exclusively versus a combination of histopathology plus molecular characterization was reevaluated. The authors reported that for 53 of the patients considered an improvement was obtained when the diagnosis made by an expert pathologist was revised according to molecular genetic testing (41). This underlines the importance of sarcoma molecular characterization and demonstrates that molecular testing could significantly increase diagnostic accuracy.

In recent years, it has been extensively demonstrated that malignant tumors are characterized by varying degrees of heterogeneity where not only the primary tumor but also the corresponding distant metastasis have distinct genetic profiles (42, 43). Considering this heterogeneity, searching for actionable mutations using only next-generation sequencing techniques may be very challenging, and the treatment of tumor cells with specific mutations by targeted therapy could select for specific subpopulations resistant to the initial therapy (44–46), making the combination of multiple drugs with different targets the most promising approach, aiming at the inhibition of tumor growth at multiple levels. For example, Patwardhan et al. reported that a selective c-Fms/KIT inhibitor in combination with an mTORC1 inhibitor could be more effective than the c-Fms/KIT inhibitor alone in reducing tumor growth in malignant peripheral nerve sheath tumors in cell lines and xenograft *in vivo* models (47). These recent findings in sarcoma biology have encouraged the sarcoma research community into developing new predictive models for improving sarcoma treatment.

TWO-DIMENSIONAL (2D) *IN VITRO* MODELS

Preclinical and translational studies of tumor mutations and aberrations as well as validation of therapeutic targets are based mainly on *in vitro* testing. Currently, the number of sarcoma models available for functional testing is still very limited, with only 2% of commercially available cell lines derived from STS (48). Moreover, the cell lines available do not represent the diversity of sarcomas, but are limited to the most common groups like osteosarcoma, leiomyosarcoma, and rhabdomyosarcoma with a total lack of more rare subtypes such as alveolar soft part sarcoma.

Due to these limitations, several groups focused on the establishment of new sarcoma cell lines. More than three decades ago, Bruland and coworkers isolated primary cells from 11 primary and metastatic human sarcoma specimens by enzymatic dissociation (49). Since the general success rate of sarcoma cell isolation was limited, they developed an alternative procedure using a non-adherent cell cultivation method (cellular spheroids) to the classical monolayer culture. With this approach, they produced stable monolayer cultures in 5 of the 11 samples used. These cells formed colonies in clonogenic soft-agar assays and developed tumors upon subcutaneous injection into nude mice. In 2002, additional cell lines were established, the majority from lung metastatic specimens derived from different sarcoma subtypes (50). In this study, all 11 cell lines analyzed expressed VEGF and basic-FGF, and they grew in anchorage-independent conditions. Moreover, when injected intramuscularly, six of the cell lines tested formed tumors and five of these spontaneously developed lung metastases, thus demonstrating the retention of tumorigenic and metastatic potential of the original tumor.

Recently, Salawa and coworkers established (48) primary cell cultures from fresh soft-tissue sarcoma samples with a success rate of 70%. For the seven long-term cell cultures that remained proliferative for at least 3 years and for more that 60 passages, they confirmed that the genomic and phenotypic characteristics were comparable to the original tumors. Since it is well known that long-term culture affects cell molecular characteristics, they analyzed the loss of heterozygosity (LOH) highlighting an increase of LOH after ~40 passages, thus demonstrating the presence of a genomic evolution commonly observed in *in vitro* cell cultures. Interestingly, three of the seven cell lines isolated were derived from undifferentiated pleomorphic sarcomas (UPSs) and the other four were derived from high-grade subtypes, suggesting a correlation between aggressive clinical course and the potential of *in vitro* growth.

Since studies based on the use of cancer cell lines often showed conflicting results, the characterization of the *in vitro* models used is very important, so that the results achieved by different laboratories can be compared. In 2010, the EuroBoNeT consortium characterized a set of 36 commonly used bone tumor cell lines (51), including osteosarcoma, EWS, and chondrosarcoma. After DNA fingerprint analysis to exclude cross-contamination of tumor cell lines, they showed that clones derived from the same original cell line (in this case, HOS) showed some differences from the parental line, suggesting a genomic evolution of the clones used in the study. Moreover, they highlighted a discrepancy between *CDKN2A* homozygous deletions in osteosarcoma and EWS cell lines (42 and 36%, respectively) compared to primary sarcoma samples, in which the frequency of this deletion is expected to be lower. This observation suggests that the cell line panel analyzed may be enriched in more aggressive tumors that

easily grow *in vitro*. Finally, they analyzed the expression of TP53, a marker accepted for response to chemotherapy. They reported that 7 of the 10 TP53wt osteosarcoma cell lines showed low levels of *TP53* mRNA transcripts and only weak or no staining for the corresponding protein. Moreover, this downregulation was present only in osteosarcoma cell lines but not in the other seven TP53wt bone tumor lines analyzed.

To select cell lines that are more representative of human osteosarcoma, the same research group further characterized the 19 osteosarcoma cell lines available in that study (52) by analyzing their ability to differentiate *in vitro* and their tumorigenic potential in nude mice. While the differentiation capacity toward osteoblasts, adipocytes, or chondrocytes was maintained in all cell lines with some cell lines able to differentiate in more than one lineage, only eight cell lines developed tumors after subcutaneous and intramuscular injection into nude mice. In mice injected with HOS-143B cell line, multiple lung metastasis was detected during autopsy, demonstrating the metastatic potential of these cells. Interestingly, the availability of the non-tumorigenic HOS parental line and the corresponding non-metastatic HOS-MNNG makes these lines an excellent model for studying osteosarcoma progression.

Since 2D *in vitro* models are inexpensive and relatively easy to generate and maintain, they have been broadly used in preclinical research. However, these models do not accurately recapitulate the three-dimensional (3D) structure of tumor tissues and the complex crosstalk between tumor cells and microenvironment.

3D *IN VITRO* MODELS

Forcing cells to grow in 2D induces alterations in cell morphology that in turn translates in changes of the gene and protein expression, as well as cell behavior compared to the tissue of origin (53–55). These limitations are partially overcome by 3D cell cultures that represent the donor-tissues' architecture including cell–cell and cell–matrix interactions and are thus valuable tools for investigating the influence of the microenvironment and gradients of nutrients and oxygen on the interplay of cells within a tumor and their response to drug treatment (56). Since little is known about the molecular biology of sarcomas including unknown contextual cross talk between signaling pathways and other components presumably including epigenetic modifications and regulatory RNA sequences, patient-derived sarcoma tumor models are desirable tools to fulfill the promises of personalized medicine.

Several reports mainly aimed at the study of the presence of cells with cancer stem cell characteristics and their role in sarcoma tumorigenesis, local relapse, metastasis, and therapy resistance were published demonstrating that sarcoma cells can grow in non-adherent conditions, forming 3D structures called spheroids (49, 57–59). In 2009, Fujii et al. showed that commercially available human sarcoma cell lines such as MG63 (osteosarcoma), HTB166 (EWS), and HT1080 (fibrosarcoma) are characterized by the ability to form sarcospheres with stem-like properties. Moreover, they showed that cells grown as spheroids were resistant to doxorubicin and cisplatin, drugs frequently used for sarcoma treatment (39).

In additional to immortalized cell lines, primary cells can also form sarcospheres when grown in non-adherent and serum-starved conditions. Salerno and coworkers demonstrated that isolated tumor spheres were tumorigenic after transplantation into mice and that the tumors formed recapitulated the corresponding human disease (58). In addition, they showed that by modification of cell culture conditions, it was possible to influence the growth of the sarcospheres. Mimicking the tumor microenvironment by reducing O_2 conditions to 1% induced a significant increase in the number and the size of the spheres demonstrating that 3D sarcoma models are useful tools for studying sarcoma development due to their flexibility.

To better model morphology, growth kinetics, and protein expression profiles of human tumors, Fong et al. (59) established an *ex vivo* 3D model of EWS by culturing TC-71 cells in porous 3D electrospun poly(ε-caprolactone) scaffolds. After a 20-day culture, a well-differentiated EWS-like phenotype was preserved in this *in vitro* 3D model as verified by expression of diagnostic markers such as CD99, keratin, and smooth muscle actin. Considering that one of the most promising new treatment strategies in EWS is the inhibition of the IGF-1R/mTOR pathway, they showed that the activation of IGF-1R/mTOR signal was higher in the 3D model, compared to the 2D counterpart, suggesting that the 3D microenvironment has a more physiological effect on the intracellular signaling cascade. Finally, they tested the sensitivity of this 3D model to doxorubicin, a cytotoxic chemotherapeutic agent used in EWS treatment. Similar to the lower sensitivity observed in xenografts, an increased resistance was observed in the 3D model compared to 2D cells. Taken together, these data demonstrated that EWS 3D models are useful and reliable tools for evaluating new IGF-1R antagonists not only as single agents but also in combined strategies. Moreover, since they better mimic the tumor microenvironment, they provide important information for identifying new signaling nodes that can represent potential targets for therapeutic intervention.

One of the main characteristics of EWS cells is the recruitment and activation of osteoclasts, leading to the destruction of bone tissue by osteoclast-mediated osteolysis. As this process is crucial, several groups focused on the development of *in vitro* models of bone osteolysis by coculturing tumor cells with osteoclasts and osteoblasts. Recently, Villasante et al. (60) engineered a healthy bone tissue by co-culturing osteoblasts derived from hMSC and osteoclasts derived from monocytes isolated from blood samples. First, hMSC were seeded within a decellularized bone scaffold and differentiated toward osteoblasts. $CD14^+$ monocytes were then cocultured with osteoblast and differentiated in osteoclasts. EWS aggregates were finally infused into the tissue-engineered bone and maintained in culture. The analysis of the bone microenvironment highlighted a decrease in bone density, connectivity, and matrix deposition in the presence of EWS cells. Moreover, the treatment with antiosteolytic drugs inhibited this process limiting osteoclast-mediated bone resorption. Taken together these data highlight the feasibility of developing bone-mimicking models for the study of bone tumors and bone metastasis development. The possibility of using patient-derived induced pluripotent stem cells for developing the bone niche suggests the potential of using this model for creating personalized models useful for precision medicine.

3D *In Vitro* Models: From Carcinoma to Sarcoma Research

In the last decade, several 3D cell culture models have been developed to study different aspects of tumor biology and to test the efficacy of new anticancer molecules. While these approaches have mainly been established using carcinoma cells, with little effort, they can be also applied to the study of sarcoma biology. The least complex and therefore most frequently used models are based on spontaneous cell aggregation where the reduction of the adhesive forces to the surface of the culture plate allows cells to adhere spontaneously to each other forming cellular spheroids (**Figure 2A**). These models can be maintained either by using non-adhesive surfaces or spinner flasks and gyratory rotators, the use of hanging drop cultures, embedding of tumor cells in hydrogel matrices, or by the use of microcarrier beads and scaffolds. To avoid cell adhesion to the substrate surface, *non-adhesive surfaces* (**Figure 3A**) can be generated by using coatings such as agarose, polyHEMA, positively charged polystyrene, or proteoglycans (61–63). More recently, culture plates with modified surface chemistry have been developed allowing for "out-of-the-box"-ready technology and more reproducible growth of cellular spheroids. Besides the biological limitations, the main technical limitation of this method is the formation of spheroids with variable size and the inability to process upscaling.

The aforementioned limitations are partially overcome using *spinner flasks or gyratory rotator* (**Figure 3B**) systems, bioreactors that allow continuous mixing of medium or a constant rotatory movement of the flask, which prevents cell adhesion (65). These methods allow massive production of spheroids, therefore representing the method of choice for growing high amounts of homogeneous spheroids for downstream applications.

A technique often used is the so-called *hanging drop* method (**Figure 3C**) that makes use of gravity to stimulate cell aggregation. Cells in suspension are plated in small drops onto the underside of a plate lid that is then carefully inverted. Due to gravity, the cells accumulate in the tip of the drop, forming spheroidal aggregates (66). For those cells that do not spontaneously aggregate, systems that facilitate cell to cell interaction have been developed. *Microcarrier beads* (**Figure 3D**) are characterized by differences

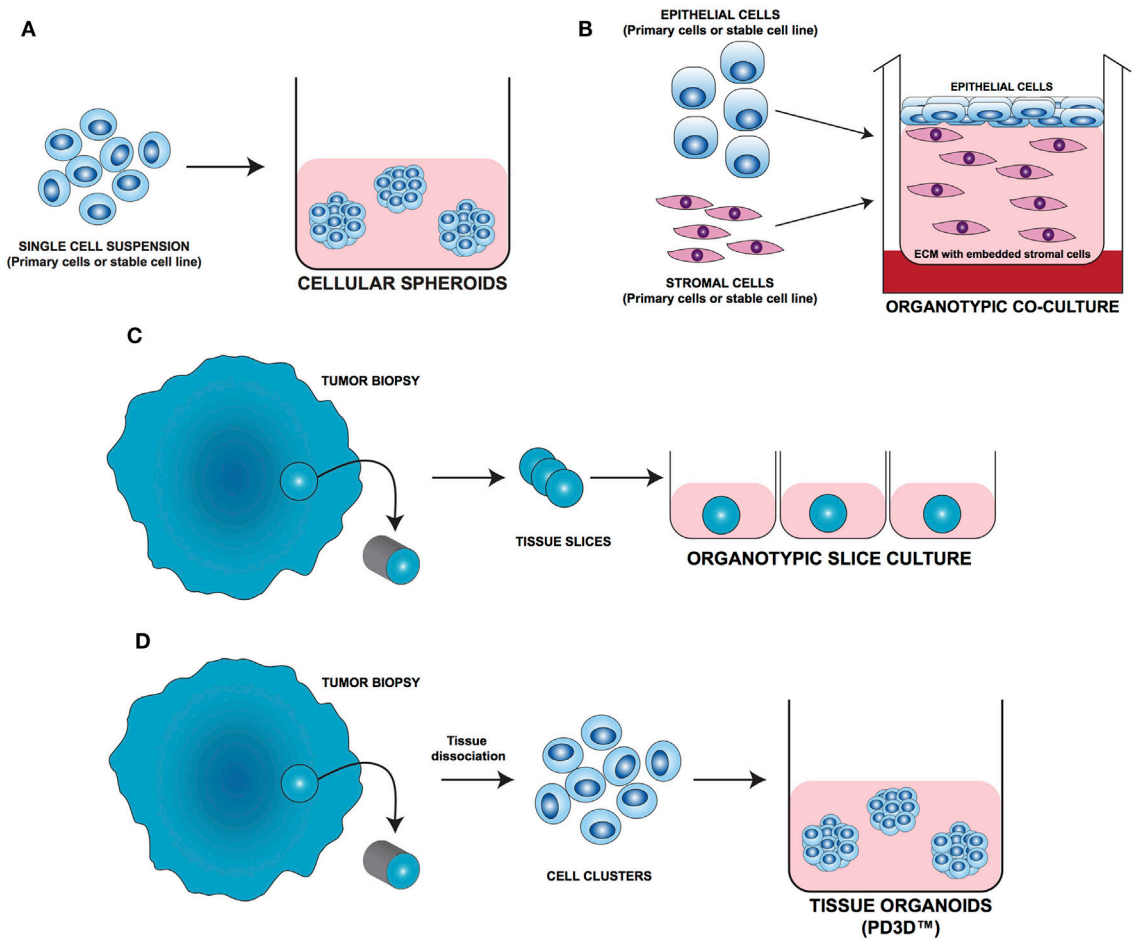

FIGURE 2 | Different approaches for 3D cell culture model development. **(A)** Cellular spheroids: single cells from primary or stable cell lines aggregate together forming 3D structures. **(B)** Organotypic coculture: epithelial cells are cocultured with stroma cells embedded in a supporting matrix. **(C)** Organotypic slice culture: tissue slices obtained from the whole organ or from fragments of it are directly cultivated *ex vivo*. **(D)** Tissue organoids (PD3D™): primary cells isolated from fresh tissue without prior cell enrichment are grown as 3D multicellular structures [Modified from Silvestri et al. (64)].

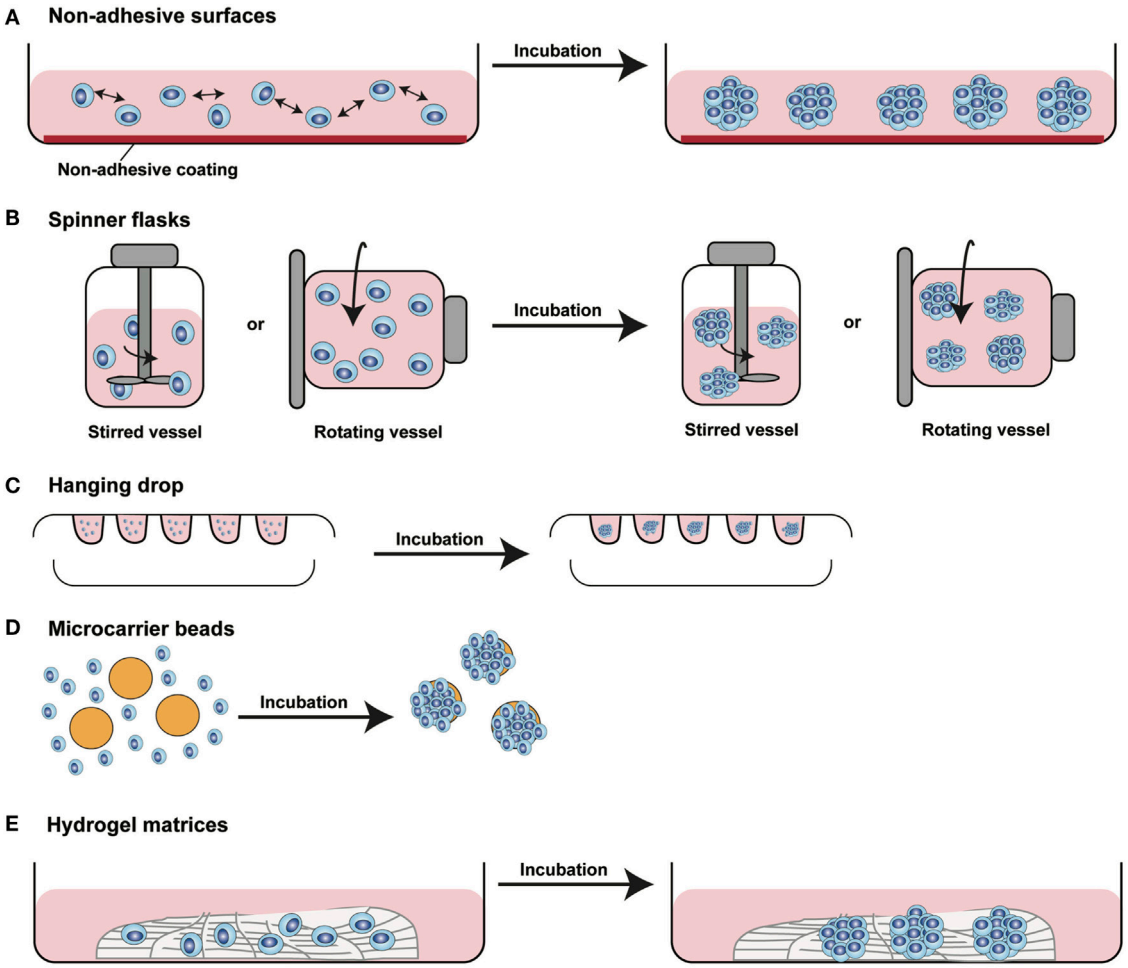

FIGURE 3 | Different methods for 3D spheroids development and growth. **(A)** Non-adhesive surfaces: culture plates with modified surfaces to reduce cell adhesion stimulate cell aggregation and formation of 3D structures. **(B)** Spinner flasks: stirred or rotating vessels are used to prevent cell adhesion to the surface of the plate allowing 3D spheroids formation. **(C)** Hanging drop: cells seeded in small drops of medium form cellular aggregates at the tip of the drop due to gravity forces. **(D)** Microcarrier beads: cells adhere to and proliferate on the surface of natural or synthetic solid beads forming 3D structures. **(E)** Hydrogel matrices: cells are seeded into matrices of natural or synthetic origin forming 3D structures by single cells aggregation or by monoclonal cell growth. [Modified from Silvestri et al. (64)].

in size and composition. Surface coating allows adhesion and proliferation of cells consequently forming minispheroids that in turn aggregate one to each other, thus forming bigger spheroids (67). Another system to facilitate cell aggregation is the use of solid scaffolds with different porosity composed by natural or synthetic materials such as collagen, chitosan, or D,D,-L,L-polylactic acid. After seeding, cells can migrate along the surface, aggregate, and create 3D structures (68).

As tumor cells do not exist as isolated entities but rather are part of a complex microenvironment, natural or synthetic *hydrogel matrices* (**Figure 3E**) that mimic the *in vivo* tissue architecture can be used to grow tumor cells in 3D structures. The choice of a naturally or synthetically composed gel can be based on the aim of the analysis, ranging from single component hydrogels, i.e., laminin, collagen, and fibronectin to more complex ones such as Matrigel™ or Puramatrix™ (69, 70). Tumor cells can also be grown together with other tissue components such as stroma and epithelial cells in organotypic cocultures (**Figure 2B**). This more complex model allows to study the influence of tumor microenvironment on tumor development and progression as well as on drug sensitivity (71–74).

One of the most important tools in medical research is the model able to mimic the physiological situation in the closest way possible. Since they are commercially available and easy to handle, most of the basic and preclinical research in the oncological field was done using immortalized cell lines. On the downside, long-term *in vivo* culturing and the immortalization process often cause alterations in the molecular and phenotypic characteristics of these cells that can strongly differ from the cell of origin. To overcome these limitations, fresh tissue directly obtained during surgery has been used for isolating and cultivating tumor cells. One of the most straight forward methods is to cultivate fragments/slices of the tumor tissue as so-called *organotypic slice cultures* (**Figure 2C**). Several research groups use this method to study drug uptake, proliferation, and cell death, as well as for molecular characterization before and after treatment

(75–77). The main advantage of this system is that the original tissue architecture is preserved, allowing the immediate study of the normal/altered physiology. Using tissue slices that can be maintained in culture for a short period of time only and without the opportunity of further expansion strongly limits the use of these models.

The currently most innovative and promising approach for *in vitro* model is represented by *tumor tissue organoids* (**Figures 2D** and **4**). Organoids are multicellular structures directly isolated from primary tissue and grown in well-defined conditions. 3D organoids maintain the complex architecture of their tissue of origin and self-organize by reproducing their unique architecture and marker expression. This innovative tool has been used by several research groups for studying tumor development and progression and for testing drug efficacy (78–81). Interestingly, it has been recently demonstrated that this tumor model can be easily applied to high-throughput drug screening (82) and to correlate patient's tumor molecular profiles to drug sensitivity (83).

MOLECULAR DRIVERS OF SARCOMA DEVELOPMENT AS NOVEL TARGETS FOR INTERVENTION

Genomic Analysis of Driver Mutations

In 2010, Barretina and colleagues (84) performed an integrative system analysis of DNA sequence, copy number, and mRNA expression on 207 soft-tissue sarcoma samples including 7 major subtypes to identify novel subtype-specific genomic alterations representing potential therapeutic targets. They first studied genomic alterations in 47 tumor/normal DNA pairs highlighting 21 totally modified genes. These results were then validated in a second study-set of 160 tumors confirming the presence of subtype-specific mutations in several genes such as *PIK3CA* in myxoid/round cell liposarcoma, *TP53* in pleomorphic liposarcoma, and *NF1* in myxofibrosarcoma and pleomorphic liposarcoma. The data obtained are of high clinical potential since they helped identify tumors that might be responsive to PI3K or mTOR inhibitors, since NF1 loss causes mTOR pathway activation.

Recently, panel sequencing of 194 cancer-related genes in 25 STS was performed to identify actionable mutations (85). This analysis revealed the presence of different mutational profiles. In particular, in 60% of the cases targetable mutations for which clinical trials are available were highlighted while for another 28% of cases mutations which are currently not targetable were present. This study demonstrates the versatility of next-generation sequencing both in patient stratification for treatment with currently available therapeutics and in the identification of potential targets for developing new molecular treatments.

In the recent years, strong efforts have been made to find new biomarkers for selecting the best treatment based on specific tumor molecular profiles. With the goal of developing an efficient approach for patient stratification for treatment, Hanes

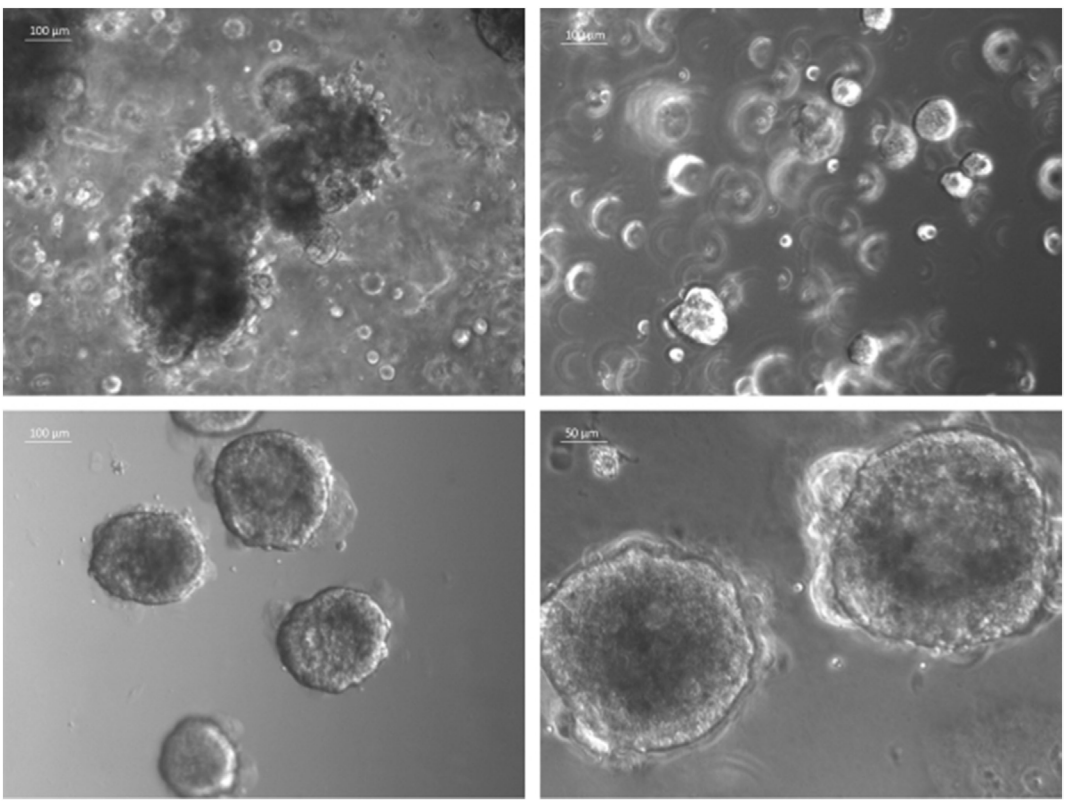

FIGURE 4 | Sarcoma spheroids growing in Matrigel-based three-dimensional cell culture.

and colleagues (86) combined tumor genomic characterization with drug testing *in vitro* in patient-derived cell lines. Three metastases from a patient with high-grade dedifferentiated liposarcoma previously treated with different chemotherapeutic agents were used for the study. Tumor tissues were analyzed by exome and transcriptome sequencing as well as DNA copy number analysis to highlight genomic aberrations that could represent potential targets for treatment. The data obtained were then used for selecting those drugs that can directly affect the altered gene or the corresponding signaling pathway in a cell line derived from the metastatic tissue. Among the altered genes observed in the tumor sample, an amplification of *FRS2*, the gene coding for fibroblast growth factor receptor substrate 2, was revealed. Based on this molecular alteration, they tested the *in vitro* efficacy of NVP-BGJ398 (infigratinib), a pan-FGFR inhibitor showing promising inhibition of proliferation induced by cell cycle arrest. Taken together, these data demonstrate the benefit of combining tumor genomic profiling with *in vitro* testing for a better selection of treatment in sarcoma patients and for selecting new promising treatments for improving sarcoma survival.

Proteomic Analysis of Intracellular Pathways Alterations

Even if specific mutations have been associated with certain sarcoma subtypes, their etiology remain largely unknown. An equally important approach in biomarker discovery is the analysis of the proteome. Since the proteome is a functional translation of the genome, the information provided by its in-depth analysis may be a key in understanding sarcoma progression and therapy failure. Several research groups focused on differential expression of proteins in tumor tissue compared to the normal counterpart using diverse technologies such as Digiwest (87), 2D-PAGE (86, 87), mass spectrometry (87), and array technology (88).

Developing new sarcoma diagnostic biomarkers, Suehara and colleagues used 2D difference electrophoresis (2D-DIGE) analysis performing global protein expression analysis in different histological subtypes of soft-tissue sarcoma. Profiling data highlighted a set of 67 proteins distinguishing the 80 sarcoma samples based on their histological classification. Moreover, a signature of five proteins was able to differentiate at time of that publication known as grade III malignant fibrous histocytomas (today classified as UPS) and leiomyosarcomas into low- and high-risk groups characterized by significantly different survival rates (88).

The same research group applied a combined 2D-DIGE and mass spectrometry approach for profiling patients with GIST characterized by good and poor clinical prognosis (89), demonstrating the potential of this marker in GIST clinical management. This analysis highlighted 43 proteins (spots) differentially expressed and corresponding to 25 distinct gene products. Among these proteins, the authors focused on pfetin, a potassium channel protein, since 8 of the 43 spots that were found derived from this protein, and 4 of these had discriminative power between the two groups. Pfetin expression and its correlation with tumor metastasis was confirmed by real-time PCR and western blot. Moreover, the authors demonstrated that pfetin expression and 5-year metastasis-free survival rate were directly correlating.

In another recent study, 59 rhabdomyosarcoma samples were microdissected to enrich tumor cell content and analyzed by reverse phase protein microarrays (90), an antibody-based technology useful in studying the level of expression of selected total and phosphoproteins. This study showed that the phosphorylation of several components of the Akt/mTOR pathway was increased in tumors from patients with short-term survival. Moreover, an altered relationship between insulin receptor substrate 1, and this pathway was highlighted in patients with poor survival. The significance of these results was demonstrated by treating mouse xenografts with CCI-779, an mTOR inhibitor, that compared to controls greatly reduced the growth of two different rhabdomyosarcoma cell lines. These data showed the utility of phosphoproteomic pathway mapping for the study of functional drivers of sarcoma progression and for selecting patients for anti-mTOR/IRS therapy. These and other proteomic studies in different sarcoma subtypes were extensively reviewed by Kondo and colleagues (91).

Genomic and proteomic approaches can be synergistically applied for a deeper understanding of tumor biology at molecular level. Integrating these profiling systems, it is possible to correlate the presence of tumor-specific mutations to functional alterations in intracellular pathways. The information obtained from a multiomics approach may help in both designing new targeted therapies and selecting the best treatment option for a specific patient.

PRECLINICAL DRUG SCREENING FOR IMPROVING SARCOMA TREATMENT

Since no innovative therapeutic approaches are available for most sarcoma subtypes, several research groups focused on the discovery of new targets for sarcoma treatment by screening of compound libraries mainly on immortalized 2D cell lines and studying their effect on sarcoma cell biology.

As mentioned before, several sarcoma types are characterized by the presence of chromosomal translocations that cause the production of altered transcription factors. About 85% of EWSs express the EWS/FLI1 fusion protein, known to cause alterations in transcriptional regulation and RNA processing. EWS/FLI1 represents a very attractive drug target since it is specifically expressed by the tumor cells, but it is absent in the healthy tissue. Since, currently, no drugs targeting transcription factors are available, one approach is to directly or indirectly inhibit the players of the altered connected pathway. To this aim, Grohar and coworkers (92) screened more than 50,000 compounds in TC32 EWS cells for the ability of altering the expression level of the EWS/FLI1 downstream target NR0B1, that was prior transfected with a luciferase construct. The 200 compounds that showed activity in primary screening were further validated by multiplex PCR assay with the aim of selecting those hits that best inhibited the expression of a predetermined set of EWS/

FLI1 downstream target genes. With this approach, they selected mithramycin as lead compound able to inhibit EWS/FLI1 activity. This effect was validated and further characterized in *in vitro* experiments and in *in vivo* xenograft models. Taken together, these data demonstrate the potential efficacy of this compound in treating EWS and the utility of applying high-throughput screening approaches for selecting new potential drug targets and new sarcoma therapies.

A similar study screened a small-molecule compound library containing FDA-approved drugs modulating the expression of EWS/FLI1 target genes on a panel of six EWS cell lines (93). To determine compound efficacy, the expression levels of few, well-characterized EWS/FLI1 target genes was measured. Among the 10 hits with the highest efficacy, several know therapeutic agents and fenretinide, currently in clinical trials for Ewing's sarcoma, have been highlighted demonstrating the robustness of this screening approach. Moreover, midostaurin, a pan-kinase inhibitor, resulted in one of the most promising novel compounds. Interestingly, the efficacy of this drug was already shown in rhabdomyosarcoma, another pediatric sarcoma type. Moreover, midostaurin is currently undergoing phase II clinical trials for leukemia in adults and children, with a low toxicity in the pediatric population that make this drug a promising candidate to be tested in pediatric sarcoma patients.

The determination of new drug targets and efficient therapeutics requires even more the investigation of sarcoma subtypes that, unlike EWS, are not characterized by a known driver molecular alteration. Several groups tested available compound libraries to better characterize the drug sensitivity of different sarcoma subtypes and to correlate the response to specific compounds with the molecular characteristics of the tumor. Teicher and coworkers (94) screened the response of 63 sarcoma cell lines to 100 FDA-approved anticancer drugs and to a library of 345 investigational oncology agents. Moreover, they correlated treatment response with cell molecular profiles obtained by exon and microRNA arrays. The authors highlighted important correlations between cell characteristics such as sarcoma subtype and gene/miRNA expression, demonstrating that this screening approach is useful in studying the efficacy of FDA-approved drugs in specific sarcoma subtypes, in defining new potential therapeutic agents and for correlating sarcoma molecular profiles with drug sensitivity.

With such screening platforms available, it will become possible to investigate combination therapies for "vertical inhibition" of a single pathway or inhibition spanning multiple pathways.

CLINICAL OPPORTUNITIES FOR PATIENT-DERIVED 3D (PD3D) *IN VITRO* MODELS

Ever since the sequencing of the first human genome, hopes were high that knowledge of the cancer genome landscape would bring an end to cancer and other diseases. Yet, sequencing alone has proven to be "remarkably unhelpful," and the belief that sequencing your DNA is going to extend your life is "a cruel illusion" as James Watson put it in a recent interview with the New York Times (95). Today, genome researchers still struggle to be able to sufficiently support clinical decision-making with meaningful sequence data, and to compensate for this deficit, they propose that "more is more" (96). Yet, these genome centrics are neither feasible in the clinical setting nor payable by the majority of patients and insurance companies. Using PD3D cell cultures and exploiting their phenomics by combining multiple layers of evidence is expected to soon become the state-of-the-art approach. All current reports share the assumption that short-term PD3D cell cultures have already proven their superior predictive value in the preclinical arena, ousting other *in vitro* models in the development of new drugs. Pauli et al. have reported that they can successfully establish 3D cell cultures from surgically removed specimen within weeks (97). Therefore, leading comprehensive cancer centers around the world have started including patient-specific cell culture data in their infrastructure, as detailed by Shraddha Chakrandhar in Nature Medicine (98). Drug screenings in an automated setup, as described in 2016 by Boehnke et al. (82), take about 1 week once enough cells are available. In parallel, ultra-deep targeted sequencing can be performed, focusing on only those mutations that are relevant for the clinical decision-making.

Of course, the panels of target genes to be sequenced has to be updated with latest clinically relevant information to ensure that oncologists can stay focused on the immediate needs of the patients. Protein extracts from before and after the drug screening can be used for methods like Digiwest, a bead-based, multiplexed western blot (87). With this method, a selection of up to 200 (phospho-)proteins can be quantified at once, providing differential information not only on expression levels but also on the activation of key signaling kinases, such as those along them TOR, WNT, MAPK, or PI3K axes. Taking into consideration the time frame in which additional information can be used to support the decision-making process and the nature of information that becomes available from measuring cellular phenomics for the discussion in tumor boards, PD3D models may indeed become an integral part in clinical oncology of the 21st century.

CONCLUSION

Recent research efforts in sarcoma has enabled important improvements in the knowledge of sarcoma histopathology that in turn defined sarcomas not as a single tumor entity but rather as different tumor subtypes with histology-specific molecular characteristics. The recent development of targeted therapies significantly contributed to the improved treatment options for sarcoma patients. Considering that this approach, first developed in carcinomas, showed efficacy in GIST, the next step in sarcoma research is to focus on the molecular characterization of the different subtypes to highlight new potential targets for therapy.

Since the availability of *in vitro* models that reliably represent the physiological tumor behavior is a prerequisite for successful sarcoma preclinical and translational research, several models have been developed for discovering new potential targets for

therapeutic intervention. In particular, patient-derived cell lines and more recently 3D organoids represent innovative tools for studying molecular pathways promoting sarcoma development and tumor progression and for drug efficacy screenings. Moreover, these models could directly impact clinical decisions if and when used as a tool for precision medicine. 3D cultures directly isolated from a patient's sarcoma could be used for testing the efficacy of drugs currently available, thus supporting clinicians in the selection of the most efficacious and promising treatment.

AUTHOR CONTRIBUTIONS

MG, AS, and CR drafted the original manuscript. CL provided the figures. JH, PR, LS, and GZ edited the draft and supported MG, AS, CR, and CL in finalizing the manuscript.

FUNDING

This study was supported by Berliner Krebsgesellschaft e.V. grant to CR (grant #201402).

REFERENCES

1. Mastrangelo G, Coindre J-M, Ducimetière F, Dei Tos AP, Fadda E, Blay J-Y, et al. Incidence of soft tissue sarcoma and beyond: a population-based prospective study in 3 European regions. *Cancer* (2012) 118:5339–48. doi:10.1002/cncr.27555
2. Ryan CW, Desai J. The past, present, and future of cytotoxic chemotherapy and pathway-directed targeted agents for soft tissue sarcoma. *Am Soc Clin Oncol Educ Book* (2013) 33:e386–93. doi:10.1200/EdBook_AM.2013.33.e386
3. Patel SR, Benjamin RS. Weichgewebe- und Knochensarkome und Knochenmetastasen. In: Suttorp N, Dietel M, editors. *Harrison's Principles of Internal Medicine (Harrisons Innere Medizin)*. Berlin: ABWWissens chaftsverlag GmbH, The McGraw-Hill Companies, Inc. (2013). p. 876–81.
4. Burningham Z, Hashibe M, Spector L, Schiffman JD. The epidemiology of sarcoma. *Clin Sarcoma Res* (2012) 2:14. doi:10.1186/2045-3329-2-14
5. Stiller CA, Trama A, Serraino D, Rossi S, Navarro C, Chirlaque MD, et al. Descriptive epidemiology of sarcomas in Europe: report from the RARECARE project. *Eur J Cancer* (2013) 49:684–95. doi:10.1016/j.ejca.2012.09.011
6. American Cancer Society. *Special Section: Rare Cancers in Adults*. Atlanta: American Cancer Society (2017).
7. The ESMO/European Sarcoma Network Working Group. Soft tissue and visceral sarcomas: ESMO Clinical Practice Guidelines for diagnosis, treatment and follow-up. *Ann Oncol* (2014) 25:iii102–12. doi:10.1093/annonc/mdu254
8. The ESMO/European Sarcoma Network Working Group. Bone sarcomas: ESMO Clinical Practice Guidelines for diagnosis, treatment and follow-up. *Ann Oncol* (2014) 25:iii113–23. doi:10.1093/annonc/mdu256
9. The ESMO/European Sarcoma Network Working Group. Gastrointestinal stromal tumours: ESMO Clinical Practice Guidelines for diagnosis, treatment and follow-up. *Ann Oncol* (2014) 25:iii21–6. doi:10.1093/annonc/mdu255
10. Gatta G, van der Zwan JM, Casali PG, Siesling S, Dei Tos AP, Kunkler I, et al. Rare cancers are not so rare: the rare cancer burden in Europe. *Eur J Cancer* (2011) 47:2493–511. doi:10.1016/j.ejca.2011.08.008
11. Schütte J, Bauer S, Brodowicz T, Grünwald V, Hofer S, Hohenberger P, et al. *Weichgewebssarkome des Erwachsenen*. (2017). Available from: www.dgho.de
12. Fletcher CDM, Krishnan Unni K, Mertens F, editors. *WHO Classification of Tumours, Pathology and Genetics of Tumours of Soft Tissue and Bone*. Lyon (2002). p. 1–415.
13. Jo VY, Fletcher CDM. WHO classification of soft tissue tumours: an update based on the 2013 (4th) edition. *Pathology* (2014) 46:95–104. doi:10.1097/PAT.0000000000000050
14. Curtiss P, Strazzulla LC, Friedman-Kien AE. An update on Kaposi's sarcoma: epidemiology, pathogenesis and treatment. *Dermatol Ther (Heidelb)* (2016) 6:465–70. doi:10.1007/s13555-016-0152-3
15. Helman LJ, Meltzer P. Mechanisms of sarcoma development. *Nat Rev Cancer* (2003) 3:685–94. doi:10.1038/nrc1168
16. Dancsok AR, Asleh-Aburaya K, Nielsen TO. Advances in sarcoma diagnostics and treatment. *Oncotarget* (2017) 8:7068–93. doi:10.18632/oncotarget.12548
17. Binh MBN, Sastre-Garau X, Guillou L, de Pinieux G, Terrier P, Lagacé R, et al. MDM2 and CDK4 immunostainings are useful adjuncts in diagnosing well-differentiated and dedifferentiated liposarcoma subtypes: a comparative analysis of 559 soft tissue neoplasms with genetic data. *Am J Surg Pathol* (2005) 29:1340–7. doi:10.1097/01.pas.0000170343.09562.39
18. Italiano A, Bianchini L, Keslair F, Bonnafous S, Cardot-Leccia N, Coindre J-M, et al. HMGA2 is the partner of MDM2 in well-differentiated and dedifferentiated liposarcomas whereas CDK4 belongs to a distinct inconsistent amplicon. *Int J Cancer* (2008) 122:2233–41. doi:10.1002/ijc.23380
19. Morrison BA. Soft tissue sarcomas of the extremities. *Proc (Bayl Univ Med Cent)* (2003) 16:285–90.
20. Hirota S, Isozaki K, Moriyama Y, Hashimoto K, Nishida T, Ishiguro S, et al. Gain-of-function mutations of c-kit in human gastrointestinal stromal tumors. *Science* (1998) 279:577–80. doi:10.1126/science.279.5350.577
21. Corless CL, Barnett CM, Heinrich MC. Gastrointestinal stromal tumours: origin and molecular oncology. *Nat Rev Cancer* (2011) 11:865–78. doi:10.1038/nrc3143
22. Kurtovic-Kozaric A, Kugic A, Hasic A, Beslija S, Ceric T, Pasic A, et al. Long-term outcome of GIST patients treated with delayed imatinib therapy. *Eur J Cancer* (2017) 78:118–21. doi:10.1016/j.ejca.2017.03.024
23. Mohseny AB, Hogendoorn PCW. Concise review: mesenchymal tumors: when stem cells go mad. *Stem Cells* (2011) 29:397–403. doi:10.1002/stem.596
24. Teicher BA. Searching for molecular targets in sarcoma. *Biochem Pharmacol* (2012) 84:1–10. doi:10.1016/j.bcp.2012.02.009
25. Danielson LS, Menendez S, Attolini CS-O, Guijarro MV, Bisogna M, Wei J, et al. A differentiation-based microRNA signature identifies leiomyosarcoma as a mesenchymal stem cell-related malignancy. *Am J Pathol* (2010) 177:908–17. doi:10.2353/ajpath.2010.091150
26. Matushansky I, Hernando E, Socci ND, Matos T, Mills J, Edgar MA, et al. A developmental model of sarcomagenesis defines a differentiation-based classification for liposarcomas. *Am J Pathol* (2008) 172:1069–80. doi:10.2353/ajpath.2008.070284
27. Cleton-Jansen A-M, Anninga JK, Briaire-de Bruijn IH, Romeo S, Oosting J, Egeler RM, et al. Profiling of high-grade central osteosarcoma and its putative progenitor cells identifies tumourigenic pathways. *Br J Cancer* (2009) 101:2064–2064. doi:10.1038/sj.bjc.6605482
28. Nielsen TO, West RB, Linn SC, Alter O, Knowling MA, O'Connell JX, et al. Molecular characterisation of soft tissue tumours: a gene expression study. *Lancet* (2002) 359:1301–7. doi:10.1016/S0140-6736(02)08270-3
29. Boeuf S, Kunz P, Hennig T, Lehner B, Hogendoorn P, Bovée J, et al. A chondrogenic gene expression signature in mesenchymal stem cells is a classifier of conventional central chondrosarcoma. *J Pathol* (2008) 216:158–66. doi:10.1002/path.2389
30. Miura M, Miura Y, Padilla-Nash HM, Molinolo AA, Fu B, Patel V, et al. Accumulated chromosomal instability in murine bone marrow mesenchymal stem cells leads to malignant transformation. *Stem Cells* (2006) 24:1095–103. doi:10.1634/stemcells.2005-0403
31. Li H, Fan X, Kovi RC, Jo Y, Moquin B, Konz R, et al. Spontaneous expression of embryonic factors and p53 point mutations in aged mesenchymal stem cells: a model of age-related tumorigenesis in mice. *Cancer Res* (2007) 67:10889–98. doi:10.1158/0008-5472.CAN-07-2665
32. Hahn WC, Counter CM, Lundberg AS, Beijersbergen RL, Brooks MW, Weinberg RA. Creation of human tumour cells with defined genetic elements. *Nature* (1999) 400:464–8. doi:10.1038/22780
33. Rich JN, Guo C, McLendon RE, Bigner DD, Wang XF, Counter CM. A genetically tractable model of human glioma formation. *Cancer Res* (2001) 61:3556–60.

34. Shima Y, Okamoto T, Aoyama T, Yasura K, Ishibe T, Nishijo K, et al. In vitro transformation of mesenchymal stem cells by oncogenic H-rasVal12. *Biochem Biophys Res Commun* (2007) 353:60–6. doi:10.1016/j.bbrc.2006.11.137
35. Li N, Yang R, Zhang W, Dorfman H, Rao P, Gorlick R. Genetically transforming human mesenchymal stem cells to sarcomas: changes in cellular phenotype and multilineage differentiation potential. *Cancer* (2009) 115:4795–806. doi:10.1002/cncr.24519
36. Mohseny AB, Szuhai K, Romeo S, Buddingh EP, Briaire-de Bruijn I, de Jong D, et al. Osteosarcoma originates from mesenchymal stem cells in consequence of aneuploidization and genomic loss of Cdkn2. *J Pathol* (2009) 219:294–305. doi:10.1002/path.2603
37. Adhikari AS, Agarwal N, Wood BM, Porretta C, Ruiz B, Pochampally RR, et al. CD117 and Stro-1 identify osteosarcoma tumor-initiating cells associated with metastasis and drug resistance. *Cancer Res* (2010) 70:4602–12. doi:10.1158/0008-5472.CAN-09-3463
38. Levings PP, McGarry SV, Currie TP, Nickerson DM, McClellan S, Ghivizzani SC, et al. Expression of an exogenous human Oct-4 promoter identifies tumor-initiating cells in osteosarcoma. *Cancer Res* (2009) 69:5648–55. doi:10.1158/0008-5472.CAN-08-3580
39. Fujii H, Honoki K, Tsujiuchi T, Kido A, Yoshitani K, Takakura Y. Sphere-forming stem-like cell populations with drug resistance in human sarcoma cell lines. *Int J Oncol* (2009) 34:1381–6. doi:10.3892/ijo_00000265
40. Honoki K. Do stem-like cells play a role in drug resistance of sarcomas? *Expert Rev Anticancer Ther* (2010) 10:261–70. doi:10.1586/era.09.184
41. Italiano A, Di Mauro I, Rapp J, Pierron G, Auger N, Alberti L, et al. Clinical effect of molecular methods in sarcoma diagnosis (GENSARC): a prospective, multicentre, observational study. *Lancet Oncol* (2016) 17:532–8. doi:10.1016/S1470-2045(15)00583-5
42. Gerlinger M, Horswell S, Larkin J, Rowan AJ, Salm MP, Varela I, et al. Genomic architecture and evolution of clear cell renal cell carcinomas defined by multiregion sequencing. *Nat Genet* (2014) 46:225–33. doi:10.1038/ng.2891
43. Gerlinger M, Rowan AJ, Horswell S, Larkin J, Endesfelder D, Gronroos E, et al. Intratumor heterogeneity and branched evolution revealed by multiregion sequencing. *N Engl J Med* (2012) 366:883–92. doi:10.1056/NEJMoa1113205
44. Rye IH, Helland Å, Saetersdal A, Naume B, Almendro V, Polyak K, et al. Intratumor heterogeneity as a predictor of therapy response in HER2 positive breast cancer. *Cancer Res* (2012) 72. doi:10.1158/0008-5472.SABCS12-P3-05-04
45. Tougeron D, Lecomte T, Pages JC, Villalva C, Collin C, Ferru A, et al. Effect of low-frequency KRAS mutations on the response to anti-EGFR therapy in metastatic colorectal cancer. *Ann Oncol* (2013) 24:1267–73. doi:10.1093/annonc/mds620
46. Bai H, Wang Z, Wang Y, Zhuo M, Zhou Q, Duan J, et al. Detection and clinical significance of intratumoral EGFR mutational heterogeneity in Chinese patients with advanced non-small cell lung cancer. *PLoS One* (2013) 8:e54170. doi:10.1371/journal.pone.0054170
47. Patwardhan PP, Surriga O, Beckman MJ, de Stanchina E, Dematteo RP, Tap WD, et al. Sustained inhibition of receptor tyrosine kinases and macrophage depletion by PLX3397 and rapamycin as a potential new approach for the treatment of MPNSTs. *Clin Cancer Res* (2014) 20:3146–58. doi:10.1158/1078-0432.CCR-13-2576
48. Salawu A, Fernando M, Hughes D, Reed MWR, Woll P, Greaves C, et al. Establishment and molecular characterisation of seven novel soft-tissue sarcoma cell lines. *Br J Cancer* (2016) 115:1058–68. doi:10.1038/bjc.2016.259
49. Bruland O, Fodstad O, Pihl A. The use of multicellular spheroids in establishing human sarcoma cell lines in vitro. *Int J Cancer* (1985) 35:793–8. doi:10.1002/ijc.2910350616
50. Hu M, Nicolson GL, Trent JC, Yu D, Zhang L, Lang A, et al. Characterization of 11 human sarcoma cell strains. *Cancer* (2002) 95:1569–76. doi:10.1002/cncr.10879
51. Ottaviano L, Schaefer K-L, Gajewski M, Huckenbeck W, Baldus S, Rogel U, et al. Molecular characterization of commonly used cell lines for bone tumor research: a trans-European EuroBoNet effort. *Genes Chromosomes Cancer* (2010) 49:40–51. doi:10.1002/gcc.20717
52. Mohseny AB, Machado I, Cai Y, Schaefer K-L, Serra M, Hogendoorn PCW, et al. Functional characterization of osteosarcoma cell lines provides representative models to study the human disease. *Lab Invest* (2011) 91:1195–205. doi:10.1038/labinvest.2011.72
53. Kenny PA, Lee GY, Myers CA, Neve RM, Semeiks JR, Spellman PT, et al. The morphologies of breast cancer cell lines in three-dimensional assays correlate with their profiles of gene expression. *Mol Oncol* (2007) 1:84–96. doi:10.1016/j.molonc.2007.02.004
54. Silberstein GB. Tumour-stromal interactions. Role of the stroma in mammary development. *Breast Cancer Res* (2001) 3:218–23. doi:10.1186/bcr299
55. Schmeichel KL, Bissell MJ. Modeling tissue-specific signaling and organ function in three dimensions. *J Cell Sci* (2003) 116:2377–88. doi:10.1242/jcs.00503
56. Akkerman N, Defize LHK. Dawn of the organoid era: 3D tissue and organ cultures revolutionize the study of development, disease, and regeneration. *Bioessays* (2017) 39:1600244. doi:10.1002/bies.201600244
57. Bai C, Yang M, Fan Z, Li S, Gao T, Fang Z. Associations of chemo- and radio-resistant phenotypes with the gap junction, adhesion and extracellular matrix in a three-dimensional culture model of soft sarcoma. *J Exp Clin Cancer Res* (2015) 34:58. doi:10.1186/s13046-015-0175-0
58. Salerno M, Avnet S, Bonuccelli G, Eramo A, De Maria R, Gambarotti M, et al. Sphere-forming cell subsets with cancer stem cell properties in human musculoskeletal sarcomas. *Int J Oncol* (2013) 43:95–102. doi:10.3892/ijo.2013.1927
59. Fong ELS, Lamhamedi-Cherradi S-E, Burdett E, Ramamoorthy V, Lazar AJ, Kasper FK, et al. Modeling Ewing sarcoma tumors in vitro with 3D scaffolds. *Proc Natl Acad Sci U S A* (2013) 110:6500–5. doi:10.1073/pnas.1221403110
60. Villasante A, Marturano-Kruik A, Robinson ST, Liu Z, Guo XE, Vunjak-Novakovic G. Tissue-engineered model of human osteolytic bone tumor. *Tissue Eng Part C Methods* (2017) 23:98–107. doi:10.1089/ten.TEC.2016.0371
61. Yuhas JM, Li AP, Martinez AO, Ladman AJ. A simplified method for production and growth of multicellular tumor spheroids. *Cancer Res* (1977) 37:3639–43.
62. Bae SI, Kang GH, Kim YI, Lee BL, Kleinman HK, Kim WH. Development of intracytoplasmic lumens in a colon cancer cell line cultured on a non-adhesive surface. *Cancer Biochem Biophys* (1999) 17:35–47. doi:10.1016/S0940-2993(99)80053-0
63. Lin R-Z, Lin R-Z, Chang H-Y. Recent advances in three-dimensional multicellular spheroid culture for biomedical research. *Biotechnol J* (2008) 3:1172–84. doi:10.1002/biot.200700228
64. Silvestri A, Schumacher D, Silvestrov M, Schäfer R, Reinhard C, Hoffmann J, et al. In vitro three-dimensional cell cultures as tool for precision medicine. In: Haybaeck J, editor. *Mechanisms of Molecular Carcinogenesis*. (Vol. 2), Cham: Springer International Publishing (2017). p. 281–313.
65. Sutherland RM, Inch WR, McCredie JA, Kruuv J. A multi-component radiation survival curve using an in vitro tumour model. *Int J Radiat Biol Relat Stud Phys Chem Med* (1970) 18:491–5. doi:10.1080/09553007014551401
66. Kelm JM, Timmins NE, Brown CJ, Fussenegger M, Nielsen LK. Method for generation of homogeneous multicellular tumor spheroids applicable to a wide variety of cell types. *Biotechnol Bioeng* (2003) 83:173–80. doi:10.1002/bit.10655
67. Johns RA, Tichotsky A, Muro M, Spaeth JP, Le Cras TD, Rengasamy A. Halothane and isoflurane inhibit endothelium-derived relaxing factor-dependent cyclic guanosine monophosphate accumulation in endothelial cell-vascular smooth muscle co-cultures independent of an effect on guanylyl cyclase activation. *Anesthesiology* (1995) 83:823–34. doi:10.1097/00000542-199510000-00023
68. Bell E. Strategy for the selection of scaffolds for tissue engineering. *Tissue Eng* (1995) 1:163–79. doi:10.1089/ten.1995.1.163
69. Hughes CS, Postovit LM, Lajoie GA. Matrigel: a complex protein mixture required for optimal growth of cell culture. *Proteomics* (2010) 10:1886–90. doi:10.1002/pmic.200900758
70. Abu-Yousif AO, Rizvi I, Evans CL, Celli JP, Hasan T. PuraMatrix encapsulation of cancer cells. *J Vis Exp* (2009) (34):e1692. doi:10.3791/1692
71. Mackenzie IC, Fusenig NE. Regeneration of organized epithelial structure. *J Invest Dermatol* (1983) 81:S189–94. doi:10.1111/1523-1747.ep12541093
72. Stark HJ, Baur M, Breitkreutz D, Mirancea N, Fusenig NE. Organotypic keratinocyte cocultures in defined medium with regular epidermal morphogenesis and differentiation. *J Invest Dermatol* (1999) 112:681–91. doi:10.1046/j.1523-1747.1999.00573.x
73. Barton CE, Johnson KN, Mays DM, Boehnke K, Shyr Y, Boukamp P, et al. Novel p63 target genes involved in paracrine signaling and keratinocyte differentiation. *Cell Death Dis* (2010) 1:e74. doi:10.1038/cddis.2010.49
74. Boehnke K, Mirancea N, Pavesio A, Fusenig NE, Boukamp P, Stark H-J. Effects of fibroblasts and microenvironment on epidermal regeneration and tissue function in long-term skin equivalents. *Eur J Cell Biol* (2007) 86:731–46. doi:10.1016/j.ejcb.2006.12.005

75. van der Kuip H, Mürdter TE, Sonnenberg M, McClellan M, Gutzeit S, Gerteis A, et al. Short term culture of breast cancer tissues to study the activity of the anticancer drug taxol in an intact tumor environment. *BMC Cancer* (2006) 6:86. doi:10.1186/1471-2407-6-86
76. Estes JM, Oliver PG, Straughn JM, Zhou T, Wang W, Grizzle WE, et al. Efficacy of anti-death receptor 5 (DR5) antibody (TRA-8) against primary human ovarian carcinoma using a novel ex vivo tissue slice model. *Gynecol Oncol* (2007) 105:291–8. doi:10.1016/j.ygyno.2006.12.033
77. Kiviharju-afHällström TM, Jäämaa S, Mönkkönen M, Peltonen K, Andersson LC, Medema RH, et al. Human prostate epithelium lacks Wee1A-mediated DNA damage-induced checkpoint enforcement. *Proc Natl Acad Sci U S A* (2007) 104:7211–6. doi:10.1073/pnas.0609299104
78. Kondo J, Endo H, Okuyama H, Ishikawa O, Iishi H, Tsujii M, et al. Retaining cell-cell contact enables preparation and culture of spheroids composed of pure primary cancer cells from colorectal cancer. *Proc Natl Acad Sci U S A* (2011) 108:6235–40. doi:10.1073/pnas.1015938108
79. Endo H, Okami J, Okuyama H, Kumagai T, Uchida J, Kondo J, et al. Spheroid culture of primary lung cancer cells with neuregulin 1/HER3 pathway activation. *J Thorac Oncol* (2013) 8:131–9. doi:10.1097/JTO.0b013e3182779ccf
80. Ashley N, Jones M, Ouaret D, Wilding J, Bodmer WF. Rapidly derived colorectal cancer cultures recapitulate parental cancer characteristics and enable personalized therapeutic assays. *J Pathol* (2014) 234:34–45. doi:10.1002/path.4371
81. Sachs N, Clevers H. Organoid cultures for the analysis of cancer phenotypes. *Curr Opin Genet Dev* (2014) 24:68–73. doi:10.1016/j.gde.2013.11.012
82. Boehnke K, Iversen PW, Schumacher D, Lallena MJ, Haro R, Amat J, et al. Assay establishment and validation of a high-throughput screening platform for three-dimensional patient-derived colon cancer organoid cultures. *J Biomol Screen* (2016) 21:931–41. doi:10.1177/1087057116650965
83. Schütte M, Risch T, Abdavi-Azar N, Boehnke K, Schumacher D, Keil M, et al. Molecular dissection of colorectal cancer in pre-clinical models identifies biomarkers predicting sensitivity to EGFR inhibitors. *Nat Commun* (2017) 8:14262. doi:10.1038/ncomms14262
84. Barretina J, Taylor BS, Banerji S, Ramos AH, Lagos-Quintana M, DeCarolis PL, et al. Subtype-specific genomic alterations define new targets for soft-tissue sarcoma therapy. *Nat Genet* (2010) 42:715–21. doi:10.1038/ng.619
85. Jour G, Scarborough JD, Jones RL, Loggers E, Pollack SM, Pritchard CC, et al. Molecular profiling of soft tissue sarcomas using next-generation sequencing: a pilot study toward precision therapeutics. *Hum Pathol* (2014) 45:1563–71. doi:10.1016/j.humpath.2014.04.012
86. Hanes R, Grad I, Lorenz S, Stratford EW, Munthe E, Reddy CCS, et al. Preclinical evaluation of potential therapeutic targets in dedifferentiated liposarcoma. *Oncotarget* (2016) 7:54583–95. doi:10.18632/oncotarget.10518
87. Treindl F, Ruprecht B, Beiter Y, Schultz S, Döttinger A, Staebler A, et al. A bead-based western for high-throughput cellular signal transduction analyses. *Nat Commun* (2016) 7:12852. doi:10.1038/ncomms12852
88. Suehara Y, Kondo T, Fujii K, Hasegawa T, Kawai A, Seki K, et al. Proteomic signatures corresponding to histological classification and grading of soft-tissue sarcomas. *Proteomics* (2006) 6:4402–9. doi:10.1002/pmic.200600196
89. Suehara Y, Kondo T, Seki K, Shibata T, Fujii K, Gotoh M, et al. Pfetin as a prognostic biomarker of gastrointestinal stromal tumors revealed by proteomics. *Clin Cancer Res* (2008) 14:1707–17. doi:10.1158/1078-0432.CCR-07-1478
90. Petricoin EF, Espina V, Araujo RP, Midura B, Yeung C, Wan X, et al. Phosphoprotein pathway mapping: Akt/mammalian target of rapamycin activation is negatively associated with childhood rhabdomyosarcoma survival. *Cancer Res* (2007) 67:3431–40. doi:10.1158/0008-5472.CAN-06-1344
91. Kondo T, Kawai A. A proteomics approach for the development of sarcoma biomarkers. *EuPA Open Proteom* (2014) 4:121–8. doi:10.1016/j.euprot.2014.06.004
92. Grohar PJ, Woldemichael GM, Griffin LB, Mendoza A, Chen Q-R, Yeung C, et al. Identification of an inhibitor of the EWS-FLI1 oncogenic transcription factor by high-throughput screening. *J Natl Cancer Inst* (2011) 103:962–78. doi:10.1093/jnci/djr156
93. Boro A, Prêtre K, Rechfeld F, Thalhammer V, Oesch S, Wachtel M, et al. Small-molecule screen identifies modulators of EWS/FLI1 target gene expression and cell survival in Ewing's sarcoma. *Int J Cancer* (2012) 131:2153–64. doi:10.1002/ijc.27472
94. Teicher BA, Polley E, Kunkel M, Evans D, Silvers T, Delosh R, et al. Sarcoma cell line screen of oncology drugs and investigational agents identifies patterns associated with gene and microRNA expression. *Mol Cancer Ther* (2015) 14:2452–62. doi:10.1158/1535-7163.MCT-15-0074
95. Apple S. *Starving the Beast*. New York: The New York Times (2016). MM64 p.
96. Schütte M, Ogilvie LA, Rieke DT, Lange BMH, Yaspo M-L, Lehrach H. Cancer precision medicine: why more is more and DNA is not enough. *Public Health Genomics* (2017). doi:10.1159/000477157
97. Pauli C, Hopkins BD, Prandi D, Shaw R, Fedrizzi T, Sboner A, et al. Personalized in vitro and in vivo cancer models to guide precision medicine. *Cancer Discov* (2017) 7:462–77. doi:10.1158/2159-8290.CD-16-1154
98. Chakradhar S. Put to the test: organoid-based testing becomes a clinical tool. *Nat Med* (2017) 23:796–9. doi:10.1038/nm0717-796

Conflict of Interest Statement: No aspect of the submitted work has received payment or services from a third party. No entity has influenced the content of the submitted work. CR is founder and CEO of cpo. AS and GZ are employed at cpo. cpo is a contract research company working as a service provider in the field of 3D *in vitro* models and drug screening. CL and LS work in research at Eli Lilly and Company. MG and PR work at the Sarcoma Center at HELIOS Kliniken Berlin-Buch. HELIOS operates multiple hospitals in Germany and Europe. PR reports grants and personal fees from Novartis, personal fees from Pfizer, personal fees from Bayer, personal fees from PharmaMar, personal fees from Amgen, personal fees from GlaxoSmthKline, personal fees from Clinigen, personal fees from Lilly, and personal fees from AstraZeneca. None of them has been influencing the submitted work. All other authors declare no conflict of interest.

frontiers in Oncology

ORIGINAL RESEARCH
published: 31 May 2017
doi: 10.3389/fonc.2017.00111

The Human NADPH Oxidase, Nox4, Regulates Cytoskeletal Organization in Two Cancer Cell Lines, HepG2 and SH-SY5Y

Simon Auer[1†], Mark Rinnerthaler[2†], Johannes Bischof[2], Maria Karolin Streubel[2], Hannelore Breitenbach-Koller[2], Roland Geisberger[3], Elmar Aigner[4,5], Janne Cadamuro[1], Klaus Richter[2], Mentor Sopjani[6], Elisabeth Haschke-Becher[1], Thomas Klaus Felder[1,5] and Michael Breitenbach[2]**

[1] Department of Laboratory Medicine, Paracelsus Medical University, Salzburg, Austria, [2] Department of Cell Biology, Division of Genetics, University of Salzburg, Salzburg, Austria, [3] Department of Internal Medicine III with Hematology, Medical Oncology, Hemostaseology, Infectious Diseases, Rheumatology, Oncologic Center, Laboratory for Immunological and Molecular Cancer Research, Paracelsus Medical University, Salzburg, Austria, [4] First Department of Medicine, Paracelsus Medical University, Salzburg, Austria, [5] Obesity Research Unit, Paracelsus Medical University, Salzburg, Austria, [6] Faculty of Medicine of the University of Prishtina, Prishtina, Kosovo

OPEN ACCESS

Edited by:
Tao Liu,
University of New South Wales, Australia

Reviewed by:
Alexander A. Mongin,
Albany Medical College, USA
Paolo E. Porporato,
Université catholique de Louvain, Belgium

***Correspondence:**
Thomas Klaus Felder
t.felder@salk;
Michael Breitenbach
michael.breitenbach@sbg.ac.at

[†]These authors have contributed equally to this work.

Specialty section:
This article was submitted to Molecular and Cellular Oncology, a section of the journal Frontiers in Oncology

Received: *06 October 2016*
Accepted: *12 May 2017*
Published: *31 May 2017*

Citation:
Auer S, Rinnerthaler M, Bischof J, Streubel MK, Breitenbach-Koller H, Geisberger R, Aigner E, Cadamuro J, Richter K, Sopjani M, Haschke-Becher E, Felder TK and Breitenbach M (2017) The Human NADPH Oxidase, Nox4, Regulates Cytoskeletal Organization in Two Cancer Cell Lines, HepG2 and SH-SY5Y. Front. Oncol. 7:111. doi: 10.3389/fonc.2017.00111

NADPH oxidases of human cells are not only functional in defense against invading microorganisms and for oxidative reactions needed for specialized biosynthetic pathways but also during the past few years have been established as signaling modules. It has been shown that human Nox4 is expressed in most somatic cell types and produces hydrogen peroxide, which signals to remodel the actin cytoskeleton. This correlates well with the function of Yno1, the only NADPH oxidase of yeast cells. Using two established tumor cell lines, which are derived from hepatic and neuroblastoma tumors, respectively, we are showing here that in both tumor models Nox4 is expressed in the ER (like the yeast NADPH oxidase), where according to published literature, it produces hydrogen peroxide. Reducing this biochemical activity by downregulating Nox4 transcription leads to loss of F-actin stress fibers. This phenotype is reversible by adding hydrogen peroxide to the cells. The effect of the Nox4 silencer RNA is specific for this gene as it does not influence the expression of Nox2. In the case of the SH-SY5Y neuronal cell line, Nox4 inhibition leads to loss of cell mobility as measured in scratch assays. We propose that inhibition of Nox4 (which is known to be strongly expressed in many tumors) could be studied as a new target for cancer treatment, in particular for inhibition of metastasis.

Keywords: NADPH oxidase, hydrogen peroxide, signaling, actin cytoskeleton, cell migration

INTRODUCTION

In an article that appeared in 2012, we showed that the monocellular yeast, *Saccharomyces cerevisiae*, contains a genuine NADPH oxidase, Yno1, and provided evidence for a function of this enzyme in regulation of the actin cytoskeleton of the yeast cell (1). We now wanted to extend this finding by studying the human NADPH oxidase Nox4, which is involved in the pathomechanism of human cancer cells. Regulation of the assembly and polarity of the actin cytoskeleton of human cells is required for all steps of tumor development and in particular is prerequisite for cell mobility and, therefore, for metastasis

of human cancer cells. This fact, and the other unique properties of Nox4 listed subsequently prompted us to choose Nox4 among the group of seven NADPH oxidase (Nox) isoenzymes expressed in human cells.

Nox4 displays the largest sequence identity and similarity of all human Nox enzymes to the yeast NADPH oxidase, Yno1. Direct pairwise sequence comparisons (2) of Yno1 with all seven human Nox enzymes shows that Nox4 is the best match for Yno1. In a sequence window of 553 amino acids, the two NADPH oxidase sequences share 29.3% identity and 50% similarity. For comparison, the second best sequence match is Nox5. In a window of 565 amino acids, Yno1 and Nox5 share 23% identity and 42% sequence similarity.

Nox4 is different from all other human Nox enzymes because it is not associated with exactly the same group of regulatory proteins which is well studied in the case of Nox2, like p47phox and p67phox. However, p22phox is required for human Nox4 expression (3, 4) and a newly discovered p22phox binding partner, Poldip2, seems to be necessary for Nox4 activation (5). Nox4 is expressed constitutively in many different cell types (6). Nox4 exists as a number of splice variants in human cells. However, the significance of the splice variants for tumor biology is not known in detail. One of the splice variants (Nox4D) lacks all transmembrane helices, is located in the nucleus and highly expressed in vascular endothelial cells (7). Four other splice variants are apparently dominant negative mutant forms lacking the NADPH and/or FADH binding sites (8, 9) with no known direct relevance for cancer growth. The K_M of Nox4 for oxygen is unusually high (on the order of the actual oxygen partial pressure in tissue) indicating that Nox4 might be a relevant oxygen sensor for human cells (10).

Nox4 was found to be expressed in several tested cancers and cancer cells lines (6). Inhibition experiments with siRNA constructs showed that Nox4 is specifically needed for metastasis and also for epithelial to mesenchymal transition (EMT), a process needed for invasiveness of tumor cells mediated by regulating the actin cytoskeleton (10, 11). Details of the mechanism by which Nox4 is involved in regulation of the action cytoskeleton, and therefore in the EMT and in migration and metastasis of tumor cells largely are unknown, however, evidence was published recently that the signaling pathway in which Nox4 is embedded could be the TIS21-PI3K-Akt1 pathway (12, 13).

Nox4 is the only human Nox, which was found to be located in the ER, as shown in the present and in a previous article (14). In the two cancer cell lines used by us, Nox4 was exclusively seen in the ER (see Results and Discussion section). In some of the other cells tested, location in the nuclear membrane, in the plasma membrane and in mitochondria was also found (6, 15). Details about the correlation of subcellular location with function or about relocation from ER to nucleus, etc. are not yet available.

The product of the Nox4 catalyzed reaction, H_2O_2, is assumed to be formed in the lumen of the ER (6), where no known SOD is present. Nox4, but none of the other human Nox enzymes, produces H_2O_2 directly (without help from superoxide dismutase) via superoxide (10). Measurements of both H_2O_2 and superoxide *in vitro* showed that about 85% of the oxygen is converted to H_2O_2 while only 15% is converted to superoxide. It is unknown presently whether the yeast enzyme, Yno1, can produce H_2O_2 directly from oxygen (1).

It is shown by a host of medical papers that the H_2O_2 produced acts as a second messenger molecule in human cells, promoting cells at several stages of the life history of tumor formation, starting from immortalization (loss of cell cycle arrest), to the EMT, tumor angiogenesis, activation of HIF1alpha leading to a hypoxia-like metabolic transition of the cells, and finally to invasiveness and the potential to metastasize (13, 16–18). Examples for signaling modules that were shown to take part in Nox4 signaling in different cell types are TGF-β and phosphotyrosine phosphatase 2B (6). Paradoxically, Nox4 expression is not only needed for proliferation but also for apoptosis of tumor cells. Pancreatic tumor cell lines became resistant to apoptotic stimuli when Nox4 was silenced by RNAi [(19) summarized in Ref. (6)]. In part, the induction of apoptosis uses the same signaling pathways as proliferation (for instance, TGF-β). This apparent contradiction is presumably resolved by considering the combinatorial nature of signaling modules and the gene expression differences in the tumor and primary non-tumor cell lines used for these experiments. These facts must be given careful consideration in the development of Nox4 as a target for cancer therapy.

A large number of pharmacological inhibitors of the human Nox enzymes have been studied (20, 21), but none of them is specific for Nox4 and very little is known about their mechanisms of action and side reactions. Relatively recently, promising natural compounds (still not specific for Nox4) were tested for their therapeutic action *in vivo* and their biochemical action *in vitro* (20).

In the present article, we present evidence that Nox4, similar to its yeast homolog, creates a ROS signal leading to restructuring of the actin cytoskeleton in two human tumor cell lines. Inhibition of Nox4 leads to a loss of cell mobility which is pictured by changing the polarity of the actin cytoskeleton and prohibits cell migration *in vitro*. Therefore, it is encouraging to block Nox4 pharmacologically as a means to counteract the metastatic potential of cancer cells.

MATERIALS AND METHODS

Cell Culture and Transfections

HepG2 cells were grown in MEM media (ThermoScientific) supplemented with 10% fetal bovine serum (FBS; Life Technologies/Gibco), 2 mM L-glutamine (Sigma-Aldrich), 1 mM sodium pyruvate (Sigma-Aldrich), 1× non-essential amino acids (Sigma-Aldrich), and 100 µg/mL gentamycin (ThermoScientific). SH-SY5Y cells obtained from ATCC were cultured in Dulbeco's Minimum Essential Medium (DMEM)/F12 (1:1 mixture) supplemented with 10% FBS, 2 mM L-glutamine, 1 mM sodium pyruvate, 1× non-essential amino acids, and 100 µg/mL gentamycin. Medium was changed every 2–3 days, and cells were subcultured at a density of 70–80%. For siRNA-mediated Nox4 knockdown, 7.5 pmol of Nox4-specific silencer RNA or scrambled control silencer RNA (siRNA, sc-41586, sc37007; Santa Cruz Biotechnology) were transfected in HepG2 and SH-SY5Y cells using Lipofectamine 2000 (ThermoScientific) reagent. Media were changed after 6 h, and cells were further incubated in growth medium for a total of 48 h. siRNA transfection efficacy was determined as > 90% of cells, using the BLOCK-iT Fluorescent Oligo (ThermoScientific).

Gene Expression Analyses

Total RNA was isolated using RNeasy Mini kits (Qiagen) and digested with DNaseI (Promega). Reverse transcription polymerase chain reaction was performed using the SuperScriptII reverse transcription kit (ThermoScientific) and random hexamer primers (ThermoScientific) followed by IQ SYBR Green (Bio-Rad Laboratories) real-time (RT) PCR analyses on the iQ Multi-Color real time PCR detector (Bio-Rad Laboratories). Oligonucleotide sequences for the amplification of Nox4 and Nox2 and the internal standard used (acidic ribosomal protein RPLP0; NCBI Reference Sequence NM_001002.3) were

For Nox4: 5′-GACTTTACAGGTATATCCGGAGCAA-3′ and 5′-TGCAGATACACTGGACAATGTAGA-3′;
For Nox2: 5′-GCCCAAAGGTGTCCAAGCT-3′ and 5′-TCCCCAACGATGCGGATAT-3′;
For RPLP0: 5′-GTTGGTTGAAACACAGCAGCT-3′ and 5′-CAAAGGCTACCAGACGACCA-3′.

Clinical Samples

Hepatocellular carcinoma specimen from a subject with non-alcoholic fatty liver disease was obtained during clinically indicated segmentectomy surgery from the resected part of the liver. Written informed consent to use part of the resected liver for molecular analyses was obtained from the patient.

The normal liver RNA samples used were commercially obtained (Ambion). Liver RNA was prepared from two male donors, age 69 (intracranial hemorrhage) and age 68 (intracranial hemorrhage) and one female donor age 25 (motor vehicle accident). All three were free of major infections.

Immunoblotting

Protein extracts were prepared using 1× RIPA lysis buffer (New England Biolabs/Cell Signaling). 16 µg from each sample were mixed with 4× Laemmli buffer (Bio-Rad Laboratories), heated to 95°C for 10 min, cooled on ice and separated on a 12% SDS PAGE gel with 10 V/cm for 30 min in the stacking gel and 15 V/cm for 75 min in the separating gel. The proteins were blotted on a methanol-activated PVDF membrane with 0.45 µm pore size (Merck Millipore), at 30 V/cm electric field strength. The membrane was washed 30 min with TBS-T (25 mM Tris-HCl pH 7.4, 0.15 M NaCl, 0.5% Tween20, and 0.05% NaN_3) before blocking unspecific binding sites with MTBS-T [5% (w/v) non-fat dry milk] for 90 min. After another washing step, the membrane was incubated with the primary antibody for 2 h. A rabbit polyclonal IgG Nox4 antibody (New England Biolabs/Cell Signaling; H-300; sc-30141; dilution 1:1,000) was used for detection of Nox4 and a rabbit monoclonal N-WASP IgG antibody (Cell Signaling; 30D10; #4848; dilution 1:2,000) for the detection of N-WASP. A rabbit polyclonal antibody to β-actin (Abcam; ab8227; dilution 1:5,000) was used for the detection of actin. A mouse monoclonal GAPDH IgG antibody (Abcam; ab9484; dilution 1:5,000) served as a loading control. Further loading controls were: cofilin using a rabbit monoclonal cofilin antibody (Cell Signaling; #5175; dilution 1:1,000), and β-actin. Following the incubation with the primary antibody the membrane was then washed with TBST-T and incubated with either goat antirabbit-HRP conjugate (Thermo Fisher Scientific; #185415; dilution 1:2,000), goat antimouse-HRP conjugate (Thermo Fisher Scientific: #31430; dilution 1:5,000), or goat antirabbit-HRP conjugate (Cell Signaling; #7074; dilution 1:2,000) as a secondary antibody. For the visualization an ECL Select Western Blotting Detection Reagent (GE Healthcare) was used according to the manufacturer's instructions. The blot was then analyzed with the Fusion Fx7 Multi-Imagingsystem (Peqlab).

Isolation of Microsomes

SH-SY5Y cells were trypsinized, taken up centrifuged and washed a total of three times in 10 mM HEPES buffer pH 7.7. Cells were taken up in a small volume (1.5 mL) of HEPES buffer and homogenized with a Dounce homogenizer. Sucrose was added to a final concentration of 0.25 M. Samples were centrifuged at 1,000 *g* for 10 min at 4°C. Supernatant was adjusted to 10 mL with the same buffer and centrifuged at 100,000 *g* for 30 min. The slightly brownish microsomal pellet was dissolved in 0.1 mL of RIPA buffer.

Fluorescence Microscopy

Nox4 cDNA was cloned into pEGFP-N3 (Takara Bio Europe/Clontech) via *Kpn*I and *Not*I using the primers 5′-GGGGTA CCCATGGCTGTGTCCTGGAG-3′ and 5′-AAGGAAAAAA GCGGCCGCTCAGCTGAAAGACTCTTT-3′. HepG2 and SH-SY5Y cells were grown on collagen type I-coated 22 mm round cover slips (Becton Dickinson) and transfected with 2 µg Nox4-EGFP fusion vector using Lipofectamine 2000. Cells were stained after 24 h with 100 nM MitoTracker Red CMXRos (ThermoScientific) or 1 µM ER-Tracker Blue-White DPX (ThermoScientific) for 30 min, rinsed three times in PBS (GE Healthcare), and fixed in 4% paraformaldehyd (Sigma-Aldrich) solution for 10 min at room temperature. Nuclei were stained with DAPI (Sigma-Aldrich) for 30 min. Cover slips were mounted with Fluorescent Mounting Medium (Agilent Technologies/Dako). A Zeiss LSM710 confocal microscope with an Axiocam digital camera was used for microscopic imaging.

For F-Actin staining, cells were grown overnight on collagen coated cover slips. Media was replaced with growth medium containing 50 µM DPI (diphenyleneiodonium chloride, Sigma-Aldrich) or 5 µM wiskostatin (Sigma-Aldrich) and incubated for 15 min at growth conditions. These DPI or wiskostatin treated cells were treated with 1 mM H_2O_2 (Sigma-Aldrich). After 15 min, cells were washed in PBS, fixed in 4% PFA, and permeabilized in 0.1% Triton X-100 (Sigma-Aldrich). F-actin filaments and cell nuclei were stained with 6 mM phalloidin-FITC conjugate (Santa Cruz Biotechnology) and 300 nM DAPI for 20 min at room temperature. After a final wash, cover slips were mounted with Fluorescent Mounting Medium. Images were analyzed using the Filaquant Software.

Flowcytometry

HepG2 cells were trypsinized and collected in MEM Media containing 10% FBS and 50 µM DPI. After 15 min of incubation, cells were washed twice with PBS, fixed in 4% PFA (10 min at room temperature) and permeabilized with 0.1% Triton X-100 (10 min at room temperature). Cells were stained in PBS containing 6 mM phalloidin-FITC conjugate. Cellular F-actin content of treated and untreated cells was analyzed in channel

FL-1 (488/530 nm) using the FACSCalibur flowcytometer and CellQuest Pro software (Becton Dickinson).

Fluorometric Assay

SH-SY5Y and HepG2 cells were grown overnight in black Nunclon-Surface 96-well plates (Fisher Scientific). Cells were treated with 50 μM DPI or DMSO for 15 min. Subsequently, cells were rinsed with PBS and fixed in 5% PFA for 10 min at room temperature. Fixed cells were washed and permeabilized with PBS containing 0.1% Triton X-100 for 10 min. After a final rinse, cells were stained with 6 mM phalloidin-FITC conjugate, followed by RNAseA (Sigma-Aldrich) digestion and counterstaining with propidium iodide (Sigma-Aldrich). F-Actin and nuclear staining were detected with a Anthos Zenyth 3100 fluorometer (Anthos Labtec Instruments) at an excitation wavelength of 485/485 nm and an emission wavelength 535/625 nm for FITC and PI, respectively. Mean values are reported as ratio between F-actin and nuclear staining normalized to control.

Actin Fractionation

The G-actin/F-actin *In Vivo* Assay Kit (Cytoskeleton) was used according to the manufacturer's instructions. Untreated or hydrogen peroxide treated siRNA transfected HepG2 cells were washed in PBS and lysed in 1 mL of F-actin stabilizing buffer [50 mM PIPES pH 6.9, 50 mM NaCl, 5 mM MgCl2, 5 mM EGTA, 5% (v/v) glycerol, 0.1% (v/v) Non-idet P40, 0.1% (v/v) Triton X-100, 0.1% (v/v) Tween 20, 0.1% (v/v) 2-mercapto-ethanol, 1 mM ATP, and 1× protease Inhibitor Cocktail] for 10 min on ice. Subsequently cells were dislodged by scraping, and whole extracts were centrifuged for 1 h at 100,000 *g* in an L7-80 ultracentrifuge (Beckman Coulter, Vienna, Austria). Supernatant fractions, containing the G-actin were removed and frozen at −80°C until further use. Pellets, containing F-actin, were incubated in 1 mL of 10 μM cytochalasin D (Sigma-Aldrich) solution on ice for 1 h and vortexed every 10 min, followed by subsequent homogenization in a 1 mL glass Dounce homogenizer (Thermo Fisher Scientific/Wheaton). Photometric total protein determination was carried out using Bradford Reagent (Sigma-Aldrich) assay and a DU 640 UV/VIS spectrometer (Beckman Coulter). 5 μg protein of each fraction were loaded and separated as described in the section Immunoblotting.

Rabbit polyclonal anti-β-actin antibody (Abcam, Cambridge, UK; # ab8227; dilution 1:500) was used as the primary antibody and incubated overnight at 4°C. Goat antirabbit-HRP conjugate (Thermo Fisher Scientific/Pierce; #185415; dilution 1:2,000) was used as secondary antibody. SuperSignal West Dura Chemiluminescent Substrate (Thermo Fisher Scientific) and Kodak 2000MM Image Station were utilized to detect specific antibody binding. Integrated optical band density measurements were calculated with the Kodak1D Image Software to determine the cellular F/G-actin ratio.

Cell Migration Assay

Cell migration activity of Nox4 or control siRNA transfected SH-SY5Y cells was studied by means of a Radius 24-well cell migration assay (Cell Biolabs) and the following media: HepG2: Eagle's Minimum Essential Medium, low glucose (1 g/L), 10% FBS, 1% v/v penicillin/streptomycin 10,000 U/mL (Pen/Strep), and non-essential amino acids (M7145 Sigma) and SH-SY5Y: DMEM, high glucose (4.5 g/L), 10% FBS, and 1% v/v Pen/Strep. Cells were seeded into the radius 24-well plate, containing a standardized 0.68 mm hydrogel spot per well, to which cells cannot attach. Cell division (proliferation) was blocked by adding 10 μg/mL mitomycin C. After 24 h, cells reached a density of approximately 80% and subsequently the biocompatible gel was removed to start the migration into the now exposed cell-free area. After 24 h, the cells were fixed and images taken with a Nikon TMS inverted microscope and MetaView software. Area closure was quantitated using the MRI Wound Healing Tool macro for ImageJ (http://dev.mri.cnrs.fr/projects/imagej-macros/wiki/Wound_Healing_Tool).

Statistical Analysis

Data are reported as arithmetic mean ± SD based on at least three biological replicas. Data were tested using ANOVA and Tukey *post hoc* analysis to determine significance of pairwise differences. Results were marked $p < 0.05$ (*), $p < 0.001$ (**), $p < 0.0001$ (***), and $p < 0.00001$ (****).

RESULTS AND DISCUSSION

The two cell lines chosen for this work are well known and widely used *in vitro* tumor models. The SH-SY5Y neuroblastoma cell line retains certain biochemical properties of dopaminergic neurons (22, 23). The HepG2 cell line retains some of the gene expression characteristics of human liver cells from which the tumor and the cell line were derived (24).

For the purpose of the present study, we first wanted to check the amount of Nox4 expression in the tumor cell lines chosen for this work. **Figure 1A** shows an estimation of the amount of the Nox4 mRNA *in vivo* (human brain and liver) compared with the two cell lines. In these experiments, equal amounts of total RNA from all four sources were analyzed using the primers for Nox4 shown in the Section "Materials and Methods." As an internal control in the same samples, the amount of the acidic ribosomal protein P0-encoding mRNA was analyzed and the values shown were normalized with respect to P0 mRNA. Clearly, the amount of Nox4 mRNA is highest in brain, but about three times smaller in the neuronal-derived cancer cell line. The amount of Nox4 mRNA in liver is smaller compared to brain, and again, the liver-derived cancer cell line contains about three times less Nox4 mRNA compared to liver. Nevertheless, the Nox4 protein is expressed in both cell lines. Next, the expression values shown in **Figure 1A** were compared with tumor tissue from a hepatocellular carcinoma. In this case a 192- and 257-fold change relative to the ribosomal P0 and GAPDH, respectively, was observed (**Figure 1B**).

Figure 1C shows that a monoclonal antibody directed against Nox4 recognizes the protein in both cell lines. The amount of protein in the two cell lines is not dramatically different, but seems to be somewhat smaller in the liver cell line.

The next question was subcellular localization of Nox4 in the two cell lines studied here. To this end, microsomes were prepared from SH-SY5Y cells and analyzed (**Figure 1F**) by

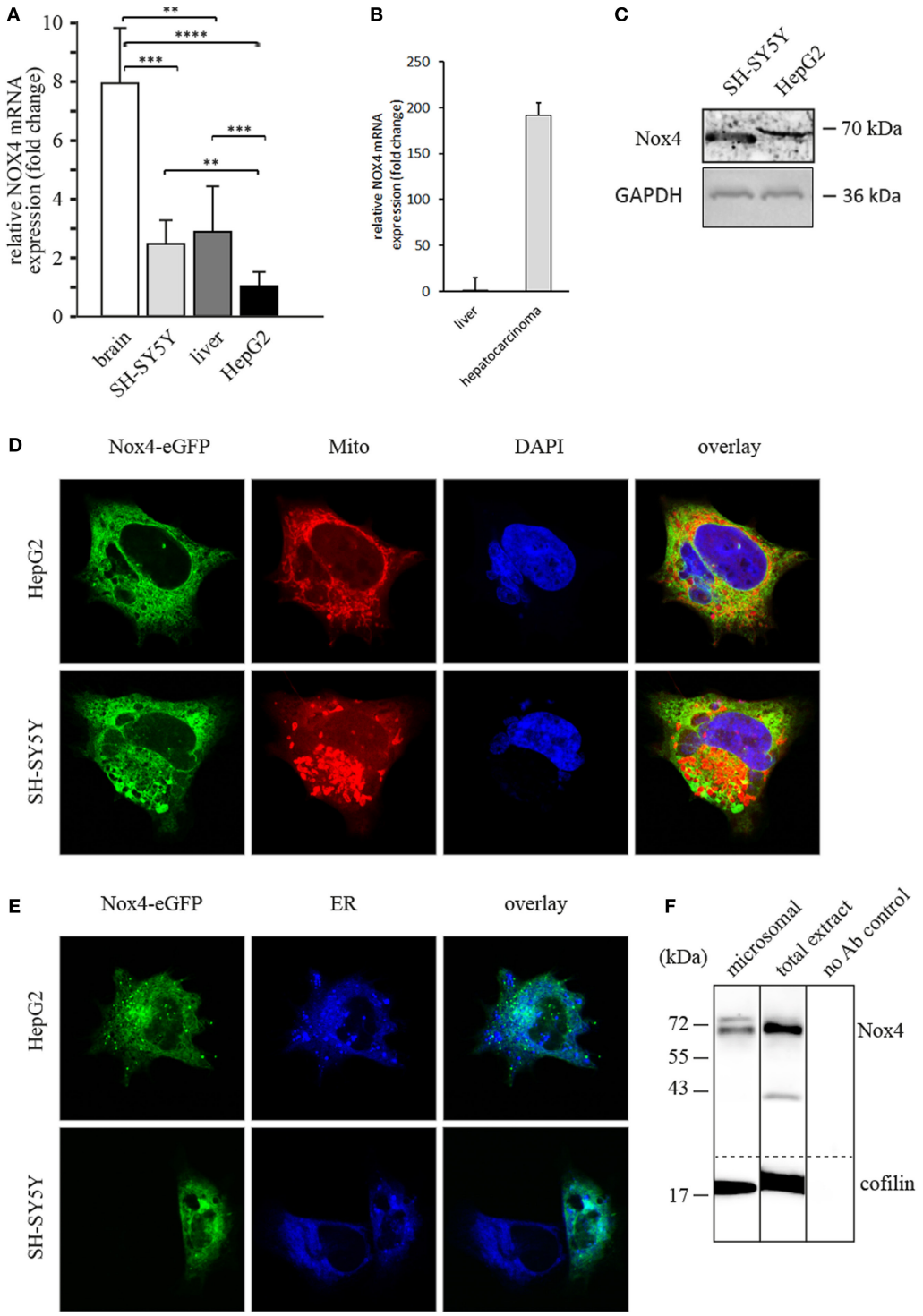

FIGURE 1 | **Nox4 expression in human tissues and cultured cells and intracellular Nox4 localization in human cell lines**. **(A)** Real-time (RT) q-PCR analyses of Nox4 in human brain and liver as well as in SH-SY5Y neuroblastoma and HepG2 hepatoma cells. Values expressed as fold change relative to a housekeeping gene (ribosomal protein P0). Determination of significance as described in the Section "Materials and Methods." **(B)** RT q-PCR analyses of Nox4 in a hepatocellular carcinoma. **(C)** Immunoblot of total protein extracts from SH-SY5Y and HepG2 cells using a polyclonal antibody against Nox4 and loading controls (GAPDH). **(D,E)** Fluorescence micrographs of HepG2 and SH-SY5Y cells transiently transfected with enhanced green fluorescence protein (eGFP) in-frame fusion construct Nox4-eGFP. DAPI, Mito or ER denotes nuclear staining with DAPI, mitochondrial staining with MitoTracker Red CMXRos, or staining of endoplasmatic reticulum with ER-Tracker Blue-White DPX, respectively. **(F)** Immunoblot of Nox4 from a total extract of SH-SY5Y cells and purified microsomes from the same extract with loading control (cofilin) and a control blot with no primary antibody.

western blot using the same monoclonal antibody directed to Nox4 that was used before (**Figure 1C**). Data were normalized to cofilin in this case. The microsomes contained Nox4 protein indicating ER localization of the enzyme. These results were now confirmed by fluorescence microscopy of formaldehyde-fixed cells. Localization of Nox4 C-terminally labeled with enhanced green fluorescence protein (eGFP), mitochondria (Mitotracker Red) and nuclei (DAPI) was analyzed (**Figure 1D**). In a second experiment, Nox4-eGFP fluorescence was compared with an ER-specific stain (ER tracker Blue-White DPX). **Figures 1D,E** show that Nox4 colocalizes with the ER marker, but not with the mitochondrial or nuclear marker. We conclude that in the two cancer cell lines used here, Nox4 is located in the ER, like Yno1 in yeast (1). The role of human Nox enzymes in the ER was recently discussed with special reference to the interaction of Nox4 with protein disulfide isomerase (25).

Human Nox4 in some of the previous publications was also found in mitochondria (26) and in the nucleus (7). As mentioned before, we assume that all three localizations which have been published for Nox4 are real. Although no data exist as to the functional significance of the nuclear and mitochondrial localization, we are providing evidence here that the ER-localized Nox4 is involved in regulation of the actin cytoskeleton (see subsequently). There is evidence that the primary product of the Nox4 activity, H_2O_2, is exported from the ER to the cytoplasm (27) where it could then fulfill its signaling function in actin cytoskeleton remodeling.

Next, we studied a possible connection between Nox4 activity and regulation of the actin cytoskeleton by staining of F-actin (after formaldehyde fixation) in growing cells in the absence and in the presence of inhibitors. As shown in **Figure 2A**, blocking NADPH oxidase activity with the unspecific inhibitor, DPI, led to a marked change in the appearance of the F-actin morphology of the SH-SY5Y cells. The normal network of F-actin fibers largely disappeared concomitantly with the appearance of granular F-actin aggregates. Interestingly, this effect was reversed by adding a low, non-toxic concentration of H_2O_2 to the cells (**Figure 2A**). To quantify this effect, we counted the number of actin microfilaments per cell (**Figure 2B**) leading to an estimate of about

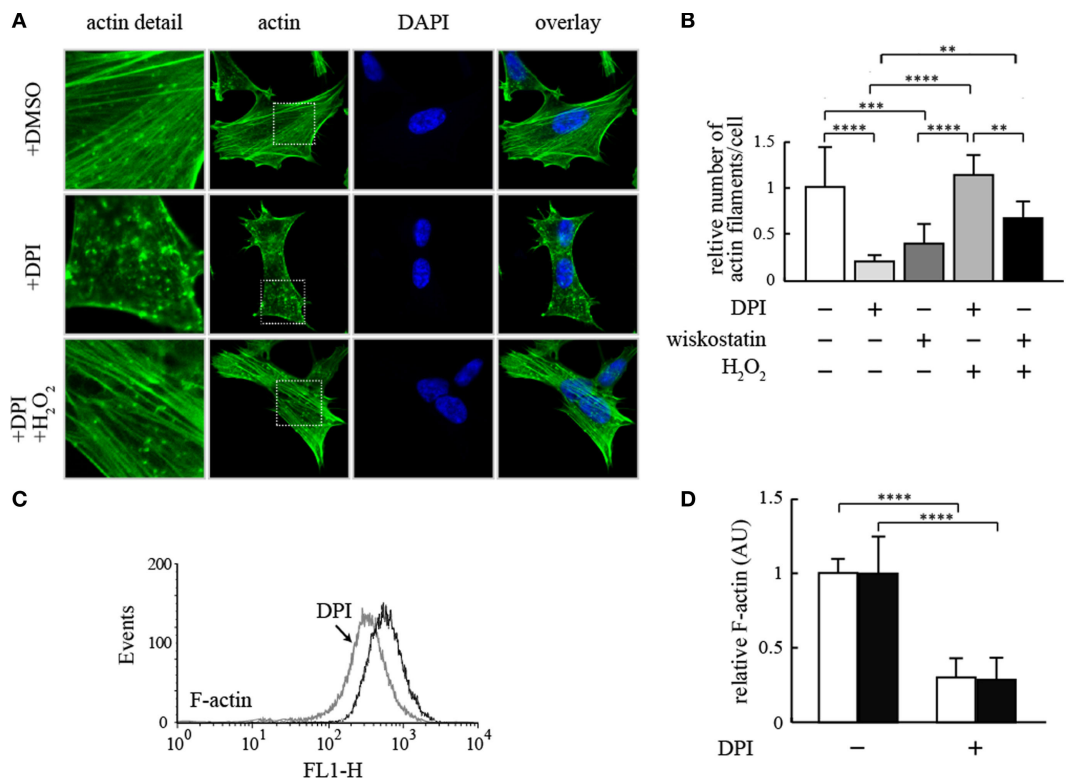

FIGURE 2 | Effect of NADPH oxidase inhibition on filamentous actin in human neuroblastoma cells. **(A)** Representative fluorescence micrographs of SH-SY5Y cells stained with phalloidin-FITC and DAPI. Cells were treated with DMSO, 50 μM DPI or 50 μM DPI, and 1 mM H_2O_2 for 15 min. Cells were washed, fixed and actin filaments and cell nuclei were stained with phalloidin-FITC and DAPI, respectively. **(B)** Actin filament number of 100 cells treated as in **(A)** or with 5 μM wiskostatin was analyzed with the software FilaQuant from fluorescence micrographs and expressed relative to the number found in untreated cells without DPI, wiskostatin, or H_2O_2. Results are mean ± SD and were marked for significance as described in the Section "Materials and Methods." **(C)** Detached HepG2 cells were treated with 50 μM DPI or DMSO, respectively. Cells were stained with phalloidin-FITC prior to FACS analysis for F-actin content. Results of one representative experiment are shown. **(D)** HepG2 and SH-SY5Y cells were treated with 50 μM DPI or DMSO for 15 min, respectively. Cells were stained with phalloidin-FITC and treated with RNAse A prior to counterstaining with propidium iodide. F-actin and nuclear staining was determined with a fluorometric assay. F-actin content is shown as normalized to nuclear staining intensity. Open bars denote HepG2 cells, whereas filled bars denote SH-SY5Y cells. Results are mean ± SD and were marked for significance as described in the Section "Materials and Methods."

25% remaining actin microfilaments. This effect was mostly due to inhibition of Nox4, which is the predominant NADPH oxidase of the neuronal cell line used (6). This fact was also shown by specifically inhibiting Nox4 by siRNA techniques (**Figures 3A,B**). A similar effect was achieved by treating the cells with wiskostatin (**Figure 2B**), an inhibitor of actin filament nucleation, especially at the branching points of the actin microfilament network, which is needed for the dynamics of the actin cytoskeleton in growing cells, in particular at the polarized moving edge of moving cells, and in the process of endocytosis. The effect of wiskostatin was partially reversible by H_2O_2 (**Figure 2B**). A similar effect was shown previously for the yeast NADPH oxidase, Yno1 (1). Taken together, the results shown so far point to a possible explanation for the mechanism of action of Nox4 in the two tumor cell lines: Nox4 seems to create a signaling substance, which is probably H_2O_2 (because the lack of Nox4 can be compensated by H_2O_2) and needed for regulation of the branching mechanism of the dynamic actin cytoskeleton of living cells.

F-actin is not only changing its morphological appearance but also in part converted into the monomeric G-actin which is no longer stainable with rhodamine-phalloidin. After staining for F-actin, the detached cells of the HepG2 culture were analyzed by FACS (**Figure 2C**), showing an appreciable loss of F-actin after DPI inhibition of NADPH oxidase. In a similar experiment, F-actin rhodamine-phalloidin fluorescence was quantitatively determined in both the HepG2 and SH-SY5Y cells with and without DPI, and the fluorescence was normalized to the fluorescence intensity of the propidium iodide stained nuclei of the cells. In both cell types, F-actin content was decreasing to about 25% of the undisturbed value after DPI inhibition (**Figure 2D**).

The effect of the Nox4-specific siRNA on Nox4 transcript levels in SH-SY5Y cells is shown in **Figure 3A**, using RT-PCR. Expressing the siRNA construct *in vivo* leads to a decrease of the Nox4 mRNA to about 45% of the normal undisturbed value. The construct has no influence on Nox2 expression, showing the specificity of the siRNA construct and there is no effect of the "scrambled" siRNA construct on the transcript levels. The decrease in mRNA is reflected by the amount of protein as determined in western blots (**Figure 3B**). It is important to note that the western blot results shown in **Figures 1B** and **3B** both show the full length protein, not one of the substantially smaller splicing isoforms. As shown in **Figure 3B**, expression of Nox4 at the protein level is strongly diminished in both cell lines by the siRNA used.

A commercial kit was now used to separate and quantitate F-actin and the monomeric form (G-actin) from the cells and to study the simultaneous action of Nox4 siRNA and wiskostatin. In undisturbed cells, there is a large majority of F-actin (**Figure 3C**, first lane). After wiskostatin treatment or in cells

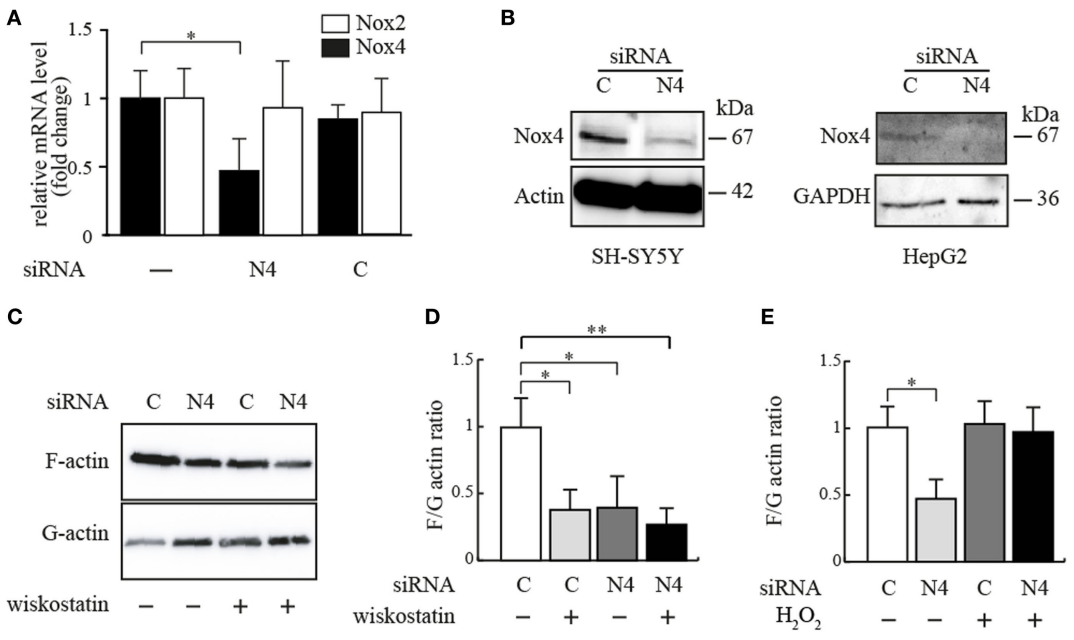

FIGURE 3 | **Effect of siRNA-mediated Nox4 knockdown on cellular F- and G-actin content**. **(A)** Nox4 mRNA expression was determined using real-time PCR in SH-SY5Y cells cultured for 48 h in the presence of either Nox4 or scrambled siRNAs. Values expressed as fold change relative to a housekeeping gene (ribosomal protein P0). Results are mean ± SD and were marked for significance as described in the Section "Materials and Methods." **(B)** Anti-Nox4 immunoblot analysis of total protein extracts isolated from Nox4 siRNA or control siRNA-treated SH-SY5Y and HepG2 cells, transiently transfected for 48 h. As loading controls, beta-actin and GAPDH immunoblots were used. **(C)** Representative immunoblot of actin after fractionation by ultracentrifugation to discriminate cellular F-actin content from G-actin in homogenates from HepG2 cells treated with Nox4 or control siRNA for 48 h in the presence or absence of 5 μM wiskostatin for 15 min. **(D)** F/G ratios calculated from densitometrical analysis of three independent experiments as in **(C)**, normalized to cells receiving control siRNA only. Results are mean ± SD and were marked for significance as described in the Section "Materials and Methods." **(E)** F/G actin ratios calculated from densitometric analysis of immunoblots for actin after fractionation of F-actin and G-actin in homogenates from HepG2 cells treated with Nox4 or control siRNA for 48 h in the presence or absence of 1 mM hydrogen peroxide for 15 min. Results are mean ± SD and were marked for significance as described in the Section "Materials and Methods."

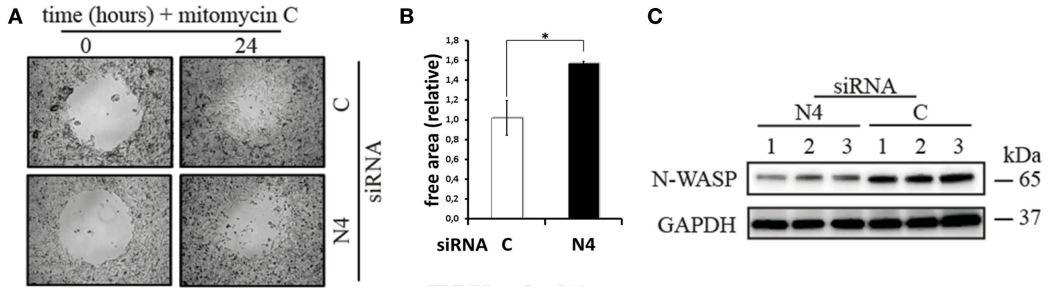

FIGURE 4 | **Cell migration assay**. **(A)** SH-SY5Y cells either transfected with Nox4 or scrambled siRNA were grown to 80% confluency in a 24-well plate containing a hydrogel spot (time point 0 h). After removing of the spot the cells transfected with scrambled siRNA but not the Nox4 siRNA started to migrate into the cell free area (time point 24 h). **(B)** The remaining free area in the open spots was determined as described in the Section "Materials and Methods." Results are mean ± SD and were marked for significance as described in the Section "Materials and Methods." **(C)** The western blot for N-WASP normalized to GAPDH indicates downregulation of N-WASP when Nox4 expression was suppressed in three independent homogenates from hepatoma cells. Equal amounts of protein were loaded onto the SDS-PAGE.

treated with Nox4 siRNA, the F/G-actin ratio is about 1 indicating approximately equal amounts of the two forms of actin (**Figure 3C**, lanes 2–4). Importantly, the combination of Nox4 siRNA and wiskostatin leads to a F/G ratio which is not different from either of the two inhibitors alone (**Figure 3D**). There is no additive effect of siRNA and wiskostatin. The standard (but cautious) interpretation of this finding is that the two inhibitors act on the same process in the cell, namely actin filament nucleation and branching, perhaps in a sequential manner. The shift from F-actin to G-actin is reversible by H_2O_2 (**Figure 3E**). Taken together, these findings mean that Nox4 exerts an activity directed to growth and/or branching of actin filaments, which is very probably mediated by the second messenger produced by Nox4, hydrogen peroxide.

The results discussed so far prompted us to investigate the influence of Nox4 inhibition and the concomitant shift in the actin cytoskeleton on mobility of the two tumor cell lines in so-called "scratch" assays (**Figure 4**). Inhibiting Nox4 in the SH-SY5Y cells led to a significant loss of mobility of the cells leading to a larger area not covered by migrating cells (**Figures 4A,B**). Possibly, this finding supports a role for Nox4 in regulating actin cytoskeleton dynamics, which is needed in the process of metastasis. This finding would mean that in neuroblastoma, the tumor from which the SH-SY5Y cell line is derived, Nox4 is a drug target worth considering. However, the effect observed is not a general one, as in the HepG2 cell line transfection with the Nox4 siRNA did not inhibit cell migration (data not shown). This is surprising as the level of Nox4 protein is very low under these conditions (**Figure 3B**) and possibly indicates that the regulation of the actin cytoskeleton nucleation and branching as well as the regulation of cell migration must be in part different in the two cell lines.

Finally, in **Figure 4C**, we show that downregulating Nox4 mRNA by siRNA leads to lowering of N-WASP, the probable drug target of wiskostatin which is mechanistically directly involved in the branching process of actin microfilaments. How can this finding be explained? We think that a direct feedback circuit probably exists which downregulates the amount of N-WASP protein in times when it is not used as a signaling target.

CONCLUSION

The experimental results presented and discussed herein lead to a still hypothetical but consistent picture of the role of the NADPH oxidase, Nox4, in cellular growth in normal and tumor cells. Nox4 which in the two tumor cell lines studied here is a NADPH oxidase of the ER, directly (without the help of superoxide dismutase) produces H_2O_2 as a growth-related signaling substance. Attenuation of this signaling module leads to characteristic changes in the actin cytoskeleton, like decomposition of actin microfilaments. A complete loss of Nox4 in HeLa cells leads to a much more drastic effect of loss of both proliferation and cell migration (28). However, these knock-out cells are still viable. Presently unknown is the recipient of H_2O_2 which presumably transmits the signal to the complicated machinery which regulates the actin cytoskeleton, in particular actin nucleation and branching (29). The point of attack of the signal is near the point where wiskostatin acts (i.e., F-actin branching and nucleation), as judged by the combination experiments with Nox4 inhibition and wiskostatin inhibition of N-WASP. As this inhibition blocks cell mobility and, therefore probably metastasis, in one of the two cell lines studied here, we suggest to study Nox4 as a drug target in cancer therapy. This must be done with great care, as the possible unwanted side effects of such treatment are unknown and some published experiments (30) not only point to a function of Nox4 in tumor growth and metastasis, but also to a function of Nox4 in the process of apoptosis, which should not be blocked in tumor therapy.

AUTHOR CONTRIBUTIONS

MB, TF, and MR wrote the manuscript. MB, MR, EH-B, EA, and TF designed experiments. MR, TF, SA, JB, MKS, HB-K, RG, JC, KR, and MS performed experiments.

FUNDING

The work presented here was funded by project P26713 of the Austrian Science Fund FWF (to MB).

REFERENCES

1. Rinnerthaler M, Buttner S, Laun P, Heeren G, Felder TK, Klinger H, et al. Yno1p/Aim14p, a NADPH-oxidase ortholog, controls extramitochondrial reactive oxygen species generation, apoptosis, and actin cable formation in yeast. *Proc Natl Acad Sci U S A* (2012) 109(22):8658–63. doi:10.1073/pnas.1201629109
2. Henikoff S, Henikoff JG. Amino-acid substitution matrices from protein blocks. *Proc Natl Acad Sci U S A* (1992) 89(22):10915–9. doi:10.1073/pnas.89.22.10915
3. Juhasz A, Ge Y, Markel S, Chiu A, Matsumoto L, van Balgooy J, et al. Expression of NADPH oxidase homologues and accessory genes in human cancer cell lines, tumours and adjacent normal tissues. *Free Radic Res* (2009) 43(6):523–32. doi:10.1080/10715760902918683
4. Ambasta RK, Kumar P, Griendling KK, Schmidt HH, Busse R, Brandes RP. Direct interaction of the novel Nox proteins with p22phox is required for the formation of a functionally active NADPH oxidase. *J Biol Chem* (2004) 279(44):45935–41. doi:10.1074/jbc.M406486200
5. Lyle AN, Deshpande NN, Taniyama Y, Seidel-Rogol B, Pounkova L, Du P, et al. Poldip2, a novel regulator of Nox4 and cytoskeletal integrity in vascular smooth muscle cells. *Circ Res* (2009) 105(3):249–59. doi:10.1161/CIRCRESAHA.109.193722
6. Guo SH, Chen XP. The human Nox4: gene, structure, physiological function and pathological significance. *J Drug Target* (2015) 23(10):888–96. doi:10.3109/1061186x.2015.1036276
7. Anilkumar N, Jose GS, Sawyer I, Santos CXC, Sand C, Brewer AC, et al. A 28-kDa splice variant of NADPH oxidase-4 is nuclear-localized and involved in Redox signaling in vascular cells. *Arterioscler Thromb Vasc Biol* (2013) 33(4):E104–33. doi:10.1161/Atvbaha.112.300956
8. Muzaffar S, Jeremy JY, Angelini GD, Shukla N. NADPH oxidase 4 mediates upregulation of type 4 phosphodiesterases in human endothelial cells. *J Cell Physiol* (2012) 227(5):1941–50. doi:10.1002/jcp.22922
9. Goyal P, Weissmann N, Rose F, Grimminger F, Schafers HJ, Seeger W, et al. Identification of novel Nox4 splice variants with impact on ROS levels in A549 cells. *Biochem Biophys Res Commun* (2005) 329(1):32–9. doi:10.1016/j.bbrc.2005.01.089
10. Nisimoto Y, Diebold BA, Constentino-Gomes D, Lambeth JD. Nox4: a hydrogen peroxide-generating oxygen sensor. *Biochemistry* (2014) 53(31):5111–20. doi:10.1021/bi500331y
11. Boudreau HE, Casterline BW, Rada B, Korzeniowska A, Leto TL. Nox4 involvement in TGF-beta and SMAD3-driven induction of the epithelial-to-mesenchymal transition and migration of breast epithelial cells. *Free Radic Biol Med* (2012) 53(7):1489–99. doi:10.1016/j.freeradbiomed.2012.06.016
12. Zhang C, Lan T, Hou J, Li J, Fang R, Yang Z, et al. NOX4 promotes non-small cell lung cancer cell proliferation and metastasis through positive feedback regulation of PI3K/Akt signaling. *Oncotarget* (2014) 5(12):4392–405. doi:10.18632/oncotarget.2025
13. Choi JA, Jung YS, Kim JY, Kim HM, Lim IK. Inhibition of breast cancer invasion by TIS21/BTG2/Pc3-Akt1-Sp1-Nox4 pathway targeting actin nucleators, mDia genes. *Oncogene* (2016) 35(1):83–93. doi:10.1038/onc.2015.64
14. Zhang L, Nguyen MV, Lardy B, Jesaitis AJ, Grichine A, Rousset F, et al. New insight into the Nox4 subcellular localization in HEK293 cells: first monoclonal antibodies against Nox4. *Biochimie* (2011) 93(3):457–68. doi:10.1016/j.biochi.2010.11.001
15. Kuroda J, Nakagawa K, Yamasaki T, Nakamura K, Takeya R, Kuribayashi F, et al. The superoxide-producing NAD(P)H oxidase Nox4 in the nucleus of human vascular endothelial cells. *Genes Cells* (2005) 10(12):1139–51. doi:10.1111/j.1365-2443.2005.00907.x
16. Sampson N, Koziel R, Zenzmaier C, Bubendorf L, Plas E, Jansen-Durr P, et al. ROS signaling by NOX4 drives fibroblast-to-myofibroblast differentiation in the diseased prostatic stroma. *Mol Endocrinol* (2011) 25(3):503–15. doi:10.1210/me.2010-0340
17. Helfinger V, Henke N, Harenkamp S, Walter M, Epah J, Penski C, et al. The NADPH oxidase Nox4 mediates tumour angiogenesis. *Acta Physiol* (2016) 216(4):435–46. doi:10.1111/apha.12625
18. Liu ZM, Tseng HY, Tsai HW, Su FC, Huang HS. Transforming growth factor beta-interacting factor-induced malignant progression of hepatocellular carcinoma cells depends on superoxide production from Nox4. *Free Radic Biol Med* (2015) 84:54–64. doi:10.1016/j.freeradbiomed.2015.03.028
19. Vaquero J, Zurita M, Aguayo C, Coca S. Relationship between apoptosis and proliferation in secondary tumors of the brain. *Neuropathology* (2004) 24(4):302–5. doi:10.1111/j.1440-1789.2004.00569.x
20. Zhang B, Liu Z, Hu X. Inhibiting cancer metastasis via targeting NAPDH oxidase 4. *Biochem Pharmacol* (2013) 86(2):253–66. doi:10.1016/j.bcp.2013.05.011
21. Krause KH, Lambeth D, Kronke M. NOX enzymes as drug targets. *Cell Mol Life Sci* (2012) 69(14):2279–82. doi:10.1007/s00018-012-1006-5
22. Xie HR, Hu LS, Li GY. SH-SY5Y human neuroblastoma cell line: in vitro cell model of dopaminergic neurons in Parkinson's disease. *Chin Med J (Engl)* (2010) 123(8):1086–92. doi:10.3760/cma.j.issn.0366-6999.2010.08.021
23. Nevo I, Sagi-Assif O, Edry Botzer L, Amar D, Maman S, Kariv N, et al. Generation and characterization of novel local and metastatic human neuroblastoma variants. *Neoplasia* (2008) 10(8):816–27. doi:10.1593/neo.08402
24. Lopez-Terrada D, Cheung SW, Finegold MJ, Knowles BB. Hep G2 is a hepatoblastoma-derived cell line. *Hum Pathol* (2009) 40(10):1512–5. doi:10.1016/j.humpath.2009.07.003
25. Laurindo FR, Araujo TL, Abrahao TB. Nox NADPH oxidases and the endoplasmic reticulum. *Antioxid Redox Signal* (2014) 20(17):2755–75. doi:10.1089/ars.2013.5605
26. Block K, Gorin Y, Abboud HE. Subcellular localization of Nox4 and regulation in diabetes. *Proc Natl Acad Sci U S A* (2009) 106(34):14385–90. doi:10.1073/pnas.0906805106
27. Wu RF, Ma ZY, Liu Z, Terada LS. Nox4-Derived H2O2 mediates endoplasmic reticulum signaling through local ras activation. *Mol Cell Biol* (2010) 30(14):3553–68. doi:10.1128/Mcb.01445-09
28. Jafari N, Kim H, Park R, Li L, Jang M, Morris AJ, et al. CRISPR-Cas9 mediated NOX4 knockout inhibits cell proliferation and invasion in HeLa cells. *PLoS One* (2017) 12(1):e0170327. doi:10.1371/journal.pone.0170327
29. Chen K, Craige SE, Keaney JF Jr. Downstream targets and intracellular compartmentalization in Nox signaling. *Antioxid Redox Signal* (2009) 11(10):2467–80. doi:10.1089/ARS.2009.2594
30. Caja L, Sancho P, Bertran E, Fabregat I. Dissecting the effect of targeting the epidermal growth factor receptor on TGF-beta-induced-apoptosis in human hepatocellular carcinoma cells. *J Hepatol* (2011) 55(2):351–8. doi:10.1016/j.jhep.2010.10.041

Conflict of Interest Statement: The authors declare that the research was conducted in the absence of any commercial or financial relationships that could be construed as a potential conflict of interest.

frontiers in Oncology

REVIEW
published: 28 August 2017
doi: 10.3389/fonc.2017.00186

Quo natas, Danio?—Recent Progress in Modeling Cancer in Zebrafish

*Stefanie Kirchberger, Caterina Sturtzel, Susana Pascoal and Martin Distel**

St. Anna Kinderkrebsforschung, Children's Cancer Research Institute, Innovative Cancer Models, Vienna, Austria

Over the last decade, zebrafish has proven to be a powerful model in cancer research. Zebrafish form tumors that histologically and genetically resemble human cancers. The live imaging and cost-effective compound screening possible with zebrafish especially complement classic mouse cancer models. Here, we report recent progress in the field, including genetically engineered zebrafish cancer models, xenotransplantation of human cancer cells into zebrafish, promising approaches toward live investigation of the tumor microenvironment, and identification of therapeutic strategies by performing compound screens on zebrafish cancer models. Given the recent advances in genome editing, personalized zebrafish cancer models are now a realistic possibility. In addition, ongoing automation will soon allow high-throughput compound screening using zebrafish cancer models to be part of preclinical precision medicine approaches.

Keywords: zebrafish, cancer, xenograft models, genetically engineered models, tumor microenvironment, compound screen

OPEN ACCESS

Edited by:
Michael Breitenbach, University of Salzburg, Austria

Reviewed by:
Lawrence Schook, University of Illinois at Chicago, United States
Miguel Ángel Medina, University of Málaga, Spain

***Correspondence:**
Martin Distel
martin.distel@ccri.at

Specialty section:
This article was submitted to Molecular and Cellular Oncology, a section of the journal Frontiers in Oncology

Received: *19 June 2017*
Accepted: *09 August 2017*
Published: *28 August 2017*

Citation:
Kirchberger S, Sturtzel C, Pascoal S and Distel M (2017) Quo natas, Danio?—Recent Progress in Modeling Cancer in Zebrafish. Front. Oncol. 7:186. doi: 10.3389/fonc.2017.00186

ZEBRAFISH AS A MODEL ORGANISM IN CANCER RESEARCH

George Streisinger established zebrafish, a small freshwater fish naturally found in rice fields and tributaries to the river Ganges, as a vertebrate model organism in his 1981 Nature publication "Production of clones of homozygous diploid zebra fish (*Brachydanio rerio*)" (1, 2). Since then, supported by large mutagenesis screens, zebrafish has become one of the major model organisms in vertebrate genetics and developmental biology (3, 4). Roughly two decades later, the potential of the zebrafish model to study human diseases began to be exploited [reviewed in Ref. (5)]. Especially, characteristics like the fast development outside the mother, transparency at embryonic and larval stages, and the high number of offspring allowing for live imaging and cost-effective compound screening make the zebrafish model an attractive complementary model to more classical mouse models.

Disease modeling in zebrafish was boosted further when the zebrafish reference genome, published in 2013, revealed that zebrafish possess >80% of all human disease-related genes, indicating that many human diseases can, in fact, be modeled in zebrafish (6). This also includes cancer and in the early 2000s, pioneering transgenic models for leukemia and rhabdomyosarcoma were established by the Crosier, Look, and Zon laboratories (7–9). From *Xiphophorus* melanoma models, it was already known for decades that fish can serve as a useful model to investigate tumor driving mechanisms [reviewed in Ref. (10)]. However, cancer research in zebrafish particularly benefits from the many genetic tools and transgenic strains established by the zebrafish community over the years. For many cell types, e.g., hematopoietic cells, a specific transgenic strain is readily available demarcating distinct cell types like neutrophils, macrophages, B cells or T cells and natural killer cells by fluorescent protein expression (11–14). Availability of such transgenic strains offers a direct readout for effects of oncogenes on distinct cell populations by confocal microscopy and also quantification

by flow cytometry. In addition, cellular interactions of labeled cells, e.g., within the tumor microenvironment (TME), can be directly monitored. Furthermore, targeted oncogene expression can be achieved using gene expression systems like Gal4/*UAS* or Cre/*loxP*. Through enhancer and gene trap screens, many cell type-specific Gal4 and Cre zebrafish strains have been established and await their application in cancer research (15–19).

MODELING APPROACHES IN ZEBRAFISH

In this review, we will focus on two fundamentally different cancer modeling approaches being pursued in zebrafish at the moment: genetic and xenograft approaches (**Figure 1**). In addition, syngeneic and allogeneic cell transplantation using genetic zebrafish models has given insight into evolution and

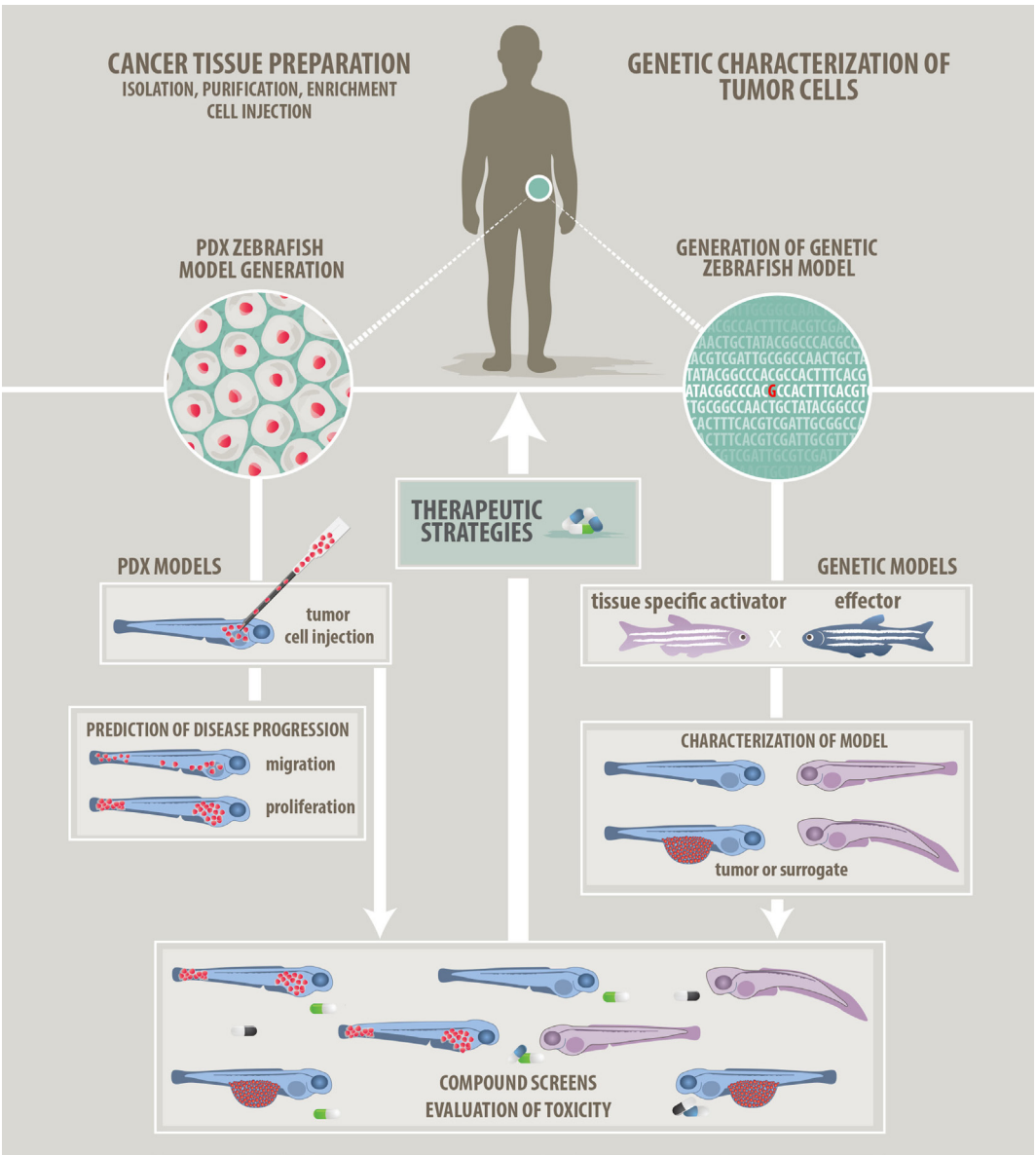

FIGURE 1 | Approaches to modeling cancer in zebrafish. We describe two main approaches how zebrafish can be used in cancer research and how zebrafish will help to develop patient-tailored therapies in the future. (*Left panel*) *Patient-derived xenograft approach*: cancer cells prepared from resected or isolated patient material will be transplanted into zebrafish larvae. Monitoring of *in vivo* proliferation, migratory behavior, and interaction with host cells like endothelial cells might allow predictions of aggressiveness and disease progression. (*Right panel*) *Genetic modeling approach*: bioinformatic analyzes of Omics data will point at candidate target genes. Genetic models featuring single or combined mutations will be generated using the zebrafish tool kit. Genetic models will be used for *in vivo* investigation of tumorigenesis. In addition, a screenable phenotype will be identified. This can be an actual tumor, hyperproliferating cells, or developmental abnormalities. Studies of the tumor microenvironment are also possible on genetic models. (*Common middle panel*) *Compound evaluation, compound screens, and development of therapeutic strategies*: testing of single compounds, compound synergies, evaluation of toxicity, and screening for new compounds will help to advise on optimized and in the future individualized therapies.

heterogeneity of cancer cells and their tumor-propagating and self-renewal potential (20, 21). This strategy has been reviewed in detail recently by Moore and Langenau (22).

Genetic approaches are based on the transfer of mutations found in cancer cells from the patient to zebrafish to investigate functional consequences of the respective mutation. This is achieved not only by expressing a mutated human gene in zebrafish but also by mutating the orthologous zebrafish gene or even by expressing cancer-related genes from other species in zebrafish like mouse *c-myc* or *xmrk* from *Xiphophorus* (8, 23). Available genetic tools and strategies for expression of oncogenes and emerging technologies to study tumor suppressors are discussed below. With next-generation sequencing (NGS) revealing the mutational landscape of many tumor genomes, new challenges have arisen. How are the many mutations best evaluated functionally if they constitute driver, modifier, or passenger mutations? Here, the zebrafish model has the potential to offer solutions through functional testing of single-mutated genes and mutation combinations.

Genetically engineered zebrafish models (GEZMs) allow for characterization of cell autonomous and non-cell autonomous mechanisms driving tumorigenesis within an intact organism. Such insights will instruct the development of therapeutic strategies. Ideally, genetic zebrafish cancer models present with an early phenotype, so that they can be used in compound screens on embryos or larvae to identify compounds able to eradicate tumor cells. Due to these obvious advantages, genetic cancer modeling in zebrafish is rapidly growing, and we will report on recent progress and discuss what still needs to be done.

Xenografting of patient-derived cancer cells into zebrafish promises to be an alternative to current patient-derived xenograft (PDX) models in mouse. In particular, transplantations into zebrafish embryos and larvae appear appealing as tumor cells can be observed directly in the transparent host and their proliferation and migratory behavior can be monitored by live microscopy. By this means, the interaction of the tumor cells with the host environment, including biological processes like neovascularization, can also be investigated. Probably most important, zebrafish larvae are ideal for higher throughput screens to identify compounds able to eradicate or differentiate tumor cells. Of particular interest is that such short-term zebrafish PDX models typically provide insights in less than 2 weeks and thus could potentially provide information relevant to patient treatment. For example, the model could assess the aggressiveness of a tumor, thereby helping estimate disease progression, or could be used to develop therapeutic strategies, based on *in vivo* compound evaluation or a compound screen, within a time frame relevant to the respective patient. However, PDX models in zebrafish (PDXz) are still in their infancy, robust PDX protocols are still missing, and several obstacles need to be overcome in reaching this rewarding aim. We will report on the progress and the challenges in the zebrafish xenograft field below.

THE TOOL KIT FOR GENETIC ZEBRAFISH CANCER MODELS

Genetic zebrafish cancer models are often based on cell type-specific expression of human oncogenes to induce tumors mimicking the related human tumor entity. For this, typical promoter-oncogene constructs as well as inducible (e.g., heat-shock) and bipartite expression systems like Gal4/*UAS*, Cre/*loxP*, and lexA/*lexAOP* are used. An advantage of the bipartite and inducible gene expression systems, and combinations of the two (e.g., Tet-ON, Cre^{ERT2}/*loxP*), is their ability to circumvent oncogene-related lethality prior to sexual maturity, which interferes with creation of transgenic strains. One example of an effective zebrafish cancer model was created by driving $KRAS^{G12V}$ specifically in the liver using the inducible Cre^{ERT2} system. The resulting fish developed various liver tumors ranging from benign adenoma to malignant hepatocellular-carcinoma and -blastoma (24). Furthermore, inducible conditional systems have been successfully used to study oncogene addiction. In a mifepristone-inducible model of zebrafish myca/b overexpression, it was shown that liver carcinogenesis was reversible upon withdrawal of the drug (25). Interestingly, regression was even independent of p53 as it also occurred in the *p53* mutant background.

While the introduction of dominant oncogenes is straightforward, studying tumor suppressors has been more difficult and initially relied on identifying fish created through random mutagenesis screens using chemicals such as ethylnitrosourea (ENU) (26, 27) or by insertional mutagenesis (28). Zinc-finger nucleases and transcription activator-like effector nucleases (TALENs) provided the first means of creating targeted knockout animals and were quickly adopted for the generation of cancer models. For example, neurofibromatosis 1 (*nf1a* and *nf1b*) zebrafish mutants were successfully created with zinc-finger nucleases (29) and tumor-suppressor retinoblastoma 1 mutants with TALENs (30).

While TALEN and zinc-finger nuclease-based methods do produce mutations, they are inefficient and labor-intensive. However, the recent advent of highly effective CRISPR/Cas9 technology provides unprecedented possibilities for genome editing in zebrafish, including for the creation of cancer models. Custom-made CRISPR guide RNAs facilitate rapid screens for tumor suppressors or cancer modifiers. Frequent bi-allelic targeting observed with CRISPR/Cas9 saves time spent backcrossing fish lines to homozygosity. Cell type-specific knockouts can be achieved by expression of Cas9 under a tissue-specific promoter allowing for spatial control of gene disruption in somatic cells (31). Although still a challenge, progress has been made in establishing knockin strategies targeting an endogenous cancer-relevant locus by homologous recombination (32–34). In the future, this will facilitate the generation of conditional knockout lines by introducing flanking *loxP* sites into tumor suppressors. Crossing such lines with tissue-specific inducible Cre lines (e.g., tamoxifen-inducible Cre^{ERT2}) will provide temporal and spatial control over the gene-disrupting event to generate driver or modifier mutations in zebrafish cancer models. In the future, even personalized CRISPR/Cas9 genetically engineered zebrafish cancer models appear feasible. A comprehensive overview focusing on genetic tools and their application in conditional zebrafish cancer models was also recently published by Mayrhofer and Mione (35).

PROGRESS IN GENETIC CANCER MODELING IN ZEBRAFISH

In the past, the zebrafish cancer field was dominated by genetic models for only a few types of cancer: melanoma (36, 37), neuroblastoma (38), rhabdomyosarcoma (9), leukemia (specifically T-ALL) (8), and liver cancer (39, 40) [reviewed in Ref. (41–44)].

Recently, researchers have created several promising new zebrafish models and improved existing ones to better address specific questions (**Table 1** lists recent models according to tumor entity). In the following, we will highlight several recent examples.

One of the key questions is how well zebrafish models can portray human cancer, and recent data in fact revealed striking similarities between zebrafish and human cancers. In one study, the molecular resemblance between human hepatocellular carcinomas (HCCs) and zebrafish liver cancer models was analyzed (62). All of the zebrafish models use the liver-specific promoter *fabp10* to drive one of the oncogenes *myc*, $KRAS^{G12V}$, or *xmrk* (23, 40, 63). Comparative transcriptome analysis using RNA-seq revealed that these three models together represented gene signatures of almost half (47%) of human HCC. They identified a conserved molecular pattern of 21 upregulated and 16 downregulated genes, which was not only common to the three zebrafish models but also consistent with human HCCs. This indicates that subtypes of human HCC are well represented by zebrafish models. It also shows the need for new models targeting the molecular mechanisms so far not covered by the existing mutations.

Primitive neuroectodermal tumors of the central nervous system (CNS-PNETs) are poorly understood, aggressive pediatric brain tumors with poor prognoses. Recently, a novel zebrafish tumor model for CNS-PNET was generated by expressing human wild-type *NRAS* or $NRAS^{Q61R}$ under the *sox10* promoter (52). The fish develop tumors in the optic tectum, cerebellum, and brain stem, and the tumors in the anterior lobes histologically and genetically resemble CNS-PNETs, specifically oligoneural and NB-*FOXR2* CNS-PNETs. In an elegant transplantation assay, the authors also showed that CNS-PNETs are sensitive to MEK inhibition.

Another new brain tumor model addresses the question of why a particular founding mutation will lead to brain lesions that are in some cases benign and in others malignant (51). The model was generated by driving *EGFP-*$HRAS^{G12V}$ expression in the central nervous system using the *zic4:KalTA4* activator strain (17), and somatic mosaic expression led to tumors mostly in the telencephalon. Interestingly, malformations with and without GFP expression could appear even in the same brains, the former an infiltrative cancer with persistent pERK activation, and the latter a sharply circumscribed heterotopia with no pERK. Comparing the tumor transcriptome to 840 human GBM markers (64) revealed that the zebrafish tumors resemble the human mesenchymal GBM subtype. Within the upregulated genes were five genes related to YAP signaling. Applying an eight gene signature featuring YAP targets to human tumors established that YAP can distinguish between mesenchymal glioblastoma and low-grade glioma and therefore could prove useful as molecular diagnostic tool. In support of the importance of Hippo signaling to tumor behavior, coexpression of a dominant-active form of YAP (YAP^{S5a}) with $HRAS^{G12V}$ in this model led to a shift from benign heterotopias to malignant lesions with increased proliferation and reduced survival.

These examples demonstrate not only the histological but also genetic resemblance of zebrafish cancer models to their human counterparts. Importantly, the zebrafish models have direct clinical implications for human patients—they can be used to develop valuable diagnostic markers that discriminate between benign and malignant tumors, and to test possible treatment strategies. Furthermore, zebrafish models are ideal for functionally characterizing candidate variant genes and for studying the synergy of mutations found in human tumors *in vivo*, as we will discuss in the next paragraph.

Functional Investigation of Mutations and of Alterations in Pathway Activity

In recent precision medicine approaches, NGS is increasingly used to evaluate tumors for mutations that may indicate potential treatment targets or may constitute risk factors like a high chance of metastasis. In addition, gene expression analysis of tumor cells reveals alterations in signaling pathway activity. Such knowledge is important for patient stratification to ideally provide individually tailored treatments. However, to understand the significance of the identified mutations, combinations of mutations and changes in activity of signaling pathways, the abnormalities need to be tested in a functional assay. Zebrafish is an ideal vertebrate model for *in vivo* analysis of such alterations for many reasons, including ease of genetic manipulation, accessibility from the one-cell stage, rapid development, and transparency of the embryos. Two recent examples of functionally testing mutations and signaling pathway alterations in zebrafish were in neuroblastoma and malignant peripheral nerve sheath tumor (MPNST) models, each revealing synergism between tested alterations.

Neuroblastoma, which affects the peripheral sympathetic nervous system, is one of the most frequent childhood cancers (8–10% of all childhood cancers). While the original zebrafish neuroblastoma models were based on the overexpression of human MYCN, a recent variation combined MYCN overexpression under the dopamine-β-hydroxylase (*dβh*) promoter with expression of mutated human ALK (45). The result was a dramatic increase in frequency of adrenal neuroblastoma, from 15 to 55%, caused by the combination of MYCN preventing differentiation of neuroblasts into chromaffin cells and ALK providing survival signals. More recently, the role of *nf1* mutations, which are associated with a poor outcome in human neuroblastoma, was also analyzed in the zebrafish *MYCN* model (46). An *nf1* mutation increased the tumor penetrance in MYCN-overexpressing fish to over 80% by blocking the apoptosis normally seen in those fish. The loss of NF1 led to aberrant Ras–Mapk pathway activation that can be rescued by expression of the GTPase-activating protein-related domain (GRD) of NF1. The authors further used their zebrafish model to develop a treatment strategy. By targeting the Ras/Mapk pathway with the FDA-approved MEK inhibitor trametinib in

TABLE 1 | Recently developed and improved zebrafish cancer models.

Cancer entity	Tissue driver: oncogene	Tumor suppressor	Modifier	Tumor frequency/survival	Effective compounds	Reference
Neuroblastoma	*dbh:MYCN*		*ALK^{F117L}*	5% neuroblastoma at 24 wpf		Zhu et al. (45)
	dbh:MYCN	*nf1a$^{-/-}$, nf1b$^{+/-}$*		*nf1a$^{-/-}$:* 60% neuroblastoma at 4 wpf; *nfla$^{-/-}$ nf1b$^{+/-}$:* 82% neuroblastoma	Trametinib, isoretinoin	He et al. (46)
Malignant peripheral nerve sheath tumor (MPNST)	*ia2:EGFP* (15 Mb deletion of chromosome 1)			30% MPNST at 30 mpf		Astone et al. (47)
	Sox10:PDGFRA$^{wt\ or\ mut}$	*tp53$^{-/-}$, nfla*", nf1b$^{-/-}$*		*PDGFRA^{wt}*: 80% at 30 wpf, *PDGFRA^{mut}*: 50% at 30 wpf	Sunitinib, trametinib	Ki et al. (48)
		tp53$^{-/-}$	*atg5^{K130R}*	*p53$^{+/-}$*: 15% tumors vs. *p53$^{+/-}$ mitfa:atg5 ^{KI30R}*: 40% tumors		Lee et al. (49)
Brain cancer		*rb1*		*33%* tumors in fish at 18 mpf injected with exon 2 or 3 transcription activator-like effector nuclease		Solin et al. (30)
	krt5:KRAS^{G12V} or gfap:KRAS^{G12V}			*krt5:KRAS^{G12V}* 26% at 1 mpf, 50% at 12 mpf; *gfap:KRAS^{G12V}: 50%* brain tumors at 12 mpf		Ju et al. (50)
	zic4:Gal4 inj. uas:HRAS^{G12V}		*YAP*	*YAP^{SSA}* (dominant-active) reduces survival from 60 to 4% in *zic4:HRAS^{G12V}*		Mayrhofer et al. (51)
	sox10:NRAS or *NRAS^{Q61R}*	*tp53$^{-/-}$*		50% CNS-PNET tumors at 6 wpf	MEK inhibitor AZD6244	Modzelewska et al. (52)
Eye cancer	*krt5:Ga14; 14xuas; zfSmoa1*			80% optical pathway glioma and retinal tumors at 12 mpf		Ju et al. (53)
Leukemia	*spi1:lox-NUP98-HOX9* × *hsp70:Cre*		*meis1, Cox2*	25% myeloproliferative neoplasms between 19 and 23 mpf	COX and HDAC inhibitors	Deveau et al. (54)
	c-myb^{hyper} (gene duplication, wt, and truncated gene version)			Myelodysplastic syndrom, 2% progress to AML or ALL, respectively, at 10–24 mpf	Flavopiridol	Liu et al. (55)
Myeloproliferative disease		*c-cbl$^{-/-}$*		*c-cbl$^{-/-}$* lethal before 15 dpf, myeloid/erythroid lineages increased		Peng et al. (56)
Mastocytosis	*actb2:KIT^{D816V}*			50% prevalance, 15 mpf median age of onset		Balci et al. (57)
Melanoma	*mitfa:BRAF^{V600E}*	*tp53$^{-/-}$*	*EDN3*	Cell line transplantations		Kim et al. (58)
	mitfa:HRAS^{G12v}			30% increase of melanocytes 5 dpf	MEK inhibitor PD185342 and rapamycin	Fernandez Del Ama et al. (59)
Uveal melanoma	*mitfa:GNAQ^{Q209P}*			33% uveal tumors at 5 mpf		Mouti et al. (60)
Thyroid cancer	*tg:BRAF^{V600E}*			64% invasive thyroid cancer at 12 mpf		Anelli et al. (37)
Liver cancer	*fabp10:LexPR* × *LexA OP:myca or LexA:mycb*			Cellular alterations from 10 days post mifepristone induction (dpi), 5% hepatocellular carcinoma (HCC) at 8 mpi		Sun et al. (25)
	fabp10:pt-beta-Catenin			4–5 mpf enlarged livers, HCC histology, decreased survival rate	JNK inhibitors and anti-depressants	Evason et al. (61)
	fabp10:LexPR × *LexA OP:Cre* × *fabp10:loxp-Stop-loxp-KRAS^{G12V}*			Induced with mifepristone at 4 wpf for 36 h ca. 60% tumor penetrance at 24 wpi		Nguyen et al. (24)

dpf: days post fertilization; wpf: weeks post fertilization; mpf: months post fertilization; dpi: days post induction.

conjunction with the use of the neuroblastoma drug isotretinoin, they worked out the ideal synergistic dosage combination for maximum effect on tumor growth.

Malignant peripheral nerve sheath tumors are very aggressive soft tissue sarcomas, thought to originate from neural crest cells. About half of them arise in children with neurofibromatosis type 1, an inherited genetic disease caused by mutations in *NF1*. Prognosis is rather poor and the recurrence rate is high. So far, the therapeutic possibilities are very limited, and chemotherapy is often ineffective, leaving complete surgical resection as the best option. In recent years, a number of zebrafish models have been developed to study the molecular mechanisms underlying the disease, as well as to screen for alternative treatment options. The first model in zebrafish was based on a mutation in the tumor-suppressor *p53* leading to MPNST in around 30% of fish after 16 months (65). The long latency in patients as well as in the zebrafish model indicated that additional mutations are needed for MPNSTs to develop. PDGFRA is found to be expressed at high levels in MPNSTs. Overexpressing either wild-type or mutant PDGFRA in $p53^{M214K}$ $nf1b^{-/-}$ zebrafish accelerated tumor development (48). Interestingly, overexpression of wild-type PDGFRA was even more detrimental than an activating mutation in PDGFRA leading to a tumor incidence of 80 vs. 50% at 30 weeks. This surprising reduction in tumor growth by constitutively active PDGFRA can be explained by the induction of senescence through a supra-optimal Erk and Akt downstream signal. In line with these observations, *PDGFRA* is rarely mutated in clinical samples. Using the RTK inhibitor, sunitinib together with the MEK inhibitor trametinib could efficiently inhibit tumor growth in this model.

Autophagy is a pathway involved in cellular degradation in response to starvation and cellular stress, but its role in tumorigenesis is controversial. A zebrafish MPNST model was recently used to analyze autophagy in tumor development (49). On a *p53* heterozygous mutant background, autophagy was inhibited by expressing dominant-negative $atg5^{K130R}$ under the *mitfa* promoter, directing expression to neural crest cells and melanocytes. Inhibition of autophagy accelerated tumorigenesis, leading mainly to MPNST and to a lesser extent to neuroendocrine and small round cell tumors. Surprisingly, given the use of the mitfa promoter, the fish did not develop melanomas. In this model, autophagy is suspected to promote genomic stability by delaying *p53* loss of heterozygosity. Inhibition of autophagy is not oncogenic by itself in this model but modulates preexisting cancer susceptibility. This shows that zebrafish models are well suited to study the contribution of cellular processes such as autophagy to cancer *in vivo* and can add an alternative perspective on data gained from mouse models and human cell lines.

Unraveling Mechanisms of Drug Resistance by Cross-Species Oncogenomics

So far, we have presented examples demonstrating the histological and genetic similarities between zebrafish and human cancers. We have also covered how mutations can be functionally analyzed, and how synergy can be studied in zebrafish cancer models. Most models were also used to develop therapeutic strategies, which might translate to the clinic. However, targeted therapies often lead to development of resistance, and the field is in dire need for a better understanding of the underlying mechanisms of drug resistance. In the following paragraph, we highlight a recent study suggesting that drug resistance mechanisms are conserved between zebrafish and human and thus can be studied in zebrafish models.

To understand the genetic alterations underlying progression of melanoma and the development of drug resistance, an elegant cross-species oncogenomics approach was applied using a zebrafish melanoma model (66). $BRAF^{V600E}$-, $NRAS^{Q31K}$-, and $HRAS^{G12V}$-mediated zebrafish models exist (36, 67, 68). The melanoma model driven by human $BRAF^{V600E}$ and mutant *p53* shows a latency of 4–6 months until melanoma manifests, indicating that additional mutations need to be acquired. Indeed, sequencing a melanoma cell line [ZMEL1 (69)] derived from this model revealed >3,000 new mutations in malignant cells. Additional treatment of ZMEL1 cells with the BRAF inhibitor vemurafenib for 4 months led to development of drug resistance. Gene expression profiling of the resistant cells (ZMEL1R) showed altered cAMP and PKA signaling, highly similar to human drug resistant samples. On the genomic level, only three additional mutations were found in drug resistant ZMEL1R cells in *bub1ba*, *col16a1*, and *pink1*. Strikingly, an increased mutation frequency in these genes is also observed in patient samples, suggesting that core drug resistance mechanisms are conserved between human and zebrafish. Zebrafish cancer models can thus be used to efficiently filter human sequencing data. Mutations conserved across species might offer new therapeutic strategies to overcome drug resistance.

Visualizing Reactivation of Developmental Programs in Melanoma Formation

Studies on melanoma in zebrafish have now advanced from establishing relevant models to a stage where new insights on the regulation of tumor initiation and cellular plasticity can be gained. A concept in the cancer field is that developmental programs are reactivated during tumorigenesis and can have important effects such as regained self-renewal capabilities and migratory behavior leading to proliferation, invasion, and metastasis (70). One advantage of zebrafish here is the ability to image the cells *in vivo* and over time. Indeed, combining a zebrafish melanoma model with a reporter for *crestin* revealed that cells reverted to an embryonic neural crest state (71). *Crestin* is a gene normally only expressed during the embryonic period in neural crest cells but is also commonly re-expressed in melanoma. Using this fluorescent *crestin* reporter, the authors could follow single melanocytes in a "cancerized field" starting to express *crestin* with these clones developing into melanoma. The functional relevance of reactivating neural crest identity was demonstrated in an experiment showing that overexpression of the neural crest regulator Sox10 in melanocytes accelerated melanoma formation. Interestingly, super-enhancers regulate the neural crest progenitor signature. This is also the case for zebrafish melanomas and human melanoma lines, which share super-enhancer signatures for the neural crest transcription factors Sox10 and Dlx2. These mechanistic insights into the regulation of the embryonic neural crest program in melanoma could be exploited to develop new therapeutic strategies directed

at the re-emergence of the neural crest signature, e.g., by targeting epigenetic mechanisms. In addition, key transcriptional regulators of reactivated developmental programs could potentially be used as biomarkers for early detection of oncogenesis.

TME STUDIES USING GENETIC ZEBRAFISH MODELS

Several aspects of tumor initiation, progression, and metastasis are intimately linked with the TME. For example, induction of angiogenesis by tumor cells in a process termed "angiogenic switch" is one of the hallmarks of cancer, and neovascularization is necessary for tumor growth (72). The TME is ideally studied *in vivo* due to its complex composition of multiple cell types, including but not limited to tumor cells, immune cells, fibroblasts, and endothelial cells. In pioneering studies, Feng and Martin showed that zebrafish is a suitable model organism to study interactions between oncogene-expressing cells and innate immune cells. Using a zebrafish melanoma model, they found that $HRAS^{G12V}$-expressing melanoblasts and goblet cells attract leukocytes by secreting H_2O_2 (73). In addition, macrophages and neutrophils provided trophic factors like prostaglandin E2, fueling proliferation of $HRAS^{G12V}$ + cells at tumor-initiating stages (74) [and summarized in Ref. (75)]. These findings reveal that, like in humans, pro-tumor immune cells also exist in zebrafish. We will focus on the latest progress in the field of TME studies in zebrafish in the following section.

In virally caused HCC, chronic inflammation is an important etiological factor and generally inflammation has been recognized as a hallmark of cancer (72). In a zebrafish $KRAS^{G12V}$ liver cancer model, neutrophils were found to be recruited to the liver (76) similar to the recruitment seen in human cancers of the digestive tract (77, 78). In this zebrafish model, neutrophils contributed to tumor growth as inhibition of neutrophil NADPH oxidase and blocking of neutrophil differentiation by a *gcsfr* morpholino led to a reduction in liver size and histological improvement. Neutrophils in the $KRAS^{G12V}$ + livers behaved more stationary within the tumor and morphological analysis revealed an increase in neutrophil numbers with hyper-segmented nuclei in the TME. Also, the TME was modulated by hepatocyte-produced TGF-β. As in mouse models, TGF-β induced a pro-tumor neutrophil cytokine expression pattern in zebrafish in this study, showing that essential mechanisms in the TME are conserved. Once the neutrophil-derived factors promoting liver carcinogenesis have been identified in this model, it will be interesting to see their role in human carcinogenesis.

The same group also found a possible explanation for the gender disparity in HCC, with men being more likely to develop HCC and also showing more aggressive disease progression than women. In their inducible $KRAS^{G12V}$ HCC model, they found increased numbers of tumor-associated neutrophils (TANs) and macrophages (TAMs) in male zebrafish, which also showed accelerated liver carcinogenesis compared to their female counterparts (79). The authors showed that male zebrafish had higher levels of cortisol, which induced expression of TGF-β. TGF-β1 in turn served as chemoattractant recruiting TANs and TAMs. Strikingly, higher cortisol and TGF-β1 levels together with higher TAN/TAM infiltration were also observed in human HCC patients indicating a causative link to tumor aggressiveness. The authors also emphasized that zebrafish is an ideal model to study cortisol-elicited effects, "as both human and zebrafish utilize cortisol as their main stress hormone whereas mouse and rat make use of corticosterone instead" (79).

Zebrafish is also a suitable model to study neo-angiogenesis as core mechanisms are conserved. Using a transgenic hypoxia reporter *Tg(phd3:EGFP)* and angiogenesis inhibitors (SU5416 and sunitinib), it was elegantly shown that like in humans liver hyperproliferation is dependent on hypoxia and angiogenesis in a *myc*-induced zebrafish liver cancer model (80). In addition to the direct influence on tumor size, neovascularization could be important for metastasis, providing tumor cells entry to the vascular system.

90% of cancer patients die from metastases (81), so a treatment to inhibit the metastatic process would be a major breakthrough in cancer therapy. During the metastatic process, tumor cells switch their phenotype. Initially, often through epithelial–mesenchymal transition (EMT) tumor cells disseminate, migrate, and enter the blood circulation. After extravasation, they switch from an invasive to a proliferative phenotype. In melanoma, the invasive phenotype is associated with low and the proliferative/differentiated with high MITF levels and this phenotype switch is likely induced by the TME (58). A recent zebrafish study looked at the fate of melanoma cells during the metastatic process focusing on the regulation of cellular plasticity and differentiation by factors of the microenvironment (58). An initially unpigmented mesenchymal zebrafish melanoma cell line derived from *mitfa:*$BRAF^{V600E}$ melanomas regained pigmentation upon transplantation indicating differentiation. This was also associated with the upregulation of a differentiation signature of MITF target genes including EDNRB receptor. Using this cell line together with human melanoma cell lines, the authors identified endothelin EDN3, likely derived from keratinocytes, to induce phenotype switching leading to increased proliferation, melanin content, and differentiation. Inactivation of EDN3 and its converting enzyme ECE2 by CRISPR/Cas9 led to reduced tumor size and increased survival rates. Targeting TME factors like EDN3 promises to be a beneficial strategy to inhibit metastatic success.

The effect of wounding on cancer progression is an understudied but important topic, as surgery is a key cancer therapy and biopsies are the gold standard for diagnosis. Based on previous studies comparing the immune responses elicited by wounding and cancer formation, a recent study set out to investigate the direct effects of wounding on melanoma propagation in zebrafish (82). Indeed, the authors found that more than 40% of repeatedly wounded *kita:*$HRAS^{G12V}$ fish developed local tumors at the sites of wounding compared to unwounded fish. Wounding close to tumor sites was associated with an inflammatory response as macrophages and neutrophils were recruited not only to the wound but increasingly to adjacent tumor cells where they persisted for longer time periods. Wounding-induced proliferation of cancer cells could be blocked by morpholinos inhibiting myeloid cell development, suggesting that myeloid cells fuel the proliferation of cancer cells. In human cancer biopsies, the extent

of ulceration, a negative prognostic marker, correlated with the number of infiltrating neutrophils but not macrophages. Based on this, improvements toward minimal invasive surgery and potential peri-operative anti-inflammatory treatment options should be considered.

These examples show that zebrafish has developed into a powerful model organism to study the TME. However, one caveat at early developmental stages best suited for *in vivo* microscopy investigations is that the adaptive immune system is not yet fully functional (83). Nevertheless, we have highlighted studies demonstrating the translational potential of zebrafish TME studies.

TOWARD PDX IN ZEBRAFISH

Xenotransplantation of patient-derived tumor cells into zebrafish embryos and larvae for short-term cultivation, analysis, and compound screening is an appealing concept, as it promises to provide patient-specific insights and patient-tailored therapeutic strategies. Several groups have embarked on establishing protocols for xenotransplantation, initially using cultured tumor cell lines. In 2005, Lee et al. were the first to inject human melanoma cells into blastula stage zebrafish embryos (84). They maintained injected embryos at 31°C and tracked melanoma cells, which survived and divided in the fish for several days. At 5 days post fertilization (dpf) cells were observed in the head, trunk, and tail of injected fish.

Other groups have chosen 24 and 48 h post fertilization (hpf) for xenotransplantation and injected several hundred cells into the yolk, the Duct of Cuvier, the caudal vein, the pericardial cavity, the perivitelline space, and the ventricles of the brain (85–87). In addition, orthotopic xenografts have shown promising results (88). Injected tumor cell lines include glioma (89), HCC (90), lung cancer (91), pancreatic cancer (92), ovarian carcinomas (93), breast cancer (94), Ewing sarcoma (95–97), prostate cancer (98), retinoblastoma (99), and leukemia (100).

Due to the absence of an adaptive immune response until 4–6 weeks post fertilization (wpf), xenografted cells are not rejected at these early time points (83, 101). Typically, transplanted zebrafish are now maintained at 32.5–35°C relatively close to the physiological temperature of human cells, but still permitting normal zebrafish development (87). To visualize xenotransplanted cells for fluorescence microscopy, they are usually dye labeled, most often using CM-DiI (102).

Typical readouts allowing for quantification of the behavior of transplanted tumor cells in the fish host are proliferation, migration, and neovascularization. Proliferation of transplanted tumor cells can be investigated in a straightforward way by using available human-specific anti-ki67 antibodies (88, 103). Neovascularization can be visualized easily by performing xenotransplantation into transgenic zebrafish strains with fluorescently labeled vasculature (104, 105). Different tools have been applied for image-based quantification of migration, including ImageJ/Fiji open source and commercial software solutions, like Image-Pro Plus-based software MetaXpress (95, 96, 100, 106).

Teng et al. showed that the migratory/spreading behavior of transplanted cells in zebrafish correlated well with their metastatic potential *in vitro* (106). A preliminary experiment using short-term-cultured primary lung cancer cells confirmed that tumor cell spreading in zebrafish can be used as readout for metastatic potential (106). As about 90% of cancer patients die from metastatic spread of primary tumors, *in vivo* models complementary to the mouse model will be beneficial (107). Using a zebrafish melanoma xenograft model, it was demonstrated that poorly invasive cell populations coinvade with inherently invasive cells, thereby maintaining heterogeneity of melanoma cells (108).

As transplantation protocols of tumor cell lines become more robust (109), the field appears to be ready for real PDXz models, which were pioneered by Marques et al., who transplanted pancreas, stomach, and colon primary tumor cells into the yolk of 48 hpf zebrafish embryos (102). More recent reports using primary cultures of breast cancer cells from bone metastases and neuroendocrine tumor cells and spheroids obtained from papillary thyroid cancer fuel the hope for personalized medicine approaches using short-term PDXz (110–112). Especially the low number of cells used for transplantation into zebrafish might allow one to use tumor cells of low abundance, such as disseminated tumor cells. Nevertheless, it needs to be investigated, how well tumor heterogeneity is preserved in PDXzs and how the zebrafish environment changes gene expression and behavior of transplanted human tumor cells. The future will also tell how well actual primary cells engraft into zebrafish embryos/larvae and if there is need for "humanizing" zebrafish to be able to provide lacking growth factors. For some slowly growing primary tumor cells, the short experimental setup proposed for PDXzs might actually be disadvantageous. Here, several immunocompromised zebrafish strains like *rag2*^{E450fs}, *jak3*^{P369fs}, *prkdc*^{D3612fs}, and *zap70*^{y442}, which can be combined with optically clear mutant strains like casper, will help to overcome adaptive immune response and imaging problems associated with performing xenograft studies in juvenile zebrafish (21, 113–115).

STRATEGIES FOR IDENTIFYING POTENTIAL THERAPEUTIC COMPOUNDS BY GEZM OR PDXz DRUG SCREENS

Toxicology and toxicity studies using various fish models have a long tradition due to the ease of substance administration directly into the water and easy-to-recognize developmental malformations as readout (116). In 2000, a pioneering screen demonstrated that small molecule effects on organ development can be studied in whole zebrafish larvae in 96 well format (117). In the following 15 years, nearly 100 zebrafish screens were conducted with differing strategies, functional focus, and compound library size as reviewed by Rennekamp and Peterson (118). Generally, phenotype-based screens have higher success rates than target-based screens, which led to great interest in compound screening using zebrafish models related to human diseases (119).

Design and especially the readout is crucial for the success of a screen. In the following, we will present recent approaches relevant to the field of cancer, including screens based on developmental surrogate readouts, high-throughput screens using GEZMs and signal pathway-targeted screens.

Screens Using Developmental Surrogate Markers

As zebrafish has been used in developmental biology for decades, the extensive knowledge can now be exploited for drug screens. During tumorigenesis, developmental programs are reactivated to escape anti-proliferative mechanisms like contact-inhibition, fate commitment, or apoptosis (72). Screens using developmental processes as readout can therefore be informative for oncology.

EMT is tightly connected to metastatic behavior of cancer cells and as metastasis is causing the majority of deaths related to cancer, therapeutic strategies blocking this process would be highly beneficial. Complex situations such as cells leaving their epithelial context are ideally modeled *in vivo*. Toward this goal, a transgenic zebrafish strain [*Tg(snai1b:GFP)*] was generated, which labels epithelial cells undergoing EMT to produce cells of the neural crest lineage (120). Applying this strain in a chemical compound screen revealed that TP-0903 is able to strongly inhibit EMT (120). Interestingly, TP-0903 is a multi-kinase inhibitor and subsequent testing of single target kinases was not able to generate the same effect. This emphasizes the tightly orchestrated activity of several kinases during EMT, which is likely true for many other biological processes. Eventually RNA sequencing and chemical rescue experiments showed that TP-0903 acts through stimulation of retinoic acid synthesis in this setting.

Another screen for potentially anti-metastatic compounds was carried out exploiting parallels between migrating posterior lateral line primordium (PLLp) cells in zebrafish and the behavior of invasive cancer cells (121, 122). Approximately 3,000 compounds were screened for their potential to affect PLLp migration in transgenic *Tg(cldnb:EGFP)* zebrafish, which express GFP in the PLLp and hereby offer a convenient readout (123). Approximately 5% of tested compounds had an effect without overt toxicity and among these was the Src inhibitor SU6656. The target of SU6656 could be rapidly validated using a CRISPR sgRNA targeting *src*. Finally, the authors showed that spreading of highly metastatic cells could be inhibited in a mouse orthotopic transplantation model, confirming that SU6656 has strong anti-metastatic activity in mammals as well.

In a leukemia-targeted screen, Ridges et al. reasoned that immature T cells might be a good surrogate for leukemic cells and thus used a transgenic strain [*Tg(lck:GFP)*], which demarcates immature T cells by GFP expression in developing zebrafish larvae (124). They screened more than 26,000 compounds on larvae in 96 well format using GFP expression in the thymic region as readout. Among the compound hits, they found lenaldekar to selectively eliminate immature T cells in larvae and also to prevent cMYC-induced T cell acute lymphoblastic leukemia (T-ALL) in adult zebrafish. Furthermore, lenaldekar was effectively inhibiting human leukemic xenograft growth in mice. This demonstrates how lead compounds can be identified in zebrafish screens.

Screens On Genetic Cancer Models

An increasing number of specific zebrafish models for solid tumors as well as leukemias have been successfully employed in small compound screens. In these phenotype-based screens, rescue of disease-related malformations is often used as readout. With this holistic approach, no prior knowledge about pathological mechanisms is required for random library screening. In addition, a whole organism screen selects for compounds with low toxicity.

One recent screen was performed on a HCC model driven by liver-specific expression of β-catenin and histologically highly similar to the human disease (61). Using this model, the authors revealed that constitutive WNT/β-catenin signaling forces proliferation and consequently measurable increase in liver size *via* JNK signaling. In a high-throughput drug repurposing screen using excessive liver growth as readout, JNK inhibitors as well as unexpectedly specific anti-depressants were identified as potent inhibitors of liver growth. This suggests JNK inhibitors and specific anti-depressants as new therapeutic strategies for β-catenin-induced liver cancers.

Repurposing studies of already approved drugs promise a fast track into the clinics, as tolerance and side-effects in humans have already been investigated for these compounds. Testing for synergy of approved drugs on zebrafish cancer models promises alternative treatment options for cancer entities where monotherapy fails.

Synergistic effects were detected in a Ras^{G12V}-driven melanoma model, which was elegantly analyzed on a standard plate reader measuring increased melanophore density. In a focused compound screen, combinations of the MAPK inhibitor PD184352 and the PI3K/mTOR inhibitors BEZ235 or rapamycin efficiently inhibited melanoma growth at low concentrations, where single compound treatment was not effective anymore (59).

Combined suppression of MAPK and PI3K/mTOR pathway also acted synergistically in a rhabdomyosarcoma zebrafish model (125). From nearly 3,000 tested drugs, the chymotrypsin-like serine protease inhibitor TPKC was found to inhibit S6k1, a downstream target of mTOR. Here, tumor growth could be suppressed with additional treatment with the MEK inhibitor PD96059.

Furthermore, He et al. highlighted in the already mentioned neuroblastoma model driven by aberrant MYCN expression and loss of NF1 that monodrug treatment is unlikely to achieve satisfying therapeutic effects. Their fish model was well suited to determine balanced and effective compound combinations. Applying isobologram analysis they worked out the best synergistic concentrations for MEK inhibitor trametinib and isotretinoin (46).

Signaling Pathway Activity-Based Screens

In a more targeted approach, comparative strategies and available transgenic signaling pathway reporter strains can be used to identify compounds able to inhibit or augment a specific signaling pathway. As many signaling pathways play crucial roles in tumorigenesis, this is directly relevant for cancer management.

The Notch signaling pathway controls cell fates and orientation during development by direct cell–cell contact and is often deregulated during cancer pathogenesis.

A screen comparing the effects on larval development of more than 200 compounds to the standard Notch inhibitor DAPT identified 2 novel Notch inhibitory compounds. These small compounds also successfully reduced proliferation of human oral cancer cell lines *in vitro* (126).

Likewise, the Hedgehog (Hh) signaling pathway is essential during development and is also connected to several malignancies, including medulloblastoma and basal cell carcinoma (BCC). A Smoothened (Smo) antagonist is approved for the treatment of advanced BCC, but additional Hh pathway inhibitors downstream of Smo could define new strategies for the treatment of other Hh-dependent malignancies. Testing 30,000 compounds for their effects on zebrafish patterning, Williams and colleagues discovered eggmanone, a small molecule, mimicking the Hh null phenotype in zebrafish embryos (127). They could show that eggmanone is an inhibitor for a phosphodiesterase 4 isoform (PDE4D3). Strikingly, PDE4 has also been implicated as a driver of CNS tumors like medulloblastoma (128). Identifying PDE4 as a potent target to inhibit Hh-signaling opens up new possibilities in Hh-dependent cancer therapy.

In another elegant compound screen, the FGF signaling reporter strain *Tg(dusp6:EGFP)*^{pt6} was used to identify compounds altering FGF signaling. (*E*)-2-benzylidene-3-(cyclohexylamino)-2,3-dihydro-1*H*-inden-1-one (BCI) augmented EGFP expression in this reporter strain. Mechanistically, BCI was found to block Dusp6 activity and enhance FGF target gene expression. Furthermore, a temporal role of Dusp6 during heart formation was discovered by treating zebrafish embryos with BCI at several developmental stages (129). Dusp6 is a phosphatase involved in the MAPK pathway, a pathway also often deregulated during cancer pathogenesis. Therefore, regulators of this target are of clinical relevance in oncology and BCI is indeed used in leukemia treatment.

Remaining Questions For Zebrafish Model-Based Compound Screening

Many small compound screens have been performed, but our understanding of pharmacokinetic processes in zebrafish is still limited. Pilot studies address the important question if zebrafish larvae metabolize drugs in a way comparable to humans. Proteomics and transcriptomics analysis show a high degree of conservation of metabolic enzymes between human and zebrafish larvae, including key metabolic cytochrome P450 (CYP) genes (130, 131). In addition, liver, kidney, and blood–brain barriers are present in zebrafish larvae (119). Investigating testosterone metabolism using zebrafish larvae and liver microsomes from adult zebrafish (ZLM) indicated that more metabolic enzymes are present in adult fish. Comparing adult fish to human, the main testosterone metabolite was identical, but differences in minor metabolites were detected (132). Another study measured the pharmacokinetics of paracetamol metabolites in zebrafish larvae at 3 dpf. Paracetamol clearance rates scaled reasonably well with higher vertebrates and were similar to young humans (133). Clearly, additional investigations are needed to acquire a more complete understanding of pharmacokinetic processes in zebrafish larvae. Nevertheless, most importantly for the use of zebrafish compound screens, pharmacological effects were so far found to be well conserved between zebrafish and mammals. For example, 22 out of 23 known cardiotoxic drugs also exhibited repolarization-related toxicity when tested in zebrafish embryos (119, 134). *Vice versa* 8 out of 10 compounds first identified in zebrafish also produced the expected effect in rodents, suggesting a good translatability (119).

SHORTCOMINGS AND CHALLENGES OF THE ZEBRAFISH MODEL

In every model, some aspects of the process of interest are not well conserved and awareness of such shortcomings of the respective model is important (**Table 2**).

TABLE 2 | Benefits and shortcomings of the zebrafish in cancer modeling.

	Benefits	Shortcomings
Embryonic development	Largely conserved development	Absent organs: breast, prostate, lung. Organ structure not as complex
	External embryonic development Fast development: major organs formed within 48 hpf, cancer studies in larvae feasible	
Physiology	Optical transparancy of larvae facilitates imaging and high-throuput screening	Patient-derived xenograft (PDX): conservation of molecular interactions between transplanted human cells and zebrafish cells unclear
	Conserved signaling pathways	Zebrafish physiological temperature: 28/29°C, for PDX increased to 34–35°C; influence on tumor cell behavior unclear Studying of some drug side-effects such as fever compromised
Genetics	>80% of human disease-related genes present	Teleost-specific whole genome duplication: gene duplications can complicate studies
	Easy genetic manipulation: many transgenic reporter and driver lines for cancer models available Transient manipulation of cancer pathways through injection into one-cell stage larvae possible	
Immune system	Underdeveloped adaptive immune system in larvae: no rejection of xenografts	Underdeveloped adaptive immune system in larvae: obstacle for studying fully functional TME
Tumor anatomy/ histology	Many tumor models show comparable histology to human cancers	Genetic tumor models for breast, prostate, or lung cancer not possible
Handling and husbandry	Abundant larvae for drug screens (up to ~200 eggs/ couple and week) Easy and cost-effective drug screens	

Physiological differences with implications for cancer modeling exist between human and zebrafish. Organs like lung, breast, and prostate are missing in zebrafish, which hampers the generation of genetic cancer models for these tumor entities in zebrafish. Furthermore, orthotopic transplantation of tumor cells from these organs is not possible in zebrafish.

In addition, there are genetic differences. A teleost-specific whole genome duplication event resulted in the presence of ~26,000 protein-coding genes in zebrafish (~20,000 in human) and thus more than one ortholog for some human genes exists (6). This gene duplication potentially leads to redundancy or specialization in gene function and can complicate loss-of-function studies of tumor-suppressor genes. On the contrary, orthologs of some cancer-related genes like oncostatin M (OSM) or leukemia inhibitory factor (*LIF*) have not yet been identified in zebrafish. As corresponding receptors are encoded in the zebrafish genome, it is likely that orthologs for *LIF and OSM* with sequence divergence but similar protein function will be discovered in the future, but other genes like *CDKN2A* might actually be missing (86).

The zebrafish genome size (1.4 Gb) is around half of the human genome size and differences are also found in non-coding regions. Type 1 (retrotransposable elements) cover 44% of the human sequence, but only 11% of the zebrafish genome. In contrast, type II (DNA transposable elements) cover 3.2% of the human but 39% of the zebrafish genome (6). It is currently unclear if this difference in types of transposable elements found in human and zebrafish genomes has implications for cancer modeling in zebrafish.

Ontogeny and function of innate and adaptive immune cells is highly conserved between human and zebrafish. However, a functional adaptive immune system is not present in zebrafish larvae within the first 4 weeks after fertilization (83, 101). Thus, the role of adaptive immune cells in tumor initiation and progression cannot be studied in zebrafish cancer models at these early stages.

Nevertheless, the absence of an adaptive immune response allows xenografts to be carried out without immunosuppression in zebrafish larvae.

A challenge for establishing PDXz models is the slightly cooler temperature in zebrafish larvae (32.5–35°C instead of 37°C), which might affect the behavior of transplanted human tumor cells. Furthermore, some zebrafish growth factors might not be conserved enough to support growth of specific tumor cells. *Vice versa*, it is known that human growth factors do not support zebrafish hematopoiesis *in vitro* (135). Therefore, similar to mouse xenograft models, humanizing zebrafish might be necessary in the future to improve xenotransplantation success rates.

Quo natas, Danio?

As outlined earlier, several novel and improved genetically engineered zebrafish cancer models have been generated over the last couple of years. Many of them have provided new mechanistic insights into tumorigenesis.

We have highlighted elegant screening strategies using zebrafish cancer models, but also developmental process- and signaling pathway-targeted approaches, which have identified chemical inhibitors and their synergistic effects, when applied in combination, of different aspects of tumorigenesis. Phenotype-based compound screening in zebrafish is also ideal for recent polypharmacology strategies to discover single drugs with effects on multiple targets. In the future, automation of the entire small compound screening process including zebrafish handling, image acquisition and image analysis will allow for higher throughput screens and several solutions are already available (136–139).

In addition to small compound screens, first automated injection examples promise that rapid testing of biologics and their delivery vehicles is also feasible in zebrafish (140).

Taken together, zebrafish models have proven to be valuable for cancer research offering unique opportunities, which are complementing mouse and human systems. Current areas of great interest in cancer research including the TME, cancer immunotherapy, epigenetics, and precision medicine will become important topics in zebrafish cancer modeling.

Live imaging together with genetic manipulation of tumor cells and their microenvironment in zebrafish will yield a better understanding of the contribution of each cell type to tumor progression. The innate immune system is already being investigated in a tumor context at larval stages. Applying fish strains, still transparent at juvenile and adult stages, will also allow for observation of adaptive immune cells by live microscopy in GEZMs. By such means, zebrafish cancer models will likely provide novel TME-targeted therapeutic strategies including immunotherapies.

While the cancer field for a long-time focused on how genetic changes lead to tumor formation, the significance of epigenetic control over gene regulation is now being recognized. Notably, pediatric cancers contain only a limited number of mutations, suggesting epigenetic aberrations as important tumor drivers. Epigenetic marks as well as the DNA methylation and histone modification machinery are well conserved in zebrafish, promising that zebrafish cancer models will become important tools to dissect the relevance of epigenetic changes in cancer cells *in vivo* (141).

Finally, with CRISPR/Cas9 genome editing possibilities, personalized genetic zebrafish cancer models harboring patient-specific mutations will be generated. The next couple of years will also reveal the potential of PDXz. Eventually, personal cancer fishes, encompassing GEZMs and PDXzs might be used to characterize individual malignancies and to test compounds in personalized cancer medicine approaches in the not too distant future.

AUTHOR CONTRIBUTIONS

SK, CS, SP, and MD all contributed to writing of this review.

ACKNOWLEDGMENTS

We thank Fikret Rifatbegovic for designing **Figure 1**. We wish to thank Marina Mione and Jennifer Hocking for their critical reading of the manuscript and insightful comments and suggestions. The authors gratefully acknowledge support by the Austrian Research Promotion Agency (FFG).

REFERENCES

1. Streisinger G, Walker C, Dower N, Knauber D, Singer F. Production of clones of homozygous diploid zebra fish (*Brachydanio rerio*). *Nature* (1981) 291:293–6. doi:10.1038/291293a0
2. Engeszer RE, Patterson LB, Rao AA, Parichy DM. Zebrafish in the wild: a review of natural history and new notes from the field. *Zebrafish* (2007) 4:21–40. doi:10.1089/zeb.2006.9997
3. Driever W, Solnica-Krezel L, Schier AF, Neuhauss SC, Malicki J, Stemple DL, et al. A genetic screen for mutations affecting embryogenesis in zebrafish. *Development* (1996) 123:37–46.
4. Haffter P, Granato M, Brand M, Mullins MC, Hammerschmidt M, Kane DA, et al. The identification of genes with unique and essential functions in the development of the zebrafish, *Danio rerio*. *Development* (1996) 123:1–36.
5. Dooley K, Zon LI. Zebrafish: a model system for the study of human disease. *Curr Opin Genet Dev* (2000) 10:252–6. doi:10.1016/S0959-437X(00)00074-5
6. Howe K, Clark MD, Torroja CF, Torrance J, Berthelot C, Muffato M, et al. The zebrafish reference genome sequence and its relationship to the human genome. *Nature* (2013) 496:498–503. doi:10.1038/nature12111
7. Kalev-Zylinska ML, Horsfield JA, Flores MV, Postlethwait JH, Vitas MR, Baas AM, et al. Runx1 is required for zebrafish blood and vessel development and expression of a human RUNX1-CBF2T1 transgene advances a model for studies of leukemogenesis. *Development* (2002) 129:2015–30.
8. Langenau DM, Traver D, Ferrando AA, Kutok JL, Aster JC, Kanki JP, et al. Myc-induced T cell leukemia in transgenic zebrafish. *Science* (2003) 299:887–90. doi:10.1126/science.1080280
9. Langenau DM, Keefe MD, Storer NY, Guyon JR, Kutok JL, Le X, et al. Effects of RAS on the genesis of embryonal rhabdomyosarcoma. *Genes Dev* (2007) 21:1382–95. doi:10.1101/gad.1545007
10. Wellbrock C, Gomez A, Schartl M. Melanoma development and pigment cell transformation in xiphophorus. *Microsc Res Tech* (2002) 58:456–63. doi:10.1002/jemt.10163
11. Langenau DM, Ferrando AA, Traver D, Kutok JL, Hezel JP, Kanki JP, et al. In vivo tracking of T cell development, ablation, and engraftment in transgenic zebrafish. *Proc Natl Acad Sci U S A* (2004) 101:7369–74. doi:10.1073/pnas.0402248101
12. Hall C, Flores MV, Storm T, Crosier K, Crosier P. The zebrafish lysozyme C promoter drives myeloid-specific expression in transgenic fish. *BMC Dev Biol* (2007) 7:42. doi:10.1186/1471-213X-7-42
13. Ellett F, Pase L, Hayman JW, Andrianopoulos A, Lieschke GJ. mpeg1 promoter transgenes direct macrophage-lineage expression in zebrafish. *Blood* (2011) 117:e49–56. doi:10.1182/blood-2010-10-314120
14. Page DM, Wittamer V, Bertrand JY, Lewis KL, Pratt DN, Delgado N, et al. An evolutionarily conserved program of B-cell development and activation in zebrafish. *Blood* (2013) 122:e1–11. doi:10.1182/blood-2012-12-471029
15. Scott EK, Mason L, Arrenberg AB, Ziv L, Gosse NJ, Xiao T, et al. Targeting neural circuitry in zebrafish using GAL4 enhancer trapping. *Nat Methods* (2007) 4:323–6. doi:10.1038/nmeth1033
16. Asakawa K, Suster ML, Mizusawa K, Nagayoshi S, Kotani T, Urasaki A, et al. Genetic dissection of neural circuits by Tol2 transposon-mediated Gal4 gene and enhancer trapping in zebrafish. *Proc Natl Acad Sci U S A* (2008) 105:1255–60. doi:10.1073/pnas.0704963105
17. Distel M, Wullimann MF, Koster RW. Optimized Gal4 genetics for permanent gene expression mapping in zebrafish. *Proc Natl Acad Sci U S A* (2009) 106:13365–70. doi:10.1073/pnas.0903060106
18. Kawakami K, Abe G, Asada T, Asakawa K, Fukuda R, Ito A, et al. zTrap: zebrafish gene trap and enhancer trap database. *BMC Dev Biol* (2010) 10:105. doi:10.1186/1471-213X-10-105
19. Jungke P, Hans S, Brand M. The zebrafish CreZoo: an easy-to-handle database for novel CreER(T2)-driver lines. *Zebrafish* (2013) 10:259–63. doi:10.1089/zeb.2012.0834
20. Blackburn JS, Liu S, Wilder JL, Dobrinski KP, Lobbardi R, Moore FE, et al. Clonal evolution enhances leukemia-propagating cell frequency in T cell acute lymphoblastic leukemia through Akt/mTORC1 pathway activation. *Cancer Cell* (2014) 25:366–78. doi:10.1016/j.ccr.2014.01.032
21. Tang Q, Moore JC, Ignatius MS, Tenente IM, Hayes MN, Garcia EG, et al. Imaging tumour cell heterogeneity following cell transplantation into optically clear immune-deficient zebrafish. *Nat Commun* (2016) 7:10358. doi:10.1038/ncomms10358
22. Moore JC, Langenau DM. Allograft cancer cell transplantation in zebrafish. *Adv Exp Med Biol* (2016) 916:265–87. doi:10.1007/978-3-319-30654-4_12
23. Li Z, Huang X, Zhan H, Zeng Z, Li C, Spitsbergen JM, et al. Inducible and repressable oncogene-addicted hepatocellular carcinoma in Tet-on xmrk transgenic zebrafish. *J Hepatol* (2012) 56:419–25. doi:10.1016/j.jhep.2011.07.025
24. Nguyen AT, Koh V, Spitsbergen JM, Gong Z. Development of a conditional liver tumor model by mifepristone-inducible Cre recombination to control oncogenic kras V12 expression in transgenic zebrafish. *Sci Rep* (2016) 6:19559. doi:10.1038/srep19559
25. Sun L, Nguyen AT, Spitsbergen JM, Gong Z. Myc-induced liver tumors in transgenic zebrafish can regress in tp53 null mutation. *PLoS One* (2015) 10:e0117249. doi:10.1371/journal.pone.0117249
26. Grunwald DJ, Streisinger G. Induction of recessive lethal and specific locus mutations in the zebrafish with ethyl nitrosourea. *Genet Res* (1992) 59:103–16. doi:10.1017/S0016672300030317
27. Moore JL, Rush LM, Breneman C, Mohideen MA, Cheng KC. Zebrafish genomic instability mutants and cancer susceptibility. *Genetics* (2006) 174:585–600. doi:10.1534/genetics.106.059386
28. McGrail M, Hatler JM, Kuang X, Liao HK, Nannapaneni K, Watt KE, et al. Somatic mutagenesis with a Sleeping Beauty transposon system leads to solid tumor formation in zebrafish. *PLoS One* (2011) 6:e18826. doi:10.1371/journal.pone.0018826
29. Shin J, Padmanabhan A, De Groh ED, Lee JS, Haidar S, Dahlberg S, et al. Zebrafish neurofibromatosis type 1 genes have redundant functions in tumorigenesis and embryonic development. *Dis Model Mech* (2012) 5:881–94. doi:10.1242/dmm.009779
30. Solin SL, Shive HR, Woolard KD, Essner JJ, Mcgrail M. Rapid tumor induction in zebrafish by TALEN-mediated somatic inactivation of the retinoblastoma1 tumor suppressor rb1. *Sci Rep* (2015) 5:13745. doi:10.1038/srep13745
31. Ablain J, Zon LI. Tissue-specific gene targeting using CRISPR/Cas9. *Methods Cell Biol* (2016) 135:189–202. doi:10.1016/bs.mcb.2016.03.004
32. Auer TO, Duroure K, De Cian A, Concordet JP, Del Bene F. Highly efficient CRISPR/Cas9-mediated knock-in in zebrafish by homology-independent DNA repair. *Genome Res* (2014) 24:142–53. doi:10.1101/gr.161638.113
33. Irion U, Krauss J, Nusslein-Volhard C. Precise and efficient genome editing in zebrafish using the CRISPR/Cas9 system. *Development* (2014) 141:4827–30. doi:10.1242/dev.115584
34. Hoshijima K, Jurynec MJ, Grunwald DJ. Precise editing of the zebrafish genome made simple and efficient. *Dev Cell* (2016) 36:654–67. doi:10.1016/j.devcel.2016.02.015
35. Mayrhofer M, Mione M. The toolbox for conditional zebrafish cancer models. *Adv Exp Med Biol* (2016) 916:21–59. doi:10.1007/978-3-319-30654-4_2
36. Patton EE, Widlund HR, Kutok JL, Kopani KR, Amatruda JF, Murphey RD, et al. BRAF mutations are sufficient to promote nevi formation and cooperate with p53 in the genesis of melanoma. *Curr Biol* (2005) 15:249–54. doi:10.1016/j.cub.2005.01.031
37. Anelli V, Santoriello C, Distel M, Koster RW, Ciccarelli FD, Mione M. Global repression of cancer gene expression in a zebrafish model of melanoma is linked to epigenetic regulation. *Zebrafish* (2009) 6:417–24. doi:10.1089/zeb.2009.0612
38. Amsterdam A, Lai K, Komisarczuk AZ, Becker TS, Bronson RT, Hopkins N, et al. Zebrafish hagoromo mutants up-regulate fgf8 postembryonically and develop neuroblastoma. *Mol Cancer Res* (2009) 7:841–50. doi:10.1158/1541-7786.MCR-08-0555
39. Lam SH, Wu YL, Vega VB, Miller LD, Spitsbergen J, Tong Y, et al. Conservation of gene expression signatures between zebrafish and human liver tumors and tumor progression. *Nat Biotechnol* (2006) 24:73–5. doi:10.1038/nbt1169
40. Nguyen AT, Emelyanov A, Koh CH, Spitsbergen JM, Lam SH, Mathavan S, et al. A high level of liver-specific expression of oncogenic Kras(V12) drives robust liver tumorigenesis in transgenic zebrafish. *Dis Model Mech* (2011) 4:801–13. doi:10.1242/dmm.007831
41. Santoriello C, Zon LI. Hooked! Modeling human disease in zebrafish. *J Clin Invest* (2012) 122:2337–43. doi:10.1172/JCI60434
42. Shive HR. Zebrafish models for human cancer. *Vet Pathol* (2013) 50:468–82. doi:10.1177/0300985812467471
43. White R, Rose K, Zon L. Zebrafish cancer: the state of the art and the path forward. *Nat Rev Cancer* (2013) 13:624–36. doi:10.1038/nrc3589

44. Yen J, White RM, Stemple DL. Zebrafish models of cancer: progress and future challenges. *Curr Opin Genet Dev* (2014) 24:38–45. doi:10.1016/j.gde.2013.11.003
45. Zhu S, Lee JS, Guo F, Shin J, Perez-Atayde AR, Kutok JL, et al. Activated ALK collaborates with MYCN in neuroblastoma pathogenesis. *Cancer Cell* (2012) 21:362–73. doi:10.1016/j.ccr.2012.02.010
46. He S, Mansour MR, Zimmerman MW, Ki DH, Layden HM, Akahane K, et al. Synergy between loss of NF1 and overexpression of MYCN in neuroblastoma is mediated by the GAP-related domain. *Elife* (2016) 5:e14713. doi:10.7554/eLife.14713
47. Astone M, Pizzi M, Peron M, Domenichini A, Guzzardo V, Tochterle S, et al. A GFP-tagged gross deletion on chromosome 1 causes malignant peripheral nerve sheath tumors and carcinomas in zebrafish. *PLoS One* (2015) 10:e0145178. doi:10.1371/journal.pone.0145178
48. Ki DH, He S, Rodig S, Look AT. Overexpression of PDGFRA cooperates with loss of NF1 and p53 to accelerate the molecular pathogenesis of malignant peripheral nerve sheath tumors. *Oncogene* (2017) 36:1058–68. doi:10.1038/onc.2016.269
49. Lee E, Wei Y, Zou Z, Tucker K, Rakheja D, Levine B, et al. Genetic inhibition of autophagy promotes p53 loss-of-heterozygosity and tumorigenesis. *Oncotarget* (2016) 7:67919–33. doi:10.18632/oncotarget.12084
50. Ju B, Chen W, Orr BA, Spitsbergen JM, Jia S, Eden CJ, et al. Oncogenic KRAS promotes malignant brain tumors in zebrafish. *Mol Cancer* (2015) 14:18. doi:10.1186/s12943-015-0288-2
51. Mayrhofer M, Gourain V, Reischl M, Affaticati P, Jenett A, Joly JS, et al. A novel brain tumour model in zebrafish reveals the role of YAP activation in MAPK- and PI3K-induced malignant growth. *Dis Model Mech* (2017) 10:15–28. doi:10.1242/dmm.026500
52. Modzelewska K, Boer EF, Mosbruger TL, Picard D, Anderson D, Miles RR, et al. MEK inhibitors reverse growth of embryonal brain tumors derived from oligoneural precursor cells. *Cell Rep* (2016) 17:1255–64. doi:10.1016/j.celrep.2016.09.081
53. Ju B, Chen W, Spitsbergen JM, Lu J, Vogel P, Peters JL, et al. Activation of Sonic hedgehog signaling in neural progenitor cells promotes glioma development in the zebrafish optic pathway. *Oncogenesis* (2014) 3:e96. doi:10.1038/oncsis.2014.10
54. Deveau AP, Forrester AM, Coombs AJ, Wagner GS, Grabher C, Chute IC, et al. Epigenetic therapy restores normal hematopoiesis in a zebrafish model of NUP98-HOXA9-induced myeloid disease. *Leukemia* (2015) 29:2086–97. doi:10.1038/leu.2015.126
55. Liu W, Wu M, Huang Z, Lian J, Chen J, Wang T, et al. c-myb hyperactivity leads to myeloid and lymphoid malignancies in zebrafish. *Leukemia* (2017) 31:222–33. doi:10.1038/leu.2016.170
56. Peng X, Dong M, Ma L, Jia XE, Mao J, Jin C, et al. A point mutation of zebrafish c-cbl gene in the ring finger domain produces a phenotype mimicking human myeloproliferative disease. *Leukemia* (2015) 29:2355–65. doi:10.1038/leu.2015.154
57. Balci TB, Prykhozhij SV, Teh EM, Da'as SI, Mcbride E, Liwski R, et al. A transgenic zebrafish model expressing KIT-D816V recapitulates features of aggressive systemic mastocytosis. *Br J Haematol* (2014) 167:48–61. doi:10.1111/bjh.12999
58. Kim IS, Heilmann S, Kansler ER, Zhang Y, Zimmer M, Ratnakumar K, et al. Microenvironment-derived factors driving metastatic plasticity in melanoma. *Nat Commun* (2017) 8:14343. doi:10.1038/ncomms14343
59. Fernandez Del Ama L, Jones M, Walker P, Chapman A, Braun JA, Mohr J, et al. Reprofiling using a zebrafish melanoma model reveals drugs cooperating with targeted therapeutics. *Oncotarget* (2016) 7:40348–61. doi:10.18632/oncotarget.9613
60. Mouti MA, Dee C, Coupland SE, Hurlstone AF. Minimal contribution of ERK1/2-MAPK signalling towards the maintenance of oncogenic GNAQQ209P-driven uveal melanomas in zebrafish. *Oncotarget* (2016) 7:39654–70. doi:10.18632/oncotarget.9207
61. Evason KJ, Francisco MT, Juric V, Balakrishnan S, Lopez Pazmino Mdel P, Gordan JD, et al. Identification of chemical inhibitors of beta-catenin-driven liver tumorigenesis in zebrafish. *PLoS Genet* (2015) 11:e1005305. doi:10.1371/journal.pgen.1005305
62. Zheng W, Li Z, Nguyen AT, Li C, Emelyanov A, Gong Z. Xmrk, kras and myc transgenic zebrafish liver cancer models share molecular signatures with subsets of human hepatocellular carcinoma. *PLoS One* (2014) 9:e91179. doi:10.1371/journal.pone.0091179
63. Li Z, Zheng W, Wang Z, Zeng Z, Zhan H, Li C, et al. A transgenic zebrafish liver tumor model with inducible Myc expression reveals conserved Myc signatures with mammalian liver tumors. *Dis Model Mech* (2013) 6:414–23. doi:10.1242/dmm.010462
64. Verhaak RG, Hoadley KA, Purdom E, Wang V, Qi Y, Wilkerson MD, et al. Integrated genomic analysis identifies clinically relevant subtypes of glioblastoma characterized by abnormalities in PDGFRA, IDH1, EGFR, and NF1. *Cancer Cell* (2010) 17:98–110. doi:10.1016/j.ccr.2009.12.020
65. Berghmans S, Murphey RD, Wienholds E, Neuberg D, Kutok JL, Fletcher CD, et al. tp53 mutant zebrafish develop malignant peripheral nerve sheath tumors. *Proc Natl Acad Sci U S A* (2005) 102:407–12. doi:10.1073/pnas.0406252102
66. Kansler ER, Verma A, Langdon EM, Simon-Vermot T, Yin A, Lee W, et al. Melanoma genome evolution across species. *BMC Genomics* (2017) 18:136. doi:10.1186/s12864-017-3518-8
67. Dovey M, White RM, Zon LI. Oncogenic NRAS cooperates with p53 loss to generate melanoma in zebrafish. *Zebrafish* (2009) 6:397–404. doi:10.1089/zeb.2009.0606
68. Santoriello C, Gennaro E, Anelli V, Distel M, Kelly A, Koster RW, et al. Kita driven expression of oncogenic HRAS leads to early onset and highly penetrant melanoma in zebrafish. *PLoS One* (2010) 5:e15170. doi:10.1371/journal.pone.0015170
69. Heilmann S, Ratnakumar K, Langdon EM, Kansler ER, Kim IS, Campbell NR, et al. A quantitative system for studying metastasis using transparent zebrafish. *Cancer Res* (2015) 75:4272–82. doi:10.1158/0008-5472.CAN-14-3319
70. Ansieau S, Morel AP, Hinkal G, Bastid J, Puisieux A. TWISTing an embryonic transcription factor into an oncoprotein. *Oncogene* (2010) 29:3173–84. doi:10.1038/onc.2010.92
71. Kaufman CK, Mosimann C, Fan ZP, Yang S, Thomas AJ, Ablain J, et al. A zebrafish melanoma model reveals emergence of neural crest identity during melanoma initiation. *Science* (2016) 351:aad2197. doi:10.1126/science.aad2197
72. Hanahan D, Weinberg RA. Hallmarks of cancer: the next generation. *Cell* (2011) 144:646–74. doi:10.1016/j.cell.2011.02.013
73. Feng Y, Santoriello C, Mione M, Hurlstone A, Martin P. Live imaging of innate immune cell sensing of transformed cells in zebrafish larvae: parallels between tumor initiation and wound inflammation. *PLoS Biol* (2010) 8:e1000562. doi:10.1371/journal.pbio.1000562
74. Feng Y, Renshaw S, Martin P. Live imaging of tumor initiation in zebrafish larvae reveals a trophic role for leukocyte-derived PGE(2). *Curr Biol* (2012) 22:1253–9. doi:10.1016/j.cub.2012.05.010
75. Feng Y, Martin P. Imaging innate immune responses at tumour initiation: new insights from fish and flies. *Nat Rev Cancer* (2015) 15:556–62. doi:10.1038/nrc3979
76. Yan C, Huo X, Wang S, Feng Y, Gong Z. Stimulation of hepatocarcinogenesis by neutrophils upon induction of oncogenic kras expression in transgenic zebrafish. *J Hepatol* (2015) 63:420–8. doi:10.1016/j.jhep.2015.03.024
77. Rao HL, Chen JW, Li M, Xiao YB, Fu J, Zeng YX, et al. Increased intratumoral neutrophil in colorectal carcinomas correlates closely with malignant phenotype and predicts patients' adverse prognosis. *PLoS One* (2012) 7:e30806. doi:10.1371/journal.pone.0030806
78. Wang J, Jia Y, Wang N, Zhang X, Tan B, Zhang G, et al. The clinical significance of tumor-infiltrating neutrophils and neutrophil-to-CD8+ lymphocyte ratio in patients with resectable esophageal squamous cell carcinoma. *J Transl Med* (2014) 12:7. doi:10.1186/1479-5876-12-7
79. Yan C, Yang Q, Gong Z. Tumor-associated neutrophils and macrophages promote gender disparity in hepatocellular carcinoma in zebrafish. *Cancer Res* (2017) 77:1395–407. doi:10.1158/0008-5472.CAN-16-2200
80. Zhao Y, Huang X, Ding TW, Gong Z. Enhanced angiogenesis, hypoxia and neutrophil recruitment during Myc-induced liver tumorigenesis in zebrafish. *Sci Rep* (2016) 6:31952. doi:10.1038/srep31952
81. Valastyan S, Weinberg RA. Tumor metastasis: molecular insights and evolving paradigms. *Cell* (2011) 147:275–92. doi:10.1016/j.cell.2011.09.024
82. Antonio N, Bonnelykke-Behrndtz ML, Ward LC, Collin J, Christensen IJ, Steiniche T, et al. The wound inflammatory response exacerbates growth of pre-neoplastic cells and progression to cancer. *EMBO J* (2015) 34:2219–36. doi:10.15252/embj.201490147

83. Lam SH, Chua HL, Gong Z, Lam TJ, Sin YM. Development and maturation of the immune system in zebrafish, *Danio rerio*: a gene expression profiling, in situ hybridization and immunological study. *Dev Comp Immunol* (2004) 28:9–28. doi:10.1016/S0145-305X(03)00103-4
84. Lee LM, Seftor EA, Bonde G, Cornell RA, Hendrix MJ. The fate of human malignant melanoma cells transplanted into zebrafish embryos: assessment of migration and cell division in the absence of tumor formation. *Dev Dyn* (2005) 233:1560–70. doi:10.1002/dvdy.20471
85. Nicoli S, Presta M. The zebrafish/tumor xenograft angiogenesis assay. *Nat Protoc* (2007) 2:2918–23. doi:10.1038/nprot.2007.412
86. Veinotte CJ, Dellaire G, Berman JN. Hooking the big one: the potential of zebrafish xenotransplantation to reform cancer drug screening in the genomic era. *Dis Model Mech* (2014) 7:745–54. doi:10.1242/dmm.015784
87. Barriuso J, Nagaraju R, Hurlstone A. Zebrafish: a new companion for translational research in oncology. *Clin Cancer Res* (2015) 21:969–75. doi:10.1158/1078-0432.CCR-14-2921
88. Welker AM, Jaros BD, Puduvalli VK, Imitola J, Kaur B, Beattie CE. Standardized orthotopic xenografts in zebrafish reveal glioma cell-line-specific characteristics and tumor cell heterogeneity. *Dis Model Mech* (2016) 9:199–210. doi:10.1242/dmm.022921
89. Yang XJ, Cui W, Gu A, Xu C, Yu SC, Li TT, et al. A novel zebrafish xenotransplantation model for study of glioma stem cell invasion. *PLoS One* (2013) 8:e61801. doi:10.1371/journal.pone.0061801
90. Hou Y, Chu M, Du FF, Lei JY, Chen Y, Zhu RY, et al. Recombinant disintegrin domain of ADAM15 inhibits the proliferation and migration of Bel-7402 cells. *Biochem Biophys Res Commun* (2013) 435:640–5. doi:10.1016/j.bbrc.2013.05.037
91. Moshal KS, Ferri-Lagneau KF, Haider J, Pardhanani P, Leung T. Discriminating different cancer cells using a zebrafish in vivo assay. *Cancers (Basel)* (2011) 3:4102–13. doi:10.3390/cancers3044102
92. Weiss FU, Marques IJ, Woltering JM, Vlecken DH, Aghdassi A, Partecke LI, et al. Retinoic acid receptor antagonists inhibit miR-10a expression and block metastatic behavior of pancreatic cancer. *Gastroenterology* (2009) 137:.e1–7. doi:10.1053/j.gastro.2009.08.065
93. Latifi A, Abubaker K, Castrechini N, Ward AC, Liongue C, Dobill F, et al. Cisplatin treatment of primary and metastatic epithelial ovarian carcinomas generates residual cells with mesenchymal stem cell-like profile. *J Cell Biochem* (2011) 112:2850–64. doi:10.1002/jcb.23199
94. Drabsch Y, He S, Zhang L, Snaar-Jagalska BE, Ten Dijke P. Transforming growth factor-beta signalling controls human breast cancer metastasis in a zebrafish xenograft model. *Breast Cancer Res* (2013) 15:R106. doi:10.1186/bcr3573
95. Ban J, Aryee DN, Fourtouna A, Van Der Ent W, Kauer M, Niedan S, et al. Suppression of deacetylase SIRT1 mediates tumor-suppressive NOTCH response and offers a novel treatment option in metastatic Ewing sarcoma. *Cancer Res* (2014) 74:6578–88. doi:10.1158/0008-5472.CAN-14-1736
96. van der Ent W, Jochemsen AG, Teunisse AF, Krens SF, Szuhai K, Spaink HP, et al. Ewing sarcoma inhibition by disruption of EWSR1-FLI1 transcriptional activity and reactivation of p53. *J Pathol* (2014) 233:415–24. doi:10.1002/path.4378
97. Franzetti GA, Laud-Duval K, Van Der Ent W, Brisac A, Irondelle M, Aubert S, et al. Cell-to-cell heterogeneity of EWSR1-FLI1 activity determines proliferation/migration choices in Ewing sarcoma cells. *Oncogene* (2017) 36:3505–14. doi:10.1038/onc.2016.498
98. Wagner DS, Delk NA, Lukianova-Hleb EY, Hafner JH, Farach-Carson MC, Lapotko DO. The in vivo performance of plasmonic nanobubbles as cell theranostic agents in zebrafish hosting prostate cancer xenografts. *Biomaterials* (2010) 31:7567–74. doi:10.1016/j.biomaterials.2010.06.031
99. Jo DH, Son D, Na Y, Jang M, Choi JH, Kim JH, et al. Orthotopic transplantation of retinoblastoma cells into vitreous cavity of zebrafish for screening of anticancer drugs. *Mol Cancer* (2013) 12:71. doi:10.1186/1476-4598-12-71
100. Zhang B, Shimada Y, Kuroyanagi J, Umemoto N, Nishimura Y, Tanaka T. Quantitative phenotyping-based in vivo chemical screening in a zebrafish model of leukemia stem cell xenotransplantation. *PLoS One* (2014) 9:e85439. doi:10.1371/journal.pone.0085439
101. Nakanishi T, Shibasaki Y, Matsuura Y. T cells in fish. *Biology (Basel)* (2015) 4:640–63. doi:10.3390/biology4040640
102. Marques IJ, Weiss FU, Vlecken DH, Nitsche C, Bakkers J, Lagendijk AK, et al. Metastatic behaviour of primary human tumours in a zebrafish xenotransplantation model. *BMC Cancer* (2009) 9:128. doi:10.1186/1471-2407-9-128
103. Benyumov AO, Hergert P, Herrera J, Peterson M, Henke C, Bitterman PB. A novel zebrafish embryo xenotransplantation model to study primary human fibroblast motility in health and disease. *Zebrafish* (2012) 9:38–43. doi:10.1089/zeb.2011.0705
104. Haldi M, Ton C, Seng WL, Mcgrath P. Human melanoma cells transplanted into zebrafish proliferate, migrate, produce melanin, form masses and stimulate angiogenesis in zebrafish. *Angiogenesis* (2006) 9:139–51. doi:10.1007/s10456-006-9040-2
105. Nicoli S, Ribatti D, Cotelli F, Presta M. Mammalian tumor xenografts induce neovascularization in zebrafish embryos. *Cancer Res* (2007) 67:2927–31. doi:10.1158/0008-5472.CAN-06-4268
106. Teng Y, Xie X, Walker S, White DT, Mumm JS, Cowell JK. Evaluating human cancer cell metastasis in zebrafish. *BMC Cancer* (2013) 13:453. doi:10.1186/1471-2407-13-453
107. Jemal A, Siegel R, Ward E, Murray T, Xu J, Thun MJ. Cancer statistics, 2007. *CA Cancer J Clin* (2007) 57:43–66. doi:10.3322/canjclin.57.1.43
108. Chapman A, Fernandez Del Ama L, Ferguson J, Kamarashev J, Wellbrock C, Hurlstone A. Heterogeneous tumor subpopulations cooperate to drive invasion. *Cell Rep* (2014) 8:688–95. doi:10.1016/j.celrep.2014.06.045
109. Tulotta C, He S, Chen L, Groenewoud A, Van Der Ent W, Meijer AH, et al. Imaging of human cancer cell proliferation, invasion, and micrometastasis in a zebrafish xenogeneic engraftment model. *Methods Mol Biol* (2016) 1451:155–69. doi:10.1007/978-1-4939-3771-4_11
110. Gaudenzi G, Albertelli M, Dicitore A, Wurth R, Gatto F, Barbieri F, et al. Patient-derived xenograft in zebrafish embryos: a new platform for translational research in neuroendocrine tumors. *Endocrine* (2017) 57:214–9. doi:10.1007/s12020-016-1048-9
111. Mercatali L, La Manna F, Groenewoud A, Casadei R, Recine F, Miserocchi G, et al. Development of a patient-derived xenograft (PDX) of breast cancer bone metastasis in a zebrafish model. *Int J Mol Sci* (2016) 17:E1375. doi:10.3390/ijms17081375
112. Cirello V, Gaudenzi G, Grassi ES, Colombo C, Vicentini L, Ferrero S, et al. Tumor and normal thyroid spheroids: from tissues to zebrafish. *Minerva Endocrinol* (2017). doi:10.23736/S0391-1977.17.02610-4
113. White RM, Sessa A, Burke C, Bowman T, Leblanc J, Ceol C, et al. Transparent adult zebrafish as a tool for in vivo transplantation analysis. *Cell Stem Cell* (2008) 2:183–9. doi:10.1016/j.stem.2007.11.002
114. Moore JC, Mulligan TS, Yordán NT, Castranova D, Pham VN, Tang Q, et al. T cell immune deficiency in zap70 mutant zebrafish. *Mol Cell Biol* (2016) 36:2868–76. doi:10.1128/MCB.00281-16
115. Moore JC, Tang Q, Yordan NT, Moore FE, Garcia EG, Lobbardi R, et al. Single-cell imaging of normal and malignant cell engraftment into optically clear prkdc-null SCID zebrafish. *J Exp Med* (2016) 213:2575–89. doi:10.1084/jem.20160378
116. Braunbeck T, Boettcher M, Hollert H, Kosmehl T, Lammer E, Leist E, et al. Towards an alternative for the acute fish LC(50) test in chemical assessment: the fish embryo toxicity test goes multi-species – an update. *ALTEX* (2005) 22:87–102.
117. Peterson RT, Link BA, Dowling JE, Schreiber SL. Small molecule developmental screens reveal the logic and timing of vertebrate development. *Proc Natl Acad Sci U S A* (2000) 97:12965–9. doi:10.1073/pnas.97.24.12965
118. Rennekamp AJ, Peterson RT. 15 years of zebrafish chemical screening. *Curr Opin Chem Biol* (2015) 24:58–70. doi:10.1016/j.cbpa.2014.10.025
119. MacRae CA, Peterson RT. Zebrafish as tools for drug discovery. *Nat Rev Drug Discov* (2015) 14:721–31. doi:10.1038/nrd4627
120. Jimenez L, Wang J, Morrison MA, Whatcott C, Soh KK, Warner S, et al. Phenotypic chemical screening using a zebrafish neural crest EMT reporter identifies retinoic acid as an inhibitor of epithelial morphogenesis. *Dis Model Mech* (2016) 9:389–400. doi:10.1242/dmm.021790
121. Gallardo VE, Liang J, Behra M, Elkahloun A, Villablanca EJ, Russo V, et al. Molecular dissection of the migrating posterior lateral line primordium during early development in zebrafish. *BMC Dev Biol* (2010) 10:120. doi:10.1186/1471-213X-10-120
122. Gallardo VE, Varshney GK, Lee M, Bupp S, Xu L, Shinn P, et al. Phenotype-driven chemical screening in zebrafish for compounds that inhibit collective cell migration identifies multiple pathways potentially involved in metastatic invasion. *Dis Model Mech* (2015) 8:565–76. doi:10.1242/dmm.018689

123. Haas P, Gilmour D. Chemokine signaling mediates self-organizing tissue migration in the zebrafish lateral line. *Dev Cell* (2006) 10:673–80. doi:10.1016/j.devcel.2006.02.019
124. Ridges S, Heaton WL, Joshi D, Choi H, Eiring A, Batchelor L, et al. Zebrafish screen identifies novel compound with selective toxicity against leukemia. *Blood* (2012) 119:5621–31. doi:10.1182/blood-2011-12-398818
125. Le X, Pugach EK, Hettmer S, Storer NY, Liu J, Wills AA, et al. A novel chemical screening strategy in zebrafish identifies common pathways in embryogenesis and rhabdomyosarcoma development. *Development* (2013) 140:2354–64. doi:10.1242/dev.088427
126. Velaithan V, Okuda KS, Ng MF, Samat N, Leong SW, Faudzi SM, et al. Zebrafish phenotypic screen identifies novel Notch antagonists. *Invest New Drugs* (2017) 35:166–79. doi:10.1007/s10637-017-0437-0
127. Williams CH, Hempel JE, Hao J, Frist AY, Williams MM, Fleming JT, et al. An in vivo chemical genetic screen identifies phosphodiesterase 4 as a pharmacological target for hedgehog signaling inhibition. *Cell Rep* (2015) 11:43–50. doi:10.1016/j.celrep.2015.03.001
128. Sengupta R, Sun T, Warrington NM, Rubin JB. Treating brain tumors with PDE4 inhibitors. *Trends Pharmacol Sci* (2011) 32:337–44. doi:10.1016/j.tips.2011.02.015
129. Molina G, Vogt A, Bakan A, Dai W, Queiroz De Oliveira P, Znosko W, et al. Zebrafish chemical screening reveals an inhibitor of Dusp6 that expands cardiac cell lineages. *Nat Chem Biol* (2009) 5:680–7. doi:10.1038/nchembio.190
130. Goldstone JV, Mcarthur AG, Kubota A, Zanette J, Parente T, Jonsson ME, et al. Identification and developmental expression of the full complement of cytochrome P450 genes in zebrafish. *BMC Genomics* (2010) 11:643. doi:10.1186/1471-2164-11-643
131. Li ZH, Alex D, Siu SO, Chu IK, Renn J, Winkler C, et al. Combined in vivo imaging and omics approaches reveal metabolism of icaritin and its glycosides in zebrafish larvae. *Mol Biosyst* (2011) 7:2128–38. doi:10.1039/c1mb00001b
132. Chng HT, Ho HK, Yap CW, Lam SH, Chan EC. An investigation of the bioactivation potential and metabolism profile of zebrafish versus human. *J Biomol Screen* (2012) 17:974–86. doi:10.1177/1087057112447305
133. Kantae V, Krekels EH, Ordas A, Gonzalez O, Van Wijk RC, Harms AC, et al. Pharmacokinetic modeling of paracetamol uptake and clearance in zebrafish larvae: expanding the allometric scale in vertebrates with five orders of magnitude. *Zebrafish* (2016) 13:504–10. doi:10.1089/zeb.2016.1313
134. Milan DJ, Peterson TA, Ruskin JN, Peterson RT, Macrae CA. Drugs that induce repolarization abnormalities cause bradycardia in zebrafish. *Circulation* (2003) 107:1355–8. doi:10.1161/01.CIR.0000061912.88753.87
135. Stachura DL, Reyes JR, Bartunek P, Paw BH, Zon LI, Traver D. Zebrafish kidney stromal cell lines support multilineage hematopoiesis. *Blood* (2009) 114:279–89. doi:10.1182/blood-2009-02-203638
136. Pardo-Martin C, Chang TY, Koo BK, Gilleland CL, Wasserman SC, Yanik MF. High-throughput in vivo vertebrate screening. *Nat Methods* (2010) 7:634–6. doi:10.1038/nmeth.1481
137. Veneman WJ, Stockhammer OW, De Boer L, Zaat SA, Meijer AH, Spaink HP. A zebrafish high throughput screening system used for *Staphylococcus epidermidis* infection marker discovery. *BMC Genomics* (2013) 14:255. doi:10.1186/1471-2164-14-255
138. van der Ent W, Veneman WJ, Groenewoud A, Chen L, Tulotta C, Hogendoorn PC, et al. Automation of technology for cancer research. *Adv Exp Med Biol* (2016) 916:315–32. doi:10.1007/978-3-319-30654-4_14
139. White DT, Eroglu AU, Wang G, Zhang L, Sengupta S, Ding D, et al. ARQiv-HTS, a versatile whole-organism screening platform enabling in vivo drug discovery at high-throughput rates. *Nat Protoc* (2016) 11:2432–53. doi:10.1038/nprot.2016.142
140. Chang TY, Shi P, Steinmeyer JD, Chatnuntawech I, Tillberg P, Love KT, et al. Organ-targeted high-throughput in vivo biologics screen identifies materials for RNA delivery. *Integr Biol (Camb)* (2014) 6:926–34. doi:10.1039/c4ib00150h
141. Chernyavskaya Y, Kent B, Sadler KC. Zebrafish discoveries in cancer epigenetics. *Adv Exp Med Biol* (2016) 916:169–97. doi:10.1007/978-3-319-30654-4_8

Conflict of Interest Statement: The authors declare that the research was conducted in the absence of any commercial or financial relationships that could be construed as a potential conflict of interest.

frontiers in Oncology

REVIEW
published: 20 July 2018
doi: 10.3389/fonc.2018.00268

Transgenic Mouse Models in Cancer Research

*Ursa Lampreht Tratar[1], Simon Horvat[2] and Maja Cemazar[1,3]**

[1] Department of Experimental Oncology, Institute of Oncology Ljubljana, Ljubljana, Slovenia, [2] Biotechnical Faculty, University of Ljubljana, Ljubljana, Slovenia, [3] Faculty of Health Sciences, University of Primorska, Isola, Slovenia

The use of existing mouse models in cancer research is of utmost importance as they aim to explore the casual link between candidate cancer genes and carcinogenesis as well as to provide models to develop and test new therapies. However, faster progress in translating mouse cancer model research into the clinic has been hampered due to the limitations of these models to better reflect the complexities of human tumors. Traditionally, immunocompetent and immunodeficient mice with syngeneic and xenografted tumors transplanted subcutaneously or orthotopically have been used. These models are still being widely employed for many different types of studies, in part due to their widespread availability and low cost. Other types of mouse models used in cancer research comprise transgenic mice in which oncogenes can be constitutively or conditionally expressed and tumor-suppressor genes silenced using conventional methods, such as retroviral infection, microinjection of DNA constructs, and the so-called "gene-targeted transgene" approach. These traditional transgenic models have been very important in studies of carcinogenesis and tumor pathogenesis, as well as in studies evaluating the development of resistance to therapy. Recently, the clustered regularly interspaced short palindromic repeats (CRISPR)-based genome editing approach has revolutionized the field of mouse cancer models and has had a profound and rapid impact on the development of more effective systems to study human cancers. The CRISPR/Cas9-based transgenic models have the capacity to engineer a wide spectrum of mutations found in human cancers and provide solutions to problems that were previously unsolvable. Recently, humanized mouse xenograft models that accept patient-derived xenografts and CD34+ cells were developed to better mimic tumor heterogeneity, the tumor microenvironment, and cross-talk between the tumor and stromal/immune cells. These features make them extremely valuable models for the evaluation of investigational cancer therapies, specifically new immunotherapies. Taken together, improvements in both the CRISPR/Cas9 system producing more valid mouse models and in the humanized mouse xenograft models resembling complex interactions between the tumor and its environment might represent one of the successful pathways to precise individualized cancer therapy, leading to improved cancer patient survival and quality of life.

Keywords: transgenic mice, genetically engineered mouse models, patient-derived xenograft models, humanized mouse models, CRISPR/Cas9, non-germline genetically engineered mouse models

OPEN ACCESS

Edited by:
Michael Breitenbach, University of Salzburg, Austria

Reviewed by:
Martin Holcmann, Medizinische Universität Wien, Austria
Reinhard Ullmann, Universität Ulm, Germany

****Correspondence:***
Maja Cemazar
mcemazar@onko-i.si

Specialty section:
This article was submitted to Molecular and Cellular Oncology, a section of the journal Frontiers in Oncology

Received: *18 April 2018*
Accepted: *29 June 2018*
Published: *20 July 2018*

Citation:
Lampreht Tratar U, Horvat S and Cemazar M (2018) Transgenic Mouse Models in Cancer Research. Front. Oncol. 8:268. doi: 10.3389/fonc.2018.00268

INTRODUCTION

The mouse as a model for human cancer research has proven to be a useful tool due to the relatively similar genomic and physiological characteristics of tumor biology between mice and humans. Mice have several similar anatomical, cellular, and molecular characteristics to humans that are known to have critical properties and functions in cancer. Additionally, the proportion of mouse genes with a human ortholog is 80% (1), thus providing an excellent experimentally tractable model system as a research tool to investigate basic mechanisms of cancer development as well as responses to treatment (2). Although conventional transgenic mouse models have remained a valuable tool to examine the molecular mechanisms of carcinogenesis, a limitation has been a low degree of heterogeneity in mouse tumors in comparison to the very heterogeneous human tumors. Several advances have been made in modeling cancer in mice, and the new models described in this review are now more capable of modeling human cancers with mutations that are controlled spatially and/or temporally. In addition, these models better address tumor heterogeneity and inter-patient variability in the clinical setting (3).

Traditionally, immunocompetent and immunodeficient mice with syngeneic and xenografted tumors transplanted subcutaneously or orthotopically have been used. These models are still widely applied for many different types of studies and are also affordable (4). However, in the early 1980s, new types of mouse models emerged with engineered mutations in their genome that revolutionized cancer research. In 1974, R. Jaenisch and B. Mintz performed an experiment wherein the viral oncogenes from simian virus (SV40) were microinjected into the blastocoel of mouse embryos. Although the resulting mice did not develop tumors, they could detect the viral DNA integrated in the genome of cells of many different tissues. These mice are considered the first transgenic mice (5). Later in the 1980s, the first transgenic mouse cancer models were produced, which were genetically engineered to express dominant oncogenes. With these so-called "oncomice," the predispositions required for the development of cancer, as well as new targets for the development of novel therapeutic approaches, could be investigated. Later, more definitive modifications in the genome were performed with knockout and knock-in mice, and since then several research papers have used the term transgenic mice as a distinct group from knockout and knock-in mice (6). Due to the confusion related to the nomenclature, in 2007, the Federation of European Laboratory Animal Science Associations released guidelines for the production and nomenclature of transgenic rodents. In these guidelines, it is stated that transgenic animals are referred to as those with spontaneous, chemically induced mutations and those with random or gene-targeting DNA recombination events (7). The National Institute of Health, National Cancer Institute (NIH NCI) refers to the term transgenic animals for models in which DNA from the mouse genome or from the genome of another species has been incorporated into each cell of the mouse model genome (8). These mice are now mostly called transgenic mice, but they are also referred to as germline genetically engineered mouse models (GEMM), including knock-in and knockout mouse models (9). Additionally, the mouse genome informatics database (10), the main database resource for the laboratory mouse, lists mutant alleles for each gene in several categories, including "transgenic models" similar to the definition in reference 8 above and "targeted," which encompasses both targeted knockout and knock-in models similar to the definition of GEMM above. In this article, we refer to the term "transgenic" as a general term for all types of genome alterations in the germ or somatic cells and/or *in vitro* and *in vivo* mouse models.

PRODUCTION OF TRANSGENIC MICE

Transgenic mice can be produced in several ways by introducing DNA into the mouse genome (**Figure 1**).

1. By retroviral infection of mouse embryos at different developmental stages. This method is not routinely used for the production of transgenic mice (11), in part due to the silencing of the transgene of viral origin following *de novo* DNA methylation after insertion of the retroviral vector (12). Another limitation is also a relatively small size of the insert that can be carried by the vector, as well as random integration, which can influence the expression of the neighboring genes, resulting in phenotypes that are unrelated to the transgene.
2. By microinjection of DNA constructs or recently by microinjecting endonuclease-based reagents (e.g., Cas9–sgRNA–ssDNA mixture) directly into the pronucleus of fertilized mouse oocytes. First, in the case of injecting DNA constructs, the transgene is randomly integrated in a small percentage of injected oocytes as one or more tandem copies into the mouse genome, and generally all the cells of such offspring possess the transgene (13–15). The method to produce transgenic progeny is relatively quick, but it includes the risk that the DNA may insert into a critical locus that can cause an unexpected, detrimental genetic mutation. Second, the transgene may insert into a locus that is subjected to gene silencing (16). Third, if the DNA construct inserts as multiple tandem copies, it can produce extreme overexpression leading to non-physiological phenotypic effects, but more often such tandem transgene integrations are silenced in subsequent generations. In the case of using a new endonuclease approach, reagents are also microinjected into the fertilized eggs, but here the genetic modification is produced at a targeted site albeit also with some off-target events. More on this novel, CRISPR-Cas9-based method is described below.
3. The third approach is called the "gene-targeted transgene approach." It includes the targeted manipulation of mouse embryonic stem (ES) cells at selected loci by introducing primarily loss-of-function mutations (11). Genetically modified ES cells are then microinjected into the mouse blastocysts and transferred to pseudopregnant recipient mice. The ES cells and donor blastocysts derive from mouse lines with different coat colors, and thus successful incorporation of targeted ES cells into the developing embryo of donor blastocyst results in chimeric offspring exhibiting variegated coat color. Chimeric offspring are further mated with wild-type mice to test for

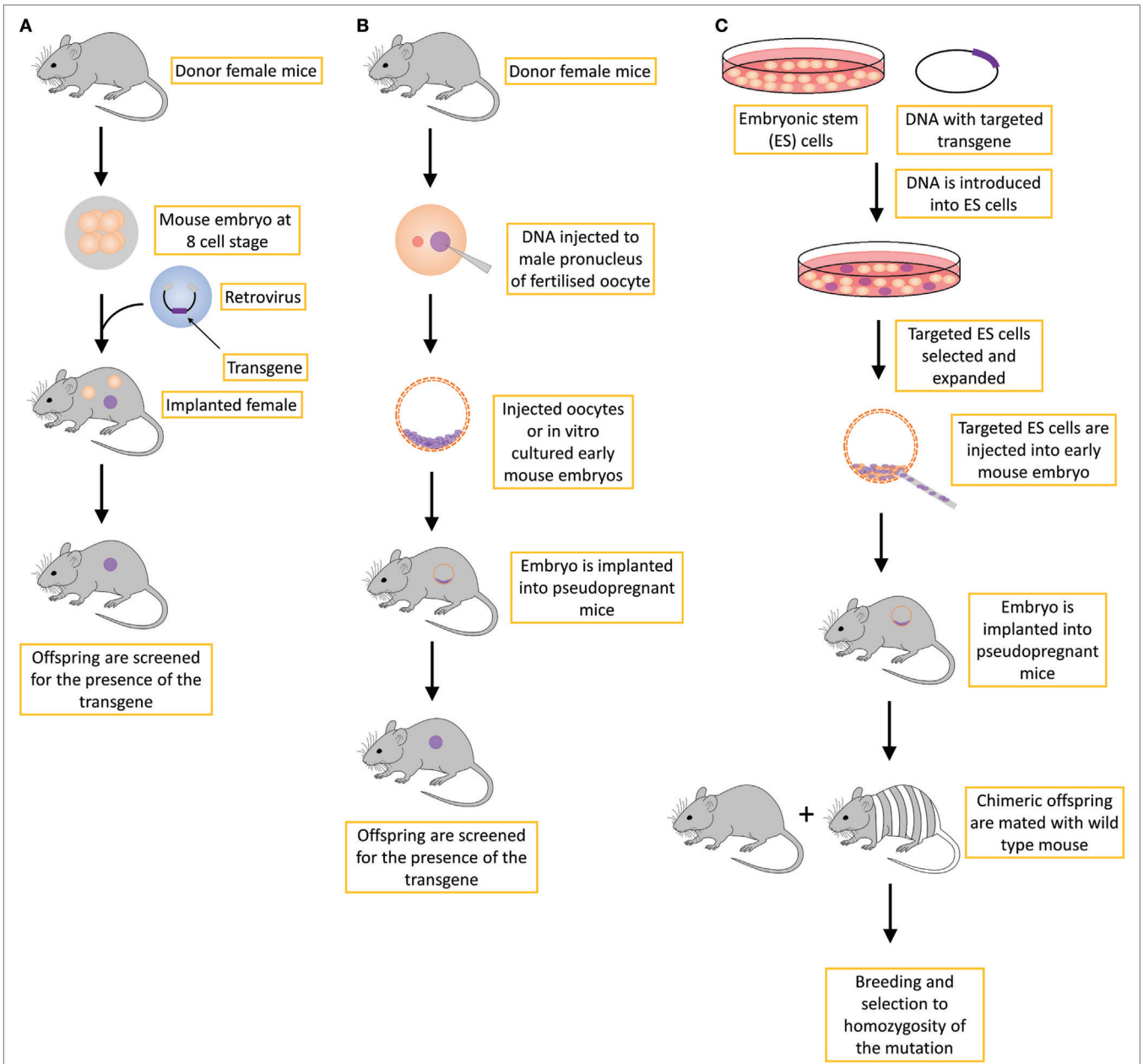

FIGURE 1 | Different strategies for creating transgenic mice include the **(A)** retroviral approach, which is not routinely used; **(B)** standard transgene approach, in which the DNA is inserted into the genome in an unspecific manner; and **(C)** gene-targeted transgene approach, which is an approach that is routinely used to create conventional knockout transgenic mice, usually with a constitutive loss-of-function mutation.

germline transmission of the transgene. If chimeric mice showing variegated coat color (meaning they are somatic chimeras) are also germline chimeras, then the cross with wild-type mice will result in a certain percent of heterozygous progeny carrying the transgene. Finally, the intercross of such heterozygotes produces homozygous mutant mice at an expected 25% frequency unless the mutation is detrimental to embryo survival and development (11, 17, 18). Various experiments are then carried out on mutant homozygotes to test the functionality of the genetic modification.

TYPES OF TRANSGENIC MICE

The production of transgenic mice described above is time-consuming as it can take several years to establish a mutation in the ES cells and develop and validate a new transgenic mouse model. Nevertheless, traditional transgenic mice are widely used in preclinical research in oncology as well as in other research fields. One of the main drawbacks of using transgenic mice in preclinical research is the long time required to generate new transgenic mouse lines. For example, the production of transgenic mice by

gene targeting (**Figure 1C**) requires very efficient targeting of ES cells, the generation of germline chimeras, at least two generations of crosses to obtain homozygotes, colony expansion of homozygous gene-targeted mice and only then can the characterization of oncological phenotypes be performed. If the gene-targeted mutation is dominant (i.e., heterozygotes express the oncological phenotype), the procedure is one generation shorter but still long. In all the methods described in **Figure 1**, the process of generating and characterizing transgenic mice takes several years, and in addition to being time- and labor-consuming, it also requires substantial financial support. In addition, one of the shortcoming of traditional transgenic mouse models (**Figures 1A,B**) is that a substantial fraction of mice can exhibit heterogeneity in their phenotypes, including differential tissue or cell type expression or the generation of additional phenotypes that are not related to the transgene due to the site in the genome-integration effects, whereby the transgene affects the expression of neighboring genes or epigenetically alters a larger region in *cis*. This additional variability in phenotypes results in an increased number of mice that are required to generate the transgenic mouse model that is stable (19). However, this phenomenon is not in line with the 3R principles, especially the principles "reduce" and "refine" (20). For all these reasons, new ways of generating transgenic mouse models have emerged, not only with alternative ways of modifying DNA that will be discussed later but also with the use of non-germline genetically engineered mouse models (nGEMM) that do not carry DNA modifications in germline cells but only in some somatic cells. In addition, classical transgenic mouse models can be improved by inducible or conditional transgenesis techniques.

Roughly, transgenic mice can be divided into two groups considering the loss or gain of function.

Loss of Function

Transgenic mice, in which the gene is depleted or silenced to cause a loss of gene function, are called knockout mice. These mice provide valuable clues about the biological function of a normal gene. In translational cancer research, this represents a powerful tool in assessing the potential validity of targeted therapy because the targets can be precisely inactivated in the setting of a developing or developed tumor. In addition, studies using knockout mice are important to elucidate the cause and effect relationship in cancer development. Such studies with knockout mice can be applied for the assessment of many gene classes, including oncogenes, tumor-suppressor genes, and metabolic ("housekeeping") genes (3). The loss-of-function models can also include dominant-negative transgenic mouse models that carry specific mutations that disrupt the activity of the wild-type gene either by overexpression or other types of modifications of gene structure. For example, dominant-negative transgenic mice have been used to probe the function of E-cadherin and its causal role in the transition from adenoma to carcinoma (21).

Two types of knockout mouse models are frequently used: constitutive (permanently inactivated target gene expression in every cell of the organism) and conditional (inducible inactivation of gene expression), which can affect a specific target tissue (tissue or cell typespecific) or can occur in a time-controlled manner (temporal) (22).

Constitutive Knockout

A constitutive knockout mouse generated by a procedure described in **Figure 1C** is often referred to as a conventional or whole-body knockout model. It defines a mouse model in which the target gene is permanently inactivated in the whole animal, in every cell of the organism (23). These mouse models can be used to assess the changes in a mouse's phenotype, such as anatomy, physiology, behavior, and other observable characteristics. In cancer research, knockout mouse models have been invaluable for the identification and validation of novel cancer genes. For example, constitutive knockout models were used to identify the role of the newly discovered gene sushi domain containing 6 [*Susd6,* human synonym; drug-activated gene overexpressed *(DRAGO)*] as a new p53-responsive gene induced after the treatment with drugs that interfere with DNA. The results of that study showed that deletion of both *Drago* alleles in *p53*−/− or *p53*+/− mice caused statistically significantly accelerated tumor development and a shortened lifespan compared with that of *p53*−/− or *p53*+/− mice that bore wild-type *Drago* alleles (24). Nevertheless, the use of constitutive knockouts in cancer research is limited because they do not imitate the sporadic development of a tumor growing from a single cell in an otherwise normal environment (clonal evolution of tumors). Additionally, simple knockouts are frequently intended to lead to a loss of protein function (and lately in non-coding RNA genes), whereas in cancer, a subset of cancer-causing mutations consistently also results in a gain of function (25). Furthermore, one of the major drawbacks of constitutive knockouts is that germline loss of function often leads to embryonic lethality, severe developmental abnormalities or adult sterility, making conclusive determinations about tumor-suppressor genes more difficult (26).

Conditional Knockout

Due to the limitations of the constitutive knockout model, modification of the knockout model emerged to lead the development of conditional knockout models. The conditional knockout model can more efficiently mimic spontaneous carcinogenesis because in humans, tumors evolve in a wild-type environment, and therefore, the timing of gene loss may be a critical factor in disease development (3). Thus, to avoid and/or improve the limitations of the constitutive knockout, conditional models, in which the gene knockout can be spatially and temporally regulated, were developed. The main actors in this technology are bacterial Cre and yeast FLP enzymes, which act as site-specific recombinases to catalyze recombination between specific 34-bp loxP and FRT sites, respectively. When Cre or FLP proteins are expressed, homologous recombination is induced between loxP or FRT sites. These sites flank the gene of interest and are oriented in the same direction, which causes the deletion of the gene of interest after recombination of flanks of genetic sequence. Expression of the recombinase can be controlled temporally or spatially, and therefore, we can control the deletion of the gene of interest in temporal and spatial manners, thus overcoming interferences due to developmental abnormalities and lethality (27).

For spatial control, mice carrying the Cre or FLP recombinase under the control of a tissue-specific or inducible promotor must first be developed, usually *via* the method described in **Figure 1B**. When these mice are crossed with gene-targeted mice carrying the gene of interest flanked by loxP or FRT sites (developed *via* the procedure in **Figure 1C**), the target gene in the progeny can be conditionally inactivated in a specific tissue or cell type or at specific times during development (3). Tissue-specific knockout models can also be produced by viral driven inducible vectors delivered locally or topically by injection to infect the cells, thereby delivering Cre or FLP enzymes to target tissues or cells. This method creates regional knockout of cells within the applied area (28). Both adenovirus and lentivirus vectors can be used (29).

For the temporal control of Cre expression, tetracycline and tamoxifen-inducible systems are mainly used (30). In the case of tetracycline-based system, a transactivator and an effector are used. The tetracycline-controlled transactivator (tTA) protein binds to the tetracycline operator (tetO) that controls the activity of Cre expression to generate conditional knockouts. When adding tetracycline to the animal's drinking water, the ingested drug binds to tTA and inhibits the association with tetO, blocking gene transcription (31). This is called a Tet-off system, wherein gene expression is inhibited in the presence of tetracycline. When using the Tet-on system, reverse tetracycline-controlled transactivator (rtTA) protein binds to tetO only if it is bound to tetracycline. Therefore, the presence of tetracycline in the animal initiates gene expression (32). One of the shortcoming of this system is the leakiness of rtTA, which compromises the desired regulation of transgene expression. The rtTA maintains some affinity for tetO sequences even in the absence of tetracycline, which results in the undesired transcription of target genes (33).

In the tamoxifen-inducible system, the Cre recombinase gene is fused to a mutated ligand-binding domain of the human estrogen receptor (Cre-ER(T)) that is specifically activated by tamoxifen. When active tamoxifen metabolite 4-hydroxytamoxifen is absent, the ER fusion protein is excluded from the nucleus. After binding to tamoxifen, the ER fusion protein is again transported to the nucleus, enabling the binding of Cre recombinase to DNA. Therefore, temporal expression of Cre can be controlled by delivering or withholding tamoxifen to the animals (34). Conditional knockout mouse model have been used in many different studies, including those manipulating genes, such as *K-Ras*, *Myc*, and *p53* (25), as well as in studies evaluating tumor-initiating cells. For example, the development of abnormal differentiated Schwann cells, which serve as neurofibroma tumor-initiating tumor cells, has been shown to result from the conditional loss of *Nf1* in fetal neural crest stem/progenitor cells of the Schwann cell lineage (35). One limitation of the tamoxifen-inducible system is the leakiness of the Cre-ER models, which causes a certain level of nuclear translocation of Cre-ER even in the absence of tamoxifen (36). Such an event can cause an undesired gain or loss of functional mutations (37).

Like any strategy, the production of conditional knockout models also has drawbacks and limitations: the procedure used to develop these models is lengthy and requires additional transgenic Cre or FLP transgenic models, with the possibility of mosaic expression of Cre or FLP-driven transgenes as many Cre lines are prone to both temporal and spatial ectopic expression, genetic background effects, or even eventual silencing of the expression of Cre or FLP-driven transgenes in mice in later generations (38). However, compared with the constitutive knockout, conditional knockout mutagenesis is advantageous because it uses subtler genetic modifications to examine the functional role(s) of gene(s) in a tissue or temporal manner. It also avoids potential embryonic lethality from the constitutive knockout approach, making it possible to study essential genes.

Gain of Function

Gain-of-function studies are often used to study oncogenes in mouse models. Knock-in models of oncogene overexpression can be used to study how the oncogene drives carcinogenesis *in vivo*.

Constitutive Random Insertion Model

The conventional random insertion mouse model can be produced by viral vector-based transfection of early mouse embryos or by pronuclear injection of the transgene directly into fertilized oocytes (**Figures 1A,B**). The transgene is then randomly incorporated into the genome. Although the procedure is very straightforward and relatively simple, the random incorporation into the genome is the main drawback of this model because it can result in an undesirable expression level or spatiotemporal distribution of transgene activity, or even deleterious effects, thus limiting the usefulness of the model. These models have been widely used to study how oncogenes such as *K-ras* drive tumorigenesis *in vivo* (39–42).

Knock-in Permissive Locus Model

To overcome the limitations of the constitutive random insertion model, several new models have been developed to study the gain of function, specifically by inserting a gene of interest into a specific region of the genome. Using homologous recombination, a more predictable and stable gain-of-function model can be obtained. The most commonly used site is the *Rosa26* locus because it does not contain any essential genes and provides stable and predictable expression of the transgene in various cell types (43, 44). *Npm1* transgenic mice can serve as a good example of a mouse model using the *Rosa26* locus and Cre-regulated expression. The *Npm1* mutation, which is the most frequent genetic alteration in acute myeloid leukemia (AML) (45), can be characterized in this knock-in permissive model. With this model, it has been shown that *Npm1* mutations affects megakaryocytic development and mimics some features of human *NPM1*-mutated AML, thus serving as a good model for further investigations of AML (46).

Conditional Knock-In Model

As previously pointed out, the constitutive gene knock-in described in Section "Constitutive Random Insertion Model" can lead to lethality, sterility, and developmental defects. Therefore, similar to the knockout mouse models, spatial and temporal control of the gene has to be regulated to also circumvent these limitations in knock-in models. Conditional knock-in models can be generated using tissue-specific promotors or by inserting a strong translational and transcriptional termination (STOP) sequence flanked by loxP or FRT sites between the promotor sequence and the gene of interest (47). When the STOP sequence

is present, transcription of the gene interest is blocked. However, when Cre or FLP recombinase are expressed and present, the STOP cassette is removed, allowing expression of the gene (28). Thus, gene expression is mediated by excision of the STOP cassette and recombinase expression. Therefore, gene expression is spatially, temporally, and inducibly mediated by Cre or FLP systems (48). Occasionally, also depending on the knock-in genome site, the STOP cassettes can be leaky, as observed in the initial *K-ras* G12D models of lung carcinoma, wherein death due to respiratory failure prior to tumor progression occurred (49). Improved STOP cassettes with less leakiness were subsequently developed. Later versions of conditional knock-in mouse model of *LSL-K-ras* G12D were shown to be good models to study the initiation and early stage pulmonary adenocarcinoma, allowing control of the timing, location, and number of tumors (28). Additionally, conditional knock-in mouse models were also used to investigate the role of *Brca1* RING function in tumor suppression and therapeutic response, where it was determined that *Brca1* RING did not affect resistance to therapy (50).

Reporter Knock-In Model

To observe the expression of the targeted gene at the transcriptional or translational level, reporter knock-in mouse models can be used. Genes encoding fluorescence proteins have been widely used as reporters in biomedical research and frequently employed to analyze the transgene activity. In reporter models, transgenes are used for the visualization of proteomic, metabolic, cellular, or genetic events *in vivo*. The most commonly used technique for visualization is fluorescent and bioluminescent optical imaging due to the increased sensitivity, relative inexpensiveness, and less time-consuming and more user-friendly features compared with those of, for example, histological, genetic, or biochemical methods. Furthermore, such models are also in line with the 3R principles in research using animals, incorporating at least two of these principles; reduction (less animals used) and refinement (less harmful methods) (20). Several transgenic mouse lines are available that express reporter genes (51). The most common reporters are green fluorescent protein (GFP) and red fluorescent protein (RFP) (52, 53) for fluorescence and firefly luciferase for bioluminescence (54). The latter can also be used for the visualization of tumor growth *in vivo*. To study tumor cell proliferation *in vivo*, mice expressing firefly luciferase under control of the human *E2F1* gene promotor, which is active during proliferation, were crossed with a mouse cancer model (55).

Recently, in cancer research, detection and imaging of the immune response has become one of the fundamental ways to follow the treatment course in live animals. Because several new treatments aim to modulate the immune response, the recruitment of immune cells to tumors is an important indicator of the effectiveness of anticancer immune therapies. This recruitment can also be used to observe tumor-induced immune suppression. The interactions between cells of the immune system and tumor targets in the context of the tumor microenvironment can be followed by intravital microscopy (56). One of the immune cells that is closely connected to progression of the various types of cancers is the regulatory T cell, the action of which is based on the immunosuppressive function of the immune response (57). For example, Bauer and colleagues used two-photon microscopy to investigate the pro-tumor role of tumor-experienced regulatory T cell interactions with dendritic cells. Transgenic mice expressing enhanced GFP (eGFP) in all T cells and mCherry in antigen-presenting cells were used. Their study showed that regulatory T cell interactions with dendritic cells in tumor-draining lymph nodes caused the death of dendritic cells (58). Intravital microscopy is a valuable tool also for assessing the dynamic changes in the tumor vasculature and following the transcriptional targeting of gene expression in various tissues (59, 60).

NEW MOUSE MODELS FOR CANCER RESEARCH

New mouse models have emerged for research in preclinical oncology, especially within the last decade with the great advancements in molecular biology as well as genomic technology and engineering. One novelty was the production of nGEMM, which showed great promise in producing transgenic mice at a low cost with less time-consuming procedures. Other novelties are alternative DNA modification techniques, which are more efficient for the faster and cheaper generation of new transgenic mice. All the different alternative modifications of DNA can be used to produce new types of transgenic mice or further modify conventional models, as described in **Figure 1**. Furthermore, apart from transgenic mice, new models used in cancer research have emerged, such as humanized mice, which have re-established borders in tumor microenvironment studies. Humanized mice implemented with patient-derived xenografts (PDX) can elucidate the interaction between the human tumor and human immune system as part of the tumor microenvironment in a mouse model.

Non-Germline Genetically Engineered Mouse Models

Non-germline genetically engineered mouse models are characterized as mouse models carrying genetically engineered alleles in somatic cells but not in germline cells (22, 61). A comprehensive review of their advantages and limitations is provided elsewhere (19), and only a brief summary is given herein. The nGEMM are produced by two major approaches: by generating chimeric or transplantation models. Non-germline chimeric mice can be a by-product of traditional knockout technology (**Figure 1C**), presenting chimeric mice that do not carry modified ES cells in the germline lineage (62). Chimeric mouse models for cancer research can also be produced only for the purpose of generating nGEMMs by injecting genetically engineered, cancer predisposed, ES cells into blastocysts from a chosen genetic background to develop cancer-prone chimeric mice in somatic tissues (63). As recipient blastocysts usually have a wild-type genetic background, and not every cell in the body is hence genetically modified, this situation better models carcinogenesis in humans. Large banks of genetically modified mouse ES cells in a large proportion of genes have already been established in genome-wide mutagenesis programs such as European Conditional Knockout Mouse Mutagenesis, North American Conditional Knockout Mouse Mutagenesis, the USA-NIH Knockout Mouse Project, and the

European Mouse Disease Clinic projects, and they are also commercially available (e.g., https://www.jax.org). Hence, ES cells obtained from these resource centers can be immediately used to generate tailored nGEMMs. As carcinogenesis is spatially and temporally restricted, tissues or developmental time specificity can be accomplished by applying induction reagents locally or in a time-restricted manner. One limitation of chimeric nGEMMs is the increased variability related to tumorigenesis between individual chimeric mice and that ES cells can populate different cell lineages and hence different target organs, which can produce heterogeneity between individual mice (49, 64). Additionally, some of the target cell lineages cannot be efficiently or cannot at all be populated by ES cells.

In transplantation models, the transplanted tissue can derive either from genetically engineered donor mice that can have a predisposing cancer mutation or from mouse or human cells that have been previously engineered *ex vivo* (mouse-to-mouse; human-to-mouse models of nGEMM) (19). Transplantation systems have first and mostly commonly been adapted to study hematopoietic carcinogenesis. Here, hematopoietic stem and progenitor cells are derived from bone marrow or fetal liver and transplanted by simple intravenous injection into lethally irradiated recipient mice (65). Irradiation models of high-dose chemotherapy in humans also create a window for successful engraftment of transplanted modified hematopoietic stem and progenitor cells into nGEMMs (66, 67). Taken together, nGEMMs are very potent for their use in cancer research, with great value in testing new therapeutics. One of the greatest advantages compared to traditional GEMM is the faster generation of new transgenic mice and improvements in modeling the tumor microenvironment, which is more similar to the situation in human carcinogenesis.

Alternative DNA Modification Techniques

Fine-tune modeling of mouse cancer models can be performed using several alternative methods that have been developed for faster and more reliable testing of genes for their oncogenic potential. The most commonly used methods are transposon-based insertional mutagenesis, RNA interference (RNAi), and engineered nucleases (68).

Transposon-Based Insertional Mutagenesis

Transposons are DNA sequences with the ability to move from one location of the genome to another. Two groups of transposons are known: retrotransposons and DNA transposons. Retrotransposons, because of their low integration efficiency, the integration of incomplete retrotranscribed elements, and the concomitant induction of chromosomal aberrations, are rarely used for the production of transgenic mice (69). In contrast, DNA transposons have shown great promise in transposon-mediated insertional mutagenesis. Mutagenesis relies on a transposase enzyme, which distinguishes specific DNA sequences and "cuts" the DNA between them. The excised DNA is then reintegrated at another site in the genome (70) (**Figure 2**). Transposon-based insertional mutagenesis can hence be used in genetic screens to identify novel cancer-causing genes, such as oncogenes or tumor-suppressor genes (71). The two most effective transposons are described: Sleeping Beauty and PiggyBac.

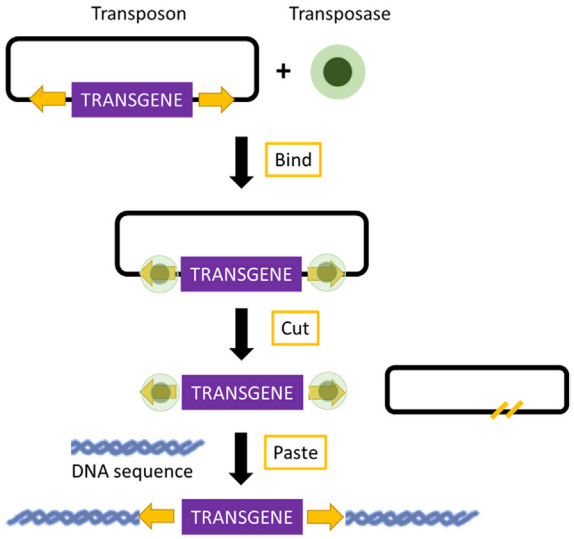

FIGURE 2 | Mechanism of transposon-based insertional mutagenesis. The transposon system is composed of a transposon (targeted sequence of DNA) and an enzyme (transposase). The transposase binds to the appropriate site along the transposon and excises the transposon. It then pastes the transposon at an appropriate location in another DNA sequence, TA site in the case of Sleeping Beauty, and a TTAA site in the case of PiggyBac.

Sleeping Beauty

The important elements of Sleeping Beauty are the transposase, which is an enzyme used for the mobilization of DNA, and the transposon, which is a mobilized sequence of DNA (72). The mechanism of Sleeping Beauty relies on a cut-and-paste mode, and when the transposase excises a transposon, it leaves behind a three-base footprint. Then, the transposon can mobilize to any location in the genome where a TA dinucleotide is present. There are more than 300 million TA sites in the genome. The TA insertion site is duplicated during the process of transposon integration (70, 73). The transposon can carry any sequence of choice, but the transposition efficiency decreases with an increased size of the sequence (70). These sequences can be mutagenic elements, which can be intended to imitate those present in retroviruses. The Sleeping Beauty transposons can be used for the induction of loss-of-function mutations as well as gain-of-function mutations (74). Due to the cut-and-paste mode, there is only a 40–50% possibility that reintegration of the excised transposon will occur into the genome. Additionally, because the number of transposons integrated in the genome decreases over time, a large number of transposable elements are required (75). Sleeping Beauty can be used for the discovery of candidate cancer genes and to search for the drivers of multiple cancer types. Because of these screens, several cancer-promoting mutations candidate have already been found, which can be used in the development of new mouse models that may prove useful for therapeutic testing. To identify candidate drivers of colorectal carcinoma, transposon-based screens are useful because cancer-promoting mutations are caused by transposon insertion events rather than genome-wide instability. Colorectal carcinoma has been modeled using mice carrying the

mutagenic *T2/Onc2 SB* transposons, conditional *Rosa26-lsl-SB11* transposase, and *villin-Cre* to activate transposition specifically in gastrointestinal tract epithelial cells. Using this technique, intraepithelial tumors, adenomas, and adenocarcinomas in the small and large intestines were generated. Moreover, analyses of the transposon insertion site of these tumors identified 77 candidate colorectal carcinoma genes, 60 of which are known to be altered or dysregulated in human colorectal carcinoma (76). Furthermore, Sleeping Beauty can also be used to induce cancer in a tissue of interest by combining it with the Cre recombinase inducible system. By employing Cre expression under the control of an albumin enhancer or promotor sequence, which is specific for liver, Sleeping Beauty transposition was limited to the liver. This system was used to screen for hepatocellular carcinoma associated genes. New genes potentially involved in carcinogenesis, such as UBE2H, were discovered, and therefore, this modified system was introduced in the search for new possible candidate genes (77).

PiggyBac

PiggyBac transposons are the only efficient alternative to Sleeping Beauty for cancer gene discovery. Compared with Sleeping Beauty, PiggyBac can carry larger cargos (up to several hundred kilobases). These cargos are inserted with higher transposition activity into mammalian genomes. Additionally, the PiggyBac system requires a TTAA insertion site instead of TA, and after the transposase excises a transposon, it does not leave any footprint, in contrast to Sleeping Beauty. This imprecise excision of PiggyBac can lead to damage at the mobilization site, thereby creating loss or gain-of-function alleles (70, 78). The PiggyBac transposons can also be used to generate transgenic rodents expressing a reporter fluorescent protein in different organs. Recently, transgenic rats carrying either the RFP gene or the eGFP gene were generated by injecting pronuclei with PiggyBac plasmids. Not only did the transgenic rats express the RFP and eGFP gene in many organs, but they also had the capability to transmit the reporter gene to the next generation through integration into the germline lineage (79).

RNA Interference

RNA interference in mice represents an alternative to knockout mice, or, more accurately, a knockdown mouse. Namely, knockdown by RNAi does not generate a completely loss-of-function allele (80). Silencing, or better, downregulating gene expression of a target gene by small interfering RNA (siRNA) has been mainly used to study gene function (81). It was used for silencing estrogen receptor alpha (*ESR1*), where stable knockdown suppressed the proliferation and enhanced apoptosis of breast cancer cells (82), or for silencing transketolase (*TKT*), which affects cell proliferation and migration as well as interactions with other metabolism-associated genes in lung cancer cells (83). However, the knockdown effect of siRNA is only transient due to the short half-life of siRNA molecules. To achieve a more sustained gene-silencing effect, plasmids encoding short hairpin RNAs (shRNA) can be used. RNAi by shRNAs permits reversible silencing of gene expression without altering the genome. To increase the expression of the shRNA, the targeting vector of interest can be inserted into the *Rosa26* locus by the recombination of a site-specific recombinase in ES cells (developed using a technique described in **Figure 1B**).

Engineered Nucleases

Thus far, three kinds of engineered nucleases have been developed and tested for DNA modulation: zinc-finger nuclease (ZNF), transcription activator-like effector (TALEN) nuclease, and the latest clustered regularly interspaced short palindromic repeat (CRISPR)/-associated (Cas9) system (84).

Briefly, ZNFs and TALENs are produced by combining a DNA-binding domain with a DNA-cleavage domain. These domains can be engineered to act as a site-specific nuclease, cutting DNA at strictly defined sites, which enables zinc-finger or TALEN nucleases to target unique sequences within complex genomes. The targeting efficiency of the ZNF system reaches 68% (85), and ZNF-mediated gene-targeting experiments are a relatively efficient means for generating non-homologous end-joining (NHEJ)-mediated knockout mice (86). Using the TALEN method to produce knockout mice is efficient in 49–77% of cases (87), which can be increased with a greater concentration of TALEN mRNA. This method has been primarily used to increase the efficiency of gene targeting, and compared to ZNFs, TALENs yield higher mutation efficiencies and survival rates.

However, the use of ZNFs and TALENs is limited because construction of the protein domains for each particular genome locus is complex and expensive. Additionally, single nucleotide substitutions or inappropriate interaction between domains can cause inaccurate cleavage of the target DNA (84). Furthermore, the targeting efficiency may be variable and much lower than reported above. However, a major drawback is that simultaneous gene targeting in multiple genes is hindered, preventing studies of oncological phenotypes wherein multiple mutations are required, in analyses of gene family members with redundant functions or in cases of cancers in which gene–gene interactions exist.

CRISPR/Cas9 System

The simplest and the most effective engineered nuclease system to generate transgenic mice is the CRISPR/Cas9 system (88). Compared with ZFNs and TALENs, the CRISPR/Cas9-mediated genome editing is more efficient, and the design, construction of reagents, as well as delivery are easier. Additionally, targeted mutations in multiple genes (so-called multiplex genome engineering) are possible with the CRISPR/Cas9 system. This system consists of a Cas9 nuclease, which can be directed to any genomic locus by an appropriate single guide RNA (sgRNA). Until now, three main types of Cas9 variants have been developed that differ in their mechanisms of action. The first system to be adapted for mouse transgenesis was the wild-type Cas9 protein from the type II CRISPR system of *Streptococcus pyogenes*, which functions *via* an association with the sgRNA with a relatively short recognition sequence (~20 nt) (89). For double-strand cleavage, this system requires the protospacer-adjacent motif (PAM), which is "NGG" or "NAG" for *S. pyogenes* Cas9 at the 3′ end of the target sequence. Recently, new forms of Cas9 enzymes have also been developed that can bind to alternative PAM sites and thereby extend the

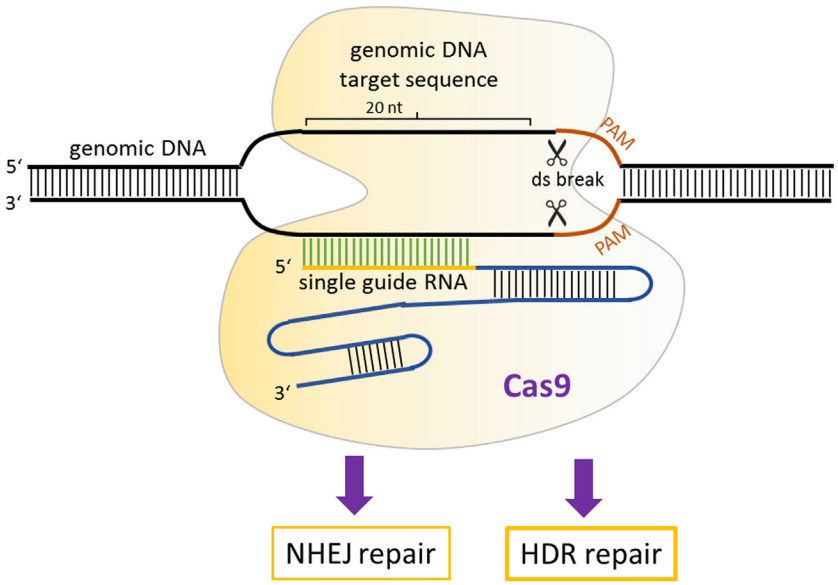

FIGURE 3 | Mechanism of CRISPR/Cas9 gene modulation. A single guide RNA directs Cas9 nuclease to a genomic locus, where it cuts the target sequence in the presence of protospacer-adjacent motif. The resulting double-stranded breaks stimulates DNA repair, which can occur *via* non-homologous end-joining or homology-directed repair-mediated repair.

range of utility of Cas9 (90). Once the double-stranded breaks occur, it can be repaired by NHEJ or by homology-directed repair (HDR) (91) (**Figure 3**). NHEJ-mediated repair frequently results in short insertions or deletions that generate loss-of-function mutations.

The second Cas9 variant was developed (92) to increase the efficiency of HDR, allowing insertions or replacements of specific nucleotides. A mutant form Cas9 protein (Cas9D10A, called nickase) was developed that cleaves only one DNA strand, downregulating the activation of NHEJ. When a homologous repair DNA template with a specific mutation or sequence to be introduced is provided in the mixture of the sgRNA and Cas9D10A mutation, it can serve as a template to repair the lesion. This activates the high-fidelity HDR pathway and hence offers the possibility to generate allele replacements and other specific modifications in the mouse genome that were essentially impossible with the classic transgenesis methods described in **Figure 1**.

The third Cas9 variant is the so-called "dead" Cas9 or nuclease-deficient Cas9 (dCas9) (93), in which certain mutations were introduced to inactivate the cleavage activity but retain the DNA-binding activity. This variant was developed to be able to target any region of the genome without cleavage and by fusing dCas9 with various activator or repressor domains, to up- or downregulate the transcription of target genes. An additional application of the dCas9 system was developed by Chen and Huang (94). By fusing dCas9 to eGFP, they developed a visualization tool and demonstrated that they could visualize several dynamic processes, such as telomere dynamics during elongation or disruption, subnuclear localization of certain loci, and dynamic behavior during mitosis in living human cells.

Application of the CRISPR/Cas9 System in Oncology

Several successful applications of the CRISPR/Cas9 system in cancer research have been published by using one of the aforementioned three systems or by combining the classic transgenic models described in **Figure 1** with CRISPR/Cas9 to generate germline or nGEMM mouse cancer models (88). Some early successful attempts to develop new *in vivo* cancer models include a new pancreatic cancer model combining viral vector delivery and CRISPR/Cas9-mediated somatic genome editing (95), and a lung cancer knock-in model (96). The latter was developed by combining a Cre-dependent Cas9 mouse model with sgRNA delivery, which generated loss-of-function mutations in *p53* and *Lkb1*, as well as nucleotide replacement leading to an oncogenic *K-rasG12D* mutation that causes lung adenocarcinoma. A conditional liver-specific mutation in cancer genes was developed by Xue et al. (97), whereas the development of novel brain tumor mouse models was reported by Zuckermann et al. (98). An important step forward in new models in cancer research was demonstrated by Maddalo et al. (99), who used CRISPR/Cas9-mediated *in vivo* somatic genome editing to engineer chromosomal rearrangements. This class of mutations plays an important role in carcinogenesis, but it is very difficult, if not impossible, to develop using classical transgenesis approaches (**Figure 1**). Authors have used viral-mediated delivery of the *Eml4–Alk* fusion gene by the CRISPR/Cas9 system to somatic cells of adult animals, which models an inversion on chromosome 2: inv(2)(p21p23) that occurs in humans. Expression of the *Eml4–Alk* fusion gene in this model results in pathological and molecular characteristics of typical ALK + human non-small cell lung cancers (NSCLC). Moreover, this mouse model responds positively to ALK inhibitors. Similarly,

using a somatic CRISPR/Cas9 approach, Cook et al. (100) demonstrated in an *ex vivo* and *in vivo* study that a chromosomal rearrangement resulting in *Bcan–Ntrk1* fusion creates a potent driver for glioblastoma development.

The adaptability of the CRISPR/Cas9 system to the scientific question and a relatively easy way to scale up the experimental design has already led to high-throughput *in vivo* screens to catalog functional tumor suppressors. One such comprehensive study by Wang et al. (101) mapped functional cancer genome variants of tumor suppressors in the mouse liver of the wild-type, immunocompetent strain. By injecting AAV pools containing a large (278) sgRNA library directed toward known and the most frequently mutated tumor-suppressor genes into Rosa-Cas9-eGFP knock-in mice, they were able to generate a mutational atlas of liver tumors. All the mice that received this AAV-sgRNA of tumor-suppressor sgRNA developed liver cancer and died within 4 months, demonstrating the validity and extremely high efficiency of this screening approach. Therefore, AAV-mediated CRISPR-Cas9 screens provide a powerful high-throughput tool for mapping functional cancer tumor suppressors in various tissues in fully immunocompetent mice.

Studies using wild-type Cas9 or nickase mutation Cas9 variant have thus far been most frequently used in mouse cancer model development. However, application of the dCas9 system in which no genome modifications are produced but an effect on the expression of target genes is observed have also started to emerge in *in vivo* models of cancer. A good example of this type of research has been described in Braun et al. (102), who aimed to examine the effect of the upregulation of *Mgmt* using dCas9 protein fused to a fourfold repeat of the VP16 transcriptional activator (VP64) in combination with sgRNAs targeting upstream regulatory regions (103). This target gene was chosen because it is known to detoxify DNA lesions caused by the chemotherapeutic agent temozolomide. Murine acute B-cell lymphoblastic leukemia cells were first infected with a combination of dCas9-VP64 and sgRNAs and transplanted into wild-type fully immunocompetent C57BL6/J mice. Positive results were obtained, as upregulation of *Mgmt* was achieved, and the mice responded to temozolomide. These findings demonstrated that the dCas9-based system could be successfully used to affect gene expression only and to model oncological genetic modifications during treatment relapse *in vivo*.

Furthermore, the simultaneous injection of Cas9 mRNA and sgRNA into the cytoplasm of zygotes has been shown to efficiently and reliably generate knockout mice with the highest targeting efficiency (67–100%) of all engineered nucleases (84). Beyond the development of novel transgenic mice, CRISPR/Cas9 can also be used to refine existing models of cancer by reengineering ES cell lines from well-known transgenic mice to harbor additional constitutive or conditional mutant alleles of oncogenes and tumor-suppressor genes (104). Therefore, CRISPR/Cas9 represents an efficient method for generating transgenic mice due to its simplicity, cost-effectiveness, high efficiency, and low fetal toxicity even at relatively high doses of Cas9 mRNA and sgRNA (105).

Humanized Mouse Xenograft Models

Patient-derived xenograft (PDX) models have been extensively used in studies of various solid and hematologic malignancies, such as breast cancer, colorectal cancer, pancreatic cancer, chronic lymphocytic leukemia, and large B cell lymphoma (106, 107). PDX models are used for the assessment of human tumor biology, identification of therapeutic targets, and are an important model for preclinical testing of new drugs for various cancers. PDX models are established by the implantation of cancer cells or tissues from patient primary tumors into immunodeficient mice. Several types of standard immunodeficient mice exist, such as athymic nude, SCID, NOD-SCID and recombination-activating gene 2 *(Rag2)* knockout mice (108). However, these mouse models are usually used to establish a xenograft cancer cell line or to grow transplantable tumor xenografts, and they are unable to grow primary cancer cells or tissues. To accomplish this goal, greater immunodeficiency is required, which is provided by the generation of NOD/SCID mice with *IL2rg* mutations (NSG) that are able to engraft almost all types of cancer due to their enhanced immunodeficiency (109). To implant patient-derived tumors into immunodeficient mice, small fragments of tumors, cell suspensions derived from blood or from the digestion of tumors into single-cell suspensions are used. The implantation can be performed heterotopically or orthotopically. Heterotopic implantation, for example, subcutaneously, has advantages over orthotopic implantation due to the simplicity of the method and more convenient measurement of tumor size. Subcutaneous and intravenous PDX models are most widely used in cancer research for solid tumors and leukemias. In contrast, if the main aim of the research is metastases of certain cancer types, than orthotopic models are superior because orthotopic implantation into host tissues can produce metastases via the normal process of cancer progression (110).

Due to recent advances in immunotherapy illuminating the importance of the immune response in tumor progression and treatment, new PDX models are necessary, namely PDX models together with the human immune system, in which the interaction between human cancers and the human immune system can be investigated, as well as potential antitumor immunotherapies (107). Several methods can be used to produce these so-called humanized mouse models. One such model can be produced by the transplantation of total peripheral blood or tumor-infiltrating lymphocytes into immunodeficient mice. However, these methods are very limited in cancer research because they cause severe graft-versus-host disease (111). Therefore, another method has been used to produce humanized mouse models through the transplantation of CD34+ human hematopoietic stem cells (HSCs) or precursor cells isolated from umbilical cord blood, bone marrow and peripheral blood, as shown in **Figure 4**. Transplantation of HSCs gives rise to various lineages of human blood cells in mice (112).

These humanized models can be used to investigate the efficacy and mechanism of cancer immunotherapy, such as programmed cell death protein 1 (PD-1)-targeted immunotherapy. Wang et al. (113) described the development of humanized NSG (huNSG) mice by transplantation of human (h)CD34+ hematopoietic progenitor and stem cells, which led to the development of human hematopoietic and immune systems. Subsequently, they implanted the PDX of NSCLC, sarcoma, bladder cancer, and triple-negative breast cancer into such humanized mice. They

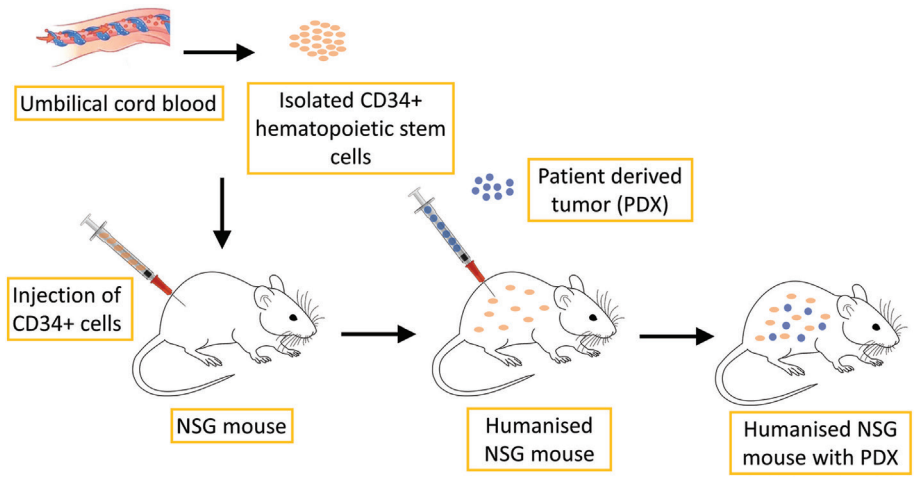

FIGURE 4 | Schematic illustration of humanized PDX mouse model production. CD34+ human hematopoietic stem cells, which are isolated from umbilical cord blood, are transplanted into NSG mice. This process leads to the development of human hematopoietic and immune systems. PDX of various tumors can then be implanted for further research.

discovered that tumor growth curves were similar in huNSG in comparison to non-human immune cell-engrafted NSG mice. Treatment with the checkpoint inhibitor pembrolizumab, an antibody that targets PD-1, caused significant growth inhibition of PDX tumors in huNSG, but not NSG mice. These results suggest that tumor-bearing huNSG mice could represent an important new model for preclinical immunotherapy research. A similar result was obtained by Pan et al, (114), who investigated the antitumor effectiveness of pembrolizumab in human bladder cancer PDX in huNSG mice. They observed that treatment with pembrolizumab inhibited tumor growth and decreased the numbers of CD4+ PD1+ and CD8+ PD1+ cells in peripheral blood and increased the numbers of CD45+ and CD8+ cells in PDXs. One limitation of NSG mice is that despite engraftment with human CD34+ cells, these mice will acquire only partially fully mature human blood cells due to incompatibility between the mouse and human cytokines necessary for blood cell development. Recent models aim to achieve the combination of transgenic or knock-in mouse models expressing human cytokines together with NSG and CD34+ cell transplantation to improve engraftment (115).

Furthermore, recent studies have demonstrated that the microbial ecosystem has a major impact on the local and distant immune response and that the efficacy of immune therapies with checkpoint inhibitors, such as pembrolizumab, can be diminished by the use of antibiotics and enhanced in the presence of specific gut microbes. To fully evaluate the interplay between immunotherapies and the microbiota, new mouse models are emerging, such as specific pathogen-free mice with defined commensal bacteria or preconditioned with antibiotics, or germ-free mice lacking commensal bacteria (116). Commensal bacteria such as *Bifidobacteria* spp. and *Akkermansia muciniphila* can increase the efficiency of anti-programmed cell death protein 1 ligand (PD-L1)-based immunotherapy against epithelial tumors by improving tumor control (117–119). Additionally, a correlation between the use of another immune checkpoint inhibitor, ipilimumab (anti CTLA-4 antibody), and colonization by Bacteroidales was observed. The efficacy of CTLA-4 blockade was improved by the microbiota composition of Bacteroidales, which affects interleukin 12-dependent Th1 immune responses, thus enabling better tumor control in mice while sparing intestinal integrity (120). One limitation of these mouse models with engrafted human microbiota is that these mice are likely unable to support colonization by all commensals of the human GI tract; therefore, it may be sufficient to focus on bacteria that successfully colonize both humans and mice.

CURRENT DIRECTIONS IN TRANSGENIC MOUSE CANCER MODELS

The mouse cancer models discussed in the previous sections clearly show a great impact of these models on the study of basic mechanisms of carcinogenesis, as well as the evaluation or development of therapies that are potentially applicable in human oncology. However, both traditional transgenic models and new opportunities offered by CRISPR/Cas9 provide great promise in even more efficient and translatable mouse models for cancer research in the future. In this section, we discuss selected fields in which we predict major developments in the near future: personalizing humanized mice, replicating specific human mutations in mouse models, analyzing and manipulating the "cancer" epigenome, and prospects in the use of mouse models for gene therapy applications in humans.

Personalizing Humanized Mice

Humanized mice have shown great potential in preclinical oncology studies. To further increase the potential of these models, there is a necessity for the immune system in humanized mice to be compatible with both its host environment and with the implanted tumor tissue to accurately model the patient's immune response during treatment. Tissue incompatibility of humanized

mice that are engrafted with an immune system from one person and implanted with the tumor of another could be the reason for the immune response observed in humanized mice, which is thus not related to the specific treatment applied to the mice. When humanized mice are produced from the engraftment of CD34+ cells, some of the mature xenoreactive T cells are also introduced into these mice. These T cells differentiate within the engrafted bone marrow, mature within the mouse and seem to display some xenoreactive tendencies (108). However, because the transplanted human immune system is weakened, it prevents complete rejection of the xenograft. One possible solution to this problem could be the production of a humanized xenograft model in which the CD34+ cells and implemented tumor tissue are derived from the same donor. Klein et al. produced humanized mice using CD34+ blood cells isolated from biopsied bone marrow of breast, lung, prostate, or esophageal cancer patient, raising the possibility of individualized analyses of antitumor T cell responses (121). Moreover, a new melanoma PDX model has been designed wherein tumor cells and tumor-infiltrating T cells from the same patient are transplanted sequentially in NOG/NSG knockout mice. This model was developed to study the most advanced and most promising current anticancer therapies, immune checkpoint inhibitors and adoptive cell transfer of autologous tumor-infiltrating T cells that have demonstrated complete durable responses in a subpopulation of patients with advanced melanoma (122).

Replicating Specific Human Cancer Mutations in Mouse Models

The conventional mouse models described in **Figure 1** will continue to be used in cancer research both on their own and in combination with other approaches such as transplantation models and humanized mice. However, as alluded previously, all three major traditional transgenesis techniques suffer due to an inability to efficiently develop precise allele replacements or insertions. Initially, CRISPR/Cas9-mediated mutagenesis was highly effective for generating loss-of-function models but not precise allele replacements or gain-of-function mutations, which are most frequent in cancer. However, recent improvements in the CRISPR/Cas9 system have immensely increased the efficiency of HDR [*e.g.*, Gutschner et al. (123); Komor et al. (124)] and hence the ability to engineer precise mutations at any site in the genome. Some successful allele replacements in the cancer research field have also been achieved *in vitro*. For example, Burgess et al. (125) developed the homozygous replacement of the oncogenic *G13D K-RAS* mutation in a human colorectal cancer cell line, which rendered them sensitive to drug treatment. One major novelty of the CRISPR/Cas9 system is the ability to simultaneously generate multiple mutations. One such successful attempt was relayed in a study by Walton et al., who managed to generate triple gene mutations that made cells deficient in *Trp53*, *Brca2*, and *Pten* genes (126). Novel gene fusion mutations are frequently found in human cancers. To model one such fusion in mice linking *Dnajb1–Prkaca* genes into one transcript, Engelholm et al. (127) employed CRISPR/Cas9 method to precisely delete a region in mice that is syngeneic to the human region on chromosome 8 to recreate a *Dnajb1–Prkaca* fusion. They demonstrated that this fusion is the only driver to induce hepatocellular carcinoma, with several features resembling human liver cancer.

Apart from precise mutations encompassing one nucleotide or smaller genomic segments, as described above, CRISPR/Cas9 technology also offers opportunities to generate large chromosomal aberrations. Recently, studies have been published with the aim to improve the efficiency of generating chromosomal rearrangements. One such strategy, named CRISpr MEdiated REarrangement strategy (128), has proven very efficient in producing desired rearrangements from one single experiment. Targeted large deletions (up to 24.4 Mb), duplications, and inversions in rodent models were developed using this approach, which will probably soon be used in cancer research to model chromosomal aberrations involved in tumor biology.

Cancer is also characterized by multiple epigenetic changes that can drive carcinogenesis and confer resistance to treatment. Epigenome editing, especially by the CRISPR/Cas9 system, now allows analyses of precise epigenetic modifications and their effects on cancer development and therapy. One great challenge ahead will be to achieve the reversion of epigenetic modifications, including DNA methylation and other mechanisms (e.g., histone acetylation) at precise sites and ensure that such an intervention is mitotically heritable. Some recent studies in cell lines have demonstrated that selective epigenetic changes (e.g., DNA methylation) can be achieved with the expected outcome on the expression of target genes (129). Apart from DNA methylation, posttranslational modifications of proteins, such as histone acetylation, also present an important epigenetic mechanism of gene expression disruption that can lead to carcinogenesis. In a recent study by Shrimp et al. (130), dCas9 fused to an activator, p300, to control the expression of lysine acetyltransferases (KATs) was applied. This pioneering study demonstrated the potential of the dCas9-p300 system for studying gene expression mechanisms in which acetylation plays a causal role, which is certainly the case in cancer biology. Further developments in this area of research may lead to the development of methods for the spatiotemporal control of acetylation at specific loci, which in turn could lead to therapeutic effects. The ability of the dCas9-effector system to activate or repress endogenous gene expression also provides a new and unique opportunity to further examine cancer-associated *cis* or *trans* acting regulatory non-coding RNAs. Thus, recent developments in CRISPR/Cas9 technology demonstrate great promise for future use and application in transgenic mouse models for studying cancer biology.

Delivery Methods

In transgenic mouse models, the delivery of components to induce mutations or to deliver modified cells *in vivo* still presents a major challenge. A brief review of the delivery methods used in cancer mouse models is provided below, with a focus on the CRISPR/Cas9 system. The development of delivery vehicles for CRISPR/Cas9-mediated transgenesis, especially in the generation of *in vivo* mouse cancer models, has been challenging because of the requirements for the delivery of multiple components in a spatially or temporally controlled manner. Nevertheless, some delivery methods have already been attempted in mouse models

of cancer and vary widely depending on the target cancer type or scientific questions asked.

Intravenous injection of Cas9-edited hematopoietic stem progenitor cells has been successfully applied to model myeloid malignancies in mice (131) and in a Burkitt lymphoma model (132). Electroporation-based delivery, a widely used method for the introduction of different molecules (chemotherapeutic drugs and genetic material) into different types of cells *in vitro* and *in vivo* (133), has also been used in *in vitro* cancer modeling, for example, in modeling alveolar rhabdomyosarcoma in mouse myoblasts (134) as well as *in vivo* for hematopoietic cell-based therapy of malignancies (135). A so-called hydrodynamic tail vein injection of CRISPR/Cas9 components has been applied in a high-throughput multiplex-mutagenesis liver cancer screen (136). Similarly, in a genome-wide screen of lung cancer in mice, subcutaneous injections were used (137). For NSCLC, basic epithelial cell transfection has also been used to target genomic rearrangements (138). To develop transgenic mouse models harboring CRISPR/Cas9-induced mutations in every cell of the body, classical microinjections into fertilized eggs or blastocysts (for modified ES cells) are frequently employed (139). Recently, some successful attempts utilizing the electroporation of pronuclear zygotes have also been reported (140, 141). Transfection with the polyethyleneimine reagent in combination with electroporation has been employed to study brain tumor model (98). Viral vector-based transfections have also been attempted *in vivo*. For example, AAV delivery has been used to study lung carcinogenesis by applying them intra-tracheally *in vivo* (96). Furthermore, lentiviral-based constructs were used in a trial involving a pancreatic ductal adenocarcinoma mouse model (142).

Although the above review of various delivery methods that have already been attempted in transgenic mouse models of cancer demonstrates some degree of initial success, several challenges remain to be solved. One such challenge is to enable the delivery of Cas9 ribonucleoprotein complexes and donor DNA *in vivo* to induce homology-directed DNA repair and repair cancer-causing mutations. A very recent study by Lee et al. (143) used gold nanoparticles conjugated to DNA and complexed with cationic endosomal disruptive polymers, and the results demonstrated correction of the DNA mutation that causes Duchenne muscular dystrophy in mice. Such an approach should be of interest for mouse cancer models, especially inherited forms of driver mutations. Finally, improvements in delivery methods to increase specificity and efficiency and to minimize off-target events and immune response are necessary to ensure the validity of mouse cancer models and to increase their translational potential.

Pitfalls and Limitations

As with every novel technology, there are pitfalls and limitations that must be overcome using the CRISPR/Cas9 system in the future. For example, in modeling small deletions and insertions, current CRISPR/Cas9-based gene editing uses NHEJ-mediated mechanisms that generate small indels, but the sequence variation in the generated allelic series is enormous. While indels usually generate loss-of-function alleles, certain indels can be in-frame or out-of-frame, generating truncated or modified gene products with different phenotypic effects. Apart from the aforementioned loss-of-function models, a greater challenge is still the development of precise cancer-driver mutations *in vivo* by the HDR mechanism. This approach continues to have room for improvements to efficiently generate gain-of-function mutations that are prevalent in carcinogenesis. As mentioned earlier, the CRISPR/Cas9 system allows multiplexing and hence sequential mutagenesis of cancer genes to model loss- or gain-of-function events that are frequently found in human cancer genomes.

The off-target editing activity of the CRISPR/Cas9 system presents a concern and potential limitation. This activity could affect the phenotype of CRISPR/Cas9-generated mouse mutants, such that the phenotype is not related to the on-target event but rather some modification(s) elsewhere in the genome. While some studies in human cells report a relatively high frequency of off-target events (144), early data in mouse embryos suggest that CRISPR/Cas9 off-target events are very rare (89, 145). To examine in detail the extent of off-target events, next-generation whole-genome sequencing has recently been used. Such studies now show that the likelihood of off-target events can be minimized by the careful design of guide RNAs and selection of genomic target sites (146). This result is further supported in a large-scale screen for off-target events in CRISPR/Cas9 transgenic mice performed by Singh et al. (105). For gRNAs selected to have low off-target hit scores, 90 founder mice were screened in 56 of the highest-scoring off-target sites, but no cases of off-target mutagenesis were recorded. To further minimize the off-target activity of Cas9, which will especially be important in eventual human therapy, researchers have attempted to modify the Cas9 protein itself, by using a truncated gRNA or by a method of "paired nicks" (147, 148). Direct use of recombinant Cas9 protein can also lower the off-target editing frequency, most likely because Cas9 protein degrades much faster once it is in the cell than the plasmid encoding Cas9 (149). Although some recent studies report advances in minimizing off-target effects (150), both future preclinical and especially clinical applications will require essentially no detectable genome-wide off-target activity. Developments in the area of high-throughput genome-wide sequencing will certainly aid in allowing the efficient identification of such off-target effects (151) and should be routinely used in future cancer model studies.

Another area that will most likely gain more attention is the combination of conventional cancer models with CRISPR/Cas9 tools to edit genes and simultaneously affect gene expression without any genome editing. Such orthogonal approaches for using the nuclease activity-deficient dCas9-effector system in combination with the editing Cas9-based system should soon be more frequently applied in mouse models of cancer. Namely, Cas9 variants isolated from different bacterial species (152, 153) or mutated forms of Cas9 from the same species that recognize different PAM sites next to the sgRNA-binding site (154) are now available. Such combinatorial approaches can be used to generate more complex mouse models of human cancers, which is certainly a complex disease.

CONCLUSION

Traditional mouse cancer models have already contributed immensely toward illuminating the mechanistic underpinnings

of carcinogenesis and will continue to be used on their own or in combination with more recently developed models. One criticism regarding the use of traditional mouse transgenic models lies in their limitations with respect to the model design and relatively slow translational potential for more rapid and improved benefits for cancer patients.

In recent years, new mouse models of human cancer were developed that may overcome these limitations by accelerating the detection of novel cancer genes, deciphering mechanisms of carcinogenesis, establishing more relevant mouse cancer models, and examining novel approaches to cancer treatments to obtain the maximum value for cancer patients. We envisage that future developments and applications in mouse transgenic cancer modeling will be focused primarily in two areas. One such area of current and future intense research will be concentrated on the use of the CRISPR/Cas9 system as the most versatile and adaptable transgenic technology to date producing transgenic mice that resemble the exact steps of human carcinogenesis. The sequence data for an individual patient tumor, which can now be obtained in a more cost-effective way, can be functionally validated using CRISPR/Cas9 transgenic *in vitro* and *in vivo* mouse models. Thus, all the improvements and results from these novel mouse cancer models will hopefully help to reveal more genotype-specific susceptibilities of particular human cancer types to finally enable more personalized, genotype-based treatments for cancer patients.

Conversely, since increasingly more is known about the importance of the tumor microenvironment, not only on tumor growth but also on the local and systemic response to therapy, there is a more extensive demand for the development of mouse models that more accurately represent the human tumor microenvironment. Humanized mouse models with implanted PDX and human microbiota would bring cancer immunotherapy research one step further, enabling the examination of the complex interaction between the tumor, immune system, and microbiome as one system in the patient. This approach could potentially be used to screen for effective immunotherapeutic agents or combinations, to study mechanisms of resistance to immunotherapies and to study approaches on how to turn immunologically cold tumors into hot ones. Although conceptually diverse, both applications have the final aim to tailor therapeutic regimens based on specific molecular profiles of tumors. The majority of the applications of these two approaches are still at the preclinical stage, but they show great promise to soon become more clinically relevant as they develop toward a more mature stage.

Taken together, forthcoming improvements in mouse cancer models might present one successful pathway to precise individualized cancer therapy, leading to improved cancer patient survival and quality of life.

AUTHOR CONTRIBUTIONS

All authors were involved with the conception and design of the manuscript, manuscript writing, and final approval of the manuscript.

ACKNOWLEDGMENTS

This work was financially supported by the Slovenian Research Agency Programs P3-0003 and P4-0220 and projects J3-8211 and J3-8202. The manuscript was edited for language by "American Journal Experts."

REFERENCES

1. Waterston RH, Lindblad-Toh K, Birney E, Rogers J, Abril JF, Agarwal P, et al. Initial sequencing and comparative analysis of the mouse genome. *Nature* (2002) 420(6915):520–62. doi:10.1038/nature01262
2. Ogilvie LA, Kovachev A, Wierling C, Lange BMH, Lehrach H. Models of models: a translational route for cancer treatment and drug development. *Front Oncol* (2017) 7:219. doi:10.3389/fonc.2017.00219
3. Walrath JC, Hawes JJ, Van Dyke T, Reilly KM. Genetically engineered mouse models in cancer research. *Adv Cancer Res* (2010) 106:113–64. doi:10.1016/S0065-230X(10)06004-5
4. House CD, Hernandez L, Annunziata CM. Recent technological advances in using mouse models to study ovarian cancer. *Front Oncol* (2014) 4:26. doi:10.3389/fonc.2014.00026
5. Smith HW, Muller WJ. Transgenic mouse models-A seminal breakthrough in oncogene research. *Cold Spring Harb Protoc* (2013) 2013:1099–108. doi:10.1101/pdb.top069765
6. Hanahan D, Wagner EF, Palmiter RD. The origins of oncomice: a history of the first transgenic mice genetically engineered to develop cancer. *Genes Dev* (2007) 21:2258–70. doi:10.1101/gad.1583307
7. FELASA Working Group, Rülicke T, Montagutelli X, Pintado B, Thon R, Hedrich HJ. FELASA guidelines for the production and nomenclature of transgenic rodents. *Lab Anim* (2007) 41:301–11. doi:10.1258/002367707781282758
8. *NCI Dictionary of Cancer Terms*. (2018). Available from: https://www.cancer.gov/publications/dictionaries/cancer-terms/def/transgenic-mice (accessed April 3, 2018)
9. Cano DA, Soto-Moreno A, Leal-Cerro A. Genetically engineered mouse models of pituitary tumors. *Front Oncol* (2014) 4:203. doi:10.3389/fonc.2014.00203
10. Smith CL, Blake JA, Kadin JA, Richardson JE, Bult CJ. Mouse genome database (MGD)-2018: knowledgebase for the laboratory mouse. *Nucleic Acids Res* (2018) 46(D1):D836–42. doi:10.1093/nar/gkx1006
11. Kumar TR, Larson M, Wang H, McDermott J, Bronshteyn I. Transgenic mouse technology: principles and methods. *Methods Mol Biol* (2009) 590:335–62. doi:10.1007/978-1-60327-378-7
12. Doyle A, McGarry MP, Lee NA, Lee JJ. The construction of transgenic and gene knockout/knockin mouse models of human disease. *Transgenic Res* (2012) 21:327–49. doi:10.1007/s11248-011-9537-3
13. Brinster RL, Chen HY, Trumbauer M, Senear AW, Warren R, Palmiter RD. Somatic expression of herpes thymidine kinase in mice following injection of a fusion gene into eggs. *Cell* (1981) 27:223–31. doi:10.1016/0092-8674(81)90376-7
14. Gordon J, Ruddle F. Integration and stable germ line transmission of genes injected into mouse pronuclei. *Science* (1981) 214:1244–6. doi:10.1126/science.6272397
15. Costantini F, Lacy E. Introduction of a rabbit β-globin gene into the mouse germ line. *Nature* (1981) 294:92–4. doi:10.1038/294092a0
16. Chicas A, Macino G. Characteristics of post-transcriptional gene silencing. *EMBO Rep* (2001) 2:992–6. doi:10.1093/embo-reports/kve231
17. Brinster RL, Palmiter RD. Induction of foreign genes in animals. *Trends Biochem Sci* (1982) 7:438–40. doi:10.1016/S0968-0004(82)80012-1
18. Zacchigna S, Ruiz de Almodovar C, Carmeliet P. Similarities between angiogenesis and neural development: what small animal models can tell us. *Curr Top Dev Biol* (2007) 80:1–55. doi:10.1016/S0070-2153(07)80001-9
19. Heyer J, Kwong LN, Lowe SW, Chin L. Non-germline genetically engineered mouse models for translational cancer research. *Nat Rev Cancer* (2010) 10:470–80. doi:10.1038/nrc2877

20. Workman P, Aboagye EO, Balkwill F, Balmain A, Bruder G, Chaplin DJ, et al. Guidelines for the welfare and use of animals in cancer research. *Br J Cancer* (2010) 102:1555–77. doi:10.1038/sj.bjc.6605642
21. Peri AK, Wilgenbus P, Dahl U, Semb H, Christofori G. A causal role for E-cadherin in the transition from adenoma to carcinoma. *Nature* (1998) 392(6672):190–3. doi:10.1038/32433
22. Kersten K, de Visser KE, van Miltenburg MH, Jonkers J. Genetically engineered mouse models in oncology research and cancer medicine. *EMBO Mol Med* (2017) 9:137–53. doi:10.15252/emmm.201606857
23. Jiang X-C. Generation of general and tissue-specific gene knockout mouse models. *Methods Mol Biol* (2013) 1027:253–71. doi:10.1007/978-1-60327-369-5_12
24. Polato F, Rusconi P, Zangrossi S, Morelli F, Boeri M, Musi A, et al. DRAGO (KIAA0247), a new DNA damage-responsive, p53-inducible gene that cooperates with p53 as oncosuppressor. *J Natl Cancer Inst* (2014) 106:1–10. doi:10.1093/jnci/dju053
25. Maddison K, Clarke AR. New approaches for modelling cancer mechanisms in the mouse. *J Pathol* (2005) 205:181–93. doi:10.1002/path.1698
26. Eisener-Dorman AF, Lawrence DA, Bolivar VJ. Cautionary insights on knockout mouse studies: the gene or not the gene? *Brain Behav Immun* (2009) 23:318–24. doi:10.1016/j.bbi.2008.09.001
27. Branda CS, Dymecki SM. Talking about a revolution: the impact of site-specific recombinases on genetic analyses in mice. *Dev Cell* (2004) 6:7–28. doi:10.1016/S1534-5807(03)00399-X
28. Jackson EL, Willis N, Mercer K, Bronson RT, Crowley D, Montoya R, et al. Analysis of lung tumor initiation and progression using conditional expression of oncogenic K-ras. *Genes Dev* (2001) 15:3243–8. doi:10.1101/gad.943001
29. DuPage M, Dooley AL, Jacks T. Conditional mouse lung cancer models using adenoviral or lentiviral delivery of Cre recombinase. *Nat Protoc* (2009) 4:1064–72. doi:10.1038/nprot.2009.95
30. Metzger D, Chambon P. Site- and time-specific gene targeting in the mouse. *Methods* (2001) 24:71–80. doi:10.1006/meth.2001.1159
31. Bäckman CM, Zhang YJ, Malik N, Shan L, Hoffer BJ, Westphal H, et al. Generalized tetracycline induced Cre recombinase expression through the ROSA26 locus of recombinant mice. *J Neurosci Methods* (2009) 176:16–23. doi:10.1016/j.jneumeth.2008.08.024
32. Sun Y, Chen X, Xiao D. Tetracycline-inducible expression systems: new strategies and practices in the transgenic mouse modeling. *Acta Biochim Biophys Sin (Shanghai)* (2007) 39(4):235–46. doi:10.1111/j.1745-7270.2007.00258.x
33. Roney IJ, Rudner AD, Couture JF, Kaern M. Improvement of the reverse tetracycline transactivator by single amino acid substitutions that reduce leaky target gene expression to undetectable levels. *Sci Rep* (2016) 6:27697. doi:10.1038/srep27697
34. Zhong ZA, Sun W, Chen H, Zhang H, Lay YAE, Lane NE, et al. Optimizing tamoxifen-inducible Cre/loxp system to reduce tamoxifen effect on bone turnover in long bones of young mice. *Bone* (2015) 81:614–9. doi:10.1016/j.bone.2015.07.034
35. Zheng H, Chang L, Patel N, Yang J, Lowe L, Burns DK, et al. Induction of abnormal proliferation by nonmyelinating Schwann cells triggers neurofibroma formation. *Cancer Cell* (2008) 13:117–28. doi:10.1016/j.ccr.2008.01.002
36. Haldar M, Hedberg ML, Hockin MF, Capecchi MR. A CreER-based random induction strategy for modeling translocation-associated sarcomas in mice. *Cancer Res* (2009) 69(8):3657–64. doi:10.1158/0008-5472.CAN-08-4127
37. Ichise H, Hori A, Shiozawa S, Kondo S, Kanegae Y, Saito I, et al. Establishment of a tamoxifen-inducible Cre-driver mouse strain for widespread and temporal genetic modification in adult mice. *Exp Anim* (2016) 65(3):231–44. doi:10.1538/expanim.15-0126
38. Smith L. Good planning and serendipity: exploiting the Cre/Lox system in the testis. *Reproduction* (2011) 141(2):151–61. doi:10.1530/REP-10-0404
39. Iwakuma T, Lozano G. Crippling p53 activities via knock-in mutations in mouse models. *Oncogene* (2007) 26:2177–84. doi:10.1038/sj.onc.1210278
40. Blackburn AC, Jerry DJ. Knockout and transgenic mice of Trp53: what have we learned about p53 in breast cancer? *Breast Cancer Res* (2002) 4:101–11. doi:10.1186/bcr427
41. Konishi H, Karakas B, Abukhdeir AM, Lauring J, Gustin JP, Garay JP, et al. Knock-in of mutant K-ras in nontumorigenic human epithelial cells as a new model for studying K-ras-mediated transformation. *Cancer Res* (2007) 67:8460–7. doi:10.1158/0008-5472.CAN-07-0108
42. To MD, Wong CE, Karnezis AN, Del Rosario R, Di Lauro R, Balmain A. Kras regulatory elements and exon 4A determine mutation specificity in lung cancer. *Nat Genet* (2008) 40:1240–4. doi:10.1038/ng.211
43. Casola S. Mouse models for miRNA expression: the ROSA26 locus. *Methods Mol Biol* (2010) 667:145–63. doi:10.1007/978-1-60761-811-9_10
44. Hohenstein P, Slight J, Ozdemir D, Burn SF, Berry R, Hastie ND. High-efficiency Rosa26 knock-in vector construction for Cre-regulated overexpression and RNAi. *Pathogenetics* (2008) 1:3. doi:10.1186/1755-8417-1-3
45. Verhaak RGW, Goudswaard CS, Van Putten W, Bijl MA, Sanders MA, Hugens W, et al. Mutations in nucleophosmin (NPM1) in acute myeloid leukemia (AML): association with other gene abnormalities and previously established gene expression signatures and their favorable prognostic significance. *Blood* (2005) 106:3747–54. doi:10.1182/blood-2005-05-2168
46. Sportoletti P, Varasano E, Rossi R, Bereshchenko O, Cecchini D, Gionfriddo I, et al. The human NPM1 mutation A perturbs megakaryopoiesis in a conditional mouse model. *Blood* (2013) 121:3447–58. doi:10.1182/blood-2012-08-449553
47. Lakso M, Sauer B, Mosinger B, Lee EJ, Manning RW, Yu SH, et al. Targeted oncogene activation by site-specific recombination in transgenic mice. *Proc Natl Acad Sci U S A* (1992) 89:6232–6. doi:10.1073/pnas.89.14.6232
48. Dragatsis I, Zeitlin S. A method for the generation of conditional gene repair mutations in mice. *Nucleic Acids Res* (2001) 29:E10. doi:10.1093/nar/29.3.e10
49. Johnson L, Mercer K, Greenbaum D, Bronson RT, Crowley D, Tuveson DA, et al. Somatic activation of the K-ras oncogene causes early onset lung cancer in mice. *Nature* (2001) 410:1111–6. doi:10.1038/35074129
50. Drost R, Bouwman P, Rottenberg S, Boon U, Schut E, Klarenbeek S, et al. BRCA1 RING function is essential for tumor suppression but dispensable for therapy resistance. *Cancer Cell* (2011) 20:797–809. doi:10.1016/j.ccr.2011.11.014
51. Abe T, Fujimori T. Reporter mouse lines for fluorescence imaging. *Dev Growth Differ* (2013) 55:390–405. doi:10.1111/dgd.12062
52. Sattarzadeh A, Saberianfar R, Zipfel WR, Menassa R, Hanson MR. Green to red photoconversion of GFP for protein tracking in vivo. *Sci Rep* (2015) 5:11771. doi:10.1038/srep11771
53. Turbofp F. Enhanced red and far-red fluorescent proteins for in vivo imaging. *Nat Methods* (2009) 6:1–2. doi:10.1038/nmeth.f.249
54. Thorne N, Inglese J, Auld DS. Illuminating insights into firefly luciferase and other bioluminescent reporters used in chemical biology. *Chem Biol* (2010) 17:646–57. doi:10.1016/j.chembiol.2010.05.012
55. Momota H, Holland EC. Bioluminescence technology for imaging cell proliferation. *Curr Opin Biotechnol* (2005) 16:681–6. doi:10.1016/j.copbio.2005.10.012
56. Torcellan T, Stolp J, Chtanova T. In vivo imaging sheds light on immune cell migration and function in cancer. *Front Immunol* (2017) 8:309. doi:10.3389/fimmu.2017.00309
57. Tanaka A, Sakaguchi S. Regulatory T cells in cancer immunotherapy. *Cell Res* (2017) 27:109–18. doi:10.1038/cr.2016.151
58. Bauer CA, Kim EY, Marangoni F, Carrizosa E, Claudio NM, Mempel TR. Dynamic Treg interactions with intratumoral APCs promote local CTL dysfunction. *J Clin Invest* (2014) 124:2425–40. doi:10.1172/JCI66375
59. Markelc B, Sersa G, Cemazar M. Differential mechanisms associated with vascular disrupting action of electrochemotherapy: intravital microscopy on the level of single normal and tumor blood vessels. *PLoS One* (2013) 8:e59557. doi:10.1371/journal.pone.0059557
60. Kamensek U, Sersa G, Cemazar M. Evaluation of p21 promoter for interleukin 12 radiation induced transcriptional targeting in a mouse tumor model. *Mol Cancer* (2013) 12:136. doi:10.1186/1476-4598-12-136
61. Zitvogel L, Pitt JM, Daillère R, Smyth MJ, Kroemer G. Mouse models in oncoimmunology. *Nat Rev Cancer* (2016) 16:759–73. doi:10.1038/nrc.2016.91
62. Huijbers IJ, Krimpenfort P, Berns A, Jonkers J. Rapid validation of cancer genes in chimeras derived from established genetically engineered mouse models. *Bioessays* (2011) 33:701–10. doi:10.1002/bies.201100018
63. Zhou Y, Rideout WM, Zi T, Bressel A, Reddypalli S, Rancourt R, et al. Chimeric mouse tumor models reveal differences in pathway activation between ERBB family– and KRAS-dependent lung adenocarcinomas. *Nat Biotechnol* (2010) 28(1):71–8. doi:10.1038/nbt.1595
64. DuPage M, Cheung AF, Mazumdar C, Winslow MM, Bronson R, Schmidt LM, et al. Endogenous T cell responses to antigens expressed in lung adenocarcinomas

delay malignant tumor progression. *Cancer Cell* (2011) 19(1):72–85. doi:10.1016/j.ccr.2010.11.011
65. Hemann MT, Fridman JS, Zilfou JT, Hernando E, Paddison PJ, Cordon-Cardo C, et al. An epi-allelic series of p53 hypomorphs created by stable RNAi produces distinct tumor phenotypes in vivo. *Nat Genet* (2003) 33:396–400. doi:10.1038/ng1091
66. Zuber J, Radtke I, Pardee TS, Zhao Z, Rappaport AR, Luo W, et al. Mouse models of human AML accurately predict chemotherapy response. *Genes Dev* (2009) 23(7):877–89. doi:10.1101/gad.1771409
67. Lauchle JO, Kim D, Le DT, Akagi K, Crone M, Krisman K, et al. Response and resistance to MEK inhibition in leukaemias initiated by hyperactive Ras. *Nature* (2009) 461(7262):411–4. doi:10.1038/nature08279
68. Bock BC, Stein U, Schmitt CA, Augustin HG. Mouse models of human cancer. *Cancer Res* (2014) 74(17):4671–6. doi:10.1158/0008-5472.CAN-14-1424
69. Goodier JL. Restricting retrotransposons: a review. *Mob DNA* (2016) 7:16. doi:10.1186/s13100-016-0070-z
70. Ranzani M, Annunziato S, Adams DJ, Montini E. Cancer gene discovery: exploiting insertional mutagenesis. *Mol Cancer Res* (2013) 11:1141–58. doi:10.1158/1541-7786.MCR-13-0244
71. Rad R, Rad L, Wang W, Cadinanos J, Vassiliou G, Rice S, et al. PiggyBac transposon mutagenesis: a tool for cancer gene discovery in mice. *Science* (2010) 330:1104–7. doi:10.1126/science.1193004
72. Aronovich EL, McIvor RS, Hackett PB. The Sleeping Beauty transposon system: a non-viral vector for gene therapy. *Hum Mol Genet* (2011) 20:R14–20. doi:10.1093/hmg/ddr140
73. Kebriaei P, Izsvák Z, Narayanavari SA, Singh H, Ivics Z. Gene therapy with the Sleeping Beauty transposon system. *Trends Genet* (2017) 33:852–70. doi:10.1016/j.tig.2017.08.008
74. Ivics Z, Li MA, Mátés L, Boeke JD, Nagy A, Bradley A, et al. Transposon-mediated genome manipulation in vertebrates. *Nat Methods* (2009) 6:415–22. doi:10.1038/nmeth.1332
75. Hou X, Du Y, Deng Y, Wu J, Cao G. Sleeping Beauty transposon system for genetic etiological research and gene therapy of cancers. *Cancer Biol Ther* (2015) 16:8–16. doi:10.4161/15384047.2014.986944
76. Tschida BR, Largaespada DA, Keng VW. Mouse models of cancer: Sleeping Beauty transposons for insertional mutagenesis screens and reverse genetic studies. *Semin Cell Dev Biol* (2014) 27:86–95. doi:10.1016/j.semcdb.2014.01.006
77. Keng VW, Villanueva A, Chiang DY, Dupuy AJ, Ryan BJ, Matise I, et al. A conditional transposon-based insertional mutagenesis screen for genes associated with mouse hepatocellular carcinoma. *Nat Biotechnol* (2009) 27(3):264–74. doi:10.1038/nbt.1526
78. Grabundzija I, Irgang M, Mátés L, Belay E, Matrai J, Gogol-Döring A, et al. Comparative analysis of transposable element vector systems in human cells. *Mol Ther* (2010) 18:1200–9. doi:10.1038/mt.2010.47
79. Li T, Shuai L, Mao J, Wang X, Wang M, Zhang X, et al. Efficient production of fluorescent transgenic rats using the piggyBac transposon. *Sci Rep* (2016) 6:33225. doi:10.1038/srep33225
80. Lee H. Genetically engineered mouse models for drug development and preclinical trials. *Biomol Ther (Seoul)* (2014) 22:267–74. doi:10.4062/biomolther.2014.074
81. Curtis CD, Nardulli AM. Using RNA interference to study protein function. *Methods Mol Biol* (2009) 505:187–204. doi:10.1007/978-1-60327-575-0_11
82. Fu HJ, Jia LT, Bao W, Zhao J, Meng YL, Wang CJ, et al. Stable knockdown of estrogen receptor a by vector-based RNA interference suppresses proliferation and enhances apoptosis in breast cancer cells. *Cancer Biol Ther* (2006) 5:842–7. doi:10.4161/cbt.5.7.2840
83. Lu H, Zhu H. Effect of siRNA-mediated gene silencing of transketolase on A549 lung cancer cells. *Oncol Lett* (2017) 14:5906–12. doi:10.3892/ol.2017.6916
84. Gaj T, Gersbach CA, Barbas CF 3rd. ZFN, TALEN and CRISPR/Cas based methods for genome engineering. *Trends Biotechnol* (2013) 31:397–405. doi:10.1016/j.tibtech.2013.04.004.ZFN
85. Carbery ID, Ji D, Harrington A, Brown V, Weinstein EJ, Liaw L, et al. Targeted genome modification in mice using zinc-finger nucleases. *Genetics* (2010) 186:451–9. doi:10.1534/genetics.110.117002
86. Lee J, Rho J-L, Devkota S, Sung YH, Lee HW. Developing genetically engineered mouse models using engineered nucleases: current status, challenges, and the way forward. *Drug Discov Today Dis Model* (2016) 20:13–20. doi:10.1016/j.ddmod.2017.07.003
87. Sung YH, Baek IJ, Kim DH, Jeon J, Lee J, Lee K, et al. Knockout mice created by TALEN-mediated gene targeting. *Nat Biotechnol* (2013) 31:23–4. doi:10.1038/nbt.2477
88. Yang H, Wang H, Jaenisch R. Generating genetically modified mice using CRISPR/Cas-mediated genome engineering. *Nat Protoc* (2014) 9:1956–68. doi:10.1038/nprot.2014.134
89. Wang H, Yang H, Shivalila CS, Dawlaty MM, Cheng AW, Zhang F, et al. One-step generation of mice carrying mutations in multiple genes by CRISPR/cas-mediated genome engineering. *Cell* (2013) 153:910–8. doi:10.1016/j.cell.2013.04.025
90. Kleinstiver BP, Prew MS, Tsai SQ, Topkar VV, Nguyen NT, Zheng Z, et al. Engineered CRISPR-Cas9 nucleases with altered PAM specificities. *Nature* (2015) 523:481–5. doi:10.1038/nature14592
91. Hsu PD, Lander ES, Zhang F. Development and applications of CRISPR-Cas9 for genome engineering. *Cell* (2014) 157:1262–78. doi:10.1016/j.cell.2014.05.010
92. Cong L, Ran FA, Cox D, Lin S, Barretto R, Habib N, et al. Multiplex genome engineering using CRISPR/Cas systems. *Science* (2013) 339:819–23. doi:10.1126/science.1231143
93. Qi LS, Larson MH, Gilbert LA, Doudna JA, Weissman JS, Arkin AP, et al. Repurposing CRISPR as an RNA-guided platform for sequence-specific control of gene expression. *Cell* (2013) 152:1173–83. doi:10.1016/j.cell.2013.02.022
94. Chen B, Huang B. Imaging genomic elements in living cells using CRISPR/Cas9. *Methods Enzymol* (2014) 546:337–54. doi:10.1016/B978-0-12-801185-0.00016-7
95. Chiou SH, Winters IP, Wang J, Naranjo S, Dudgeon C, Tamburini FB, et al. Pancreatic cancer modeling using retrograde viral vector delivery and in vivo CRISPR/Cas9-mediated somatic genome editing. *Genes Dev* (2015) 29:1576–85. doi:10.1101/gad.264861.115
96. Platt RJ, Chen S, Zhou Y, Yim MJ, Swiech L, Kempton HR, et al. CRISPR-Cas9 knockin mice for genome editing and cancer modeling. *Cell* (2014) 159:440–55. doi:10.1016/j.cell.2014.09.014
97. Xue W, Chen S, Yin H, Tammela T, Papagiannakopoulos T, Joshi NS, et al. CRISPR-mediated direct mutation of cancer genes in the mouse liver. *Nature* (2014) 514:380–4. doi:10.1038/nature13589
98. Zuckermann M, Hovestadt V, Knobbe-Thomsen CB, Zapatka M, Northcott PA, Schramm K, et al. Somatic CRISPR/Cas9-mediated tumour suppressor disruption enables versatile brain tumour modelling. *Nat Commun* (2015) 6:7391. doi:10.1038/ncomms8391
99. Maddalo D, Manchado E, Concepcion CP, Bonetti C, Vidigal JA, Han YC, et al. In vivo engineering of oncogenic chromosomal rearrangements with the CRISPR/Cas9 system. *Nature* (2014) 516:423–8. doi:10.1038/nature13902
100. Cook PJ, Thomas R, Kannan R, De Leon ES, Drilon A, Rosenblum MK, et al. Somatic chromosomal engineering identifies BCAN-NTRK1 as a potent glioma driver and therapeutic target. *Nat Commun* (2017) 8:15987. doi:10.1038/ncomms15987
101. Wang G, Chow RD, Ye L, Guzman CD, Dai X, Dong MB, et al. Mapping a functional cancer genome atlas of tumor suppressors in mouse liver using AAV-CRISPR–mediated direct in vivo screening. *Sci Adv* (2018) 4:eaao5508. doi:10.1126/sciadv.aao5508
102. Braun CJ, Bruno PM, Horlbeck MA, Gilbert LA, Weissman JS, Hemann MT. Versatile in vivo regulation of tumor phenotypes by dCas9-mediated transcriptional perturbation. *Proc Natl Acad Sci U S A* (2016) 113:E3892–900. doi:10.1073/pnas.1600582113
103. Maeder ML, Linder SJ, Cascio VM, Fu Y, Ho QH, Joung JK. CRISPR RNA-guided activation of endogenous human genes. *Nat Methods* (2013) 10:977–9. doi:10.1038/nmeth.2598
104. Dow LE, Lowe SW. Life in the fast lane: mammalian disease models in the genomics era. *Cell* (2012) 148:1099–109. doi:10.1016/j.cell.2012.02.023
105. Singh P, Schimenti JC, Bolcun-Filas E. A mouse geneticist's practical guide to CRISPR applications. *Genetics* (2015) 199:1–15. doi:10.1534/genetics.114.169771
106. Dobrolecki LE, Airhart SD, Alferez DG, Aparicio S, Behbod F, Bentires-Alj M, et al. Patient-derived xenograft (PDX) models in basic and translational

breast cancer research. *Cancer Metastasis Rev* (2016) 35:547–73. doi:10.1007/s10555-016-9653-x
107. Lai Y, Wei X, Lin S, Qin L, Cheng L, Li P. Current status and perspectives of patient-derived xenograft models in cancer research. *J Hematol Oncol* (2017) 10:106. doi:10.1186/s13045-017-0470-7
108. Morton CL, Houghton PJ. Establishment of human tumor xenografts in immunodeficient mice. *Nat Protoc* (2007) 2:247–50. doi:10.1038/nprot.2007.25
109. Shultz LD, Goodwin N, Ishikawa F, Hosur V, Lyons BL, Greiner DL. Human cancer growth and therapy in immunodeficient mouse models. *Cold Spring Harb Protoc* (2014) 2014:694–708. doi:10.1101/pdb.top073585
110. Paez-Ribes M, Man S, Xu P, Kerbel RS. Development of patient derived xenograft models of overt spontaneous breast cancer metastasis: a cautionary note. *PLoS One* (2016) 11:e0158034. doi:10.1371/journal.pone.0158034
111. Ali N, Flutter B, Sanchez Rodriguez R, Sharif-Paghaleh E, Barber LD, Lombardi G, et al. Xenogeneic graft-versus-host-disease in NOD-scid IL-2Rγnull mice display a T-effector memory phenotype. *PLoS One* (2012) 7:e44219. doi:10.1371/journal.pone.0044219
112. Tanner A, Taylor SE, Decottignies W, Berges BK. Humanized mice as a model to study human hematopoietic stem cell transplantation. *Stem Cells Dev* (2014) 23:76–82. doi:10.1089/scd.2013.0265
113. Wang M, Yao L-C, Cheng M, Cai D, Martinek J, Pan C-X, et al. Humanized mice in studying efficacy and mechanisms of PD-1-targeted cancer immunotherapy. *FASEB J* (2018) 32(3):1537–49. doi:10.1096/fj.201700740R
114. Pan C, Shi W, Ma A-H, Zhang H, Lara P, Keck JG, et al. Humanized mice (humice) carrying patient-derived xenograft (PDX) as a platform to develop immunotherapy in bladder cancer (BCa). *J Clin Oncol* (2017) 35:381. doi:10.1200/JCO.2017.35.6_suppl.381
115. Walsh NC, Kenney LL, Jangalwe S, Aryee K-E, Greiner DL, Brehm MA, et al. Humanized mouse models of clinical disease. *Annu Rev Pathol* (2017) 12:187–215. doi:10.1146/annurev-pathol-052016-100332
116. Zitvogel L, Ma Y, Raoult D, Kroemer G, Gajewski TF. The microbiome in cancer immunotherapy: diagnostic tools and therapeutic strategies. *Science* (2018) 359:1366–70. doi:10.1126/science.aar6918
117. Sivan A, Corrales L, Hubert N, Williams JB, Aquino-Michaels K, Earley ZM, et al. Commensal *Bifidobacterium* promotes antitumor immunity and facilitates anti-PD-L1 efficacy. *Science* (2015) 350:1084–9. doi:10.1126/science.aac4255
118. Matson V, Fessler J, Bao R, Chongsuwat T, Zha Y, Alegre ML, et al. The commensal microbiome is associated with anti-PD-1 efficacy in metastatic melanoma patients. *Science* (2018) 359:104–8. doi:10.1126/science.aao3290
119. Routy B, Le Chatelier E, Derosa L, Duong CPM, Alou MT, Daillère R, et al. Gut microbiome influences efficacy of PD-1-based immunotherapy against epithelial tumors. *Science* (2018) 359:91–7. doi:10.1126/science.aan3706
120. Vétizou M, Pitt JM, Daillère R, Lepage P, Waldschmitt N, Flament C, et al. Anticancer immunotherapy by CTLA-4 blockade relies on the gut microbiota. *Science* (2015) 350:1079–84. doi:10.1126/science.aad1329
121. Werner-Klein M, Proske J, Werno C, Schneider K, Hofmann HS, Rack B, et al. Immune humanization of immunodeficient mice using diagnostic bone marrow aspirates from carcinoma patients. *PLoS One* (2014) 9:e97860. doi:10.1371/journal.pone.0097860
122. Jespersen H, Lindberg MF, Donia M, Söderberg EMV, Andersen R, Keller U, et al. Clinical responses to adoptive T-cell transfer can be modeled in an autologous immune-humanized mouse model. *Nat Commun* (2017) 8:707. doi:10.1038/s41467-017-00786-z
123. Gutschner T, Haemmerle M, Genovese G, Draetta GF, Chin L. Post-translational regulation of Cas9 during G1 enhances homology-directed repair. *Cell Rep* (2016) 14:1555–66. doi:10.1016/j.celrep.2016.01.019
124. Komor AC, Kim YB, Packer MS, Zuris JA, Liu DR. Programmable editing of a target base in genomic DNA without double-stranded DNA cleavage. *Nature* (2016) 533:420–4. doi:10.1038/nature17946
125. Burgess MR, Hwang E, Mroue R, Bielski CM, Wandler AM, Huang BJ, et al. KRAS allelic imbalance enhances fitness and modulates MAP kinase dependence in cancer. *Cell* (2017) 168:817–29.e15. doi:10.1016/j.cell.2017.01.020
126. Walton JB, Farquharson M, Mason S, Port J, Kruspig B, Dowson S, et al. CRISPR/Cas9-derived models of ovarian high grade serous carcinoma targeting Brca1, Pten and Nf1, and correlation with platinum sensitivity. *Sci Rep* (2017) 7:1–11. doi:10.1038/s41598-017-17119-1
127. Engelholm LH, Riaz A, Serra D, Dagnaes-Hansen F, Johansen JV, Santoni-Rugiu E, et al. CRISPR/Cas9 engineering of adult mouse liver demonstrates that the Dnajb1–Prkaca gene fusion is sufficient to induce tumors resembling fibrolamellar hepatocellular carcinoma. *Gastroenterology* (2017) 153:1662–73.e10. doi:10.1053/j.gastro.2017.09.008
128. Birling M-C, Schaeffer L, André P, Lindner L, Maréchal D, Ayadi A, et al. Efficient and rapid generation of large genomic variants in rats and mice using CRISMERE. *Sci Rep* (2017) 7:43331. doi:10.1038/srep43331
129. Vojta A, Dobrinic P, Tadic V, Bockor L, Korac P, Julg B, et al. Repurposing the CRISPR-Cas9 system for targeted DNA methylation. *Nucleic Acids Res* (2016) 44:5615–28. doi:10.1093/nar/gkw159
130. Shrimp JH, Grose C, Widmeyer SRT, Thorpe AL, Jadhav A, Meier JL. Chemical control of a CRISPR-Cas9 acetyltransferase. *ACS Chem Biol* (2018) 13:455–60. doi:10.1021/acschembio.7b00883
131. Heckl D, Kowalczyk MS, Yudovich D, Belizaire R, Puram RV, McConkey ME, et al. Generation of mouse models of myeloid malignancy with combinatorial genetic lesions using CRISPR-Cas9 genome editing. *Nat Biotechnol* (2014) 32:941–6. doi:10.1038/nbt.2951
132. Aubrey BJ, Kelly GL, Kueh AJ, Brennan MS, O'Connor L, Milla L, et al. An inducible lentiviral guide RNA platform enables the identification of tumor-essential genes and tumor-promoting mutations invivo. *Cell Rep* (2015) 10:1422–32. doi:10.1016/j.celrep.2015.02.002
133. Savarin M, Kamensek U, Cemazar M, Heller R, Sersa G. Electrotransfer of plasmid DNA radiosensitizes B16F10 tumors through activation of immune response. *Radiol Oncol* (2017) 51:30–9. doi:10.1515/raon-2017-0011
134. Lagutina IV, Valentine V, Picchione F, Harwood F, Valentine MB, Villarejo-Balcells B, et al. Modeling of the human alveolar rhabdomyosarcoma Pax3-foxo1 chromosome translocation in mouse myoblasts using CRISPR-Cas9 nuclease. *PLoS Genet* (2015) 11:e1004951. doi:10.1371/journal.pgen.1004951
135. Mandal PK, Ferreira LMR, Collins R, Meissner TB, Boutwell CL, Friesen M, et al. Efficient ablation of genes in human hematopoietic stem and effector cells using CRISPR/Cas9. *Cell Stem Cell* (2014) 15:643–52. doi:10.1016/j.stem.2014.10.004
136. Weber J, Öllinger R, Friedrich M, Ehmer U, Barenboim M, Steiger K, et al. CRISPR/Cas9 somatic multiplex-mutagenesis for high-throughput functional cancer genomics in mice. *Proc Natl Acad Sci U S A* (2015) 112:13982–7. doi:10.1073/pnas.1512392112
137. Chen S, Sanjana NE, Zheng K, Shalem O, Lee K, Shi X, et al. Genome-wide CRISPR screen in a mouse model of tumor growth and metastasis. *Cell* (2015) 160:1246–60. doi:10.1016/j.cell.2015.02.038
138. Choi PS, Meyerson M. Targeted genomic rearrangements using CRISPR/Cas technology. *Nat Commun* (2014) 5:3728. doi:10.1038/ncomms4728
139. Dow LE, Fisher J, O'Rourke KP, Muley A, Kastenhuber ER, Livshits G, et al. Inducible in vivo genome editing with CRISPR-Cas9. *Nat Biotechnol* (2015) 33:390–4. doi:10.1038/nbt.3155
140. Qin W, Dion SL, Kutny PM, Zhang Y, Cheng AW, Jillette NL, et al. Efficient CRISPR/cas9-mediated genome editing in mice by zygote electroporation of nuclease. *Genetics* (2015) 200:423–30. doi:10.1534/genetics.115.176594
141. Hashimoto M, Takemoto T. Electroporation enables the efficient mRNA delivery into the mouse zygotes and facilitates CRISPR/Cas-based genome editing. *Sci Rep* (2015) 5:1–8. doi:10.1038/srep11315
142. Mazur PK, Herner A, Mello SS, Wirth M, Hausmann S, Sánchez-Rivera FJ, et al. Combined inhibition of BET family proteins and histone deacetylases as a potential epigenetics-based therapy for pancreatic ductal adenocarcinoma. *Nat Med* (2015) 21:1163–71. doi:10.1038/nm.3952
143. Lee K, Conboy M, Park HM, Jiang F, Kim HJ, Dewitt MA, et al. Nanoparticle delivery of Cas9 ribonucleoprotein and donor DNA in vivo induces homology-directed DNA repair. *Nat Biomed Eng* (2017) 1:889–901. doi:10.1038/s41551-017-0137-2
144. Fu Y, Foden JA, Khayter C, Maeder ML, Reyon D, Joung JK, et al. High-frequency off-target mutagenesis induced by CRISPR-Cas nucleases in human cells. *Nat Biotechnol* (2013) 31(9):822–6. doi:10.1038/nbt.2623
145. Yang H, Wang H, Shivalila CS, Cheng AW, Shi L, Jaenisch R. XOne-step generation of mice carrying reporter and conditional alleles by CRISPR/cas-mediated genome engineering. *Cell* (2013) 154(6):1370–9. doi:10.1016/j.cell.2013.08.022
146. Veres A, Gosis BS, Ding Q, Collins R, Ragavendran A, Brand H, et al. Low incidence of off-target mutations in individual CRISPR-Cas9 and TALEN

targeted human stem cell clones detected by whole-genome sequencing. *Cell Stem Cell* (2014) 15(1):27–30. doi:10.1016/j.stem.2014.04.020
147. Ran FA, Hsu PD, Wright J, Agarwala V, Scott DA, Zhang F. Genome engineering using the CRISPR-Cas9 system. *Nat Protoc* (2013) 8(11):2281–308. doi:10.1038/nprot.2013.143
148. Jinek M, East A, Cheng A, Lin S, Ma E, Doudna J. RNA-programmed genome editing in human cells. *Elife* (2013):e00471. doi:10.7554/eLife.00471
149. Ramakrishna S, Kwaku Dad AB, Beloor J, Gopalappa R, Lee SK, Kim H. Gene disruption by cell-penetrating peptide-mediated delivery of Cas9 protein and guide RNA. *Genome Res* (2014) 24(6):1020–7. doi:10.1101/gr.171264.113
150. Yin H, Song CQ, Suresh S, Kwan SY, Wu Q, Walsh S, et al. Partial DNA-guided Cas9 enables genome editing with reduced off-target activity. *Nat Chem Biol* (2018) 14:311–6. doi:10.1038/nchembio.2559
151. Zischewski J, Fischer R, Bortesi L. Detection of on-target and off-target mutations generated by CRISPR/Cas9 and other sequence-specific nucleases. *Biotechnol Adv* (2017) 35:95–104. doi:10.1016/j.biotechadv.2016.12.003
152. Dahlman JE, Abudayyeh OO, Joung J, Gootenberg JS, Zhang F, Konermann S. Orthogonal gene knockout and activation with a catalytically active Cas9 nuclease. *Nat Biotechnol* (2015) 33:1159–61. doi:10.1038/nbt.3390
153. Kiani S, Chavez A, Tuttle M, Hall RN, Chari R, Ter-Ovanesyan D, et al. Cas9 gRNA engineering for genome editing, activation and repression. *Nat Methods* (2015) 12:1051–4. doi:10.1038/nmeth.3580
154. Kleinstiver BP, Prew MS, Tsai SQ, Nguyen NT, Topkar VV, Zheng Z, et al. Broadening the targeting range of *Staphylococcus aureus* CRISPR-Cas9 by modifying PAM recognition. *Nat Biotechnol* (2015) 33:1293–8. doi:10.1038/nbt.3404

Conflict of Interest Statement: The authors declare that the research was conducted in the absence of any commercial or financial relationships that could be construed as a potential conflict of interest.

frontiers in Oncology

REVIEW
published: 23 August 2017
doi: 10.3389/fonc.2017.00190

The Oncopig Cancer Model: An Innovative Large Animal Translational Oncology Platform

*Kyle M. Schachtschneider[1†], Regina M. Schwind[1†], Jordan Newson[2], Nickolas Kinachtchouk[2], Mark Rizko[3], Nasya Mendoza-Elias[3], Paul Grippo[4], Daniel R. Principe[4], Alex Park[3], Nana H. Overgaard[5], Gregers Jungersen[5], Kelly D. Garcia[6], Ajay V. Maker[7], Laurie A. Rund[8], Howard Ozer[4], Ron C. Gaba[1] and Lawrence B. Schook[1,8]**

[1] Department of Radiology, University of Illinois at Chicago, Chicago, IL, United States, [2] Albion College, Albion, MI, United States, [3] College of Medicine, University of Illinois at Chicago, Chicago, IL, United States, [4] Department of Medicine, University of Illinois at Chicago, Chicago, IL, United States, [5] Division of Immunology and Vaccinology, National Veterinary Institute, Technical University of Denmark, Kongens Lyngby, Denmark, [6] Biologic Resources Laboratory, University of Illinois at Chicago, Chicago, IL, United States, [7] Department of Surgical Oncology, University of Illinois at Chicago, Chicago, IL, United States, [8] Department of Animal Sciences, University of Illinois, Urbana, IL, United States

OPEN ACCESS

Edited by:
Michael Breitenbach,
University of Salzburg, Austria

Reviewed by:
Giuseppe Alberto Palumbo,
Policlinico Universitario di Catania, Italy
Reinhard Ullmann,
Institut für Radiobiologie der Bundeswehr in Verbindung mit der Universität Ulm, Germany

***Correspondence:**
Lawrence B. Schook
schook@illinois.edu

†These authors have contributed as co-first authors.

Specialty section:
This article was submitted to Molecular and Cellular Oncology, a section of the journal Frontiers in Oncology

Received: 17 June 2017
Accepted: 10 August 2017
Published: 23 August 2017

Citation:
Schachtschneider KM, Schwind RM, Newson J, Kinachtchouk N, Rizko M, Mendoza-Elias N, Grippo P, Principe DR, Park A, Overgaard NH, Jungersen G, Garcia KD, Maker AV, Rund LA, Ozer H, Gaba RC and Schook LB (2017) The Oncopig Cancer Model: An Innovative Large Animal Translational Oncology Platform. Front. Oncol. 7:190. doi: 10.3389/fonc.2017.00190

Despite an improved understanding of cancer molecular biology, immune landscapes, and advancements in cytotoxic, biologic, and immunologic anti-cancer therapeutics, cancer remains a leading cause of death worldwide. More than 8.2 million deaths were attributed to cancer in 2012, and it is anticipated that cancer incidence will continue to rise, with 19.3 million cases expected by 2025. The development and investigation of new diagnostic modalities and innovative therapeutic tools is critical for reducing the global cancer burden. Toward this end, transitional animal models serve a crucial role in bridging the gap between fundamental diagnostic and therapeutic discoveries and human clinical trials. Such animal models offer insights into all aspects of the basic science-clinical translational cancer research continuum (screening, detection, oncogenesis, tumor biology, immunogenicity, therapeutics, and outcomes). To date, however, cancer research progress has been markedly hampered by lack of a genotypically, anatomically, and physiologically relevant large animal model. Without progressive cancer models, discoveries are hindered and cures are improbable. Herein, we describe a transgenic porcine model—the Oncopig Cancer Model (OCM)—as a next-generation large animal platform for the study of hematologic and solid tumor oncology. With mutations in key tumor suppressor and oncogenes, $TP53^{R167H}$ and $KRAS^{G12D}$, the OCM recapitulates transcriptional hallmarks of human disease while also exhibiting clinically relevant histologic and genotypic tumor phenotypes. Moreover, as obesity rates increase across the global population, cancer patients commonly present clinically with multiple comorbid conditions. Due to the effects of these comorbidities on patient management, therapeutic strategies, and clinical outcomes, an ideal animal model should develop cancer on the background of representative comorbid conditions (tumor macro- and microenvironments). As observed in clinical practice, liver cirrhosis frequently precedes development of primary liver cancer or hepatocellular carcinoma. The OCM has the capacity to develop tumors in combination with such relevant comorbidities. Furthermore,

studies on the tumor microenvironment demonstrate similarities between OCM and human cancer genomic landscapes. This review highlights the potential of this and other large animal platforms as transitional models to bridge the gap between basic research and clinical practice.

Keywords: cancer models, pigs, oncopig, clinical needs, oncology, translational medicine

INTRODUCTION

Cancer is a global epidemic causing more than 8 million annual deaths worldwide. The more than 13 million new cancer diagnoses made each year carry an economic burden of $290B. Cancer is expected to be the second leading cause of death in the United States in 2017. The American Cancer Society (ACS) estimates approximately 1,688,780 new cancer diagnoses will be made and 600,920 Americans will die from cancer. The Agency for Healthcare Research and Quality (AHRQ) estimates that direct medical costs of cancer in the United States in 2014 exceeded $87B. Many of these diagnoses, deaths, and costs could be avoided by shortening the gap between pre-clinical research and regulatory approval for safe and effective therapies. Large animal models that closely recapitulate human cancer and comorbid diseases represent a critical tool in the global cancer-fighting toolbox.

Cancers are deadliest when diagnosed at late stages, a problem that is caused by lack of early detection tests. Cancers of the colon, esophagus, liver and intrahepatic bile ducts, lung and bronchus, non-Hodgkin lymphoma, oral cavity, ovary, pancreas, and uterine cervix are diagnosed at regional or distant stages in more than 50% of cases, resulting in poor survival for many patients. The journey for advancing cancer diagnostics and therapeutics is both lengthy as well as expensive. On average, it takes approximately 8 years, at a cost of $1.2B, per approved antineoplastic agent to complete the required series of clinical trials leading to regulatory approval. This timeline and cost does not include pre-clinical development and testing, thereby establishing that the total time from development to approval exceeds a decade, per agent. Approximately 10% of drugs that begin pre-clinical testing advance into human testing. Roughly 75% of research and development costs are attributed to failures throughout the drug discovery process, leading to the perception that drug discovery and development is one of the most precarious financial undertakings in science and biomedical research. However, with better models that recapitulate human conditions, fewer of these failures may be observed in human clinical trial participants. Better models offer the promise of shortening the timeline for pre-clinical and clinical trials, as well as substantially reducing the cost. Perhaps the most outstanding opportunity is to observe such failures in a large animal model, saving years in patient accrual to human clinical trials and millions of dollars to conduct such trials.

The concerns of bringing new drugs to market are recognized by pharmaceutical companies, physicians, researchers, and perhaps most importantly, patients. In recent years, the U.S. Food and Drug Administration (FDA) has worked diligently to decrease the timelines for approval while increasing the number of new drug approvals. Since 2015, 39 new indications on more than 20 newly approved drugs have come into effect. In considering a new agent for approval, the FDA does not calculate the cost-effectiveness of the agent under review. Many newly approved therapies carry a substantial cost exceeding $60,000–$120,000 annually, high price tags for marginal clinical benefits. Unfortunately, due to the lengthy timeline and expensive costs of developing drugs, many costs are passed on to insurance companies and patients. Utilization of large animal models that best mimic human diseases improves the potential for those agents, which reach human trials to have a better chance for success, eventually leading to fewer development costs for the market to bear.

With specific regard to cancer therapy, costs are compounded as patients eventually fail first-line therapy, thereby moving onto second-, third-, and fourth-line therapies, and so on, until treatment options are exhausted. As patients and physicians desperately hope for cures, off-label treatments are frequently employed on a case-by-case basis. The army of available antineoplastic agents, which has grown substantially following the sequence of the human genome, further increases costs while confounding guideline-driven treatment. Pre-clinical or co-clinical large animal models play an important role in the process of new drug trials and approvals. As the biomedical research community works to make the promise of precision medicine a reality, better animal models are more critical now than ever before.

Animal models, and specifically mouse models, have played a major role in our understanding of the genetic basis of cancer and the role of specific genes and gene mutations in the development and progression of cancer. However, gaining a complete understanding of cancer, which reflects an astonishing number of variant diseases, and translating this knowledge to more efficacious treatments and cures have been elusive. In a clinical landscape that is already challenging, the promise of precision cancer medicine serves to further complicate cancer therapeutics. Precision medicine, simply defined as the right treatment for the right patient, at the right time, demands highly relevant translational models to recapitulate human disease. As clinical practice is being driven more and more by molecular pathology, the treatment landscape becomes unique for each individual cancer patient, rather than cohorts of patients treated as one. This review highlights the advantages and disadvantages of currently available small and large animal cancer models and introduces the Oncopig Cancer Model (OCM) as a qualified alternative to currently available cancer models applicable to a wide variety of cancer types.

CURRENT SMALL ANIMAL MODELS

Advances in cancer care are dependent upon the use of pre-clinical *in vivo* model systems to test safety and efficacy. In general, an

ideal animal model for biomedical research should: (1) mimic the human disease on a molecular basis, (2) derive from a relevant cell line that lends itself to *in vitro* study, (3) be reliable and predictable, (4) manifest survival differences, (5) allow for accurate treatment assessment, (6) be readily imaged, and (7) occur in similar background settings as the human disease (1). A variety of *in vivo* systems have been used to study cancer biology including the development of genetically modified rodents, immunodeficient mouse models engrafted with human tumors, and the use of carcinogens and radiation to induce tumors (2–5). However, due to vast differences between humans and rodents such as mice, the ability to model complex diseases such as cancer and translate results to clinical practice is quite limited (6). This section focuses on the benefits and drawbacks of currently used small animal cancer models.

Mouse Models

Murine models offer several advantages such as the availability of a wealth of genetic information, reduced genetic variation, short generation intervals, high fecundity, and ease of maintenance and handling at a more affordable cost. There are also vast numbers of commercially available mouse lines with know genetics, making them highly suitable to model a wide variety of human diseases. While murine models represent the most commonly used small animal cancer models, there are several drawbacks associated with their use. Humans are 3,000 times larger than mice, live 30–50 times longer and, therefore, undergo about 105 more cell divisions in a lifetime (7). Without genetic modification, mice develop cancers of mainly mesenchymal origin, such as sarcomas and lymphomas, whereas humans have a bias toward the development of epithelial cancers (carcinomas) with age (7). The small size and short lifespan of mice, while advantageous for reducing study times and housing needs, means that loss of certain tumor suppressor genes is insufficient to result in the development of cancer in a highly penetrant manner, particularly when such mutations are heterozygous. Accordingly, investigators have used the Cre-Lox system to homozygously inactivate tumor suppressors in a tissue or cell type-specific manner. While this is often sufficient to drive tumor formation, such a situation does not mimic the cancer disease progression for patients in which rare loss of heterozygosity (LOH), a genetic condition in which one copy of a heterozygous genomic region (i.e., gene or genetic locus and portion of chromosome) is lost due to a mutational event occurs. LOH is a common phenomenon in human cancer, which can result in the loss of tumor suppressor gene functions through elimination of the allele encoding the functional copy of a gene in a subset of cells in the body, often leading to the development of a tumor or the progression of an existing tumor. Because mouse chromosomes are telocentric, LOH often occurs in murine models by loss of the entire chromosome carrying the wild-type tumor suppressor gene allele in cells heterozygous for a tumor suppressor gene mutation (8). However, in human tumors, LOH usually occurs via sub-chromosomal deletions covering the wild-type tumor suppressor gene locus (9, 10).

On a cellular level, murine cells have lower thresholds for genetic and/or epigenetic changes that lead to transformation in culture, which further demonstrates fundamental differences in the mechanistic properties of cancer development between mice and humans (11). Arguably, the most profound difference between mouse models and humans is the essentially 100% homozygosity of every locus in inbred mouse lines, which makes extrapolation back to human populations challenging (12). Mouse cells are immortalized much more readily than human cells (7). It has also been suggested that mouse cells respond to oncogenic *Ras* expression differently than human cells; *RAS* oncogenes require Ras-like (Ral) signaling in human cells, whereas the requirement for this signaling pathway is much reduced in *Ras* oncogene transformation of mouse cells (13). Laboratory mouse strains have very long telomeres and express *Tert*, in contrast to human cells (11, 14). Moreover, mice do not develop the same forms of genetic instability that human cells do during tumorigenesis, perhaps due to their shorter lifespan that could restrict the number of sequential mutations that accumulate in human tumors (14).

Organ systems also vary between mice and humans such that certain types of cancer cannot be accurately modeled. For example, anatomical and physiologic variances between the mouse and human pancreas make modeling pancreatic cancers in mice difficult. The human pancreas is a retroperitoneal and segmented organ divided into a distinct head, body, and tail (15). In contrast, the mouse pancreas is diffuse, dendritic, and poorly lobulated (16). While the vascular supply between mice and humans are largely homologous, there are also substantial differences in several of the functional cell types between the two species. In humans, the exocrine pancreatic acini are organized into lobules that secrete to a small, intercalated duct. These then drain to larger, interlobular ducts, which then join to form the main pancreatic duct. This then joins the bile duct and empties to the duodenum. The mouse pancreas has a large interlobular duct that drains the three respective lobes. The splenic and gastric ducts then merge with the common bile duct and empty more proximally to the duodenum (15). The endocrine component of the pancreas also differs. While humans have 1,000–3,000 times more endocrine islets than mice, humans have a larger proportion of glucagon producing α-cells than mice, who have a larger relative percentage of insulin producing β-cells. Human islets are also rich with both parasympathetic and sympathetic innervation and uniformly distributed, while mice have comparatively sparse autonomic innervation and random islet distribution (15). However, despite these differences, the Pdx-Cre x LSL-$Kras^{G12D}$-$Trp53^{R172H}$ (KPC) mouse has been the benchmark for pancreatic cancer research for the better part of a decade (17). By targeting expression of $Kras^{G12D}$ and $Trp53^{R172H}$ mutations to the exocrine pancreas via the Pdx1 promoter, this model produces reliable and clinically relevant cancer histotypes.

Fundamental differences in how tumorigenesis occurs in mice and humans also exist. For example, humans carrying one mutant and one wild-type allele for the tumor suppressor gene *APC* develop polyps in the large intestine that progressively leads to invasive carcinoma. In contrast, mice with the same heterozygous state for *Apc* develop polyps in the small intestine that rarely show disease progression (18). Such differences in cancer development are due to inherent biological differences

between man and mice and are not limited to intestinal polyps but are observed in many mouse models of cancer. This is well illustrated by variations in tumor spectrum when certain tumor suppressor genes known to cause specific cancers in humans are knocked out in mice.

The body size limitation of mice makes the development of novel imaging modalities and surgical techniques nearly impossible yet these are key techniques needed to diagnose and treat a wide variety of tumor types in patients. Moreover, the rate of metabolism is substantially higher in mice compared to humans (7). These differences mean that the pathways by which tumor progression occurs can vary dramatically when comparing mouse models to human cancer. As a consequence, the tumors that develop in a mouse model may respond differently to therapy. For these genetic and physiological reasons, including vast differences in drug metabolism and xenobiotic receptors, rodents also poorly model toxicity, sensitivity, and efficacy when used in pre-clinical drug studies (19). The ability to establish toxicity and drug sensitivity pre-clinically in animal models is immensely important because less than 8% of cancer drugs translate successfully in Phase I clinical trials from animal models (20). While mice have provided numerous insights into the biology of cancer, their historical limitations emphasize the need to develop new models for cancer translational research.

In addition to genetic-based cancer models, induction of tumorigenesis via administration of carcinogenic agents is utilized to study cancer in small animal models. However, a major disadvantage of this method is the time from administration of the carcinogenic agent to tumor formation, which can range from 30 to 50 weeks (21). Another route of establishing *in vivo* tumors is xenograft of tumor cell lines into mice. Although this mechanism is temporally practical, the ensuing pathogenesis is not always representative of human disease (21, 22).

Rat Models

Rats represent another rodent commonly utilized as pre-clinical cancer models. In addition to some of the abovementioned advantages of murine models, rats have the added benefit of larger size, rendering them more amenable to interventions such as surgery and radiological imaging (23). Rats are commonly used to model colon and bone cancers, largely by exposure to chemical carcinogens (23, 24). In addition, surgical manipulations have been utilized to develop rat models of metaplastic reflux-induced esophageal cancer (25). Recent genome-wide association studies in rats have also identified correlations between rat and human genetic markers of cancer risk (26). However, these models are often limited in their ability to recapitulate human cancer pathophysiology. For example, transgenic and xenograft-induced rat breast cancer models exhibit spontaneous necrosis and failure to metastasize (27, 28). In addition, engrafted rat pancreatic neuroendocrine tumors (PNET) exhibit increased tumor growth following treatment with an mTOR inhibitor, a response that contrasts the results of mTOR inhibitor clinical trials (29).

Zebrafish Models

Zebrafish are one of the few non-mammalian species that have been extensively utilized as cancer models. As a potential model organism, zebrafish exhibit several advantages. The short lifespan and high reproductive capacity of zebrafish render them amenable to high-throughput screening for genetic mutations (30). In addition, the zebrafish genome shares high homology with humans (31), allowing the use of zebrafish tumorigenic mutations to gain insights into human tumorigenesis. The use of gene-editing techniques including Clustered Regularly Interspaced Short Palindromic Repeats (CRISPR) has facilitated mutagenesis of numerous gene loci in this highly reproductive species (32). Zebrafish cell lines also represent valuable *in vitro* models, including models of broad spectrum leukemia using mutant *c-Myc* transgenic zebrafish (33) and malignant melanoma using *BRAF* mutant zebrafish (34). Nevertheless, zebrafish cancer models are not without limitations. Zebrafish exhibit great diversity both across and within strains that results in high levels of individual-specific variation (31). In addition, genomic comparisons between human melanoma patients and zebrafish models have identified reduced mutational burden in zebrafish tumor cells, suggesting significant differences in genomic stability between humans and zebrafish (35). Moreover, attempts to model certain cancers including acute myeloblastic leukemia and pancreatic carcinoma have either failed to develop or exhibit limited metastatic capacity (35). Therefore, zebrafish cancer models exhibit limitations that prevent their use as consistent models of the wide variety of human cancer phenotypes.

Small Animal Hepatocellular Carcinoma (HCC) Models

In addition to small animal models that are utilized to model many different human cancers, there are animal models whose ability to model human disease is limited to one cancer or cancer subtype. For example, the rabbit VX2 model is one of the most commonly utilized small animal HCC models. In this model, virally infected VX2 carcinoma cell cultures are injected into rabbits resulting in tumor formation in the rabbit liver (36). However, these tumors have unknown biology, varying tumor kinetics, and unknown genome organization (36), highlighting the limitations of this model as a relevant human HCC model. Another drawback of this model is spontaneous tumor necrosis, which confounds the evaluation of treatment response after pharmacological or interventional treatment. This represents a significant drawback for this model, given its use by interventional radiologists for novel locoregional therapy testing. Another commonly used HCC mode is the woodchuck model, which produces HCC tumors in response to woodchuck hepatitis virus (WHV) infection. WHV infection shares many disease characteristics with the human hepatitis B virus (HBV), which causes liver cirrhosis and leads to HCC development in humans. Similarities between WHV and HBV are seen in the morphology of the virus, its life cycle, and the resulting development of HCC after 2–4 years of infection (37). This model has been used to develop radiofrequency ablation of primary HCC tumors in pre-clinical trials (38); however, several limitations exist, including differential behavior (woodchuck's hibernate for a period of 4–6 months) and variable diet and WHV infection period when using wild specimens (39).

CURRENT LARGE ANIMAL MODELS

Large animal models of cancer comprise a smaller portion of cancer models than small animal cancer models. While small animal models offer several advantages such as the availability of a wealth of genetic information, reduced genetic variation, short generation intervals, high fecundity, and ease of maintenance and handling at a more affordable cost, they do not provide the anatomical scale required to develop interventional treatments. Large animal models such as pigs offer a more anatomically similar organism to develop these interventional treatment (40–42) and offer cancer cell biology more analogous to human cancer cell biology (43, 44). This section focuses on the benefits and drawbacks of currently used and up and coming large animal cancer models.

Canine Cancer Models

Client owned dogs provide a unique opportunity to study spontaneously developing tumors in a context that is beneficial for both pets and people. In order to utilize client owned dogs to help researchers better understand tumor biology and facilitate translation of novel human cancer treatments to clinical settings, the National Cancer Institute's Center for Cancer Research started the Comparative Oncology Program (COP) in 2003.[1] Use of these animals as comparative cancer models is beneficial due to their many biological similarities with humans along with the large genetic diversity observed within the canine population. Tumors commonly presenting in dogs include osteosarcoma, soft tissue sarcomas (STS), lung carcinoma, oral melanoma, mammary carcinoma, oral squamous cell carcinoma, nasal tumors, and malignant non-Hodgkin's lymphoma—likely the best cancer model provided by canines because it has considerable analogy to the human variant. Canine cancer models are unique because they spontaneously present with tumors with several characteristics similar to those observed in humans (i.e., osteosarcoma in large breed dogs) (45). Indeed, cancer occurs naturally in dogs with rates reported to range between 5 and 33% (46, 47). It is estimated that 45% of dogs 10 and older die of cancer (45), which is comparable to the estimated 60% of humans who are diagnosed with cancer of the age of 65 years (48). This natural occurrence and history of cancer permits the rapid study of DNA damage and epigenetic alterations that accumulate over time to result in tumor formation, especially given the high homology observed between the canine and human genome (49). Because of these advantages, researchers have been able to utilize canine cancer models to identify relevant genetic alterations and drivers of cancer similar to those observed in human cancers. Additionally, canine subjects bypass the phases of clinical trial testing, accelerating the pace of drug development (50). Many drugs have undergone pre-clinical trials using canine cancer models including Resiniferatoxin, a drug that acts as an agonist for pain caused by bone cancer, due to the canine's highly noticeable response of self-mutilation of areas in pain (51).

There are several disadvantages with using dogs to model human cancers. Canine cancer models tend to consist of lymphoid and sarcoma tumor types as opposed to carcinomas. Cancer drug development studies conducted in canines are also not always translatable to humans, as dogs have varying drug sensitivity compared to humans (52). Another contention surrounding the use of canine cancer models in translational research is the issue of outbred versus inbred models; because modern dog breeds are a product of line inbreeding, their ability to provide a relevant model of diverse and heterogeneous human cancers is questionable (47). Finally, accrual of client dogs to clinical trials—as with human patients—presents a barrier to the timeliness of study conduct.

Non-Human Primate Models

To date, published reviews or studies on cancer in non-human primates are relatively scarce and limited to single case reports and small case studies. However, there has been a steady increase in the number of reviews published on cancer in non-human primates (53–56). These reviews likely represent an increase in the recognition of cancer in non-human primates, but they also likely represent an increase in the longevity of non-human primates maintained in research facilities attributed to factors such as improved health care and nutrition and improvements in record keeping, including breeding history, genetic background, and clinical course of disease.

Potentially, non-human primates offer advantages for studying cancer because of their anatomical, physiological, and genetic similarities with humans, being the only bipedal mammalian animal model for research and having 1:1 homology with the majority of human protein-coding genes (57). It is difficult to determine the concordance of toxicities identified in non-human primates relative to humans and other species because of a lack of clinical data. It is tempting to assume that in response to drug delivery, non-human primates will have pharmacological or physiological responses most similar to humans; however, this sweeping generalization cannot be made (58). Despite the lack of evidence, because of receptor and epitope similarity, non-human primates may be an appropriate species for testing certain classes of drugs, for example, large molecule and biological compounds due to the high degree of cross reactivity in those compounds between humans and non-human primates (59).

Porcine Cancer Models

Swine cancer models are also highly relevant due to their similarity in size, anatomy, pathophysiology, metabolism, genetics, epigenetics, and pathology, as well as their reduced cost compared to non-human primate models (60–68). Swine subjects age at approximately 3–5 times the rate of humans and have similar clinical laboratory and histological findings (66). This life cycle permits enough time to develop, characterize, and modulate cancer in the swine model from weaning to adolescence (69) but also sufficiently short-lived that reasonable research aims and budgets can be outlined and accomplished. Advances in DNA sequencing and our understanding of the role of non-coding DNA sequences have provided insights into the mechanisms underlying altered gene expression and other drivers of cancer development. Swine genetics in particular lends itself to clinically translatable studies due to many available outbred lines. The outbred nature of

[1] https://ccr.cancer.gov/Comparative-Oncology-Program.

pigs is key in imitating the variety of genetic profiles underlying human patient populations and cancer types. In addition, the pig genome has high homology with the human genome (70, 71) and epigenetic regulation is highly conserved (67). This elucidation of the porcine genetic profile combined with advances in genetic engineering has permitted the creation of genetically modified pig cancer models that not only follow an analogous disease course as humans (72) but also respond to cancer drug therapy similarly to humans in randomized controlled trials. High-throughput genome sequencing and a collection of precision-genetic tools combined with tools for bioinformatics analyses and profiling of gene expression/proteomics can be applied to pigs (67, 68, 71, 73–77). The ability to modify mammalian genomes through transgenesis, targeted nucleases, and CRISPR, united with the development of advanced reproductive technologies including cloning, allows researchers to create complex and unique cancer models in swine that are more applicable to human malignancies (73, 78). Current porcine models utilized for cancer research include an APC^{I311} porcine model of familial adenomatous polyposis that produces polyps but not tumors (79), a heterozygous *TP53* knockout model of spontaneous osteosarcomas (80), and a chemically induced porcine HCC model, which takes over 1 year to develop clinically relevant tumors (81, 82).

In addition to recent advances in making precise genetic modifications to pig genomes, there has been significant progress in technologies for testing consequences of genetic changes. Imaging modalities such as computed tomography (CT), magnetic resonance imaging (MRI), and positron emission tomography (PET) can be easily applied to large animals such as pigs, whereas application of analogous clinical protocols is difficult and impractical using rodents (83). By applying these imaging modalities to swine cancer models, detection techniques, progression monitoring, and therapeutic response assessments may be improved. The pig's size permits radiation-directed therapies to be tested and optimized. Surgical resection is the first line of therapy and often the standard of care for many cancers. The pig's anatomy allows refinement of surgical techniques and studies of local tumor recurrence both of which are difficult or impossible to perform in rodents. In addition, tumor natural history is an area that is difficult to study in rodents due to their short lifespan, about 1/30th that of humans (7). Swine can live up to 10 years, thereby enabling researchers to carefully follow the development of tumors, tumor progression, invasion, and metastasis in the absence of intervention over time. Additionally, the identification of biomarkers may be more feasible in these animals due to the facile nature of accessing blood and tissue samples, the abundance of sample material and the ability to perform longitudinal blood sampling over longer periods of time. Understanding tumor heterogeneity may be well suited for a large animal, as samples could be collected from many different tumors over time and followed for variations in somatic mutations, gene expression, epigenetic alterations, or differential responses to treatment (66, 78).

One of the main drawbacks of rodent cancer models has been their inability to identify safe and effective drugs to treat cancer. Mouse cancer models have been poor predictors of drug safety, toxicity, and efficacy (84). Furthermore, routes of administration in mice are largely limited to intravenous (i.v.), intraperitoneal (i.p.), or oral gavage. Pigs have been widely used in pre-clinical drug toxicology and are a standard large animal model for pre-clinical toxicology prior to human studies (63). The size and ease in handling pigs allows drugs to be administered in the same manner that patients are administered, including orally, i.v., i.p., by inhalation, dermal absorption, subcutaneous, intramuscular, and transmucosal routes. Longitudinal blood sampling can be performed to assess drug exposure and metabolism over long periods of time, and the amount of blood samples that can be taken from swine in a short period of time enhances the ability of pharmacologists to get precise kinetic data following drug exposure. There are significant homologies between swine and human xenobiotic receptors that regulate drug metabolism and pharmacokinetic properties (85). The cytochrome P450 (CYP) superfamily of proteins plays a critical role in the processing and metabolism of drugs, and again, many studies have shown parallels in the structure and function of these molecules in pigs and humans (85). Importantly, for pediatric cancer drug studies, juvenile pigs have been shown to have similar pharmacokinetic responses to certain drugs that cannot be modeled in other animals (86). Finally, pigs are easily subject to models of relevant comorbidities including non-alcoholic steatohepatitis (NASH) and alcohol-induced cirrhosis. The use of pigs in pre-clinical drug testing may identify safer and more effective therapies as well as establish dosing and routes of administration for new drugs prior to human clinical trials. Practically speaking, enrollment of pigs to clinical research studies eliminates the accrual barrier observed in candidate dogs and human clinical trial patients because cohorts of pigs are accessible. Furthermore, a facile porcine genome engineering platform enables future humanization of drug metabolism in swine models (66).

THE OCM

The OCM is a novel transgenic swine model that recapitulates human cancer through development of site and cell specific tumors following Cre recombinase induced expression of heterozygous $KRAS^{G12D}$ and $TP53^{R167H}$ transgenes (87). Details regarding the generation of the OCM can be found in Schook et al. (87). Briefly, porcine *KRAS* and *TP53* cDNA were cloned and site-directed mutagenesis was performed to introduce the oncogenic G12D and R167H mutations, respectively. The two cDNAs were then introduced into a Cre-inducible vector containing a CAG promoter followed by a Lox-Stop-Lox (LSL) sequence—which prevents expression of the transgenes until it is removed by Cre recombinase—followed by a single copy of the $KRAS^{G12D}$ and $TP53^{R167H}$ transgenes separated by an internal ribosome entry site (IRES) sequence (**Figure 1A**). Normal Minnesota minipig embryotic fibroblasts were transfected with the resulting plasmid, and stably transfected cells were used as the source of nuclei for somatic cell nuclear transfer (SCNT). A single male Oncopig was selected from the resulting litter to develop the Oncopig herd (**Figure 1B**) due to the insertion of the transgene construct at a single location on chromosome 18. The breeding scheme depicted in **Figure 1B** allows the production of a herd of male and female Oncopigs homozygous for both the transgene and an MHC haplotype. The resulting homozygous males can be

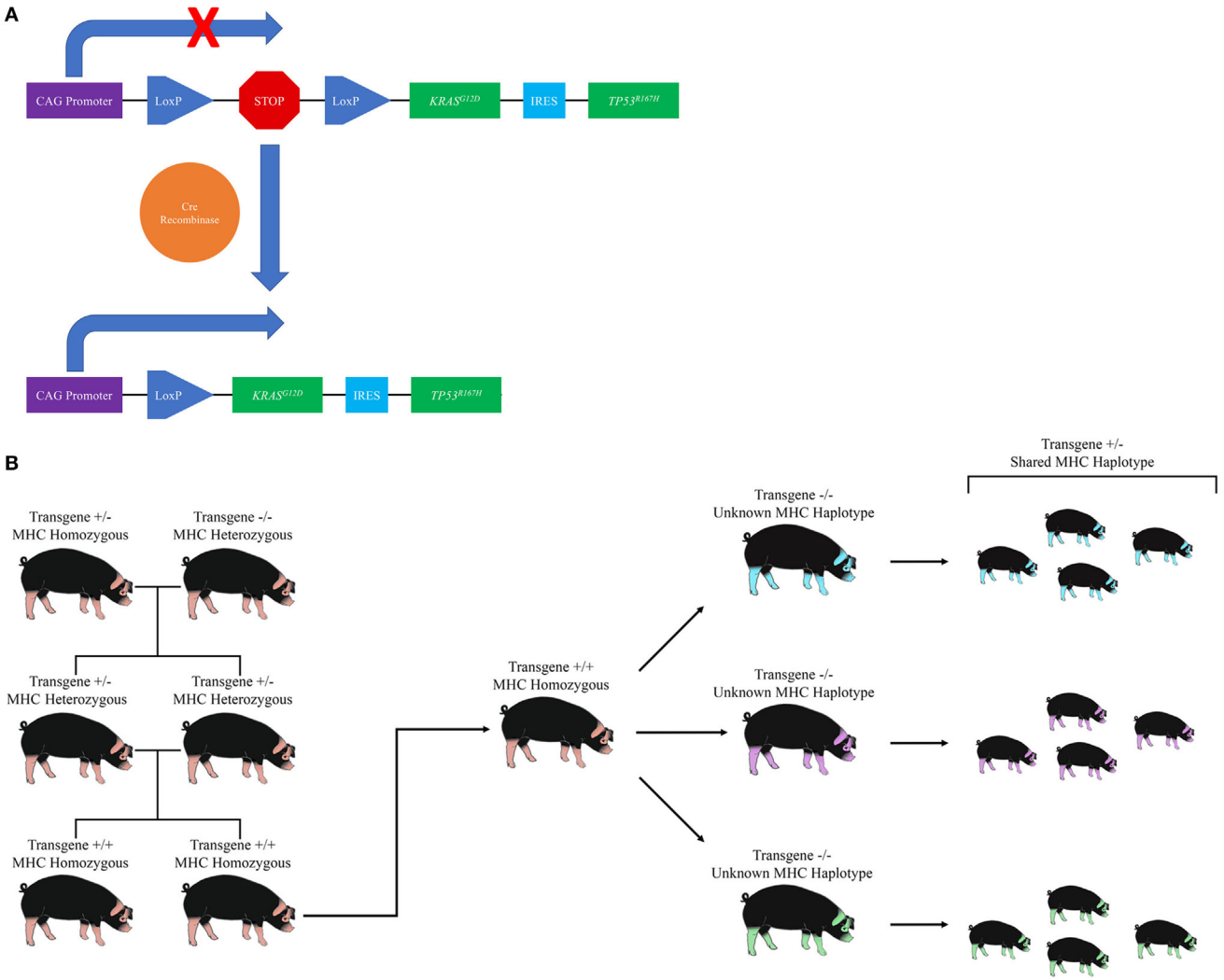

FIGURE 1 | Development and utilization of the Oncopig Cancer Model (OCM). **(A)** Diagram of the Oncopig transgene cassette located on chromosome 18. A Lox-Stop-Lox sequence prevents expression of *KRAS*^{G12D} and *TP53*^{R167H}. Exposure to Cre recombinase results in site specific recombination between the two recognition sites (LoxP), resulting in removal of the Stop sequence and subsequent expression of *KRAS*^{G12D} and *TP53*^{R167H}. **(B)** Diagram of the breeding scheme used to produce Oncopigs for experimental use. The original male Oncopig homozygous for an MHC haplotype and carrying a single transgene cassette located on chromosome 18 is bred to a non-transgenic female to produce offspring heterozygous for the transgene cassette and MHC haplotype. The resulting heterozygous offspring are further bred to produce Oncopig offspring homozygous for both the transgene cassette and an MHC haplotype. Male homozygous offspring can then be bred to a variety of transgenic or non-transgenic pig breeds (depicted through varying color) to produce genetically diverse Oncopigs for experimental purposes, all of which harbor a single copy of the transgene cassette and a shared MHC haplotype.

bred to a wide range of available pig breeds, allowing the production of genetically diverse experimental Oncopigs possessing a single copy of the mutated transgenes, the WT alleles, and a shared MHC haplotype important for immunological studies as described below (**Figure 1B**).

The *KRAS*^{G12D} and *TP53*^{R167H} mutations were chosen because the resulting amino acid substitutions are commonly found in human cancers, with *RAS* and *TP53* mutated in one-quarter and one-third of all human cancers, respectively (88, 89). These mutations are also observed simultaneously in human cancers, making this a highly relevant model from a genomics perspective. Utilization of two mutations commonly observed in human tumors allows production of tumors driven by the same molecular alterations as humans in a species with similar anatomy, physiology, metabolism, and genetics. In addition, the heterozygous outbred nature of the OCM means that this model more closely mimics the human condition in comparison to commonly used inbred, homozygous germline mouse models. This model, as a transitional animal model from mice or other small animals to humans, fulfills the currently unmet clinical modeling needs for relevant investigation of both hematologic and solid tumor cancers. With its genetic malleability and predictable behavior, the OCM offers a comprehensive toolset for modeling both human cancers and comorbid disease. Together, this makes the OCM

an ideal platform to develop a wide range of cancer models to test new treatments, develop standards, and improve early detection rates. The OCM is a transformational research tool for the investigation of therapeutic efficacy while significantly reducing the costs, variables seen in human subjects, and lengthy conduct of human clinical trials. The following sections discuss progress made to date on modeling various cancer types in the OCM.

Soft Tissue Sarcomas

Soft tissue sarcomas are a group of rare mesenchymal tumors that carry a 5-year survival rate of 50%. STS consist of over 50 subtypes and arise from a number of tissue types including fat, muscle, blood vessels, and nerves (90). As the survival rate for STS has remained unchanged for decades, there is a critical need for further research into STS characterization and treatment. This research is currently limited by the availability of STS cell lines and tissue samples (91), highlighting the need for transitional STS models for improved STS detection, diagnosis, and treatment. As *TP53* represents one of the most frequently mutated genes in human STS (92, 93), the OCM represents an ideal model to develop STS cell lines and *in vivo* models critical for improving survival rates for patients with STS. To date, both STS cell lines and *in vivo* STS tumors have been developed and characterized in the OCM (76, 87).

Utilization of human tumor cell lines is critical for expanding our understanding of tumor biology and developing new cancer therapies (94). However, given the high number of diverse human STS subtypes and limited cell line availability, additional STS model cell lines are required to investigate the mechanisms underlying variable targeted therapy responses observed across STS subtypes (91, 95). As an initial proof of concept to demonstrate the ability to transform Oncopig mesenchymal cells, fibroblasts isolated from Oncopig skin biopsies were transformed via exposure to Cre recombinase *in vitro* (87). The resulting STS cell lines expressed both $KRAS^{G12D}$ and $TP53^{R167H}$ transgenes and displayed tumorigenic phenotypes, including altered morphology, reduced cell cycle length, increased cell migration, and soft agar colony formation (87). Injection of the STS cell lines in SCID mice resulted in tumor formation (87), and transcriptional profiling of Oncopig STS cell lines via RNA-seq identified transcriptional hallmarks of human STS, including altered TP53 signaling, Wnt signaling activation, and evidence of epigenetic reprogramming, including altered expression of DNA and histone methyltransferases (76). In addition, *FOSL1*, a key transcriptional regulator of human STS, was identified as a master regulator in the Oncopig STS cell lines (76), further demonstrating the similarities between Oncopig and human STS at the molecular level. These *in vitro* phenotypes and transcriptional profiles are consistent across replicates and in lines cultured for extended periods of time (76), highlighting the stability of Oncopig cell lines. As the OCM supports the transformation of any cell type, it provides a platform for the production of stable STS cell lines originating from a wide variety of mesenchymal cell types for *in vitro* STS research.

While cell lines are useful for understanding fundamental tumor biology and testing potential new therapies, *in vivo* transitional models are also critical to translate basic *in vitro* discoveries into clinical practice. STS tumor formation has been successfully demonstrated via direct injection of adenoviral vector encoding Cre recombinase (AdCre) into Oncopig skeletal muscle, resulting in tumors blindly pathologically characterized as leiomyosarcomas (76, 87, 96). These tumors develop rapidly and consistently and also recapitulate transcriptional hallmarks of human leiomyosarcomas, including altered TP53 signaling, Wnt signaling activation, and evidence of epigenetic reprogramming (76). Master regulators of Oncopig leiomyosarcomas were also consistent with human leiomysoarcomas, including *MEF2C*, which acts as a tumor suppressor in human leiomyosarcoma (97). The Oncopig leiomyosarcoma model therefore represents a qualified alternative tumor model for pre-clinical treatment and imaging testing, as well as an ideal training tool for surgical and procedural specialties. In fact, the OCM is already being utilized for device testing. Using the Oncopig leiomyosarcoma model, researchers have tested the efficacy of 3D spatially registered real-time image-guided catheter-based ultrasound (CBUS) thermal ablation therapies (96). By inducing leiomyosarcoma formation and then treating these tumors, the ability to utilize 3D tracked ultrasound image guidance to precisely place catheters and treat tumors was demonstrated, resulting in complete ablation of the tumor (96). This demonstrates the ability to utilize the OCM as a pre-clinical model for device testing not possible in small animal models.

Pancreatic Cancer

Despite modest improvements in recent years, pancreatic cancers remain highly lethal with an overall 5-year survival of 8% (98). Genetically modified mice have allowed tremendous insights into disease etiology, particularly on a genetic level, as well as *in vivo* characterization and mechanisms. The KPC mouse model has been the gold standard for pre-clinical pancreatic cancer research for over a decade. Yet, such models are limited in scope for more direct translational application to humans regarding epigenetic events and therapies given their anatomical and physiological variances compared to humans. Given the greater anatomical and physiological similarities between pigs and humans, an Oncopig pancreatic ductal adenocarcinoma (PDAC) model will provide a more clinically relevant model, allowing insight into surgical and interventional radiology techniques not possible in currently used mouse models. While such a porcine model is certainly not without limitations, the domestic pig may more faithfully recapitulate human PDAC and expand our understanding of disease pathology beyond what is possible using current small animal PDAC models.

A porcine PDAC model is currently being developed using the OCM. Successful induction of both predominant pancreatic cancer histotypes—exocrine and neuroendocrine—via direct delivery of AdCre to the main pancreatic duct has been demonstrated in the OCM. This approach led to locally invasive disease sharing histological hallmarks of human PDAC including a dense fibroblastic stroma and acinar-to-ductal metaplasia (99), which may provide a more clinically relevant model than currently used small animal PDAC models. This is particularly important for the neuroendocrine component, which is relatively underrepresented in research compared to exocrine/ductal cancers. Murine models of PNET produce a variety of PNET types with varying behaviors

ranging from indolent to highly aggressive (100, 101). While these models have proved to be valuable prototypes of disease, they are limited in the extent to which they can represent human PNET. The low incidence and heterogeneous presentations of PNET itself combined with the low availability of pre-clinical models have slowed progress in terms of early diagnosis and the development of targeted therapies. In fact, one of the most significant clinical challenges in the management of pancreatic caner is its late presentation, demonstrated by the diagnosis of more than 80% of pancreatic cancer cases at regional and distant stages. As stage is the key prognostic factor in pancreatic cancer survival (98), a means of improved early detection is extremely attractive to clinicians. Given the size and orientation of the pig pancreas, near identical imaging modalities can be used to longitudinally follow disease progression immediately after induction in the Oncopig PDAC model, which may improve our understanding of early events in the carcinogenic process and facilitate earlier detection.

Furthermore, the Oncopig PDAC model also allows investigation into several clinical avenues that are not possible or must be significantly altered to perform in rodents. For instance, patients with locally surgically resectable tumors have improved survival compared to those with inoperable disease (98). However, in rodents, the study of many novel surgical techniques is impossible due to the differences in size and anatomy. In this capacity, the Oncopig PDAC model may allow investigation of new surgical interventions as well as nanotechnology and localized drug delivery methods for pancreatic cancers.

HCC and Comorbidities

Worldwide, HCC is the fifth most common cancer and the third most common cause of cancer-related deaths, occurring more often in men than in women. In the United States, 40,710 new cancers of the liver and intrahepatic bile duct are expected in 2017, with an estimated 28,920 deaths. HCC is the main form of primary liver cancer that carries a 5-year survival rate of 17.5%. This low survival rate is predominantly due to the low number (15%) of patients who are eligible for surgery or other curative therapies at the time of diagnosis (102), highlighting the need for improved HCC early detection and treatment strategies. A number of locoregional therapies (LRTs) including cryoablation, radiofrequency ablation, and transarterial chemoembolization are currently used to treat HCC patients who are ineligible for surgery; however, the optimum treatment strategy is dictated by the physician's specialty as opposed to evidence-based consensus (103). This highlights the need for improved HCC animal models to test LRTs and combination therapies to better understand the intrinsic tumor biology underlying differential treatment responses. An Oncopig HCC model would provide an ideal transitional model to address this need as well as refine techniques to help improve early detection rates.

The OCM, as an HCC investigational tool, offers a novel, physiologically and anatomically relevant cancer model for which a multitude of innovative therapeutic modalities can be applied and tested. This model is a critical transitional, translational, and transformational research tool for the investigation of therapeutic efficacy, variables seen in human subjects, and lengthy conduct of human clinical trials. Importantly, it can be utilized to conduct correlative studies for more efficient and consistent investigation of new therapies. Its size allows utilization of the same methods and instruments used in human clinical practice, and the segmental nature of the pig liver (similar to human anatomy) allows each Oncopig to serve as its own therapeutic control. Although the information gained from human clinical studies has been used to marginally enhance the efficacy of current standard of care LRTs, such trials have provided only limited capability for the investigation of the fundamental processes contributing to procedure effectiveness and disease relapse.

An Oncopig HCC model has been initiated to serve as a transitional model linking murine results with clinical outcomes. Oncopig HCC cell lines have been created by isolating hepatocytes from Oncopig livers followed by *in vitro* transformation (77). These cell lines recapitulate human HCC characteristics, including an epithelial-mesenchymal transition, secretion of alpha-fetoprotein (AFP), and transcriptional similarities including *TERT* reactivation, apoptosis evasion, angiogenesis activation, and Wnt signaling activation (77). In addition, direct comparison between Oncopig and 18 commonly used human HCC cell lines revealed conservation of master regulators of gene expression (77). The Oncopig HCC cells also form hypervascular tumors histologically characterized as Edmondson Steiner grade 2 HCC with trabecular patterning when implanted into both SCID mice and Oncopigs subcutaneously (77). In addition, T-lymphocyte infiltration is observed, indicating that these are "hot" tumors potentially appropriate for immunotherapy trials. This is an important aspect of this model, as it is clear that HCC-specific antigens are recognized by the immune system and contemporary clinical studies have indicated that manipulating the immune response can be deleterious to HCC tumor growth (78). Together this suggests that the Oncopig HCC model is a qualified alternative for improving HCC detection, treatment, and biomarker discovery.

In addition to the formation of clinically relevant tumors, an ideal HCC animal model must also mimic relevant comorbidities observed in humans. Alcoholic liver disease and NASH represent common chronic liver ailments, both of which are progressive and incite liver cirrhosis—a precancerous state of liver scarring—that increases the risk for HCC development. A protocol for the induction of alcohol-related liver cirrhosis within 8 weeks using intravascular administration of an ethanol-ethiodized oil emulsion via the hepatic artery has been successfully tested and validated in the OCM (77). This provides the opportunity to assess the role of chronic alcohol-induced liver cirrhosis in HCC tumorigenesis. In addition, researchers have utilized the Ossabaw pig to generate a porcine NASH liver disease model (104). As Ossabaw pigs are genetically predisposed to obesity and diabetes, exposure to a "Western" or "NASH diet" results in the development of severe metabolic syndrome with markedly abnormal liver histology that closely mimics human NASH within 8–24 weeks (104). While this represents a promising porcine NASH model, natural progression to HCC would take years to develop. However, crossbreeding the OCM and Ossabaw would result in a unique "Oncobaw" cross characterized by capacity for inducible tumors as well as development of NASH liver disease,

providing a distinctive platform to study HCC in the NASH liver microenvironment.

Oncopig Immunological Profiling

The hallmarks of cancer have recently been updated to include the ability of cancer cells to avoid immune recognition and subsequent destruction (105). The impact of having immune cell infiltrates at the tumor site has especially been evaluated in colorectal cancer patients, where intratumoral T cells with cytotoxic nature and memory phenotypes allowed prediction of prognosis for patients at an early stage of disease (106). In addition to the *type* of immune cell infiltrates, the outcome for colorectal cancer patients was also found to be dependent on both the *density* and *location* of the immune cells within the tumor (107). Together, these three concepts formed the basis of the *Immunoscore*, which has already become an integrated part of the prognostic approach for colorectal cancers in humans (108). The mechanisms underlying the ability of the cancer cells to avoid immune destruction have been proposed to differ dependent on the degree of immune cell infiltrates (109). For this reason, an immunological characterization of the OCM tumor landscape is considered crucial to subsequently use this information for design of pre-clinical immunotherapeutic studies. Recently, both infiltration of several T-cell subsets within OCM tumors and endogenous anti-tumor immune responses have been demonstrated (Overgaard et al., 2017, submitted). This indicates that the OCM develops "hot" tumors and a porcine version of the *Immunoscore* will indeed be both interesting and useful when selecting which therapies to test in the OCM. Adaptation of an *in vivo* cytotoxicity assay in line with what has previously been demonstrated for mice and monkeys (110–112) would allow a direct measure of anti-tumor cytotoxic immune responses and identification of epitopes involved in the cytotoxic recognition of tumor cells. While T-cell infiltration has been observed in Oncopig tumors developed via either AdCre or transformed cell line injection, comparisons of the resulting tumor heterogeneity and immune microenvironments induced by the two tumor formation methods have not been performed. These future comparisons will be important for ensuring Oncopig tumor heterogeneity, the surrounding microenvironment, and subsequent immunological responses mimic those observed in humans.

In addition, adoptive transfer of T cells between MHC-matched Oncopig littermates is now a possibility with the development of a NGS-based approach for porcine MHC class I allele typing (113). Those animal pairs suddenly enable adoptive T-cell therapies to be tested in a large and fully immunocompetent animal model. Finally, in addition to the adaptive immune system, the porcine innate immune system has been heavily studied and found to be similar to humans in terms of anatomy, organization, and response (114). For example, pattern recognition receptors such as toll-like receptors (TLRs) have been heavily studied in pigs (115–117), providing insights into their evolution, variability across breeds, and similarities with humans. In addition, vast knowledge regarding porcine cellular and humoral innate immune responses and their similarities with humans exist (114). While this work has not been performed in the Oncopig, the extensive knowledge of both the porcine adaptive and innate immune system represents a significant advantage for this and other porcine cancer models, given the emerging role of the immune system in tumor development and treatment.

UTILIZING THE OCM TO ADDRESS UNMET CLINICAL NEEDS

Animal research has played a vital role in advancing biomedical science. However, laboratory animals may experience significant adverse effects as a result of experimentally induced cancers and the effects of investigative or treatment regimes are substantial (118, 119). Therefore, the use of animals in research comes with ethical responsibilities (120). The three R's (Reduce, Replace, and Refine) as defined by Russell and Burch (121) provide a practical strategy for applying an ethical framework to animal research. These guiding principles indicate that researchers must seek to (1) replace animal use with alternative techniques, (2) reduce the number of animals used to the minimum required to obtain meaning information, and (3) refine experimental procedures to ensure animal suffering is reduced as much as possible.

Consistent with the three Rs, the Oncopig model allows the discrete induction of localized tumors that can be closely followed to meet scientific objectives while minimizing comorbidities and mortality. However, in order for the OCM to be utilized to its full potential, an understanding of how the various Oncopig-based cancer models can be applied to specific unmet clinical and pre-clinical human cancer needs is required. This section describes significant and pressing unmet clinical needs that (1) need to be addressed to improve disease burden and survival rate and (2) can be effectively addressed by utilizing the OCM as a translational model to bridge the gap between small animal models and human clinical trials.

Early Detection

As the biomedical research community investigates the diagnostic and prognostic value of liquid biopsies, a large animal model becomes increasingly important for both metabolic similarities and ease of sampling. Candidate biomarkers from serum, plasma, or peripheral blood must be accurately and reproducibly measurable, clinically feasible, cost-effective, and prospectively validated in randomized clinical trials. Due to the inducible nature of the OCM, this model represents an ideal large animal model for the identification of candidate early detection biomarkers. **Figure 2** outlines a variety of biomarkers that have been validated in the clinic and can be more rigorously tested in the OCM. Putative biomarkers in blood consist of soluble factors such as serum proteins and circulating tumor DNA, or other cellular factors such as tumor cells, T-cell subsets, and other immune cell populations. The serum factors may be single or could include a panel of factors preferably measured by a single, validated assay. To date, most published analyses of peripheral blood biomarkers in immunotherapy have been retrospective and hypothesis generating, although important information has been gained that illuminates the mechanisms of clinical benefit with some approaches and has helped inform subsequent clinical trial design.

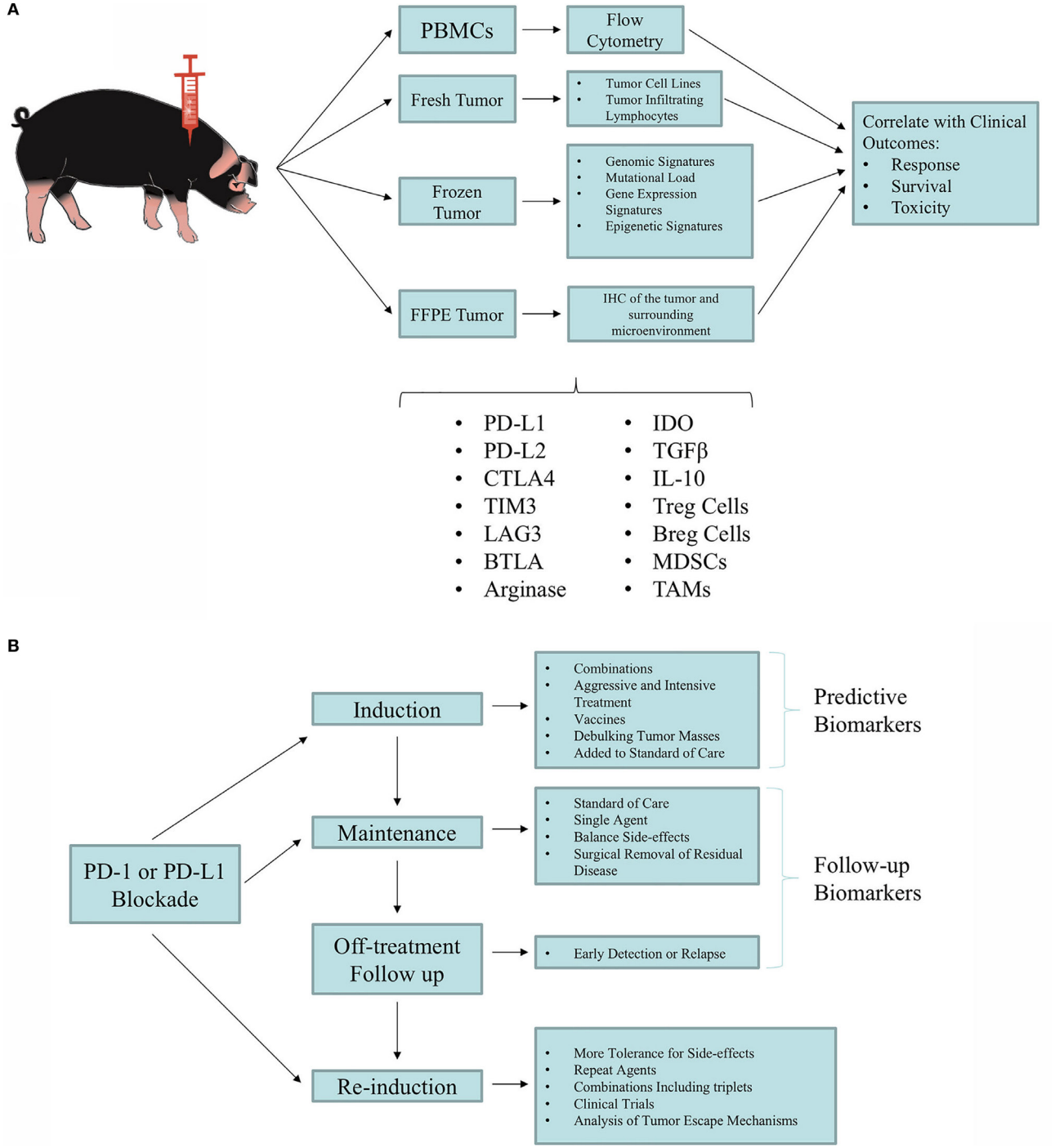

FIGURE 2 | Utilization of the Oncopig Cancer Model (OCM) for biomarker discovery and validation. **(A)** Tumor and blood samples are taken from Oncopigs for biomarker screening studies. Samples are processed immediately (fresh), flash-frozen, or formalin-fixed paraffin-embedded (FFPE). Blood samples can immediately undergo Ficoll density centrifugation for isolation of peripheral blood mononuclear cells (PBMCs). Fresh tumor samples can be used to produce tumor cell lines and isolate tumor-infiltrating lymphocytes (TILs). The flash-frozen samples can be used for deep sequencing (i.e., whole-exome sequencing, RNA-seq, miRNA-seq, and DNA methylation analysis). FFPE samples can be utilized for immunohistochemistry (IHC) of the tumor and the tumor microenvironment. Results obtained from these analyses can be correlated with patient outcomes to identify predictive biomarkers. **(B)** Proposed testing of clinical management with immunotherapy. As new immunotherapy agents and combinations are developed, optimal combinations and subtype susceptibility must be determined. Patients experiencing durable responses that are sustained even off treatment require new concepts in risk management and mitigation, while making the most of the clinical benefit. Overall, a phased approach can be tested in which aggressive combination regimens that achieve frequent responses can be followed by maintenance with less aggressive and safer regimens, reaching the point of weaning responsive animals off treatment. Identifying biomarkers will be crucial for optimal clinical management. Adapted from Ref. (122).

Immunogenicity and Immunotherapy

After decades of research, the hope of effective immunotherapy for solid tumors became a reality with the development of immune checkpoint inhibitors (78, 123). This elegant approach leverages the immune system, which has the capability to recognize a diverse array of both foreign and tumor-derived antigens, to exact a tumor-specific response capable of arresting malignant growth. Novel immunotherapeutic regimens that both counteract these immunosuppressive mechanisms and amplify tumor-specific immunity have the potential to profoundly improve clinical outcomes for cancer patients. The recent demonstration that cancer immunotherapy extends patient survival has reinvigorated interest in elucidating the role of immunity in tumor pathogenesis. Since ipilimumab entered the treatment landscape in 2011, immunotherapy has continued to revolutionize cancer therapy. In fact, immunotherapy was named the American Society of Clinical Oncology (ASCO) top cancer advance of the year for 2016 (124). A number of U.S. FDA-approved agents have become available for an increasing number of difficult-to-treat cancers, such as melanoma, renal cell carcinoma (RCC), HCC, and lung cancer, among others. In contrast with most chemotherapy and targeted therapies, immunotherapy offers the possibility of durable responses, sometimes even without continued treatment (125–127). However, objective responses among patients treated with single-agent regimens are seen in less than one-half of patients treated. Combination of immune checkpoint inhibitor therapy raises response rates but also increases toxicity and cost (128). Thus, to optimize selection of appropriate patients for immunotherapy and avoid unnecessary toxicity and health care costs, there is a clear need to identify truly predictive, and not simply prognostic, biomarkers of response. The OCM can address some of the issues regarding selection of agents and expected immune responsiveness as novel agents are developed.

Understanding which factors predict clinical benefit with immunotherapy in a relevant animal model can improve the selection of tumor types and patient subsets who will respond, illuminate the mechanism of action of novel immunotherapeutic approaches, and potentially inform which patients require single-agent versus combination strategies (**Table 1**). Examples of biomarkers in the immunotherapy landscape include (1) soluble factors such as serum proteins, (2) tumor-specific factors such as receptor expression patterns and components of the microenvironment, (3) identification of immune cell subsets such as Treg, and (4) host genomic factors (129–131). Despite the interest in biomarker development for immunotherapy, validated biomarkers have remained an elusive goal and the availability of the OCM enables biomarker validation of serum, immune cell, tumor, and tumor microenvironment to be correlated with response.

Our incomplete understanding of the mechanisms of action of specific immunotherapies makes it difficult to identify a surrogate marker that adequately captures the process across different classes of drugs (133). Many published analyses of potential predictive biomarkers for immunotherapy are retrospective, with limited extension into large prospective trials. In addition, there has been substantial variability in standardization, measurement, and interpretation of early biomarker assays (134). Furthermore, biomarker development in immunotherapy is challenged by the fact that immunotherapy targets are often inducible and dynamic

TABLE 1 | Potential predictive biomarkers for immunotherapy.

Type	Source	Biomarker	Clinical significance
Liquid	Serum	IL-6	High-dose IL-2 treatment failure and shorter overall survival associated with high levels in metastatic renal cell carcinoma
		CRP	High-dose IL-214 resistance associated with high levels; decreasing levels during ipilimumab therapy associated with disease control and survival
		VEGF	Lack of response to high-dose IL-2 is associated with high levels and decreased overall survival
		LDH	Ipilimumab therapeutic benefit predicted by low pretreatment levels; decreasing levels during ipilimumab therapy associated with disease control and survival
		sCD25	Ipilimumab therapy resistance predicted by high levels
		NY-SEO-1 antibody	Greater likelihood to respond to CTLA-4 blockade predicted by seropositivity
Cellular	Peripheral blood	Neutrophils/leukocytes	High-dose IL-2 treatment failure and shorter overall survival associated with high counts
		Lymphocytes	High-dose IL-2 therapy response associated with immediate lymphocytosis
		CD8+ T cells	Clinical benefit to CTLA-4 blockade associated with presence
		Absolute lymphocyte count	Increasing counts during ipilimumab therapy associated with improved overall survival
		Eosinophils	Increasing counts during ipilimumab therapy associated with improved overall survival
		CD4 + ICOS + T cells	Increase in frequency after ipilimumab therapy
		Myeloid-derived suppressor cells	Ipilimumab therapy benefit predicted by low frequency
	Tumor	PD-L1	
	Tumor-infiltrating lymphocytes	CD4 + ICOShigh T cells	Clinical benefit of ipilimumab correlated with increased frequency
		CD8 + T cells	PD-1/PD-L1 expression predicts response to PD-1 blockade
Genomic	Tumor	Tumor mutation loads	Predicts clinical benefit of ipilimumab and PD-1 blockade
		Mismatch repair	Predicts clinical benefit of PD-1 blockade

Adapted from Ref. (132).

over time and location. This is a function of the complex tumor microenvironment and the contribution of immuno-editing to the immune milieu. The tumor microenvironment involves complicated interactions between several types of infiltrating immune cells such as monocytes, neutrophils, dendritic cells, T and B cells, eosinophils, basophils, mast cells, and natural killer cells, as well as the heterogeneous tumor cells themselves and their companion stromal cells, including tumor-associated macrophages, fibroblasts, adipocytes, endothelial cells, and others (135). The local environment is further complicated by "micro-niches" created by alterations in perfusion, oxygenation, electrolyte levels, and the subsequent development of resistant tumor cells surviving in nutrient- and oxygen-deprived conditions (135, 136). Thus, these micro-niches likely represent distinct microenvironments with different cell types and factors, all within one tumor deposit. Finally, incomplete immune editing may result in selective pressure on tumor cells, resulting in resistant tumor cell clones and immune escape (132, 135).

Despite these challenges, clinical research of immunotherapy over the last several years has confirmed the importance of tumor-infiltrating lymphocytes as both prognostic and predictive indicators for patients with cancer and for treatment with immunotherapy. There have also been several trials of T-cell checkpoint inhibitors in which PD-L1 expression in the tumor microenvironment has been associated with more favorable outcomes, although this has not been uniformly demonstrated. Other groups have used a larger panel of gene signatures, including Treg, CD8, cytokines, chemokines, and other factors, that correlate with therapeutic responses. These studies collectively suggest that there may be host, tumor, and immune factors that can be used for biomarker development. The importance of the tumor microenvironment has been appropriately stressed, but, practically, the ability to use serum or peripheral blood biomarkers is challenging and would be bolstered through utilization of the OCM.

Therapeutic Screening and Development

During early drug development, the primary goal of testing is to determine if the compound exhibits pharmacological activity that justifies commercial development. If so, the drug then moves into testing for safety. Minimum requirements for drug toxicity testing in non-clinical studies are regulated by agencies such as the FDA in the USA, the Committee for Medicinal Products for Humane Use in Europe, and the ministry of Health, Labor and Welfare in Japan. Common expectations for these agencies are provided by the International Committee on Harmonization (ICH[2]), which has developed standards for acceptable practices in drug development. ICH requires toxicity testing in two relevant animal species (137). Relevant animal species usually include one rodent, either a rat or mouse, and one large animal species. However, many of the available pre-clinical animal cancer models offer limited benefit for therapeutic screening, dosing, and development due to their lack of similar size and drug metabolism compared to humans.

[2]http://www.ich.org/home.html.

Several factors are considered when selecting the large animal species. Ethical and legal considerations encourage use of the lowest sentient species that will accomplish the scientific goals (121). Other criteria used in selecting a species include the generation of a similar metabolic profile to humans, appropriateness of the species for use in the laboratory environment, prior history of the species with similar classes of drugs, historical database, genetic and phenotypic variability of the species, and/or breed, ease of handling, source, and supply. Swine are not typically used during early drug development because of their large mass and the relative lack of drug until production scales up (138). However, swine have been used in safety assessment and are increasingly used because of similarities to humans in cardiovascular anatomy and physiology, integumentary system, digestive system, renal system, and immune system (139). The porcine *PXR* gene regulates hepatic genes involved in metabolism and transport. *PXR* activates *CYP3A*, which is involved in more than 50% of xenobiotic metabolism, by binding to its regulatory region. The porcine *PXR* gene is 87% homologous to human *PXR*, which represents a significant advantage compared to the 77% homology observed between human *PXR* and mouse *Pxr*. The OCM therefore represents an ideal model for the investigation of absorption, distribution, metabolism, excretion, and toxicity. In addition, the similar size between the OCM and humans, in contrast to small animal models, allows more accurate testing of optimal dose in a pre-clinical setting. Finally, as cancers in humans develop over many years on the background of comorbid disease, utilization of the OCM enables therapeutic screening and development in a setting closely mimicking molecular and clinical backgrounds. Therefore, the OCM represents an ideal model for the investigation of drug metabolism and toxicity predictive of human outcomes.

Prognostic Indicators

In an ever-changing world of medical research and disease treatment, prognostic indicators evolve as treatment avenues evolve. One key unmet clinical need that biomedical models can bridge is the investigation of prognostic indicators, thereby allowing clinicians to more accurately forecast patients' benefits resulting from treatment. As mentioned earlier, the OCM allows ample biospecimen (blood, saliva, urine, tissue, etc.) sampling and analysis. Furthermore, given the outbred nature of this model and the adequate supply, the OCM allows cohort investigation, which can provide sufficient unique analysis and volume to determine such prognostic indicators as progression-free survival (PFS) and time to progression (TTP). Based on the incidence of comorbid diseases, such as alcoholic cirrhosis and NASH, the OCM will allow precise diagnosis and prognostication.

Improved Imaging

The importance of diagnostic imaging in both research and treatment cannot be overstated. Medical imaging, in clinical practice, is used to diagnose, assess, and prognosticate patients' health over time. The size and anatomy of the OCM provides the ability to easily image—with various modalities including CT, MRI, PET, and ultrasound—in a similar setting as clinical practice. As a model of

disease, OCM imaging can be correlated with physical dissection to validate imaging findings, which cannot be done in human patients. Furthermore, the long lifespan and relatively low cost of the OCM permits frequent imaging and longitudinal studies from premalignant through metastatic disease states, which can assist in prognostic assessment and therapeutic response evaluation. The similar anatomy of the OCM allows deep investigation of angiographic imaging, which is limited or impossible in small animal models but is important for inducing disease as well as therapeutic research, as discussed in the following section.

Device Testing and Surgical Practice

Advancements in surgical technologies are necessary to improve outcomes for patients; however, pre-clinical models in which to test new strategies are limited. One aspect of testing new techniques or devices is the engineering capabilities or technical feasibility of the instrument or procedure; however, equally as important are the ergonomics and ability to translate the findings to human patients. Thus, selecting the appropriate animal model is one of the most important components of pre-clinical testing for these indications, and the animal model chosen should reflect the target patient population.

For a surgical device, technique, simulation, or practice, it is imperative that the anatomy, physiology, and disease state of the animal be similar to humans. As the size of medical devices and instruments used are optimized for human sized organs, a large animal model is ideal within ethical, safety, and financial considerations. Given the similarity of size of the swine organs, skin characteristics, and physiology/immunity; porcine models have become standard in multiple settings including cardiac/atherosclerosis (140), hernia, foregut, transplant (141), hepatobiliary (142), and minimally invasive surgery training and research programs (143, 144). As pigs are true ominvores, the physiology of digestion and liver metabolism are quite homologous, thus rendering the pig a valuable model for translational surgical research. However, what has been missing up until this time is a reliable model in which cancer treatment and resection could be tested. Though clearly this is valuable for an anti-tumor systemic treatment model, it is invaluable for the surgeon who wishes to test a catheter-based, resection-based, or technical procedure since the same instruments used in the human can be utilized in the animal. Furthermore, the OCM allows realistic tumor modeling in which tissue characteristics as a result of tumor growth are reliably recreated and margins can be assessed, both of which have been difficult to model by either orthotopic injections or biomaterial injections (145).

The OCM platform has already been applied to establish STS, HCC, and PDAC in target organs and, using the same sequence of gene mutations, is being used to create colon and other cancer models. Open, laparoscopic, and robotic liver, stomach, pancreas, small bowel, colon, and gallbladder resections have been performed on the OCM using the same instruments, devices, and techniques used in humans, including vascular staplers and energy devices. The size of sutures used in the OCM is the same as humans, and tissue characteristic are near identical from a surgical perspective. Therefore, we see the OCM as an ideal model for surgical technique and device testing in the management of cancers in multiple organs, recapitulating the human situation and allowing realistic and accurate practice in an animal model.

Development of Standards

The importance of standards development in the field of medical research is understood by veterinary and human clinical researchers alike. The National Cancer Institute supports standards' development throughout the cancer continuum, including such initiatives as the Veterinary Cooperative Oncology Group (VCOG), the cancer Data Standards Registry and Repository (caDSR), the National Clinical Trials Network (NCTN), and the Genomic Data Commons (GDC), to name a few. Standards, which can refer to data elements, data types and formats, programmatic interfaces, and operating procedures, enable potential data sharing across institutions, diseases, and research studies. With this in mind, the OCM platform was designed to develop and adhere to standards from the beginning. The OCM is part of a centralized platform that includes participating in clinical laboratory assessments, central data submission and management, a central imaging repository, and shared standard operating procedures. With the development and implementation of such standards, any present or future collaborator on OCM projects will have an additional dimension of comparative assessment for study validation.

FUTURE MODELING CAPABILITIES

In addition to the work currently underway to utilize the OCM to model the abovementioned cancer types, opportunity exists to utilize the OCM to model a wide range of additional cancers. While successful *in vitro* transformation and *in vivo* tumor formation has already been demonstrated in the OCM for three cancer types (STS, PDAC, and HCC), the ability to induce tumorigenesis in any cell type in a temporal and spatial manner provides the framework for modeling cancer types of all origins. While an exhaustive attempt to isolate and transform all OCM cell types has not been performed, to date researchers have not encountered an OCM cell isolate that has not been rendered tumorigenic following exposure to Cre recombinase (unpublished data; **Table 2**). The ability to transform all OCM cell types attempted to date highlights the potential for utilization in studies focused on

TABLE 2 | Oncopig cell isolates successfully transformed *in vitro*.

Cell type/origin	Isolated	Transformed
Fibroblasts	Yes	Yes
Hepatocytes	Yes	Yes
Pancreatic ductal cells	Yes	Yes
Dermal epithelial cells	Yes	Yes
Splenocytes	Yes	Yes
Ovarian surface epithelial cells	Yes	Yes
Fallopian tube secretory epithelial cells	Yes	Yes
Renal proximal tubule epithelial cells	Yes	Yes
Bone marrow (no specific cell isolation)	Yes	Yes
Testis (no specific cell isolation)	Yes	Yes
Skeletal muscle (no specific cell isolation)	Yes	Yes

List of OCM cell types for which isolation and transformation have been attempted.

additional cancer types, including colorectal, ovarian, fallopian tube, renal, bladder, and skin cancers.

In addition, the OCM is emerging as an excellent candidate for modeling leukemia, lymphoma, and other hematological cancers and their clinically associated comorbidities including obesity, myelodysplasia, age-related changes, and toxin-induced malignancies. Hematological malignancies in swine—reviewed in Ref. (146)—were first reported as early as 1865 (147) but as of yet, there is no porcine model of hematological malignancies that can be reliably induced and consistently reproduced. There is a wide spectrum of potential immunotherapy targets, cellular therapies, and gene targets that can be used to eradicate or control malignant hematopoietic stem cells. However, these therapies present significant safety challenges for patients that cannot be addressed by traditional procedures and require the development of new biomarker protocols and test systems, for which the rigorous use of large animal species will be required. A significant hindrance to development of therapies for hematological malignancies is the limited ability to detect, monitor, and quantify the etiology of hematological malignancies *in vivo*. Indeed, while current imaging strategies increase the predictive accuracy of new drug candidates, they are unsuitable for evaluating minimal residual disease, the foremost problem in current AML therapy. Temporal imaging of the OCM over the course of a disease or treatment regime would allow researchers a better appreciation of disease pathology, response to treatment, and drug pharmacokinetics. In addition, the OCM permits access to blood and bone marrow components, lymph nodes, spleen, and thymic tissue, allowing transformation of these multiple sources of hematopoietic cells. Moreover, the recent development of a porcine CD34 monoclonal antibody (Ozer et al., 2017, submitted) as well as the cloning of additional porcine hematopoietic cytokines and growth factors will enable studies of the regulatory aspects of leukemia and lymphoma development.

The ability to model these and other cancer types in the OCM is further facilitated by the ability to cross the OCM with other breeds, such as the Ossabaw, as well as other transgenic porcine models like the APC^{1311} porcine model of familial adenomatous polyposis (79). In addition, the successful utilization of CRISPR technology in pigs provides the opportunity to add additional mutations to the OCM background, allowing modeling of the same cancer type with varying underlying driver mutations, as well as cancer types with known genetic backgrounds. Finally, utilization of nanoparticle delivery systems can be utilized to selectively target Cre exposure *in vivo* to specific organs and cell types (148), allowing autochthonous tumor formation of known cellular origin. Together, this highlights the current and future capabilities of the highly customizable OCM to drive transitional cancer research and address unmet clinical needs.

AUTHOR CONTRIBUTIONS

KS, RS, JN, NK, MR, NM-E, PG, DP, AP, NO, GJ, KG, AM, LR, HO, RG, and LS wrote and approved the manuscript.

REFERENCES

1. Aravalli RN, Golzarian J, Cressman ENK. Animal models of cancer in interventional radiology. *Eur Radiol* (2009) 19:1049–53. doi:10.1007/s00330-008-1263-8
2. Cheon D-J, Orsulic S. Mouse models of cancer. *Annu Rev Pathol* (2011) 6:95–119. doi:10.1146/annurev.pathol.3.121806.154244
3. Frese KK, Tuveson DA. Maximizing mouse cancer models. *Nat Rev Cancer* (2007) 7:654–8. doi:10.1038/nrc2192
4. Rivina L, Schiestl R. Mouse models of radiation-induced cancers. *Adv Genet* (2013) 84:83–122. doi:10.1016/B978-0-12-407703-4.00003-7
5. Liu Y, Yin T, Feng Y, Cona MM, Huang G, Liu J, et al. Mammalian models of chemically induced primary malignancies exploitable for imaging-based preclinical theragnostic research. *Quant Imaging Med Surg* (2015) 5:708–29. doi:10.3978/j.issn.2223-4292.2015.06.01
6. Cheng Y, Ma Z, Kim B-H, Wu W, Cayting P, Boyle AP, et al. Principles of regulatory information conservation between mouse and human. *Nature* (2014) 515:371–5. doi:10.1038/nature13985
7. Rangarajan A, Weinberg RA. Opinion: comparative biology of mouse versus human cells: modelling human cancer in mice. *Nat Rev Cancer* (2003) 3:952–9. doi:10.1038/nrc1235
8. Luongo C, Dove WF. Somatic genetic events linked to the Apc locus in intestinal adenomas of the Min mouse. *Genes Chromosomes Cancer* (1996) 17:194–8. doi:10.1002/1098-2264(199611)17:3<194::AID-GCC2870170302>3.0.CO;2-E
9. Petursdottir TE, Thorsteinsdottir U, Jonasson JG, Moller PH, Huiping C, Bjornsson J, et al. Interstitial deletions including chromosome 3 common eliminated region 1 (C3CER1) prevail in human solid tumors from 10 different tissues. *Genes Chromosomes Cancer* (2004) 41:232–42. doi:10.1002/gcc.20072
10. Thiagalingam S, Laken S, Willson JK, Markowitz SD, Kinzler KW, Vogelstein B, et al. Mechanisms underlying losses of heterozygosity in human colorectal cancers. *Proc Natl Acad Sci U S A* (2001) 98:2698–702. doi:10.1073/pnas.051625398
11. Holliday R. Neoplastic transformation: the contrasting stability of human and mouse cells. *Cancer Surv* (1996) 28:103–15.
12. Kaiser J. The cancer test. *Science* (2015) 348:1411–3. doi:10.1126/science.348.6242.1411
13. Hamad NM, Elconin JH, Karnoub AE, Bai W, Rich JN, Abraham RT, et al. Distinct requirements for Ras oncogenesis in human versus mouse cells. *Genes Dev* (2002) 16:2045–57. doi:10.1101/gad.993902
14. Kim S, Kaminker P, Campisi J. Telomeres, aging and cancer: in search of a happy ending. *Oncogene* (2002) 21:503–11. doi:10.1038/sj.onc.1205077
15. Dolenšek J, Rupnik MS, Stožer A. Structural similarities and differences between the human and the mouse pancreas. *Islets* (2015) 7:e1024405. doi:10.1080/19382014.2015.1024405
16. Liu X-Y, Xue L, Zheng X, Yan S, Zheng S-S. Pancreas transplantation in the mouse. *Hepatobiliary Pancreat Dis Int* (2010) 9:254–8.
17. Hingorani SR, Wang L, Multani AS, Combs C, Deramaudt TB, Hruban RH, et al. Trp53R172H and KrasG12D cooperate to promote chromosomal instability and widely metastatic pancreatic ductal adenocarcinoma in mice. *Cancer Cell* (2005) 7:469–83. doi:10.1016/j.ccr.2005.04.023
18. Karim BO, Huso DL. Mouse models for colorectal cancer. *Am J Cancer Res* (2013) 3:240–50.
19. Swanson KS, Mazur MJ, Vashisht K, Rund LA, Beever JE, Counter CM, et al. Genomics and clinical medicine: rationale for creating and effectively evaluating animal models. *Exp Biol Med (Maywood)* (2004) 229:866–75. doi:10.1177/153537020422900902
20. Mak IW, Evaniew N, Ghert M. Lost in translation: animal models and clinical trials in cancer treatment. *Am J Transl Res* (2014) 6:114–8.
21. De Minicis S, Kisseleva T, Francis H, Baroni GS, Benedetti A, Brenner D, et al. Liver carcinogenesis: rodent models of hepatocarcinoma and cholangiocarcinoma. *Dig Liver Dis* (2013) 45:450–9. doi:10.1016/j.dld.2012.10.008
22. Shao DM, Wang QH, Chen C, Shen ZH, Yao M, Zhou XD, et al. N-acetylglucosaminyltransferase V activity in metastatic models of human hepatocellular carcinoma in nude mice. *J Exp Clin Cancer Res* (1999) 18:331–5.

23. Johnson RL, Fleet JC. Animal models of colorectal cancer. *Cancer Metastasis Rev* (2013) 32:39–61. doi:10.1007/s10555-012-9404-6
24. Bao Y, Hua B, Hou W, Shi Z, Li W, Li C, et al. Involvement of protease-activated receptor 2 in nociceptive behavior in a rat model of bone cancer. *J Mol Neurosci* (2014) 52:566–76. doi:10.1007/s12031-013-0112-7
25. Miyashita T, Miwa K, Fujimura T, Ninomiya I, Fushida S, Shah FA, et al. The severity of duodeno-esophageal reflux influences the development of different histological types of esophageal cancer in a rat model. *Int J Cancer* (2013) 132:1496–504. doi:10.1002/ijc.27824
26. Sanders J, Samuelson DJ. Significant overlap between human genome-wide association-study nominated breast cancer risk alleles and rat mammary cancer susceptibility loci. *Breast Cancer Res* (2014) 16:R14. doi:10.1186/bcr3607
27. Szpirer C. Cancer research in rat models. *Methods Mol Biol* (2010) 597:445–58. doi:10.1007/978-1-60327-389-3_30
28. Rashid OM, Takabe K. Animal models for exploring the pharmacokinetics of breast cancer therapies. *Expert Opin Drug Metab Toxicol* (2015) 11:221–30. d oi:10.1517/17425255.2015.983073
29. Pool SE, Bison S, Koelewijn SJ, van der Graaf LM, Melis M, Krenning EP, et al. mTOR inhibitor RAD001 promotes metastasis in a rat model of pancreatic neuroendocrine cancer. *Cancer Res* (2013) 73:12–8. doi:10.1158/0008-5472.CAN-11-2089
30. Ceol CJ, Houvras Y, Jane-Valbuena J, Bilodeau S, Orlando DA, Battisti V, et al. The histone methyltransferase SETDB1 is recurrently amplified in melanoma and accelerates its onset. *Nature* (2011) 471:513–7. doi:10.1038/nature09806
31. Howe K, Clark MD, Torroja CF, Torrance J, Berthelot C, Muffato M, et al. The zebrafish reference genome sequence and its relationship to the human genome. *Nature* (2013) 496:498–503. doi:10.1038/nature12111
32. Varshney GK, Sood R, Burgess SM. Understanding and editing the zebrafish genome. *Adv Genet* (2015) 92:1–52. doi:10.1016/bs.adgen.2015.09.002
33. Langenau DM, Traver D, Ferrando AA, Kutok JL, Aster JC, Kanki JP, et al. Myc-induced T cell leukemia in transgenic zebrafish. *Science* (2003) 299:887–90. doi:10.1126/science.1080280
34. Patton EE, Widlund HR, Kutok JL, Kopani KR, Amatruda JF, Murphey RD, et al. BRAF mutations are sufficient to promote nevi formation and cooperate with p53 in the genesis of melanoma. *Curr Biol* (2005) 15:249–54. doi:10.1016/j.cub.2005.01.031
35. Yen J, White RM, Stemple DL. Zebrafish models of cancer: progress and future challenges. *Curr Opin Genet Dev* (2014) 24:38–45. doi:10.1016/j.gde.2013.11.003
36. Parvinian A, Casadaban LC, Gaba RC. Development, growth, propagation, and angiographic utilization of the rabbit VX2 model of liver cancer: a pictorial primer and "how to" guide. *Diagn Interv Radiol* (2014) 20:335–40. doi:10.5152/dir.2014.13415
37. Tennant BC, Toshkov IA, Peek SF, Jacob JR, Menne S, Hornbuckle WE, et al. Hepatocellular carcinoma in the woodchuck model of hepatitis B virus infection. *Gastroenterology* (2004) 127:S283–93. doi:10.1053/j.gastro.2004.09.043
38. Burke CT, Cullen JM, State A, Gadi S, Wilber K, Rosenthal M, et al. Development of an animal model for radiofrequency ablation of primary, virally induced hepatocellular carcinoma in the woodchuck. *J Vasc Interv Radiol* (2011) 22:1613–8.e1. doi:10.1016/j.jvir.2011.08.020
39. Tennant BC, Gerin JL. The woodchuck model of hepatitis B virus infection. *ILAR J* (2001) 42:89–102. doi:10.1093/ilar.42.2.89
40. Meurens F, Summerfield A, Nauwynck H, Saif L, Gerdts V. The pig: a model for human infectious diseases. *Trends Microbiol* (2012) 20:50–7. doi:10.1016/j.tim.2011.11.002
41. Schook L, Beattie C, Beever J, Donovan S, Jamison R, Zuckermann F, et al. Swine in biomedical research: creating the building blocks of animal models. *Anim Biotechnol* (2005) 16:183–90. doi:10.1080/10495390500265034
42. Tumbelson M, Schook L. In: Tumbelson M, Schook L, editors. *Advances in Swine in Biomedical Research*. New York: Plenum Press (1996).
43. Paoloni MC, Khanna C. Comparative oncology today. *Vet Clin North Am Small Anim Pract* (2007) 37:1023–32. doi:10.1016/j.cvsm.2007.08.003
44. Breen M. Update on genomics in veterinary oncology. *Top Companion Anim Med* (2009) 24:113–21. doi:10.1053/j.tcam.2009.03.002
45. Gardner HL, Fenger JM, London CA. Dogs as a model for cancer. *Annu Rev Anim Biosci* (2016) 4:199–222. doi:10.1146/annurev-animal-022114-110911
46. Rowell JL, McCarthy DO, Alvarez CE. Dog models of naturally occurring cancer. *Trends Mol Med* (2011) 17:380–8. doi:10.1016/j.molmed.2011.02.004
47. Pang LY, Argyle DJ. Using naturally occurring tumours in dogs and cats to study telomerase and cancer stem cell biology. *Biochim Biophys Acta* (2009) 1792:380–91. doi:10.1016/j.bbadis.2009.02.010
48. Berger NA, Savvides P, Koroukian SM, Kahana EF, Deimling GT, Rose JH, et al. Cancer in the elderly. *Trans Am Clin Climatol Assoc* (2006) 117:147–55; discussion 155–6.
49. Pinho SS, Carvalho S, Cabral J, Reis CA, Gartner F. Canine tumors: a spontaneous animal model of human carcinogenesis. *Transl Res* (2012) 159:165–72. doi:10.1016/j.trsl.2011.11.005
50. Gordon I, Paoloni M, Mazcko C, Khanna C. The comparative oncology trials consortium: using spontaneously occurring cancers in dogs to inform the cancer drug development pathway. *PLoS Med* (2009) 6:e1000161. doi:10.1371/journal.pmed.1000161
51. Brown DC, Agnello K, Iadarola MJ. Intrathecal resiniferatoxin in a dog model. *Pain* (2015) 156:1. doi:10.1097/j.pain.0000000000000115
52. American Cancer Society. *Cancer Facts & Figures 2017*. Atlanta, GA: American Cancer Society (2017). p. 1–71. Available from: https://www.cancer.org/research/cancer-facts-statistics/all-cancer-facts-figures/cancer-facts-figures-2017.html
53. Lapin BA. Use of nonhuman primates in cancer research. *J Med Primatol* (1982) 11:327–41.
54. McClure H. Neoplastic diseases of nonhuman primates: literature review and observations in an autopsy series of 2176 animals. In: Montali R, Magaki G, editors. *The Comparative Pathology of Zoo Animals*. Washington, DC: Smithsonian Institution Press (1980). p. 549–65.
55. Remick AK, Van Wettere AJ, Williams CV. Neoplasia in prosimians: case series from a captive prosimian population and literature review. *Vet Pathol* (2009) 46:746–72. doi:10.1354/vp.08-VP-0154-R-FL
56. Simmons HA, Mattison JA. The incidence of spontaneous neoplasia in two populations of captive rhesus macaques (*Macaca mulatta*). *Antioxid Redox Signal* (2011) 14:221–7. doi:10.1089/ars.2010.3311
57. Rogers J, Gibbs RA. Content and dynamics. *Nat Rev Genet* (2014) 15:347–59. doi:10.1038/nrg3707.Comparative
58. Weber H. Factors affecting the choice of spoecies. In: Wolfe-Coote S, editor. *The Laboratory Primate*. Boston, MA: Elsevier Academic Press (2005). p. 259–72.
59. Chapman KL, Pullen N, Andrews L, Ragan I. The future of non-human primate use in mAb development. *Drug Discov Today* (2010) 15:235–42. doi:10.1016/j.drudis.2010.01.002
60. Swindle MM, Makin A, Herron AJ, Clubb FJ, Frazier KS. Swine as models in biomedical research and toxicology testing. *Vet Pathol* (2012) 49:344–56. doi:10.1177/0300985811402846
61. Whyte JJ, Prather RS. Genetic modifications of pigs for medicine and agriculture. *Mol Reprod Dev* (2011) 78:879–91. doi:10.1002/mrd.21333
62. Schook LB, Kuzmuk K, Adam S, Rund L, Chen K, Rogatcheva M, et al. DNA-based animal models of human disease: from genotype to phenotype. *Dev Biol (Basel)* (2008) 132:15–25.
63. Ganderup NC, Harvey W, Mortensen JT, Harrouk W. The minipig as nonrodent species in toxicology—where are we now? *Int J Toxicol* (2012) 31:507–28. doi:10.1177/1091581812462039
64. Flisikowska T, Kind A, Schnieke A. The new pig on the block: modelling cancer in pigs. *Transgenic Res* (2013) 22:673–80. doi:10.1007/s11248-013-9720-9
65. Helke KL, Swindle MM. Animal models of toxicology testing: the role of pigs. *Expert Opin Drug Metab Toxicol* (2013) 9:127–39. doi:10.1517/17425255.2013.739607
66. Watson AL, Carlson DF, Largaespada DA, Hackett PB, Fahrenkrug SC. Engineered swine models of cancer. *Front Genet* (2016) 7:78. doi:10.3389/fgene.2016.00078
67. Schachtschneider KM, Madsen O, Park C, Rund LA, Groenen MA, Schook LB. Adult porcine genome-wide DNA methylation patterns support pigs as a biomedical model. *BMC Genomics* (2015) 16:743. doi:10.1186/s12864-015-1938-x
68. Choi M, Lee J, Le MT, Nguyen DT, Park S, Soundrarajan N, et al. Genome-wide analysis of DNA methylation in pigs using reduced representation bisulfite sequencing. *DNA Res* (2015) 22:343–55. doi:10.1093/dnares/dsv017
69. Yeom S-C, Cho S-Y, Park C-G, Lee W-J. Analysis of reference interval and age-related changes in serum biochemistry and hematology in the specific pathogen free miniature pig. *Lab Anim Res* (2012) 28:245–53. doi:10.5625/lar.2012.28.4.245

70. Schook LB, Beever JE, Rogers J, Humphray S, Archibald A, Chardon P, et al. Swine genome sequencing consortium (SGSC): a strategic roadmap for sequencing the pig genome. *Comp Funct Genomics* (2005) 6:251–5. doi:10.1002/cfg.479
71. Groenen MAM, Archibald AL, Uenishi H, Tuggle CK, Takeuchi Y, Rothschild MF, et al. Analyses of pig genomes provide insight into porcine demography and evolution. *Nature* (2012) 491:393–8. doi:10.1038/nature11622
72. Flisikowska T, Kind A, Schnieke A. Pigs as models of human cancers. *Theriogenology* (2016) 86:433–7. doi:10.1016/j.theriogenology.2016.04.058
73. Schook LB, Rund L, Begnini KR, Remiao MH, Seixas FK, Collares T. Emerging technologies to create inducible and genetically defined porcine cancer models. *Front Genet* (2016) 7:28. doi:10.3389/fgene.2016.00028
74. Schachtschneider KM, Liu Y, Rund LA, Madsen O, Johnson RW, Groenen MAM, et al. Impact of neonatal iron deficiency on hippocampal DNA methylation and gene transcription in a porcine biomedical model of cognitive development. *BMC Genomics* (2016) 17:856. doi:10.1186/s12864-016-3216-y
75. Ji P, Schachtschneider KM, Schook LB, Walker FR, Johnson RW. Peripheral viral infection induced microglial sensome genes and enhanced microglial cell activity in the hippocampus of neonatal piglets. *Brain Behav Immun* (2016) 54:243–51. doi:10.1016/j.bbi.2016.02.010
76. Schachtschneider KM, Liu Y, Makelainen S, Madsen O, Rund LA, Groenen MAM, et al. Oncopig soft-tissue sarcomas recapitulate key transcriptional features of human sarcomas. *Sci Rep* (2017) 7(1):2624. doi:10.1038/s41598-017-02912-9
77. Schachtschneider KM, Schwind RM, Darfour-Oduro KA, De AK, Rund LA, Singh K, et al. A validated, transitional and translational porcine model of hepatocellular carcinoma. *Oncotarget* (2017). doi:10.18632/oncotarget.18872
78. Harding JJ, El Dika I, Abou-Alfa GK. Immunotherapy in hepatocellular carcinoma: primed to make a difference? *Cancer* (2016) 122:367–77. doi:10.1002/cncr.29769
79. Flisikowska T, Merkl C, Landmann M, Eser S, Rezaei N, Cui X, et al. A porcine model of familial adenomatous polyposis. *Gastroenterology* (2012) 143:1173–5.e1–7. doi:10.1053/j.gastro.2012.07.110
80. Saalfrank A, Janssen K-P, Ravon M, Flisikowski K, Eser S, Steiger K, et al. A porcine model of osteosarcoma. *Oncogenesis* (2016) 5:e210. doi:10.1038/oncsis.2016.19
81. Li X, Zhou X, Guan Y, Wang Y-XJ, Scutt D, Gong Q-Y. N-nitrosodiethylamine-induced pig liver hepatocellular carcinoma model: radiological and histopathological studies. *Cardiovasc Intervent Radiol* (2006) 29:420–8. doi:10.1007/s00270-005-0099-8
82. Mitchell J, Tinkey PT, Avritscher R, Van Pelt C, Eskandari G, Konnath George S, et al. Validation of a preclinical model of diethylnitrosamine-induced hepatic neoplasia in Yucatan miniature pigs. *Oncology* (2016) 91:90–100. doi:10.1159/000446074
83. Sieren JC, Meyerholz DK, Wang X-J, Davis BT, Newell JD, Hammond E, et al. Development and translational imaging of a TP53 porcine tumorigenesis model. *J Clin Invest* (2014) 124:4052–66. doi:10.1172/JCI75447
84. Gould SE, Junttila MR, de Sauvage FJ. Translational value of mouse models in oncology drug development. *Nat Med* (2015) 21:431–9. doi:10.1038/nm.3853
85. Myers MJ, Farrell DE, Howard KD, Kawalek JC. Identification of multiple constitutive and inducible hepatic cytochrome P450 enzymes in market weight swine. *Drug Metab Dispos* (2001) 29:908–15.
86. Roth WJ, Kissinger CB, McCain RR, Cooper BR, Marchant-Forde JN, Vreeman RC, et al. Assessment of juvenile pigs to serve as human pediatric surrogates for preclinical formulation pharmacokinetic testing. *AAPS J* (2013) 15:763–74. doi:10.1208/s12248-013-9482-6
87. Schook LB, Collares TV, Hu W, Liang Y, Rodrigues FM, Rund LA, et al. A genetic porcine model of cancer. *PLoS One* (2015) 10:e0128864. doi:10.1371/journal.pone.0128864
88. Pylayeva-Gupta Y, Grabocka E, Bar-Sagi D. RAS oncogenes: weaving a tumorigenic web. *Nat Rev Cancer* (2011) 11:761–74. doi:10.1038/nrc3106
89. Malkin D. Li-Fraumeni syndrome. *Genes Cancer* (2011) 2:475–84. doi:10.1177/1947601911413466
90. Linch M, Miah AB, Thway K, Judson IR, Benson C. Systemic treatment of soft-tissue sarcoma—gold standard and novel therapies. *Nat Rev Clin Oncol* (2014) 11:187–202. doi:10.1038/nrclinonc.2014.26
91. Taylor BS, Barretina J, Maki RG, Antonescu CR, Singer S, Ladanyi M. Advances in sarcoma genomics and new therapeutic targets. *Nat Rev Cancer* (2011) 11:541–57. doi:10.1038/nrc3087
92. Barretina J, Taylor BS, Banerji S, Ramos AH, Lagos-Quintana M, Decarolis PL, et al. Subtype-specific genomic alterations define new targets for soft-tissue sarcoma therapy. *Nat Genet* (2010) 42:715–21. doi:10.1038/ng.619
93. Dodd RD, Mito JK, Kirsch DG. Animal models of soft-tissue sarcoma. *Dis Model Mech* (2010) 3:557–66. doi:10.1242/dmm.005223
94. Sharma SV, Haber DA, Settleman J. Cell line-based platforms to evaluate the therapeutic efficacy of candidate anticancer agents. *Nat Rev Cancer* (2010) 10:241–53. doi:10.1038/nrc2820
95. Salawu A, Fernando M, Hughes D, Reed MWR, Woll P, Greaves C, et al. Establishment and molecular characterisation of seven novel soft-tissue sarcoma cell lines. *Br J Cancer* (2016) 115:1058–68. doi:10.1038/bjc.2016.259
96. Clif Burdette E, Ghoshal G, Williams E, Neubauer P, Frith L, Roady P, et al. Image-guided catheter-based ultrasound thermal ablation of tumors in genetically engineered oncogenic pigs. *Society for Thermal Medicine Annual Meeting*. Cancun (2017). Abstract #0130.
97. Di Giorgio E, Clocchiatti A, Piccinin S, Sgorbissa A, Viviani G, Peruzzo P, et al. MEF2 is a converging hub for histone deacetylase 4 and phosphatidylinositol 3-kinase/Akt-induced transformation. *Mol Cell Biol* (2013) 33:4473–91. doi:10.1128/MCB.01050-13
98. Siegel R, Ma J, Zou Z, Jemal A. Cancer statistics, 2014. *CA Cancer J Clin* (2014) 64:9–29. doi:10.3322/caac.21208
99. Diaz A, Principe D, DeCant B, Grippo PJ, Rund L, Schook LB. Abstract 4178: pigs as a new weapon against cancer: modeling solid tumors in porcine. *Cancer Res* (2016) 76(14 Suppl):4178. doi:10.1158/1538-7445.AM2016-4178
100. Sadanandam A, Wullschleger S, Lyssiotis CA, Grotzinger C, Barbi S, Bersani S, et al. A cross-species analysis in pancreatic neuroendocrine tumors reveals molecular subtypes with distinctive clinical, metastatic, developmental, and metabolic characteristics. *Cancer Discov* (2015) 5:1296–313. doi:10.1158/2159-8290.CD-15-0068
101. Yu R. Animal models of spontaneous pancreatic neuroendocrine tumors. *Mol Cell Endocrinol* (2016) 421:60–7. doi:10.1016/j.mce.2015.08.004
102. El-Serag HB, Marrero JA, Rudolph L, Reddy KR. Diagnosis and treatment of hepatocellular carcinoma. *Gastroenterology* (2008) 134:1752–63. doi:10.1053/j.gastro.2008.02.090
103. Hyder O, Dodson RM, Nathan H, Herman JM, Cosgrove D, Kamel I, et al. Referral patterns and treatment choices for patients with hepatocellular carcinoma: a United States population-based study. *J Am Coll Surg* (2013) 217:896–906. doi:10.1016/j.jamcollsurg.2013.07.007
104. Lee L, Alloosh M, Saxena R, Van Alstine W, Watkins BA, Klaunig JE, et al. Nutritional model of steatohepatitis and metabolic syndrome in the Ossabaw miniature swine. *Hepatology* (2009) 50:56–67. doi:10.1002/hep.22904
105. Hanahan D, Weinberg RA. Hallmarks of cancer: the next generation. *Cell* (2011) 144:646–74. doi:10.1016/j.cell.2011.02.013
106. Pagès F, Kirilovsky A, Mlecnik B, Asslaber M, Tosolini M, Bindea G, et al. In situ cytotoxic and memory T cells predict outcome in patients with early-stage colorectal cancer. *J Clin Oncol* (2009) 27:5944–51. doi:10.1200/JCO.2008.19.6147
107. Galon J, Costes A, Sanchez-Cabo F, Kirilovsky A, Mlecnik B, Lagorce-Pagès C, et al. Type, density, and location of immune cells within human colorectal tumors predict clinical outcome. *Science* (2006) 313:1960–4. doi:10.1126/science.1129139
108. Galon J, Fox BA, Bifulco CB, Masucci G, Rau T, Botti G, et al. Immunoscore and immunoprofiling in cancer: an update from the melanoma and immunotherapy bridge 2015. *J Transl Med* (2016) 14:273. doi:10.1186/s12967-016-1029-z
109. Gajewski TF, Schreiber H, Fu Y-X. Innate and adaptive immune cells in the tumor microenvironment. *Nat Immunol* (2013) 14:1014–22. doi:10.1038/ni.2703
110. Steptoe RJ, Ritchie JM, Wilson NS, Villadangos JA, Lew AM, Harrison LC. Cognate CD4+ help elicited by resting dendritic cells does not impair the induction of peripheral tolerance in CD8+ T cells. *J Immunol* (2007) 178:2094–103. doi:10.4049/jimmunol.178.4.2094

111. Wells JW, Cowled CJ, Farzaneh F, Noble A. Combined triggering of dendritic cell receptors results in synergistic activation and potent cytotoxic immunity. *J Immunol* (2008) 181:3422–31. doi:10.4049/jimmunol.181.5.3422
112. Nieuwenhuis I, Beenhakker N, Bogers WMJM, Otting N, Bontrop RE, Dubois P, et al. No difference in Gag and Env immune-response profiles between vaccinated and non-vaccinated rhesus macaques that control immunodeficiency virus replication. *J Gen Virol* (2010) 91:2974–84. doi:10.1099/vir.0.022772-0
113. Sørensen MR, Ilsøe M, Strube ML, Bishop R, Erbs G, Hartmann SB, et al. Sequence-based genotyping of expressed swine leukocyte antigen class I alleles by next-generation sequencing reveal novel swine leukocyte antigen class I haplotypes and alleles in Belgian, Danish, and Kenyan fattening pigs and Göttingen minipigs. *Front Immunol* (2017) 8:701. doi:10.3389/fimmu.2017.00701
114. Mair KH, Sedlak C, Käser T, Pasternak A, Levast B, Gerner W, et al. The porcine innate immune system: an update. *Dev Comp Immunol* (2014) 45:321–43. doi:10.1016/j.dci.2014.03.022
115. Darfour-Oduro KA, Megens H-J, Roca AL, Groenen MAM, Schook LB. Adaptive evolution of toll-like receptors (TLRs) in the family Suidae. *PLoS One* (2015) 10:e0124069. doi:10.1371/journal.pone.0124069
116. Darfour-Oduro KA, Megens H-J, Roca AL, Groenen MAM, Schook LB. Evolutionary patterns of toll-like receptor signaling pathway genes in the Suidae. *BMC Evol Biol* (2016) 16:33. doi:10.1186/s12862-016-0602-7
117. Darfour-Oduro KA, Megens H-J, Roca A, Groenen MAM, Schook LB. Evidence for adaptation of porcine toll-like receptors. *Immunogenetics* (2016) 68:179–89. doi:10.1007/s00251-015-0892-8
118. Montgomery C. Oncologic and toxicologic research: alleviation and control of pain and distress in laboratory animals. *Cancer Bull* (1990) 42:230–7.
119. van Loo PLP, Everse LA, Bernsen MR, Baumans V, Hellebrekers LJ, Kruitwagen CLJJ, et al. Analgesics in mice used in cancer research: reduction of discomfort? *Lab Anim* (1997) 31:318–25. doi:10.1258/002367797780596211
120. Perry P. The ethics of animal research: a UK perspective. *ILAR J* (2007) 48:42–6. doi:10.1093/ilar.48.1.42
121. Russell WMS, Burch RL. In: Russell WMS, Burch RL, editors. *The Principles of Humane Experimental Technique*. London: Methuen & Co. Ltd. (1959).
122. Melero I, Berman DM, Aznar MA, Korman AJ, Gracia JLP, Haanen J. Evolving synergistic combinations of targeted immunotherapies to combat cancer. *Nat Rev Cancer* (2015) 15:457–72. doi:10.1038/nrc3973
123. Postow MA, Harding J, Wolchok JD. Targeting immune checkpoints: releasing the restraints on anti-tumor immunity for patients with melanoma. *Cancer J* (2012) 18:153–9.
124. Dizon DS, Krilov L, Cohen E, Gangadhar T, Ganz PA, Hensing TA, et al. Clinical cancer advances 2016: annual report on progress against cancer from the American Society of Clinical Oncology. *J Clin Oncol* (2016) 34:987–1011. doi:10.1200/JCO.2015.65.8427
125. Ansell SM, Lesokhin AM, Borrello I, Halwani A, Scott EC, Gutierrez M, et al. PD-1 blockade with nivolumab in relapsed or refractory Hodgkin's lymphoma. *N Engl J Med* (2015) 372:311–9. doi:10.1056/NEJMoa1411087
126. Gettinger SN, Horn L, Gandhi L, Spigel DR, Antonia SJ, Rizvi NA, et al. Overall survival and long-term safety of nivolumab (anti-programmed death 1 antibody, BMS-936558, ONO-4538) in patients with previously treated advanced non-small-cell lung cancer. *J Clin Oncol* (2015) 33:2004–12. doi:10.1200/JCO.2014.58.3708
127. Larkin J, Lao CD, Urba WJ, McDermott DF, Horak C, Jiang J, et al. Efficacy and safety of nivolumab in patients with *BRAF* V600 mutant and *BRAF* wild-type advanced melanoma. *JAMA Oncol* (2015) 1:433. doi:10.1001/jamaoncol.2015.1184
128. Postow MA, Chesney J, Pavlick AC, Robert C, Grossmann K, McDermott D, et al. Nivolumab and ipilimumab versus ipilimumab in untreated melanoma. *N Engl J Med* (2015) 372:2006–17. doi:10.1056/NEJMoa1414428
129. Schumacher TN, Kesmir C, van Buuren MM. Biomarkers in cancer immunotherapy. *Cancer Cell* (2015) 27:12–4. doi:10.1016/j.ccell.2014.12.004
130. Rizvi NA, Hellmann MD, Snyder A, Kvistborg P, Makarov V, Havel JJ, et al. Mutational landscape determines sensitivity to PD-1 blockade in non-small cell lung cancer. *Science* (2015) 348:124–8. doi:10.1126/science.aaa1348
131. Van Allen EM, Miao D, Schilling B, Shukla SA, Blank C, Zimmer L, et al. Genomic correlates of response to CTLA-4 blockade in metastatic melanoma. *Science* (2015) 350:207–11. doi:10.1126/science.aad0095
132. Spencer KR, Wang J, Silk AW, Ganesan S, Kaufman HL, Mehnert JM. Biomarkers for immunotherapy: current developments and challenges. *Am Soc Clin Oncol Educ Book* (2016) 36:e493–503. doi:10.14694/EDBK_160766
133. Strimbu K, Tavel JA. What are biomarkers? *Curr Opin HIV AIDS* (2010) 5:463–6. doi:10.1097/COH.0b013e32833ed177
134. Fox BA, Schendel DJ, Butterfield LH, Aamdal S, Allison JP, Ascierto P, et al. Defining the critical hurdles in cancer immunotherapy. *J Transl Med* (2011) 9:214. doi:10.1186/1479-5876-9-214
135. Nelson D, Fisher S, Robinson B. The "Trojan Horse" approach to tumor immunotherapy: targeting the tumor microenvironment. *J Immunol Res* (2014) 2014:1–14. doi:10.1155/2014/789069
136. Das B, Tsuchida R, Malkin D, Koren G, Baruchel S, Yeger H. Hypoxia enhances tumor stemness by increasing the invasive and tumorigenic side population fraction. *Stem Cells* (2008) 26:1818–30. doi:10.1634/stemcells.2007-0724
137. Food and Drug Administration, HHS. International conference on harmonisation; guidance on M3(R2) nonclinical safety studies for the conduct of human clinical trials and marketing authorization for pharmaceuticals; availability. Notice. *Fed Regist* (2010) 75:3471–2.
138. Smith D, Trennery P. *Non-Rodent Selection in Pharmaceutical Toxicology*. A "Points to Consider" document developed by the ABPI in conjunction with UK Home Office. (2002). Available from: http://www.abpi.org.uk/our-work/library/guidelines/Pages/non-rodent.aspx
139. Stricker-Krongrad A, Shoemake CR, Pereira ME, Gad SC, Brocksmith D, Bouchard GF. Miniature swine breeds in toxicology and drug safety assessments. *Toxicol Pathol* (2016) 44:421–7. doi:10.1177/0192623315613337
140. Iqbal J, Chamberlain J, Francis SE, Gunn J. Role of animal models in coronary stenting. *Ann Biomed Eng* (2016) 44:453–65. doi:10.1007/s10439-015-1414-4
141. Cooper DKC, Satyananda V, Ekser B, van der Windt DJ, Hara H, Ezzelarab MB, et al. Progress in pig-to-non-human primate transplantation models (1998-2013): a comprehensive review of the literature. *Xenotransplantation* (2014) 21:397–419. doi:10.1111/xen.12127
142. Huisman F, van Lienden KP, Damude S, Hoekstra LT, van Gulik TM. A review of animal models for portal vein embolization. *J Surg Res* (2014) 191:179–88. doi:10.1016/j.jss.2014.05.089
143. Fritscher-Ravens A, Cuming T, Dhar S, Parupudi S, Patel K, Ghanbari A, et al. Endoscopic ultrasound-guided fine needle aspiration training: evaluation of a new porcine lymphadenopathy model for in vivo hands-on teaching and training, and review of the literature. *Endoscopy* (2013) 45:114–20. doi:10.1055/s-0032-1325931
144. Willingham FF, Gee DW, Sylla P, Kambadakone A, Singh AH, Sahani D, et al. Natural orifice versus conventional laparoscopic distal pancreatectomy in a porcine model: a randomized, controlled trial. *Gastrointest Endosc* (2009) 70:740–7. doi:10.1016/j.gie.2009.03.021
145. Matthes K, Thakkar SJ, Lee S-H, Gromski MA, Lim RB, Janschek J, et al. Development of a pancreatic tumor animal model and evaluation of NOTES tumor enucleation. *Surg Endosc* (2011) 25:3191–7. doi:10.1007/s00464-011-1686-1
146. Duran-Struuck R, Matar AJ, Huang CA. Myeloid leukemias and virally induced lymphomas in miniature inbred swine: development of a large animal tumor model. *Front Genet* (2015) 6:332. doi:10.3389/fgene.2015.00332
147. Bostock DE, Owen LN. Porcine and ovine lymphosarcoma: a review. *J Natl Cancer Inst* (1973) 50:933–9. doi:10.1093/jnci/50.4.933
148. Friedman AD, Claypool SE, Liu R. The smart targeting of nanoparticles. *Curr Pharm Des* (2013) 19:6315–29. doi:10.2174/13816128113199990375

Conflict of Interest Statement: The authors declare that the research was conducted in the absence of any commercial or financial relationships that could be construed as a potential conflict of interest.

frontiers in Oncology

PERSPECTIVE
published: 19 September 2017
doi: 10.3389/fonc.2017.00219

Models of Models: A Translational Route for Cancer Treatment and Drug Development

*Lesley A. Ogilvie[1], Aleksandra Kovachev[1], Christoph Wierling[1], Bodo M. H. Lange[1] and Hans Lehrach[1,2]**

[1] Alacris Theranostics GmbH, Berlin, Germany, [2] Max Planck Institute for Molecular Genetics, Berlin, Germany

Every patient and every disease is different. Each patient therefore requires a personalized treatment approach. For technical reasons, a personalized approach is feasible for treatment strategies such as surgery, but not for drug-based therapy or drug development. The development of individual mechanistic models of the disease process in every patient offers the possibility of attaining truly personalized drug-based therapy and prevention. The concept of virtual clinical trials and the integrated use of *in silico*, *in vitro*, and *in vivo* models in preclinical development could lead to significant gains in efficiency and order of magnitude increases in the cost effectiveness of drug development and approval. We have developed mechanistic computational models of large-scale cellular signal transduction networks for prediction of drug effects and functional responses, based on patient-specific multi-level omics profiles. However, a major barrier to the use of such models in a clinical and developmental context is the reliability of predictions. Here we detail how the approach of using "models of models" has the potential to impact cancer treatment and drug development. We describe the iterative refinement process that leverages the flexibility of experimental systems to generate highly dimensional data, which can be used to train and validate computational model parameters and improve model predictions. In this way, highly optimized computational models with robust predictive capacity can be generated. Such models open up a number of opportunities for cancer drug treatment and development, from enhancing the design of experimental studies, reducing costs, and improving animal welfare, to increasing the translational value of results generated.

Keywords: preclinical models, computational model, mechanistic modeling, genetically engineered mouse models, transgenic mice, model optimization

OPEN ACCESS

Edited by:
Michael Breitenbach, University of Salzburg, Austria

Reviewed by:
Michael Gerhard Löffler, University of Salzburg, Austria
Hans-Werner Mewes, Technische Universität München, Germany

***Correspondence:**
Hans Lehrach
lehrach@molgen.mpg.de

Specialty section:
This article was submitted to Molecular and Cellular Oncology, a section of the journal Frontiers in Oncology

Received: *26 June 2017*
Accepted: *01 September 2017*
Published: *19 September 2017*

Citation:
Ogilvie LA, Kovachev A, Wierling C, Lange BMH and Lehrach H (2017) Models of Models: A Translational Route for Cancer Treatment and Drug Development. Front. Oncol. 7:219. doi: 10.3389/fonc.2017.00219

MECHANISTIC MODELS IN ONCOLOGY

Despite major breakthroughs in cancer research and therapy, the disease still remains one of the world's major healthcare challenges. A challenge that is exacerbated in Europe due to an aging population (1) and associated increase in cancer incidence (2). Ultimately, identification of successful therapies is hampered by the high level of complexity and genetic heterogeneity existing even within single tumor types, causing a large fraction of patients to remain refractory to treatment even with the most effective drugs we have available today (3–7).

Whenever we deal with complex problems mistakes are unavoidable, often with catastrophic consequences. Computer models can be used to simulate complex situations prior to testing in reality, allowing us to make these inevitable mistakes *in silico* and helping us to successfully avoid their deleterious impacts.

Although used in many areas from the aviation industry to climate prediction, a computational modeling strategy is still not being applied within two areas that have a fundamental impact on our health, wellbeing, and even our survival: drug-based treatment and drug development. Both are areas in which we still proceed statistically, prescribing drugs that ultimately only help a very small fraction of the patients receiving them and that could have negative consequences. Adverse drug effects lead to nearly 200,000 deaths per year in Europe (8), with enormous associated economic costs (9).

To overcome this problem, we have to be able to generate sufficiently accurate models of an individual patient—a virtual self—that allow us to observe the effects of different therapies. The basis is a generic computational model with the ability to predict effects and side effects of different drugs and their combinations, which is individualized based on a detailed characterization of a patient by molecular, sensor, and other techniques. In oncology, for example, we should ideally reflect the heterogeneity of the tumor by modeling individual tumor cells, including the stroma, to determine response. In addition, aspects of the liver should also be considered to determine the pharmacogenetics of the drug. Side effects can be evaluated by incorporating a selection of normal cell types and if we want to predict the effects and side effects of immunotherapies, we should also include elements of the immune system.

Currently, we are building large-scale mechanistic computational models of the signal transduction networks in cells (or cell collectives), based on the ever-expanding biological knowledge base, e.g., on signaling pathways in human cells. For this, we are using PyBioS, currently in its third iteration (PyBioS3), an integrated software platform for the design, modeling, and simulation of cellular systems (10, 11). The current model integrates about 50 cancer-related signaling pathways and makes use of a large and growing information base on functional consequences of genetic variants and mechanistic drug action. See Ref. (12–16), for further details of the modeling system and it applications.

To provide personalized predictions, the models are typically individualized with next generation sequencing-derived omics data (e.g., genome and transcriptome) from a patient and in the case of cancer also from individual tumors. For drug response predictions, the drugs to be "screened" are regarded as molecular entities that typically affect molecular networks. This information is translated into systems of ordinary differential equations, which can be solved numerically to make predictions regarding the functional response of the system in response to perturbations, such as specific genetic variants and/or drugs and their combinations. Adaptation of the model to biological observations and experimental data calls for optimization approaches. As the models become more complex, it is becoming increasingly important to use advanced parameter estimation strategies (17–20) to fit the model to the data. This can be done based on data generated on the types of preclinical models discussed in this issue.

Cancer is suited particularly well to this type of approach, as it is fundamentally a cellular disease. In tandem, high levels of funding for cancer research in the last decades has generated much of the knowledge required to establish generic computational models, such as information on the basic mechanisms of cancer and drug action, including molecular targets [e.g., (21–25)]. Diseased tissues can also be obtained as surgical or biopsy material. This means we can actually observe the changes—often dramatic—occurring in the tumor genome and transcriptome, making it easier to understand the likely functional consequences. Last but not least, computing power is now at a level (26) that makes predictive modeling on a large scale a realistic prospect.

PREDICTING UNCERTAINTY

The use of such computational models for personalizing medicine in the clinic does, however, still face a number of challenges. One of the main barriers to routine implementation of computational models in clinical scenarios is the accuracy of the prediction. Just how reliable can predictive computational models be?

The generic mechanistic model we have created integrates major molecular species, i.e., representations of genes, proteins, protein complexes, metabolites, etc., and biochemical/cellular processes, together making up an *in silico* representation of the cellular signaling network. Furthermore, it integrates modifications of the molecular species that are associated with cancer onset and development, such as mutated genes and proteins, reflecting gain-of-function or loss-of-function of oncogenes or tumor suppressor genes. Understanding how such a complex system functions as a whole is inferred from examination of its individual parts and their interactions [e.g., see Ref. (27, 28)].

To ensure that such mechanistic models are predictive we need a detailed assessment of the most important underlying biological reactions. However, within the large-scale networks generated, much of this information, such as binding affinities, (de)phosphorylation rates and synthesis, and degradation rates, is not easily obtained experimentally. To overcome the lack of information on parameters needed for this, we originally used a Monte Carlo strategy, selecting multiple random parameter vectors for multiple solutions (12). The unknown kinetic parameters are repeatedly sampled from probability distributions of values and used in multiple parallel simulations.

As the models grow in size, representing more signaling pathways and cellular components, so does the inherent complexity of the model and the associated number of unknown parameters involved in each process (e.g., kinetic constants, component concentrations). The signal transduction model we are currently working with comprises hundreds of genes, their modifications, and associated interactions, equating to tens of thousands of parameters. To infer the unknown parameters within this growing large-scale network, parameter optimization and reverse engineering strategies are used to increase the accuracy of predictions. This essentially means using data generated in experimental systems, e.g., mouse models, organotypic cultures, and cell culture, as well as data from patients (if available), for evaluating drug effects and other functional responses on the phenotypic and molecular level. We are generating this type of data within

the scope of a number of national and international projects, such as the Horizon2020 project CanPathPro (www.canpathpro.eu); focused on the development of a combined experimental and systems biology platform for predictive modeling of cancer signaling, Treat20Plus, a German Federal Ministry of Education and Research funded project that uses a computational modeling approach to predict treatment outcome for metastatic skin cancer patients, and the recently concluded OncoTrack project [www.oncotrack.eu (15)], an IMI EU funded collaborative effort that aimed to develop and validate biomarkers for colon cancer, leveraging "virtual patient" models, and multi-level omics data to provide a personalized approach to the treatment of colon cancer. Using such data, we can train the model's parameters and structure, and validate the predictions made in an iterative fashion.

When using models of such scale, we are faced with the problem that the number of unknown parameters significantly outnumbers the datasets that can be accumulated, leading to limited identifiability of parameters. To identify model parameters, statistical methods such as Bayesian and frequentist estimation as well as global and local optimization techniques can be applied (29, 30). Partitioning of the datasets into training, validation, and test sets, i.e., cross validation, facilitates identification of optimized parameter vectors and provides an unbiased estimate of how these vectors actually perform with an independent dataset (31). However, due to the limited number of training datasets available, overfitting is likely to occur, e.g., predictions become overly influenced by "noise" in the dataset rather than the inherent trends, resulting in poor predictive performance. A number of approaches can be used to overcome overfitting, such as increasing the amount of data (real or *in silico*) and/or using regularization parameters, but with complex models these strategies may bring limited improvements. An alternative strategy is to reduce the number of parameters by simplifying the model using model reduction methods (32, 33). These approaches face the challenge of identifying simplified models that exhibit dynamics comparable with the original. Ensembles of parameters that fit the data can further reduce overfitting effects. Moreover, techniques from artificial intelligence, such as deep learning, can help to learn directly from the data in an unsupervised fashion, without even knowing the underlying model (34).

MODELS OF MODELS: THE USE OF PRECLINICAL MODELS FOR OPTIMIZING *IN SILICO* PREDICTIONS

We see preclinical experimental models, including PDXs and transgenic mice [genetically engineered mouse models (GEMMs)] as well as cell and organotypic cultures, as being an integral part of the development and optimization of mechanistic computational models with more robust predictive capacity.

In particular, the contribution of mouse models to the understanding of fundamental biological processes, cancer research, and drug development has been significant, albeit with inevitable pitfalls (35, 36). PDX models have been shown to recapitulate the major molecular features of the tumor of origin, and therefore have immense utility in translational cancer research and personalized medicine applications (37, 38). Similarly, transgenic cancer mouse models, in which gene deletion or expression can be targeted in a spatial or temporal manner, are becoming an increasingly useful tool for understanding biological processes and disease development. These genetically engineered mice develop tumors *de novo*, which closely mimic both the histopathological and molecular features of human tumors, and provide an experimentally tractable *in vivo* platform for investigating disease mechanisms and determining response to therapies (36, 39).

While each preclinical system has its particular merits and pitfalls, it is clear they can provide a flexible and accurate experimental test bed for training and validating computational models. As part of a number of research projects (e.g., CanPathPro, Treat20Plus, and OncoTrack), the flexibility of preclinical systems is being leveraged to iteratively improve the accuracy of *in silico* predictions, regarding the functional consequences of molecular alterations on the signal transduction network, and the corresponding response to *in silico* drug treatment.

Even at the level of cell culture, an opportunity is provided to engage in a depth and breadth of experimentation that may not be feasible, cost and time-wise, using more complex preclinical models such as PDXs and GEMMs. Due to the simplicity and low cost of cellular systems, in-depth experimentation is made possible. A systematic comparison of predicted and observed responses of different cell models—in the case of oncology, tumor cells—to a variety of drugs and their combinations can be conducted in a quantitative and time-resolved manner. The observed phenotypic responses, e.g., does the cell respond to a drug or not, can be evaluated in the context of their specific molecular profiles. In addition, cell lines or organoids can be used for time-resolved analysis of the molecular changes (e.g., transcriptome, proteome, metabolome, and other omics-strategies) triggered by adding a drug or drugs under investigation. In-depth data are generated that is likely to be required for model optimization in high-dimensional parameter spaces. This detailed comparison of a cellular model at the phenotypic and molecular level with the predicted behavior of its computational avatar provides an essential data foundation that enables fine-scale optimization and increased predictive accuracy of *in silico* models. Computational models can be optimized in an iterative fashion through *in silico* perturbation experiments and subsequent validation of parameter information and functional response within experimental systems. See **Figure 1**, for a typical iterative workflow.

A stepwise process is taken in which the generic cellular signaling model is first adapted to the cancer being studied, with additional relevant pathways and mutations being added as modular elements [see (13, 16)]. Next, multi-tiered omics data from model samples (e.g., tumor and control samples from PDXs and transgenic mice or organotypic/tumor cell culture samples) is acquired and analyzed for alterations such as single nucleotide polymorphisms, gene fusions, and mutations. These data are integrated into the signaling network in modular format to individualize and calibrate the model.

Given that many parameters will be unknown, estimation strategies are applied [as detailed above and in Ref. (13, 16)] and the effects of perturbations (e.g., genetic variants and/or drugs), in combination with omics data (e.g., transcriptome of

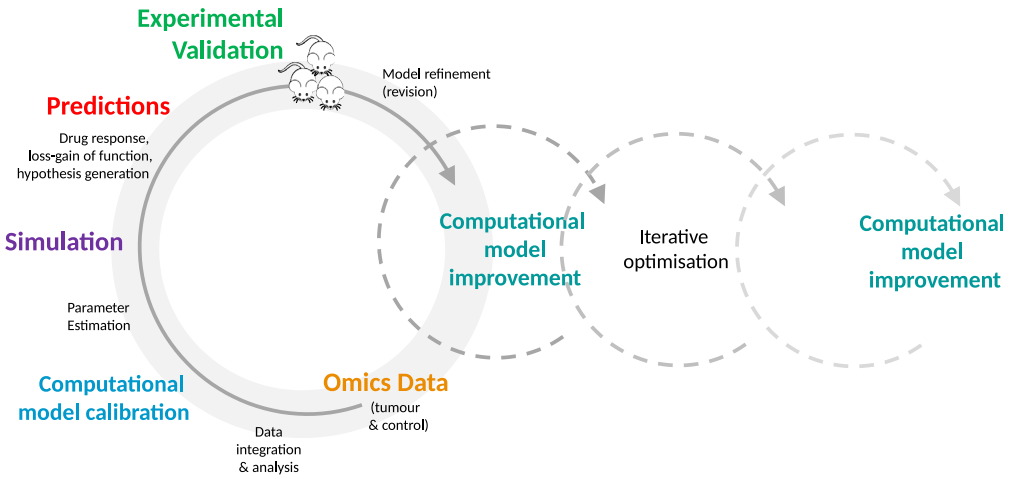

FIGURE 1 | The iterative optimization cycle. From data integration and analysis to computational model development and optimization. Multi-tiered omics data generated from experimental models (e.g., mice or cell lines) are integrated into the generic signaling model and used to train the model. The estimated model parameters are then used to simulate the effect of perturbations, such as molecular alterations and drugs. The resulting predictions are validated in the experimental model by comparison with the expected values. This process is repeated on an iterative basis, enabling identification of key parameters, furthering mechanistic understanding of disease processes and drug action, and increasing the predictive accuracy of the model.

the respective samples), on network components are simulated. The generated simulation data are analyzed to make predictions regarding functional effects within the network, using indicators such as Myc levels or caspase activity as a proxy for phenotypic effects (e.g., cell proliferation, apoptosis). These predictions, including drug response, can subsequently be validated in an experimental system such as a PDX or cell culture. This detailed comparison of experimental results and predictions enables us to further refine our definition of the computational parameter space used for modeling, identifying parameters that are key to generating accurate predictions and that influence the phenotype of interest.

We are taking such an iterative approach within CanPathPro (www.canpathpro.eu), an EU Horizon2020 funded project, which focuses on the development of a combined experimental and systems biology platform for predictive modeling of cancer signaling. GEMMs, GEMM-derived cell lines, and organotypic cultures are used to provide an accurate route toward mapping the functional changes (e.g., deregulated pathways, pathway modules, and expression signatures) associated with a variety of mutated or over-expressed oncogenes and tumor suppressor genes that lead to different lung or breast cancer phenotypes.

For *in silico* experiments, a generic mouse-specific computational model has been generated based on the human-specific ModCell™ model (12, 13), leveraging the conservation and homologies existing between human and mouse genes, proteins, network structure, individual signaling relevant protein–protein interactions, and post-translational events (40–45). The mouse-specific computational model is then "personalized" with multi-layered omics data (e.g., exome, transcriptome, quantitative proteome, and phosphoproteome data), from individual tumor and control mouse tissues at different disease stages. This provides the model with essential information on parameters, such as presence or absence of mutations (including their frequencies), protein synthesis rates (derived from RNA-Seq data), and protein decay rates (e.g., derived from pulse chase experiments). Local and global optimization methods are employed to infer unknown parameters and ensembles of models with different parameter sets are used to simulate multiple hypothetical loss-/gain-of-function and under-/over-expression experiments or alternative interactions among the model components. These simulations lead to the formulation of testable hypotheses, such as determination of a specific cancer phenotype, pathway activity, and/or cross-talk. The perturbations that have the strongest effect on measurable read-out components are most likely to be used to reject or accept a hypothesis. Selected hypotheses can then be tested experimentally, first in cell lines and organotypic cultures and then in mouse models. Based on the outcome of these validation experiments, the quality and precision of the computational model predictions can be improved (see also **Figure 1** for a depiction of the iterative process). These systematic and detailed investigations will enhance the design of experiments and facilitate identification of new mechanistic interactions as well as synergistic and cross-talk effects between the cancer pathways.

Overall, the abundance of data that can be generated within preclinical systems provides a platform for validating computational model predictions, identifying the areas of the parameter space that correspond most closely to reality. More accurate identification of this space can reduce the gap between prediction and reality, improving the ability of the model to make accurate predictions, and potentially improving the translational capacity of results for the human system.

MODELS OF MODELS: ACCELERATING DRUG DEVELOPMENT

The drug development pipeline is notoriously fraught with difficulties. Preclinical models are a pivotal part of this pipeline,

bridging the translational gap from bench to bedside, however, approval rates of new drugs, especially in oncology, remain critically low—only ~5% of cancer drugs currently in Phase I trials will make it to market (46). A process with associated costs that amount to billions of dollars (47, 48). The reasons for such high attrition rates are complex and include the typically low response rate of patients to drugs, leading to the failure of late stage non-stratified clinical trials, usually after hundreds of millions to billions of dollars expenditure. Another key factor is the poor predictivity of preclinical models. Approximately 85% of drugs that have been successful in preclinical tests fail in early clinical trials, with cancer drugs making up the largest proportion of failures [reviewed in Ref. (49)]. Given that preclinical testing remains an integral part of the regulatory roadmap for drug development and approval, better approaches for improving the translational capacity of results generated are required.

In addition to virtual humans (either individual patients, or patients in large clinical trials), there is also the potential to model the large number of experimental models which are used during the preclinical phase of drug development. A highly optimized computational model opens up a range of opportunities for enhancing the design of experimental studies, thereby minimizing the number of experimental animals required, significantly reducing costs and improving animal welfare, and importantly, increasing the translational value of results generated.

The current strategy of directly extrapolating results of models to humans tends to ignore the enormous differences in the biology of models and human. It is really not very surprising that this will lead to imprecise predictions. After all, even the comparatively minor differences between different patients can cause enormous differences in response to already approved drugs (50). In a sense, we are trying to do the equivalent of directly transferring the results of a model plane in a wind tunnel to a large passenger plane, without taking into account key information on scaling effects and different aerodynamics.

To increase the translational success from experimental models to humans, we should first compare the results obtained from experimental models to the predictions obtained by computational modeling, e.g., the effects of a drug on a computer model of the animal or cell model, adapting this computer model first. This adaptation can then be transferred to the human model of each individual patient; an equivalent strategy to that used in airplane design.

Deployment of *in silico* models at multiple stages throughout the drug development process (**Figure 2**) provides an opportunity to streamline the pipeline. During the early stages of drug development, *in silico* models can be deployed for selecting the most relevant drugs (and indeed models) for further development. Computational model-based knowledge gains in our understanding of the functional effects of disease-related molecular alterations could provide an effective pre-screening framework for selection of top priority candidates. By simulating the perturbation(s) occurring within the cellular transduction network, such as genetic alterations and drug treatment, *in silico* modeling has the capacity to improve understanding of disease progression and drug action. Model-based predictions of drug response/resistance and/or mode of action, based on the molecular profile of a specific experimental model, can in turn be independently validated in a preclinical experimental system using a variety of genetic manipulation techniques (e.g., RNA interference, over-expression analyses, etc.). In tandem, scope is provided to undertake experimental studies *in silico* that would not be possible due to cost and animal welfare constraints; for instance, more in-depth temporal investigations and extended screening of drug combinations.

A more robust translational route can be taken that combines the flexibility of optimized computational model predictions with experimental data, ultimately delivering benefits for patients.

OUTLOOK

Ultimately, the goal of any modeling approach is to generate results that will have a positive impact on patient outcomes and wellbeing, making it theoretically possible to identify the optimal

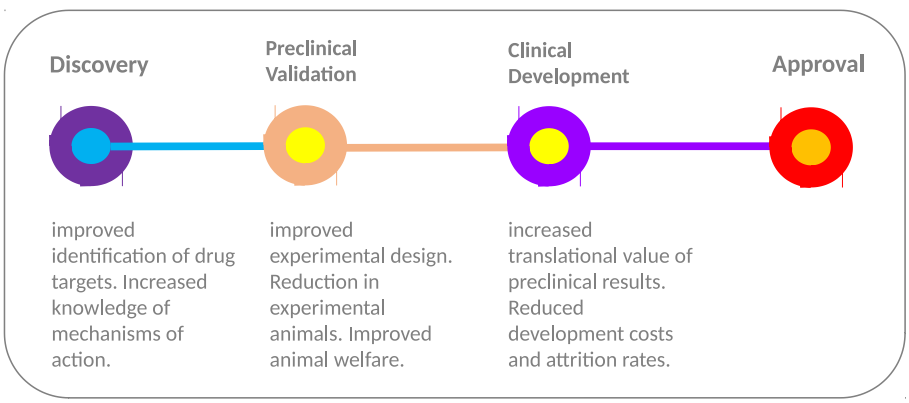

FIGURE 2 | From discovery to approval. The use of computational models throughout the drug development process provides the scope to improve experimental design and increase the translational value of early and preclinical stage results. The "models of models" approach provides a flexible test bed, enabling extended testing not feasible in animal models due to welfare and economic concerns. In combination with highly optimized computational models with more robust predictive capacity, the approach has the potential to increase the translational value of preclinical results and improve the high level of drug attrition rates, especially within the cancer arena.

therapy or preventive measure for every individual patient. Cancer models, whether experimental or computational, allow us to conduct investigations that are not possible on patients due to welfare, ethical, and economic considerations, generating information that will, in the short or long term, benefit patients. However, most model systems fail to fully recapitulate the human situation. In tandem with issues of experimental design, these inherent shortcomings will impact the translational value of models, exemplified by the high rates of attrition when preclinical findings are translated to clinical scenarios. It is also clear that existing computer models do not reflect the full complexity of the biological systems being simulated. Our own mechanistic models incorporate only a fraction of all human protein coding genes (ca. 2.5%) and do not reflect all aspects that play a role in a patient's response to drugs, such as the immune system, metabolism, and the microbial milieu associated with tumors. As our knowledge accumulates on these aspects, including the molecular mechanisms underlying interactions between tumor cells, their surrounding soma cells, and infiltrating cells of the immune system, more complex computational models can be developed that reflect the true complexity and heterogeneity of tumors. We are continually working on these components, but for now take a pragmatic approach that has enabled the generation of a generic mechanistic model of a large-scale cellular signaling network capable of predicting patient-specific responses to miRNA-based treatments (14). Within the framework of a number of preclinical and clinical studies, issues of accuracy, sensitivity, and uncertainty are being addressed, as the model is expanded, optimized, and validated.

The tandem use of *in silico* and preclinical models—models of models—provides a necessary and complementary approach for improving the translational value of both model types. By leveraging the flexibility of experimental systems to generate datasets from multiple experimental set-ups, we have the potential to develop highly optimized and validated computational models, with robust predictive potential. This extends from improving the predictive accuracy of the *in silico* model through iterative rounds of experimentation and validation to enhancing preclinical experimental study design, opening up the possibility of minimizing the number of animals or experiments required, thereby improving animal welfare and reducing costs.

AUTHOR CONTRIBUTIONS

LO wrote the first draft of the manuscript. LO, AK, CW, BL, and HL contributed to the writing of the manuscript. LO, AK, CW, BL, and HL jointly developed the structure and arguments for the paper. All authors reviewed and approved the final manuscript.

ACKNOWLEDGMENTS

The authors would like to thank their colleagues at Alacris Theranostics GmbH and the Dahlem Centre for Genome Research and Medical Systems Biology (DCGMS), for fruitful discussions and constructive criticism. This work has received funding from the European Union's Horizon 2020 research and innovation programme under grant agreement No. 686282 (CanPathPro).

REFERENCES

1. European Commission. *The 2015 Ageing Report. Economic and Budgetary Projections for the EU 28 Member States (2013–2060)*. Report No.: 3 Directorate-General for Economic and Financial Affairs, European Economy (2015).
2. Ferlay J, Soerjomataram I, Ervik M, Dikshit R, Eser S, Mathers C, et al. *GLOBOCAN 2012 v1.0, Cancer Incidence and Mortality Worldwide: IARC CancerBase No. 11*. Lyon, France: International Agency for Research on Cancer (2013).
3. Gerlinger M, Swanton C. How Darwinian models inform therapeutic failure initiated by clonal heterogeneity in cancer medicine. *Br J Cancer* (2010) 103(8):1139–43. doi:10.1038/sj.bjc.6605912
4. Meacham CE, Morrison SJ. Tumour heterogeneity and cancer cell plasticity. *Nature* (2013) 501:328–37. doi:10.1038/nature12624
5. Burrell RA, McGranahan N, Bartek J, Swanton C. The causes and consequences of genetic heterogeneity in cancer evolution. *Nature* (2013) 501:338–45. doi:10.1038/nature12625
6. Fisher R, Pusztai L, Swanton C. Cancer heterogeneity: implications for targeted therapeutics. *Br J Cancer* (2013) 108(3):479–85. doi:10.1038/bjc.2012.581
7. Gerlinger M, Rowan AJ, Horswell A, Math M, Larkin J, Endesfelder D, et al. Intratumor heterogeneity and branched evolution revealed by multiregion sequencing. *N Engl J Med* (2016) 366(10):883–92. doi:10.1056/NEJMoa1113205
8. European Commission. *Proposal for a Regulation Amending, as Regards Pharmacovigilance of Medicinal Products for Human Use. Regulation (EC) No 726/2004. Impact Assessment*. (2008). Available from: http://ec.europa.eu/health/files/pharmacos/pharmpack_12_2008/pharmacovigilance-ia-vol1_en.pdf
9. Sultana J, Cutroneo P, Trifirò G. Clinical and economic burden of adverse drug reactions. *J Pharmacol Pharmacother* (2013) 4:S73–7. doi:10.4103/0976-500X.120957
10. Wierling C, Herwig R, Lehrach H. Resources, standards and tools for systems biology. *Brief Funct Genomic Proteomic* (2007) 6(3):240–51. doi:10.1093/bfgp/elm027
11. Klipp E, Liebermeister W, Wierling C, Lehrach H, Herwig R. *Systems Biology: A Textbook*. Weinheim: Wiley-VCH GmbH & Co. KgaA (2009).
12. Wierling C, Kühn A, Hache H, Daskalaki A, Maschke-Dutz E, Peycheva S, et al. Prediction in the face of uncertainty: a Monte Carlo-based approach for systems biology of cancer treatment. *Mutat Res* (2012) 746(2):163–70. doi:10.1016/j.mrgentox.2012.01.005
13. Wierling C, Kessler T, Ogilvie LA, Lange BM, Yaspo ML, Lehrach H. Network and systems biology: essential steps in virtualising drug discovery and development. *Drug Discov Today Technol* (2015) 15:33–40. doi:10.1016/j.ddtec.2015.07.002
14. Röhr C, Kerick M, Fischer A, Kühn A, Kashofer K, Timmermann B, et al. High-throughput miRNA and mRNA sequencing of paired colorectal normal, tumor and metastasis tissues and bioinformatic modeling of miRNA-1 therapeutic applications. *PLoS One* (2013) 8(7):e67461. doi:10.1371/journal.pone.0067461
15. Henderson D, Ogilvie LA, Hoyle N, Keilholz U, Lange B, Lehrach H. Personalized medicine approaches for colon cancer driven by genomics and systems biology: OncoTrack. *Biotechnol J* (2014) 9(9):1104–14. doi:10.1002/biot.201400109
16. Ogilvie LA, Wierling C, Kessler T, Lehrach H, Lange BM. Predictive modeling of drug treatment in the area of personalized medicine. *Cancer Inform* (2015) 14:95–103. doi:10.4137/CIN.S1933
17. Banga JR, Balsa-Canto E. Parameter estimation and optimal experimental design. *Essays Biochem* (2008) 45:195–210. doi:10.1042/BSE0450195
18. Ashyraliyev M, Fomekong-Nanfack Y, Kaandorp JA, Blom JG. Systems biology: parameter estimation for biochemical models. *FEBS J* (2009) 276(4):886–902. doi:10.1111/j.1742-4658.2008.06844.x
19. Cedersund G, Samuelsson O, Ball G, Tegnér J, Gomez-Cabrero D. Optimization in biology parameter estimation and the associated optimization problem. In: Geris L, Gomez-Cabrero D, editors. *Uncertainty in Biology: A Computational Modeling Approach*. Cham: Springer (2016). p. 177–97.
20. Penas DR, González P, Egea JA, Doallo R, Banga JR. Parameter estimation in large-scale systems biology models: a parallel and self-adaptive cooperative strategy. *BMC Bioinformatics* (2017) 18(1):52. doi:10.1186/s12859-016-1452-4

21. Hanahan D, Weinberg RA. The hallmarks of cancer. *Cell* (2000) 100(1):57–70. doi:10.1016/S0092-8674(00)81683-9
22. Hanahan D, Weinberg RA. Hallmarks of cancer: the next generation. *Cell* (2011) 144(5):646–74. doi:10.1016/j.cell.2011.02.013
23. Santos R, Ursu O, Gaulton A, Bento AP, Donadi RS, Bologa CG, et al. A comprehensive map of molecular drug targets. *Nat Rev Drug Discov* (2017) 16(1):19–34. doi:10.1038/nrd.2016.230
24. Csermely P, Korcsmáros T, Kiss HJ, London G, Nussinov R. Structure and dynamics of molecular networks: a novel paradigm of drug discovery: a comprehensive review. *Pharmacol Ther* (2013) 138(3):333–408. doi:10.1016/j.pharmthera.2013.01.016
25. Karaman MW, Herrgard S, Treiber DK, Gallant P, Atteridge CE, Campbell B, et al. A quantitative analysis of kinase inhibitor selectivity. *Nat Biotechnol* (2008) 26(1):127–32. doi:10.1038/nbt1358
26. Processing Power Compared. Visualizing a 1 trillion-fold increase in computing performance. *Experts Exchange*. (2015). Available from: http://pages.experts-exchange.com/processing-power-compared/
27. Kitano H. Systems biology: a brief overview. *Science* (2002) 295(5560):1662–4. doi:10.1126/science.1069492
28. Klipp E, Liebermeister L, Wierling C, Kowald A. *Systems Biology. A Textbook*. Weinheim: Wiley-Blackwell (2016). 504 p.
29. Villaverde AF, Banga JR. Reverse engineering and identication in systems biology: strategies, perspectives and challenges. *J R Soc Interface* (2014) 11(91):20130505. doi:10.1098/rsif.2013.0505
30. Fröhlich F, Kaltenbacher B, Theis FJ, Hasenauer J. Scalable parameter estimation for genome-scale biochemical reaction networks. *PLoS Comput Biol* (2017) 13(1):e1005331. doi:10.1371/journal.pcbi.1005331
31. Hastie T, Tibshirani R, Friedman J. *The Elements of Statistical Learning: Data Mining, Inference and Prediction*. 2nd ed. New York: Springer Series in Statistics (2008). p. 241–9.
32. Henriques D, Villaverde AF, Rocha M, Saez-Rodriguez J, Banga JR. Data-driven reverse engineering of signaling pathways using ensembles of dynamic models. *PLoS Comput Biol* (2017) 13(2):e1005379. doi:10.1371/journal.pcbi.1005379
33. Rao S, Van der Schaft A, Van Eunen K, Bakker BM, Jayawardhana B. A model reduction method for biochemical reaction networks. *BMC Syst Biol* (2014) 8(1):52. doi:10.1186/1752-0509-8-52
34. Angermueller C, Pärnamaa T, Parts L, Stegle O. Deep learning for computational biology. *Mol Syst Biol* (2016) 12(7):878. doi:10.15252/msb.20156651
35. Day CP, Merlino G, Van Dyke T. Preclinical mouse cancer models: a maze of opportunities and challenges. *Cell* (2000) 163(1):39–53. doi:10.1016/j.cell.2015.08.068
36. Kersten K, de Visser KE, van Miltenburg MH, Jonkers J. Genetically engineered mouse models in oncology research and cancer medicine. *EMBO Mol Med* (2017) 9(2):137–53. doi:10.15252/emmm.201606857
37. Schütte M, Risch T, Abdavi-Azar N, Boehnke K, Schumacher D, Keil M, et al. Molecular dissection of colorectal cancer in pre-clinical models identifies biomarkers predicting sensitivity to EGFR inhibitors. *Nat Commun* (2017) 8:14262. doi:10.1038/ncomms14262
38. Morgan KM, Riedlinger GM, Rosenfeld J, Ganesan S, Pine SR. Patient-derived xenograft models of non-small cell lung cancer and their potential utility in personalized medicine. *Front Oncol* (2017) 7:2. doi:10.3389/fonc
39. van Miltenburg MH, Jonkers J. Using genetically engineered mouse models to validate candidate cancer genes and test new therapeutic approaches. *Curr Opin Genet Dev* (2012) 22(1):21–7. doi:10.1016/j.gde.2012.01.004
40. Kitano H. Biological robustness. *Nat Rev Genet* (2004) 5(11):826–37. doi:10.1038/nrg1471
41. Pires-daSilva A, Sommer RJ. The evolution of signalling pathways in animal development. *Nat Rev Genet* (2003) 4(1):39–49. doi:10.1038/nrg977
42. Cheng Y, Ma Z, Kim BH, Wu W, Cayting P, Boyle AP, et al. Principles of regulatory information conservation between mouse and human. *Nature* (2014) 515(7527):371–5. doi:10.1038/nature13985
43. Stergachis AB, Neph S, Sandstrom R, Haugen E, Reynolds AP, Zhang M, et al. Conservation of trans-acting circuitry during mammalian regulatory evolution. *Nature* (2014) 515(7527):365–70. doi:10.1038/nature13972
44. Tan CS, Bodenmiller B, Pasculescu A, Jovanovic M, Hengartner MO, Jørgensen C, et al. Comparative analysis reveals conserved protein phosphorylation networks implicated in multiple diseases. *Sci Signal* (2009) 2(81):ra39. doi:10.1126/scisignal.2000316
45. Kiel C, Aydin D, Serrano L. Association rate constants of ras-effector interactions are evolutionarily conserved. *PLoS Comput Biol* (2008) 4(12):e1000245. doi:10.1371/journal.pcbi.1000245
46. Thomas DW, Burns J, Audette J, Carroll A, Dow-Hygelund C, Hay M. *Clinical Development Success Rates 2006–2015*. Biotechnology Innovation Organization (BIO) (2016). Available from: https://www.bio.org/sites/default/files/Clinical Development Success Rates 2006-2015 - BIO, Biomedtracker, Amplion 2016.pdf [Accessed 30 May 2017].
47. Herper M. *The Cost of Creating a New Drug Now $5 Billion, Pushing Big Pharma to Change*. New Jersey: Forbes, Pharma & Healthcare (2013). Available from: https://www.forbes.com/sites/matthewherper/2013/08/11/how-the-staggering-cost-of-inventing-new-drugs-is-shaping-the-future-of-medicine/#3df7a07e13c3
48. DiMasi JA, Grabowski HG, Hansen RW. *Innovation in the Pharmaceutical Industry: New Estimates of R&D Costs*. Boston: Tufts Center for the Study of Drug Development (2014). Available from: http://csdd.tufts.edu/news/complete_story/cost_study_press_event_webcast
49. Mak IW, Evaniew N, Ghert M. Lost in translation: animal models and clinical trials in cancer treatment. *Am J Transl Res* (2014) 6(2):114–8.
50. Schork NJ. Personalized medicine: time for one-person trials. *Nature* (2015) 520(7549):609–11. doi:10.1038/520609a

Conflict of Interest Statement: All authors are affiliated with Alacris Theranostics GmbH, which aims to develop "virtual patient" models for use in therapy choice and drug development.

The reviewer, ML, and handling editor declared their shared affiliation.

frontiers in Oncology

ORIGINAL RESEARCH
published: 30 August 2017
doi: 10.3389/fonc.2017.00189

Modeling Cancer Cell Growth Dynamics *In vitro* in Response to Antimitotic Drug Treatment

Alexander Lorz[1,2], *Dana-Adriana Botesteanu*[3,4] *and Doron Levy*[4]*

[1]CEMSE Division, King Abdullah University of Science and Technology (KAUST), Thuwal, Saudi Arabia, [2]Sorbonne Universités, UPMC Univ Paris 06, UMR 7598, Laboratoire Jacques-Louis Lions, Paris, France, [3]Women's Malignancies Branch, Center for Cancer Research, National Cancer Institute, Bethesda, MD, United States, [4]Department of Mathematics and Center for Scientific Computation and Mathematical Modeling (CSCAMM), University of Maryland, College Park, MD, United States

Investigating the role of intrinsic cell heterogeneity emerging from variations in cell-cycle parameters and apoptosis is a crucial step toward better informing drug administration. Antimitotic agents, widely used in chemotherapy, target exclusively proliferative cells and commonly induce a prolonged mitotic arrest followed by cell death via apoptosis. In this paper, we developed a physiologically motivated mathematical framework for describing cancer cell growth dynamics that incorporates the intrinsic heterogeneity in the time individual cells spend in the cell-cycle and apoptosis process. More precisely, our model comprises two age-structured partial differential equations for the proliferative and apoptotic cell compartments and one ordinary differential equation for the quiescent compartment. To reflect the intrinsic cell heterogeneity that governs the growth dynamics, proliferative and apoptotic cells are structured in "age," i.e., the amount of time remaining to be spent in each respective compartment. In our model, we considered an antimitotic drug whose effect on the cellular dynamics is to induce mitotic arrest, extending the average cell-cycle length. The prolonged mitotic arrest induced by the drug can trigger apoptosis if the time a cell will spend in the cell cycle is greater than the mitotic arrest threshold. We studied the drug's effect on the long-term cancer cell growth dynamics using different durations of prolonged mitotic arrest induced by the drug. Our numerical simulations suggest that at confluence and in the absence of the drug, quiescence is the long-term asymptotic behavior emerging from the cancer cell growth dynamics. This pattern is maintained in the presence of small increases in the average cell-cycle length. However, intermediate increases in cell-cycle length markedly decrease the total number of cells and can drive the cancer population to extinction. Intriguingly, a large "switch-on/switch-off" increase in the average cell-cycle length maintains an active cell population in the long term, with oscillating numbers of proliferative cells and a relatively constant quiescent cell number.

Keywords: apoptosis, cell-cycle variations, intrinsic heterogeneity, mitotic arrest, OVCAR-8, partial differential equations, population dynamics

OPEN ACCESS

Edited by:
Michael Breitenbach, University of Salzburg, Austria

Reviewed by:
Robert Friis, University of Bern, Switzerland
Reinhard Schuster, Medizinische Dienste der Krankenversicherung, Germany

***Correspondence:**
Doron Levy
dlevy@math.umd.edu

Specialty section:
This article was submitted to Molecular and Cellular Oncology, a section of the journal Frontiers in Oncology

Received: *27 April 2017*
Accepted: *09 August 2017*
Published: *30 August 2017*

Citation:
Lorz A, Botesteanu D-A and Levy D (2017) Modeling Cancer Cell Growth Dynamics In vitro in Response to Antimitotic Drug Treatment. Front. Oncol. 7:189. doi: 10.3389/fonc.2017.00189

1. INTRODUCTION

Intratumoral cancer heterogeneity represents a major obstacle to improving the overall response and survival of cancer patients (1–4). While most tumors initially respond well to drug therapies, many will relapse at a certain point following treatment (5, 6). One of the major reasons behind therapeutic failure is attributed to cancer cell-intrinsic factors, such as variations in cell-cycle parameters (e.g., cell-cycle duration, apoptosis length, mitotic index, percentage of apoptotic cells) and the presence of quiescent cancer cells, both of which decrease the efficacy of therapies that rely on active cell cycling (7–10).

Antimitotic cancer drugs represent a highly diverse and successful class of antimitotic agents, reported to have a broad spectrum of potent anti-tumor activity in various hematological and solid malignancies (7, 11–17). Examples of such drugs include microtubule-targeting agents, e.g., taxanes and vinca alkaloids, and newer agents that disrupt mitosis without affecting microtubule dynamics, e.g., kinesin spindle protein inhibitors and inhibitors of mitotic kinases (18–28).

While the primary drug target depends on the antimitotic agent used, pre-clinical data from in vitro experiments showed that prolonged mitotic arrest occurs in 100% of the cell populations under study irrespective of the agent used (29–33). However, these data also revealed that while all proliferating cells will undergo mitotic arrest when exposed to high concentrations of antimitotic drugs, there is considerable cell-to-cell variation of apoptotic response to antimitotic drugs in human cancer cell lines. Such observations have been reported in multiple single-cell studies involving individual cancer cells in culture in the presence of various antimitotic drugs, including kinesin-5 inhibitors (30, 32) taxol (29, 31–37), and nocodazole (32, 38–40). In the presence of identical drug exposure times and concentrations, the extent of heterogeneity in cellular response reported both within and across cancer cell lines is considerable (29–33, 35–37). For example, in Ref. (32), the authors analyzed 15 different cancer cell lines for their long-term response to different antimitotic drugs. They found that cellular responses to identical drugs are heterogeneous, e.g., within each distinct cell line, cells exhibit different responses following prolonged mitotic arrest, such as undergoing apoptosis after exiting mitosis, dying after completing several mitoses, or dying in interphase.

Investigating the role of intrinsic cell heterogeneity emerging from variations in cell-cycle parameters and apoptosis in cancer cell growth dynamics *in vitro* is a crucial first step toward better informing antimitotic drug administration. Several mathematical models have been formulated to investigate the dynamic variations among different cellular phenotypes and their role in the emergence of adaptive evolution and chemotherapeutic resistance (41–45) or the impact of cancer cell size, age, and cell-cycle phase in predicting the long-term *in vitro* population growth dynamics (46–55).

For example, in Ref. (46), the authors modeled the cancer cell population dynamics using a system of four partial differential equations (PDEs) representing the four cell-cycle phases (i.e., G_0, G_1, S, and M) with relative DNA content as the structuring variable. The goal therein was to obtain the steady DNA distributions for each cell-cycle phase and match the flow cytometry DNA profiles of the human melanoma NZM13 cell line at various time points following the addition of paclitaxel.

In Ref. (48), the authors derived two novel mathematical models, a stochastic agent-based model and an integro-differential equation model, in order to study the effect of cell-cycle-induced intrinsic tumor heterogeneity on the overall growth dynamics. Both models characterized the growth of cancer cells as dynamic interactions between the proliferative, quiescent, and apoptotic states. The models were designed to predict the cancer growth as a function of the intrinsic heterogeneity in the duration of the cell-cycle and apoptosis process and also included cellular density dependency effects. An extension of these models to spatial models was done in Ref. (49).

In this paper, we reformulated the models of Ref. (48). Specifically, we assumed that cells are structured by their age, i.e., how long each cell will spend in the cell cycle or apoptosis. The advantages of the present approach lie in the ability to access directly the cellular age in each compartment and to study the impact of prolonged mitotic arrest induced by antimitotic agents on the long-term population growth dynamics. Our model comprises of two PDEs for the proliferative and apoptotic cell compartments structured in cellular age and one ordinary differential equation for the quiescent compartment. We modeled the prolonged mitotic arrest induced by the drug as an increase in the average cell-cycle length duration, a consequence of the slowing or blocking of mitosis at the metaphase-anaphase transition (30, 34, 38, 56). We assumed that if the total time a cell spends in the cell cycle is greater than the cell-cycle age threshold, apoptotic cell death is triggered, a phenomenon observed *in vitro* (18, 30, 33, 34, 37, 38, 56–61). We used numerical simulations to subsequently study the impact of increasing the cell-cycle length on the overall population survival.

Our results suggest that at confluence and in the absence of any drug, quiescence is the long-term asymptotic behavior emerging from the cancer cell growth dynamics. This pattern is maintained in the presence of a small increase in the average cell-cycle length. However, an intermediate increase in cell-cycle length markedly decreases the total number of cancer cells present and can drive the cell population to extinction. A large "switch-on/switch-off" increase in the average cell-cycle length maintains an active cell population in the long term, with oscillating numbers of proliferative cells and a relatively constant quiescent cell number. Intriguingly, our results suggest that a large "switch-on/switch-off" increase in the average cell-cycle length may maintain an active cancer cell population in the long term.

This work is aimed at understanding cancer cell growth dynamics in the context of cancer heterogeneity emerging from variations in cell-cycle and apoptosis parameters. The mathematical modeling framework proposed herein merits consideration as one of the few mathematical models to investigate dynamic cancer cell responses to prolonged mitotic arrest induced by antimitotic drug exposure. Our proposed modeling framework can serve as a basis for future studies of the heterogeneity observed *in vitro* of cancer cell responses in the presence of antimitotic drugs.

2. MATERIALS AND METHODS

2.1. Model Setup

The system (1)–(3) is a novel physiologically motivated mathematical model that assumes continuous distributions on cellular age, i.e., the times spent in the cell-cycle and apoptosis process. The model consists of proliferative (i.e., cells actively dividing, in either a G_1, G_2 or M-like state), quiescent (i.e., a G_0-like state), and apoptotic compartments, as illustrated in **Figure 1**.

The proliferative compartment is structured by the time remaining to be spent by cells in the cell cycle before successfully completing mitosis and doubling. The apoptotic compartment is structured by the time remaining for cells to fully degrade and complete apoptosis. Accordingly, the dynamics of the cancer cell population is governed by the following system:

$$\partial_t P(t,a) - \partial_a P(t,a) = \alpha_{QP}(t)Q(t)f_P(a)\mathbb{1}_{[0,\bar{a}]} - \alpha_{PA}(t)P(t,a), \tag{1}$$

$$\partial_t Q(t) = 2P(t,0) - (\alpha_{QP}(t) + \alpha_{QA}(t))Q(t), \tag{2}$$

$$\partial_t A(t,a) - \partial_a A(t,a) = \left[\alpha_{QA}(t)Q(t) + \alpha_{PA}(t)\int P(t,a)\,da + \alpha_{QP}(t)Q(t)\int f_P(a)\mathbb{1}_{(\bar{a},\infty)}\,da\right] f_A(a). \tag{3}$$

Initial conditions for this system are described in the following.

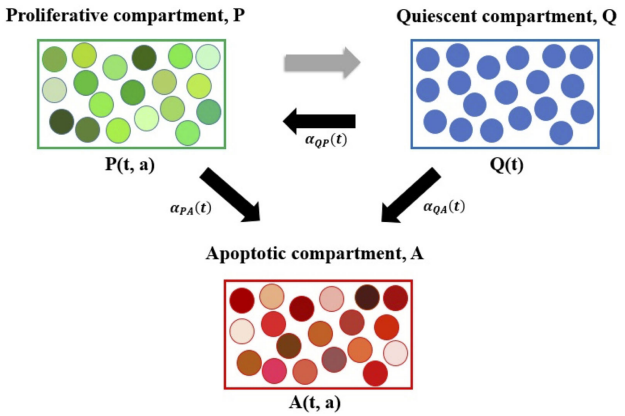

FIGURE 1 | Diagram representing the age-structured mathematical modeling framework. Here, P denotes the proliferative compartment, with $P(t, a)$ cells present at time t with time a remaining to be spent in this compartment. Proliferative cells can either transition to A or to Q at $a = 0$ upon completion of the cell cycle. Q denotes the quiescent compartment, with $Q(t)$ cells present at time t. Quiescent cells can either transition to P with rate $\alpha_{QP}(t)$ or to A with rate $\alpha_{QA}(t)$. A denotes the apoptotic compartment, with $A(t, a)$ cells present at time t and time a remaining to be spent in this compartment before completing apoptosis. For illustration purposes, cells within each compartment are grouped together. The various shades of green represent the different times remaining to be spent by cells in the proliferative compartment (i.e., in the cell cycle) before transitioning. Similarly, the various shades of red represent the different times remaining to be spent by cells in the apoptotic compartment, before completing apoptosis and being removed from the numerical simulations. The three explicit transition rates (i.e., $\alpha_{QP}(t)$, $\alpha_{PA}(t)$, and $\alpha_{QA}(t)$) are illustrated using black arrows pointing in the direction of the respective transition. The implicit transition from P to Q representing the successful completion of the cell cycle is denoted by a gray arrow.

2.2. Model Description

In these equations, $P(t, a)$ represents the number of proliferative cells at time t that still spend a in this compartment before doubling. The rates of change of $P(t, a)$ with respect to the experimental time course t and age a are represented by ∂_t and ∂_a, respectively. The term $\partial_a P(t, a)$ in equation (1) implies that the time remaining until proliferating cells complete the cell cycle decreases as time t advances.

When entering the cell cycle, each cell is assigned its individual amount of time to be spent cycling, i.e., a, which is randomly selected from the Gaussian distribution function with mean μ and SD σ and probability density function $f_P(a)$. When reaching $a = 0$, cells in P exit the cell cycle. The maximum length of time spent in P before exiting thus corresponds to the maximum length of the mitotic arrest induced by an antimitotic drug. We assumed that the transition of cells back to Q is due to a successful (i.e., non-aberrant) mitosis.

Cells in Q act as a reservoir for the other two compartments, i.e., they move into either the apoptotic or proliferative compartment with rates $\alpha_{QA}(t)$ or $\alpha_{QP}(t)$, respectively. Intuitively, quiescent cells do not actively progress through the cell cycle nor are committed to undergo apoptosis (i.e., they remain in a G_0-like state).

Cells can undergo apoptosis immediately after exiting the cell cycle, after completing several mitoses, or during interphase. Once cells enter A, they are irreversibly committed to completing apoptosis and cannot transition back to either P or Q. When apoptosis is completed, cells are removed from the numerical simulation. The term $\partial_a A(t, a)$ in equation (3) implies that the time remaining until cells complete apoptosis decreases as time t advances.

Cells undergoing apoptosis take time to fully degrade (62, 63); until apoptosis is completed, the cells still take up space and can inhibit the growth of neighboring cells *in vitro* (37, 63). Upon entering the apoptosis compartment, the time remaining to be spent there is randomly chosen from a probability distribution, e.g., Gamma distribution $\Gamma(\omega, \lambda)$ with shape parameter ω, rate parameter λ, and probability density function $f_A(a)$. The choice for this probability distribution is explained in greater detail in Section 2.5.

We noted that the two age-structured PDEs for the proliferative and apoptotic cell compartments enable us to monitor a cell's progress through the cell cycle (in the case of a cell in P) or advancement through apoptosis until complete degradation (in the case of a cell in A). Additionally, we assumed that if, upon entering P, the time a cell will spend in P, a, is greater than the threshold $\bar{a}$ (i.e., the cell-cycle age threshold corresponding to a prolonged mitotic arrest), the cell will undergo apoptosis and will thus immediately transition to A. This phenomenon has been observed *in vitro* when the sustained prolonged mitotic arrest caused by antimitotic drug exposure leads to apoptotic cell death via the gradual accumulation of cell death signals that ultimately trigger apoptosis. Examples include the phosphorylation and subsequent inactivation of the anti-apoptotic Bcl-2 proteins (Bcl-2, Bcl-xL, and Mcl-1), PARP cleavage, and the activation of caspases 3, 7, and 9 (33, 34, 36–38, 58, 64–66).

2.3. Initial Conditions

Initial conditions for the system (1)–(3) are as follows:

$$P(0, a) = 0, \tag{4}$$

$$Q(0) = \rho(0)K, \tag{5}$$

$$A(0, a) = 0. \tag{6}$$

where $\rho(0)$ represents the initial *in vitro* plating density. Here, three different initial conditions are used, i.e., $Q(0) = 0.1K$, $Q(0) = 0.45K$, and $Q(0) = 0.8K$, corresponding to 10, 45, or 80% of the plating carrying capacity K, respectively, according to experimental setup in Ref. (48). We noted that the $Q(0) = 0.1K$ and $0.8K$ cases are identical to the initial conditions reported in Ref. (48). For comparison purposes, we considered in this work, an intermediate case, $Q(0) = 0.45K$, which corresponds to the mean value of the two experimental datasets reported in Ref. (48). Therein, the growth dynamics measuring total cellular density every 24 h for a period of 96 h in the two different seeding densities (i.e., 10 and 80% of the *in vitro* plating density) was subsequently recorded. For a more detailed description of the experimental design, we referred to Ref. (48) Appendix B.1.2.

We noted that equation (1) does not require a boundary condition at $a = 0$, since this is a PDE that models a transport process with outward flux only, i.e., once proliferating cells reach $a = 0$, they double, after which both daughter cells return to quiescence before entering another cell cycle.

2.4. Inter-Compartmental Dynamics

Following (48), the transition rates that describe the processes of mitotic exit followed by quiescence, mitotic exit, or quiescence followed by the onset of apoptosis are, respectively:

$$\alpha_{QP}(t) = c\frac{[\beta(\rho(t))N_{tot}(t) - P(t)]_+}{Q(t)}, \tag{7}$$

$$\alpha_{PA}(t) = c\gamma\frac{[dN_{tot}(t) - A(t)]_+}{P(t)}, \tag{8}$$

$$\alpha_{QA}(t) = c(1-\gamma)\frac{[dN_{tot}(t) - A(t)]_+}{Q(t)}. \tag{9}$$

$P(t)$, $Q(t)$, and $A(t)$ represent the total number of cells at time t in the proliferative, quiescent, and apoptotic compartments. Herein, the total number of proliferative and apoptotic cells are integrated over the cellular age, i.e., $\int P(t, a)\ da$ and $\int A(t, a)\ da$, respectively. The total number of cells that occupy the plate at time t is described by $N_{tot}(t) = P(t) + Q(t) + A(t)$. The total number of non-apoptotic cells at time t is described by $N(t) = P(t) + Q(t)$. Cell density is denoted by $\rho(t) = N_{tot}(t)/K$, with K representing *in vitro* confluence. Here, $\rho = 1$ when $N_{tot}(t) = K$, which implies that cells have reached confluence at time t. For a complete explanation and derivation of the transition rates in (7)–(9), we referred to Ref. (48).

We noted that the functional forms in equations (7)–(9) are time and density dependent and reflect the *in vitro* experimental conditions used in Ref. (48), where OVCAR-8 cells were seeded at different cell densities and initially synchronized to be quiescent using starvation media.

Additionally, we assumed that for a given *in vitro* cell density at time t, there exists an equilibrium distribution of cells actively in the cell cycle. This is represented in the model by the function $\beta(\rho(t))$, i.e., the fraction of proliferating cells as a function of the *in vitro* cell density $\rho(t)$ at equilibrium. Experimentally, in order to determine $\beta(\rho(0))$, in Ref. (48), OVCAR-8 human ovarian carcinoma cells seeded at different cell densities were initially synchronized as quiescent, using two distinct cell-cycle arrest experiments performed by changing the starvation media and duration of the experiment. For a more detailed description of the experimental design, we referred to Ref. (48) Appendix B.1.1.

In the model, $\beta(\rho(t))$ is described by:

$$\beta(\rho(t)) = \beta_m e^{\frac{-\theta(\rho-\rho_m)^2}{\rho(1+\varepsilon-\rho)^2}}, \tag{10}$$

$$\theta := \frac{\varepsilon^2 \log\left(\frac{\beta_m}{d}\right)}{(1-\rho_m)^2}. \tag{11}$$

A complete list of the variables and parameters used throughout the modeling framework (1)–(11) and their interpretation can be found in **Table 1**. We noted that the parameters and functional forms described earlier are adapted from Ref. (48).

2.5. Intra-Compartmental Dynamics

The age-structured mathematical model proposed above incorporates an intrinsic form of cell heterogeneity in the *in vitro* cancer cell growth dynamics, specifically in the distribution of times individual cells spend in the cell-cycle and apoptosis process.

To the best of our knowledge, there are no *in vitro* studies describing the distribution of times individual OVCAR-8 cells spend in the cell-cycle. In Ref. (48), Greene et al. chose to model the amount of time OVCAR-8 cells spend in the proliferative compartment, P, as a normal distribution, $\mathcal{N}(\mu, \sigma)$, with probability density function $f_P(a)$. In our model, the density function is renormalized to integrate to 1 on the interval $[0, \infty)$. Based on the temporal OVCAR-8 growth dynamics reproduced in Figure 4 in Ref. (48), the mean cell-cycle length obtained when fitting to the experimental data is $\mu = 19.12$ h, when the initial plating density is set at $Q(0) = 10\%$ of the maximum plating density, K. When the initial plating density is $Q(0) = 80\%$ of the maximum plating density, K, the mean cell-cycle length obtained when fitting to the experimental data is $\mu = 15.23$ h. When fitting the system (1)–(4) to the experimental data for both plating density conditions, the mean cell-cycle length obtained is $\mu = 18.33$ h. Experimentally, the doubling time reported for OVCAR-8 cells decreases with higher plating density and varies between 14.57 (67) and 26.1 h (68).

The amount of time cells spend in the apoptosis compartment, A, is assumed to follow a Gamma distribution, $\Gamma(\omega, \lambda)$, where ω and λ denote the shape and rate parameters, respectively, with probability density function $f_A(a)$. These parameters are set at $\omega = 4.9436$ and $\lambda = 0.19117$, respectively, to match the experimental results of Ref. (62) on the length of the apoptotic process. They are identical to the ones used in Ref. (48) to characterize this

TABLE 1 | List of variables and parameters used throughout the model.

Variable	Value	Definition
t	[0, 200] (hours)	Time
a	[0, 80] (hours)	Maximum time remaining to be spent in P or A
$P(t, a)$	[0, ∞) (cells)	Number of proliferative cells at time t with time a to spend in P
$Q(t)$	[0, ∞) (cells)	Number of quiescent cells at time t
$A(t, a)$	[0, ∞) (cells)	Number of apoptotic cells at time t with time a to spend in A
$N_{tot}(t)$	[0, ∞) (cells)	Total number of cells at time t
$N(t)$	[0, ∞) (cells)	Total number of non-apoptotic cells at time t
K	40,401 (cells)	*In vitro* carrying capacity
$f_P(a)$	[0, ∞)	PDF of $\mathcal{N}(\mu, \sigma)$, describing the cell-cycle length without drug
μ	[15.23, 19.12] (hours)	Mean cell-cycle length without drug
σ	3 (hours)	SD of the cell-cycle length without drug
$f_{P,c}(a)$	[0, ∞)	PDF of $\mathcal{N}(\mu + c(t), \sigma)$, describing the cell-cycle length with drug
$c(t)$	[0, ∞) (hours)	Drug-induced mitotic arrest extending the average cell-cycle length
$f_A(a)$	[0, ∞)	PDF of $\Gamma(\omega, \lambda)$ describing the length of apoptosis
ω	4.9436	Shape parameter for the Gamma-distributed length of apoptosis
λ	0.19117	Rate parameter for the Gamma-distributed length of apoptosis
$\bar{a}$	[24.23, 28.12] (hours)	Cell-cycle age threshold corresponding to a prolonged mitotic arrest
$\alpha_{QP}(t)$	[0, ∞)	Transition rate from Q to P
$\alpha_{PA}(t)$	[0, ∞)	Transition rate from P to A
$\alpha_{QA}(t)$	[0, ∞)	Transition rate from Q to A
c	[0.37, 0.64] (hour^{-1})	Cellular reaction rate
γ	[0.0005, 0.9999]	Transition probability to enter A
$\rho(t)$	[0, ∞)	*In vitro* cell density at time t
d	0.03	Fraction of total number of cells in A
$\beta(\rho(t))$	[0, 1]	Fraction of total number of cells in P as a function of $\rho(t)$
β_m	[0, 1]	Maximum of $\beta(\rho(t))$
ρ_m	[0, 1]	Maximizing density of $\beta(\rho(t))$
ε	[0, 1]	Parameter governing the shape of $\beta(\rho(t))$

process. We noted, however, that the study of Ref. (62) investigated the individual responses of PC12 rat adrenal gland tumor cells to serum deprivation. Therein, the authors performed a comprehensive study on the fate of distinct cells undergoing apoptosis following serum removal. To the best of our knowledge, no such studies performed on human cancer cell lines have reported a distribution of the time individual cells spend in apoptosis at such a fine resolution, either in the absence or the presence of antimitotic drugs. We thus chose to model the probability density function of the length of apoptosis process based on the experimental data in Ref. (62). The remaining model parameters listed in **Table 1** are obtained following the parameter estimation procedure described in Ref. (48).

2.6. Cellular Response to Antimitotic Drugs

In our model, we considered an antimitotic drug whose effect on the cellular dynamics is to induce mitotic arrest, extending the average cell-cycle length. We assumed the administered drug to be homogeneously distributed, such that all cells in P are equally susceptible to its effect. Specifically, the impact of the drug is to increase the time cells spend in the proliferative compartment, P, corresponding to a sustained mitotic arrest. Upon exiting quiescence and entering the cell cycle, a cell can undergo one of two fates: (i) if the time chosen to be spent in P is lower than the threshold $\bar{a}$, the cell enters P, progresses through the cell cycle, and either successfully completes mitosis with rate α_{QP}, or undergoes apoptosis with rate α_{PA}; (ii) otherwise, the cell commits to undergoing apoptosis and immediately moves to the apoptotic compartment A. The parameter $\bar{a}$ serves as the cell-cycle age threshold corresponding to a prolonged mitotic arrest, after which cells exit the cell cycle and undergo apoptosis.

It is a well-known phenomenon *in vitro* that a sustained mitotic arrest (i.e., slowing or blocking of mitosis at the metaphase–anaphase transition, thus increasing cell-cycle length) predisposes cancer cells to undergoing apoptosis following mitotic exit (7, 11, 18, 30, 33, 34, 36–38, 56, 66). This was revealed using time-lapse microscopy data, where exposure of cancer cells to saturating antimitotic drug concentrations delayed to various extents the cells from exiting drug-induced mitotic arrest and undergoing subsequent apoptosis.

In our model formulation, the antimitotic drug acts directly on the cell-cycle dynamics by increasing the average cell-cycle length, and as a consequence, causing cells to transition to the apoptotic compartment. To include the effect of such a drug, we shifted the expected value μ of the normal distribution by the function $c(t)$ corresponding to the cell-length increase induced by the antimitotic drug, i.e., $f_{P,c}(a)$ is the probability density function of the normal distribution $\mathcal{N}(\mu + c(t), \sigma)$. The system (1)–(12) remains otherwise unchanged. Here, $c(t)$ can, for example, be modeled as a constant or bang–bang function throughout the duration of the simulation time $t = 200$ h, corresponding to either a sustained, constant mitotic arrest or a switch-on/switch-off arrest.

Experimentally, the sustained, constant mitotic arrest corresponds to the large cell-to-cell variations in the duration of mitotic arrest and the timing of drug-induced cell death via apoptosis observed *in vitro* when single cells are exposed to saturating drug concentrations using various antimitotics for prolonged periods of time, e.g., 96 hours or more (32, 33, 37). We further investigated the impact of an *in silico* switch-on/switch-off mitotic arrest on the overall cancer cell growth dynamics. This type of "bang–bang" mitotic arrest could, for example, be induced *in vitro* by the periodic addition and wash-off of the antimitotic drug under study, along with growth media refreshment. In this setting, when the drug is withdrawn, proliferating cells do not necessarily revert to the cell-cycle length assigned to them in the absence of the drug. Rather, these cells can still undergo a period of mitotic arrest, in which the progression through the cell cycle can be slowed down or blocked, leading to an increase in the cell-cycle length, after which the cell cycle is completed and cells exit proliferation.

We noted that our age-structured modeling framework allows us to estimate the number of cells present in each compartment at any given time and to temporally trace the distribution of the times remaining to be spent in the proliferative phase during the cell cycle or in the apoptotic phase. This framework enables us to dynamically estimate the amount of time remaining to be spent in each of these processes and to track cells in their progression through each cellular phase.

3. RESULTS

3.1. Cancer Cell Growth Dynamics in the Absence of the Drug

We illustrate in **Figure 2** the cancer cell growth dynamics modeled by the system (1)–(3), with transition rates (7)–(9) and initial conditions (4)–(6). Specifically, we consider three sets of initial conditions, i.e., $Q(0) = 0.1K$ in **Figures 2A,D,G**, $Q(0) = 0.45K$ in **Figures 2A,D,G**, and $Q(0) = 0.8K$ in **Figures 2B,E,H**, corresponding to 10, 45, or 80% of the plating carrying capacity, K, respectively.

The initial plating density, with all cells being experimentally synchronized as quiescent, as described in Section (2.3), substantially alters the overall growth dynamics throughout the simulation time. This can be observed in the relative and absolute numbers of proliferating cells (solid green line) or quiescent cells (solid blue line) and in the total number of cells, i.e., proliferating and quiescent cells (solid magenta line). In the $Q(0) = 0.1K$ case, the ratio $Q/P = \frac{Q(t)}{\int P(t,a)\,da}$ (henceforth referred to as Q/P) is greater than 1 until around $t = 2$ h, after which it becomes smaller than 1 until around $t = 63$ h. Afterward, the ratio Q/P increases with time. In the $Q(0) = 0.45K$ case, the ratio Q/P becomes less than 1 only for a brief period of time, $t \in [7, 13]$, after which it continues to increase with time. In the $Q(0) = 0.8K$ case, the number of quiescent cells only decreases for a brief period of time, $t \in [0, 11]$, after which the number of quiescent cells continues to increase until almost reaching carrying capacity. The ratio Q/P remains >1 throughout the duration of the simulation.

For comparison purposes, we also illustrate the distribution of the times remaining to be spent in the proliferative (P) or apoptotic (A) compartment at the end of simulation time ($t = 200$ h), for each of the initial plating densities: $Q(0) = 0.1K$ in **Figure 2G**, $Q = 0.45K$ in **Figure 2H**, and $Q(0) = 0.8K$ in **Figure 2I**. The solid green lines correspond to the distribution of the time remaining to be spent by cells in P, and the solid red lines correspond to the times remaining to be spent by cells in A.

In each of the three scenarios, all cells are synchronized to be quiescent at the start of the simulation time $t = 0$ h. The long-term dynamics of the system (1)–(3) reveals that the majority of cells are quiescent at the end of the simulation time $t = 200$ h, with $N_{tot}(t)$ close to the carrying capacity. There are few remaining proliferating cells, suggesting that once cells approach confluence, proliferation will be inhibited. The initial plating density does not alter the quantitative nor qualitative dynamics of the apoptotic cell compartment throughout the simulation time (solid red lines). We conclude that at confluence and in the absence of the drug, quiescence is the long-term asymptotic behavior emerging from the cancer cell growth dynamics.

3.2. Cancer Cell Growth Dynamics under Antimitotic Drug Action

We now investigate the dynamic behavior of the system (1)–(3) using two distinct antimitotic drug effects, i.e., a sustained, constant mitotic arrest and a switch-on/switch-off arrest, with three different levels of increase in the average cell-cycle length.

In the numerical simulations depicted later, the function $c(t)$, corresponding to the drug-induced mitotic arrest extending the average cell-cycle length, can take two functional forms: it is set to be a constant function $c(t) = 2c_{arrest}$ set at either 2, 10, or 20 h (solid lines) or a bang–bang function $c(t) = 2c_{arrest}$ for $0 \leq t \leq 2$ and $c(t) = 0$ for $2 \leq t \leq 4$ h, repeated periodically with period 4 until $t = 200$ h (dashed lines).

3.2.1. Cancer Cell Growth Dynamics Given Small Increases in Cell-Cycle Length

We studied the cancer cell growth dynamics given the action of the drug as modeled by the system (1)–(3), with initial conditions (4)–(6). To begin with, we considered small increases in the average cell-cycle length setting $c_{arrest} = 2$ h.

There is a relatively small difference between the two distinct antimitotic drug effects (see **Figure 3**, solid versus dashed lines for each color representing the different cellular compartments). Specifically, in both cases, the number of proliferative cells (solid and dashed green lines in **Figure 3A**) initially increases and then starts to decrease at around $t = 73$ h. The number of quiescent cells (solid and dashed blue lines in **Figure 3A**) initially decreases and continues to oscillate until around $t = 40$ h, when it begins to increase with time. These oscillations are due to the transitions from Q to P and back to Q. Initially, the ratio Q/P becomes less than 1 ($t \in [2, 73]$), after which it steadily increases beyond 1 throughout the rest of the simulation time. The total number of apoptotic cells integrated over the cellular age, $\int A(t, a)\,da$ (solid and dashed red lines in **Figure 3D**), steadily increases with respect to time. In **Figure 3G**, we show the distribution of the times remaining to be spent by proliferating cells (green lines) and apoptotic cells (red lines) at the end of simulated time $t = 200$ h, given small increases in average cell-cycle length, using the sustained, constant mitotic arrest (solid lines) and switch-on/switch-off arrest (dashed lines).

The two antimitotic drug effects have no noticeable difference with regard to the cellular dynamics in either of the three compartments. Compared with the cancer cell growth dynamics in the absence of the drug (see **Figures 2** and **3**), the ratio Q/P becomes greater than 1 and subsequently increases at a slightly later time point, i.e., at around $t = 73$ versus $t = 63$ h in the absence of the drug.

Similar results are obtained when considering $Q(0) = 0.45K$ (see **Figures 3B,E,H**) and when considering $Q(0) = 0.8K$ (see **Figures 3C,F,I**). We conclude that nearing confluence and in the presence of small increases in average cell-cycle length, quiescence emerges as the long-term asymptotic behavior resulting from the cancer cell growth dynamics.

3.2.2. Cancer Cell Growth Dynamics Given Intermediate Increases in Cell-Cycle Length

We now consider intermediate increases in the average cell-cycle length, setting $c_{arrest} = 10$ h. Results are shown in **Figure 4**.

The case $Q(0) = 0.1K$ is illustrated in **Figures 4A,D,G**. Specifically, the number of proliferative cells (solid and dashed green lines) fluctuates significantly at the beginning of the numerical simulation for both antimitotic drug effects considered. However, at around $t = 77.5$ h, the number of proliferative cells exposed to

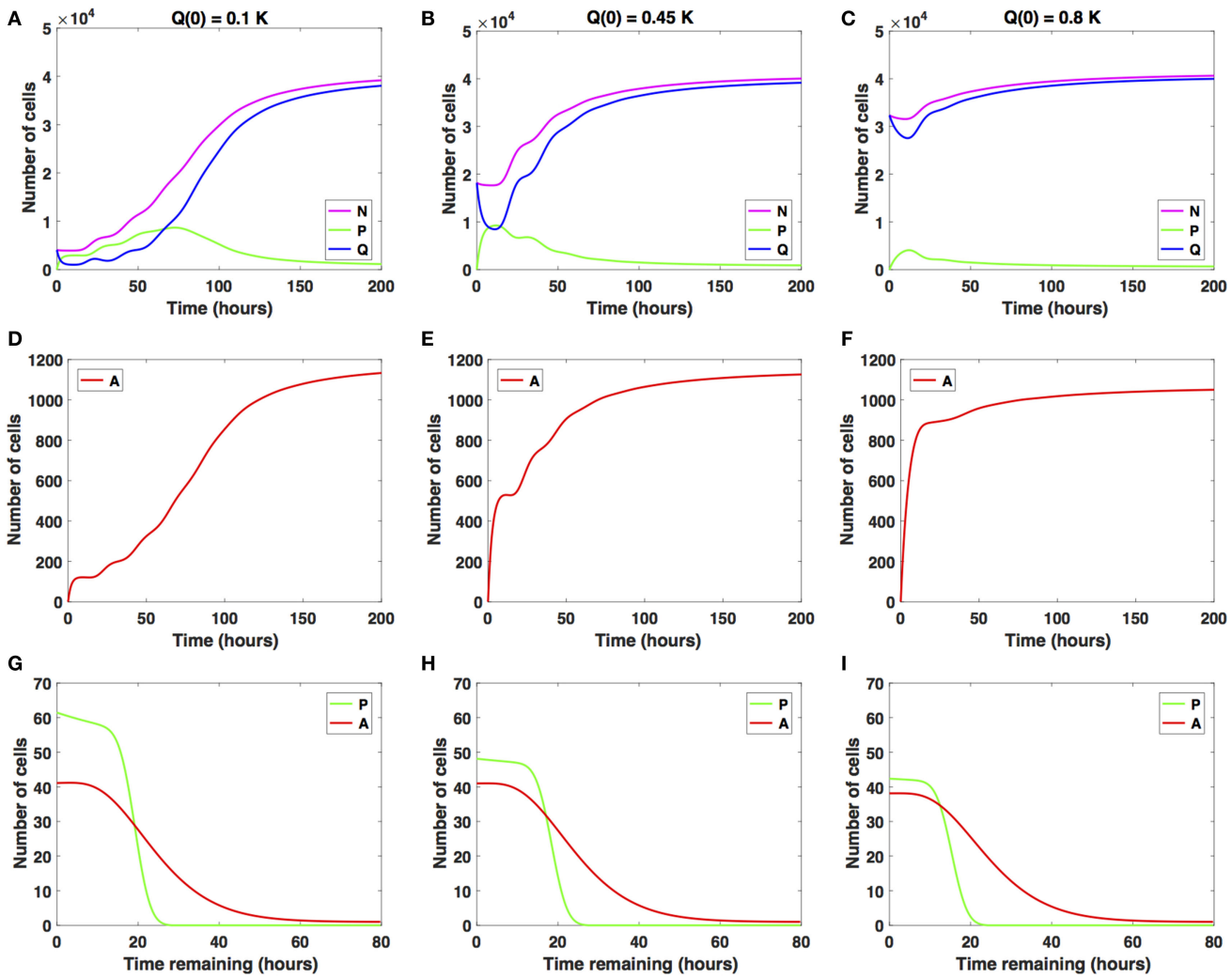

FIGURE 2 | Numerical solutions for the system (1)–(3) in the absence of the drug with **(A,D,G)** $Q(0) = 10\%$, **(B,E,H)** $Q(0) = 45\%$, and **(C,F,I)** $Q(0) = 80\%$ of the *in vitro* carrying capacity, K. **(A–C)** show the dynamics of the proliferating (P), quiescent (Q), and total number of non-apoptotic cells (N). **(D–F)** show the dynamics of the apoptotic cells (A). **(G–I)** illustrate the distribution of the times remaining to be spent by cells in the proliferative (P) and apoptotic (A) compartments as seen at the end of the simulation time, $t = 200$ h, with **(G)** $Q(0) = 10\%$, **(H)** $Q(0) = 45\%$, and **(I)** $Q(0) = 80\%$ of plating carrying capacity, K.

the sustained, constant mitotic arrest starts to decrease with time. The number of proliferative cells exposed to the switch-on/switch-off arrest oscillates slightly around the number of quiescent cells.

After the initial decrease in absolute numbers at around $t = 15$ h, the quiescent cells exposed to the sustained, constant mitotic arrest exhibit a pattern of damped oscillations. They continue to slightly decrease in numbers throughout simulation time (solid blue line). The quiescent cells exposed to the switch-on/switch-off arrest seem to have reached a steady state at around $t = 88$ h. Interestingly, for the sustained, constant mitotic arrest, the ratio Q/P becomes greater than 1 and increases slightly with time starting at around $t = 78$ h. However, for the switch-on/switch-off arrest, the same ratio remains consistently around 1 throughout simulation time, suggesting the existence of a steady-state equilibrium between the proliferative and quiescent populations. A similar pattern can be observed in the dynamics of the total number of proliferating and quiescent cells (solid and dashed magenta lines).

The total number of apoptotic cells (solid and dashed red lines in **Figure 4D**) oscillates with time. **Figure 4G** shows the distribution of the times remaining to be spent by proliferating cells (green lines) and by apoptotic cells (red lines) at $t = 200$ h. Similar results are obtained when considering $Q(0) = 0.45K$ (see **Figures 4B,E,H**).

However, for $Q(0) = 0.8K$, the dynamics of the proliferative (green lines), quiescent (blue lines), and apoptotic (red lines) cell compartments are quantitatively and qualitatively distinct between the two distinct antimitotic drug effects (see **Figures 4C,F,I**).

Specifically, the number of proliferative cells (solid green line in **Figure 4C**) in the sustained, constant mitotic arrest case starts to decrease around $t = 50$ h. Given the switch-on/switch-off

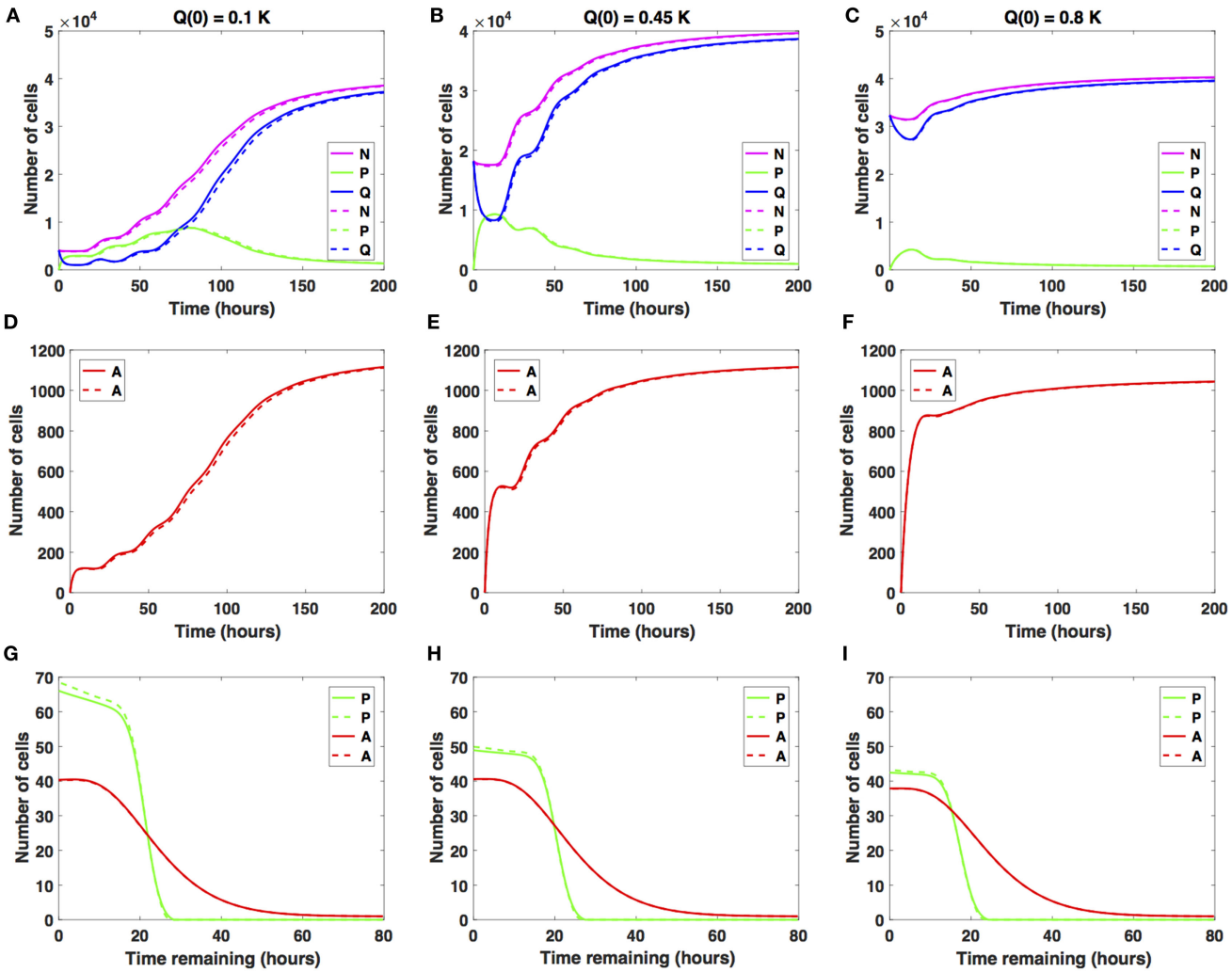

FIGURE 3 | Numerical solutions for the system (1)–(3) given small increases in the average cell-cycle length with **(A,D,G)** $Q(0) = 10\%$, **(B,E,H)** $Q(0) = 45\%$, and **(C,F,I)** $Q(0) = 80\%$ of the *in vitro* carrying capacity, K. The cellular dynamics in each compartment given a sustained, constant mitotic arrest or a switch-on/switch-off arrest is illustrated using solid or dashed lines, respectively. **(A–C)** show the dynamics of the proliferating (P), quiescent (Q), and the total number of non-apoptotic cells (N). **(D–F)** show the dynamics of the apoptotic cells (A). **(G–I)** illustrate the distribution of the times remaining to be spent by cells in the proliferative (P) and apoptotic (A) compartments as seen at the end of the simulation time, $t = 200$ h, with **(G)** $Q(0) = 10\%$, **(H)** $Q(0) = 45\%$, and **(I)** $Q(0) = 80\%$ of plating carrying capacity, K.

arrest however, the number of proliferative cells oscillates slightly (dashed green line) starting around $t = 20$ h and continues until the end of the simulated time. The number of quiescent cells (dashed green and blue lines, respectively) continues to steadily decrease for both antimitotic drug effects, with the quiescent cells decaying at a faster rate in the sustained arrest case than in the switch-on/switch-off one (see **Figure 4C**). A similar pattern can be observed in the dynamics of the total number of cells (proliferating and quiescent), as represented by the solid and dashed magenta lines in **Figure 4C**. The total number of apoptotic cells (solid and dashed red lines in **Figure 4F**) starts to decrease at around $t = 18$ h. In **Figure 4I**, we show the distribution of the times remaining to be spent by proliferating cells (green lines) and apoptotic cells (red lines) at $t = 200$ h.

The two antimitotic drug effects at intermediate increases in cell-cycle length have a marked distinct impact on the cellular dynamics in each of the three cellular compartments for the $Q(0) = 0.8K$ case. Specifically, the number of quiescent cells decreases in time, and implicitly, the total number of cells decreases at a slower (dashed magenta line) or faster rate (solid magenta line). The dynamics of the cell population illustrated in **Figure 4C** is overall substantially different from the oscillatory dynamics observed in the $Q(0) = 0.45K$ and $Q(0) = 0.1K$ cases. We conclude that in the presence of intermediate increases in the cell-cycle length, the sustained, constant mitotic arrest markedly decreases the total number of cancer cells present. A switch-on/switch-off arrest maintains an active cell population in the long-term, with proliferative cell numbers exhibiting a steady

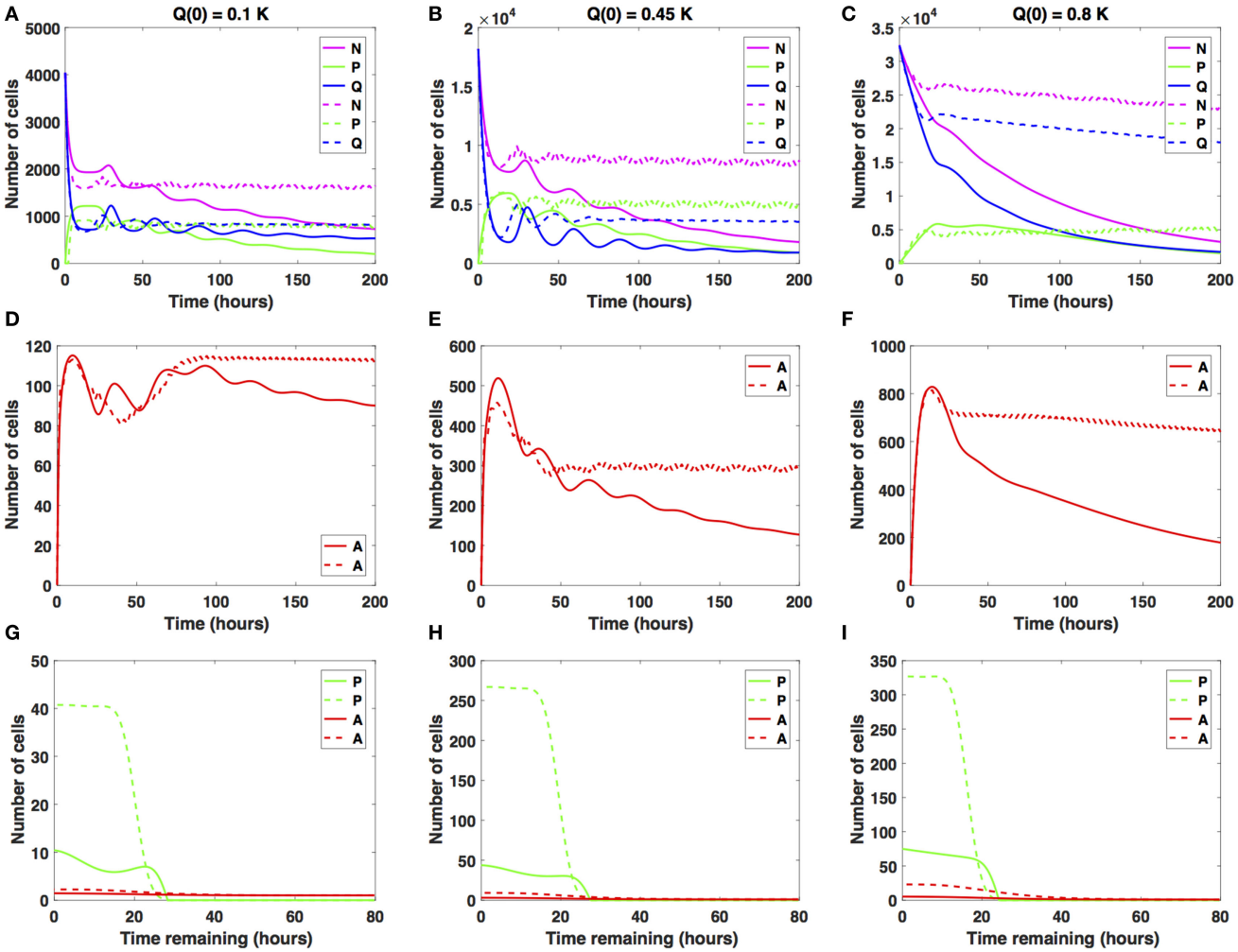

FIGURE 4 | Numerical solutions for the system (1)–(3) given intermediate increases in the average cell-cycle length with **(A,D,G)** $Q(0) = 10\%$, **(B,E,H)** $Q(0) = 45\%$, and **(C,F,I)** $Q(0) = 80\%$ of the *in vitro* carrying capacity, K. The cellular dynamics in each compartment given a sustained, constant mitotic arrest or a switch-on/switch-off arrest is illustrated using solid or dashed lines, respectively. Panels **(A–C)** show the dynamics of the proliferating (P), quiescent (Q), and total number of non-apoptotic cells (N). **(D–F)** show the dynamics of the apoptotic cells (A). **(G–I)** illustrate the distribution of the times remaining to be spent by cells in the proliferative (P) and apoptotic (A) compartments as seen at the end of the simulation time, $t = 200$ h, with **(G)** $Q(0) = 10\%$, **(H)** $Q(0) = 45\%$, and **(I)** $Q(0) = 80\%$ of the plate carrying capacity, K.

oscillatory state and quiescent cell numbers remaining relatively constant in time.

3.2.3. Cancer Cell Growth Dynamics Given Large Increases in Cell-Cycle Length

We now consider increases in the average cell-cycle length, setting $c_{arrest} = 20$ h. Results are shown in **Figure 5**.

When the initial density is low ($Q(0) = 0.1K$), the number of proliferative cells given the sustained, constant mitotic arrest case (solid green line in **Figure 5A**) remains essentially zero for the entire simulation. Given the large increase in the average cell-cycle length induced by the drug, any cells that transition from Q to P subsequently transition to A, instead of doubling successfully at the end of the cell cycle. However, given the switch-on/switch-off arrest (dashed green line in **Figure 5A**), proliferative cell numbers exhibit a steady oscillatory state throughout the duration of the simulated time. The ratio Q/P oscillates around 1 as time increases for the duration of simulation. A similar pattern can be observed in the dynamics of the total number of cells (proliferating and quiescent), as shown by the magenta lines in **Figure 5D**.

The total number of apoptotic cells (solid and dashed red lines in **Figure 5G**) oscillates with time. In **Figure 5J**, we show the distribution of times remaining to be spent by proliferating cells (green lines) and apoptotic cells (red lines) at $t = 200$ h.

Our numerical simulations suggest that in the presence of a sustained, constant mitotic arrest, the cancer cell population is nearly driven to extinction (see solid lines in **Figures 5A,D**). Intriguingly, in the presence of a long-term switch-on/switch-off arrest, it is possible to maintain an active cancer cell population even when starting with a small initial plating density ($Q(0) = 0.1K$) and large increase in the average cell-cycle length. The balance between the quiescent and proliferative cell-turnover is maintained over time

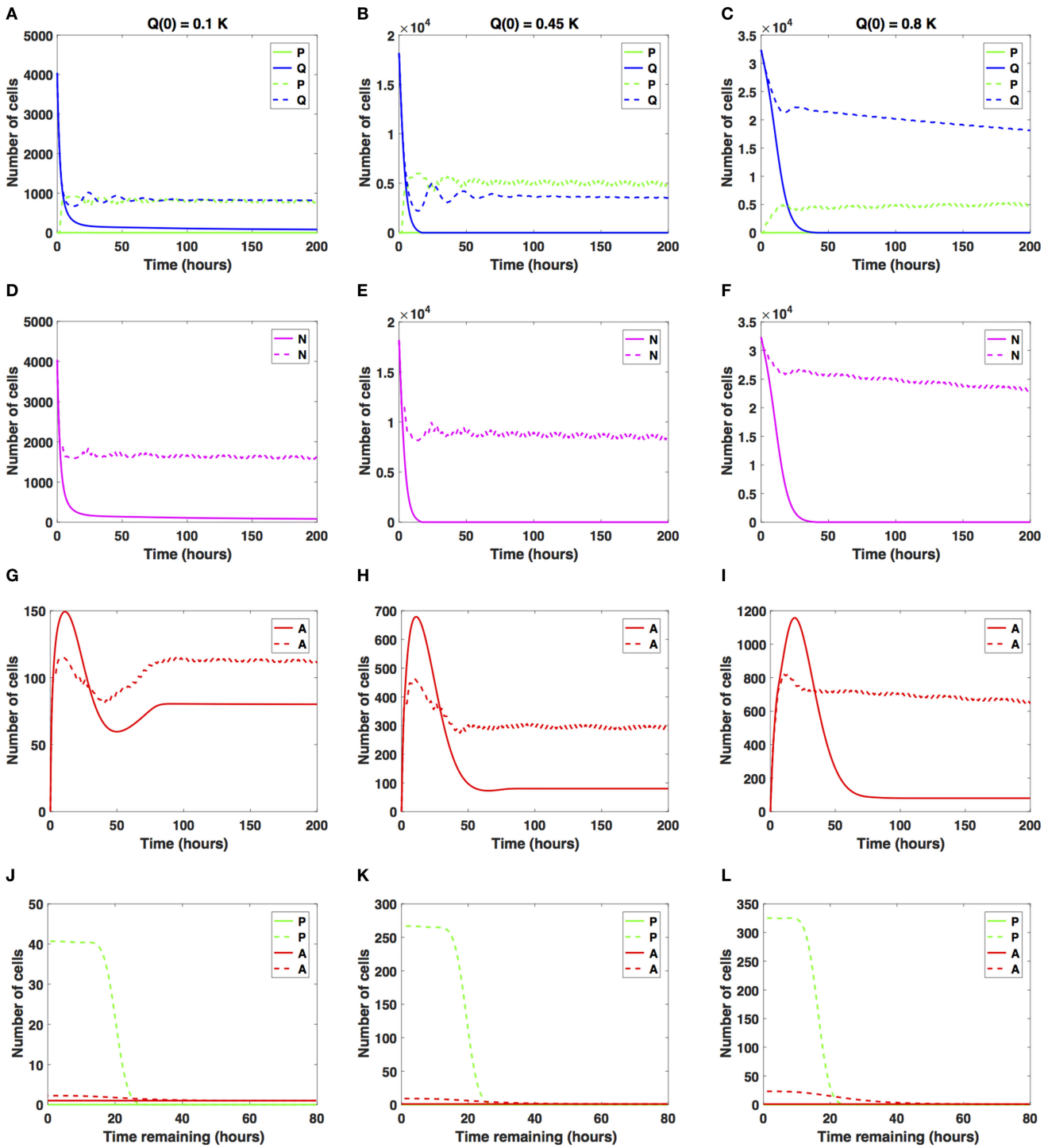

FIGURE 5 | Numerical solutions for the system (1)–(3) given large increases in the average cell-cycle length with **(A,D,G,J)** $Q(0) = 10\%$, **(B,E,H,K)** $Q(0) = 45\%$, and **(C,F,I,L)** $Q(0) = 80\%$ of the *in vitro* carrying capacity, K. The cellular dynamics in each compartment given a sustained, constant mitotic arrest or a switch-on/switch-off arrest is illustrated using solid or dashed lines, respectively. **(A–F)** show the dynamics of the proliferating (P), quiescent (Q), and the total number of non-apoptotic cells (N). **(G–I)** show the dynamics of the apoptotic cells (A). Panels **(J–L)** illustrate the distribution of the times remaining to be spent by cells in the proliferative (P) and apoptotic (A) compartments as seen at the end of the simulation time, $t = 200$ h, with **(J)** $Q(0) = 10\%$, **(K)** $Q(0) = 45\%$, and **(L)** $Q(0) = 80\%$ of the plate carrying capacity, K.

(see dashed lines in **Figures 5A,D**). Similar results are obtained when considering $Q(0) = 0.45K$, shown in **Figures 5B,E,H,K**.

However, when $Q(0) = 0.8K$, the dynamics of the proliferative (green lines), quiescent (blue lines), and apoptotic (red lines) cell compartments are quantitatively and qualitatively distinct between the two antimitotic drug effects, with a clear difference between the sustained, constant, and switch-on/switch-off mitotic arrest (see **Figures 5C,F,I,L,** solid versus dashed lines for each color representing the different cellular compartments).

Specifically, the number of proliferative cells, given the sustained, constant mitotic arrest (solid green line in **Figure 5C**), remains essentially zero for the entire simulation, similar to the 10 and 45% initial density cases. However, given the switch-on/switch-off mitotic arrest (dashed green line in **Figure 5C**), proliferative cell numbers exhibit a steady oscillatory state throughout the duration of the simulation. The number of quiescent cells (dashed green and blue lines, respectively) continues to steadily decrease for both drug effects, with quiescent cells decaying at a faster rate in the sustained, constant arrest case than in the switch-on/switch-off one (see **Figure 5C**). A similar pattern can be observed in the dynamics of the total number of cells (proliferating and quiescent), as represented by the solid and dashed magenta lines in **Figure 5F**. The total number of apoptotic cells (solid and dashed red lines in **Figure 5I**) oscillates with time.

Our numerical simulations suggest that in the presence of a large sustained increase in the average cell-cycle length induced by the drug, the cancer cell population is nearly driven to extinction, despite the large initial starting density (see solid lines in **Figures 5C,F**). Conversely, in the presence of a long-term switch-on/switch-off arrest, it is possible to maintain an active cancer cell population even when starting with a large initial plating density ($Q(0) = 0.8K$) and a large increase in the average cell-cycle length. The dynamic balance between the quiescent and proliferative cell turnover is maintained over time (see dashed lines in **Figures 5C,F**). We conclude that in the presence of large increases in the average cell-cycle length induced by the drug, a sustained, constant mitotic arrest drives both the proliferating and quiescent cell numbers to extinction. A switch-on/switch-off arrest maintains an active cell population in the long-term, with proliferative and quiescent cell numbers exhibiting a steady oscillatory state in time.

4. DISCUSSION

The dynamics of cellular response to antimitotic drug exposure has only recently begun to be investigated *in vitro* using time-lapse microscopy on single cells in culture (18, 29, 30, 32–38, 56, 58, 64, 65). Several studies have demonstrated that antimitotic drugs characteristically induce a period of prolonged mitotic arrest (that can last for as long as 72 hours or more) followed predominantly by cell death via apoptosis (32). As such, mitotic arrest constitutes the first cellular response to antimitotic drug exposure, but the mechanisms behind the drug-induced prolonged mitotic arrest and subsequent cancer cell death remain, however, unclear (30–33, 35–37, 64, 65, 69).

To investigate this issue, multiple antimitotic drugs and different drug concentrations have been used in cancer cell studies. Accordingly, multiple *in vitro* single-cell live imaging studies have demonstrated that cancer cells display widely varying responses to antimitotic drugs given different exposure times and drug concentrations (30–33, 35–37, 56, 64, 65, 69). These findings provided strong evidence that the duration of the mitotic arrest is not identical for all cells, both across and within distinct cancer cell lines, in the presence of various antimitotic drugs such as nocodazole, kinesin-5 (Eg5) inhibitors, monastrol, or taxol (29–32, 35, 36).

Even within identical types of cell cultures or drugs used, cells exhibit a considerable degree of heterogeneity in response to prolonged antimitotic drug exposure. For example, cells may either exit mitosis and remain in interphase for an indefinite period of time, undergo programmed cell death (i.e., apoptosis) after exiting mitosis or interphase, or proceed through mitosis via multipolar spindle formation (29, 31–33, 35–37, 69). In the case of multipolar spindle formation, cells divide into daughter cells by segregating their chromosomes in more than two different directions, dying during the second mitosis, or remaining in interphase for the duration of the experiments (33, 69, 70).

Motivated by these experimental findings, we introduce a novel mathematical modeling framework of cancer cell dynamics given drug exposure that incorporates an intrinsic form of heterogeneity in response to prolonged antimitotic drug exposure via the duration of times cells spend in the cell cycle and apoptosis process. The system (1)–(3) is an age-structured, physiologically motivated modeling framework for describing *in vitro* cancer cell growth dynamics given a drug that induces mitotic arrest, thus extending the average cell-cycle length. To reflect the intrinsic cell heterogeneity, cells in the proliferative and in the apoptotic compartment are structured by the amount of time they spend in each phase. Herein, we considered a drug that extends the average cell-cycle length and studied its impact on the long-term cancer cell growth dynamics and response to antimitotic drug exposure using two distinct antimitotic drug effects, i.e., a sustained, constant mitotic arrest and a switch-on/switch-off arrest and three different levels of increase in the average cell-cycle lengths.

Our numerical simulations suggest that at confluence and in the absence of any drug, quiescence is the long-term asymptotic behavior emerging from the cancer cell growth dynamics. Upon drug addition, the cancer cell dynamics significantly changes. Specifically, the prolonged mitotic arrest induced by the antimitotic drug results in a strong growth-inhibitory activity *in vitro* in a time-dependent manner. In the presence of small increases in the average cell-cycle length, quiescence emerges as the long-term asymptotic behavior resulting from the cancer cell growth dynamics. Our numerical simulations suggest that quiescence can emerge relatively quickly and can thus constitute an intrinsic resistance mechanism to antimitotic drug exposure. The small increases in the average cell-cycle length result in a period of slowing down of the cell cycle from which cancer cells can recover and continue proliferating until reaching confluence. From a therapeutic point of view, the presence of quiescent cancer cells has serious implications for chemotherapy regimens, which rely on active cell cycling to target and kill proliferating cells. The long-term maintenance of a quiescent cancer cell population acts as a reservoir for proliferating cells and can ultimately lead to cancer recurrence and shorter disease-free survival periods (7–9, 71, 72).

However, in the presence of intermediate increases in the average cell-cycle length, a sustained, constant mitotic arrest markedly decreases the total number of cancer cells present and can drive the cell population to extinction. A switch-on/switch-off arrest maintains an active cell population in the long term, with proliferative cell numbers exhibiting a steady oscillatory state and quiescent cell numbers remaining relatively constant in time. The transient behavior in the cancer cell growth dynamics signals the emergence and maintenance of a steady quiescent cell population, which in turn represents a form of intrinsic, non-genetic resistance that results from variations in cell-cycle parameters (73, 74). This can potentially decrease the efficacy of therapies that rely on active cell cycling for their killing effects, such as traditional chemotherapies (75–77). Moreover, given large increases in the average cell-cycle length induced by antimitotics, cells do not resume proliferation and are driven to extinction by a sustained, constant mitotic arrest. Intriguingly, a switch-on/switch-off arrest may maintain an active cancer cell population in the long term. This suggests that unless exposed to saturating drug concentrations for prolonged periods of time, cancer cells may not experience a mitotic arrest for long enough in order to trigger apoptosis, which may have therapeutic implications as clinical responses depend on apoptosis rates and not exclusively on mitotic arrest (18, 69).

Additionally, the fate of cells following drug treatment also depends on the cell type. For instance, cell lines sensitive to mitotic cell death tend to reach the MOMP threshold before cyclin B1 levels reach the threshold required for cells to slip out of mitosis (29, 32, 33, 35, 37, 69). Conversely, cell lines resistant to mitotic cell death tend to have a faster rate of cyclin B1 degradation and/or slow rate of intrinsic cell death activation (34, 36, 38, 58). These molecular-based variations in sensitivity to apoptosis and mitotic arrest are likely to substantially contribute to the observed heterogeneity in cell responses and potentially represent the crucial factor in determining cell fate in response to antimitotic drug exposure.

AUTHOR CONTRIBUTIONS

Conceived and designed the experiments: AL, D-AB, and DL. Acquired, analyzed, and interpreted the data: AL, D-AB, and DL. Drafted the manuscript: AL, D-AB, and DL. Approved the final version of the manuscript: AL, D-AB, and DL.

FUNDING

The work of AL was supported by the King Abdullah University of Science and Technology (KAUST) baseline and start-up funds (BAS/1/1648-01-01 and BAS/1/1648-01-02). The work of D-AB was partially supported by the Intramural Research Program of the National Institutes of Health, Center for Cancer Research, National Cancer Institute, as part of a seed grant from the UMD-NCI Partnership for Cancer Technology. The work of DL was supported in part by the John Simon Guggenheim Memorial Foundation, the Simons Foundation, and the Jayne Koskinas Ted Giovanis Foundation. The funders had no role in the study design, data collection and analysis, decision to publish, or preparation of the manuscript.

REFERENCES

1. Lloyd MC, Cunningham JJ, Bui MM, Gillies RJ, Brown JS, Gatenby RA. Darwinian dynamics of intratumoral heterogeneity: not solely random mutations but also variable environmental selection forces. *Cancer Res* (2016) 76(11):3136–44. doi:10.1158/0008-5472.CAN-15-2962
2. Gerlinger M, Rowan AJ, Horswell S, Larkin J, Endesfelder D, Gronroos E, et al. Intratumor heterogeneity and branched evolution revealed by multiregion sequencing. *N Engl J Med* (2012) 366(10):883–92. doi:10.1056/NEJMoa1113205
3. Pribluda A, Cecile C, Jackson EL. Intratumoral heterogeneity: from diversity comes resistance. *Clin Cancer Res* (2015) 21(13):2916–23. doi:10.1158/1078-0432.CCR-14-1213
4. Sottoriva A, Spiteri I, Piccirillo SG, Touloumis A, Collins VP, Marioni JC, et al. Intratumor heterogeneity in human glioblastoma reflects cancer evolutionary dynamics. *Proc Natl Acad Sci U S A* (2013) 110(10):4009–14. doi:10.1073/pnas.1219747110
5. Sherman-Baust CA, Becker KG, Wood Iii WH, Zhang Y, Morin PJ. Gene expression and pathway analysis of ovarian cancer cells selected for resistance to cisplatin, paclitaxel, or doxorubicin. *J Ovarian Res* (2011) 4(1):21. doi:10.1186/1757-2215-4-21
6. Borst P. Cancer drug pan-resistance: pumps, cancer stem cells, quiescence, epithelial to mesenchymal transition, blocked cell death pathways, persisters or what? *Open Biol* (2012) 2(5):120066. doi:10.1098/rsob.120066
7. Chen JG, Horwitz SB. Differential mitotic responses to microtubule-stabilizing and -destabilizing drugs. *Cancer Res* (2002) 62(7):1935–8. doi:10.4161/cc.7.4.5313
8. Janssen A, Beerling E, Medema R, van Rheenen J. Intravital FRET imaging of tumor cell viability and mitosis during chemotherapy. *PLoS One* (2013) 8(5):e64029. doi:10.1371/journal.pone.0064029
9. Hornick JE, Bader JR, Tribble EK, Trimble K, Breunig JS, Halpin ES, et al. Live-cell analysis of mitotic spindle formation in taxol-treated cells. *Cell Motil Cytoskeleton* (2008) 65(8):595–613. doi:10.1002/cm.20283
10. Chien J, Kuang R, Landen C, Shridhar V. Platinum-sensitive recurrence in ovarian cancer: the role of tumor microenvironment. *Front Oncol* (2013) 3:251. doi:10.3389/fonc.2013.00251
11. Schiff PB, Horwitz SB. Taxol stabilizes microtubules in mouse fibroblast cells. *Proc Natl Acad Sci U S A* (1980) 77(3):1561–5. doi:10.1073/pnas.77.3.1561
12. Ozols RF, Bundy BN, Greer BE, Fowler JM, Clarke-Pearson D, Burger RA, et al. Phase III trial of carboplatin and paclitaxel compared with cisplatin and paclitaxel in patients with optimally resected stage III ovarian cancer: a Gynecologic Oncology Group study. *J Clin Oncol* (2003) 21(17):3194–200. doi:10.1200/JCO.2003.02.153
13. Piccart M, Cardoso F. Progress in systemic therapy for breast cancer: an overview and perspectives. *Eur J Cancer* (2003) 1(2):56–69. doi:10.1016/S1359-6349(03)00009-0
14. Bonomi P, Kim K, Kusler J. Comparison of survival for stage IIIB versus IV non-small cell lung cancer (NSCLC) patients with etopiside-cisplatin versus taxol-cisplatin: an Eastern Cooperative Oncology (ECOG) Group trial. *J Clin Oncol* (2000) 16(2):623–31. doi:10.1200/JCO.2000.18.3.623
15. Woessner R, Tunquist B, Lemieux C, Chlipala E, Jackinsky S, Dewolf W, et al. ARRY-520, a novel KSP inhibitor with potent activity in hematological and taxane-resistant tumor models. *Anticancer Res* (2009) 29(11):4373–80.
16. Hirschmann-Jax C, Foster AE, Wulf GG, Nuchtern JG, Jax TW, Gobel U, et al. A distinct "side population" of cells with high drug efflux capacity in human tumor cells. *Proc Natl Acad Sci U S A* (2004) 101(39):14228–33. doi:10.1073/pnas.0400067101
17. Aneja R, Zhou J, Vangapandu SN, Zhou B, Chandra R, Joshi HC. Drug-resistant T-lymphoid tumors undergo apoptosis selectively in response to an antimicrotubule agent, EM011. *Blood* (2006) 107(6):2486–92. doi:10.1182/blood-2005-08-3516
18. Shi J, Mitchison TJ. Cell death response to anti-mitotic drug treatment in cell culture, mouse tumor model and the clinic. *Endocr Relat Cancer* (2017) 24(9):T83–96. doi:10.1530/ERC-17-0003

19. Marzo I, Naval J. Antimitotic drugs in cancer chemotherapy: promises and pitfalls. *Biochem Pharmacol* (2013) 86(6):703–10. doi:10.1016/j.bcp.2013.07.010
20. Jackson JR, Patrick DR, Dar MM, Huang PS. Targeted anti-mitotic therapies: can we improve on tubulin agents? *Nat Rev Cancer* (2007) 7(2):107–17. doi:10.1038/nrc2049
21. Perez EA. Microtubule inhibitors: differentiating tubulin-inhibiting agents based on mechanisms of action, clinical activity, and resistance. *Mol Cancer Ther* (2009) 8(8):2086–95. doi:10.1158/1535-7163.MCT-09-0366
22. Fanale D, Bronte G, Passiglia F, Calo V, Castiglia M, Di Piazza F, et al. Stabilizing versus destabilizing the microtubules: a double-edge sword for an effective cancer treatment option? *Anal Cell Pathol (Amst)* (2015) 2015:690916. doi:10.1155/2015/690916
23. Mukhtar E, Adhami VM, Mukhtar H. Targeting microtubules by natural agents for cancer therapy. *Mol Cancer Ther* (2014) 13(2):275–84. doi:10.1158/1535-7163.MCT-13-0791
24. Ye XS, Fan L, Van Horn RD, Nakai R, Ohta Y, Akinaga S, et al. A novel Eg5 inhibitor (LY2523355) causes mitotic arrest and apoptosis in cancer cells and shows potent antitumor activity in xenograft tumor models. *Mol Cancer Ther* (2015) 14(11):2463–72. doi:10.1158/1535-7163.MCT-15-0241
25. Brogdon CF, Lee FY, Canetta RM. Development of other microtubule-stabilizer families: the epothilones and their derivatives. *Anticancer Drugs* (2014) 25(5):599–609. doi:10.1097/CAD.0000000000000071
26. Cheetham P, Petrylak DP. Tubulin-targeted agents including docetaxel and cabazitaxel. *Cancer J* (2013) 19(1):59–65. doi:10.1097/PPO.0b013e3182828d38
27. Islam MN, Iskander MN. Microtubulin binding sites as target for developing anticancer agents. *Mini Rev Med Chem* (2004) 4(10):1077–104. doi:10.2174/1389557043402946
28. Jordan MA, Wilson L. Microtubules as a target for anticancer drugs. *Nat Rev Cancer* (2004) 4(4):253–65. doi:10.1038/nrc1317
29. Shi J, Orth JD, Mitchison T. Cell type variation in responses to antimitotic drugs that target microtubules and kinesin-5. *Cancer Res* (2008) 68(9):3269–76. doi:10.1158/0008-5472.CAN-07-6699
30. Huang HC, Mitchison TJ, Shi J. Stochastic competition between mechanistically independent slippage and death pathways determines cell fate during mitotic arrest. *PLoS One* (2010) 5(12):e15724. doi:10.1371/journal.pone.0015724
31. Bekier ME, Fischbach R, Lee J, Taylor WR. Length of mitotic arrest induced by microtubule-stabilizing drugs determines cell death after mitotic exit. *Mol Cancer Ther* (2009) 8(6):1646–54. doi:10.1158/1535-7163.MCT-08-1084
32. Gascoigne KE, Taylor SS. Cancer cells display profound intra- and interline variation following prolonged exposure to antimitotic drugs. *Cancer Cell* (2008) 14(2):111–22. doi:10.1016/j.ccr.2008.07.002
33. Aspinall CF, Zheleva D, Tighe A, Taylor SS. Mitotic entry: non-genetic heterogeneity exposes the requirement for Plk1. *Oncotarget* (2015) 6(34):36472–88. doi:10.18632/oncotarget.5507
34. Hain KO, Colin DJ, Rastogi S, Allan LA, Clarke PR. Prolonged mitotic arrest induces a caspase-dependent DNA damage response at telomeres that determines cell survival. *Sci Rep* (2016) 6:26766. doi:10.1038/srep26766
35. Orth JD, Tang Y, Shi J, Loy CT, Amendt C, Wilm C, et al. Quantitative live imaging of cancer and normal cells treated with Kinesin-5 inhibitors indicates significant differences in phenotypic responses and cell fate. *Mol Cancer Ther* (2008) 7(11):3480–9. doi:10.1158/1535-7163.MCT-08-0684
36. Brito DA, Rieder CL. The ability to survive mitosis in the presence of microtubule poisons differs significantly between human nontransformed (RPE-1) and cancer (U2OS, HeLa) cells. *Cell Motil Cytoskeleton* (2009) 66(8):437–47. doi:10.1002/cm.20316
37. Topham C, Tighe A, Ly P, Bennett A, Sloss O, Nelson L, et al. MYC is a major determinant of mitotic cell fate. *Cancer Cell* (2015) 28:129–40. doi:10.1016/j.ccell.2015.06.001
38. Colin DJ, Hain KO, Allan LA, Clarke PR. Cellular responses to a prolonged delay in mitosis are determined by a DNA damage response controlled by Bcl-2 family proteins. *Open Biol* (2015) 5(3):140156. doi:10.1098/rsob.140156
39. Choi HJ, Zhu BT. Role of cyclin B1/Cdc2 in mediating Bcl-XL phosphorylation and apoptotic cell death following nocodazole-induced mitotic arrest. *Mol Carcinog* (2014) 53(2):125–37. doi:10.1002/mc.21956
40. Choi HJ, Fukui M, Zhu BT. Role of cyclin B1/Cdc2 up-regulation in the development of mitotic prometaphase arrest in human breast cancer cells treated with nocodazole. *PLoS One* (2011) 6(8):e24312. doi:10.1371/journal.pone.0024312
41. Chisholm RH, Lorenzi T, Lorz A, Larsen AK, de Almeida LN, Escargueil A, et al. Emergence of drug tolerance in cancer cell populations: an evolutionary outcome of selection, nongenetic instability, and stress-induced adaptation. *Cancer Res* (2015) 75(6):930–9. doi:10.1158/0008-5472.CAN-14-2103
42. Enderling H, Chaplain MA. Mathematical modeling of tumor growth and treatment. *Curr Pharm Des* (2014) 20(30):4934–40. doi:10.2174/1381612819666131125150434
43. Wang W, Quan Y, Fu Q, Liu Y, Liang Y, Wu J, et al. Dynamics between cancer cell subpopulations reveals a model coordinating with both hierarchical and stochastic concepts. *PLoS One* (2014) 9(1):e84654. doi:10.1371/journal.pone.0084654
44. Powathil G, Chaplain M, Swat M. Investigating the development of chemotherapeutic drug resistance in cancer: a multiscale computational study. *IET Syst Biol* (2015) 1(1):1–23.
45. Lorz A, Lorenzi T, Hochberg ME, Clairambault J, Perthame B. Populational adaptive evolution, chemotherapeutic resistance and multiple anti-cancer therapies. *ESAIM Math Model Numer Anal* (2013) 47(8):377–99. doi:10.1051/m2an/2012031
46. Basse B, Baguley BC, Marshall ES, Joseph WR, van Brunt B, Wake G, et al. A mathematical model for analysis of the cell cycle in cell lines derived from human tumors. *J Math Biol* (2003) 47(4):295–312. doi:10.1007/s00285-003-0203-0
47. Spinelli L, Torricelli A, Ubezio P, Basse B. Modelling the balance between quiescence and cell death in normal and tumour cell populations. *Math Biosci* (2006) 202(2):349–70. doi:10.1016/j.mbs.2006.03.016
48. Greene JM, Levy D, Fung KL, Souza PS, Gottesman MM, Lavi O. Modeling intrinsic heterogeneity and growth of cancer cells. *J Theor Biol* (2015) 367:262–77. doi:10.1016/j.jtbi.2014.11.017
49. Greene JM, Levy D, Herrada SP, Gottesman MM, Lavi O. Mathematical modeling reveals that changes to local cell density dynamically modulate baseline variations in cell growth and drug response. *Cancer Res* (2016) 76(10):2882–90. doi:10.1158/0008-5472.CAN-15-3232
50. Rundell W. Determining the birth function for an age structured population. *Math Popul Stud* (1989) 1(4):377–95. doi:10.1080/08898488909525285
51. Pilant M, Rundell W. Determining the initial age distribution for an age structured population. *Math Popul Stud* (1991) 3(1):3–20. doi:10.1080/08898489109525320
52. Bekkal Brikci F, Clairambault J, Ribba B, Perthame B. An age-and-cyclin-structured cell population model for healthy and tumoral tissues. *J Math Biol* (2008) 57(1):91–110. doi:10.1007/s00285-007-0147-x
53. Gyllenberg M, Webb F. A nonlinear structured population model of tumor growth with quiescence. *J Math Biol* (1990) 28(6):671–94. doi:10.1007/BF00160231
54. Arino O, Kimmel M. Asymptotic analysis of models of cell production systems. *Math Model* (1986) 7(6):1269–300. doi:10.1016/0270-0255(86)90081-3
55. Arino O, Kimmel M. Asymptotic analysis of a cell cycle model based on unequal division. *SIAM J Appl Math* (1987) 47(6):128–45. doi:10.1137/0147008
56. Kueh HY, Zhu Y, Shi J. A simplified Bcl-2 network model reveals quantitative determinants of cell-to-cell variation in sensitivity to anti-mitotic chemotherapeutics. *Sci Rep* (2016) 6:36585. doi:10.1038/srep36585
57. Blagosklonny MV. Mitotic arrest and cell fate: why and how mitotic inhibition of transcription drives mutually exclusive events. *Cell Cycle* (2007) 6(1):70–4. doi:10.4161/cc.6.1.3682
58. Orth JD, Loewer A, Lahav G, Mitchison TJ. Prolonged mitotic arrest triggers partial activation of apoptosis, resulting in DNA damage and p53 induction. *Mol Biol Cell* (2012) 23(4):567–76. doi:10.1091/mbc.E11-09-0781
59. Allan LA, Clarke PR. Phosphorylation of caspase-9 by CDK1/cyclin B1 protects mitotic cells against apoptosis. *Mol Cell* (2007) 26(2):301–10. doi:10.1016/j.molcel.2007.03.019
60. Hou Y, Allan LA, Clarke PR. Phosphorylation of XIAP by CDK1-cyclin-B1 controls mitotic cell death. *J Cell Sci* (2017) 130(2):502–11. doi:10.1242/jcs.192310
61. Jiang X, Li H, Zhao P, Xie J, Khabele D, Xu J, et al. Early detection of treatment-induced mitotic arrest using temporal diffusion magnetic resonance spectroscopy. *Neoplasia* (2016) 18(6):387–97. doi:10.1016/j.neo.2016.04.006

62. Messam CA, Pittman RN. Asynchrony and commitment to die during apoptosis. *Exp Cell Res* (1998) 238(2):389–98. doi:10.1006/excr.1997.3845
63. Vorobjev I, Barteneva NS. Temporal heterogeneity metrics in apoptosis induced by anticancer drugs. *J Histochem Cytochem* (2015) 63(7):494–510. doi:10.1369/0022155415583534
64. Eichhorn JM, Kothari A, Chambers TC. Cyclin B1 overexpression induces cell death independent of mitotic arrest. *PLoS One* (2014) 9(11):e113283. doi:10.1371/journal.pone.0113283
65. Eichhorn JM, Sakurikar N, Alford SE, Chu R, Chambers TC. Critical role of anti-apoptotic Bcl-2 protein phosphorylation in mitotic death. *Cell Death Dis* (2013) 4:e834. doi:10.1038/cddis.2013.360
66. Gascoigne KE, Taylor SS. How do anti-mitotic drugs kill cancer cells? *J Cell Sci* (2009) 122(15):2579–85. doi:10.1242/jcs.039719
67. Dixit R, Gold B. Inhibition of N-methyl-N-nitrosourea-induced mutagenicity and DNA methylation by ellagic acid. *Proc Natl Acad Sci U S A* (1986) 83(21):8039–43. doi:10.1073/pnas.83.21.8039
68. (DTP-NCI), D. T. P. *NCI-60 Human Tumor Cell Lines*. (2015). Available at: http://dtp.nci.nih.gov/
69. Zasadil LM, Andersen KA, Yeum D, Rocque GB, Wilke LG, Tevaarwerk AJ, et al. Cytotoxicity of paclitaxel in breast cancer is due to chromosome missegregation on multipolar spindles. *Sci Transl Med* (2014) 6(229):229ra43. doi:10.1126/scitranslmed.3007965
70. Weaver BA. How taxol/paclitaxel kills cancer cells. *Mol Biol Cell* (2014) 25(18):2677–81. doi:10.1091/mbc.E14-04-0916
71. Coller HA, Sang L, Roberts JM. A new description of cellular quiescence. *PLoS Biol* (2006) 4(3):e83. doi:10.1371/journal.pbio.0040083
72. Kangwan N, Park JM, Kim EH, Hahm KB. Chemoquiescence for ideal cancer treatment and prevention: where are we now? *J Cancer Prev* (2014) 19(2):89–86. doi:10.15430/JCP.2014.19.2.89
73. Moore N, Lyle S. Quiescent, slow-cycling stem cell populations in cancer: a review of the evidence and discussion of significance. *J Oncol* (2011) 2011:11. doi:10.1155/2011/396076
74. Visvader JE, Lindeman GJ. Cancer stem cells in solid tumours: accumulating evidence and unresolved questions. *Nat Rev Cancer* (2008) 8(10):755–68. doi:10.1038/nrc2499
75. Dickson MA, Schwartz GK. Development of cell-cycle inhibitors for cancer therapy. *Curr Oncol* (2009) 16(2):36–43.
76. Shapiro GI, Harper JW. Anticancer drug targets: cell cycle and checkpoint control. *J Clin Invest* (1999) 104(12):1645–53. doi:10.1172/JCI9054
77. Deep G, Agarwal R. New combination therapies with cell-cycle agents. *Curr Opin Investig Drugs* (2008) 9(6):591–604.

Conflict of Interest Statement: The authors declare that the research was conducted in the absence of any commercial or financial relationships that could be construed as a potential conflict of interest.

Advantages of publishing in Frontiers

OPEN ACCESS
Articles are free to read for greatest visibility and readership

FAST PUBLICATION
Around 90 days from submission to decision

HIGH QUALITY PEER-REVIEW
Rigorous, collaborative, and constructive peer-review

TRANSPARENT PEER-REVIEW
Editors and reviewers acknowledged by name on published articles

Frontiers
Avenue du Tribunal-Fédéral 34
1005 Lausanne | Switzerland

Visit us: www.frontiersin.org
Contact us: info@frontiersin.org | +41 21 510 17 00

REPRODUCIBILITY OF RESEARCH
Support open data and methods to enhance research reproducibility

DIGITAL PUBLISHING
Articles designed for optimal readership across devices

FOLLOW US
@frontiersin

IMPACT METRICS
Advanced article metrics track visibility across digital media

EXTENSIVE PROMOTION
Marketing and promotion of impactful research

LOOP RESEARCH NETWORK
Our network increases your article's readership